공학석사 학위논문

On the Analysis of High Viscous Horizontal Slug Flow Characteristics by Changing Pipe Diameter

관 직경 변화에 따른

고점성도 수평 슬러그 유동 특성 분석

2014 년 12 월

서울대학교 대학원

에너지시스템공학부

김 태 우

Abstract

On the Analysis of High Viscous Horizontal Slug Flow Characteristics by Changing Pipe Diameter

Taewoo Kim

Department of Energy Systems Engineering

The Graduate School

Seoul National University

The analysis of slug characteristics for high viscous horizontal flow was experimentally carried out by changing the pipe diameter. Slug flow is the general pattern of oil-gas two-phase flow in a horizontal pipe. Each slug characteristic plays an important role in predicting the pressure gradient and average liquid holdup, contributing to designing production systems.

Most of the existing prediction models were developed to evaluate low and medium viscous flow, so an experimental verification is needed to predict the flow parameters of high viscous flow. Furthermore, previous studies for high viscous flow have only been conducted in 50.8-mm-ID (2-in.) pipes. The scalability of the observed behavior in larger diameters is still under consideration.

628 experimental tests were conducted in a 76.2-mm-ID (3-in.) horizontal pipe. Six different oil viscosities were considered. Among them, data sets with 587 cP, 181 cP, and 155 cP were used to analyze the pipe diameter effects compared with the 50.8-mm-ID (2-in.) pipe experimental data. Superficial liquid velocity varied from 0.02 m/s to 0.35 m/s and superficial gas velocity varied from 0.1 m/s to 3.6 m/s to match the experimental matrices of previous studies.

Statistically calibrated two-wire type capacitance sensors were used to measure the liquid holdup. The pressure and pressure gradient were obtained using different transducers. Flow pattern, pressure gradient, average liquid holdup, slug liquid holdup, film liquid holdup, slug length, slug length distribution, and slug frequency were measured and analyzed. Not only data obtained from this study, but also previous data from 2-in. ID pipes were used to compare with the 3-in. ID pipes results.

The pipe diameter and oil viscosity affect the flow transition boundary, while the pressure drop decreases and the average liquid holdup increases for larger pipe diameters. Moreover, the slug liquid holdup and slug frequency increase, and the film liquid holdup and slug length decrease as the pipe diameter increases.

The experimental results were also used to evaluate different flow pattern maps, existing models and correlations for two-phase slug flow. Some degree of discrepancy was observed between experimental and predicted results, especially for predicting the pressure gradient. This indicates that the coupled effect of high viscosity with pipe diameter is yet to be completely understood and needs to be modified.

The simplified Lockhart and Martinelli's separated pressure gradient prediction model was suggested in this study by subtracting the accelerational pressure gradient from the original equation. This model presents lower absolute average relative errors than the original model and relatively acceptable average relative errors in the entire range of datasets, emphasizing the importance of separating liquid and gas Reynolds numbers in high viscous experimental data.

Keywords: two-phase flow, pipe diameter, high viscosity, horizontal flow, pipe flow, slug flow, pressure gradient, average liquid holdup, slug characteristics, slug liquid holdup, film liquid holdup, translational velocity, slug length, slug frequency, pressure gradient prediction model.

Student ID: 2012-23280

Table of Contents

List of Tables

List of Figures

Chapter 1 Introduction

In the petroleum industry, gas-liquid two-phase flow in pipes is extensively observed during production and transportation. For production system design, it is crucial to predict the flow behavior such as flow pattern, pressure drop, average liquid holdup, and slug characteristics correctly. Slug flow covers a great part of flow patterns in oil and gas horizontal flow. For that reason, slug flow parameters play a significant role in predicting pressure gradient and average liquid holdup especially for suggesting empirical closure relationship. Every flow variables, for example, liquid and gas flow rates, fluid properties, and pipe geometries can influence flow behaviors.

The importance of heavy oils has been highlighted as conventional oil and gas reservoirs become depleted. Thus, transition to alternative oils such as heavy oil (characterized by large viscosities) has been occurring with the demand increase of hydrocarbon resources and the deterioration in discoveries of new conventional hydrocarbon reservoirs.

Unfortunately, there is a lack of knowledge about viscosity and pipe geometry effect on two-phase flow. Most of the existing prediction models were proposed to evaluate low and medium viscous flow. Furthermore, only few studies for high viscous oil have been carried out in 50.8-mm-ID (2-in.) pipes. Scalability of the observed behavior to larger diameters is still under consideration.

Accordingly, the main objective of the present study is to investigate the pipe diameter effects on flow pattern, pressure drop, average liquid holdup, and slug characteristics. This last includes slug liquid holdup, film liquid holdup, translational velocity, slug length, and slug frequency. A 76.2-mm-ID (3-in.) and 18.9-m-long

horizontal test section was used in this experimental study. The experiments were conducted with various oil viscosities, namely, 587 cP, 420 cP, 300 cP, 220 cP, 181 cP, and 155 cP, corresponding to oil temperatures of 61 °F, 70 °F, 80 °F, 90 °F, 96.5 °F, and 100 °F. The selected oil viscosities cover medium to high oil viscosities. 628 experimental data points were completed with elaborate instrumentations and video recordings, resulting in a comprehensive data set. Among them, oil viscosities of 587 cP, 181 cP, and 155 cP were used to analysis the pipe diameter effects comparing with the previous 50.8-mm-ID (2-in.) pipes experimental data.

All of the slug characteristics including pressure gradient and average liquid holdup were qualitatively analyzed to investigate multiple effects of pipe diameter and oil viscosity. Different flow transition boundaries were observed, while pressure drop decreases and average liquid holdup increases for larger pipe diameter. Slug liquid holdup and slug frequency also increase, and film liquid holdup and slug length decrease as a pipe diameter increases.

The existing correlations and models for various flow parameters such as pressure gradient, average liquid holdup, slug liquid holdup, film liquid holdup, translational velocity, slug length, and slug frequency were quantitatively tested to evaluate their performance against the experimental data. Based on statistical parameters, some degrees of discrepancy were observed, indicating that the existing closure relationships are needed to be modified by changing inner coefficients or variations. Most closure relationships were developed by using experimental data due to the complexity of oil-gas two-phase flow. Nevertheless, the proper correlations and models showing lower errors were able to be suggested by this study for specific cases with the necessity of further experiments.

Among the compared closure relationships, there is no model which

can properly predict pressure gradient. Assuming this is mainly occurred by misapplication of Reynolds numbers, the simplified Lockhart and Martinelli's separated model is proposed, presenting fair agreement when compared with the experimental data of 2- and 3-in. ID pipes.

This study is comprised as follows and some other related information is provided in appendices:

Chapter 1 provides an introduction to the dissertation, defining the problems, research objective, summary, and structure of the dissertation.

Chapter 2, Literature Review, arranges and summarizes the relevant literatures which were used and consulted in this project.

Chapter 3, Experimental System, describes details on the facility, and explains the components of this facility such as fluids, instrumentations, data acquisition system, and procedure of data analysis.

Chapter 4, Pipe Diameter Effect on Slug Characteristics for High Viscous Horizontal Flow, shows comparison between the results of 50.8-mm-(2-in.) and 76.2-mm-ID (3-in.) pipes to determine the effect of pipe diameter on slug flow parameters.

Chapter 5, Model and Correlation Evaluation, presents the evaluation of existing two-phase flow models against experimental results with 50.8-mm-(2-in.) and 76.2-mm-ID (3-in.) pipes.

Chapter 6, Simplified Lockhart and Martinelli's Separated Pressure Gradient Prediction Model, gives the procedure of simplification, and the verification with present data.

Chapter 7, gives all the combined key conclusions from this research. Recommendations are suggested for the further study.

Chapter 2 Literature Review

Numbers of studies related to oil and gas two-phase flow in horizontal pipes have been conducted. Most of them accomplished with 50.8-mm-ID (2-in.) pipes. Moreover, there were very few studies for the pipe diameter effects on comprehensive two-phase flow characteristics. Thus, this study is the very first research for scale-up and viscosity effects on comprehensive two-phase flow parameters such as pressure gradient, average liquid holdup, and slug characteristics. This section presents a literature review of the previous studies which showed the effects of oil viscosity on two-phase flow characteristics in horizontal pipes. Literatures are classified into the experimental study and the model development study.

2.1 Experimental studies

There are numerous publications for the two-phase pipe flow experiments using various liquids such as water (μ_L=1cP), low (μ_L<10cP) viscous, medium (10cP< μ_L <180cP) viscous, and high (μ_L>180cP) viscous oils.

Shoham (1982) conducted an experimental study for air-water flow in the 50.8-mm-ID pipes to observe the specific flow patterns over the entire range of inclination angles. The observed flow patterns were stratified smooth, stratified wavy, elongated bubble, slug, annular, and dispersed bubble flows. Flow patterns in horizontal and near-horizontal conditions are shown in Figure 2.1.

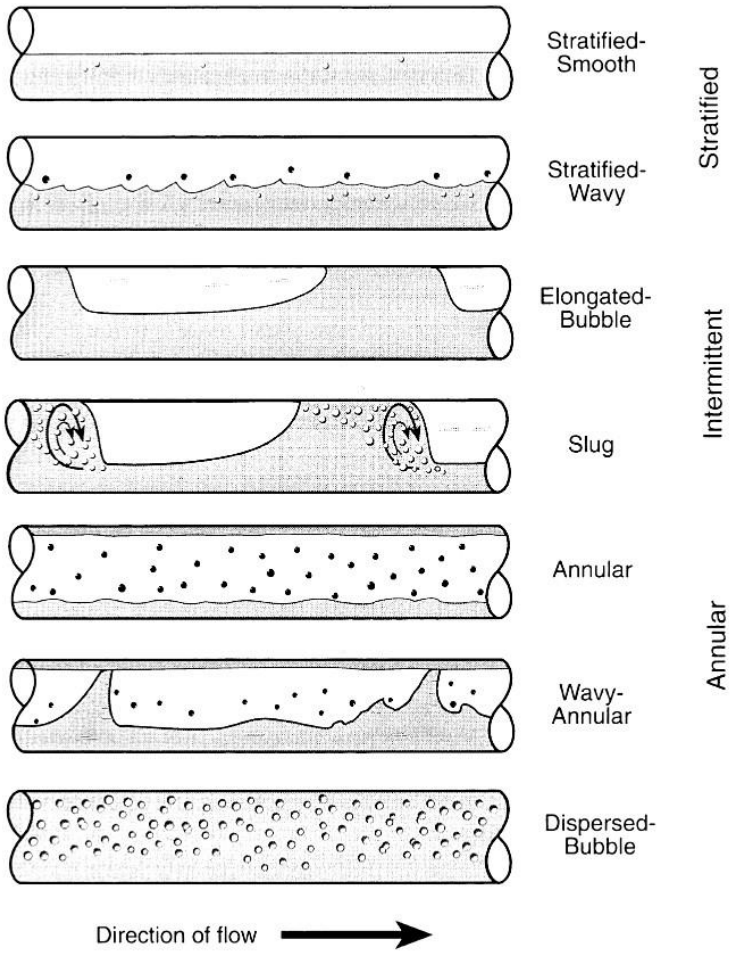

Figure 2.1 Flow patterns in horizontal and near-horizontal pipes (Shoham, 2006).

Kokal (1987) investigated flow characteristics using the oil-air two-phase in horizontal and slightly inclined pipes. Additionally, different pipe diameters (25.4-, 50.8-, and 76.2-mm-ID pipes) were used to investigate the effect of the pipe diameter on transition boundaries. Comparing with theoretical predictions, pipe diameter had a distinct effect on all transition boundaries.

Nädler & Mewes (1995) reported experimental results of the effect of liquid viscosity on the phase distribution in two-phase air-liquid slug flow in horizontal pipes. Water and viscous oil (14 mPas< μ_L<37 mPas) were used as test fluids with the 50.8-mm-ID pipes. They used a gamma ray densitometer to measure the liquid holdup. They observed that the average liquid holdup increased by the liquid viscosity increase.

Marcano *et al*. (1998) performed an experimental study for translational velocity, slug length, pressure drop, slug length distribution, and slug frequency. His work showed that the slug length has a log-normal distribution.

Colmenares *et al*. (2001) experimentally studied the flow characteristics and the existing model comparison for viscous oils in horizontal condition. It was observed that the slug flow region was expanded with an increase of oil viscosity. Additionally, slug frequency and film liquid holdup increased, while slug length decreased as oil viscosity increased.

With air-water and air-glycerin (27 cP) as test fluids, Rosa *et al*. (2004) investigated the influence of liquid viscosity on slug characteristics in horizontal condition. Average slug length and coalescence rate decreased with liquid viscosity increase. Conversely, slug frequency and bubble front velocity increased as liquid viscosity increased.

Gokcal (2005 and 2008) conducted experimental studies to understand the effects of high oil viscosity on two-phase oil-gas flow behaviors in horizontal 50.8-mm-ID pipes. He found that, at high oil viscosities (μ_L>180cP), the dominant flow regimes were intermittent flow (elongated bubble and slug flow), and oil viscosity had a marked effect on flow behavior. As oil viscosity

increased, pressure gradient and average liquid holdup increased, and flow pattern map showed a little discrepancy in prediction of the transition boundary. For the slug flows, slug length decreased and slug frequency increased with oil viscosity increase.

Kora (2010) experimentally studied the effects of high oil viscosity on slug liquid holdup in horizontal 50.8-mm-ID pipes. In her study, the existing slug liquid holdup correlations and models poorly agreed with the experimental results, especially, at mixture velocities higher than 2 m/s. Slug liquid holdup slightly decreased with increasing oil viscosity. Experimental data for liquid film heights were acquired with respect to oil viscosity increase, but no significant change was observed.

Ben-Mansour *et al*. (2010) investigated the effect of high viscous oil on drift velocity in different pipe diameters. Experimental and simulation results were compared, reporting that the drift velocity increased with an increase in pipe diameter. Additionally, the height of liquid film increased with liquid viscosity increase and pipe diameter decrease.

A recent experimental study of Brito (2012) addressed the effect of medium oil viscosity on two-phase oil-gas flow behavior in 50.8-mm-ID horizontal pipes. The trend of her results were in agreement with Gokcal (2005 and 2008) and Kora (2010), which were conducted with a larger range of superficial liquid and gas velocities. Additionally, a total of 21 tests were conducted at 587 cP to determine the effect of mixing tee geometry on two-phase oil-gas flow behavior in horizontal pipes. The more suitable shape of mixing tee was able to be designed and installed to gauge superficial liquid and gas velocities more precisely.

2.2 Modeling development studies

There are various models developed for each flow parameters. The models used in this study (see Ch. 5.) are enumerated and explained in this section. The previous model development studies are categorized into the following subsections: flow pattern, pressure gradient & average liquid holdup, slug liquid holdup, film liquid holdup, translational velocity, slug length, and slug frequency.

2.2.1 Flow pattern

Taitel & Dukler (1976) developed a theoretical model to predict the relationship between the fluid variables at which flow regime transitions take place. The new generalized map did account for all of the operational factors and thus permitted the prediction of flow regime with confidence at every conditions.

Barnea (1987) presented and summarized the models for predicting flow pattern transitions in steady gas-liquid flow in pipes. He proposed the models which incorporates the effect of fluid properties, pipe size and inclination angle in a unified way. The developed models are not restricted to a specific range of pipe inclinations.

Zhang *et al*. (2003a and b) proposed a unified hydrodynamic model based on the dynamics of slug flow. The proposed model is applicable to all pipe geometries and fluid properties. This model can predict the flow pattern transitions, pressure gradient, and liquid holdup for all inclination angles using

the momentum equations for slug flow. It shows suitable predictions for flow pattern and hydrodynamic behaviors.

2.2.2 Pressure gradient and average liquid holdup

Xiao *et al*. (1990) proposed a comprehensive mechanistic model for gas-liquid two-phase flow in horizontal and near horizontal pipelines. With establishing a pipeline data bank, they presented their model can detect the existing flow pattern, and can predict the flow characteristics, primarily liquid holdup and pressure drop. The model was evaluated against the data bank and compared with the most commonly used correlations for two-phase flow in pipelines.

Gokcal *et al*. (2006) modified the closure relationships included in the Zhang *et al*. (2003) model. The modified model showed better agreement with the experimental results for pressure gradient and liquid holdup in high viscous oils.

2.2.3 Slug characterization

Gokcal (2005, 2008), Kora (2010), Jeyachandra (2011), and Brito (2012) demonstrated that the effect of high viscous oil on two-phase flow and the most commonly observed flow pattern is slug flow. The following sections present the previous studies into slug liquid holdup, film liquid holdup, translational velocity, slug length, and slug frequency.

2.2.3.1 Slug liquid holdup

Gregory *et al.* (1978) developed a simple empirical correlation using the mixture velocity, which can be used to predict the slug liquid holdup. It was shown to be a significant performance over the entire range of flow rates in which slug flow occurs. This model is shown in Eq. (1).

$$H_{LLS} = \frac{1}{1+(\frac{v_m}{\alpha})^{\beta}} \tag{1}$$

where α=8.66 and β=1.39 were used for the conditions of 25.4- and 50.8-mm-ID pipes when v_{SG}<10 m/s.

Barnea & Brauner (1985) assumed that the gas in a developed liquid slug appears as dispersed bubbles. Following this assumption, the gas holdup that the liquid slug can accommodate as dispersed bubbles is to be determined from a balance between breakage forces due to turbulence and coalescence forces due to gravity and/or surface tension. The developed model is presented in Eq. (2) based on the above assumption.

$$H_{LLS} = 1 - 0.058\left[2\left(\frac{0.4\sigma}{(\rho_L-\rho_G)}\right)^{1/2}\left(\frac{2f_s v_m{}^3}{D_p}\right)^{2/5}\left(\frac{\rho_L}{\sigma}\right)^{3/5} - 0.725\right]^2 \tag{2}$$

where σ is the surface tension, and f_s is the friction factor for the slug.

Based on the experiments conducted with 146-mm-ID pipes at inclination angle of 0° and 4°, Ferschneider (1983) proposed an empirical correlation for the slug liquid holdup as follows:

$$H_{LLS} = \frac{1}{\left[1+\left(\frac{v_m}{\sqrt{(1-\rho_G/\rho_L)gD_p}}\right)^2 \Big/ \left(\frac{A}{B_O{}^{\beta}}\right)^2\right]^2} \tag{3}$$

where A is a coefficient and B_O is the Bond number.

Andreussi & Bendiksen (1989) conducted a series of experiments with pipes of 50.8- and 90-mm-ID, at inclinations ranging from -3° to 0.5°, using air-water as test fluids. A semi-empirical correlation for the slug liquid holdup was developed and compared with available data as follows:

$$H_{LLS} = \frac{v_m - v_{mf}}{\beta v_m + v_{m0}} \tag{4}$$

where

$$v_{mf} = \frac{(v'_{mf} - v_D)}{(C_0 - 1)} \tag{5}$$

$$v_{m0} = (C_2 - S_D \sin\theta)\frac{v_{G0}}{C_1(C_0 - 1)} + \frac{v_D}{C_0 - 1}\left(1 + \frac{1}{C_1}\right) \tag{6}$$

and

$$v_{G0} = 1.53\left[\frac{g\sigma}{\rho_L{}^2}(\rho_L - \rho_G)\right]^{1/4} \tag{7}$$

where v'_{mf} is the limiting velocity corresponding to the mixture velocity below

which the film flow is continuously merged into the slug, S_D is a distribution slip-ratio, β, C_0, C_1, and C_2 are the experimental coefficients.

Felizola (1992) suggested an empirical correlation for inclination angles from 0° to vertical based on experimental results from 50.8-mm-ID pipes. This correlation includes mixture velocity and pipe inclination angle into consideration as follows:

$$H_{LLS} = A_1 + A_2 v_m + v_m^{\,2} \tag{8}$$

where A_1, A_2, and A_3 are constants depending on inclination angle.

Andreussi *et al*. (1993) developed an empirical correlation to predict the slug liquid holdup which includes the effect of inclination angle, pipe diameter, and physical properties. The slug gas void fraction data was acquired, experimentally. The correlation and coefficients are presented in Eqs (9) to (12).

$$H_{LLS} = 1 - \frac{N_{Fr_m} + N_{F_0}}{N_{Fr_m} + N_{F_1}} \tag{9}$$

where

$$N_{F_0} = \max\left[0;2.6\left(1-2\left(\frac{2.5}{D_p}\right)^2\right)\right] \tag{10}$$

$$N_{F_1} = 2400\left[1-\frac{\sin(\theta)}{3}\right] B_O^{\,-3/4} \tag{11}$$

and

$$N_{Fr_m} = \frac{v_m}{\sqrt{g\,D_p}} \tag{12}$$

where B_O is the Bond number.

Gomez *et al*. (2000) presented a correlation based on the experimental data: Schmidt (1977), Kouba (1986), Rothe *et al*. (1986), Kokal (1987), Brandt & Fuches (1989), and Felizola (1992). The correlation was simple due to being presented in a dimensionless form, and it correctly captured the inclination effect. It is given as follows:

$$H_{LLS} = 1.0\, e^{-(0.45\theta_R + 2.48\cdot 10^{-6}\,\mathrm{Re}_{LS})}, \quad 0 \le \theta_R \le 1.57 \tag{13}$$

$$\mathrm{Re}_{LS} = \frac{\rho_L v_m D_p}{\mu_L} \tag{14}$$

where θ_R is the inclination angle in radians.

Abdul-Majeed (2000) proposed an empirical equation for estimating the slug liquid holdup in horizontal and slightly inclined two-phase flow as a function of mixture velocity, liquid viscosity, and inclination angle. The proposed equation is based on the experimental data: Kouba (1986), Felizola & Shoham (1992), Roumazeilles (1994), Kokal (1987), Rothe *et al*. (1986), Fuchs & Brandt (1989), and Gregory *et al*. (1978). The equation is shown in Eqs (15) and (16).

$$H_{LLS} = (1.009 - C\,v_m)A \qquad \begin{aligned} A &= 1.0 \ (\theta \le 0) \\ A &= 1.0 - \sin\theta \ (\theta > 0) \end{aligned} \tag{15}$$

$$C = 0.006 + 1.3377 \frac{\mu_G}{\mu_L} \tag{16}$$

Zhang *et al*. (2003) developed a unified model which can accurately predict the slug liquid holdup at all inclination angles using the mechanistic correlations. This model is based on a balance between the turbulent kinetic energy of the liquid phase and the surface free energy of dispersed gas bubbles in a slug body, yielding

$$H_{LLS} = \frac{1}{1 + \frac{T_{sm}}{3.16\,[(\rho_L - \rho_G) g \sigma]^{1/2}}} \tag{17}$$

where

$$T_{sm} = \frac{1}{C_e}\left(\frac{f_S}{2}\rho_S {v_S}^2 + \frac{D_p}{4}\frac{\rho_L H_{LF}(v_T - v_F)(v_S - v_F)}{L_S} + \frac{D_p}{4}\frac{\rho_C (1 - H_{LF})(v_T - v_C)(v_S - v_C)}{L_S}\right) \tag{18}$$

and

$$C_e = \frac{2.5 - |\sin\theta|}{2} \tag{19}$$

Kora (2010) proposed two empirical correlations based on the oil liquid viscosity. As can be seen in the section 6.4.1 of this study, these models showed a great agreement between measured and calculated data. The models and correlations are shown in Eqs (20) to (24).

$$H_{LLS} = 1.0120 e^{(-0.085 N_{Fr} N_{\mu}^{0.2})}, \quad for \quad 0.15 < N_{Fr}\, N_{\mu}^{0.2} < 1.5 \tag{20}$$

$$H_{LLS} = 0.9473 e^{(-0.041 N_{Fr} N_{\mu}^{0.2})}, \quad for \quad N_{Fr}\, N_{\mu}^{0.2} \geq 1.5 \tag{21}$$

and

$$H_{LLS} = 1.0, \quad for \quad N_{Fr}\, N_{\mu}^{0.2} \leq 0.15 \tag{22}$$

where

$$N_{Fr} = \frac{v_m}{(g\, D_p)^{0.5}} \sqrt{\frac{\rho_L}{\rho_L - \rho_G}} \tag{23}$$

$$N_{\mu} = \frac{v_m \mu_L}{g\, D_p^{\,2} (\rho_L - \rho_G)} \tag{24}$$

2.2.3.2 Film liquid holdup

Zhang *et al*. (2003) proposed not only the slug liquid holdup prediction model, but also the model which can predict the film liquid holdup based on an empirical correlation of liquid entrainment fraction. The model and closure relationships are shown in Eqs (25) to (30).

$$H_{LF} = \frac{v_{SL}(1 - F_E)}{v_F} \tag{25}$$

$$F_E = \frac{0.003 We_{SG}^{1.8} N_{Fr_{SG}}^{-0.92} \mathrm{Re}_{SL}^{0.7} \mathrm{Re}_{SG}^{-1.24} \left(\frac{\rho_L}{\rho_G}\right)^{0.38} \left(\frac{\mu_L}{\mu_G}\right)^{0.97}}{1 + 0.003 We_{SG}^{1.8} N_{Fr_{SG}}^{-0.92} \mathrm{Re}_{SL}^{0.7} \mathrm{Re}_{SG}^{-1.24} \left(\frac{\rho_L}{\rho_G}\right)^{0.38} \left(\frac{\mu_L}{\mu_G}\right)^{0.97}} \quad (26)$$

where

$$We_{SG} = \frac{\rho_G v_{SG}^2 D_p}{\sigma} \quad (27)$$

$$N_{Fr_{SG}} = \frac{v_{SG}}{\sqrt{g D_p}} \quad (28)$$

$$\mathrm{Re}_{SL} = \frac{\rho_L v_{SL} D_p}{\mu_L} \quad (29)$$

and

$$\mathrm{Re}_{SG} = \frac{\rho_G v_{SG} D_p}{\mu_G} \quad (30)$$

2.2.3.3 Translational velocity

Nicklin *et al*. (1962) defined the translational velocity as the sum of the bubble velocity, namely the drift velocity, and the maximum velocity in the slug body as follows:

$$v_T = C_0 v_m + v_D \tag{31}$$

where v_T is the translational velocity, C_0 is the distribution parameter; i.e. the flow coefficient, v_m is the mixture velocity, and v_D is the drift velocity.

2.2.3.3.1 Flow Coefficient (C_0)

In Nicklin *et al*. (1962) study of the rise velocity of Taylor bubbles, they have found that for liquid Reynolds numbers greater than 8,000, C_0=1.2, whereas at lower Reynolds numbers C_0 approached 2.0.

Rouhani & Axelsson (1970) proposed the flow coefficient as a function of two-phase flow quality (x), pipe diameter, liquid density, and the mixture mass flux.

$$\begin{aligned} C_0 &= 1 + 0.2\,(1-x)(gD_p\rho_L{}^2/G^2)^{0.25} && (for\ \alpha \le 0.1) \\ C_0 &= 1 + 0.2\,(1-x) && (for\ \alpha > 0.1) \\ C_0 &= 1 + 0.12\,(1-x) && (for\ \theta = 0) \end{aligned} \tag{32}$$

Bonnecaze *et al*. (1971), and Shipley (1982) proposed a constant value for the flow coefficient as C_0=1.2. Similarly, Greskovich & Cooper (1975), and Gomez *et al*. (2000) also designed the flow coefficient as a constant value in vicinity of 1.2 applicable to bubbly and slug flow regimes.

Bendiksen (1984) conducted experimental study to investigate the effect of inclination angle on the flow coefficient for different ranges of liquid flow rates. The flow coefficient applicable for relatively low liquid flow rates is

$$C_0(\theta) = C_0(0°) + (C_0(90°) - C_0(0°))\sin^2\theta \tag{33}$$

where $C_0(0°)=1$ and $C_0(90°)=1.2$.

Clark & Flemmer (1985) developed the flow coefficients considering the effect of void fraction, which are given by

$$C_0 = 0.934(1 + 1.42\alpha) \tag{34}$$

Beattie & Sugawara (1986) conducted an experimental study by using steam-water up-flow in 76.2-mm-ID pipes. They proposed the flow coefficient based on the Fanning friction factor obtained from mixture Reynolds number (based on mixture properties), yielding:

$$C_0 = 1 + 2.6\sqrt{f_{tp}} \tag{35}$$

where

$$f_{tp} = 0.0716\,\mathrm{Re}_{tp}^{-0.237} + 0.008 \tag{36}$$

Kataoka & Ishii (1987) empirically developed the flow coefficient correlation for a round tube in the moderate Reynolds number range, using the density of fluids, yielding:

$$C_0 = 1.2 - 0.2\sqrt{\rho_G / \rho_L} \tag{37}$$

Mishima & Hibiki (1996) measured the rise velocity of slug bubbles for air-water flows in capillary tubes with inner diameters in the range from 1 to 4 mm. The void fraction was correlated well by the drift flux model with a new equation for the flow coefficient as a function of inner diameter, yielding:

$$C_0 = 1.2 + 0.51\, e^{(-0.691(D_p/1000))} \tag{38}$$

Petalas & Aziz (2000) proposed the flow coefficient which includes the effect of inclination angle and slug Reynolds number. They indicated that C_0 value of 1.2 which is generally taken, is determined from the following empirically derived correlation:

$$C_0 = (1.64 + 0.12 \sin\theta)\, \mathrm{Re}_{mL}^{-0.031} \tag{39}$$

where

$$\mathrm{Re}_{mL} = \frac{\rho_L v_m D_p}{\mu_L} \tag{40}$$

Gokcal (2008) investigated the effect of high oil viscosity on drift velocity in horizontal condition. It was observed that the flow coefficient obtained by experimental study was in the vicinity of 1.87.

The recent correlation of Choi *et al*. (2012) took account into the effect of fluid properties, pipe diameter and two-phase flow rates on the flow coefficient through two-phase mixture Reynolds number, yielding:

$$C_0 = \frac{2}{1 + (\mathrm{Re}_{tp}/1000)^2} + \frac{1.2 - 0.2\sqrt{\frac{\rho_G}{\rho_L}}(1 - e^{(-18\alpha)})}{1 + (1000/\mathrm{Re}_{tp})^2} \tag{41}$$

2.2.3.3.2 Drift velocity (v_D)

In case of drift velocity, Nicklin *et al*. (1962) experimentally measured in

vertical pipes and found the proportionality constant to be 0.35. This is in agreement with Dumitrescu (1943) who proposed that the drift velocity of the gas phase to be proportional to Eq. (42) with the proportionality constant being 0.351 (Bhagwat and Ghajar, 2014).

$$v_D = C\sqrt{gD_p} \tag{42}$$

where C is a proportionality constant.

Greskovich & Cooper (1975), Eq. (43), Shipley (1982), Eq. (44), and Mishima & Hibiki (1996), Eq. (45), proposed similar form of the drift velocity equation without accounting for the effect of fluid properties on the drift velocity. Among them, Shipley (1982) includes the effect of void fraction on the drift velocity, and Mishima & Hibiki (1996) suggested the value of 0 for the drift velocity. These correlations are shown in Eqs (43) to (45), respectively.

$$v_D = 0.671\sqrt{gD_p}(\sin\theta)^{0.263} \tag{43}$$

$$v_D = 0.24 + 0.35(v_{SG}/v_m)^2\sqrt{gD_p\alpha} \tag{44}$$

and

$$v_D = 0 \tag{45}$$

Rouhanni & Axelsson (1970), Eq. (46), Clark & Flemmer (1985), Eq. (47), Gomez *et al*. (2000), Eq. (48), and Choi *et al*. (2012), Eq. (49), reported analogous drift velocity equation. Especially Choi *et al*. (2012) combined the empirical correlation considering the effect of inclination angle. Gomez *et al*. (2000) included the void fraction effect on the drift velocity with considering

the effect of inclination angle. Eqs (46) to (49) presented these correlations, respectively.

$$v_D = 1.18\,(\,g\,\sigma\,\Delta\rho/\rho_L{}^2)^{0.25} \tag{46}$$

$$v_D = 1.53\,(\,g\,\sigma\,\Delta\rho/\rho_L{}^2)^{0.25} \tag{47}$$

$$v_D = 1.53\,(\,g\,\sigma\,\Delta\rho/\rho_L{}^2)^{0.25}\sqrt{1-\alpha}\,\sin\theta \tag{48}$$

and

$$v_D = 0.0246\ \ \cos\ \theta + 1.606\ \ (\,g\,\sigma\,\Delta\rho/\rho_L{}^2)^{0.25}\sin\,\theta \tag{49}$$

Bonnecaze *et al*. (1971), Eq. (50), Hibiki & Ishii (2003), Eq. (51), and Beattie & Sugawara (1986), Eq. (52), used drift velocity correlations based on slug flow incorporate the effect of pipe diameter and phase densities but ignore the effect of surface tension on the drift velocity. On the other hands, for bubbly flow, i.e. elongated bubble flow, the effect of surface tension was included without considering the pipe diameter effect on drift velocity.

$$v_D = 0.35\sqrt{gD_p\Delta\rho/\rho_L}, \qquad where\ \Delta\rho = (\rho_L - \rho_G) \tag{50}$$

$$\begin{aligned}
&v_D = 1.41(g\sigma\Delta\rho/\rho_L{}^2)^{0.25}(1-\alpha)^{1.75}, && for\ \ Bubbly\ flow\\
&v_D = 0.35\sqrt{gD_p\Delta\rho/\rho_L}, && for\ \ Slug\ \ flow\\
&v_D = (1-\alpha)/(\alpha + 4\frac{\sqrt{\rho_G/\rho_L}\,(\sqrt{gD_p\Delta\rho(1-\alpha)})}{0.015\rho_G}), && for\ \ Annular\ flow
\end{aligned} \tag{51}$$

and

$$v_D = 0.35\sqrt{gD_p\Delta\rho/\rho_L}, \quad where\ \Delta\rho = (\rho_L - \rho_G) \tag{52}$$

Kataoka & Ishii (1987) developed the correlation using the viscosity number, $N_{\mu l}$, and density ratio between liquid and gas. They indicated that the drift velocity is closely related to the drag coefficient for bubbles and the drag coefficient mainly depends on the liquid phase properties, yielding:

$$\begin{aligned} v_D &= 0.03(\rho_G/\rho_L)^{-0.157}(g\sigma\Delta\rho/\rho_L{}^2)^{0.25}N_{\mu_L}{}^{-0.562}, \quad for\ D_h{}^* \le 40 \\ v_D &= 0.92(\rho_G/\rho_L)^{-0.157}(g\sigma\Delta\rho/\rho_L{}^2)^{0.25}N_{\mu_L}{}^{-0.562}, \quad for\ D_h{}^* > 40 \end{aligned} \tag{53}$$

where

$$\begin{aligned} D_h{}^* &= D_h/\sqrt{\sigma/(g\Delta\rho)} \\ N_{\mu_L} &= \mu_L/(\rho_L\sigma\sqrt{(\sigma/g\Delta\rho)})^{0.5} \end{aligned} \tag{54}$$

Conducting the experimental study, Gokcal (2008) developed a new model to predict the drift velocity for gas and high viscous oil two-phase flow in horizontal condition which includes the effect of viscosity on drift velocity.

Moreiras (2012) investigated the effects of oil viscosity, pipe diameter, and pipe inclination angle on drift velocity based on Froude number. The unified correlation was proposed using the different Froude numbers at each inclinations, namely, from horizontal to vertical.

2.2.3.4 Slug length

Dukler & Hubbard (1975) developed a new model for the slug length by calculating the mass of liquid crossing the plane in the time it takes for the slug

to pass, T_s, and the time it takes for the film to pass, T_f, indicating that the average slug length is found to be approximately 30D.

$$l_s = \frac{v_s}{f_s(H_{LLS} - H_{LFe})}\left[\frac{W_L}{\rho_L A v_s} - H_{LFe} + C(H_{LLS} - H_{LFe})\right] \tag{55}$$

where

$$C = 0.021[\ln(\mathrm{Re}_s)] + 0.022 \tag{56}$$

Similar with the results of Dukler & Hubbard (1975), other authors obtained similar expressions: (1) Andreussi (1975) L_s=2D, (2) Nicholson *et al*. (1978) L_s=30D, (3) Gregory *et al*. (1978) L_s=30D, (4) Barnea & Brauner (1985) L_s=32D, and (5) Manolis (1995) L_s=20D (Brito, 2012).

Brill *et al*. (1981) investigated that the nature of the statistical distribution of liquid-slug lengths is the right-skewed log-normal shape, using the data from Prudhoe Bay Field in Alaska and TUFFP databank. A linear regression was run on the dependent variable L_s vs. the independent variables D and v_m, yielding:

$$\ln(L_s) = -3.851 + 0.059\ln\left(\frac{v_m}{0.3048}\right) + 5.445[\ln(D_p)]^{0.5} \tag{57}$$

Neglecting the effect of mixture velocity, Norris (1981) modified the Brill *et al*. (1981) correlation, which is shown by Eq. (58).

$$\ln(L_s) = -2.099 + 4.859[\ln(D_p)]^{0.5} \tag{58}$$

Scott (1986) observed that how slug length varied as a function of pipe

diameter correcting the Brill *et al*. (1981) and Norris (1981) correlations to conform to the expanded data base. Additionally, description of the slug growth on the basis of observations from the Prudhoe Bay data was performed. All these results were combined into a comprehensive slug-length and –growth correlation, yielding:

$$\ln(L_s) = -25.4144 + 28.4948[\ln(D_p)]^{0.1} \tag{59}$$

Nydal *et al*. (1992) conducted an experimental study investigating air-water slug flow in 53- and 90-mm-ID horizontal pipes. He noted that the slug lengths were seen to be quite constant for a large range of velocities corresponding to the pipe diameter as follow:

$$\frac{L_s}{D} = 15 \ to \ 20, \quad for \ 5cm \ ID \ pipe \tag{60}$$

$$\frac{L_s}{D} = 12 \ to \ 16, \quad for \ 9cm \ ID \ pipe \tag{61}$$

Marcano *et al*. (1998) developed the empirical correlations using a 78-mm-ID, 1378-ft long horizontal flowline. Analysis of the data yielded important information on slug translational velocity, liquid holdup, slug length, frequency, and slug length distribution. Similar with Brill *et al*. (1981) the slug length distribution histograms indicated a right-skewed, bell-shaped tendency. The developed mean dimensionless slug length is given by:

$$\frac{L_s}{D} = \exp(\mu + 0.5\sigma^2) \tag{62}$$

where

$$\mu = 4.073 - 0.218\ln(v_{SL}) - 0.178\ln(v_m) \tag{63}$$

$$\sigma = 0.661 - 0.018\ln(v_{SL}) - 0.119\ln(v_m) \tag{64}$$

Gokcal (2008) performed an experimental study using gas and high viscous oil (181 – 587 cP) two-phase horizontal flow data. Based on Gokcal's (2008) experimental data, Al-safran *et al*. (2011) indicated that the statistical analysis showed a significant effect of liquid phase viscosity on slug length distribution including maximum slug length and slug length variation. A new dimensional analysis based model was proposed to predict average slug length for high viscous liquid slug flow, yielding:

$$\frac{L_s}{D} = 2.63\left(\frac{D_p^{3/2}\sqrt{\rho_L(\rho_L - \rho_G)g}}{\mu_L}\right)^{0.321} \tag{65}$$

2.2.3.5 Slug frequency

Gregory & Scott (1969) measured the slug frequency for the system carbon dioxide-water in a 19-mm-ID tube. Based on the Hubbard's (1965) experimental data and the Eq. (66) which is a slug velocity dependence, Gregory & Scott (1969) developed a new correlation, Eq. (67), including the pipe diameter effect.

$$f_s = \frac{A}{v_s} + Bv_s + C \tag{66}$$

$$f_s = 0.0226\left[\frac{v_{SL}}{g\,D_p}\left(\frac{19.75}{v_m} + v_m\right)^{1.2}\right] \tag{67}$$

where *A*, *B*, and *C* are constants corresponding to the plot of slug velocity vs. slug frequency.

Greskovich & Shrier (1972) indicated that Eq. (67) proposed by the Gregory & Scott (1969) yielded a standard deviation of 15.8% from their (Greskovich & Shirer, 1972) experimental data. And therefore a new correlation was developed by including the two parameters, no-slip liquid holdup and Froude number as follows:

$$f_s = 0.0226\left[\lambda_L\left(\frac{2.02}{D_p} + N_{Fr}\right)^{1.2}\right] \tag{68}$$

Taitel & Dukler (1977) modelled the complicated entrance phenomenon using open channel flow equations for the purpose of analytically predicting the slug frequency.

Heywood & Richardson (1979) performed experimental study using the co-current flow of air and water in 42-mm-ID bore horizontal pipelines. By using the γ-ray absorption method, which enabled probability density functions (PDF) and power spectral densities (PSD) of holdup, they estimated the average film and slug holdups, average slug length and frequency. For the slug frequency correlation, they suggested two formulas which are similar with

Greskovich & Shrier (1972), yielding:

$$f_s = 0.0434\left[\lambda_L\left(\frac{2.02}{D_p}+N_{Fr}\right)^{1.02}\right] \tag{69}$$

$$f_s = 0.0364\left[\lambda_L\left(\frac{2.02}{D_p}+N_{Fr}\right)^{1.08}\right] \tag{70}$$

Hill & Wood (1990-Part 2) modified and improved the previous correlation (Hill & Wood, 1990-Part 1) considering the effect of time required for the film to rebuild its equilibrium height and form a slug.

$$\frac{f_s D_p}{v_m} = 0.275*10^{\,2.68h_L} \tag{71}$$

where h_L is the liquid thickness for stratified flow in inch.

Tronconi (1990) proposed a slug frequency prediction correlation by assuming that the slug frequency is one half of the frequency of the unstable waves precursors of slugs, as determined according to published analyses of finite amplitude waves in conduits. Simple generalized equations were provided to estimate the slug frequency as follows:

$$f_s = 0.61\frac{\rho_G}{\rho_L}\frac{v_G}{h_G} \tag{72}$$

where h_G is the equilibrium gas depth, v_G is the actual gas velocity.

Stapelberg & Mewes (1994) conducted an experimental study which

took into account the influence of a second immiscible liquid upon gas-liquid slug flow. The previous existing models were extended based on the experimental data obtained by Heywood & Richardson (1979).

$$f_s = [N_{Fr_{\min}} + A(N_{Fr_M}{}^{0.1} - 1.17 N_{Fr_L}{}^{0.064})]^2 \sqrt{\frac{g}{D_p}} \tag{73}$$

where

$$N_{Fr_L} = \frac{J_L}{\sqrt{g\, D_p}} \tag{74}$$

$$N_{Fr_{\min}} = 0.048\ N_{Fr_L}{}^{0.81} \tag{75}$$

and

$$A = 0.73\ N_{Fr_L}{}^{2.34} \tag{76}$$

Zabaras (1999) investigated the performance of the existing slug frequency prediction models and developed a correlation based on the Gregory & Shrier (1972) experimental data, including the effect of inclination angle, yielding:

$$f_s = 0.0226 \left[\lambda_L \left(\frac{2.02}{D_p} + N_{Fr_M}{}^2 \right) \right]^{1.2} [0.836 + 2.75 \sin^{0.25} \theta] \tag{77}$$

As previously stated, Gokcal (2008) conducted an experimental study using gas and high viscous oil (181 – 587 cP) two-phase horizontal flow data.

With providing the dimensionless slug length prediction correlation, Al-safran *et al*. (2011) also proposed a new correlation which can predict the slug frequency for gas and high viscous oil two-phase flow behavior as follows:

$$f_s = 2.623\left(\frac{N_f^{-0.612} v_{SL}}{D_p}\right) \tag{78}$$

where

$$N_f = \frac{N_{Fr}}{N_\mu} = \frac{D_p^{3/2}\sqrt{\rho_L(\rho_L - \rho_G)g}}{\mu_L} \tag{79}$$

Chapter 3 Experimental System

The High Viscosity Oil/Gas Two-Phase Flow Loop was utilized in this study. This facility was previously used by Gokcal (2005 and 2008) and Kora (2010) to investigate the effect of high oil viscosity on slug flow characteristics. Later, Jeyachandra (2011) studied the effect of inclination angle for gas and high viscous oil two-phase flow. Finally, Brito (2012) determined the effect of medium oil viscosity on two-phase oil-gas flow behavior in horizontal pipes using the same facility. They conducted their experiments on 2-in. ID test section, and 3-in. ID pipe was used just as return line of test fluids. In this study, 3-in. ID pipe was used as a test section. New instrumentations were installed to 3-in. ID pipes section and additional calibrations were conducted to verify the reliability of the obtained data. Detailed information of experimental fluids, facility, instrumentation and data acquisition system are explained in this section. Experimental procedure and data analysis methods are also presented.

3.1 Experimental fluids

Oil has been used as the liquid phase, and compressed air is selected for the gas phase. The following sections describe the properties of each fluid.

3.1.1 Oil properties

The oil used in this study is a Newtonian fluid, environmentally safe and has

wide range of viscosities for the considered temperature range. The relationship between viscosity and temperature was determined by a rheometer, RheoScope 1™. Sensitivity analysis on the temperature gradient (20 min to 4 hours) and the initial temperature (60 ℉ and 120 ℉) was conducted 8 times. The density at a given temperature was checked using a Coriollis flow meter and additional measurement was conducted using a WEIGHT PER GALLON CUPS. The behavior aspects of oil viscosity and density vs. temperature are plotted in Figures 3.1 and 3.2, respectively. The following viscosity and density vs. temperature correlations were obtained by Data-Fit ver. 9.0 software provided by Oakdale engineering.

$$\mu_{ExperimentalOil} = 94.05 + 2519214T^{2} + 1.4\times10^{27} \times 2.72^{T} \quad (80)$$

$$\rho_{Experimental\ Oil} = -0.31T + 90265 \quad (81)$$

where T is a temperature in ℉, μ_{Oil} is an oil viscosity in cP, and ρ_{Oil} is an oil density in kg/m^3. Additional physical properties of this mineral oil are given in Table 3.1.

Table 3.1 Physical properties of experimental oil

API Gravity	30.5 @ 70 ℉
Oil Viscosity	420 cP @ 70 ℉
Oil Density	880 kg/m^3 @ 70 ℉
Surface Tension	0.03 N/m

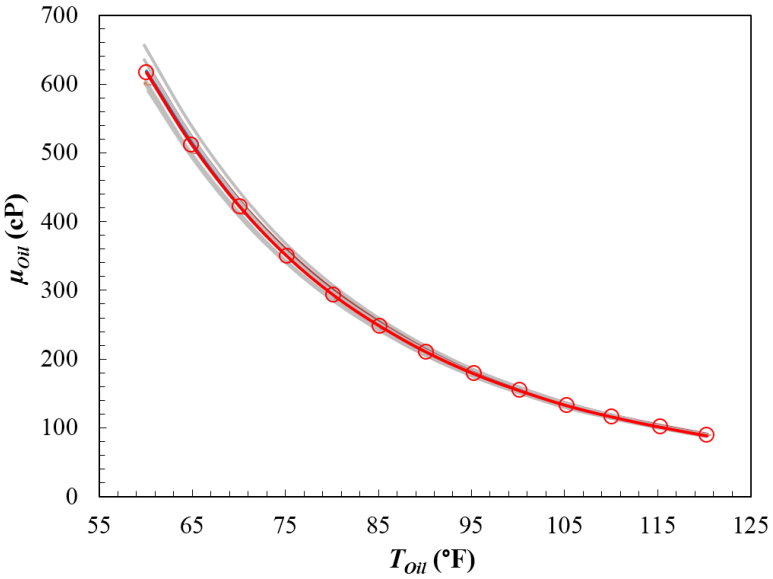

Figure 3.1. Temperature vs. oil viscosity. Eight repetitive tests were conducted by a rheometer. Red line with circle markers is the average value of the tests.

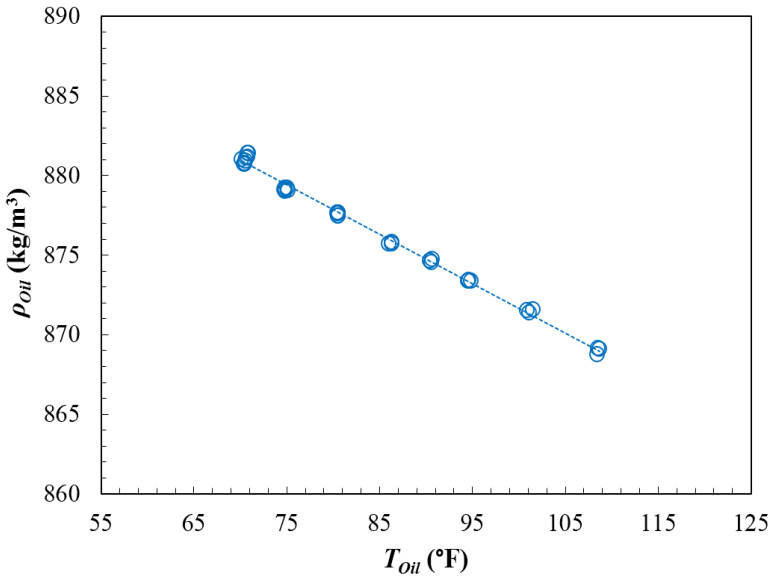

Figure 3.2. Temperature vs. oil density. The used temperature range was from 70 °F to 110 °F and step-size of 5 °F.

3.1.2 Gas properties

In this study, compressed air was used for the gas phase. Rasmussen (1997) gas density correlation was used to compute air density at different temperatures as follows

$$\rho_{air} = \frac{0.0034834P(1-0.378X_w)}{ZT} \tag{82}$$

$$P_{sv} = \exp\ (0.000012378\ \ T^2 - 0.01912\ \ T + 33.937 - 6343\,T^{-1}) \tag{83}$$

$$f = 1.00062 + 0.0000000314\ \ P + 0.00000056\ \ T_t^{\,2} \tag{84}$$

$$X_w = \frac{h}{100}\frac{P_{sv}}{P} f \tag{85}$$

$$\begin{aligned} Z = 1 - \frac{P_{sv}}{T}(A_0 + A_1 T_t + A_2 T_t) + (A_3 + A_4 T_t) X_w + (A_5 + A_6 T_t) X_w{}^2 \\ + \left(\frac{P}{T}\right)^2 (A_7 + A_8 X_w{}^2) \end{aligned} \tag{86}$$

where T is a system temperature in Kelvin, T_t is a system temperature in ℃, P is a system pressure in Pascal, P_{sv} is a saturation water vapour pressure in Pascal, X_w is a mole fraction of water vapour in air, h is a relative humidity in %, f is an enhancement factor, ρ_{air} is an air density in kg/m^3, and Z is a compressibility factor for humid air. A_i coefficients are defined in Table 3.2.

Table 3.2 A_i coefficients for Rasmussen (1997) gas density correlation

A_0	0.00000158123
A_1	-0.00000002933
A_2	0.0000000001104
A_3	0.000005707
A_4	-0.00000002051
A_5	0.00019898
A_6	-0.000002376
A_7	0.0000000000183
A_8	-0.00000000765

From Eq. (87) to Eq. (91) are Lee's correlation (Londono, 2002) and air viscosity was calculated by these formulas.

$$\mu_{air} = AK\frac{Exp(X\rho_{air}{}^{Y})}{1000} \tag{87}$$

$$Y = 2.4 - 0.2X \tag{88}$$

$$X = 3.5 + \frac{986}{T} + 0.01W \tag{89}$$

$$AK = \frac{(9.4 + 0.02\ W)(T^{1.5})}{(209 + 19\ W + T)} \tag{90}$$

$$W = 29\gamma_{air} \tag{91}$$

where γ_{air} is a gas specific gravity, ρ_{air} is an air density in kg/m^3, μ_{air} is an air viscosity in cP, T is a temperature in °F, and Z is a gas compressibility factor.

3.2 Experimental facility

This experiment was conducted in the TUFFP high viscosity two-phase flow loop. The loop is equipped with a heating system and an air conditioner allowing the operation at constant temperature. Figure 3.5 illustrates the schematic of the modified facility. The test section was designed as a 3-in. ID and 5.6-m-long pipe consisting of an opaque PVC pipe section. This section is connected to 2-in. ID pipe with a flexible hose. The experimental oil is stored in the 3.03 m^3 main storage tank. This oil is pumped to the 2-in. ID pipe section by 20 hp Kral Screw pump. A photograph of the main storage tank is given in Figure 3.3. Compressed air is jet to the system by 20 hp Gardner Denver dry rotary screw compressor with a capacity of 1030 CFM at 100 psig. Oil and gas are mixed at a geometry mixing tee in the entrance of the flow loop. An oil transfer tank (1.32 m^3) is located at the end of the 3-in. ID pipes, where the gravitational separation of two-phase occurs. Separated air is released to the atmosphere from this tank. A transfer pump sends the gathered oil back to main storage tank. Figure 3.4 shows the oil transfer tank and pump. The loop can be subdivided into the heating system, the metering system, and the test section.

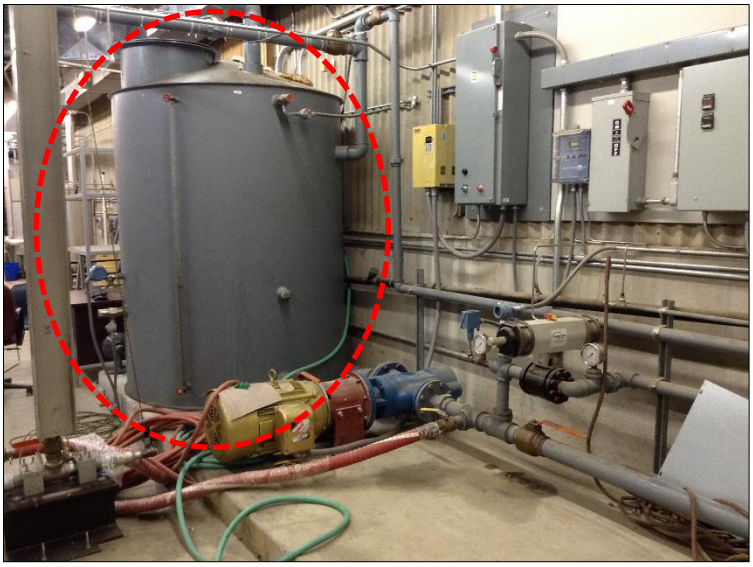

Figure 3.3 The main oil storage tank and the screw pump to transfer oil to the 2-in. ID pipe inlet section.

Figure 3.4 The oil transfer tank located at the end of the 3-in. ID pipes.

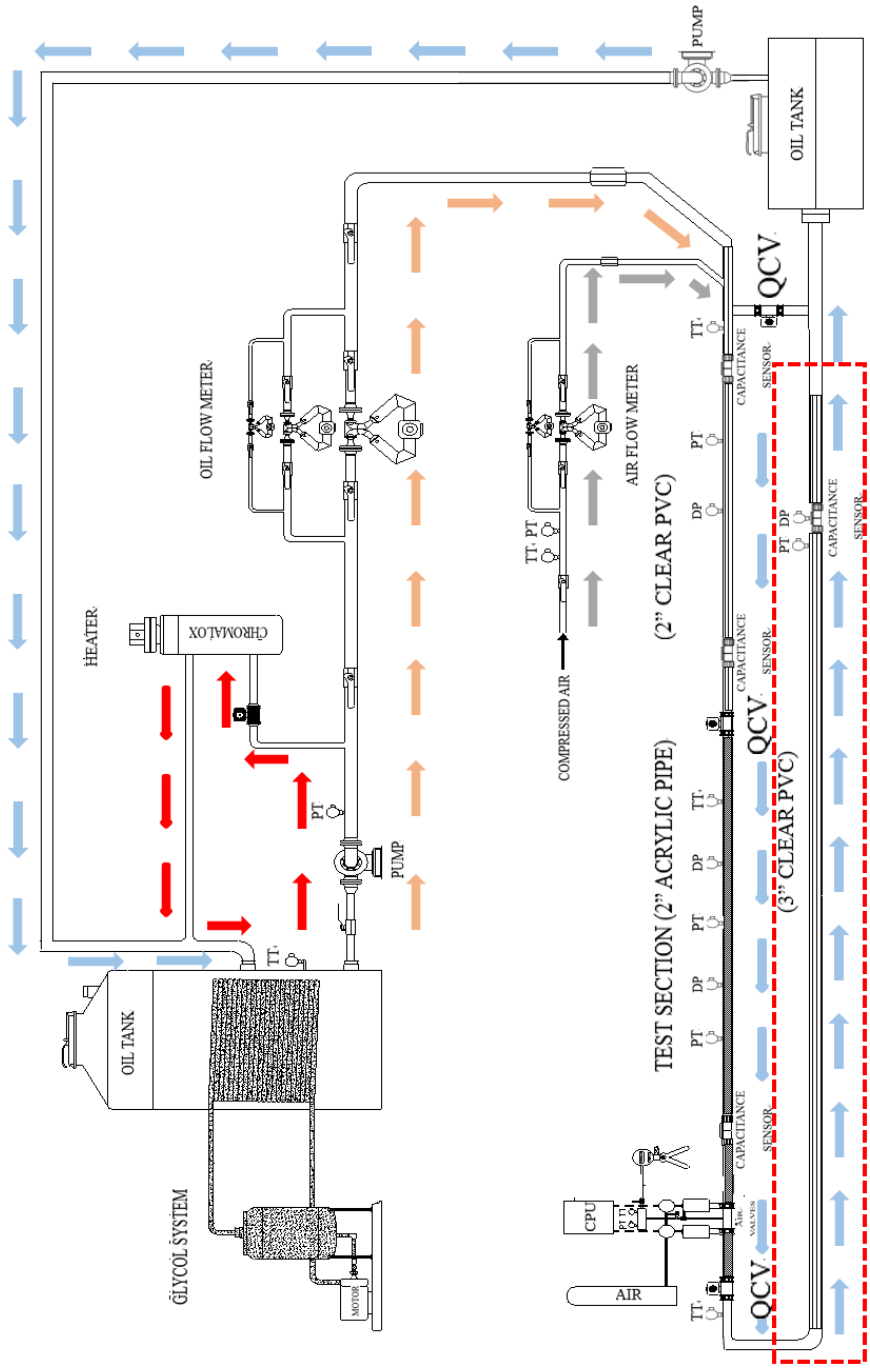

Figure 3.5 Facility schematic

3.2.1 The heating system

In this experimental study, it is crucial to conduct experiments at constant temperatures. The heating system is used to increase the oil temperature to the desired value. This system consists of a 2-in. ID circulation pipe, a 20 KW Chromalox circulation heater, a heater control panel and control valves. The oil is circulated through the heater until the oil reaches the desired temperature. Figure 3.6 shows a photograph of the Chromalox heater.

The set temperature of the air conditioner can be considered as the ambient temperature for the tests, which has to be maintained during the experimental program.

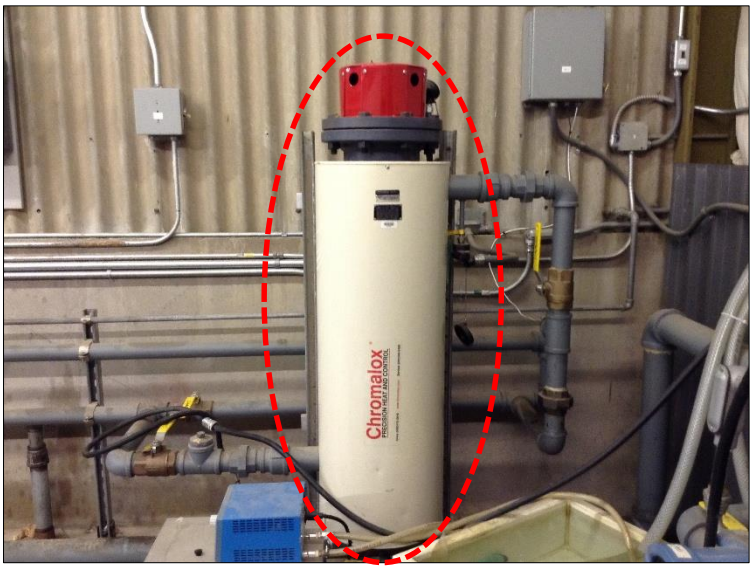

Figure 3.6 The Chromalox heating system to increase the oil temperature.

3.2.2 The metering section

Before air and oil are mixed, there are three Micro Motion™ mass flow meters; CMF25, CMF100, and CMF300, having different sizes to measure the different ranges of mass flow rates and densities. The gas flow rate is measured by CMF25 and CMF50 depending on the ranges. Temperature and pressure are also measured to calculate the superficial gas velocity. The pictures of the metering system is shown in Figure 3.7.

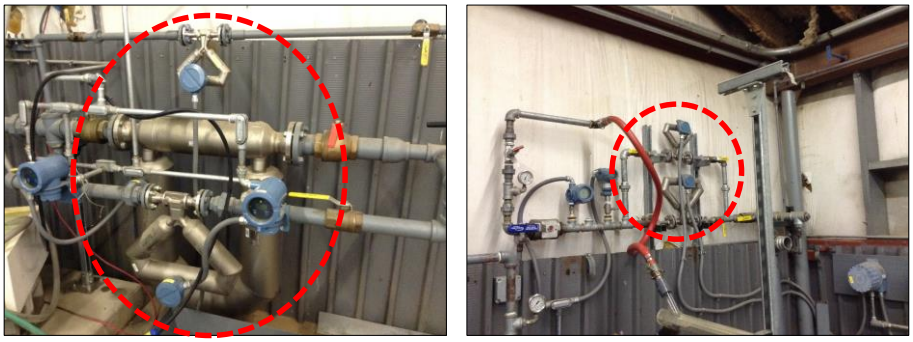

(a) CMF25, CMF100, and CMF300 (b) CMF25 and CMF50

Figure 3.7 The Metering system to gauge (a) the liquid mass flow rate, (b) the gas mass flow rate

3.2.3 The test section

Figure 3.8 illustrates the pictures of test section. This section consists of the 3-in. ID and 5.6-m-long PVC pipes. The test section is positioned at the end of the 3-in. ID pipes to increase the degree of steady state flow.

Because the oil viscosity changes with the temperature, it is significantly important to measure the fluid temperature. One of the Resistance Temperature Detector (RTD) temperature transducer placed at the end of the 2-in. ID pipes was used for the oil viscosity calculations. The maximum allowable operating pressure of the 2-in. ID pipe is about 100 psig. For safety purposes, a pressure relief valve is installed which can withstand up to 110 psig. This valve is set to operate at 30 psig.

A differential pressure transducer is located at the center of 3-in. ID pipe test section, which has the length of 5.6 m. A pressure transducer is also installed close by a differential pressure transducer to get averaged pressure value on the test section. Two capacitance sensors are installed at the center of the test section to measure the average liquid holdup, slug and film liquid holdup, translational velocity, slug length, and slug frequency.

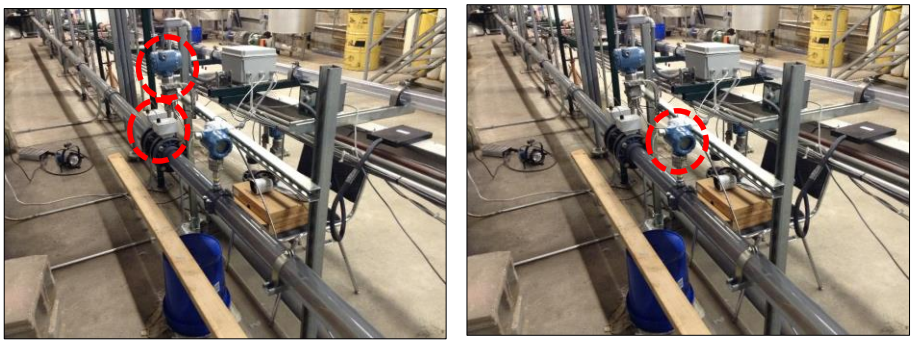

Figure 3.8 Test section of the 3-in. ID pipes. Two capacitance sensors (CP), one pressure transducer (PT), and one differential pressure transducer (DP) are equipped. Additionally, two fast-cameras are placed on the side and upper of the test section.

3.3 Instrumentation

3.3.1 Mass flow meter

There are five Micro Motion™ mass flow meters to measure the oil and gas (air) flow rates, and densities. Calibration of these meters was performed by the manufacturer. The systematic uncertainty for the gas (CMF25, and CMF50) and liquid (CMF25, CMF100, and CMF300) flow meters is reported as ±0.1%. The superficial liquid and gas velocities are calculated using values measured by mass flow meters, pressure transducer, and temperature transducer.

3.3.2 Video cameras

The PHOTRON high speed video camera is utilized to observe the flow behavior. The system includes a video camera (FASTCAM SA3), transfer cable, and a processor capable of capturing up to 2000 fps at full resolution (1,024 by 1,024 pixel resolution). The high speed snapshots were taken at 250 fps with a special light source in this study.

A security system with four cameras (SAMSUNG) is installed along the test section. Two of cameras are located on the 2-in. ID pipe section and the others are positioned on the 3-in. ID pipe section. These cameras are used to investigate the flow pattern variance depending on the experimental condition.

3.3.3 Temperature transducer

The resistance temperature detector (RTD) temperature transducer are installed on the 2-in. ID pipes, the mixing tee, and the main oil storage tank to measure the temperature at different locations. Temperature transducer placed at the end of the 2-in. ID pipe section was used to acquire a proper two-phase temperature for the 3-in. ID pipe section. This equipment was calibrated by manufacturer, and had an uncertainty value of ±0.5℃.

3.3.4 Pressure transducer and differential pressure transducer

Pressure data are obtained by a Rosemount pressure transducer. The pressure transducer is located at the center of the 3-in. ID pipe test section. Additionally Rosemount differential pressure transducer is placed to measure a pressure gradient value. The distance of the differential pressure measuring points is 5.6-m along the test section. The pressure and differential pressure transducers were calibrated using a pressure calibrator with an uncertainty value of ±0.05%.

3.3.5 Capacitance sensor

The capacitance sensors were used based on difference in dielectric values between two different phases. Kora (2010) and Jeyachandra (2011) measured the liquid holdup using two-wire and ring type capacitance sensors, respectively. Brito (2012) reported that two-wire capacitance sensor is more suitable for

measuring liquid holdup due to its linear response and low sensitivity to temperature change. Similar to Brito's (2012) study, only the two-wire capacitance sensors were used to determine the liquid holdup in this project. The schematic of the two-wire capacitance sensor is shown in Figure 3.9.

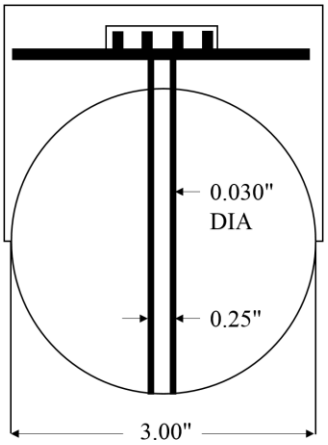

Figure 3.9 Schematic of the two-wire capacitance sensor. The sensor consists of two parallel copper wires placed perpendicular to the flow with a distance of 0.25-in.; an electronic circuit to filter, amplify and convert the measured capacitance to a voltage; and housing (Kora, 2010).

To verify suitability of the measurements, the capacitance sensors were statically calibrated following the different oil viscosities. This calibration was conducted under static conditions. The voltage value was non-dimensionalized using Eq. (92). Table 3.3 summarizes static calibration curve coefficients to calculate a liquid holdup from a dimensionless voltage for each oil viscosities.

$$V' = \frac{V_{read} - V_{\min}}{V_{\max} - V_{\min}} \tag{92}$$

Table 3.3 Static calibration curve coefficients for the different oil viscosities.

				$H_{LStatic} = aV' + b$	
Name	**Sensor Type**	**Oil Viscosity**	**Br (±)**	**a**	**b**
Cap 1	Two-Wire	587 cP	0.0096	1.0224	-0.0342
	Two-Wire	420 cP	0.0014	0.9847	0.0112
	Two-Wire	300 cP	0.0025	0.9866	0.001
	Two-Wire	220 cP	0.0046	1.0152	0.0038
	Two-Wire	181 cP	0.0027	1.0098	0.0086
	Two-Wire	155 cP	0.0067	1.0051	0.0419
Cap 8	Two-Wire	587 cP	0.0094	1.0207	-0.0569
	Two-Wire	420 cP	0.0023	0.9814	0.0099
	Two-Wire	300 cP	0.0018	0.9885	0.0157
	Two-Wire	220 cP	0.0033	0.9885	0.04
	Two-Wire	181 cP	0.0021	1.0226	-0.0005
	Two-Wire	155 cP	0.0064	1.0551	-0.0133

3.4 Data acquisition system

Two data acquisition systems are connected to the facility. The first one is the low-speed data acquisition system for pressure, temperature, flow rates, and superficial liquid and gas velocities. The other one is the high-speed data acquisition system for the output voltage from the capacitance sensors. Flow variables (low-speed data; pressure, temperature, and flow rates) measured by flow meters, pressure and temperature transducers are saved with a sampling rate of 25 samples/s. The high-speed data (voltage values) are stored with a

sampling rate of 1000 samples/s.

These data are transferred to a PC which includes the LabVIEW™ express 7.1 software package to display data on the monitor. An I/O board connected to instruments with 32 analogue input channels converts analogue signals to digital signals (-10 to +10 Volts).

3.5 Experimental procedure

The following procedure abides by the rules to obtain the more accurate flow characteristics data. Because the experiments are preformed simultaneously in both of the 2- and 3-in. ID pipes, this sequential guideline includes the experimental procedure for the 2-in. ID pipes.

1. Start the air compressor.
2. Check the temperature of oil in main storage tank. Use the heating system to increase the temperature of oil if it is necessary.
3. Check the ambient temperature which is displayed on the air conditioner input monitor. Use the air conditioner to adjust the ambient temperature to minimize the oil temperature change during the experimental study.
4. Start the data acquisition program, and monitor readings of all instruments.
5. Check all valves in order to avoid operational problems.
6. Start the oil pump and maintain desired superficial oil velocity.
7. Circulate single-phase oil until oil reaches to oil transfer tank.

8. Stop the flow and verify that a differential pressure transducer indicates zero psi.
9. Open the air valve and increase the superficial air velocity up to desired value.
10. Circulate fluids until steady state flow is observed.
11. Check the temperature transducer which is located at the end of the 2-in. ID pipes. The temperature should be kept constant for oil viscosity control.
12. After checking the operation of low and high speed data acquisition systems, save the temperature, pressure, and flow rate data with these programs.
13. Repeat these steps for different superficial air and oil velocities, and viscosities.
14. Stop air flow.
15. Shut down the oil pump.
16. Log out from the data acquisition systems.
17. Shut down the air compressor.

3.6 Data analysis

Data management is a major task for this study due to the large amount of data acquired. Therefore, data processing must be automated (Brito, 2012). The modified VBA Excel macro program which was initially coded by Brito (2012) was used to process the raw data recorded by pressure, temperature, and differential pressure transducers, mass flow meters, and capacitance sensors.

Average, standard deviation, and uncertainty of all parameters are calculated by this program. Calculated parameters are pressure gradient (dP/dL), average liquid holdup ($H_{LAverage}$), slug (H_{LLS}) and film liquid holdup (H_{LF}), translational velocity (v_T), slug length (L_S/D), and slug frequency (f_S). Quality and consistency of the results can be increased by following the above procedure, reducing the random error and the time needed for data analysis.

3.7 Uncertainty analysis

A deviation from accuracy is called error or uncertainty. Since the true value cannot be predicted exactly, an error exists and uncertainty should be analyzed for every measurements. The confidence of the acquired experimental data can be constructed by uncertainty analysis.

There are random and systematic errors. Those can be found in every data. A random error is inherent and must be quantified through the analysis. Systematic error, which means the difference between the measured values and a true value, is a constant for all experiments.

3.7.1 Random uncertainty

Experimental results are used to calculate random uncertainty. A set of N data points are acquired in a population. Then, the standard deviation of a population is

$$S_X = \sqrt{\frac{\sum_{i=1}^{N}(X_i - \overline{X})^2}{N-1}} \tag{93}$$

In order to find the error percentage in the average, the standard deviation of the population average is estimated by

$$S_{\overline{X}} = \frac{S_X}{\sqrt{N}} \tag{94}$$

where $S_{\overline{X}}$ is the random uncertainty with a confidence level of 68% which is equivalent to one standard deviation.

The 95% confidence interval of a measurement can be determined by using the student-t distribution. A value of t=1.96 represents 95% cumulative probability. Therefore, the random uncertainty of measurement, X, is given by the uncertainty interval like following.

$$\overline{X} - t_{95}S_{\overline{X}} \le X \le \overline{X} + t_{95}S_{\overline{X}} \tag{95}$$

3.7.2 Systematic uncertainty

Systematic error is constant for all experiments, which can be obtained by using a particular instrument. This error is often provided by the manufacturer. Table 3.4 shows the different sources of systematic error.

Table 3.4 Instrument systematic uncertainties.

Measured Parameter	Instruments	Systematic Uncertainty
Pressure	Rosemount Pressure Transducer	±1.3%
Prssure Drop	Rosemount Differential Pressure Transducer	±1.4%
Temperature	RTD	±0.5 ℃
Liquid Density	Micro Motion™	±0.5 kg/m^3
Gas Density	Micro Motion™	±0.2 kg/m^3
Liquid Flow Rate	Micro Motion™	±0.1%
Gas Flow Rate	Micro Motion™	±0.1%

3.7.3 Combined random and systematic uncertainties

The overall measurement uncertainty is estimated by combining the random and systematic uncertainties. The accuracy of the experimental measurements is quantified through these values. The equation to calculate the combined uncertainty is

$$U_{95} = \pm t_{95}[(B_R/2)^2 + (S_{\bar{X}})^2]^{1/2} \tag{96}$$

where B_R is the combined systematic uncertainty of the overall uncertainty analysis.

In the Excel macro program, the Taylor series uncertainty propagation method is adopted to calculate the uncertainty propagation into the gas and liquid density and viscosity, superficial gas and liquid velocities, mixture velocity, and mixture Reynolds number. Additionally, the Monte Carlo Analysis is used to calculate uncertainty related with the threshold value selection on the slug parameters (Brito, 2012).

3.7.4 Uncertainty analysis for calibrations

The uncertainties related to the static calibration of the capacitance sensors are calculated by using a simplified uncertainty analysis reported by Dieck (2006). The dynamic calibration was not conducted in this study, as a result, the degree of uncertainties only occurred by the static calibration of the capacitance sensor are very small which can be almost neglected. Eqs (97) and (98) are the formulas used to determine this uncertainty value.

$$U_{ASME} = \pm 2\,[b^2 + (S_X / \sqrt{N})]^{1/2} \tag{97}$$

and

$$S_X \approx SEE = [\{\sum_{i=1}^{N} (Y_i - Y_{iC})\}/(N-K)]^{1/2} \tag{98}$$

where U_{ASME} is the calibration uncertainty value, b is the systematic standard uncertainty of the instrument under calibration (it assumed to be zero in this study), S_x is the standard deviation of the calibration data, N is the number of data points, Y_i is the ith data point in the calibration corresponding to X_i, Y_{iC} is the value of the curve fit corresponding to X_i, K is the number of curve fit coefficients, and N-K is the degree of freedom for *SEE*.

Chapter 4 Pipe Diameter Effect on Slug Characteristics for High Viscous Horizontal Flow

The following sub-sections compare the results between previous 2-in. ID experiments and current 3-in. ID experimental study. Various flow characteristics are compared, i.e., flow pattern map, pressure gradient, average liquid holdup and slug characteristics (such as translational velocity, slug length and slug frequency). The experimental data by Gokcal (2008), Kora (2010) and Brito (2012) are selected for comparison.

Flow pattern map, pressure gradient, average liquid holdup and translational velocity results obtained using oil viscosities of 181 cP and 587 cP were compared with Gokcal's (2008) experimental data. Kora's (2010) data were considered with these oil viscosity range to compare slug and film liquid holdup. At last, for slug length and frequency, Brito's (2012) experimental data were used to make a comparison between 2- and 3-in. ID pipes with 155 cP oil viscosity data.

Effect of high viscous oil on two-phase flow in 3-in. ID horizontal pipes is treated in Appendix B, including experimental matrix, single-phase, and two-phase flow tests. Appendix B shows similar results with Gokcal (2008), Kora (2010), and Brito (2012).

4.1 Flow pattern map

As mentioned in the section B.3.1, three different flow patterns have been observed, namely, Elongated Bubble (EB), Slug (SL) and Annular (AN) flow. Based on this, three transition boundaries (Elongated Bubble-Slug, Slug-Annular, and Slug-Dispersed Bubble flow) were observed in this study. Similarly, Elongated Bubble (EB), Slug (SL) and Annular (AN) flow were investigated in 2-in. section with observed transition boundaries. The observed flow patterns of 2- and 3-in. ID pipes were compared with Taitel and Dukler (1976), Barnea (1987) and TUFFP Unified models. Figures 4.1 to 4.6 show the comparison between the observed flow patterns for each oil viscosity and the flow pattern prediction model. All of the flow pattern prediction models show that slug flow region expands and elongated bubble flow region shrinks with increase of oil viscosity. In general, the entire intermittent flow area expands as the stratified region shrinks. As above, it is observed that the slug flow region expands when oil viscosity increases in both 2- and 3-in. ID pipes. The reasons of this trend can be summarized slug front eddy formation is delayed as the viscosity decreases and development of continuous gas core is postponed with increasing oil viscosity.

Taitel and Dukler model satisfactorily predicts intermittent flow region and transition boundary between slug and dispersed bubble flow for 3-in. cases, however, as oil viscosity increases, it is not acceptable to predict transition boundary from slug to dispersed bubble flow for 2-in. cases. Prediction for transition boundary from slug to annular flow is not suitable for both cases.

For all oil viscosities, Barnea model shows a large discrepancy in predicting the transition boundary between slug flow and annular flow in both cases. As liquid viscosity decreases, small differences are observed for the transition boundary from elongated bubble flow to slug flow in 3-in. case. On the other hand, the transition boundary from elongated bubble flow to slug flow is properly predicted for 2-in. case.

TUFFP Unified model is appropriate to predict intermittent flow regime for both pipe diameters. Similarly, transition boundary between slug and annular flow is reasonably predicted for relatively low oil viscosity. As oil viscosity increases, there is a wide gap to predict transition from slug to annular flow in both cases.

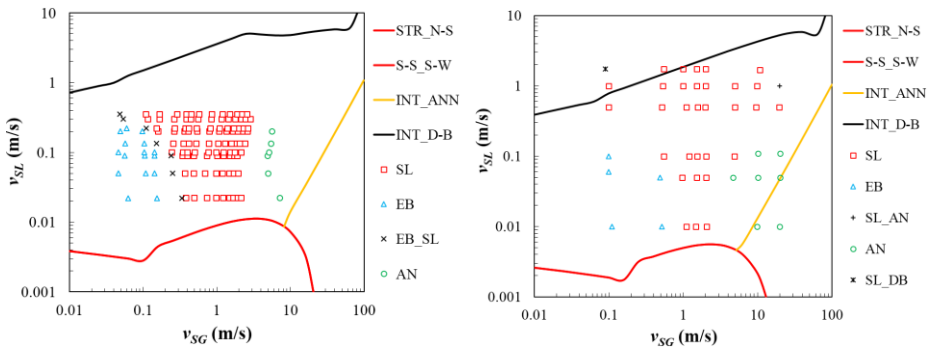

(a) 3-in. ID pipes results (b) 2-in. ID pipes results

Figure 4.1 Taitel & Dukler flow pattern (1976) prediction model with observed flow pattern data for μ_{Oil} = 181 cP, (a) 3- and (b) 2-in. ID pipes.

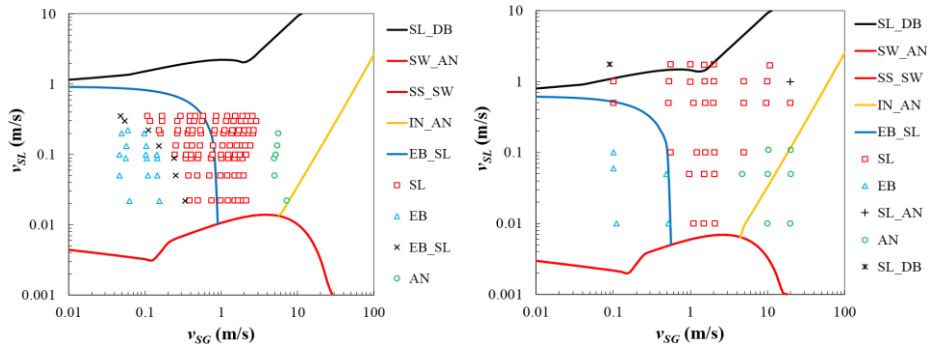

(a) 3-in. ID pipes results (b) 2-in. ID pipes results

Figure 4.2 Barnea flow pattern (1980) prediction model with observed flow pattern data for μ_{Oil} = 181 cP, (a) 3- and (b) 2-in. ID pipes.

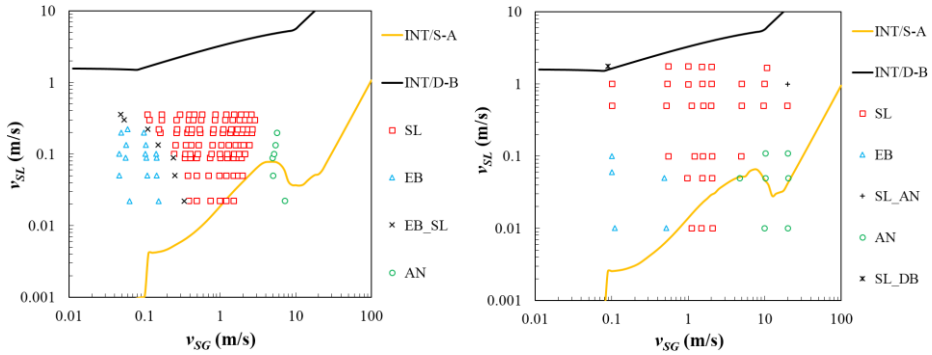

(a) 3-in. ID pipes results (b) 2-in. ID pipes results

Figure 4.3 TUFFP Unified flow pattern prediction model with observed flow pattern data for μ_{Oil} = 181 cP, (a) 3- and (b) 2-in. ID pipes.

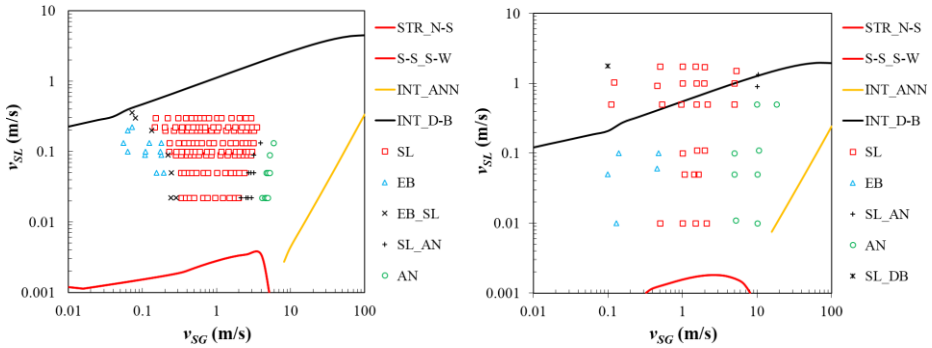

(a) 3-in. ID pipes results (b) 2-in. ID pipes results

Figure 4.4 Taitel & Dukler flow pattern (1976) prediction model with observed flow pattern data for μ_{Oil} = 587 cP, (a) 3- and (b) 2-in. ID pipes.

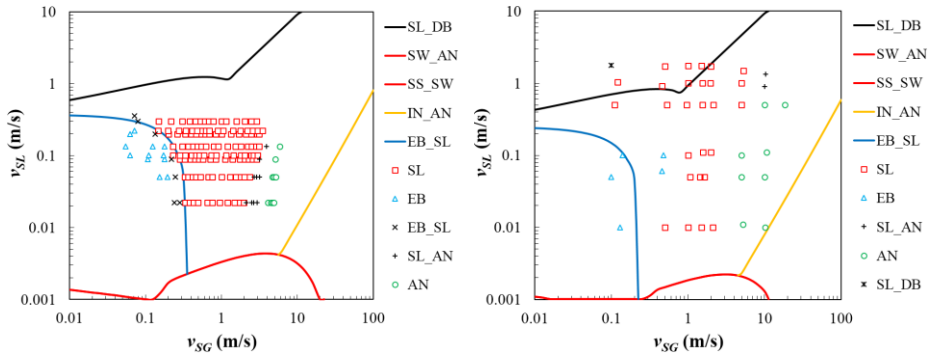

(a) 3-in. ID pipes results (b) 2-in. ID pipes results

Figure 4.5 Barnea flow pattern (1980) prediction model with observed flow pattern data for μ_{Oil} = 587 cP, (a) 3- and (b) 2-in. ID pipes.

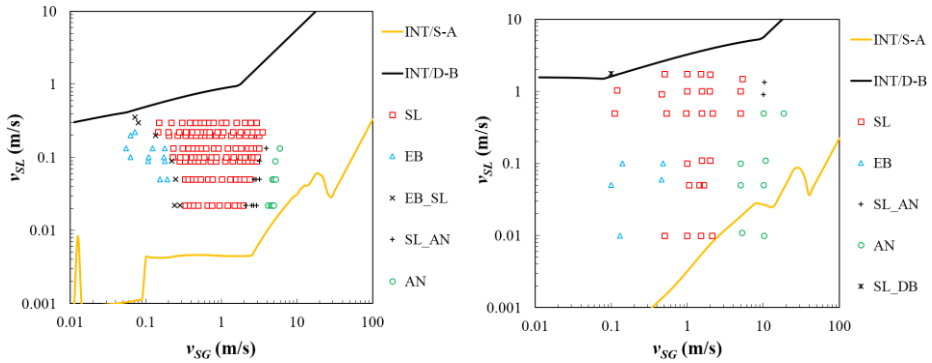

(a) 3-in. ID pipes results (b) 2-in. ID pipes results

Figure 4.6 TUFFP Unified flow pattern prediction model with observed flow pattern data for μ_{Oil} = 587 cP, (a) 3- and (b) 2-in. ID pipes.

4.2 Pressure gradient

Figures 4.7 and 4.8 present the measured pressure gradient against the superficial gas velocity reported by Gokcal (2008) and Brito (2012) at different oil viscosities when v_{SL}=0.1 m/s and 0.3 m/s. These experimental data were obtained from 2-in. ID pipes. Figures 4.9 and 4.10 show the pressure gradient difference between 2- and 3-in. ID pipes for different oil viscosities (181 cP and 587 cP).

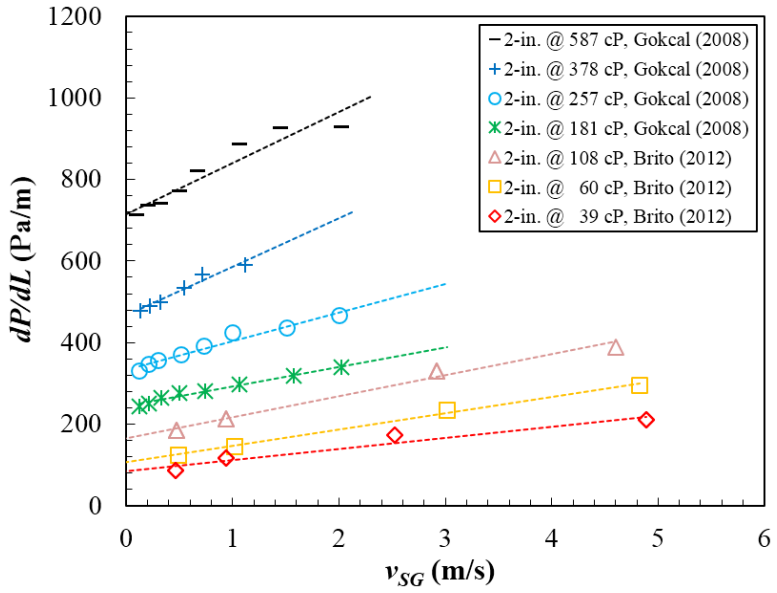

Figure 4.7 Pressure gradient vs. superficial gas velocity for v_{SL}=0.1 m/s and d=2-in. These experimental data were acquired by Gokcal (2008) and Brito (2012).

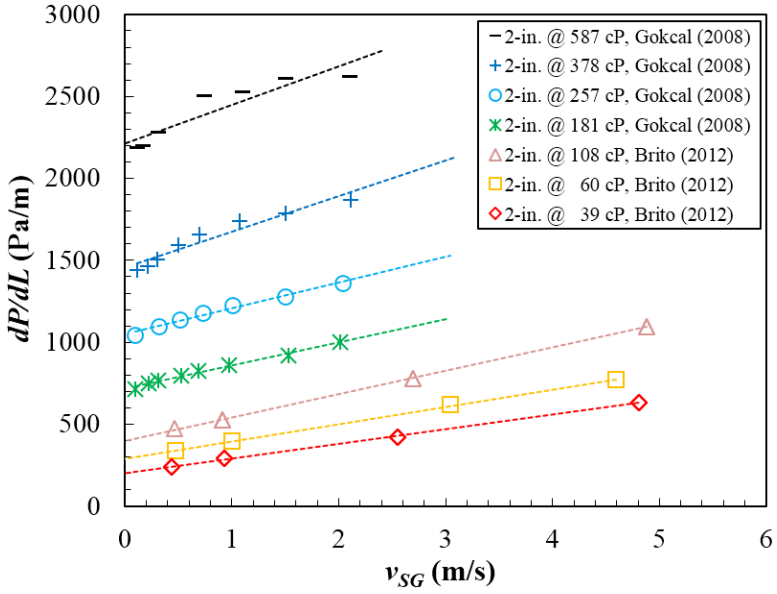

Figure 4.8 Pressure gradient vs. superficial gas velocity for v_{SL}=0.3 m/s and d=2-in.

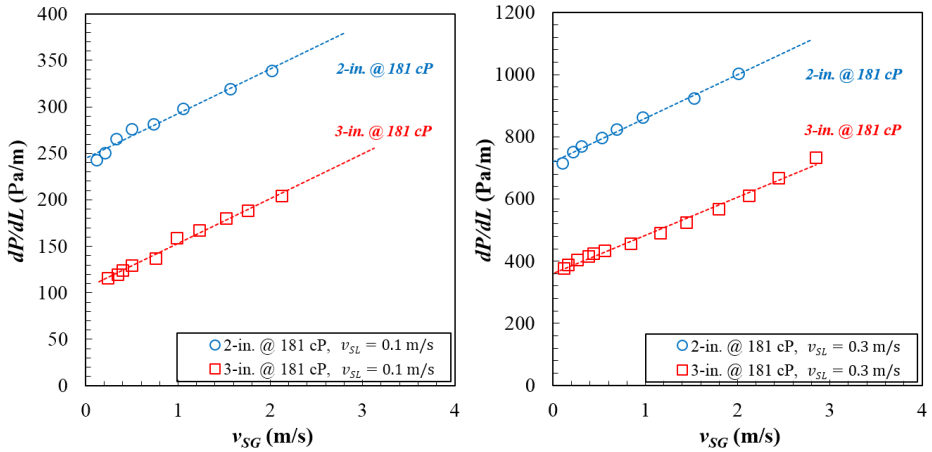

(a) v_{SL} = 0.1 m/s (b) v_{SL} = 0.3 m/s

Figure 4.9 Pressure gradient in 2- and 3-in. ID pipes vs. superficial gas velocity for μ_{Oil} = 181 cP, (a) v_{SL}=0.1 m/s and (b) v_{SL}=0.3 m/s.

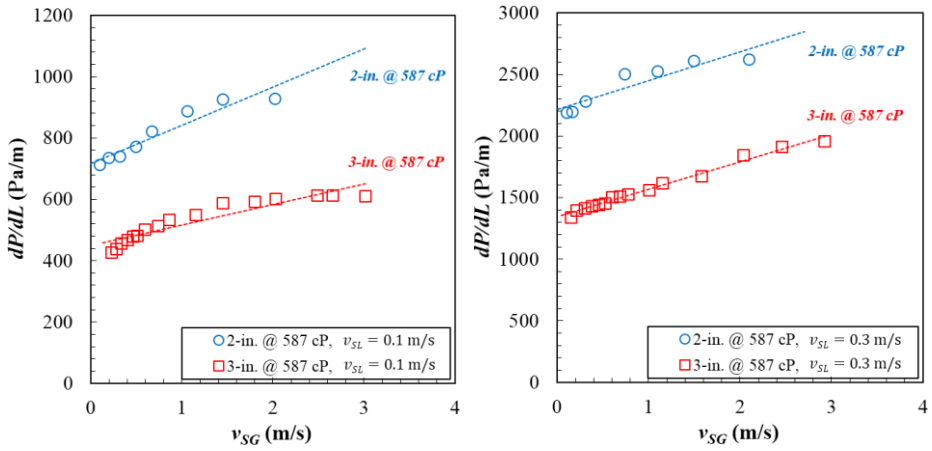

(a) v_{SL} = 0.1 m/s (b) v_{SL} = 0.3 m/s

Figure 4.10 Pressure gradient in 2- and 3-in. ID pipes vs. Superficial gas velocity for μ_{Oil} = 587 cP, (a) v_{SL}=0.1 m/s and (b) v_{SL}=0.3 m/s.

Pressure gradient increases with increasing superficial gas velocity in both cases. Similarly, at a given superficial liquid and gas velocity, pressure gradient increases for higher oil viscosities. For a constant superficial liquid and gas velocity and oil viscosity, pressure gradient decreases for a larger pipe diameter. To explain this phenomena, a simplified slug flow model is considered, which was proposed by Brito (2013). Based on Taitel and Barnea (1990), Eq. (99), and definition of the slug length ratio, Eq. (100), a simplify pressure gradient correlation was developed in Eq. (102) using the shear stress in the liquid slug in Eq. (101). From Eq. (99), gas shear in the film zone is neglected.

$$-\left.\frac{dp}{dL}\right|_U = \rho_S \sin(\theta)\frac{L_S}{L_U} + \frac{\tau_S \pi d}{A_P}\frac{L_S}{L_U} + \rho_F \sin(\theta)\frac{L_F}{L_U} + \frac{\tau_F S_F}{A_P}\frac{L_F}{L_U} + \frac{\tau_G S_G}{A_P}\frac{L_F}{L_U} \tag{99}$$

$$\frac{L_S}{L_U} = \frac{(v_{SL} - v_{LTB}H_{LTB})}{(v_{LLS}H_{LLS} - v_{LTB}H_{LTB})} \tag{100}$$

$$\tau_S = 8\frac{\mu_S v_m}{D_p} \tag{101}$$

$$\left.\frac{dp}{dL}\right|_U = \frac{32\mu_S v_m v_{SL}}{{D_p}^2 v_{LLS}H_{LLS}} \tag{102}$$

where v_{LLS} is a liquid velocity in the slug body in m/s, H_{LLS} is a liquid holdup in the slug body, v_{LTB} is a liquid velocity in the end of film region in m/s, H_{LTB} is a liquid holdup in the end of film region, μ_S is a mixture viscosity in Pa·s.

As can be seen, as pipe diameter increases, total pressure gradient decreases being inversely proportional to the square of pipe diameter.

4.3 Average liquid holdup

Figures 4.11 and 4.12 show the measured average liquid holdup against the superficial gas velocity reported by Gokcal (2008) and Brito (2012) at different oil viscosities when v_{SL}=0.1 m/s and 0.3 m/s. These data were attained from 2-in. ID pipes.

The comparison of average liquid holdup between 2- and 3-in. ID pipes at different oil viscosities are presented in Figures 4.13 and 4.14. For all oil viscosities and constant superficial liquid velocity, the average liquid holdup decreases as superficial gas velocity increases; and, for a given superficial gas velocity, average liquid holdup increases when superficial liquid velocity and oil viscosity increase in both 2- and 3-in. cases.

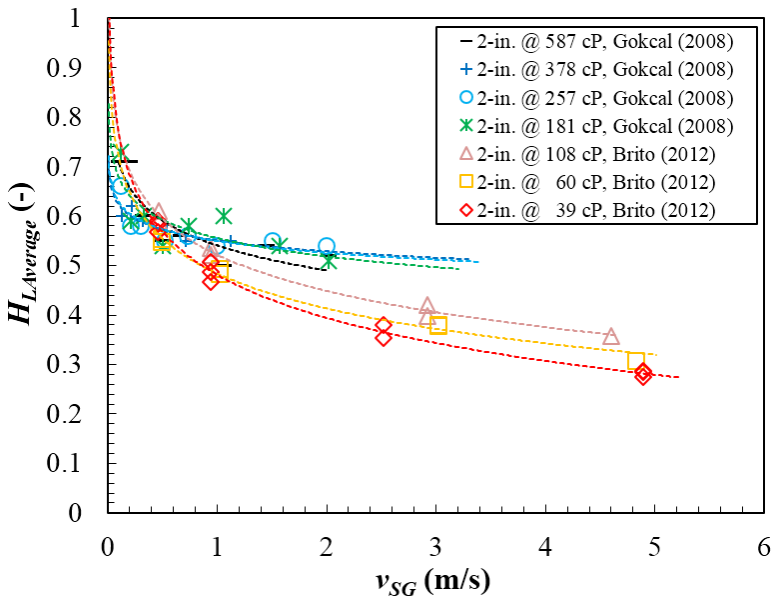

Figure 4.11 Average liquid holdup vs. superficial gas velocity for v_{SL}=0.1 m/s and d=2-in. These experimental data were acquired by Gokcal (2008) and Brito (2012).

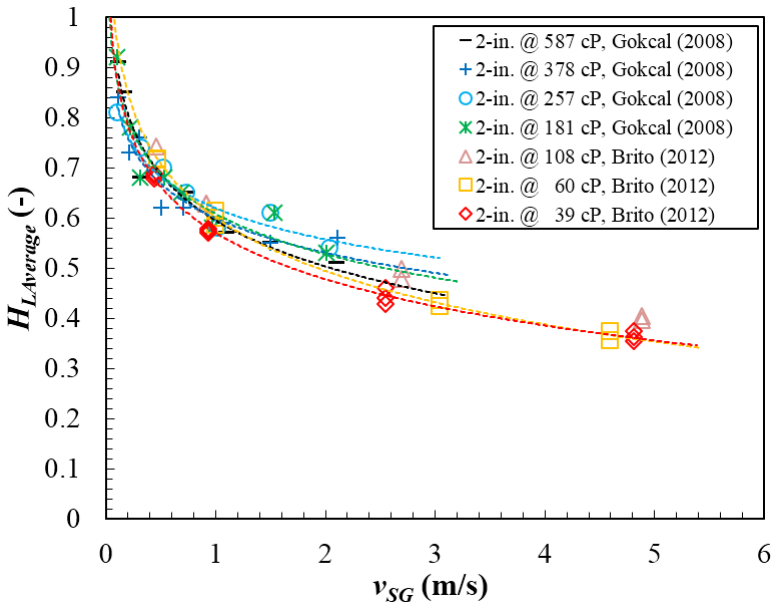

Figure 4.12 Average liquid holdup vs. superficial gas velocity for v_{SL}=0.3 m/s and d=2-in.

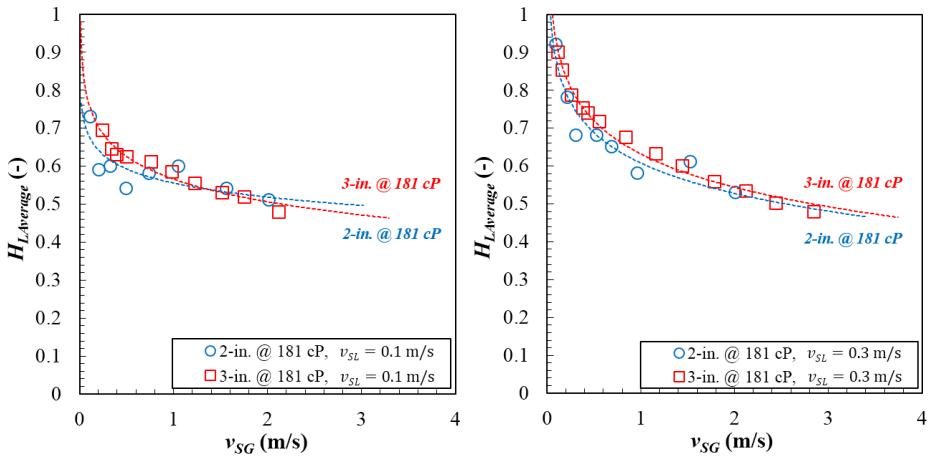

(a) v_{SL} = 0.1 m/s (b) v_{SL} = 0.3 m/s

Figure 4.13 Average liquid holdup in 2- and 3-in. ID pipes vs. superficial gas velocity for μ_{Oil} = 181 cP, (a) v_{SL}=0.1 m/s and (b) v_{SL}=0.3 m/s.

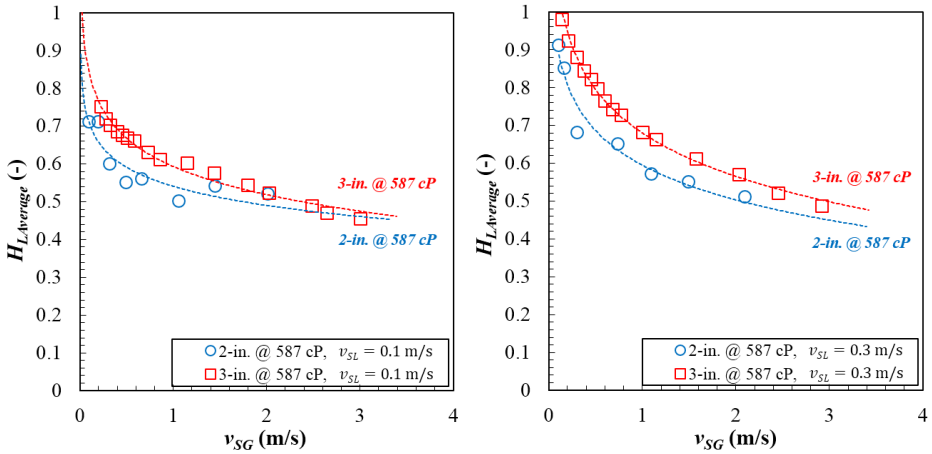

(a) v_{SL} = 0.1 m/s (b) v_{SL} = 0.3 m/s

Figure 4.14 Average liquid holdup in 2- and 3-in. ID pipes vs. superficial gas velocity for μ_{Oil} = 587 cP, (a) v_{SL}=0.1 m/s and (b) v_{SL}=0.3 m/s.

As can be seen, the average liquid holdups in 3-in. ID pipe cases are little higher than in 2-in. ID pipe cases especially, for higher oil viscosity (587 cP). The average liquid holdup discrepancy due to pipe diameter increase can be explained with following reasons.

1. In slug flow regime, the film liquid holdup presented in the section 4.4.2 can affect the average liquid holdup significantly. As the film liquid holdup increases, the average liquid holdup can be increased.
2. The effect of film liquid holdup has to be considered with the ratio of slug length to slug unit length. Although the film liquid holdup between 2- and 3-in. cases are almost same, the average liquid holdup can be increased with the increasing proportion of slug length for larger pipe diameter.

Figure 4.15 illustrates the ratio of slug length to slug unit length against no-slip liquid holdup (v_{SL}/v_m). In this study, at relatively lower oil viscosity (181 cP), the film liquid holdup slightly decreases for larger pipe diameter and, at relatively higher oil viscosity (587 cP), the gap between the results of 2- and 3-in. cases decreases. The portion of slug length to slug unit length marginally increases at relatively low oil viscosity (155 cP). Thus, it can be surmised that, at comparatively low oil viscosity, the impact of slug length ratio on the average liquid holdup is greater than does to the film liquid holdup. On the other hand, at relatively high oil viscosity, the effect of film liquid holdup on the average liquid holdup is more decisive than does to the slug length ratio.

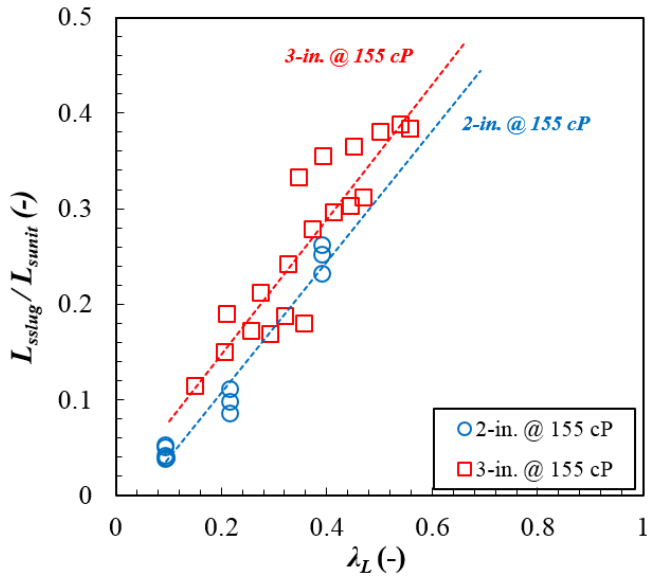

Figure 4.15 Slug length(L_{sslug})/Slug unit length(L_{sunit}) vs. no-slip liquid holdup($\lambda_L=v_{SL}/v_m$) for μ_{Oil} = 155 cP.

For a constant superficial gas and liquid velocity, and relatively low oil viscosity (181 cP), the average liquid holdup of 3-in. ID pipe is slightly higher than 2-in. ID pipe results. However, at a higher oil viscosity (587 cP), the difference of average liquid holdup increases in less-slip condition. Figure 4.16 shows this discrepancy more clearly using x-axis as no-slip liquid holdup, namely, v_{SL}/v_m. As stated in section B.3.3, with increase of no-slip liquid holdup, the average liquid holdups become closer to the inlet liquid fraction, indicating that the slippages between the phases decreases. In other words, for high no-slip liquid holdup, namely in less-slip conditions, the gas phase tends to be dragged more easily by the liquid phase especially for lower oil viscosity and smaller pipe diameter. Consequently, the average liquid holdup difference between 2- and 3-in. ID pipes increases as oil viscosity increases, based on pipe diameter difference. This is mainly occurring in the film region, and an analogous trend is also observed in the film liquid holdup comparison presented in the section 4.4.2.

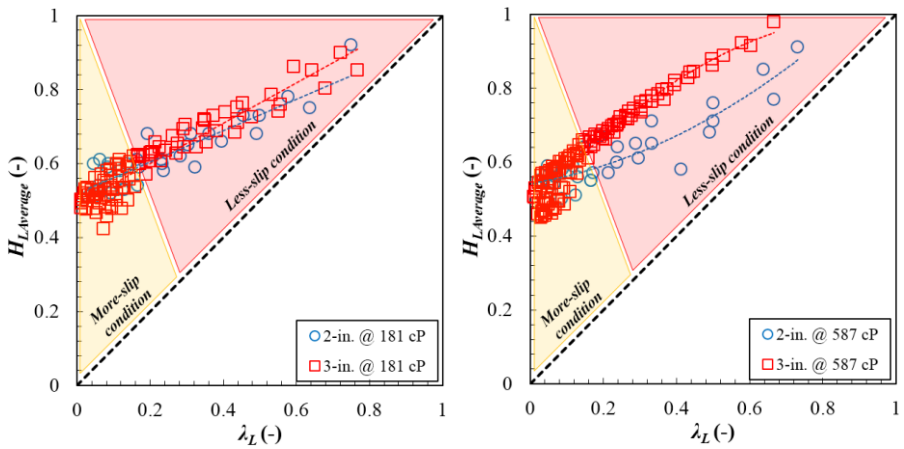

(a) μ_{Oil}= 181 cP (b) μ_{Oil} = 587 cP

Figure 4.16 Average liquid holdup in 2- and 3-in. ID pipes vs. no-slip liquid holdup($\lambda_L=v_{SL}/v_m$) for (a) μ_{Oil} = 181 cP and (b) μ_{Oil} = 587 cP.

4.4 Slug flow characterizations

This section presents the slug characteristics comparison between 2- and 3-in. ID pipes. The slug flow characterization consists of the following subcategories: slug liquid holdup, film liquid holdup, translational velocity, slug length, slug length distribution, and slug frequency.

In previous studies, Gokcal (2008) did not acquire data for slug liquid holdup and film liquid holdup, Kora's (2010) experimental data were used to compare these parameters on this account. For the slug length and frequency, because Gokcal (2008) used different methodology to measure these parameters, Brito's (2012) experimental data were utilized to compare these parameters.

4.4.1 Slug liquid holdup

The slug liquid holdup decreases with increasing superficial gas velocity in 2-in. cases, and this is similar in 3-in. cases. These results are plotted in Figures 4.17 and 4.18. In the 2-in. cases, the slug liquid holdup slightly decreases with increasing oil viscosity due to the increased amount of entrained gas in the slug region, however, the amount of reduction is very small. On the other hands, there is no significant change with oil viscosity increase in the 3-in. cases.

The comparison of slug liquid holdup between 2- and 3-in. ID pipes at different oil viscosities are presented from Figures 4.19 to 4.21. When the oil viscosity is 181 cP, the slug liquid holdups of 2- and 3-in. ID pipes are almost

same, however, as oil viscosity increases, the results of 3-in. cases are slightly higher than 2-in. cases. To explain this phenomena, the different effect of gas amount which pass through the top of the slug region, and gas bubble amount which was entrained in the slug region have to be considered. However, because the quantification of these components was challenge in this study, future research is needed to investigate these effects.

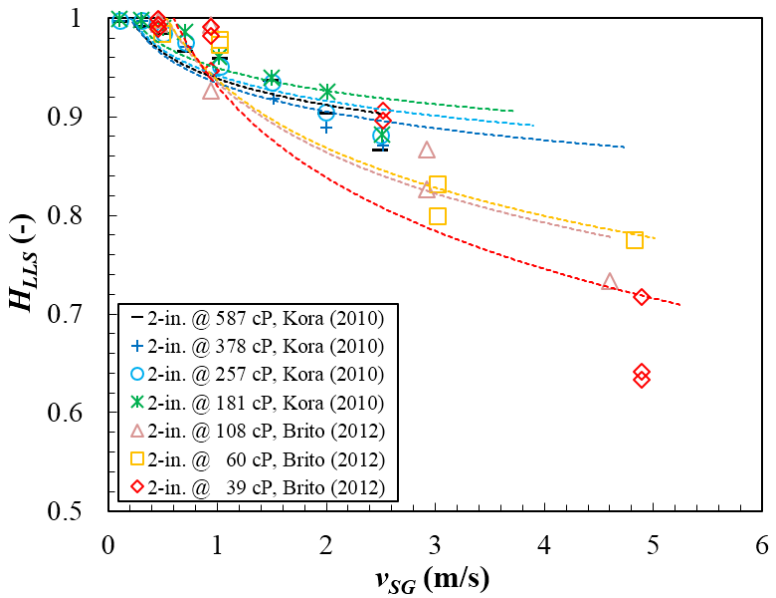

Figure 4.17 Slug liquid holdup vs. superficial gas velocity for v_{SL}=0.1 m/s and d=2-in. These experimental data were acquired by Kora (2010) and Brito (2012).

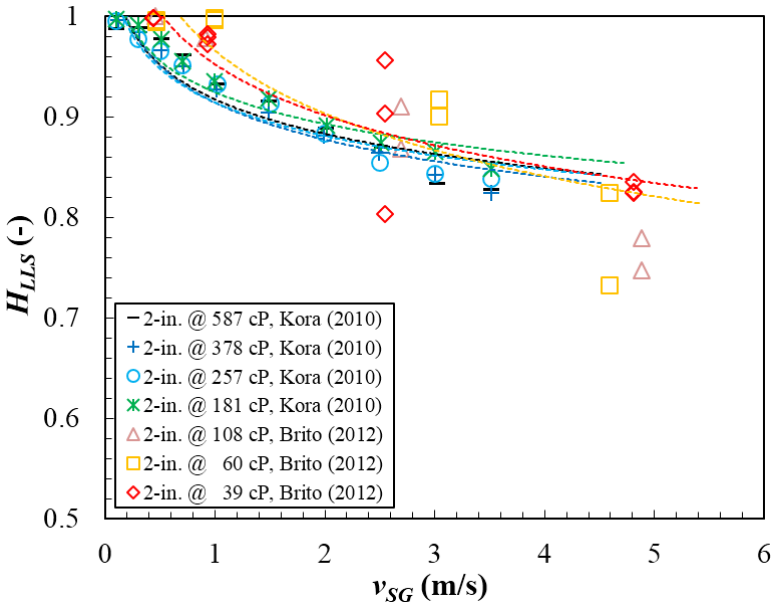

Figure 4.18 Slug liquid holdup vs. superficial gas velocity for v_{SL}=0.3 m/s and d=2-in. These experimental data were acquired by Kora (2010) and Brito (2012).

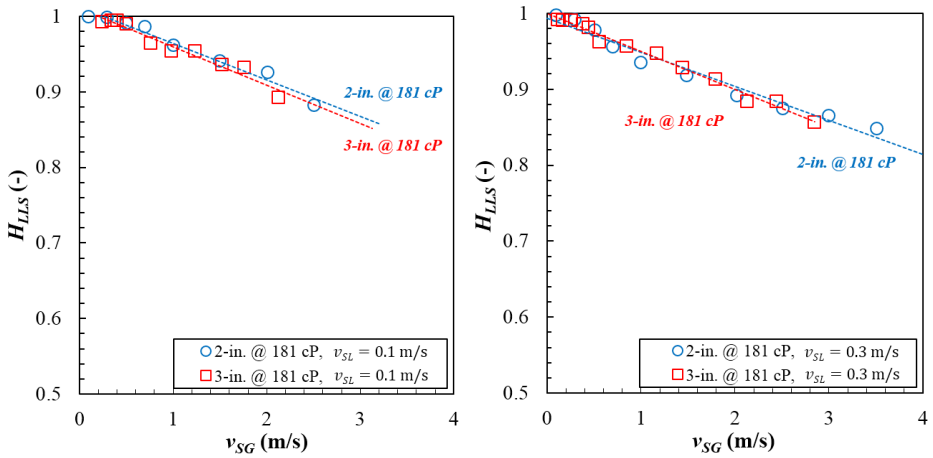

Figure 4.19 Slug liquid holdup in 2- and 3-in. ID pipes vs. superficial gas velocity for μ_{Oil} = 181 cP, (a) v_{SL}=0.1 m/s and (b) v_{SL}=0.3 m/s.

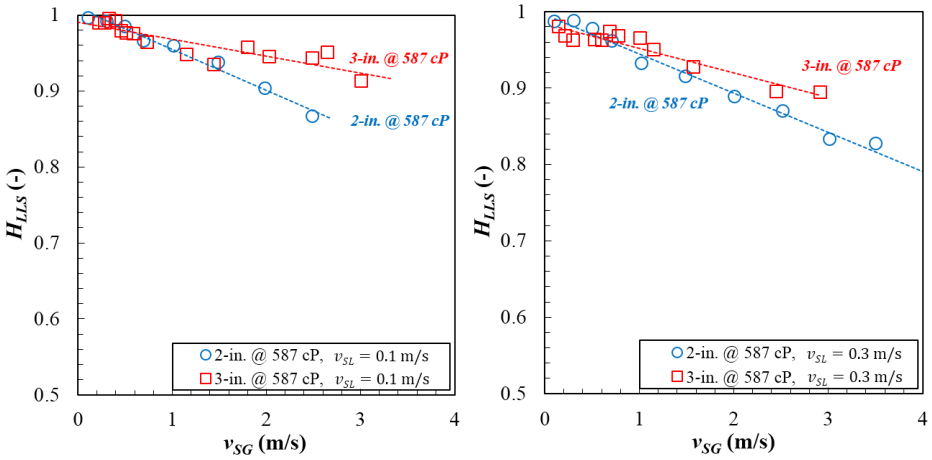

Figure 4.20 Slug liquid holdup in 2- and 3-in. ID pipes vs. superficial gas velocity for μ_{Oil} = 587 cP, (a) v_{SL}=0.1 m/s and (b) v_{SL}=0.3 m/s.

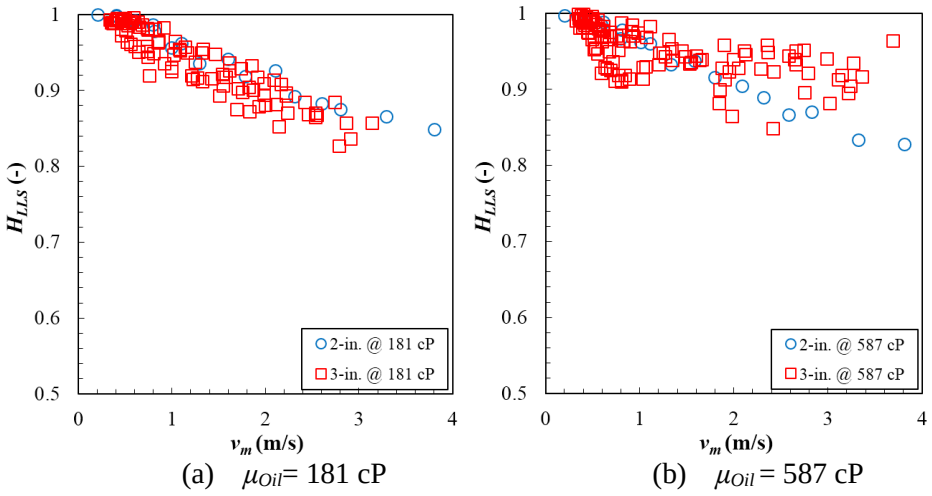

Figure 4.21 Slug liquid holdup in 2- and 3-in. ID pipes vs. mixture velocity for (a) μ_{Oil} = 181 cP and (b) μ_{Oil} = 587 cP.

4.4.2 Film liquid holdup

As can be seen in Figures 4.22 and 4.23, for a given superficial liquid velocity and oil viscosity, the film liquid holdup decreases with increase of superficial gas velocity. At constant superficial liquid and gas velocities, the film liquid holdup increases when oil viscosity increases in 3-in. ID case, while the opposite trend is observed in 2-in. ID case.

For constant superficial gas and liquid velocities, and relatively low oil viscosity (181 cP), the film liquid holdup of 2-in. are higher than 3-in. results. On the other hand, at a higher oil viscosity (587 cP), the difference of film liquid holdup between 2- and 3-in. decreases (See Figures 4.24 and 4.25.). In addition, Figure 4.26 shows that the film liquid holdups of 3-in. are slightly higher than those of 2-in. case when v_{SL}/v_m is higher than 0.3. This area is regarded as pseudo-slug region. The discrepancy of film liquid holdup between 2- and 3-in. ID pipes decreases as oil viscosity increases owing to the different effect of drag force. This trend is similar to the average liquid holdup. In addition, as superficial liquid velocity increases (from 0.1 to 0.3 m/s), the film liquid holdup difference decreases when the superficial gas velocities are higher than 1 m/s.

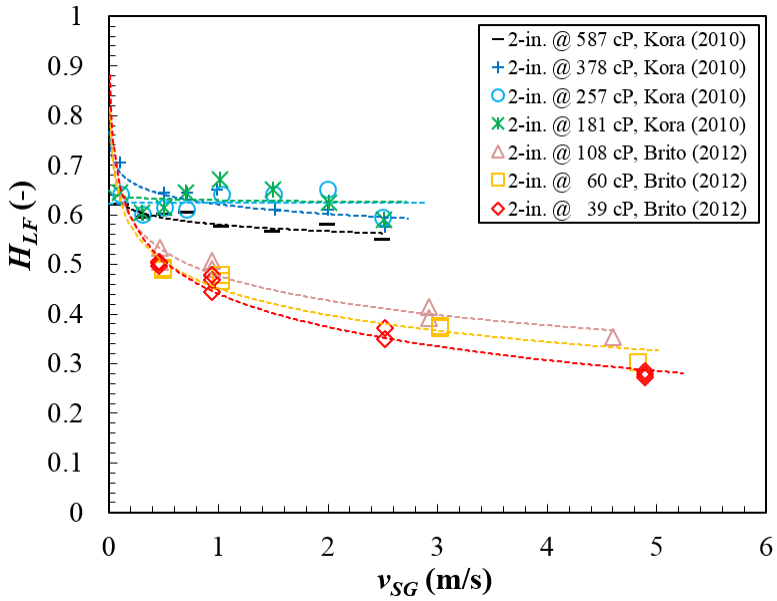

Figure 4.22 Film liquid holdup vs. superficial gas velocity for v_{SL}=0.1 m/s and d=2-in. These experimental data were acquired by Kora (2010) and Brito (2012).

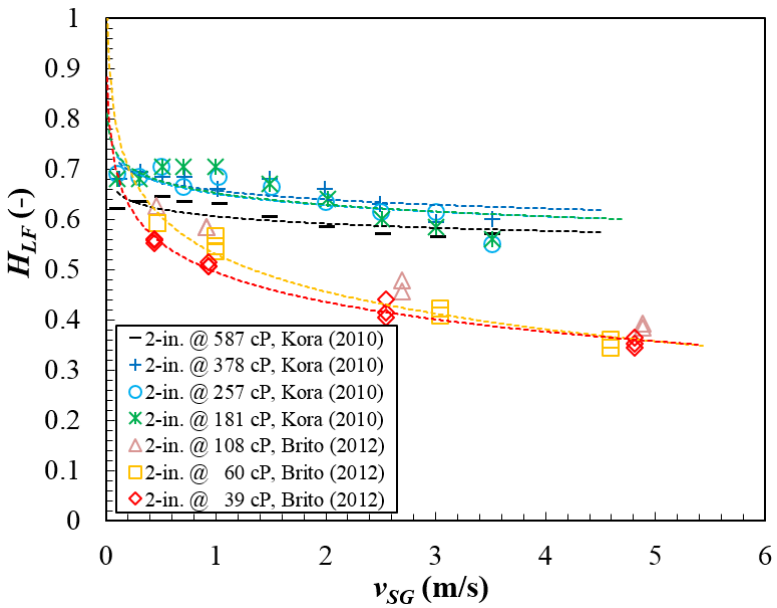

Figure 4.23 Film liquid holdup vs. superficial gas velocity for v_{SL}=0.3 m/s and d=2-in. These experimental data were acquired by Kora (2010) and Brito (2012).

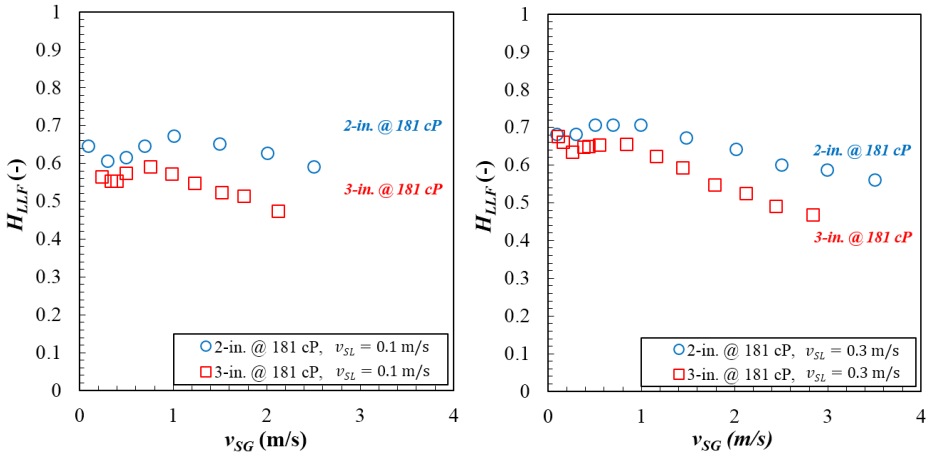

(a) v_{SL} = 0.1 m/s (b) v_{SL} = 0.3 m/s

Figure 4.24 Film liquid holdup in 2- and 3-in. ID pipes vs. superficial gas velocity for μ_{Oil} = 181 cP, (a) v_{SL}=0.1 m/s and (b) v_{SL}=0.3 m/s.

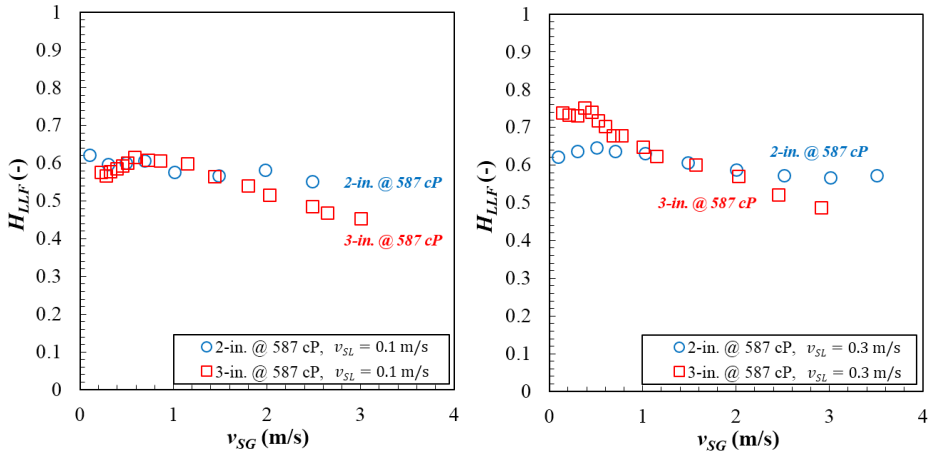

(a) v_{SL} = 0.1 m/s (b) v_{SL} = 0.3 m/s

Figure 4.25 Film liquid holdup in 2- and 3-in. ID pipes vs. superficial gas velocity for μ_{Oil} = 587 cP, (a) v_{SL}=0.1 m/s and (b) v_{SL}=0.3 m/s.

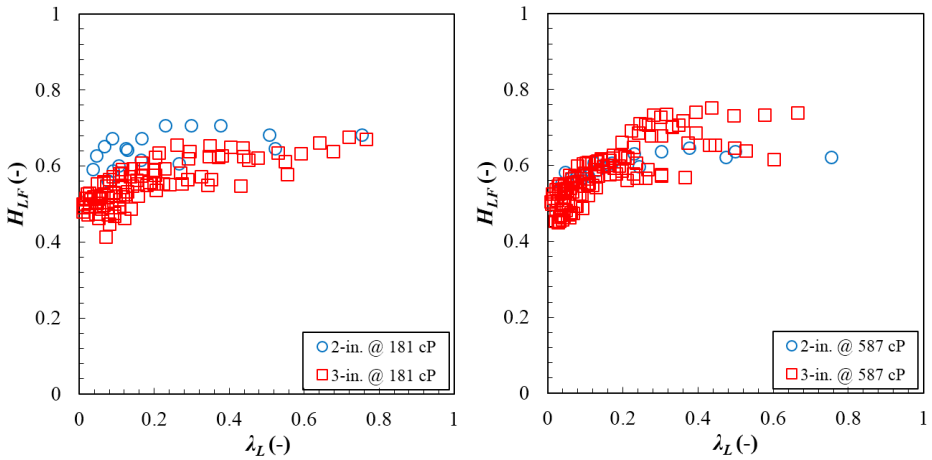

(a) μ_{Oil}= 181 cP (b) μ_{Oil} = 587 cP

Figure 4.26 Film liquid holdup in 2- and 3-in. ID pipes vs. mixture velocity for (a) μ_{Oil} = 181 cP and (b) μ_{Oil} = 587 cP.

4.4.3 Translational velocity

Figures 4.27 and 4.28 present the translational velocity vs. the mixture velocity reported by Gokcal (2008) and Brito (2012). These data sets correspond to different oil viscosities, superficial gas and liquid velocities. Both data sets were obtained from 2-in. ID pipes.

The comparison of translational velocity between 2- and 3-in. ID pipes at different oil viscosities are presented in Figures 4.29 and 4.30. For all oil viscosities, translational velocity increases when mixture velocity increases. For constant oil viscosity and mixture Reynolds number, translational velocity of 2-in. is higher than 3-in case. At low mixture velocities, v_m < 1.0 m/s, the translational velocity of 3-in. is slightly higher than that of 2-in. ID pipes due

to the small difference of drift velocity (see Figure 4.31). The drift velocity from this study are similar with Ben-Mansour *et al*. (2010). It is observed that the drift velocity increases for larger pipe diameter. The decrease in the drift velocity with viscosity change is steeper in smaller pipes. The plots tend to have an asymptotic level at very high viscosity which leads to a small variation in drift velocity with viscosity change.

In both cases, the slope of the resultant lines are approximately 2.0 representing the C_0 coefficient. This indicates that the experiments were in the laminar flow regime. Conversely, for $v_m > 2.0$ m/s, translational velocity slightly decreases as pipe diameter increases due to the effect of different cross-sectional areas. In general, the top portion of the slug region is barely reaching the top of the pipe. This is a symptom of unstable slugs or pseudo-slugs. Additionally, this phenomenon arouse the increase of data scattering. In this study, flow regime for this section is regarded as Pseudo-slug flow region. The degree of scattering can be visualized more clearly by using mixture Reynolds number (see Figures 4.29(b) and 4.30(b)).

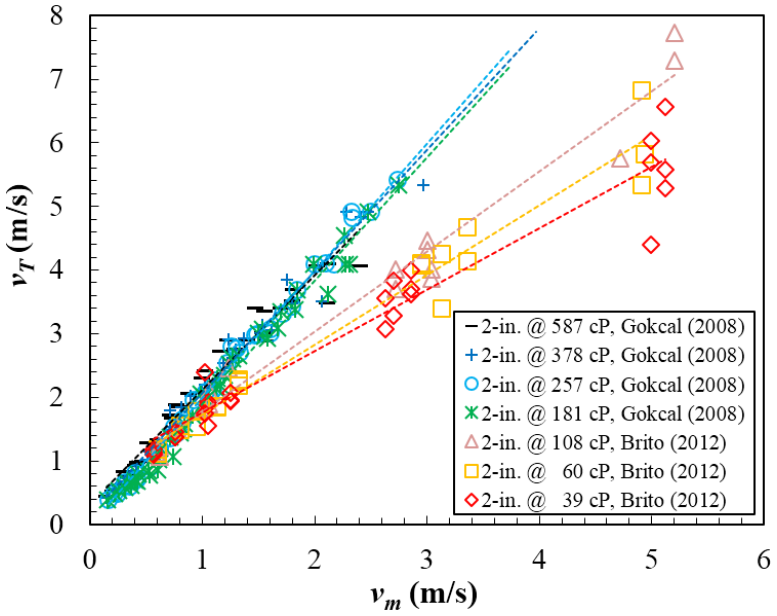

Figure 4.27 Translational velocity vs. mixture velocity for *d*=2-in. These experimental data were acquired by Gokcal (2008) and Brito (2012).

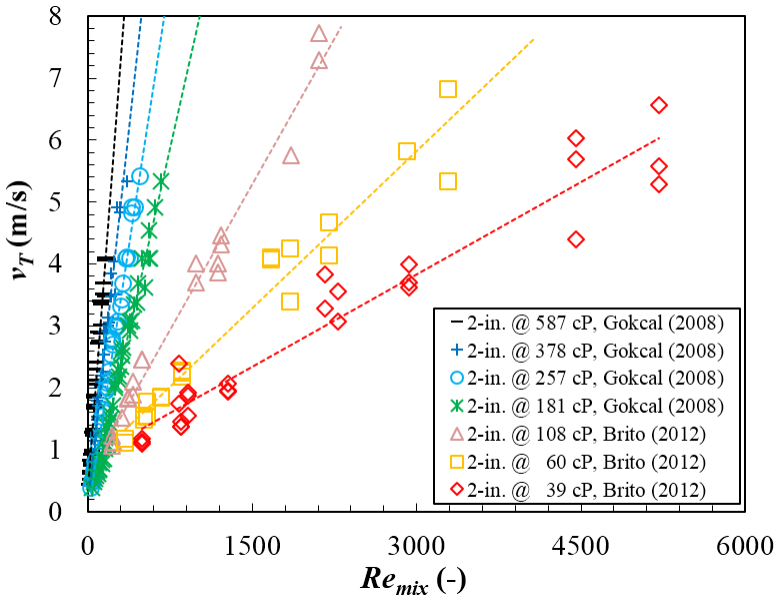

Figure 4.28 Translational velocity vs. mixture Reynolds number for *d*=2-in. These experimental data were acquired by Gokcal (2008) and Brito (2012).

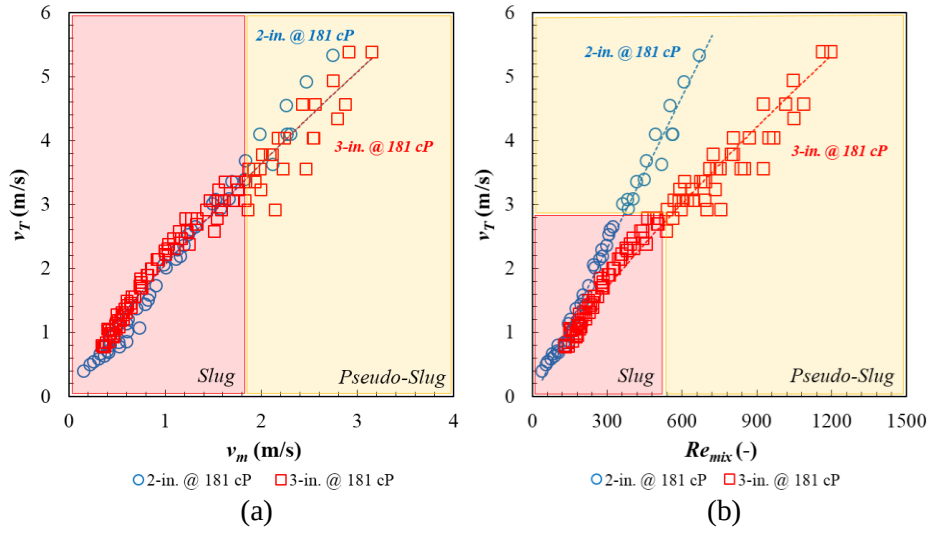

Figure 4.29 Translational velocity vs. (a) mixture velocity and (b) mixture Reynolds number for μ_{Oil} = 181 cP.

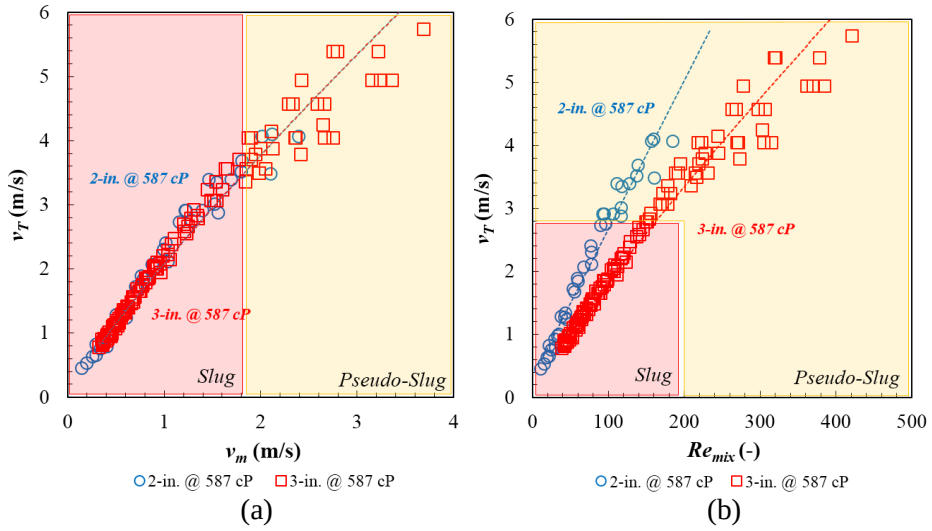

Figure 4.30 Translational velocity vs. (a) mixture velocity and (b) mixture Reynolds number for μ_{Oil} = 587 cP.

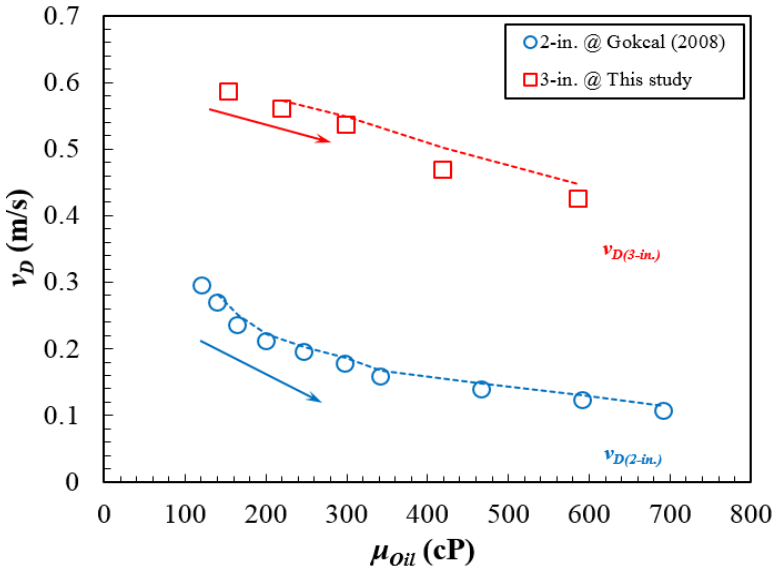

Figure 4.31 Drift velocity in 2- and 3-in. ID pipes vs. oil viscosity. In this study, drift velocity was calculated by using $v_T = C_0 v_m + v_D$ propsed by Nicklin *et al*. (1962), on the other hand, 2-in. results were measured by Gokcal (2008).

4.4.4 Slug length

In previous study, Gokcal (2008) investigated slug length and slug frequency. However, sensors and methodology differ from current study. Gokcal (2008) used laser sensors to measure slug length, while similar capacitance sensors as Brito (2012) were used in this project. For such a reason, Brito's (2012) experimental data for slug length and frequency were used to investigate the effect of pipe diameter.

As can be seen in Figure 4.32, dimensionless slug length (L_s/D) decreases as mixture velocity increases, and L_s/D decreases when oil viscosity increases in both 2- and 3-in. ID pipes.

For a constant mixture velocity and oil viscosity, L_s/D values of 3-in. are slightly higher than 2-in. ID pipes. Figures 4.33 and 4.34 present this trend when oil viscosity is 155 cP. The opposite results were reported by Nydal *et al*. (1992) who proposed Eqs. (60) and (61). However, Nydal *et al*.'s (1992) experimental study was carried out with low viscous liquid and large data scattering was observed. Finally, as gas velocity increases (keeping liquid flow rate constant), slugs moves faster and shorter slugs are required to satisfy mass balance.

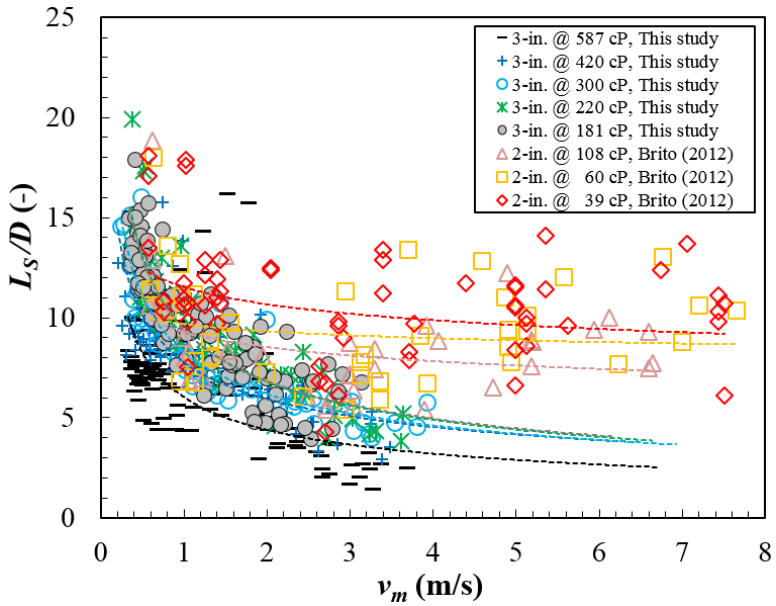

Figure 4.32 Dimensionless slug length vs. mixture velocity for different oil viscosities. 3-in. data were measured in this study and 2-in. results were acquired by Brito (2012).

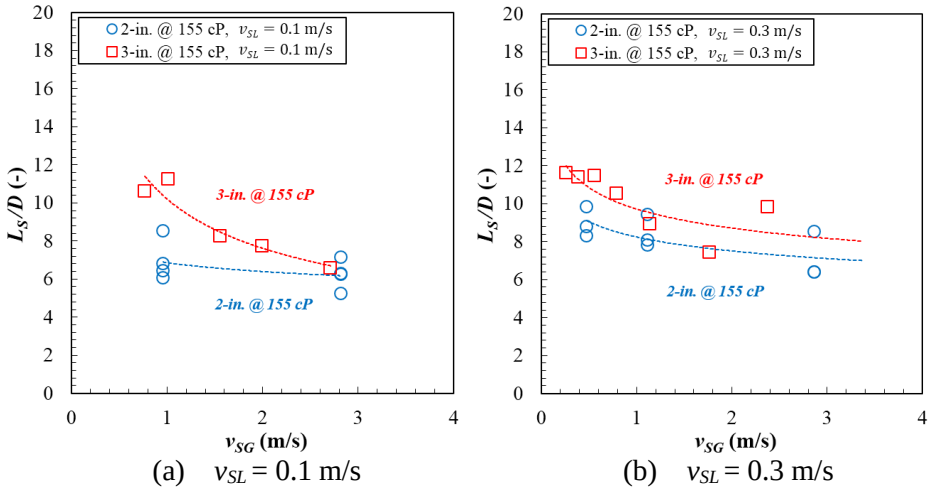

Figure 4.33 Dimensionless slug length in 2- and 3-in. ID pipes vs. superficial gas velocity for μ_{Oil} = 155 cP, (a) v_{SL}=0.1 m/s and (b) v_{SL}=0.3 m/s.

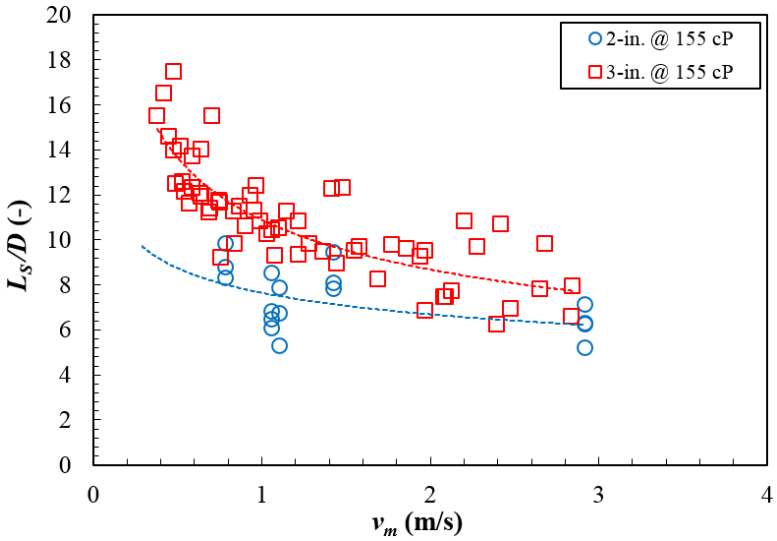

Figure 4.34 Dimensionless slug length in 2- and 3-in. ID pipes vs. mixture velocity for μ_{Oil} = 155 cP.

4.4.5 Slug length distribution

Figures 4.35 and 4.36 show the statistical distribution of slug lengths when the oil viscosity is 155 cP. As stated in section B.3.4.5, the proper high ranked functions are gamma (or gamma 3p), log-normal (or log-normal 3p), and weibull in both pipe diameter cases. Additionally, the degree of right-skewed are similar in both cases supporting the results of previous experimental studies (such as Brill *et al*. (1981), Marcano *et al*. (1998), Gokcal (2008), and Brito (2012)).

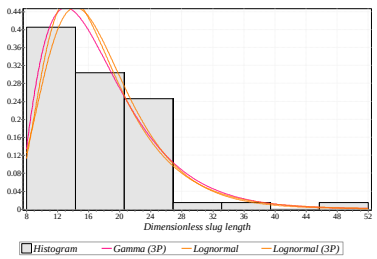

(a)μ_{Oil}=155cP, v_{SL}=0.3m/s, v_{SG}=0.4m/s

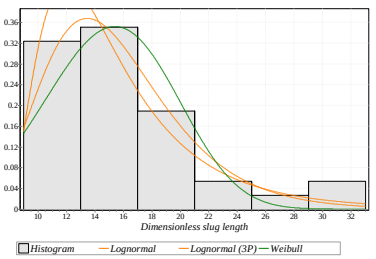

(b)μ_{Oil}=155cP, v_{SL}=0.3m/s, v_{SG}=1.0m/s

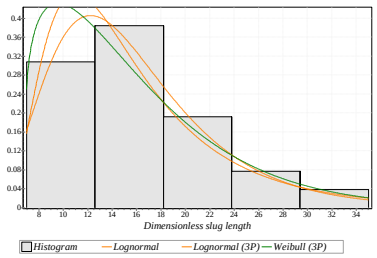

(c)μ_{Oil}=155cP, v_{SL}=0.3m/s, v_{SG}=2.0m/s

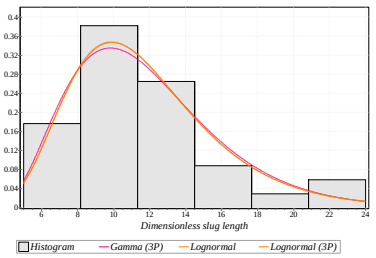

(d)μ_{Oil}=155cP, v_{SL}=0.3m/s, v_{SG}=3.0m/s

Figure 4.35 Dimensionless slug length distribution for μ_{Oil}=155 cP and *d*=3-in.

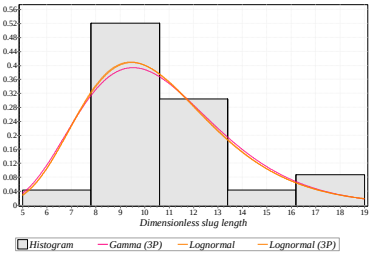

(a)μ_{Oil}=155cP, v_{SL}=0.3m/s, v_{SG}=0.1m/s

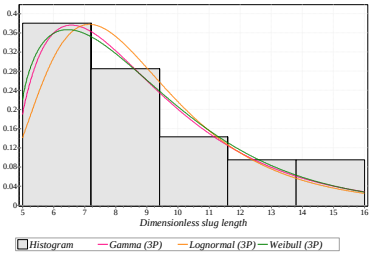

(b)μ_{Oil}=155cP, v_{SL}=0.3m/s, v_{SG}=0.5m/s

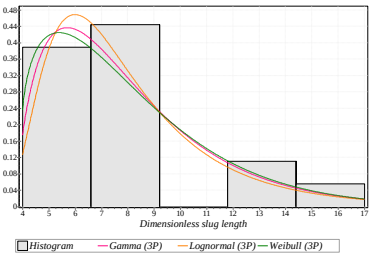

(c)μ_{Oil}=155cP, v_{SL}=0.3m/s, v_{SG}=1.0m/s

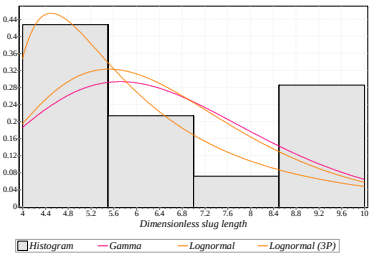

(d)μ_{Oil}=155cP, v_{SL}=0.3m/s, v_{SG}=3.0m/s

Figure 4.36 Dimensionless slug length distribution for μ_{Oil}=155 cP and d=2-in.

4.4.6 Slug frequency

Similar with previous sections, Figures 4.37 and 4.38 show the slug frequency versus the superficial gas velocity reported by Gokcal (2008) and Brito (2012) at different oil viscosities and for v_{SL}=0.1 m/s and 0.3 m/s. These data were acquired from 2-in. ID pipes.

As same as referred to in the section B.3.4.6, for the case of 2-in. ID pipes, the slug frequency increases when superficial liquid velocity increases. For superficial velocity from 0.02 m/s to 0.4 m/s, slug frequency initially increases and reaches a maximum as superficial gas velocity increases. Further increase of superficial gas velocity results in slug frequency decreases. This

phenomenon is the same for 3-in. ID pipes as previously stated.

As can be seen in Figures 4.39 and 4.40, for the same oil viscosity, superficial liquid and gas velocities, slug frequency of 2-in. is larger than 3-in. ID pipes. Owing to the mass balance relationship between slug frequency and slug length, slug frequency for 2-in. is larger as compare with 3-in. ID pipe. Consequently, when the pipe diameter increases, the slug length decreases and more slug per unit of time (frequency) are required to transport the same liquid flow rate per unit of area.

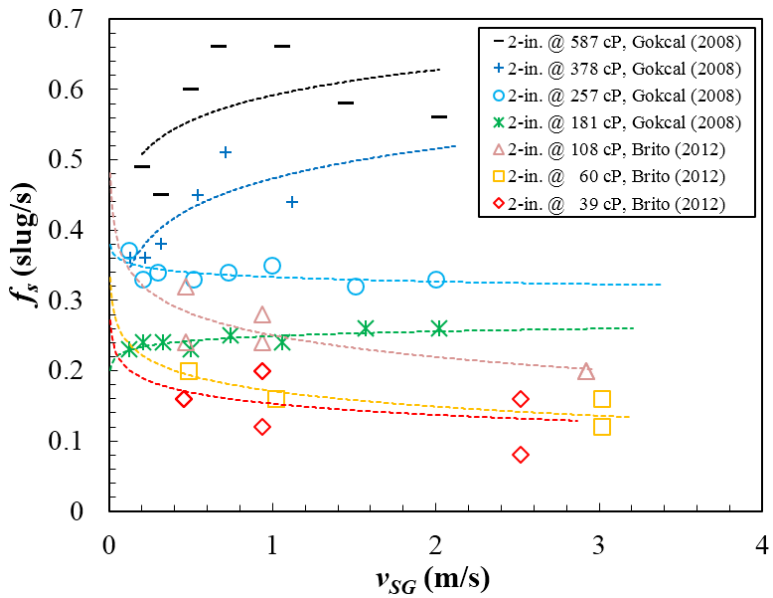

Figure 4.37 Slug frequency vs. superficial gas velocity for v_{SL}=0.1 m/s and d=2-in. These experimental data were acquired by Gokcal (2008) and Brito (2012).

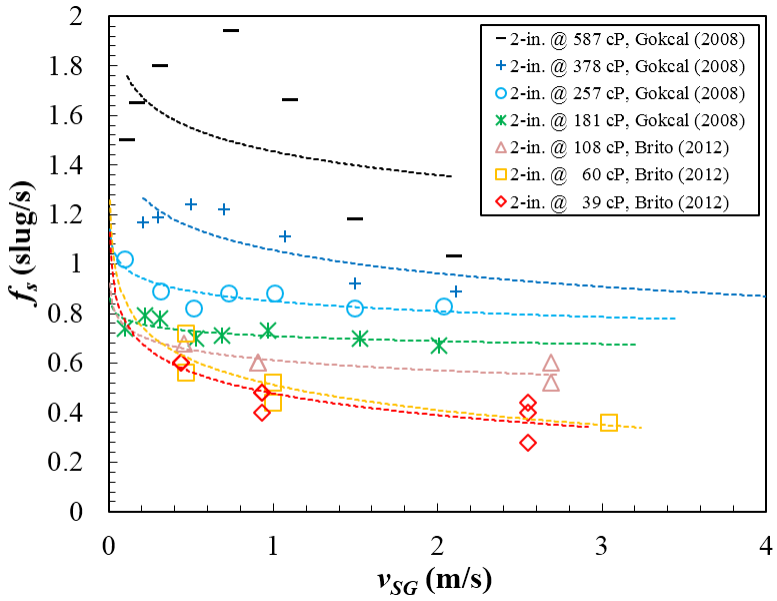

Figure 4.38 Slug frequency vs. superficial gas velocity for v_{SL}=0.3 m/s and d=2-in. These experimental data were acquired by Gokcal (2008) and Brito (2012).

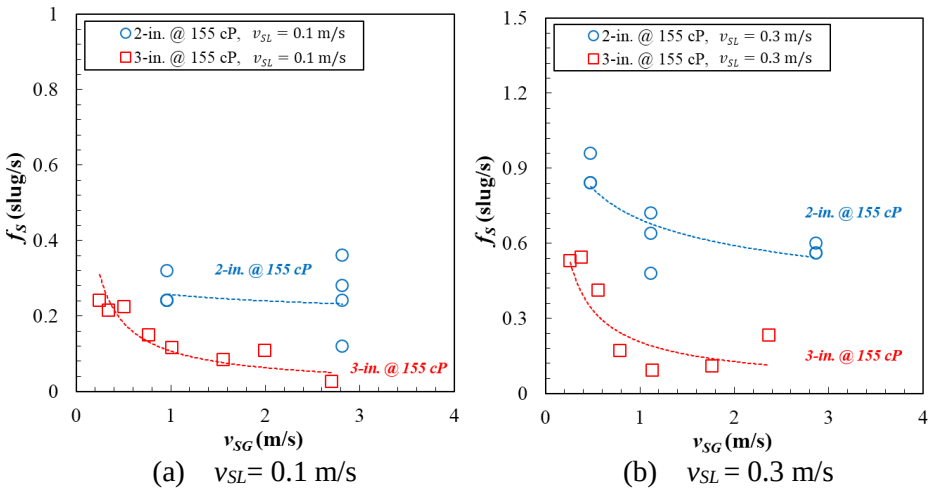

Figure 4.39 Slug frequency in 2- and 3-in. ID pipes vs. superficial gas velocity for μ_{Oil} = 155 cP, (a) v_{SL}=0.1 m/s and (b) v_{SL}=0.3 m/s.

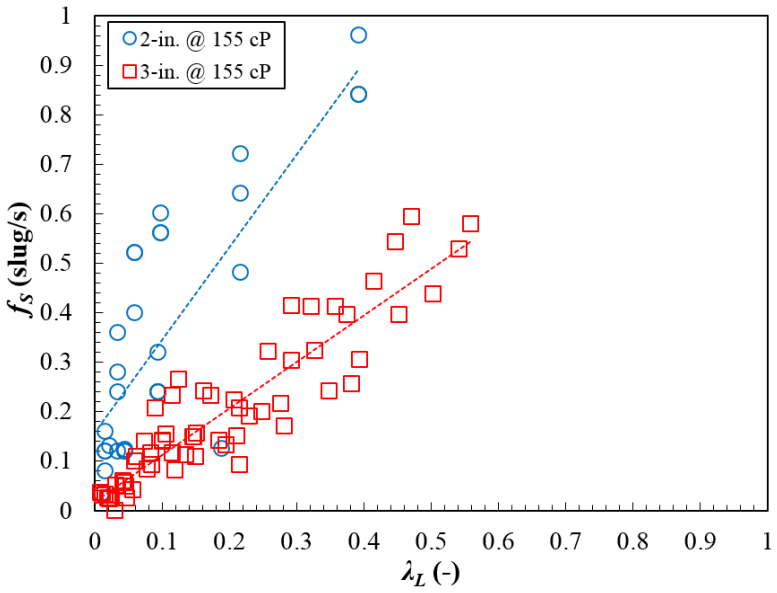

Figure 4.40 Slug frequency in 2- and 3-in. ID pipes vs. $\lambda_L(v_{SL}/v_m)$ for μ_{Oil} = 155 cP.

Chapter 5 Model and Correlation Evaluation

This chapter presents the evaluation of the existing models and correlations with the acquired high viscosity two-phase flow data. The high viscosity and pipe diameter effects on two-phase flow were analyzed. Pressure gradient, average liquid holdup, and slug characteristics such as slug liquid holdup, film holdup, translational velocity, slug length, and slug frequency are compared with the existing models and correlations.

5.1 Statistical parameters

Six statistical parameters were used to evaluate the performance of pressure gradient, average liquid holdup, and slug flow characteristics prediction models. Actual error, e_i, and relative error, e_j, are expressed in Eqs (103) and (104) to calculate the statistical parameters defined in Eqs (105) to (110).

$$e_i = \left(\frac{q_{i,Cal} - q_{i,Mea}}{q_{i,Mea}} \right) \times 100 \tag{103}$$

$$e_j = (q_{i,Cal} - q_{i,Mea}) \tag{104}$$

Based on the relative and actual errors, six statistical parameters are defined as follows.

Average relative error

$$\varepsilon_1 = \frac{1}{N}\sum_{i=1}^{N}(e_i) \tag{105}$$

Absolute average relative error

$$\varepsilon_2 = \frac{1}{N}\sum_{i=1}^{N}(|e_i|) \tag{106}$$

Standard deviation of relative error

$$\varepsilon_3 = \sqrt{\frac{\sum_{i=1}^{N}(e_i - \varepsilon_1)^2}{N-1}} \tag{107}$$

Average actual error

$$\varepsilon_4 = \frac{1}{N}\sum_{i=1}^{N}(e_j) \tag{108}$$

Absolute average actual error

$$\varepsilon_5 = \frac{1}{N}\sum_{i=1}^{N}(|e_j|) \tag{109}$$

Standard deviation of actual error

$$\varepsilon_6 = \sqrt{\frac{\sum_{i=1}^{N}(e_i - \varepsilon_4)^2}{N-1}} \tag{110}$$

where N is the number of data points.

The average relative error, ε_1, and the average actual error, ε_4, show the total error between the predicted and measured parameters. Positive and negative values indicate whether the existing models over-estimate or under-estimate, respectively. These two parameters can be either positive or negative, and can hide the true error cancelling each other. Therefore, the absolute average relative error, ε_2, and the absolute average actual error, ε_5, are more reliable than ε_1 and ε_4, eliminating the masking effect. They indicate how large the error is on the average. The standard deviations, ε_3 and ε_6, represent the degree of scattering with respect to their corresponding average errors, ε_1 and ε_4. These six parameters were used to evaluate the performance of the existing models and correlations with the acquired data.

5.2 Pressure gradient

Next sections present the results of the new 3-in. data and its comparison with 2-in. previous studies.

5.2.1 3-in. ID pipes

The measured pressure gradient was compared with TUFFP Unified, OLGA, and Xiao *et al*. (1990) models for 3-in. ID pipes case. Figures 5.2 is the graphical presentations of the three models' prediction against the measured pressure gradient for all experimental data sets and oil viscosities.

When the entire dataset is compared against TUFFP Unified model,

the average and absolute average relative errors are $\varepsilon_{1\,(3\text{-}in.)}$ = -22% and $\varepsilon_{2\,(3\text{-}in.)}$ = 26%, respectively. Figures 5.2 to 5.8 show that enormous under-prediction occurs at the entire experimental range of the measured pressure gradient and oil viscosity.

OLGA model also presents a negative value of $\varepsilon_{1\,(3\text{-}in.)}$ for all the cases. For the entire data sets, average relative error and actual errors correspond to -31 % and -185 Pa/m, respectively.

Similarly, Xiao *et al*. (1990) model produces a negative value of $\varepsilon_{1\,(3\text{-}in.)}$ (-32%). Same as the previous two models, Xiao *et al*. (1990) model under-estimates for the entire data sets.

In summary, TUFFP Unified, OLGA, and Xiao *et al*. (1990) models were compared with the experimental pressure gradient data and statistical parameters were used to evaluate the existing model performance. The three models give negative $\varepsilon_{1\,(3\text{-}in.)}$ values of -22%, -31%, and -32% with relatively small $\varepsilon_{3\,(3\text{-}in.)}$ values of 16%, 17%, and 17%, respectively. Nevertheless, TUFFP Unified model shows the lowest absolute average relative error. The details of the error analysis are provided in Appendix F.

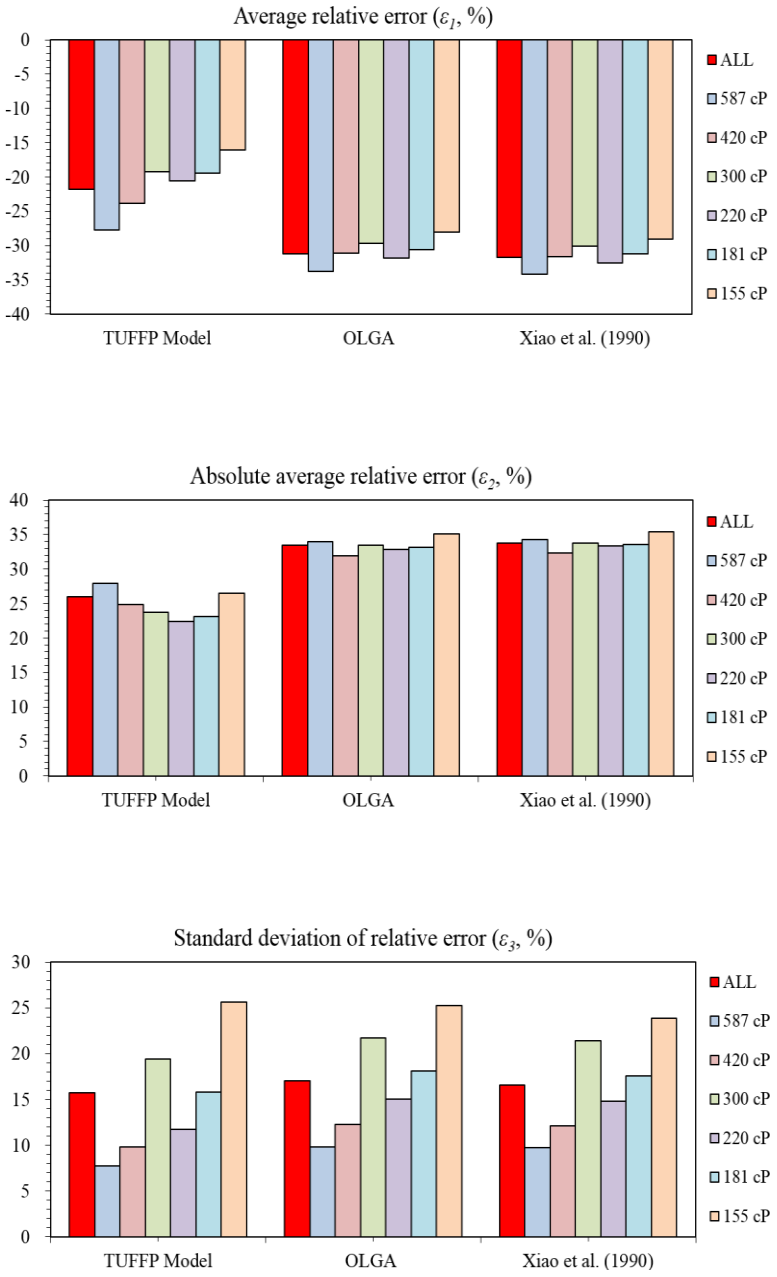

Figure 5.1 Model evaluation using the pressure gradient experimental data acquired from 3-in. ID pipes.

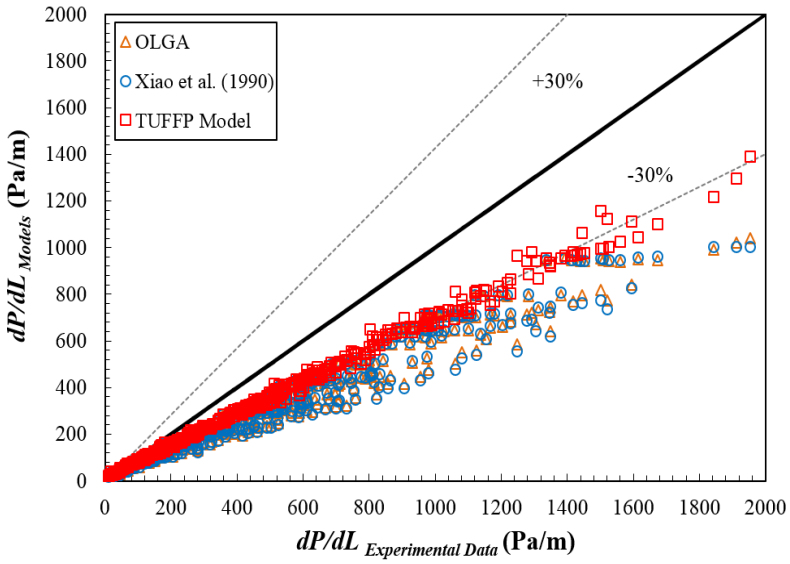

Figure 5.2 Comparison between TUFFP, OLGA, and Xiao *et al*. (1990) model prediction and measured pressure gradients for 'all' oil viscosities when the pipe diameter is 3-in.

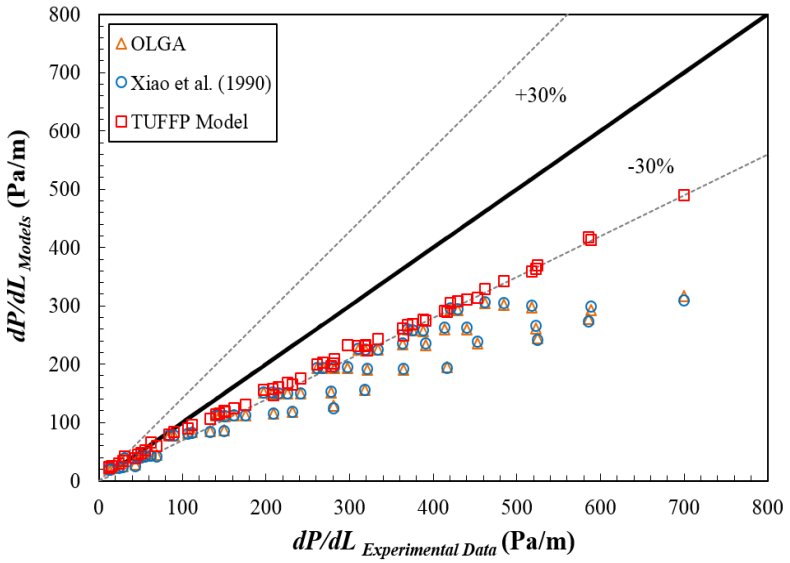

Figure 5.3 Comparison between TUFFP, OLGA, and Xiao *et al*. (1990) model prediction and measured pressure gradients for μ_{Oil} = 155 cP when the pipe diameter is 3-in.

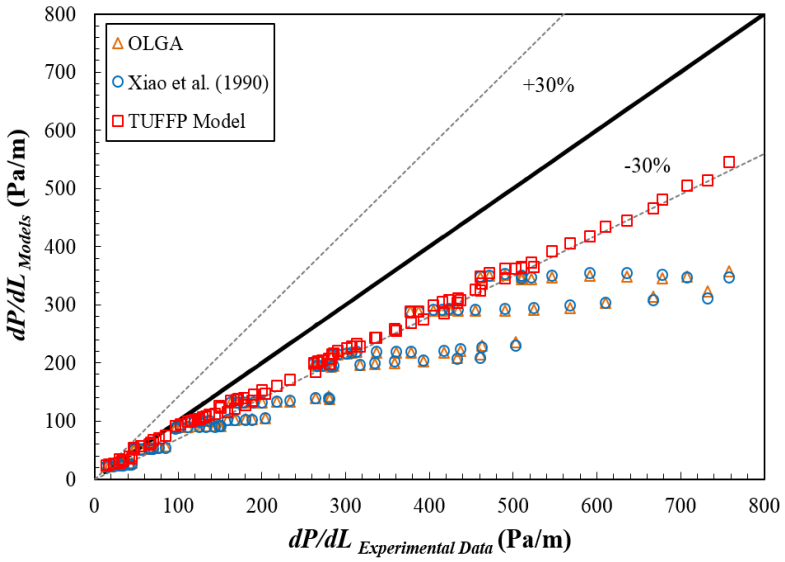

Figure 5.4 Comparison between TUFFP, OLGA, and Xiao *et al*. (1990) model prediction and measured pressure gradients for μ_{Oil} = 181 cP when the pipe diameter is 3-in.

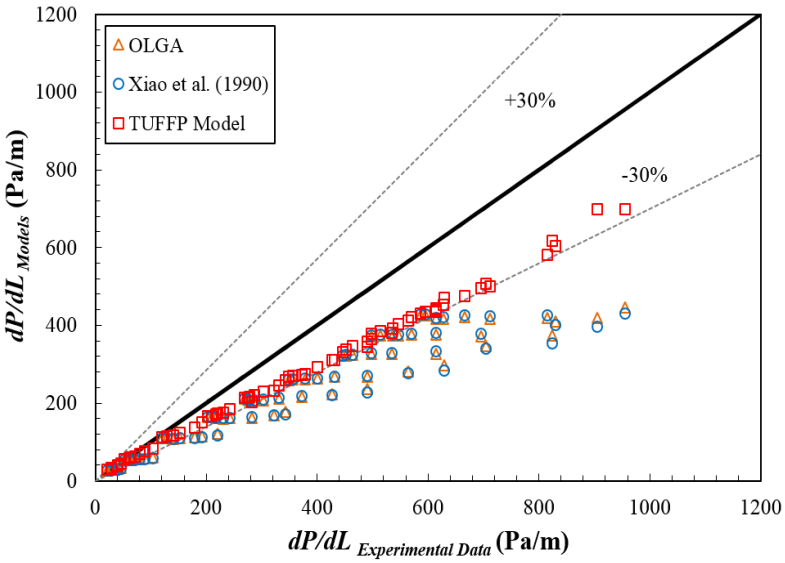

Figure 5.5 Comparison between TUFFP, OLGA, and Xiao *et al*. (1990) model prediction and measured pressure gradients for μ_{Oil} = 220 cP when the pipe diameter is 3-in.

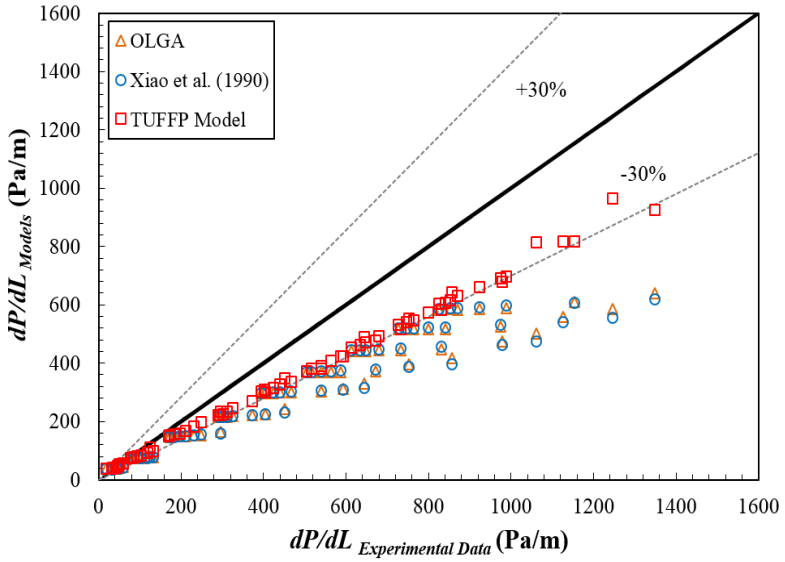

Figure 5.6 Comparison between TUFFP, OLGA, and Xiao *et al*. (1990) model prediction and measured pressure gradients for μ_{Oil} = 300 cP when the pipe diameter is 3-in.

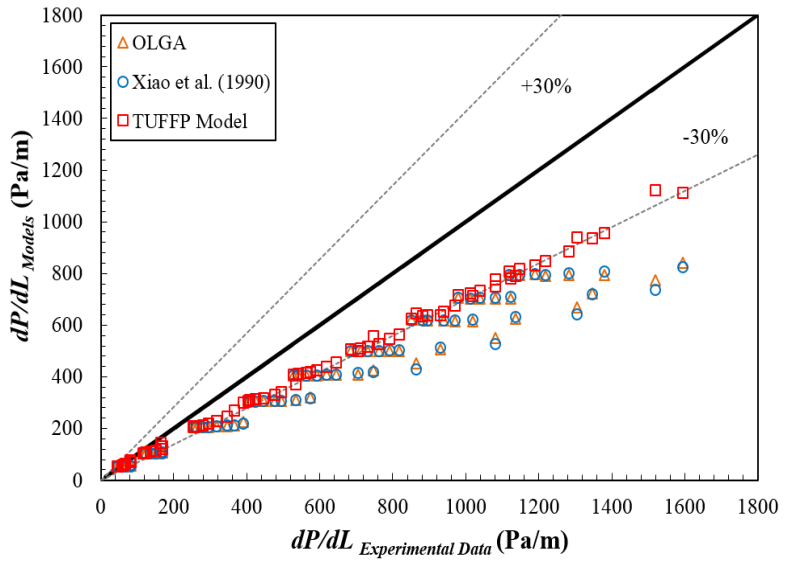

Figure 5.7 Comparison between TUFFP, OLGA, and Xiao *et al*. (1990) model prediction and measured pressure gradients for μ_{Oil} = 420 cP when the pipe diameter is 3-in.

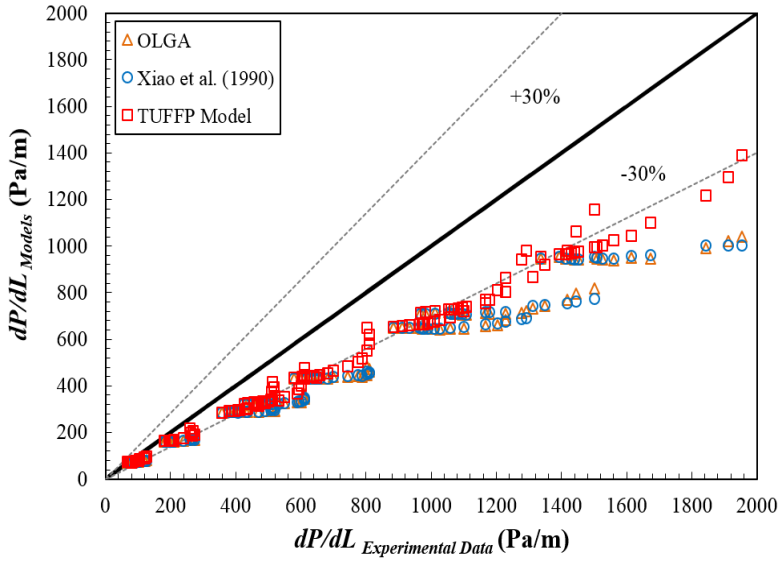

Figure 5.8 Comparison between TUFFP, OLGA, and Xiao *et al*. (1990) model prediction and measured pressure gradients for μ_{Oil} = 587 cP when the pipe diameter is 3-in.

5.2.2 2-in. ID pipes

Figures 5.10 to 5.12 present the three models' predictions (TUFFP Unified, OLGA, and Xiao *et al*. (1990)) against the Gokcal's (2008) measured pressure gradient data obtained from 2-in. ID pipes. Figure 5.9 shows the results of the model evaluation for the pressure gradient.

TUFFP Unified model gives the average relative and actual errors by -7.1% and -80 Pa/m, respectively. This model little more under-estimates for relatively lower oil viscosity (181 cP) than the results of higher oil viscosity (587 cP). For the relatively lower pressure gradient (dP/dL < 200 Pa/m), the degree of under-estimation decreases comparing to the result of higher pressure

gradient (dP/dL > 200 Pa/m). OLGA and Xiao *et al*. (1990) models also under-predict the pressure gradient for all the range of the oil viscosities indicating that the existing three models need to be modified to predict slightly higher than these results. The average relative errors of OLGA and Xiao *et al*. (1990) models are -14% and -13 %, respectively.

In summary, although all of the three models under-estimate the pressure gradient, TUFFP Unified gives the lowest absolute average relative error of 7.5% indicating that this model is the best to predict the pressure gradient when the pipe diameter is 2-in. The details of the error analysis are provided in Appendix F.

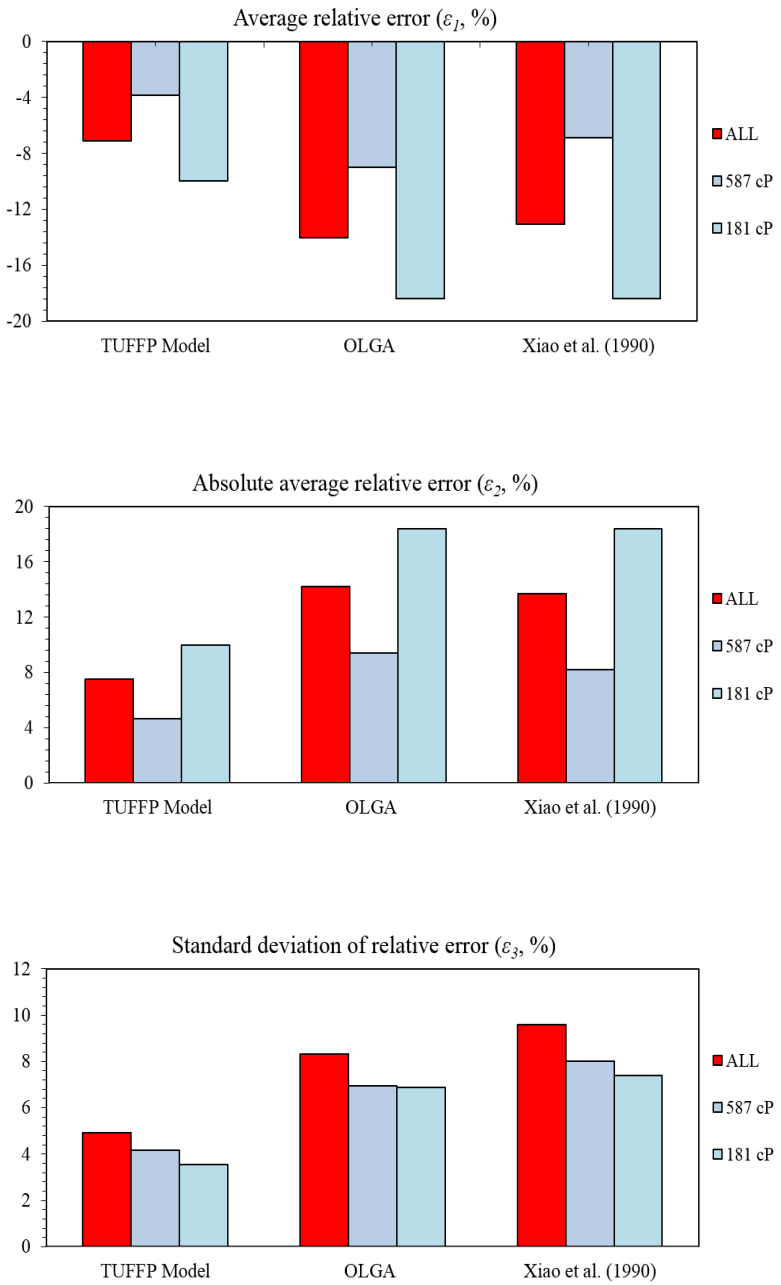

Figure 5.9 Model evaluation using the pressure gradient experimental data reported by Gokcal (2008) from 2-in. ID pipes.

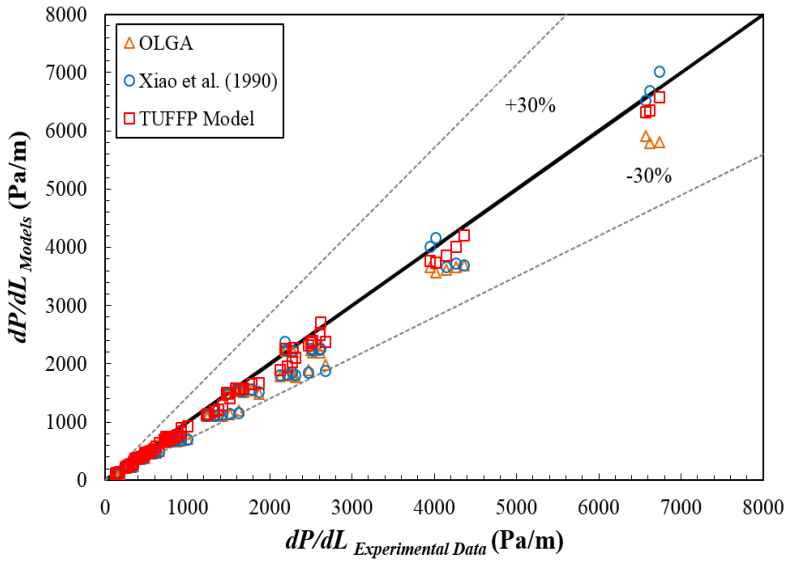

Figure 5.10 Comparison between TUFFP, OLGA, and Xiao *et al.* (1990) model prediction and Gokcal's (2008) measured pressure gradients for 'all' oil viscosities when the pipe diameter is 2-in.

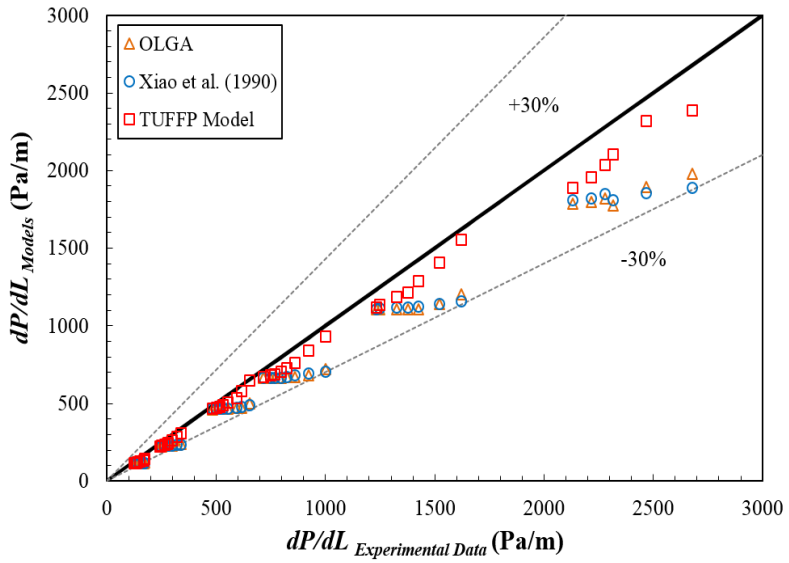

Figure 5.11 Comparison between TUFFP, OLGA, and Xiao *et al.* (1990) model prediction and Gokcal's (2008) measured pressure gradients for μ_{Oil} = 181 cP when the pipe diameter is 2-in.

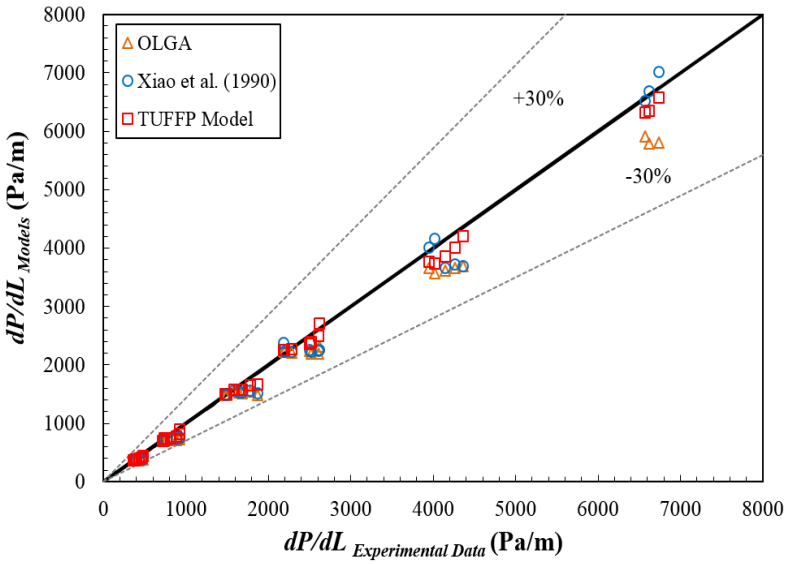

Figure 5.12 Comparison between TUFFP, OLGA, and Xiao *et al*. (1990) model prediction and Gokcal's (2008) measured pressure gradients for μ_{Oil} = 587 cP when the pipe diameter is 2-in.

5.2.3 Combined data of 2- and 3-in. ID pipes

Figures 5.15 to 5.17 show the comparison of TUFFP Unified, OLGA, and Xiao *et al*. (1990) models against the measured pressure gradient data obtained from both 2- and 3-in. ID pipes. The results of the error analysis are shown in Figures 5.13 and 5.14.

As previously stated, all of the models under-estimate for entire data sets. Because all of the models calculate the pressure gradient using a force balance over a slug unit, the used variables for this term need to be reinvestigated for more accurate prediction of the pressure gradient.

Nevertheless, TUFFP Unified model gives the best pressure gradient prediction for the considered pipe diameter (2- and 3-in.) and oil viscosity range.

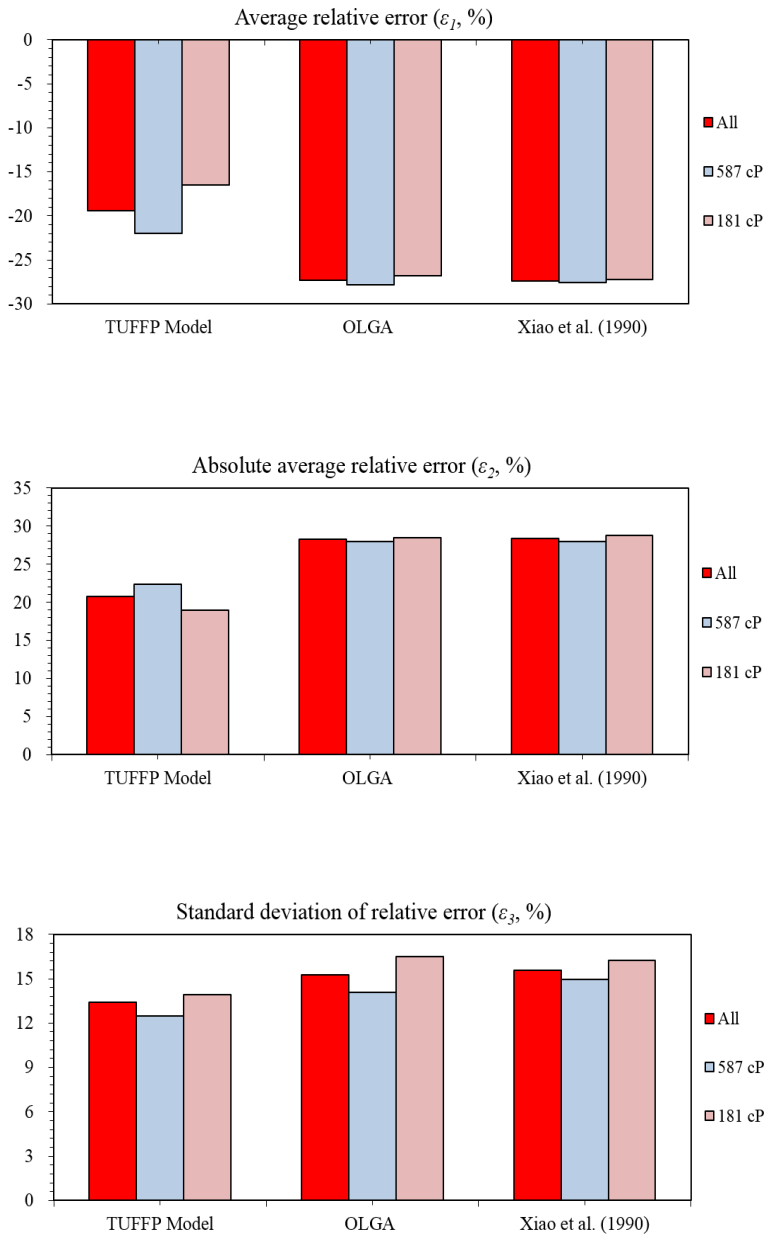

Figure 5.13 Model evaluation using the pressure gradient experimental data acquired from both 2- and 3-in. ID pipes.

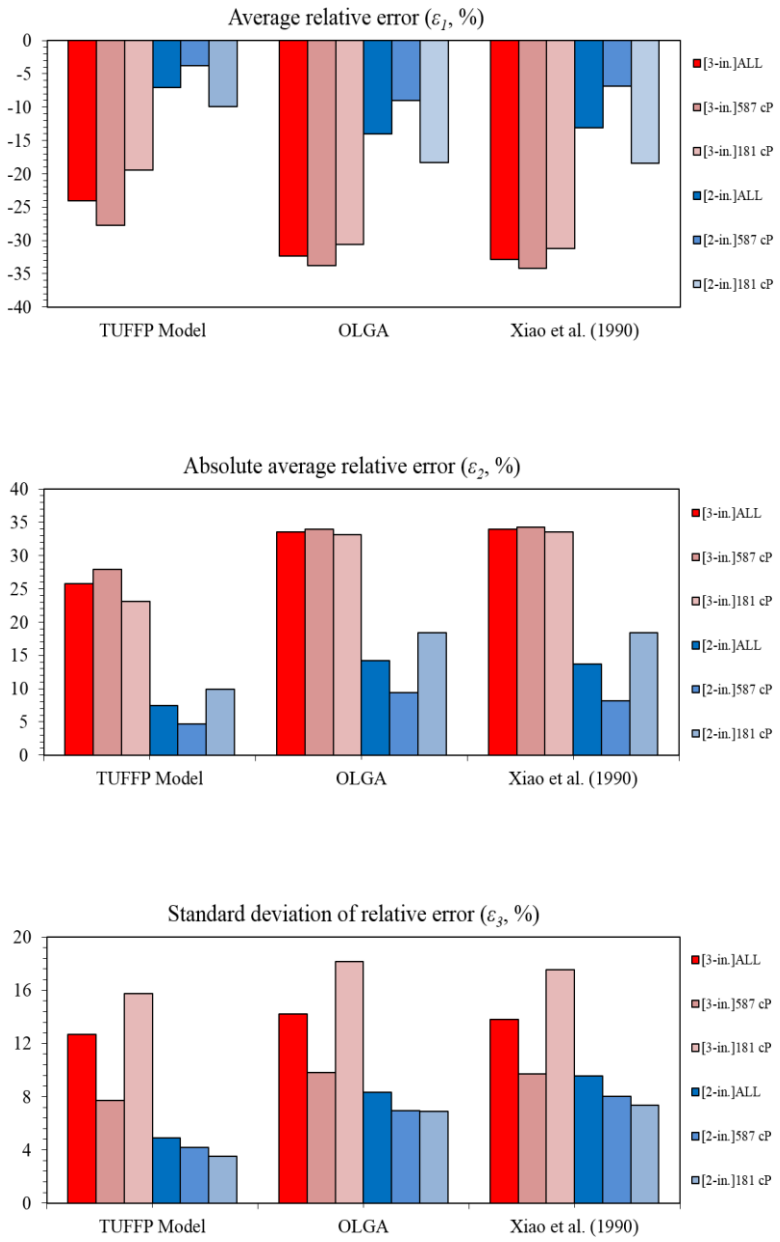

Figure 5.14 Model evaluation using the pressure gradient experimental data acquired from 2- and 3-in. ID pipes, respectively.

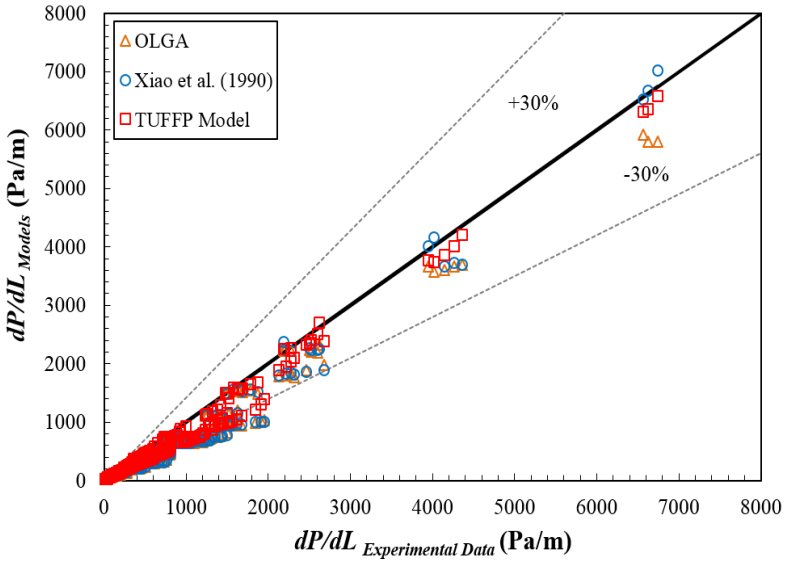

Figure 5.15 Comparison between TUFFP, OLGA, and Xiao *et al*. (1990) model prediction and measured pressure gradients for 'all' oil viscosities acquired from both 2- and 3-in. ID pipes.

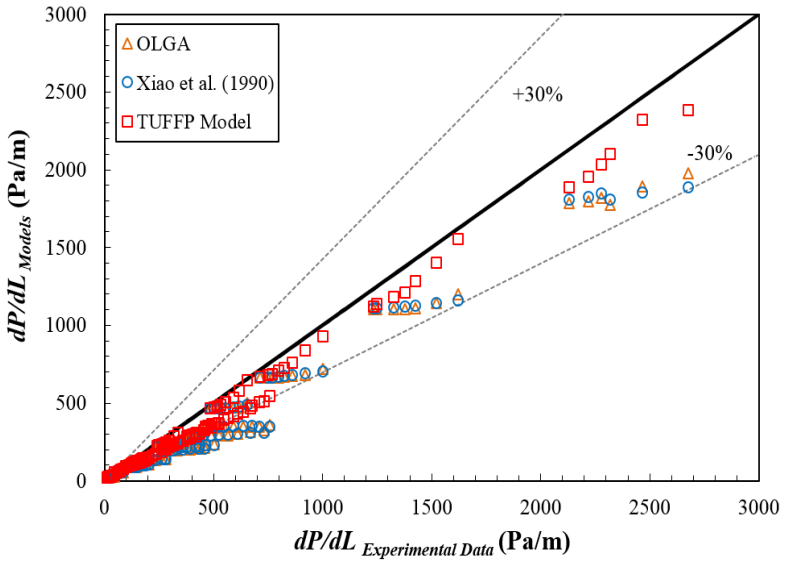

Figure 5.16 Comparison between TUFFP, OLGA, and Xiao *et al*. (1990) model prediction and measured pressure gradients for μ_{Oil} = 181 cP acquired from both 2- and 3-in. ID pipes.

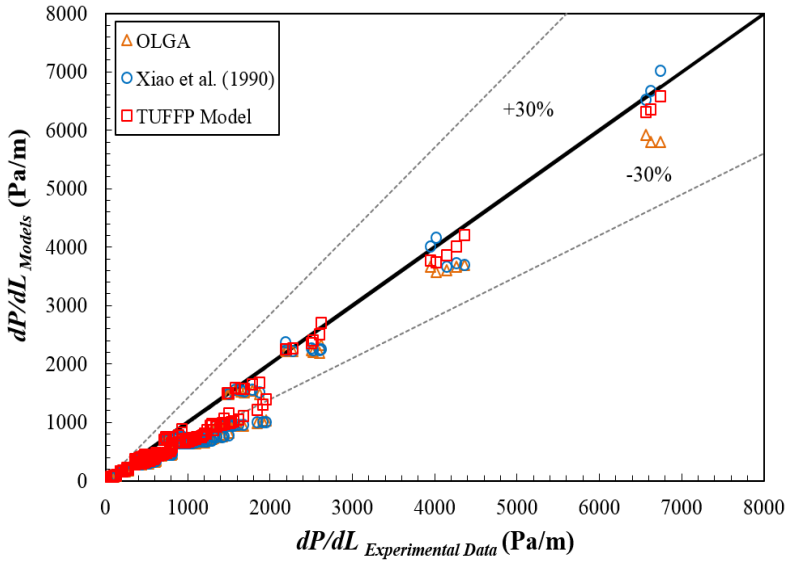

Figure 5.17 Comparison between TUFFP, OLGA, and Xiao *et al*. (1990) model prediction and measured pressure gradients for μ_{Oil} = 587 cP acquired from both 2- and 3-in. ID pipes.

5.3 Average liquid holdup

Next sections present the model comparison for 2- and 3-in. experimental data

5.3.1 3-in. ID pipes

Model evaluation results for the average liquid holdup are shown in Figure 5.18. Experimental results for the average liquid holdup were compared with predictions by TUFFP Unified, OLGA, and Xiao *et al*. (1990) models.

TUFFP unified model gives a positive value of $\varepsilon_{1\ (3\text{-in.})}$ for most oil viscosities (155, 181, 220, 420, and 587 cP). This means that an average liquid

holdup tends to be over-estimated for the considered oil viscosities. The degree of over-estimation decreases with oil viscosity increase. Thus, this model is more suitable to predict the average liquid holdup for higher oil viscosities with the 3-in. ID pipes. For 'all' oil viscosities, the absolute average relative error reported by TUFFP unified model is 7.5%.

OLGA and Xiao *et al*. (1990) models show a similar behavior. They over-estimate the average liquid holdup for 'all' oil viscosities except 300 cP. OLGA and Xiao *et al*. (1990) model show the average relative errors for all data by 6.9% and 1.8%, respectively.

Figures 5.19 through 5.25 are graphical representations of the measured average liquid holdup against the calculated average liquid holdup by the existing models. The absolute average relative errors of all models slightly increase as oil viscosity decreases. Among the three models, TUFFP Unified model presents the lowest absolute average relative errors, $\varepsilon_{2\ (3\text{-in.})}$, for all viscosities.

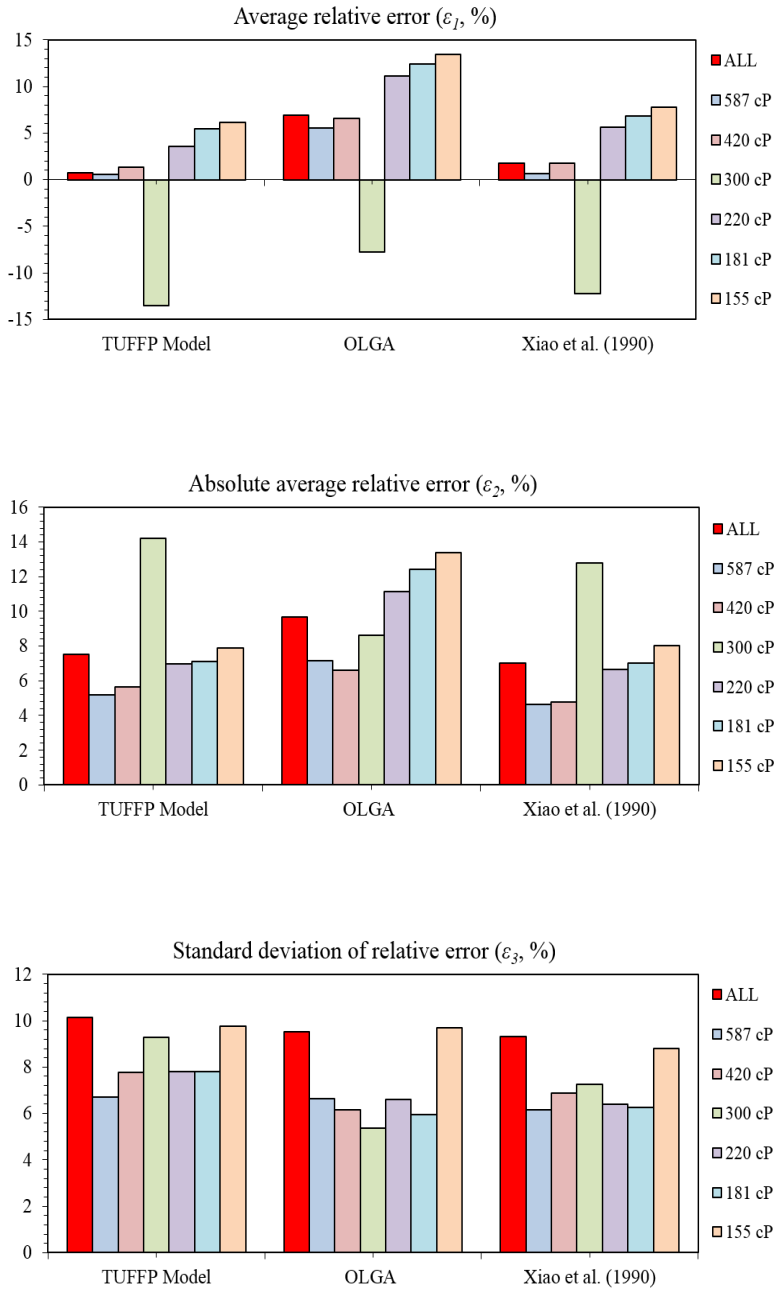

Figure 5.18 Model evaluation using the average liquid holdup experimental data from 3-in. ID pipes.

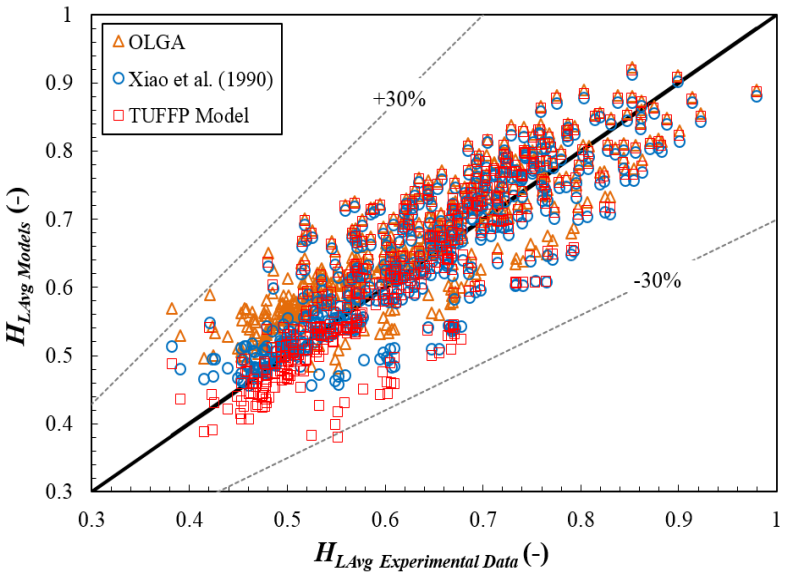

Figure 5.19 Comparison between TUFFP, OLGA, and Xiao *et al*. (1990) model prediction and measured average liquid holdups for 'all' oil viscosities when the pipe diameter is 3-in.

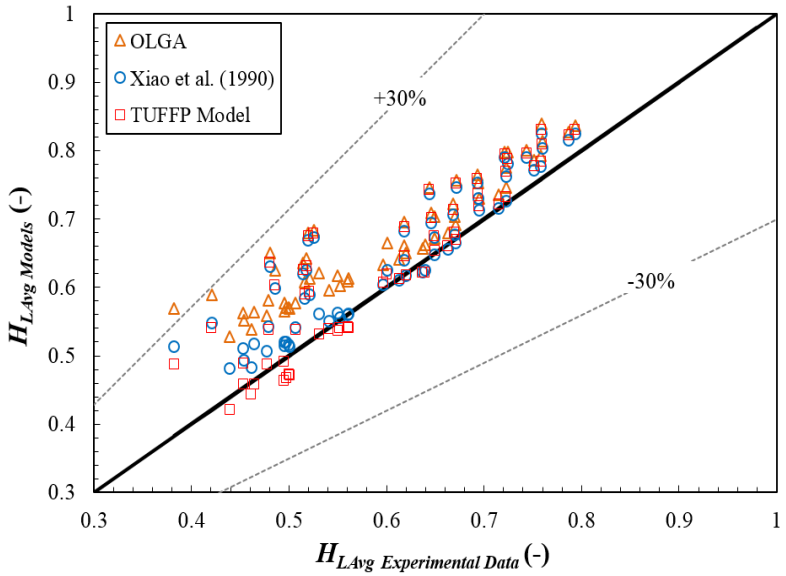

Figure 5.20 Comparison between TUFFP, OLGA, and Xiao *et al*. (1990) model prediction and measured average liquid holdups for μ_{Oil} = 155 cP when the pipe diameter is 3-in.

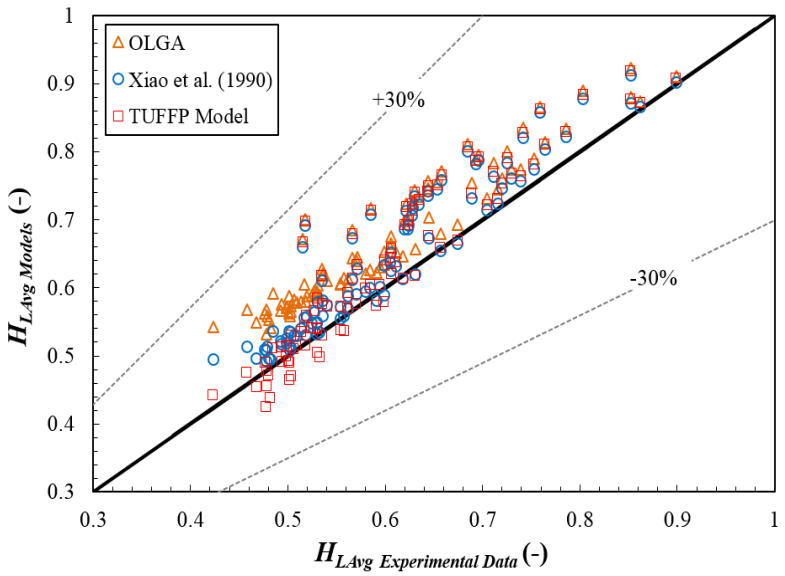

Figure 5.21 Comparison between TUFFP, OLGA, and Xiao *et al*. (1990) model prediction and measured average liquid holdups for μ_{Oil} = 181 cP when the pipe diameter is 3-in.

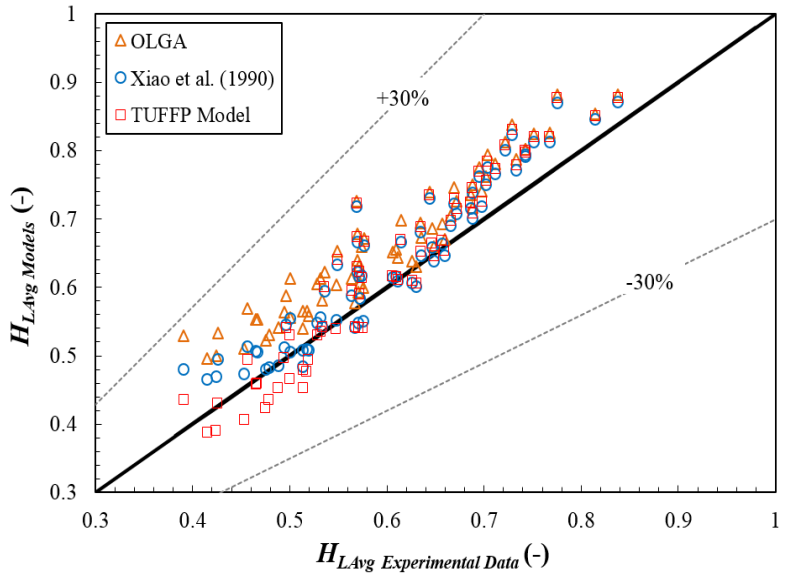

Figure 5.22 Comparison between TUFFP, OLGA, and Xiao *et al*. (1990) model prediction and measured average liquid holdups for μ_{Oil} = 220 cP when the pipe diameter is 3-in.

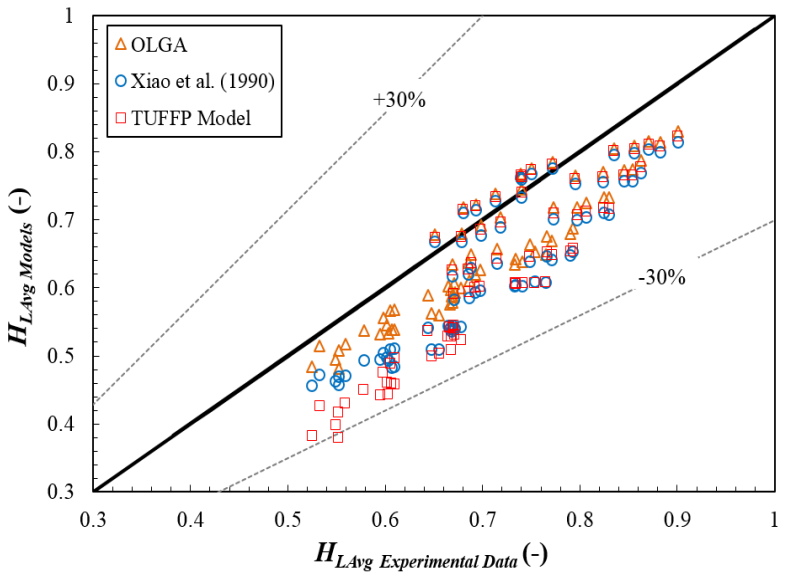

Figure 5.23 Comparison between TUFFP, OLGA, and Xiao *et al*. (1990) model prediction and measured average liquid holdups for μ_{Oil} = 300 cP when the pipe diameter is 3-in.

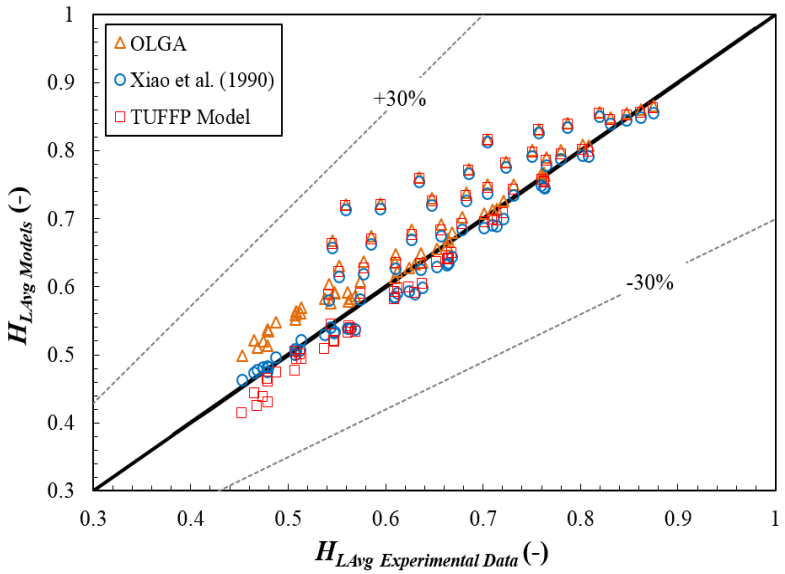

Figure 5.24 Comparison between TUFFP, OLGA, and Xiao *et al*. (1990) model prediction and measured average liquid holdups for μ_{Oil} = 420 cP when the pipe diameter is 3-in.

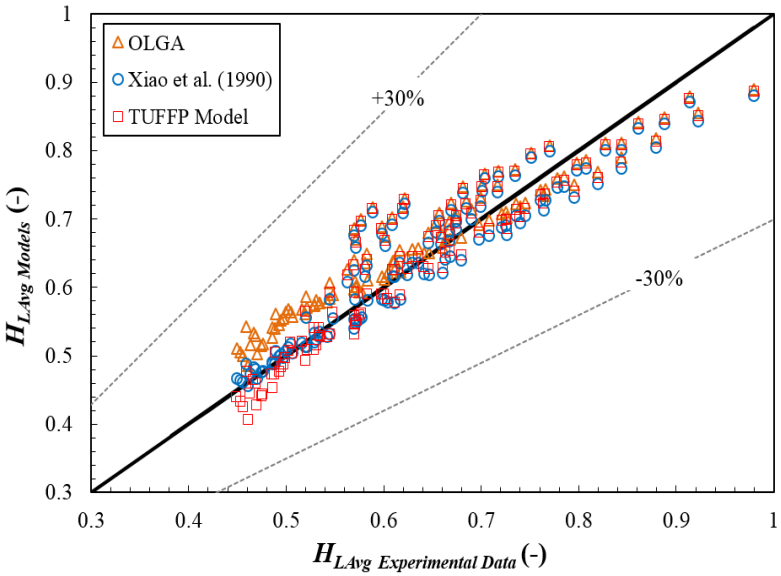

Figure 5.25 Comparison between TUFFP, OLGA, and Xiao *et al*. (1990) model prediction and measured average liquid holdups for μ_{Oil} = 587 cP when the pipe diameter is 3-in.

5.3.2 2-in. ID pipes

The model evaluation results are shown in Figure 5.26 for TUFFP Unified, OLGA, and Xiao *et al*. (1990) mechanistic models. In Figures 5.27 to 5.29, these three models are compared with Gokcal's (2008) experimental data acquired from 2-in. ID pipes.

TUFFP Unified model produces positive values of $\varepsilon_{1\ (2\text{-in.})}$ (7.4%) and $\varepsilon_{4\ (2\text{-in.})}$ (0.05) for 'all' oil viscosities, indicating over-estimation of the average liquid holdup. The degree of over-estimation slightly increases with increasing oil viscosity.

When the dataset was compared against OLGA model, the average

relative and actual errors are 11% and 0.07, respectively. Similar with TUFFP Unified model, the degree of over-estimation increases as oil viscosity increases.

By Xiao *et al*. (1990) mechanistic model, the average relative and actual errors are 5.5% and 0.03 for 'all' oil viscosities, showing that this model gives the lowest average relative error. The absolute average relative error of this model is 9.7%.

In summary, TUFFP Unified and Xiao *et al*. (1990) models give proper predictions for the average liquid holdup when the pipe diameter is 2-in. The details of the error analysis are provided in Appendix F.

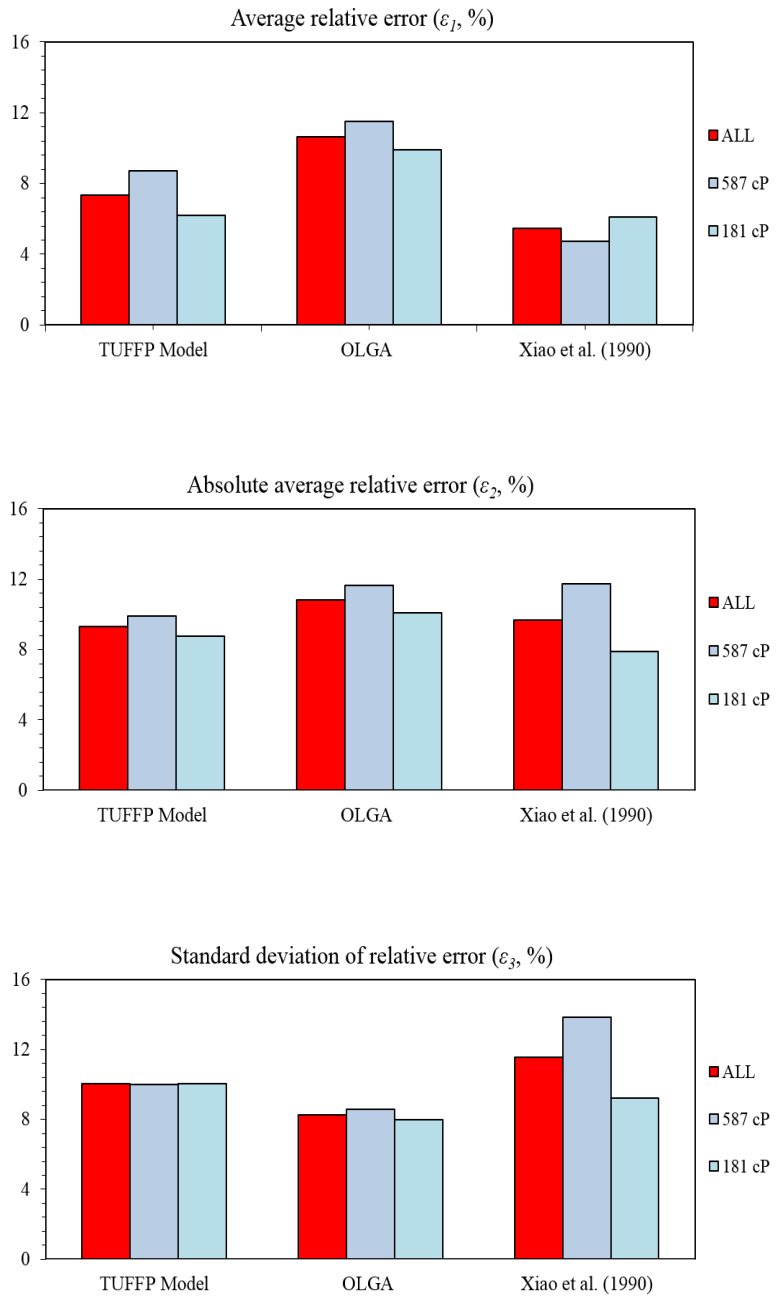

Figure 5.26 Model evaluation using the average liquid holdup experimental data reported by Gokcal (2008) from 2-in. ID pipes.

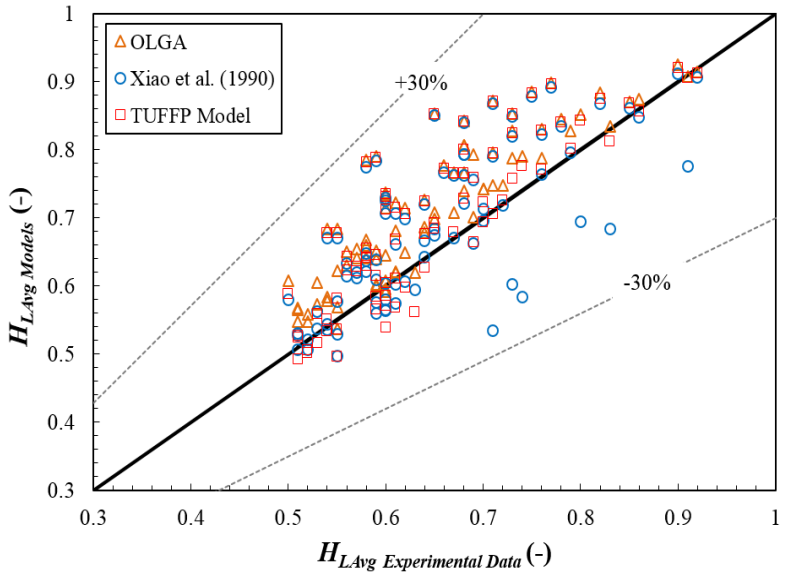

Figure 5.27 Comparison between TUFFP, OLGA, and Xiao *et al*. (1990) model prediction and Gokcal's (2008) measured average liquid holdups for 'all' oil viscosities when the pipe diameter is 2-in.

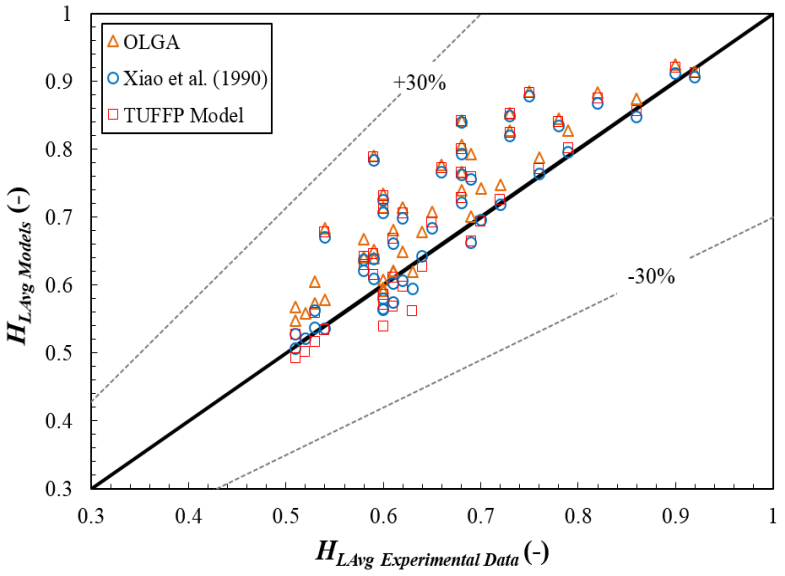

Figure 5.28 Comparison between TUFFP, OLGA, and Xiao *et al*. (1990) model prediction and Gokcal's (2008) measured average liquid holdups for μ_{Oil} = 181 cP when the pipe diameter is 2-in.

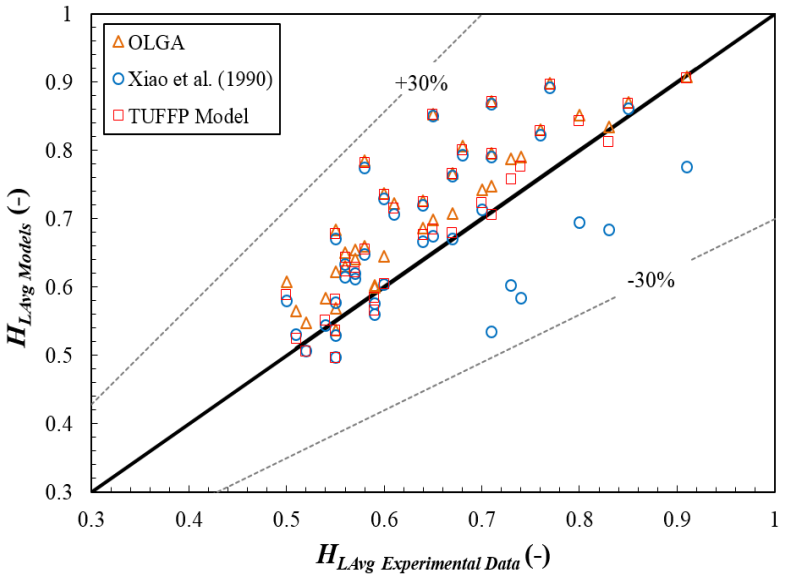

Figure 5.29 Comparison between TUFFP, OLGA, and Xiao *et al*. (1990) model prediction and Gokcal's (2008) measured average liquid holdups for μ_{Oil} = 587 cP when the pipe diameter is 2-in.

5.3.3 Combined data of 2- and 3-in. ID pipes

Figures 5.32 to 5.34 show the comparison of TUFFP Unified, OLGA, and Xiao *et al*. (1990) models versus the measured average liquid holdup data obtained from both 2- and 3-in. ID pipes. The results of the error analysis are shown in Figures 5.30 and 5.31. The details of the error analysis are provided in Appendix F.

As can be seen in Figure 5.30, all of the models slightly over-estimate the average liquid holdup for 'all' oil viscosities. The average relative errors, $\varepsilon_{1\ (2\text{-in. + 3-in.})}$, of TUFFP Unified, OLGA, and Xiao *et al*. (1990) models are 4.0%, 9.2%, and 4.0%, respectively. The absolute average relative errors, $\varepsilon_{2\ (2\text{-in. + 3-in.})}$, are 6.9%, 9.9%, and 6.8%, respectively. The degree of over-estimation

decreases with increasing oil viscosity, indicating that the models are suitable for predicting the average liquid holdup at relatively higher oil viscosities.

In summary, when the data of 2- and 3-in. are combined, TUFFP Unified and Xiao *et al*. (1990) models present lower absolute average relative errors and this means that these two models are proper to predict the average liquid holdup.

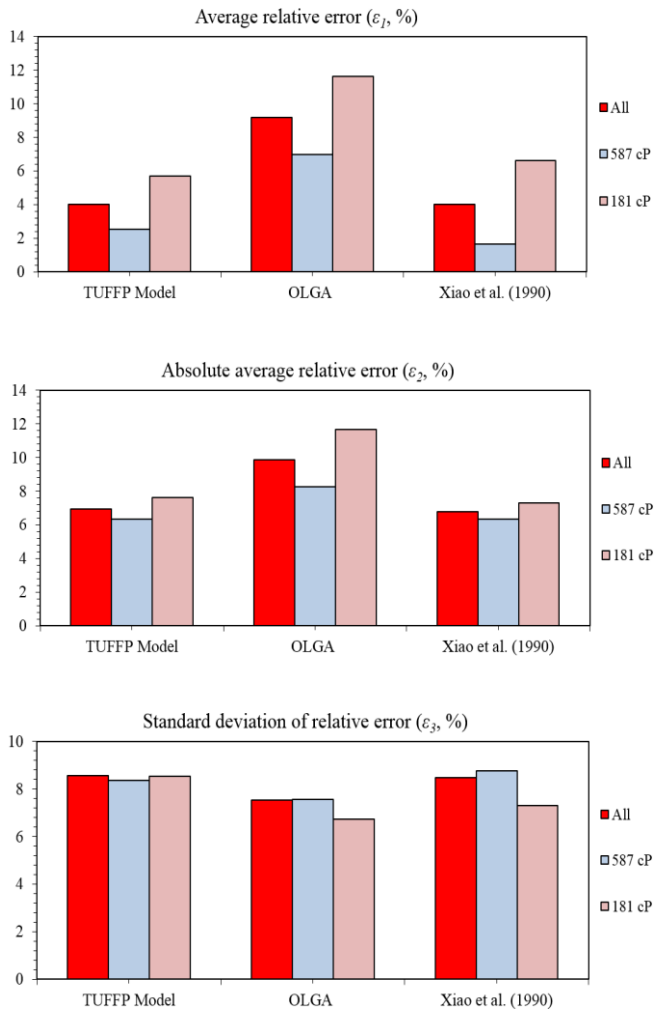

Figure 5.30 Model evaluation using the average liquid holdup experimental data acquired from both 2- and 3-in. ID pipes.

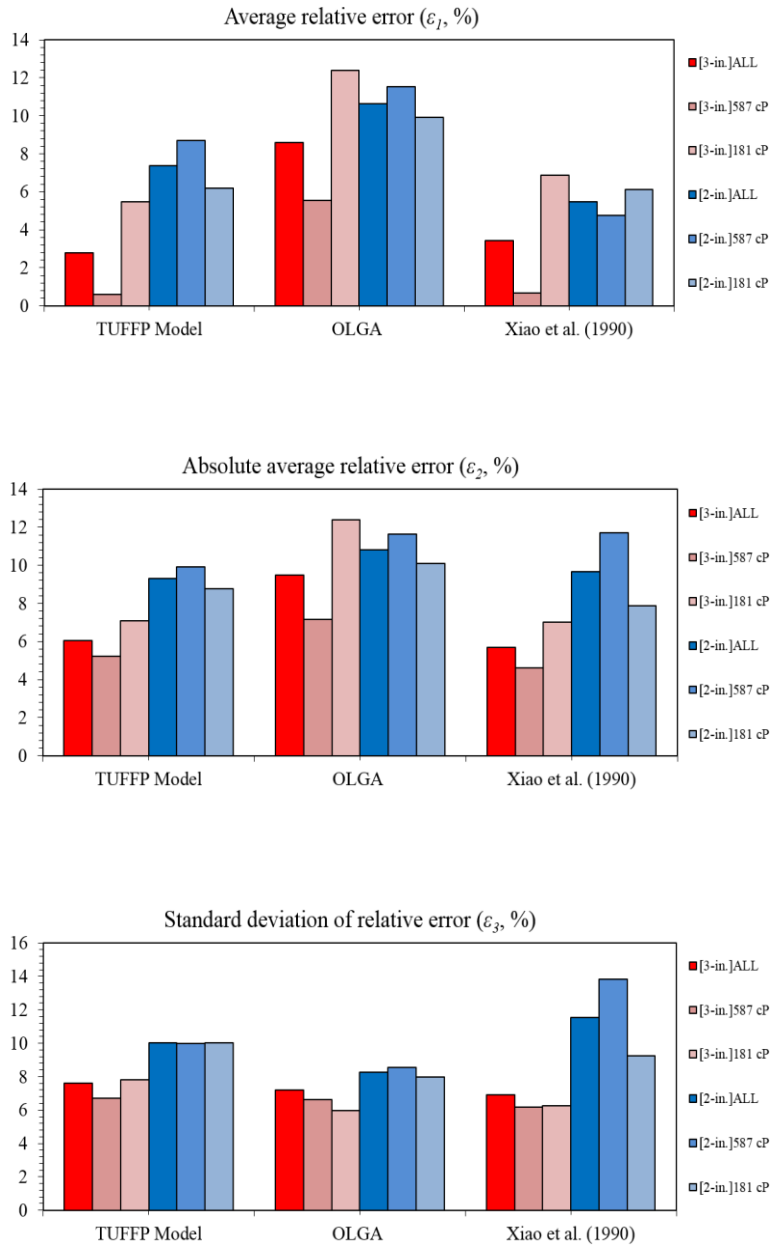

Figure 5.31 Model evaluation using the average liquid holdup experimental data acquired from 2- and 3-in. ID pipes, respectively.

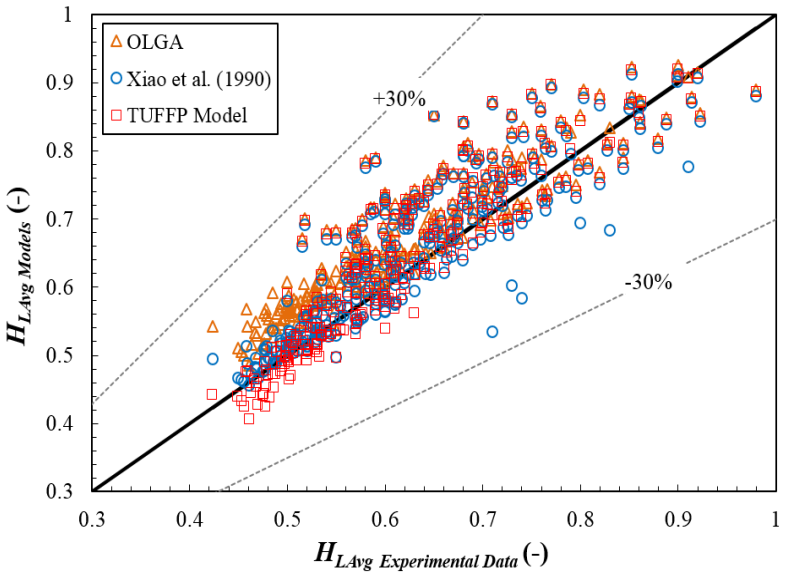

Figure 5.32 Comparison between TUFFP, OLGA, and Xiao *et al*. (1990) model prediction and measured average liquid holdups for 'all' oil viscosities acquired from both 2- and 3-in. ID pipes.

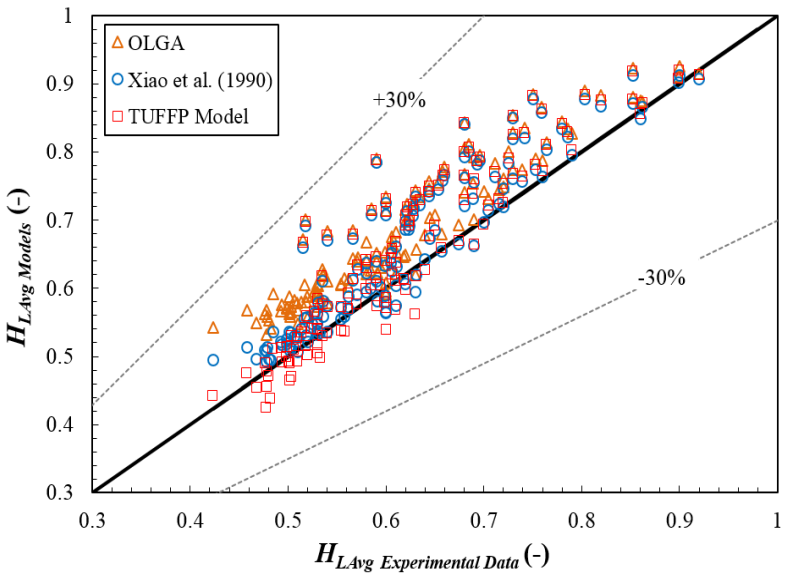

Figure 5.33 Comparison between TUFFP, OLGA, and Xiao *et al*. (1990) model prediction and measured average liquid holdups for μ_{Oil} = 181 cP acquired from both 2- and 3-in. ID pipes.

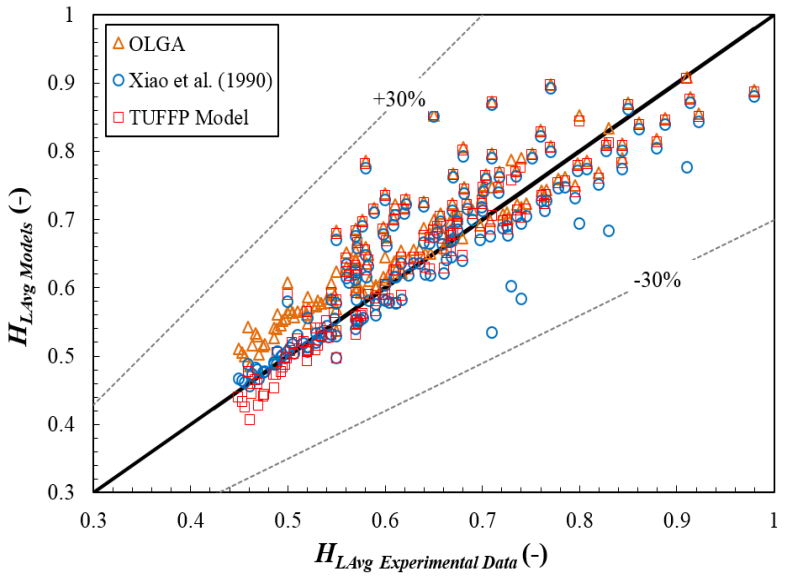

Figure 5.34 Comparison between TUFFP, OLGA, and Xiao *et al*. (1990) model prediction and measured average liquid holdups for μ_{Oil} = 587 cP acquired from both 2- and 3-in. ID pipes.

5.4 Slug flow characterizations

Comparison between acquired experimental data and available models and correlations for slug characterizations is presented in the next sections.

5.4.1 Slug liquid holdup

Comparison with model and correlations for slug liquid holdup is presented below.

5.4.1.1 3-in. ID pipes

The performance of available slug liquid holdup models and correlations are reviewed. The model evaluation results for slug liquid holdup are shown in Figure 5.35. Models and correlations reported by Gregory *et al*. (1978), Gomez *et al*. (2000), Barnea & Brauner (1985), Andreussi & Bendiksen (1989), Abdul-Majeed (2000), Kora (2010), Felizola (1992), and TUFFP Unified models are considered. Figures 5.36 to 5.42 show the comparison of these models against the measured slug liquid holdup experimental data.

Among compared models and correlations, Gregory *et al*. (2.9%), Kora (3.2%), and TUFFP Unified (3.8%) models have lower absolute average relative errors for 'all' oil viscosities. Figure 5.43 shows the predictions of these three models against the measured slug liquid holdup for all experimental data sets. Gregory *et al*. (1978) and TUFFP Unified models slightly under-predict the slug liquid holdup for 'all' oil viscosities, showing the negative $\varepsilon_{1\ (3\text{-in.})}$ values of -1.0% and -0.8%, respectively. Kora's (2010) correlation shows an average relative error value of 2.6%. Although the average relative error of this model increases when oil viscosity decreases, in general, reasonable predictions are reported for all the range of oil viscosities. This is in agreement with Brito's (2012) experimental results. These three models (Gregory *et al*. (1978), Kora (2010), and TUFFP Unified) show the best agreement with the experimental results.

Although Barnea & Brauner (1985) model gives the lowest average relative error value of 0.3%, this model shows a slightly higher absolute average relative error of 5.8%. Among the existing models, Gomez *et al*. (2000) and

Abdul-Majeed (2000) models show almost constant values for the slug liquid holdup due to the consideration of the liquid viscosity. The error values calculated for the different models are shown in Figure 5.35. The details of the error analysis are presented in Appendix F.

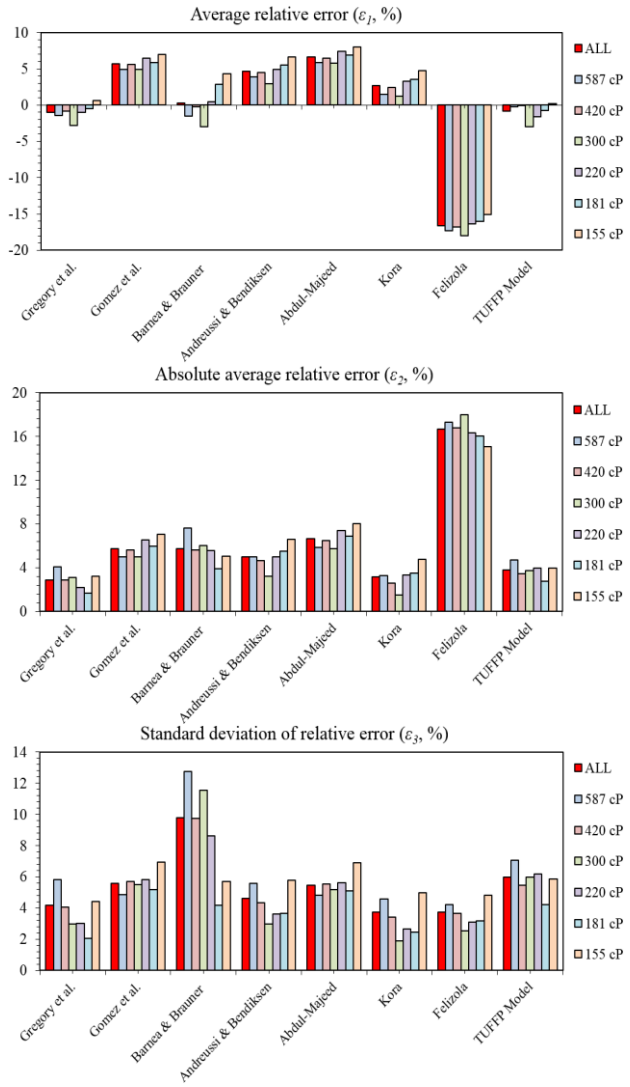

Figure 5.35 Model evaluation using the slug liquid holdup experimental data acquired from 3-in. ID pipes.

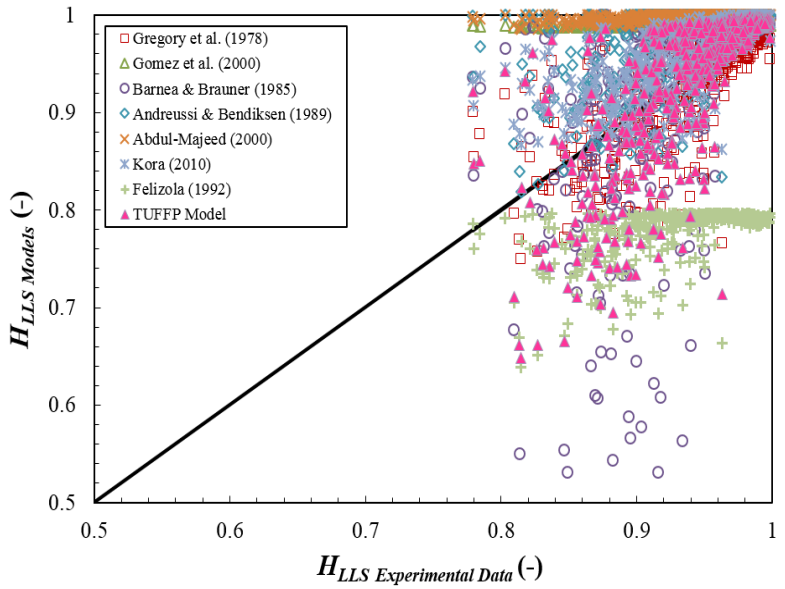

Figure 5.36 Comparison of model predictions against the measured slug liquid holdup for 'all' oil viscosities when the pipe diameter is 3-in.

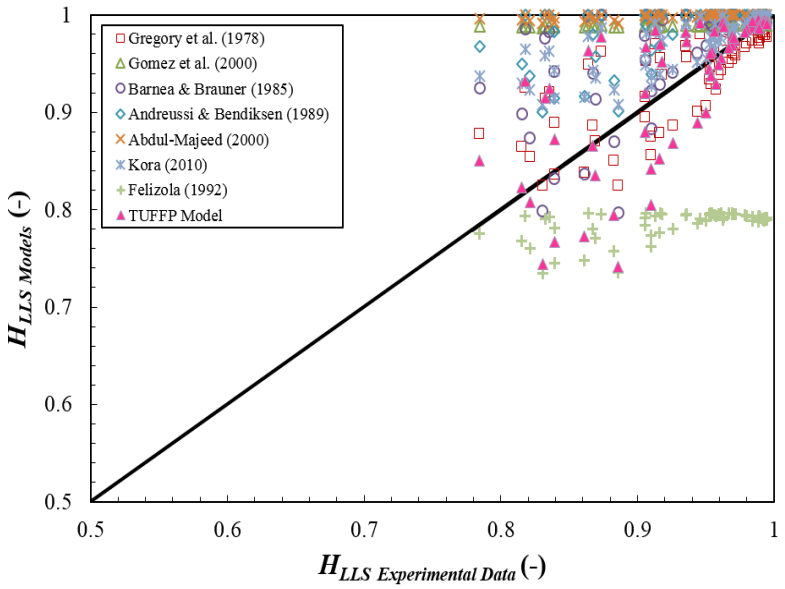

Figure 5.37 Comparison of model predictions against the measured slug liquid holdup for μ_{Oil} = 155 cP when the pipe diameter is 3-in.

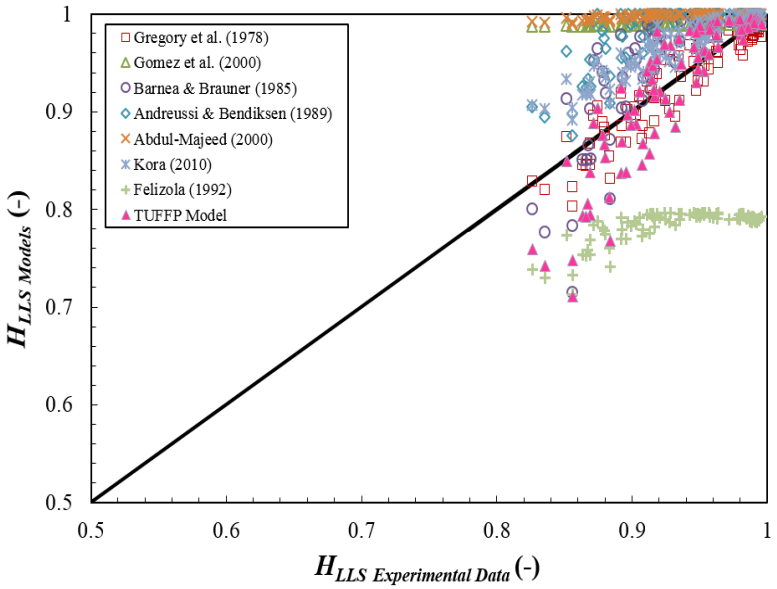

Figure 5.38 Comparison of model predictions against the measured slug liquid holdup for μ_{Oil} = 181 cP when the pipe diameter is 3-in.

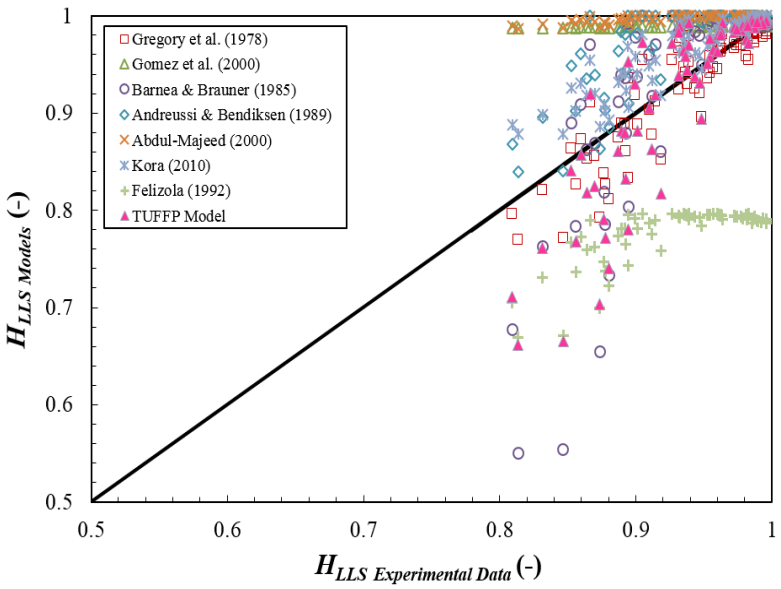

Figure 5.39 Comparison of model predictions against the measured slug liquid holdup for μ_{Oil} = 220 cP when the pipe diameter is 3-in.

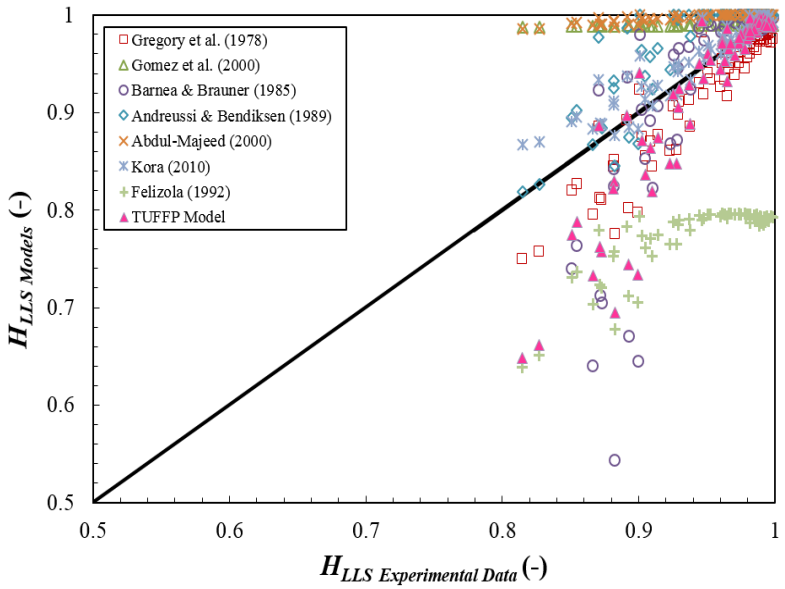

Figure 5.40 Comparison of model predictions against the measured slug liquid holdup for μ_{Oil} = 300 cP when the pipe diameter is 3-in.

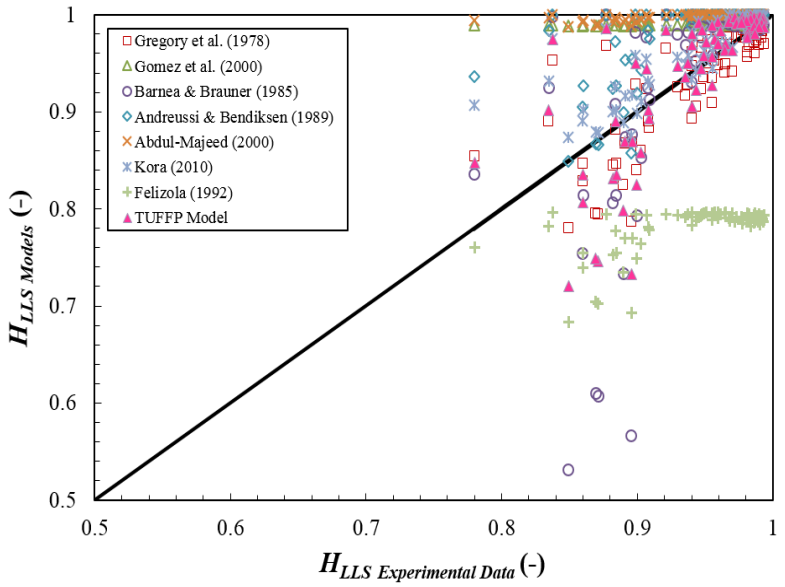

Figure 5.41 Comparison of model predictions against the measured slug liquid holdup for μ_{Oil} = 420 cP when the pipe diameter is 3-in.

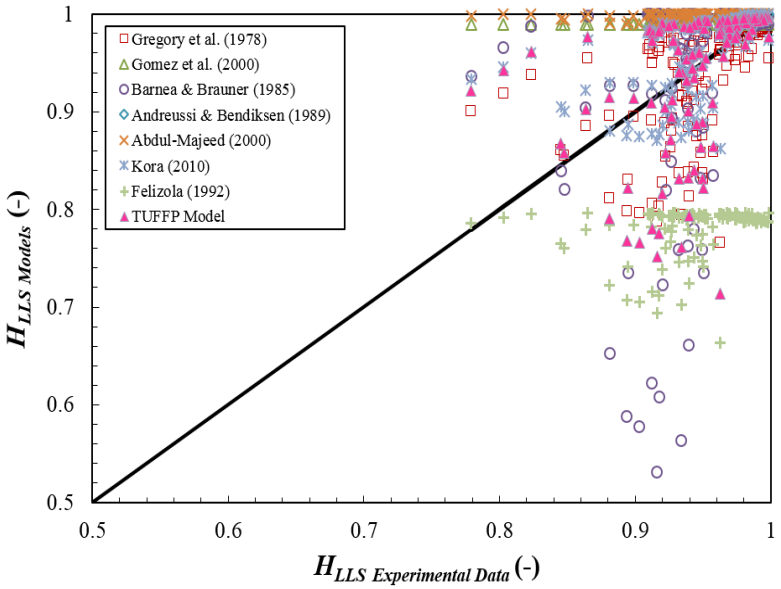

Figure 5.42 Comparison of model predictions against the measured slug liquid holdup for μ_{Oil} = 587 cP when the pipe diameter is 3-in.

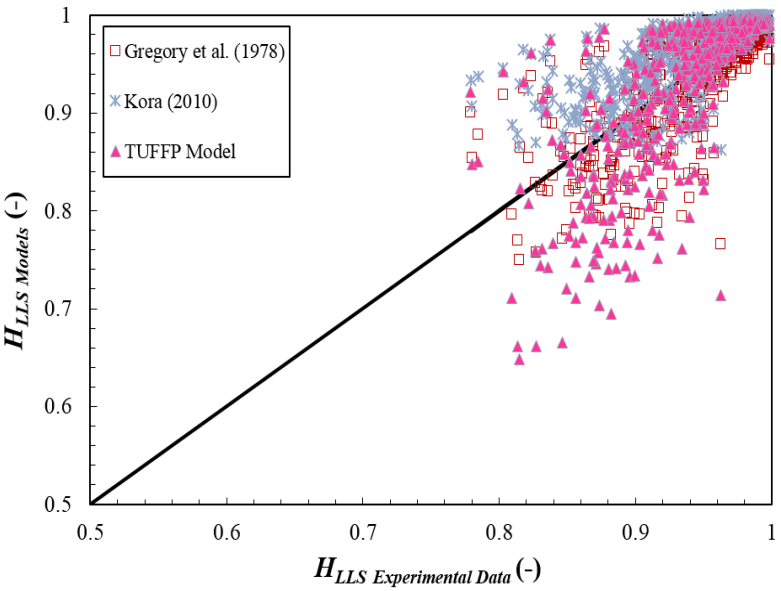

Figure 5.43 Comparison of the best three model predictions against the measured slug liquid holdup for 'all' oil viscosities when the pipe diameter is 3-in.

5.4.1.2 2-in. ID pipes

Same as the 3-in. ID pipes case, models and correlations reported by Gregory *et al*. (1978), Gomez *et al.* (2000), Barnea & Brauner (1985), Andreussi & Bendiksen (1989), Abdul-Majeed (2000), Kora (2010), Felizola (1992), and TUFFP Unified models are compared with Kora's (2010) experimental data for the slug liquid holdup. The model evaluation results for the slug liquid holdup are presented in Figure 5.44. The measured slug liquid holdup against to model predictions are shown in Figures 5.45 to 5.47.

Andreussi & Bendiksen (2.0%), Kora (0.8%), and TUFFP Unified (5.1%) models present lower absolute average relative error. Kora (2010) and TUFFP Unified models slightly under-predict the slug liquid holdup value for 'all' oil viscosities, showing the negative $\varepsilon_{1\ (2\text{-}in.)}$ values of -0.6% and -4.3%, respectively. On the other hands, Andreussi & Bendiksen (1989) model over-predicts the slug liquid holdup for 'all' oil viscosities, presenting a positive $\varepsilon_{1\ (2\text{-}in.)}$ value of 0.8%. Similar with these three models, Gregory *et al*. (1978) model also produces a suitable prediction for the slug liquid holdup, showing the average relative error ($\varepsilon_{1\ (2\text{-}in.)}$) and the absolute average relative error ($\varepsilon_{2\ (2\text{-}in.)}$) values of -3.7% and 3.7%, respectively. The details of the error analysis are tabled in Appendix F.

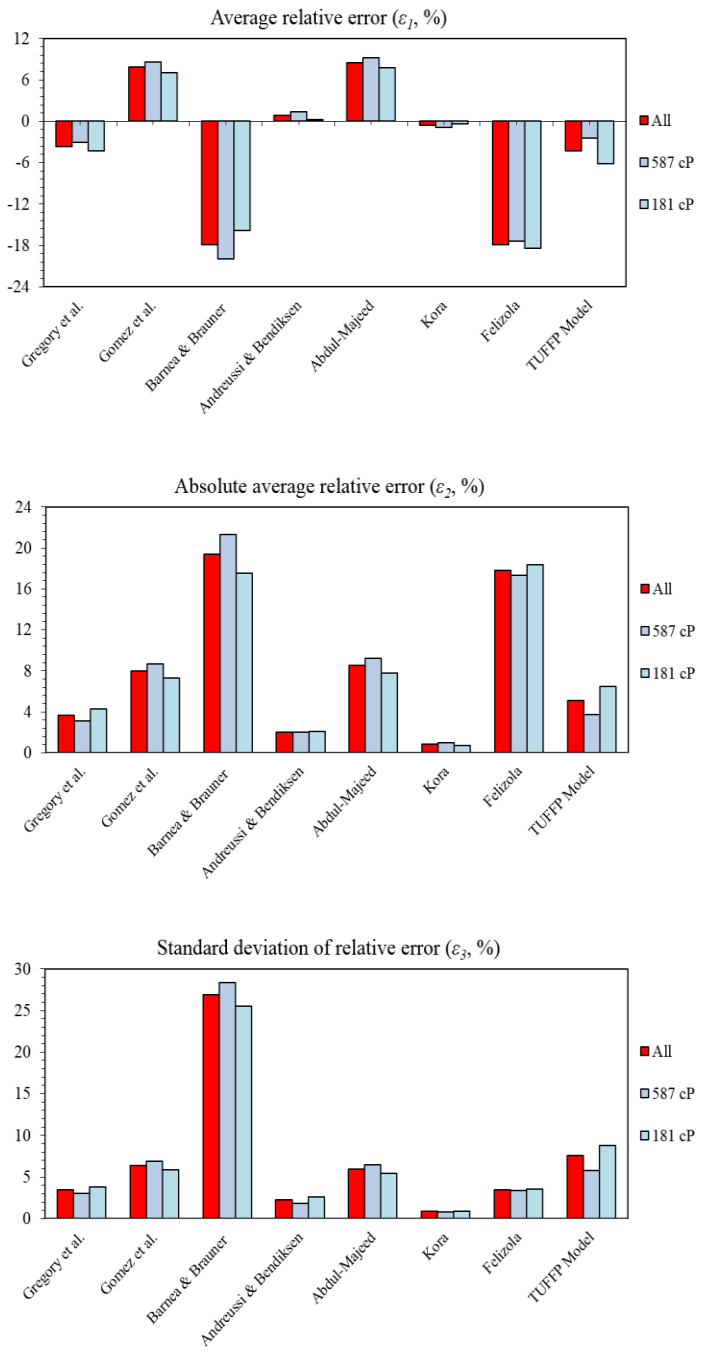

Figure 5.44 Model evaluation using the slug liquid holdup experimental data reported by Kora (2010) from 2-in. ID pipes.

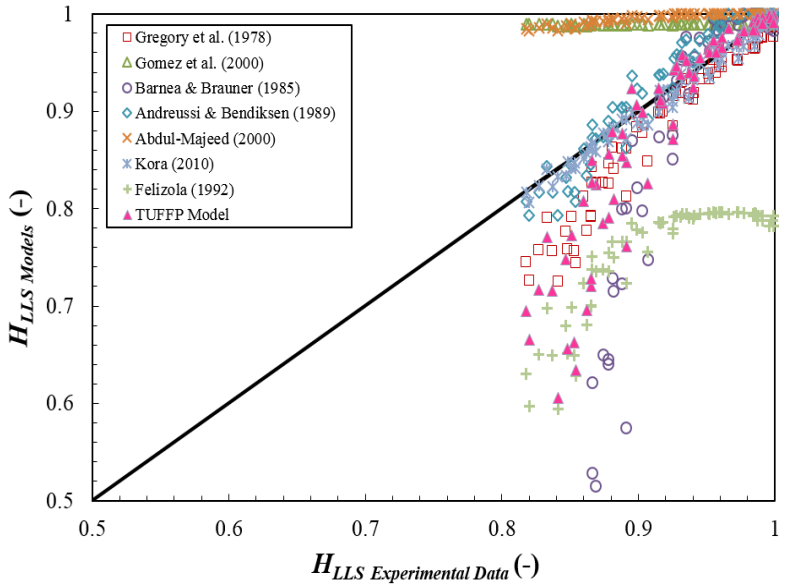

Figure 5.45 Comparison of model predictions against the Kora's (2010) measured slug liquid holdup for 'all' oil viscosities when the pipe diameter is 2-in.

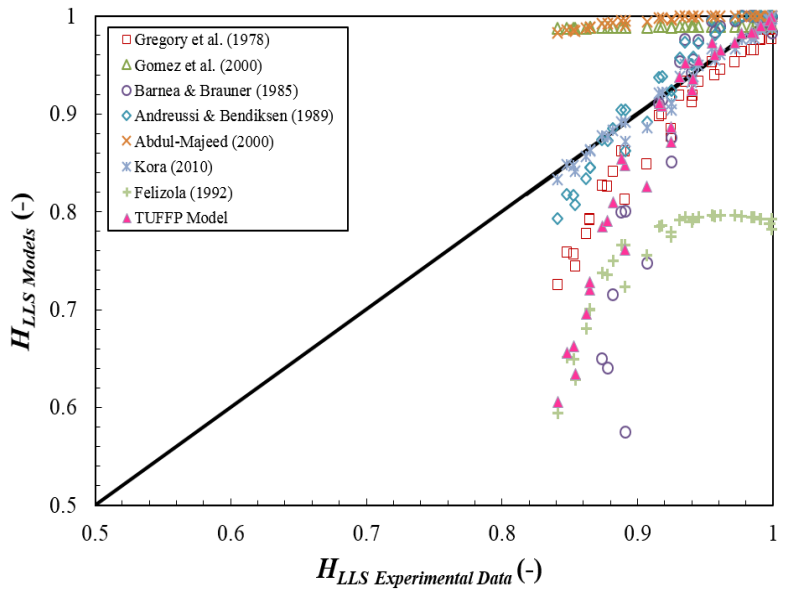

Figure 5.46 Comparison of model predictions against the Kora's (2010) measured slug liquid holdup for μ_{Oil} = 181 cP when the pipe diameter is 2-in.

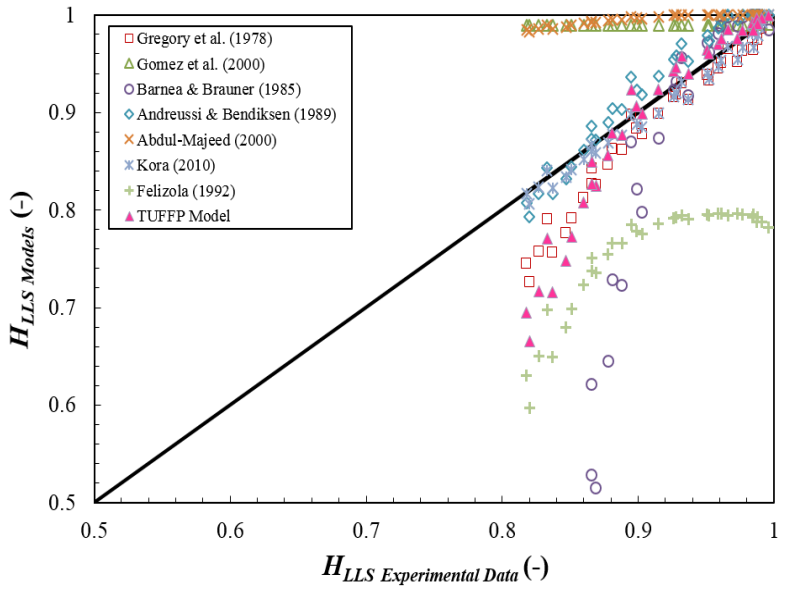

Figure 5.47 Comparison of model predictions against the Kora's (2010) measured slug liquid holdup for μ_{Oil} = 587 cP when the pipe diameter is 2-in.

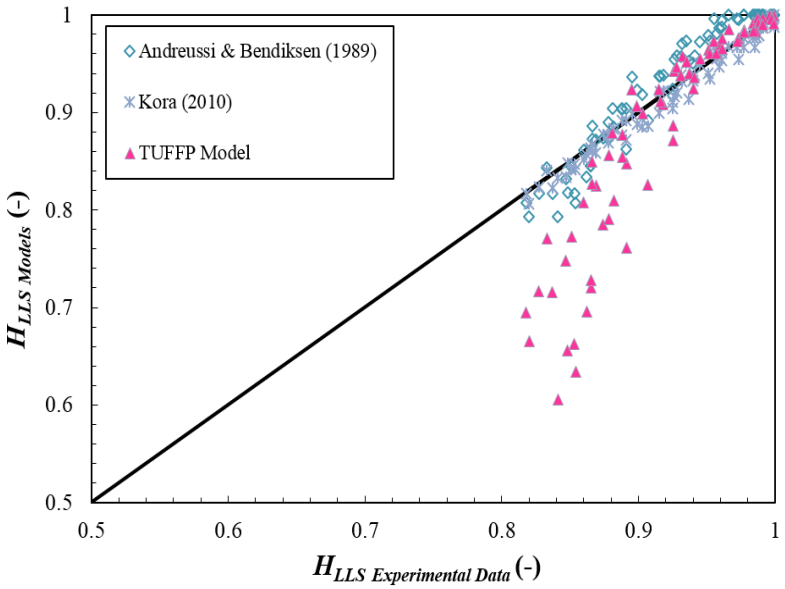

Figure 5.48 Comparison of the best three model predictions against the Kora's (2010) measured slug liquid holdup for 'all' oil viscosities when the pipe diameter is 2-in.

5.4.1.3 Combined data of 2- and 3-in. ID pipes

Figures 5.51 to 5.53 show the comparison of the Gregory *et al*. (1978), Gomez *et al*. (2000), Barnea & Brauner (1985), Andreussi & Bendiksen (1989), Abdul-Majeed (2000), Kora (2010), Felizola (1992), and TUFFP Unified models versus the measured slug liquid holdup data obtained from both 2- and 3-in. ID pipes. The results of the error analysis are shown in Figures 5.49 and 5.50. The details of the error analysis are tabled in Appendix F.

In Figure 5.49, when the data of 2- and 3-in. are combined, Gregory *et al*. (3.2%), Kora (2.8%), and TUFFP Unified (4.2%) models show lower absolute average relative errors for 'all' oil viscosities and this result is similar with 3-in. ID pipes case. The graphical presentation of these three models prediction against the measured slug liquid holdup for all experimental data sets is shown in Figure 5.54. Among the models, Kora (2010) and Gregory *et al*. (1978) produce lower absolute average relative errors ($\varepsilon_{2\,(2\text{-in.}..+\,3\text{-in.})}$), and average relative errors ($\varepsilon_{1\,(2\text{-in.}\,+\,3\text{-in.})}$). Since Gregory *et al*. (1978) model does not consider the fluid properties, this low error demonstrates the strong correlation of the mixture velocity and the slug liquid holdup. This result is in agreement with Kora's (2010) and Brito's (2012) experimental investigation. For TUFFP Unified model, the slug liquid holdup is not properly predicted when this parameter has low value ($H_{LLS} < 0.85$) in both 2- and 3-in. ID pipes cases. TUFFP Unified model severely under-predicts the slug liquid holdup in this area ($H_{LLS} < 0.85$).

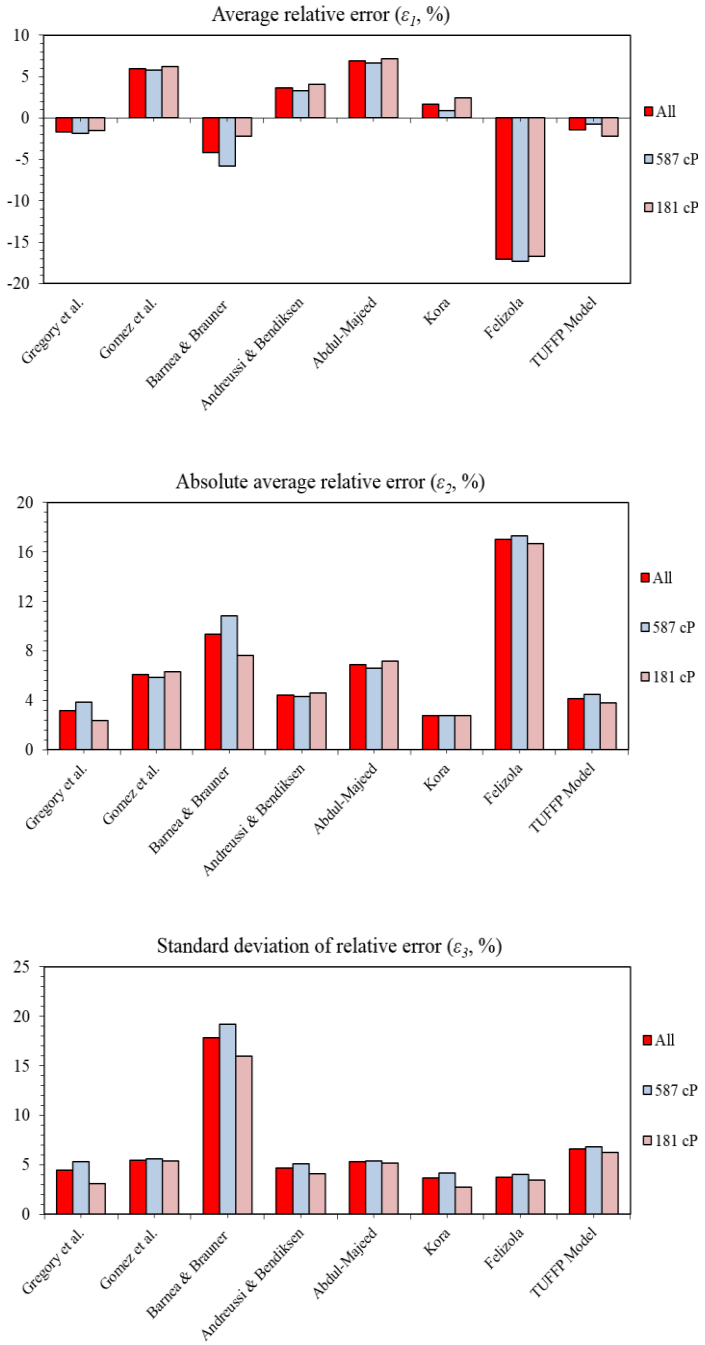

Figure 5.49 Model evaluation using the slug liquid holdup experimental data acquired from both 2- and 3-in. ID pipes.

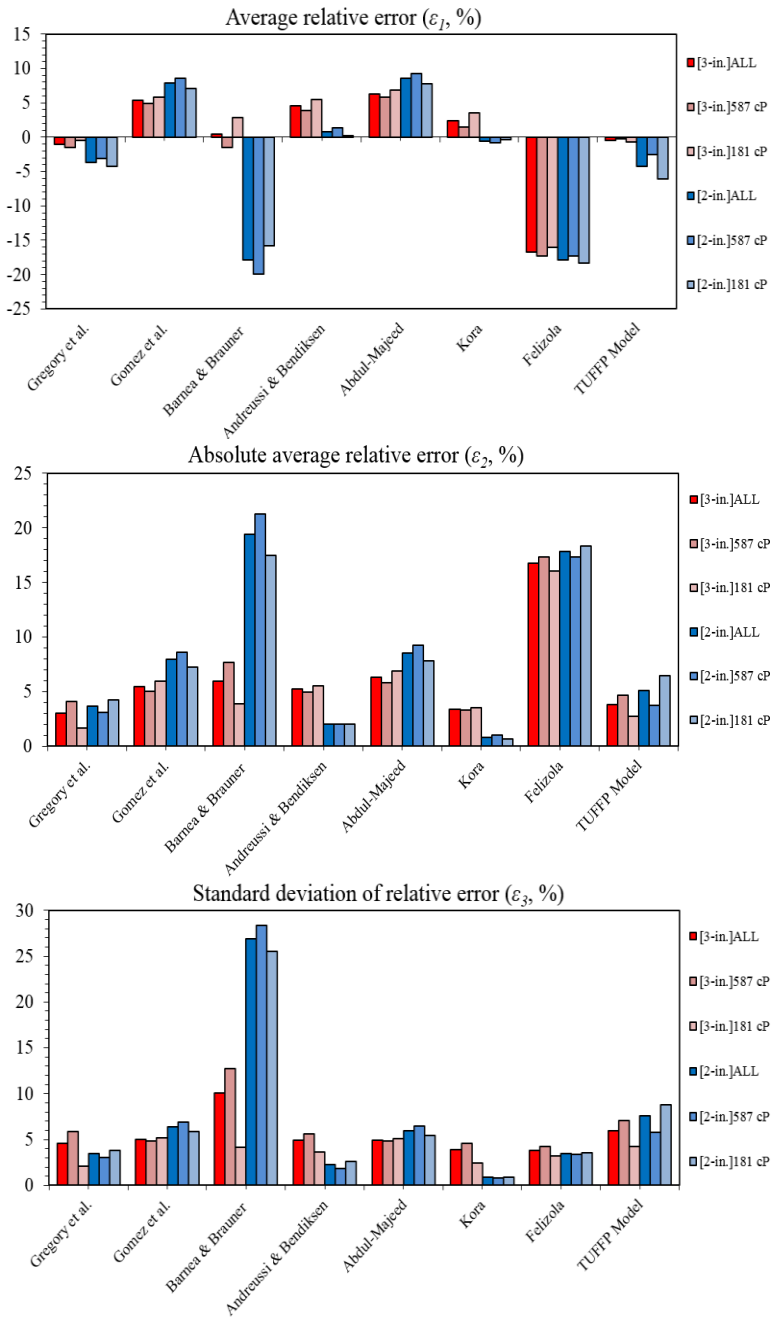

Figure 5.50 Model evaluation using the slug liquid holdup experimental data acquired from 2- and 3-in. ID pipes, respectively.

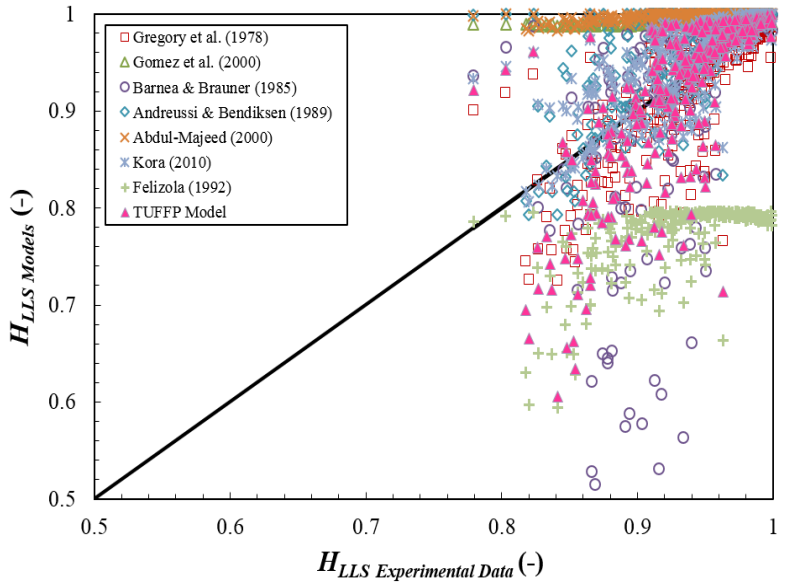

Figure 5.51 Comparison of model predictions against the measured slug liquid holdup for 'all' oil viscosities acquired from both 2- and 3-in. ID pipes.

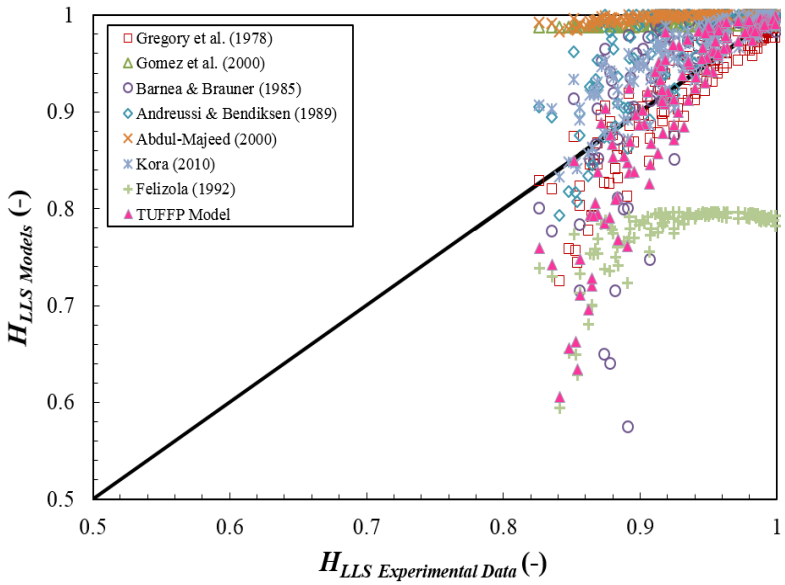

Figure 5.52 Comparison of model predictions against the measured slug liquid holdup for μ_{Oil} = 181 cP acquired from both 2- and 3-in. ID pipes.

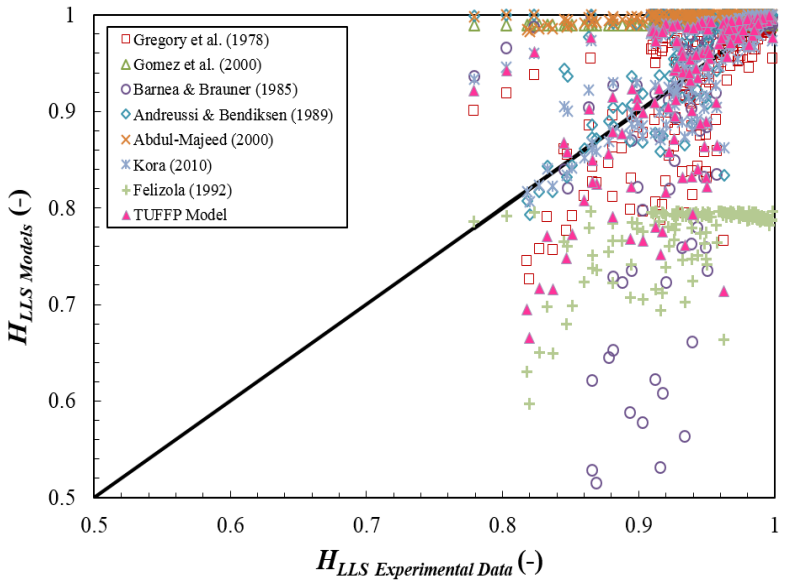

Figure 5.53 Comparison of model predictions against the measured slug liquid holdup for μ_{Oil} = 587 cP acquired from both 2- and 3-in. ID pipes.

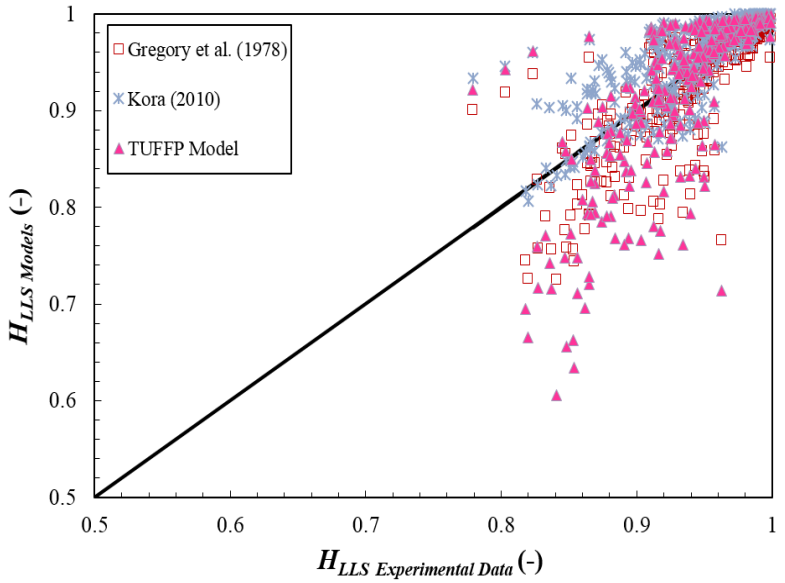

Figure 5.54 Comparison of model predictions against the measured slug liquid holdup for 'all' oil viscosities acquired from both 2- and 3-in. ID pipes.

5.4.2 Film liquid holdup

Comparison between film holdup experimental data and models is presented in this section.

5.4.2.1 3-in. ID pipes

Model evaluation results for the average film liquid holdup are shown in Figure 5.55. Experimental results for the average film liquid holdup were compared with predictions by TUFFP Unified model. These results are plotted in Figures 5.56 to 5.62.

TUFFP Unified model presents an absolute average relative error of 10.43% for 'all' oil viscosities. The average relative error presents a positive value of 3%, indicating that this model slightly over-estimates the film liquid holdup for 'all' oil viscosities. Although $\varepsilon_{2\ (3\text{-}in.)}$ value is not significantly changed, the average relative error, $\varepsilon_{1\ (3\text{-}in.)}$, decreases with increasing oil viscosity. This means that the degree of over-estimation decreases with an increase of oil viscosity, indicating that TUFFP Unified model is more suitable for higher oil viscosity. This tendency is similar with Brito's (2012) experimental result.

The degree of scattering increases as the film liquid holdup increases. For the relatively low film liquid holdup ($H_{LF} < 0.5$), the standard deviation of the obtained data is small, while increases for higher film liquid holdup ($H_{LF} > 0.5$). It can be concluded that, because the film liquid holdup is relative with the superficial liquid velocity, the degree of scattering increases with increasing of

the superficial liquid velocity, namely in less-slip condition. As a result, the TUFFP Unified model cannot reflect this phenomenon and it need to be carefully modified.

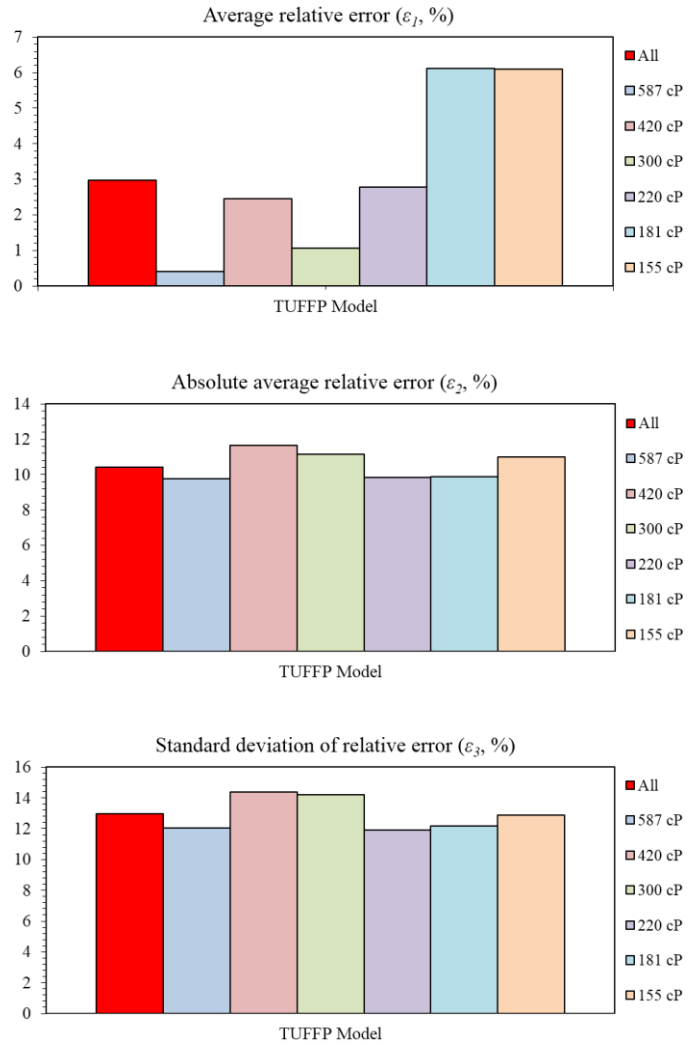

Figure 5.55 Model evaluation using the film liquid holdup experimental data acquired from 3-in. ID pipes.

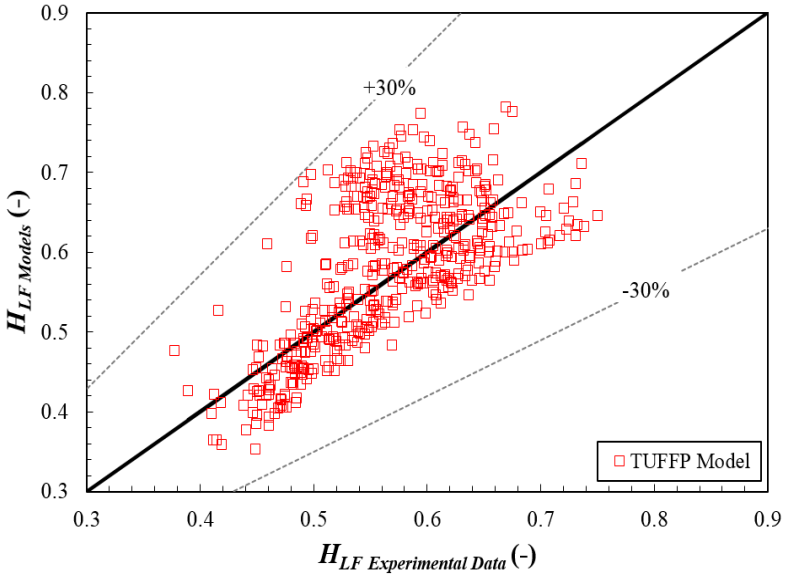

Figure 5.56 Comparison between TUFFP Unified model prediction and measured film liquid holdups for 'all' oil viscosities when the pipe diameter is 3-in.

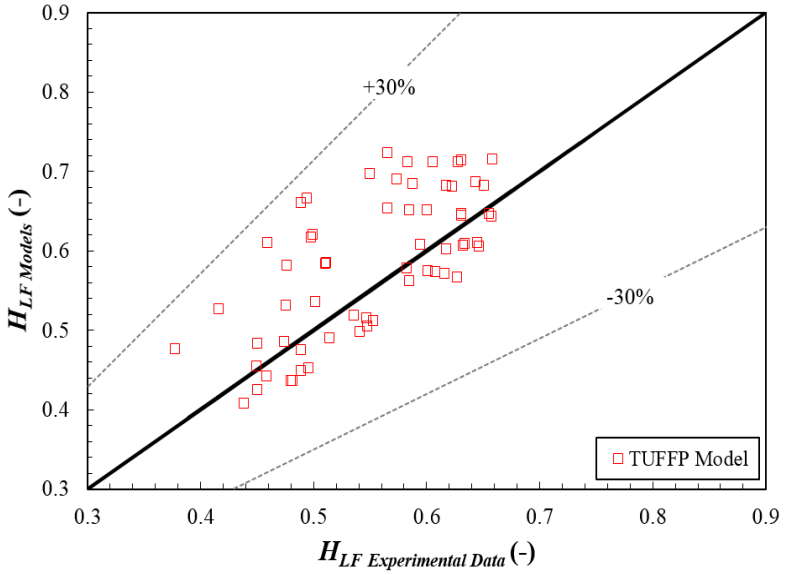

Figure 5.57 Comparison between TUFFP Unified model prediction and measured film liquid holdups for μ_{Oil} = 155 cP when the pipe diameter is 3-in.

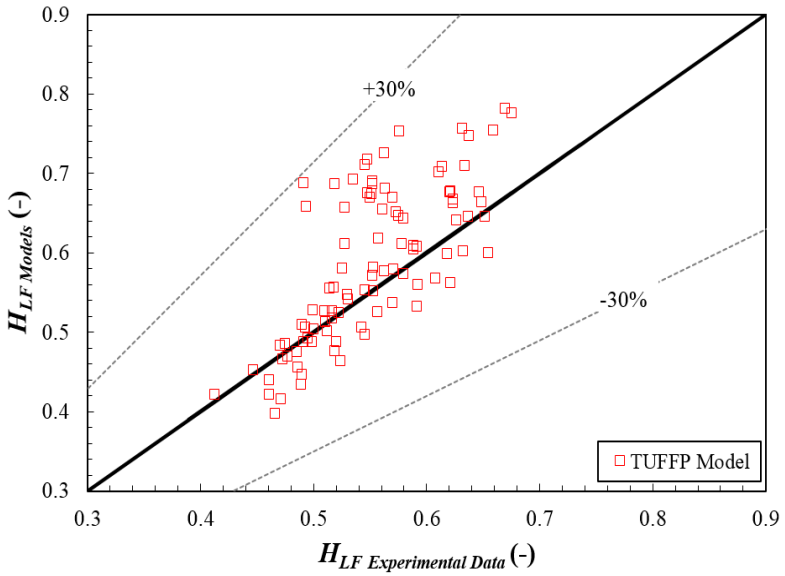

Figure 5.58 Comparison between TUFFP Unified model prediction and measured film liquid holdups for μ_{Oil} = 181 cP when the pipe diameter is 3-in.

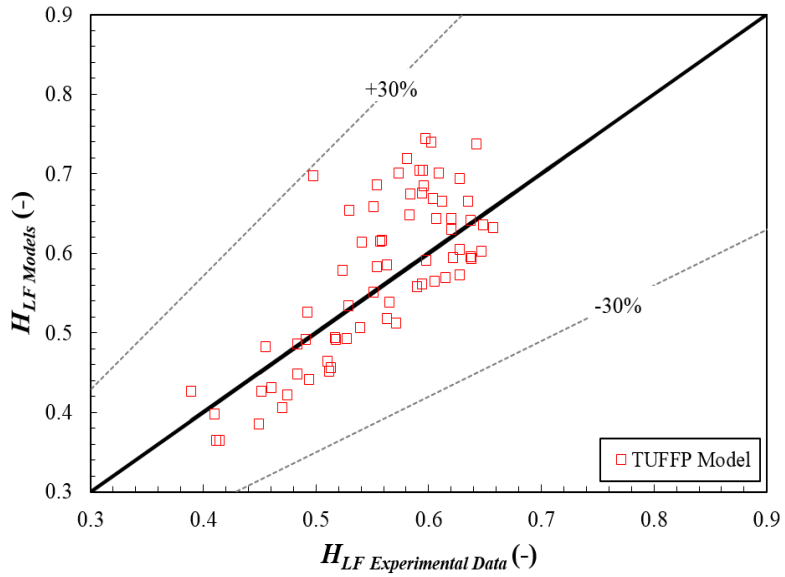

Figure 5.59 Comparison between TUFFP Unified model prediction and measured film liquid holdups for μ_{Oil} = 220 cP when the pipe diameter is 3-in.

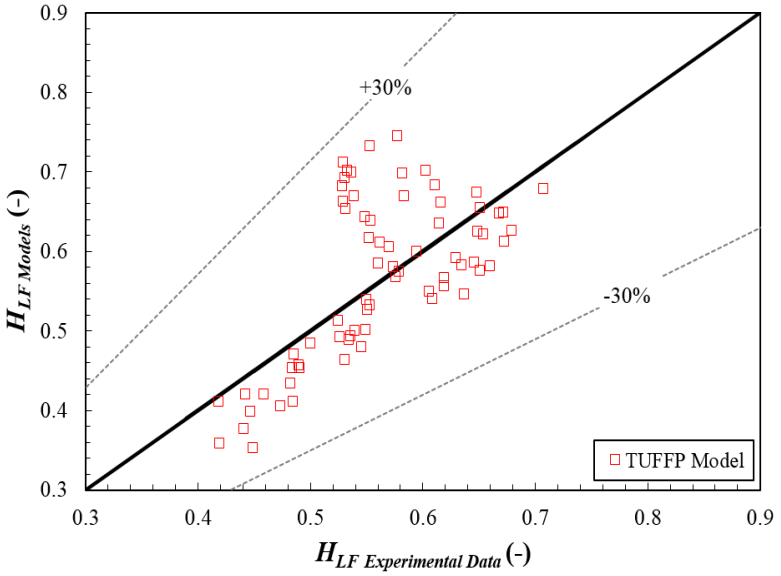

Figure 5.60 Comparison between TUFFP Unified model prediction and measured film liquid holdups for μ_{Oil} = 300 cP when the pipe diameter is 3-in.

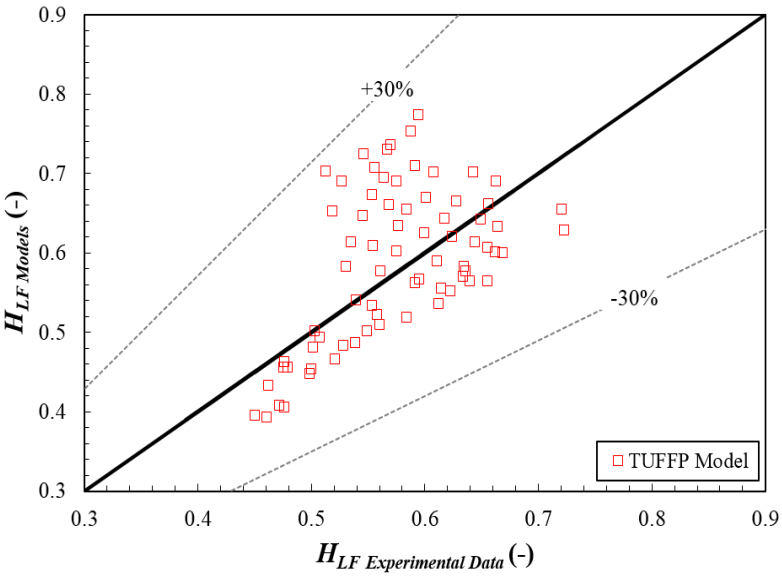

Figure 5.61 Comparison between TUFFP Unified model prediction and measured film liquid holdups for μ_{Oil} = 420 cP when the pipe diameter is 3-in.

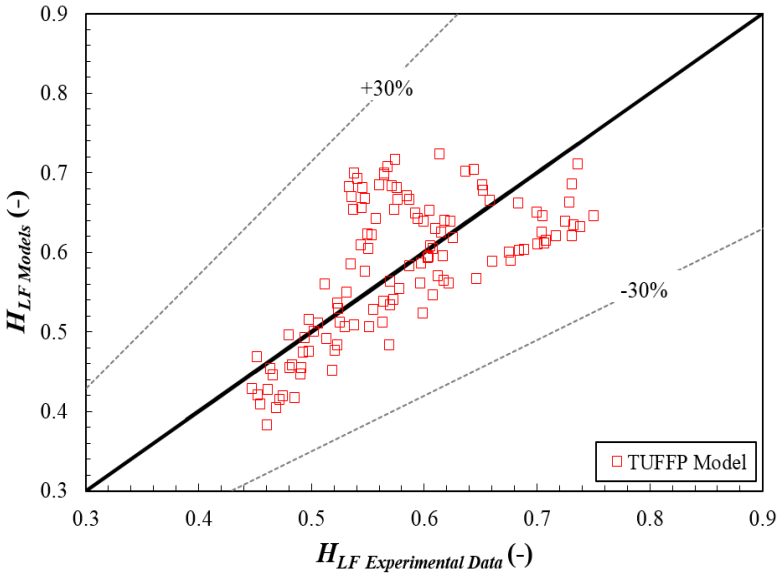

Figure 5.62 Comparison between TUFFP Unified model prediction and measured film liquid holdups for μ_{Oil} = 587 cP when the pipe diameter is 3-in.

5.4.2.2 2-in. ID pipes

Model evaluation results for the average film liquid holdup obtained from 2-in. ID pipes are shown in Figure 5.63. Same as 3-in. ID pipes case, experimental results for the average film liquid holdup were compared with predictions by TUFFP Unified model. These results are plotted in Figures 5.64 to 5.67. TUFFP Unified model produces an absolute average relative error of 18% for 'all' oil viscosities. The average relative error has a negative value of -16%, indicating that this model under-estimates the film liquid holdup for 'all' oil viscosities. There is no significant change in both of the average relative error, $\varepsilon_{1\ (2\text{-in.})}$, and the absolute average relative error, $\varepsilon_{2\ (2\text{-in.})}$, with increasing of oil viscosity.

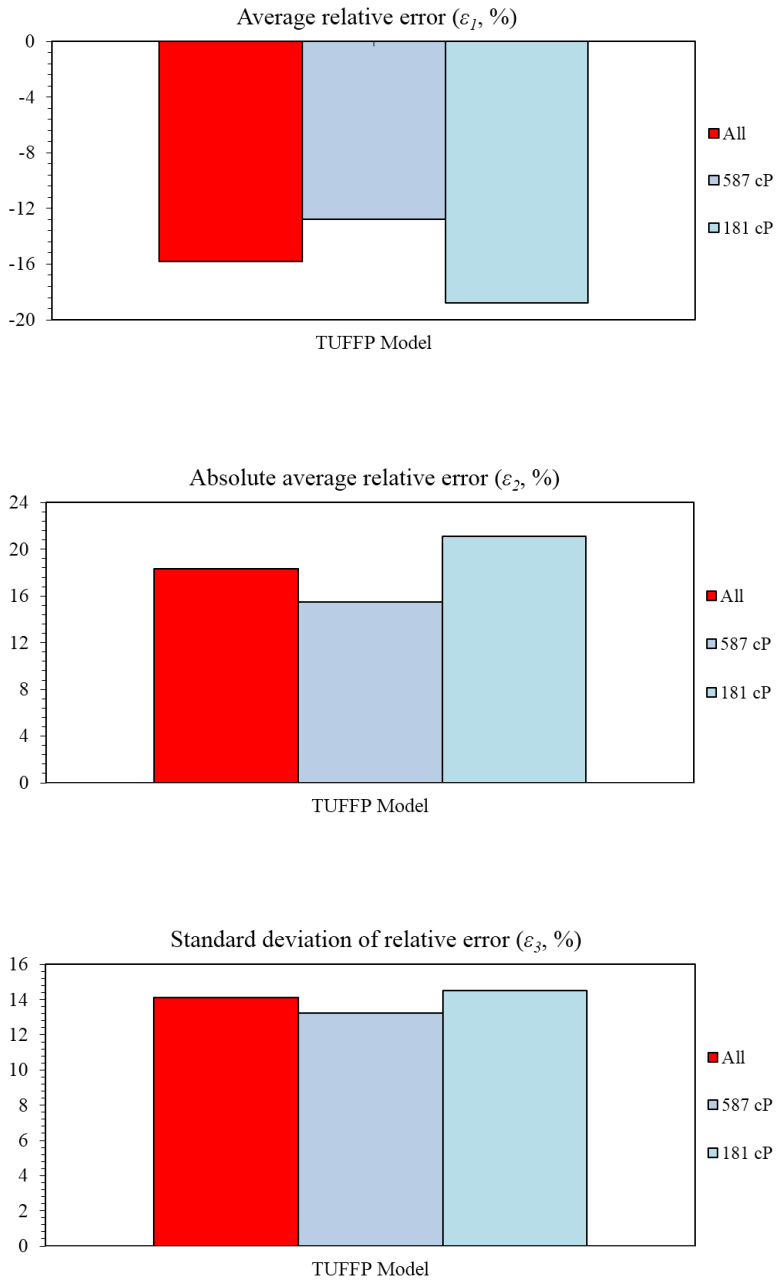

Figure 5.63 Model evaluation using the film liquid holdup experimental data reported by Kora (2010) from 2-in. ID pipes.

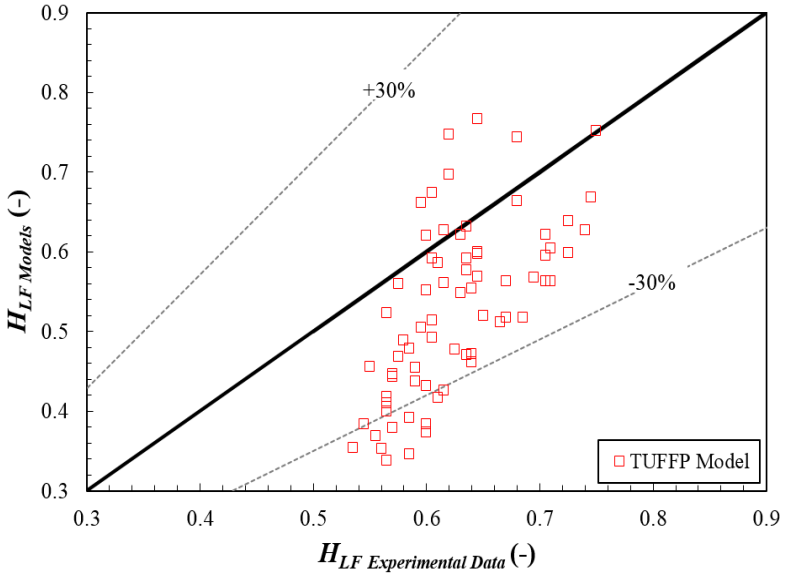

Figure 5.64 Comparison between TUFFP Unified model prediction and Kora's (2008) measured film liquid holdups for 'all' oil viscosities when the pipe diameter is 2-in.

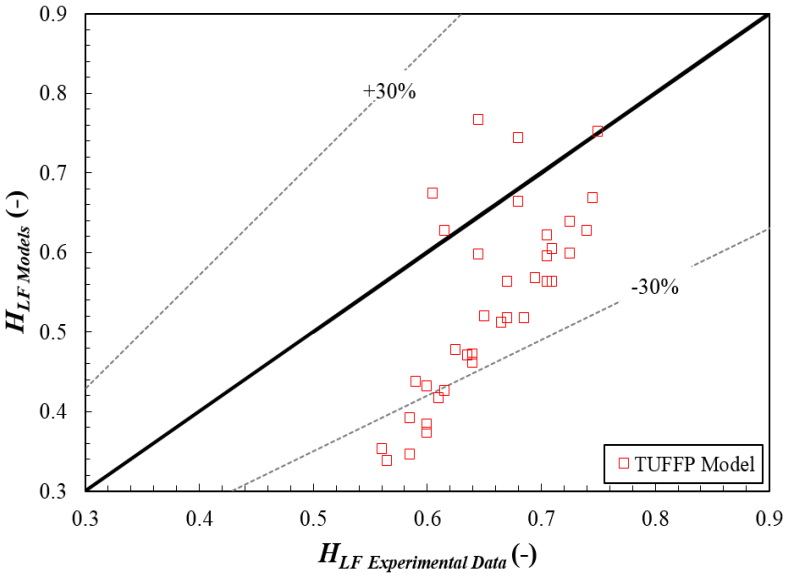

Figure 5.65 Comparison between TUFFP Unified model prediction and Kora's (2008) measured film liquid holdups for μ_{Oil} = 181 cP when the pipe diameter is 2-in.

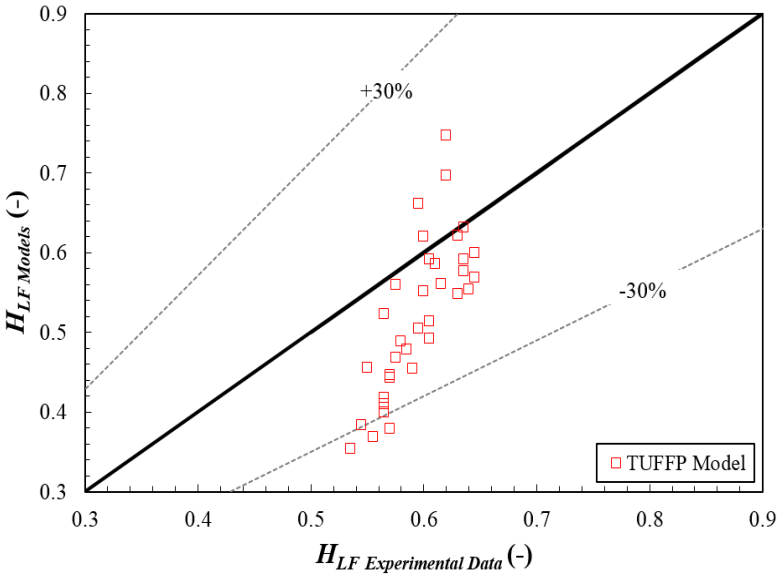

Figure 5.66 Comparison between TUFFP Unified model prediction and Kora's (2008) measured film liquid holdups for μ_{Oil} = 587 cP when the pipe diameter is 2-in.

5.4.2.3 Combined data of 2- and 3-in. ID pipes

Figures 5.67 and 5.68 present TUFFP model evaluation for both 2- and 3-in. results. In Figure 5.67, when the data of 2- and 3-in. are combined, the average relative error, $\varepsilon_{1\ (2\text{-in.}+3\text{-in.})}$, and the absolute average relative error, $\varepsilon_{2\ (2\text{-in.}+3\text{-in.})}$, show the values of -1.7%, and 12%, respectively. The absolute and average relative errors of 'all' oil viscosities from both 2- and 3-in. are relatively low. However, in Figure 5.68, film liquid holdup is severely under-estimated for 2-in. ID pipes ($\varepsilon_{1\ (2\text{-in.})}$=-16%) while it is properly predicted for 3-in. ID pipes ($\varepsilon_{1\ (3\text{-in.})}$=3%). For 3-in. ID pipes case, the degree of over-estimation decreases as oil viscosity increases. As a result, it can be inferred that TUFFP model gives better prediction of film liquid holdup for higher pipe diameter and oil viscosity.

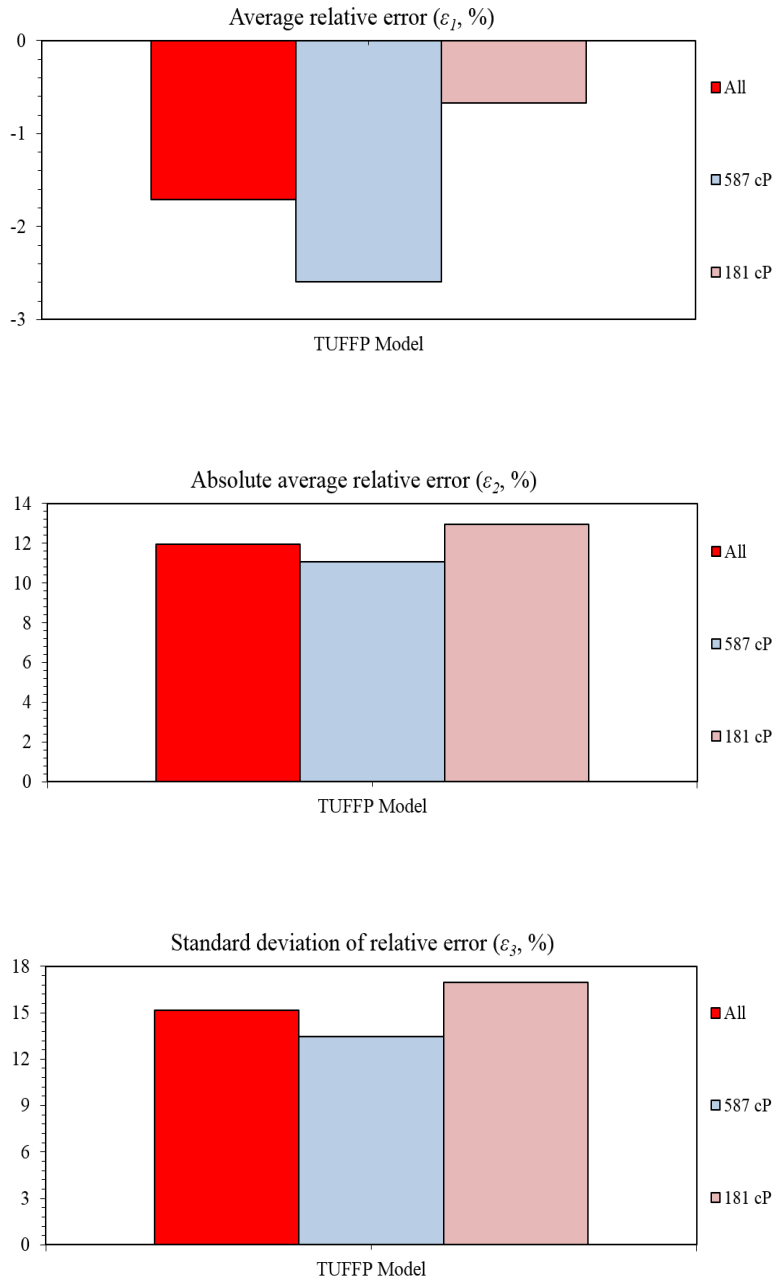

Figure 5.67 Model evaluation using the film liquid holdup experimental data acquired from both 2- and 3-in. ID pipes.

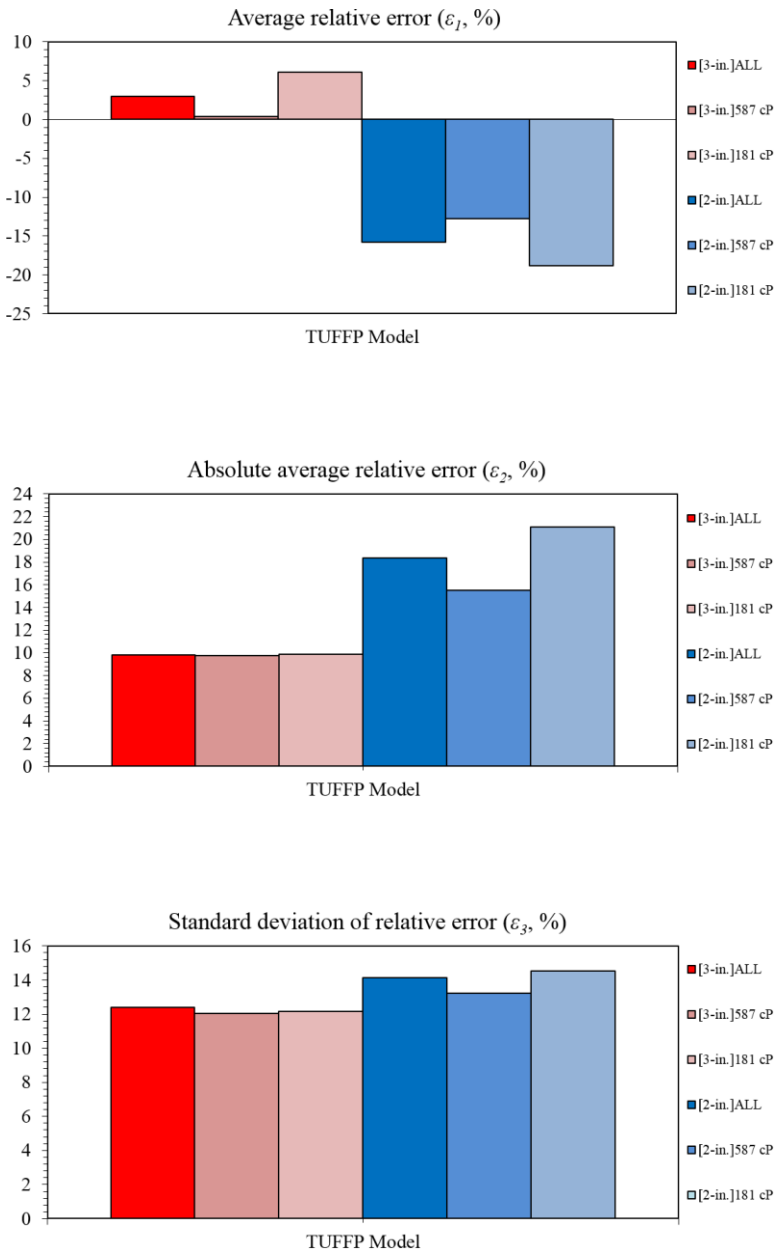

Figure 5.68 Model evaluation using the film liquid holdup experimental data acquired from 2- and 3-in. ID pipes, respectively.

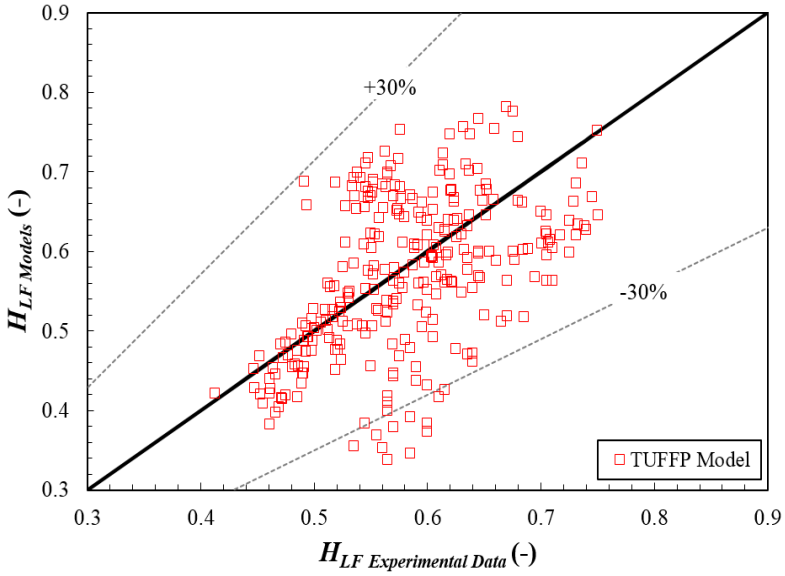

Figure 5.69 Comparison between TUFFP Unified model prediction against the measured film liquid holdup for 'all' oil viscosities acquired from both 2- and 3-in. ID pipes

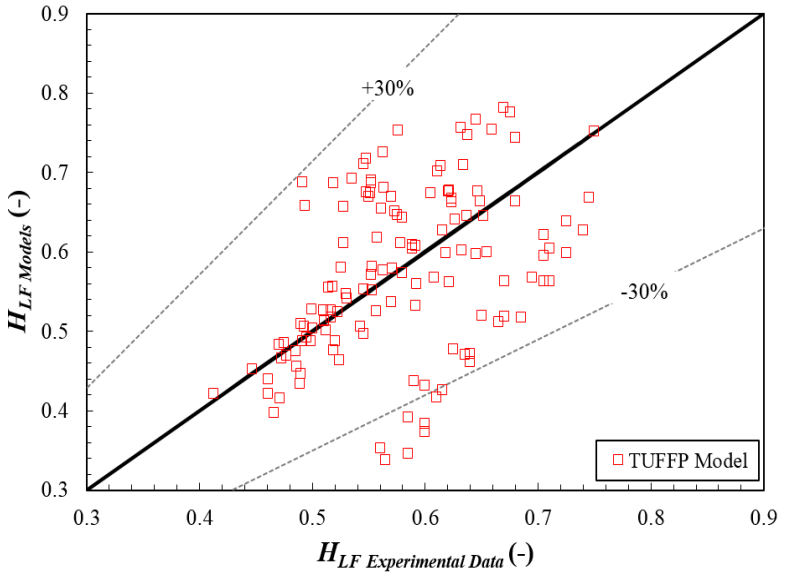

Figure 5.70 Comparison between TUFFP Unified model prediction against the measured film liquid holdup for μ_{Oil}=181 cP acquired from both 2- and 3-in. ID pipes

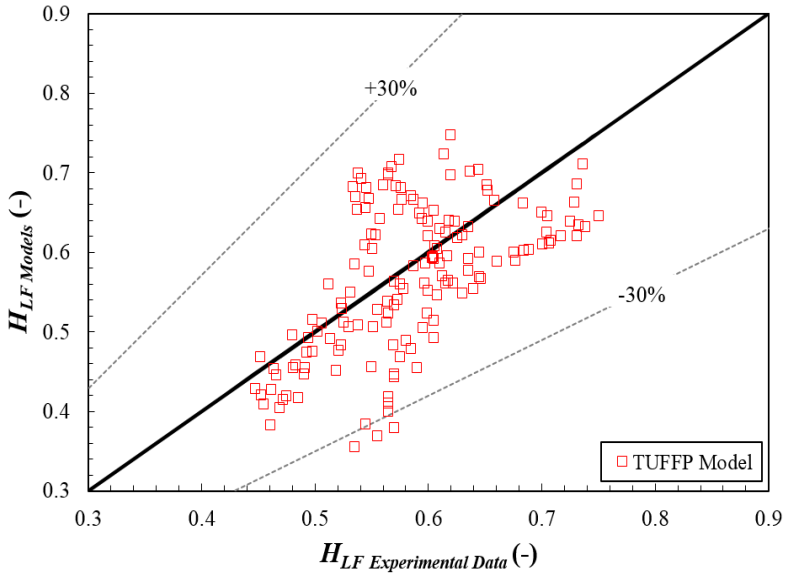

Figure 5.71 Comparison between TUFFP Unified model prediction against the measured film liquid holdup for μ_{Oil}=587 cP acquired from both 2- and 3-in. ID pipes

5.4.3 Translational velocity

Comparison between predicted and measured translational velocity is presented in this section.

5.4.3.1 3-in. ID pipes

A total of 16 correlations have been identified in the literature (see Table B.2); Fabre (1994), Petalas & Aziz (2000), Shoham (1982), Choi *et al*. (2012), Bonnecaze *et al*. (1971), Shipley (1982), Gomez *et al*. (2000), Rouhani & Axelsson (1970), Hibiki & Ishii (2003), Mishima & Hibiki (1996), Clark &

Flemmer (1985), Greskovich & Cooper (1975), Beattie & Sugawara (1986), Kataoka & Ishii (1987), Gokcal (2008), and Bendiksen (1984) models. The model evaluations for the translational velocity in 3-in. ID pipes are shown in Figure 5.72.

Choi *et al*. (2012) model presents the lowest $\varepsilon_{1\ (3\text{-}in.)}$ and $\varepsilon_{2\ (3\text{-}in.)}$ values for 'all' oil viscosities by -6.4% and 10%, respectively. This indicates an insignificant under-prediction of the translational velocity and a small error around the average. $\varepsilon_{1\ (3\text{-}in.)}$ and $\varepsilon_{2\ (3\text{-}in.)}$ slightly decrease with increasing oil viscosity, showing that this model gives better prediction for the translational velocity when the oil viscosity is high. Petalas & Aziz (2000) correlation presents the second best agreement with the experimental results. It can be observed that when the oil viscosity decreases, both Choi *et al*. (2012) and Petalas & Aziz (2000) models tend to have higher $\varepsilon_{1\ (3\text{-}in.)}$ values, indicating larger under-estimation of the translational velocity.

In contrast, Greskovich & Cooper (1975) model produces the highest $\varepsilon_{1\ (3\text{-}in.)}$ and $\varepsilon_{2\ (3\text{-}in.)}$ values of -51% and 51%, respectively, indicating a severe under-estimation of the translational velocity. As stated in section B.3.4.3, the existing models considering the other components such as void fraction, pipe diameter, and Reynolds number show lower $\varepsilon_{1\ (3\text{-}in.)}$ and $\varepsilon_{2\ (3\text{-}in.)}$. Figure 5.73 through Figure 5.79 show comparisons between the predicted and measured translational velocities for different oil viscosities. The comparison of the best five models are plotted in Figure 5.80.

In summary, various existing models are compared against the experimental data for the translational velocity. Statistical parameters are calculated to evaluate the model performance (See Appendix F for more details

of the statistical parameter values). It can be concluded that the Choi *et al*. (2012) model presents the lowest absolute average relative error for 'all' oil viscosities, but the errors increase as the oil viscosity decreases. This trend makes this model less suitable for low viscous oils.

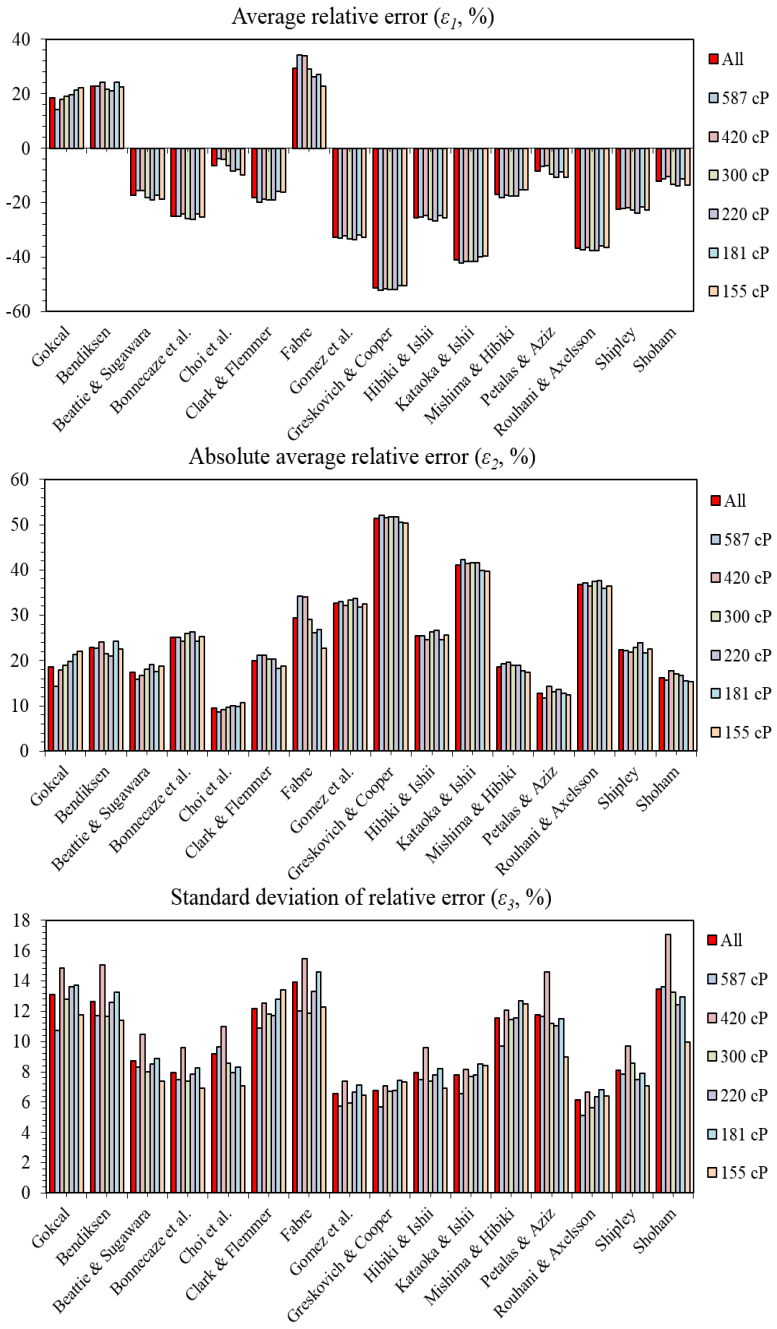

Figure 5.72 Model evaluation using the translational velocity data acquired from 3-in. ID pipes.

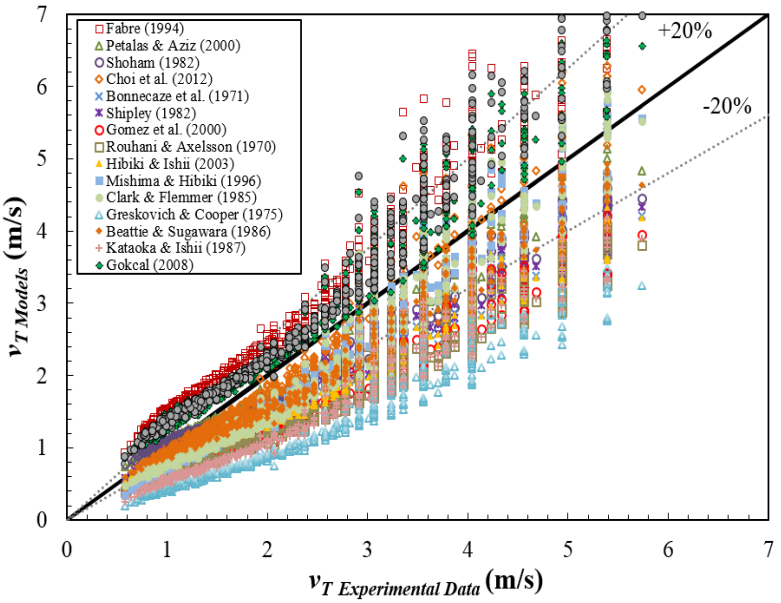

Figure 5.73 Comparison of model predictions against the measured translational velocity for 'all' oil viscosities when the pipe diameter is 3-in.

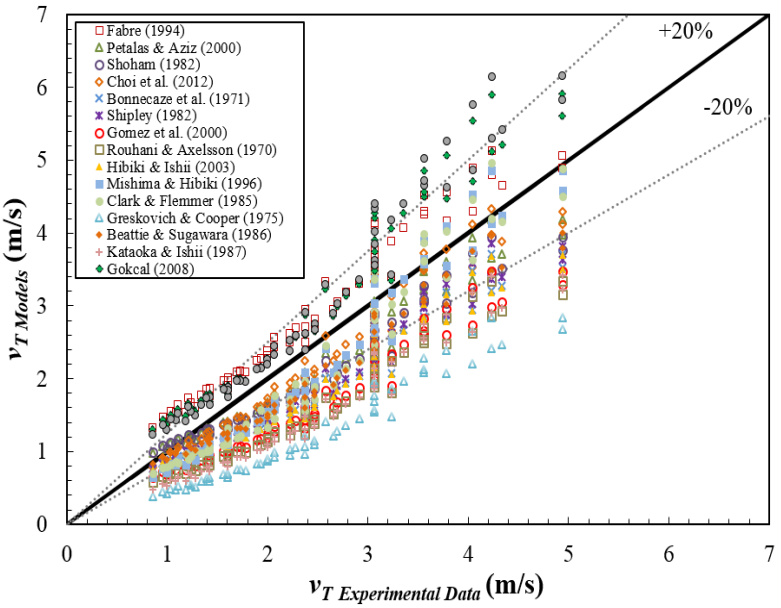

Figure 5.74 Comparison of model predictions against the measured translational velocity for μ_{Oil} = 155 cP when the pipe diameter is 3-in.

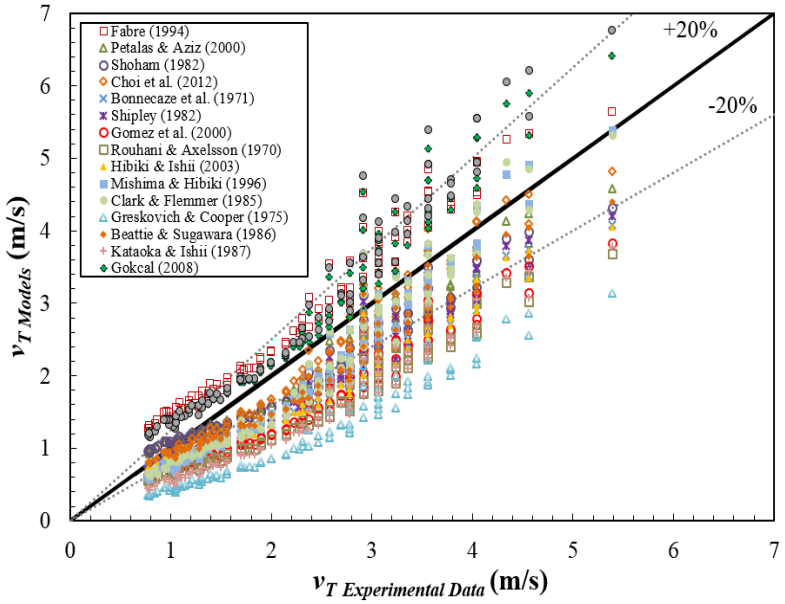

Figure 5.75 Comparison of model predictions against the measured translational velocity for μ_{Oil} = 181 cP when the pipe diameter is 3-in.

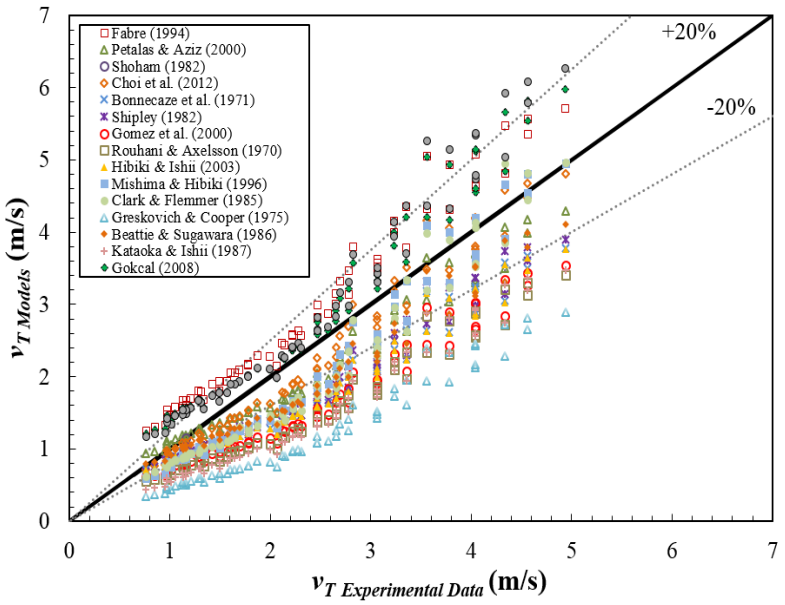

Figure 5.76 Comparison of model predictions against the measured translational velocity for μ_{Oil} = 220 cP when the pipe diameter is 3-in.

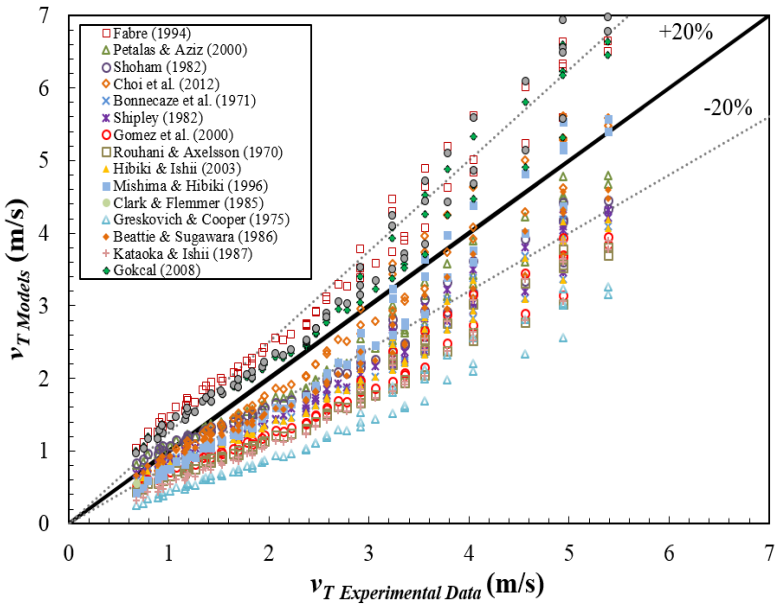

Figure 5.77 Comparison of model predictions against the measured translational velocity for μ_{Oil} = 300 cP when the pipe diameter is 3-in.

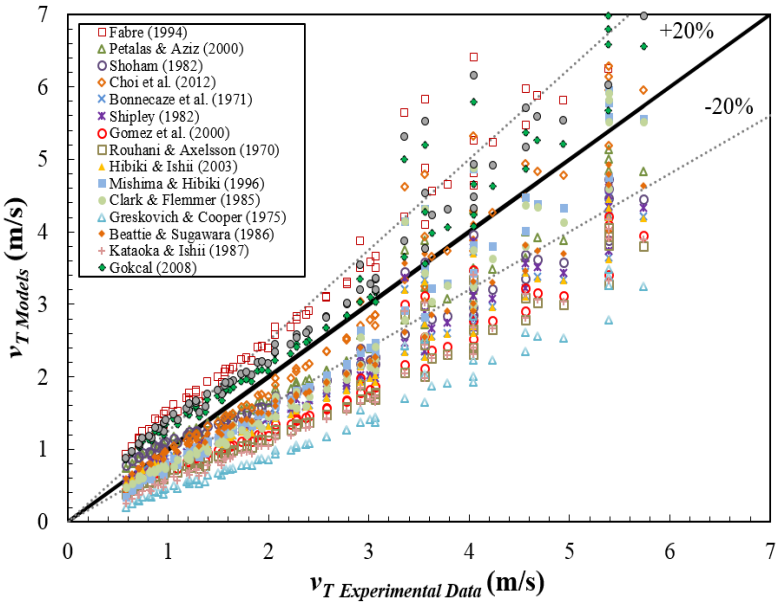

Figure 5.78 Comparison of model predictions against the measured translational velocity for μ_{Oil} = 420 cP when the pipe diameter is 3-in.

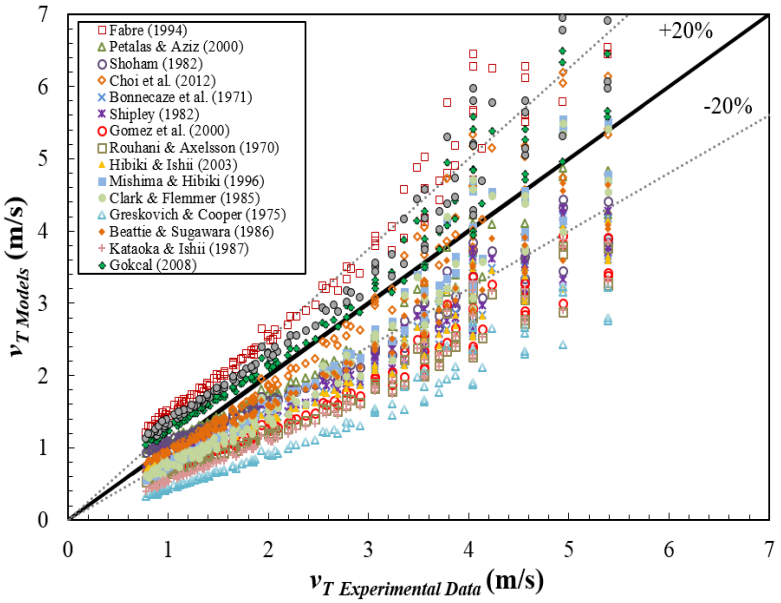

Figure 5.79 Comparison of model predictions against the measured translational velocity for μ_{Oil} = 587 cP when the pipe diameter is 3-in.

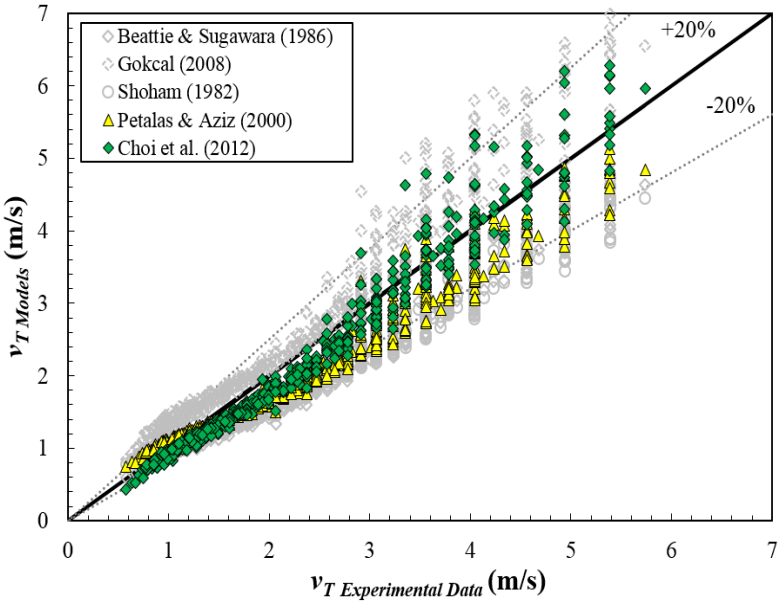

Figure 5.80 Comparison of the best five model predictions against the measured translational velocity for 'all' oil viscosities when the pipe diameter is 3-in.

5.4.3.2 2-in. ID pipes

Similar with 3-in. ID pipes case, the model evaluations for the translational velocity are shown in Figure 5.81 for the Fabre (1994), Petalas & Aziz (2000), Shoham (1982), Choi *et al*. (2012), Bonnecaze *et al*. (1971), Shipley (1982), Gomez *et al*. (2000), Rouhani & Axelsson (1970), Hibiki & Ishii (2003), Mishima & Hibiki (1996), Clark & Flemmer (1985), Greskovich & Cooper (1975), Beattie & Sugawara (1986), Kataoka & Ishii (1987), Gokcal (2008), and Bendiksen (1984) models.

The model with the smallest average relative error ($\varepsilon_{1\ (2\text{-in.})}$ = -0.1%) and the smallest absolute average relative error ($\varepsilon_{2\ (2\text{-in.})}$ = 10%) corresponds to Choi *et al*. (2012). Shoham (1982) correlation presents the second best agreement with the experimental results showing $\varepsilon_{1\ (2\text{-in.})}$ and $\varepsilon_{2\ (2\text{-in.})}$ of -0.2% and 25%. Gokcal (2008) model gives relatively higher standard deviation of relative error, $\varepsilon_{3\ (2\text{-in.})}$, of 18% with the average relative and absolute average relative errors of -5% and 9%, respectively. For the relatively low oil viscosity (181 cP), these three models over-predict the translational velocity, while under-predict it for higher oil viscosity (587 cP).

Greskovich & Cooper (1975) model presents the highest average relative and absolute average relative errors of -50% and 50%, respectively. This result is similar with 3-in. ID pipes case. The details of the error analysis are tabled in Appendix F.

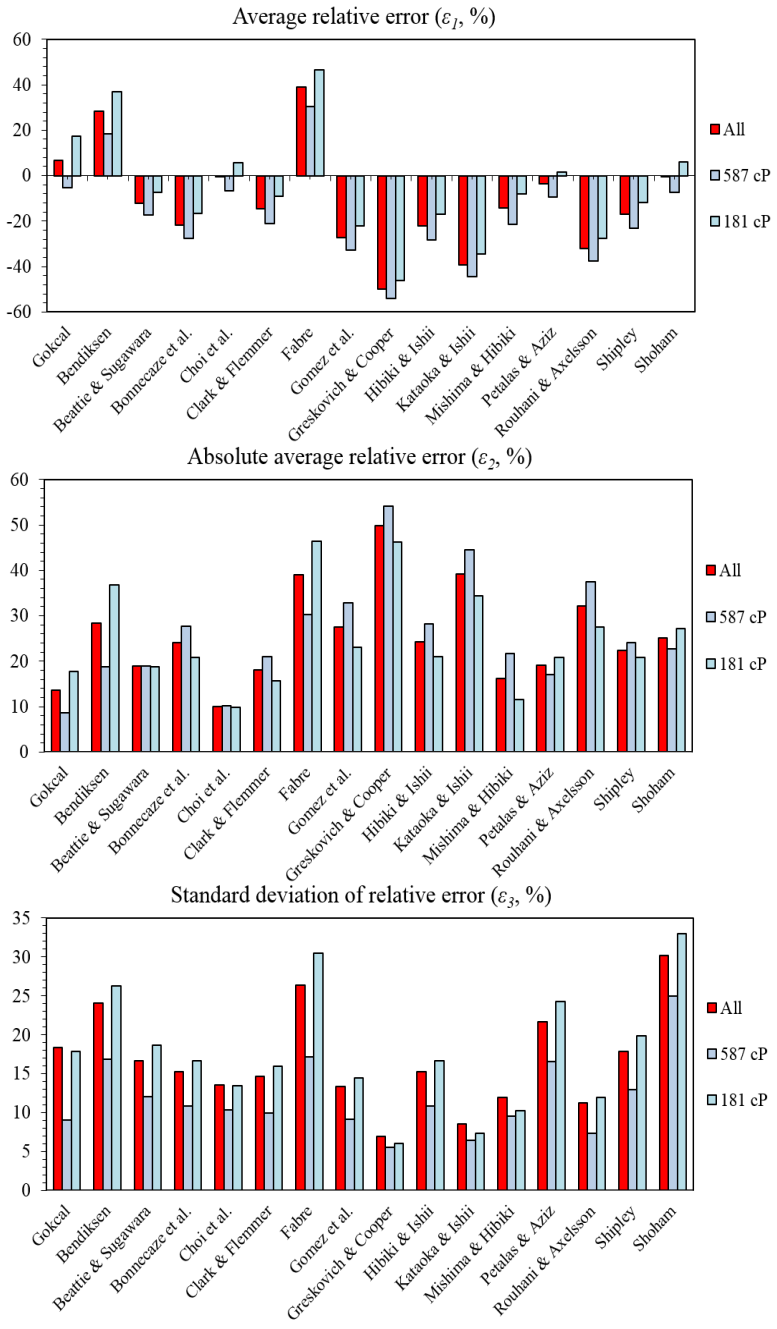

Figure 5.81 Model evaluation using the translational velocity data reported by Gokcal (2008) from 2-in. ID pipes.

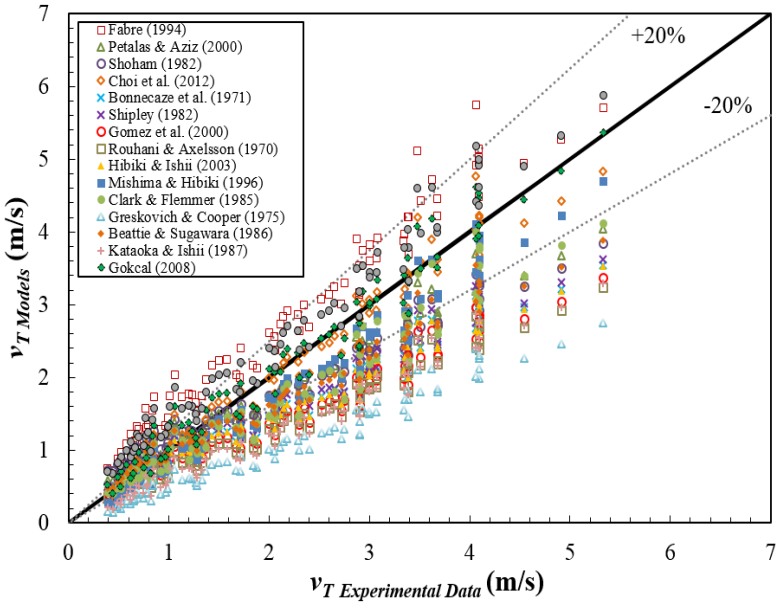

Figure 5.82 Comparison of model predictions against the Gokcal's (2008) measured translational velocity for 'all' oil viscosities when the pipe diameter is 2-in.

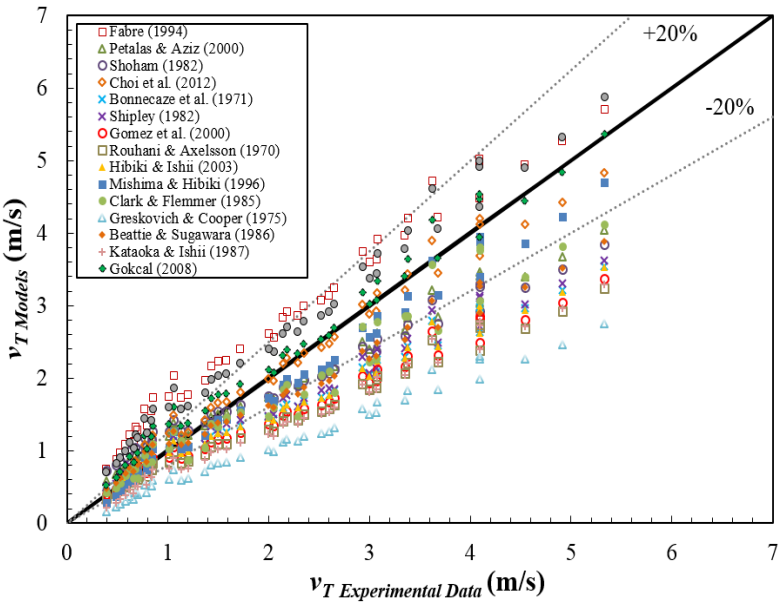

Figure 5.83 Comparison of model predictions against the Gokcal's (2008) measured translational velocity for μ_{Oil} = 181 cP when the pipe diameter is 2-in.

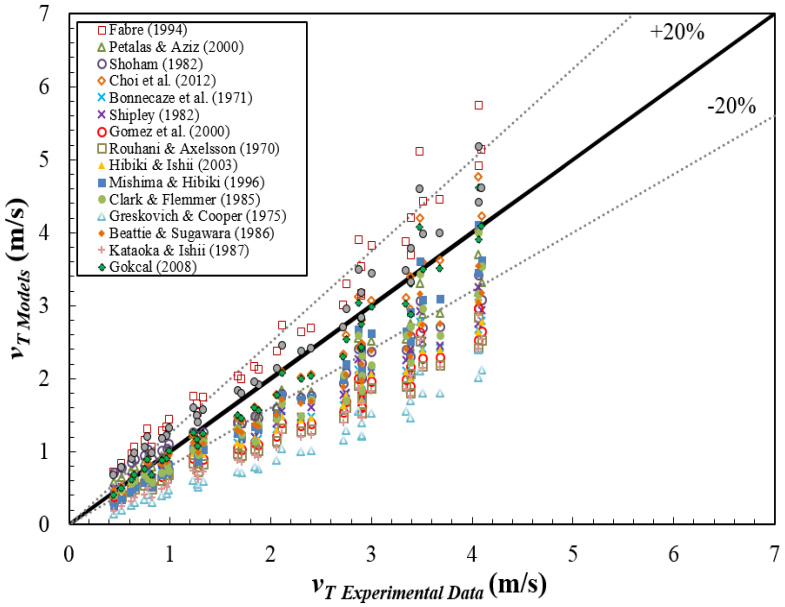

Figure 5.84 Comparison of model predictions against the Gokcal's (2008) measured translational velocity for μ_{Oil} = 587 cP when the pipe diameter is 2-in.

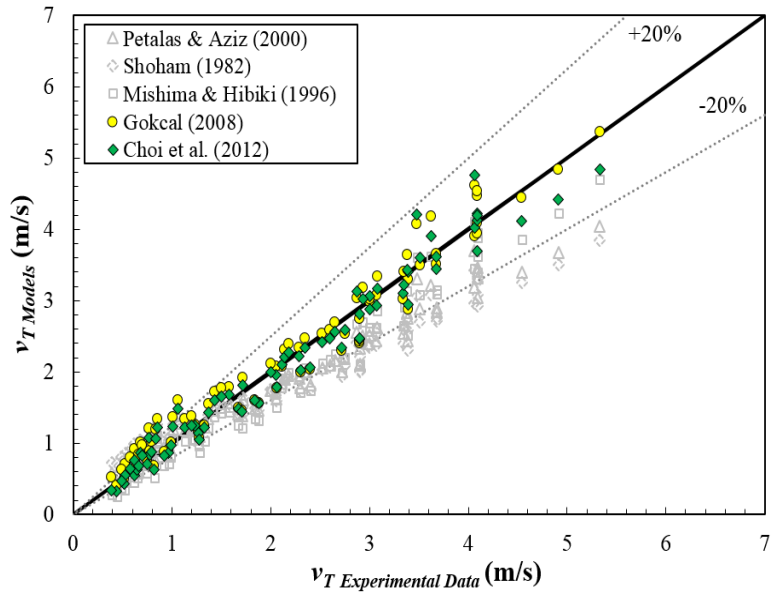

Figure 5.85 Comparison of the best five model predictions against the Gokcal's (2008) measured translational velocity for 'all' oil viscosities when the pipe diameter is 2-in.

5.4.3.3 Combined data of 2- and 3-in. ID pipes

Figures 5.86 and 5.87 present the statistical performance of the existing models and correlations. In Figure 5.86, when the data of 2- and 3-in. are combined, Choi *et al*. (2012), Petalas & Aziz (2000), and Shoham (1982) models produce the negative $\varepsilon_{1\ (2\text{-in.}+3\text{-in.})}$ values of -4.1%, -6.4%, and -8.1%, respectively. In contrast, Gokcal (2008) model shows a positive $\varepsilon_{1\ (2\text{-in.}+3\text{-in.})}$ value of 14% with the absolute average relative error, $\varepsilon_{2\ (2\text{-in.}+3\text{-in.})}$, of 16%. Figure 5.88 through Figure 5.90 present the comparison of the existing models against the translational velocity experimental data acquired from both 2- and 3-in. ID pipes.

In summary, Choi *et al*. (2012) model shows the best agreement with all of the experimental data and Petalas & Aziz (2000), Shoham (1982), and Gokcal (2008) models also give the suitable predictions.

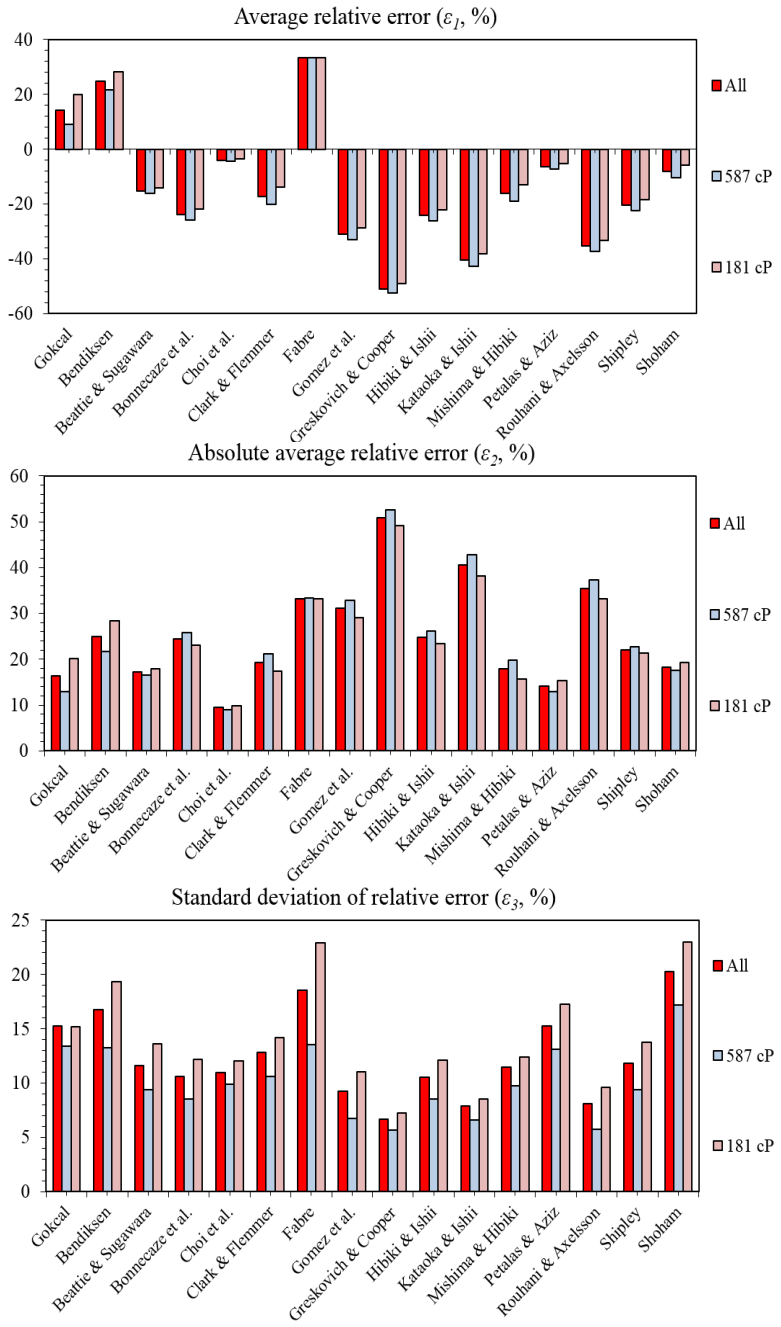

Figure 5.86 Model evaluation using the translational velocity data acquired from both 2- and 3-in. ID pipes.

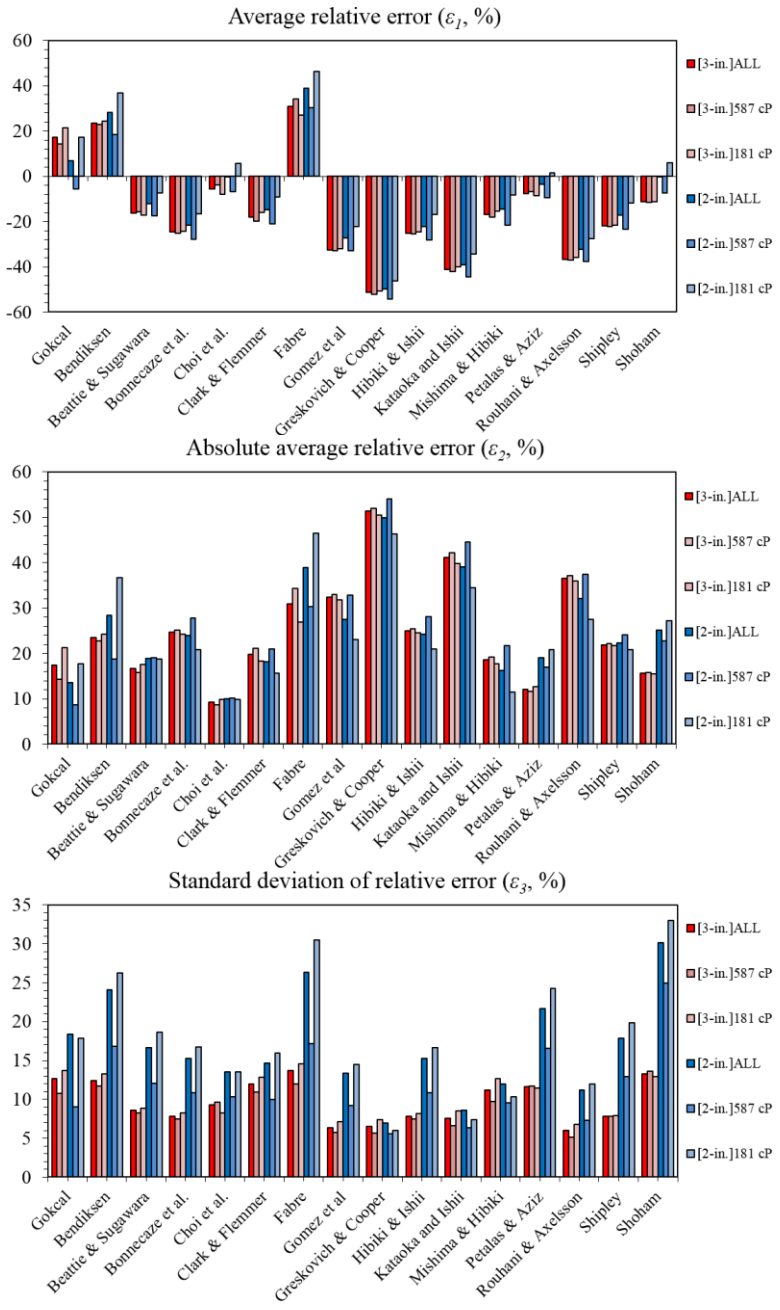

Figure 5.87 Model evaluation using the translational velocity data acquired from 2- and 3-in. ID pipes, respectively.

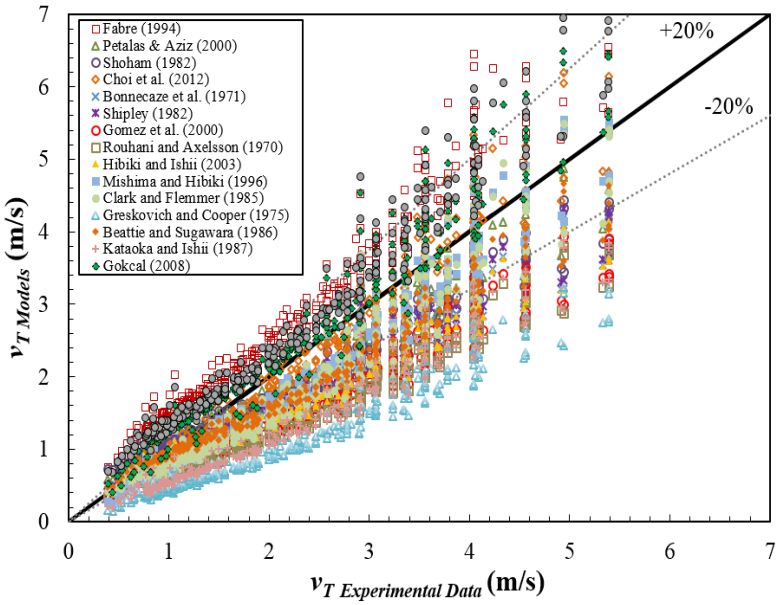

Figure 5.88 Comparison of model predictions against the measured translational velocity for 'all' oil viscosities acquired from both 2- and 3-in. ID pipes.

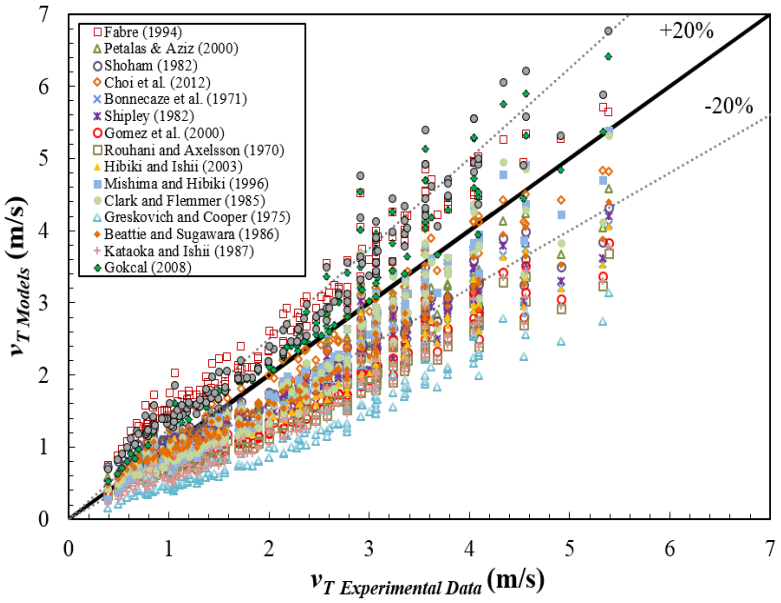

Figure 5.89 Comparison of model predictions against the measured translational velocity for μ_{Oil} = 181 cP acquired from both 2- and 3-in. ID pipes.

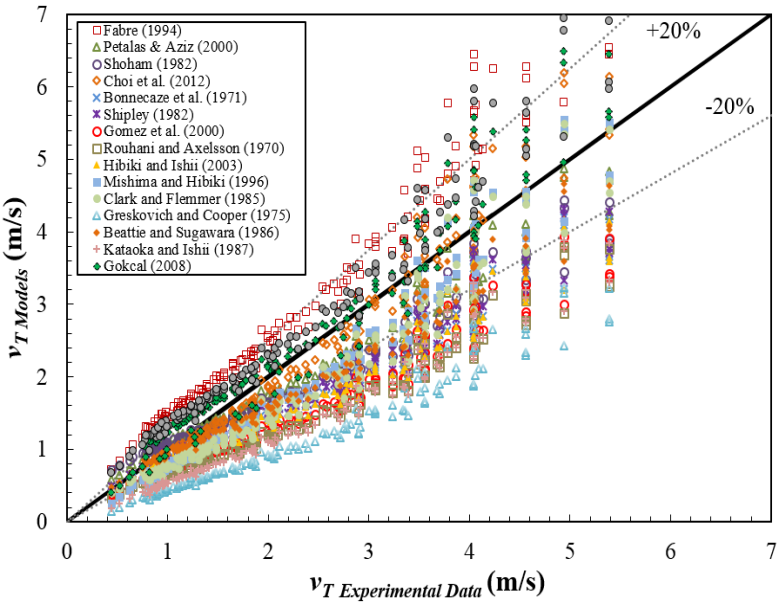

Figure 5.90 Comparison of model predictions against the measured translational velocity for μ_{Oil} = 587 cP acquired from both 2- and 3-in. ID pipes.

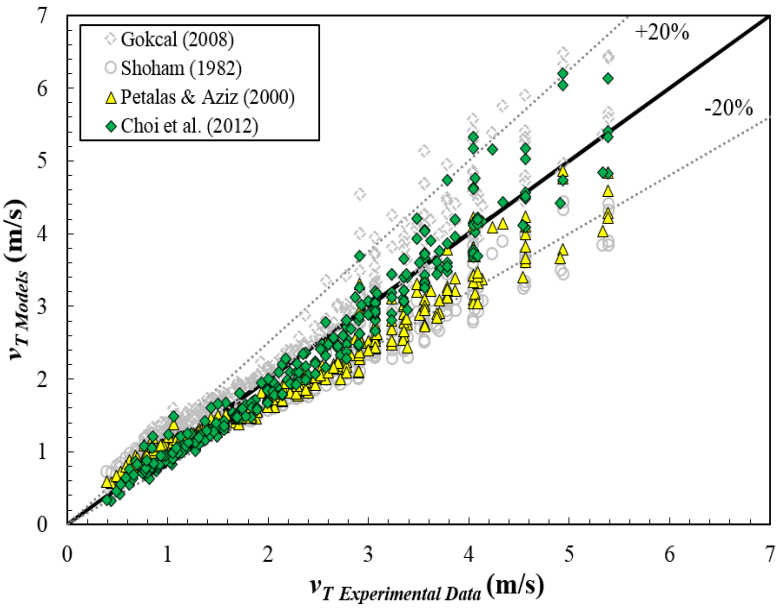

Figure 5.91 Comparison of the best four model predictions against the measured translational velocity for 'all' oil viscosities acquired from both 2- and 3-in. ID pipes.

5.4.4 Slug length

In 3-in. case, the model evaluation results for the slug length are shown in Figure 5.92. Figures 5.93 shows the comparison between the measured slug length against the model predictions by Dukler & Hubbard (1975), Andreussi (1975), Nicholson *et al*. (1978), Gregory *et al*. (1978), Nydal *et al*. (1992), Manolis (1995), Scott *et al*. (1986), Brill *et al*. (1981), TUFFP Unified, Norris (1981), Marcano *et al*. (1998), Barnea & Brauner (1985), and Al-safran *et al*. (2011). A graphical presentation using the dimensionless slug length is shown in Figure 5.94. Among these models, Brill *et al*. (1981), Marcano *et al*. (1998), and Al-safran *et al*. (2011) models are considering the other components, for example, not only the pipe diameter but also the mixture velocity and the fluid properties that affect the slug length (see Figures 5.93 and 5.94).

As can be seen in Figure 5.92, all of the models present the high positive values of $\varepsilon_{1\ (3\text{-in.})} > 100\%$, indicating that they are severely over-predicting the slug length. It can be observed that none of these models is completely suitable to predict the slug length. Nevertheless, if it has to be said, Nydal *et al*. (1992) and Al-safran *et al*. (2011) are the models with lower absolute average relative error, $\varepsilon_{2\ (3\text{-in.})}$, values of 121% and 177%, respectively.

Similar with the 3-in. ID pipes case, there is no model giving a satisfactory result when the pipe diameter is 2-in. Figure 5.95 to 5.97 present the comparison between the model predictions and the measured slug length experimental data from 2-in. ID pipes with the statistical model evaluations.

This is in agreement with Brito's (2012) study. None of the models consider all possible variables affecting the slug length, such as pipe geometry,

flow conditions, and fluid properties. As Brito (2012) discussed, further study is necessary to develop and modify a satisfactory correlation to predict the slug length for high oil viscosities.

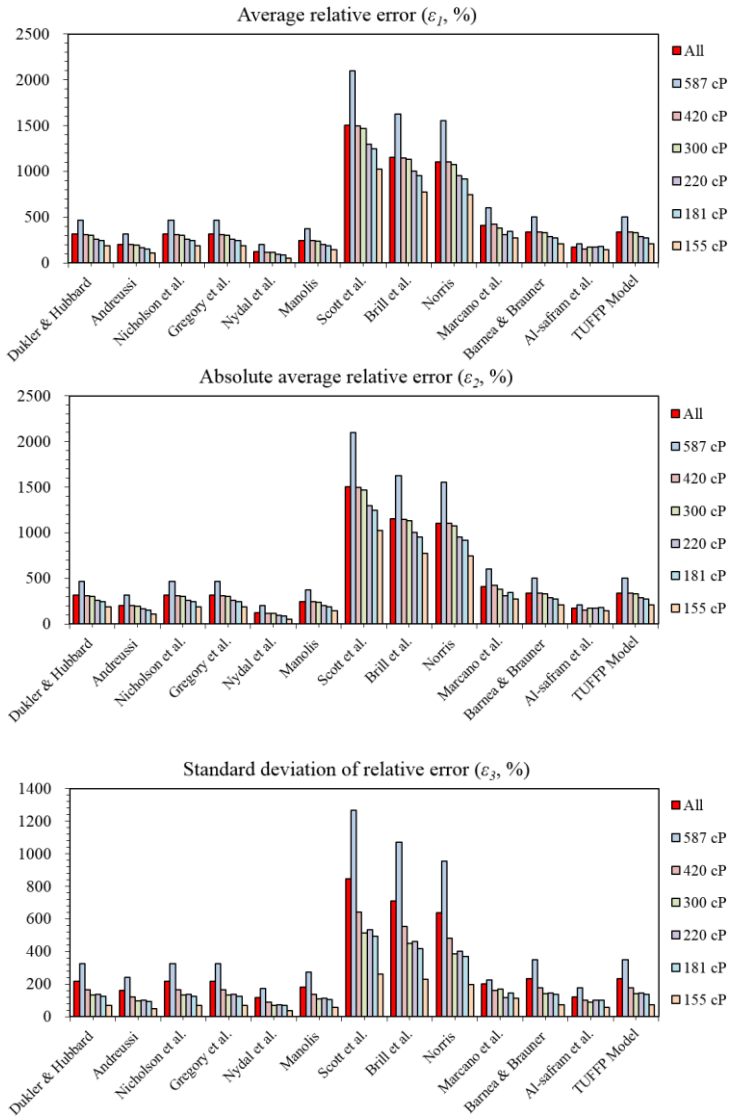

Figure 5.92 Model evaluation using the slug length experimental data acquired from 3-in. ID pipe.

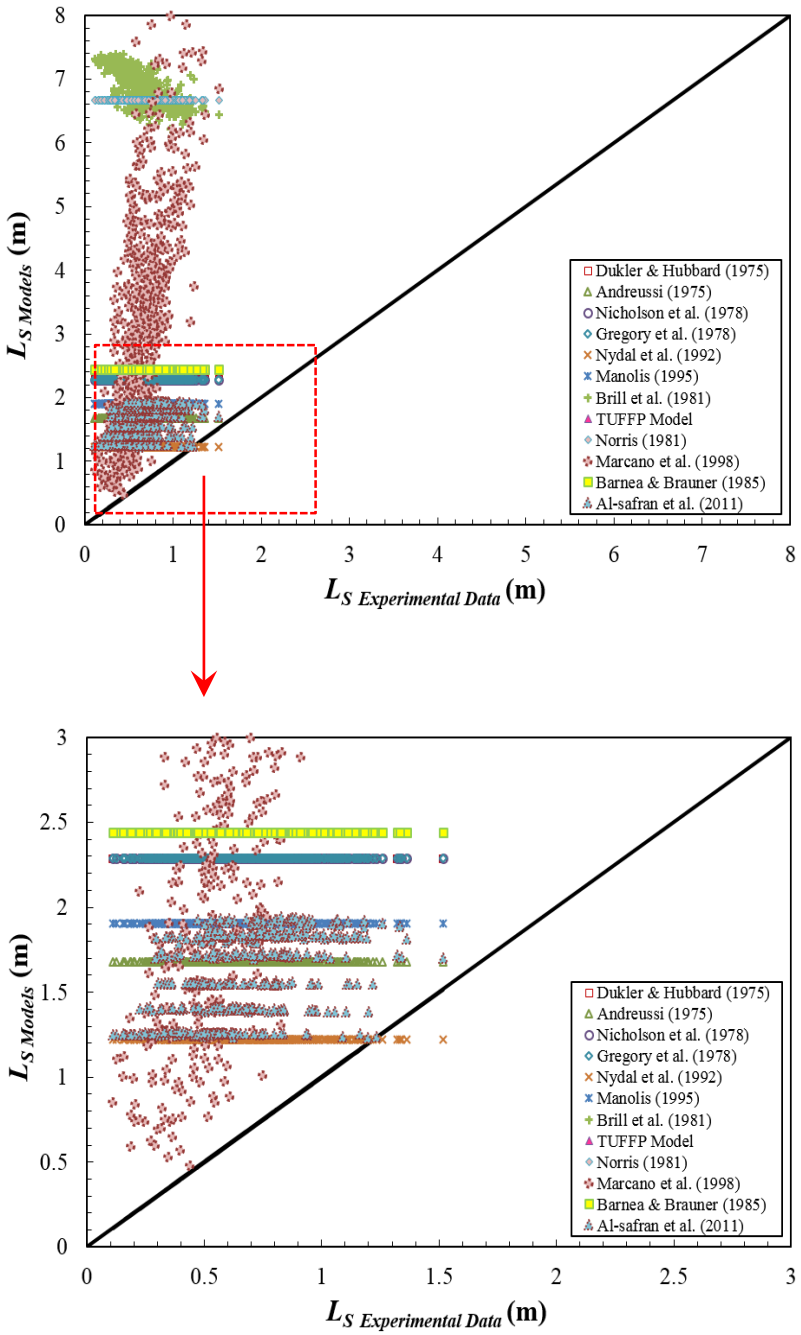

Figure 5.93 Comparison of model predictions against the measured slug length for 'all' oil viscosities when the pipe diameter is 3-in.

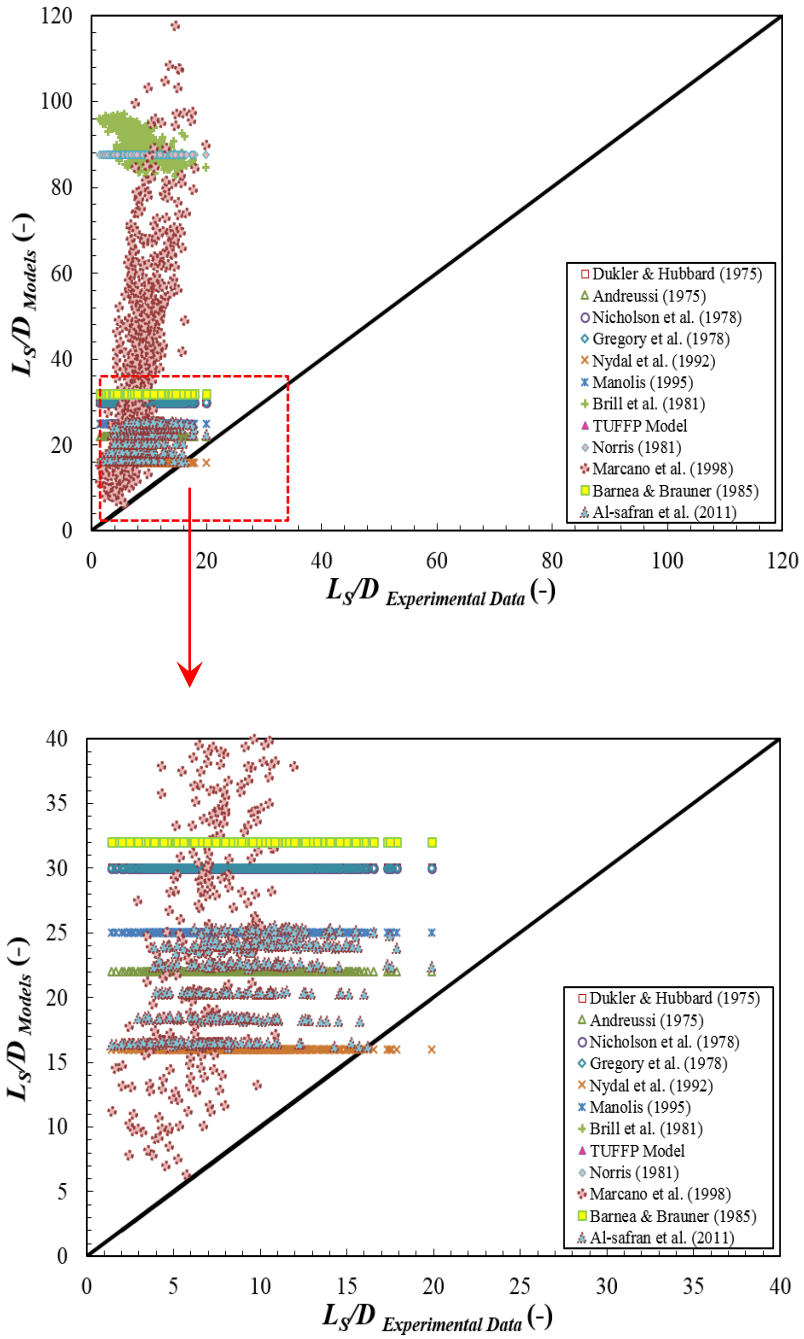

Figure 5.94 Comparison of model predictions against the measured dimensionless slug length for 'all' oil viscosities when the pipe diameter is 3-in.

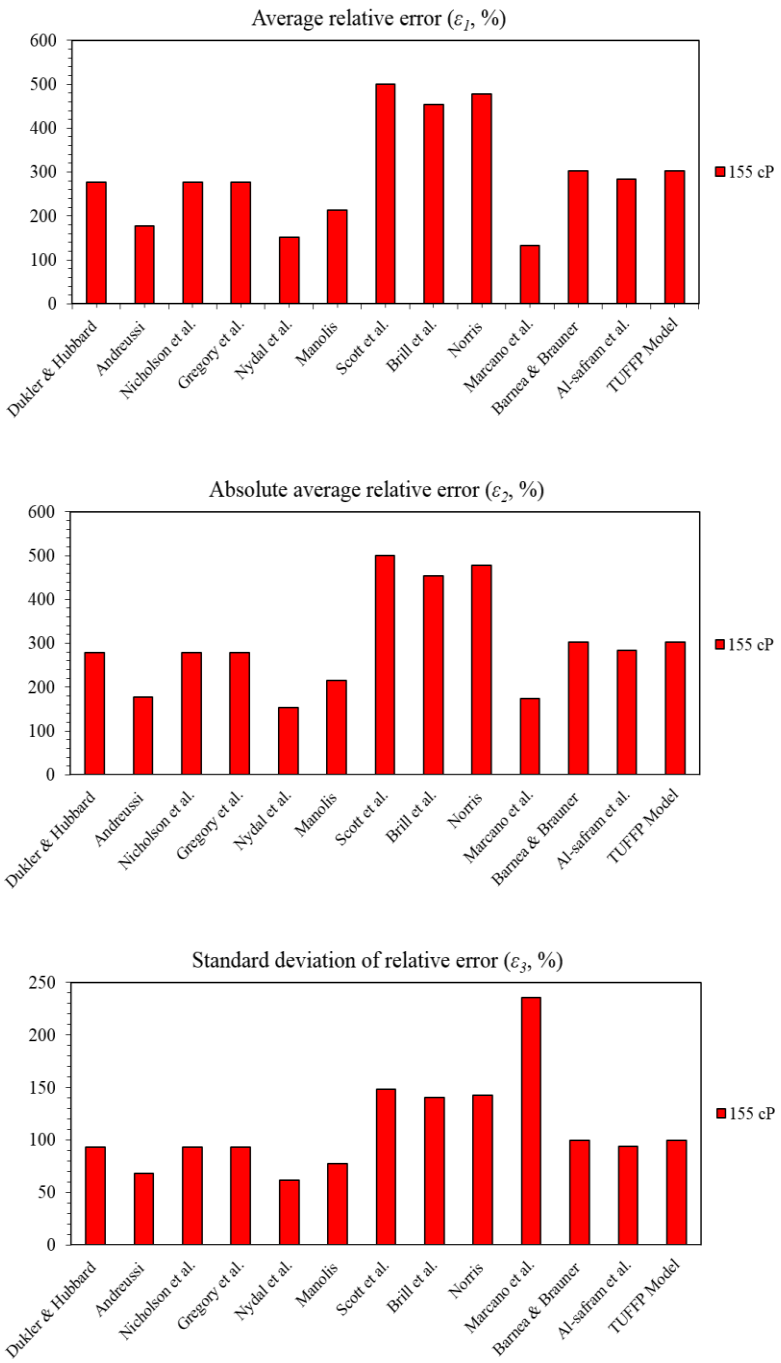

Figure 5.95 Model evaluation using the slug length experimental data reported by Brito (2012) from 2-in. ID pipes.

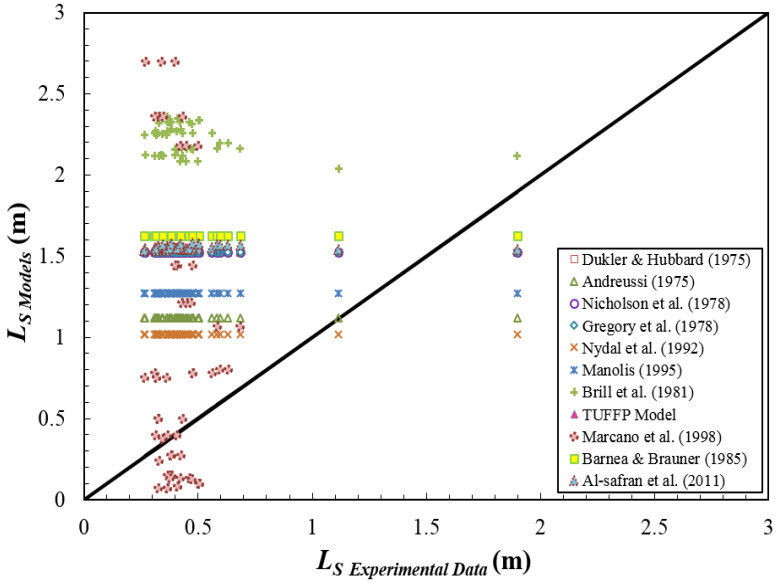

Figure 5.96 Comparison of model predictions against the Brito's (2012) measured slug length for μ_{Oil} = 155 cP when the pipe diameter is 2-in.

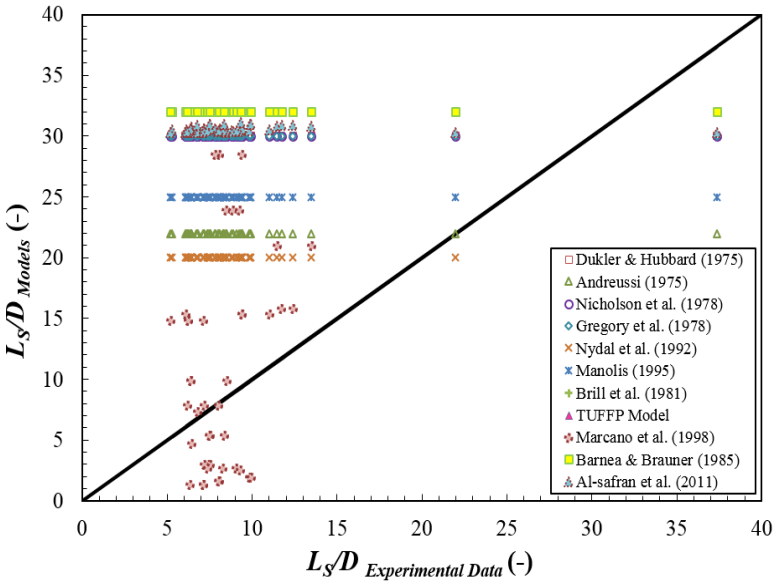

Figure 5.97 Comparison of model predictions against the Brito's (2012) measured dimensionless slug length for μ_{Oil} = 155 cP when the pipe diameter is 2-in.

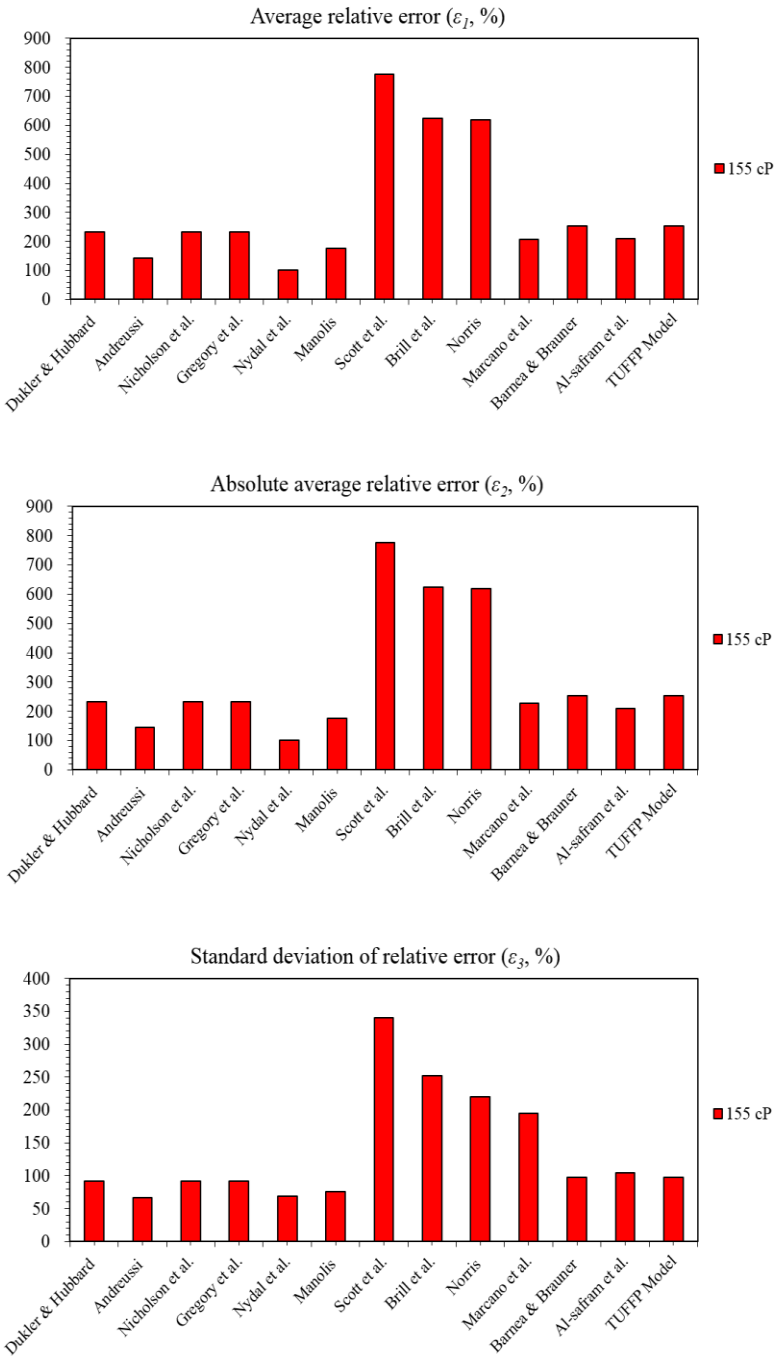

Figure 5.98 Model evaluation using the slug length experimental data acquired from both 2- and 3-in. ID pipes.

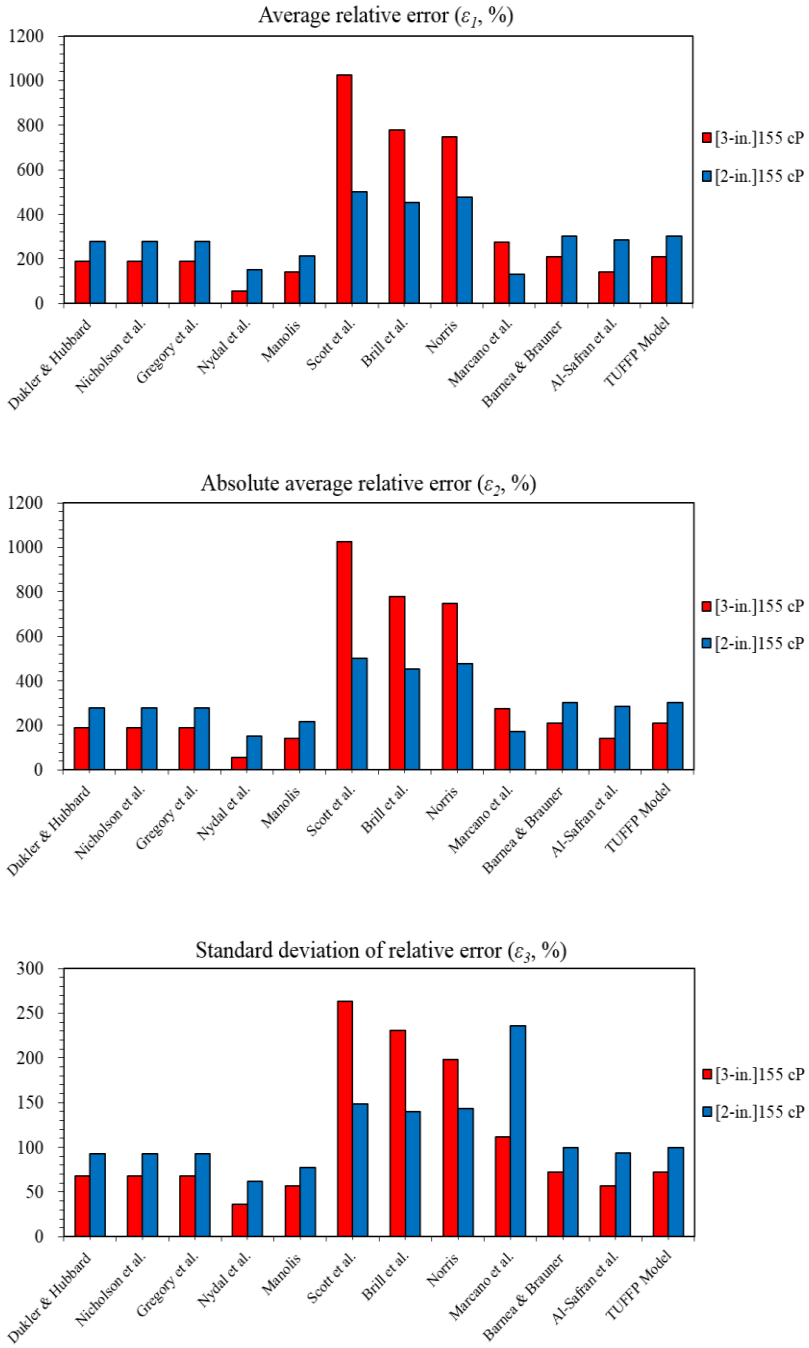

Figure 5.99 Model evaluation using the slug length experimental data acquired from 2- and 3-in. ID pipe, respectively.

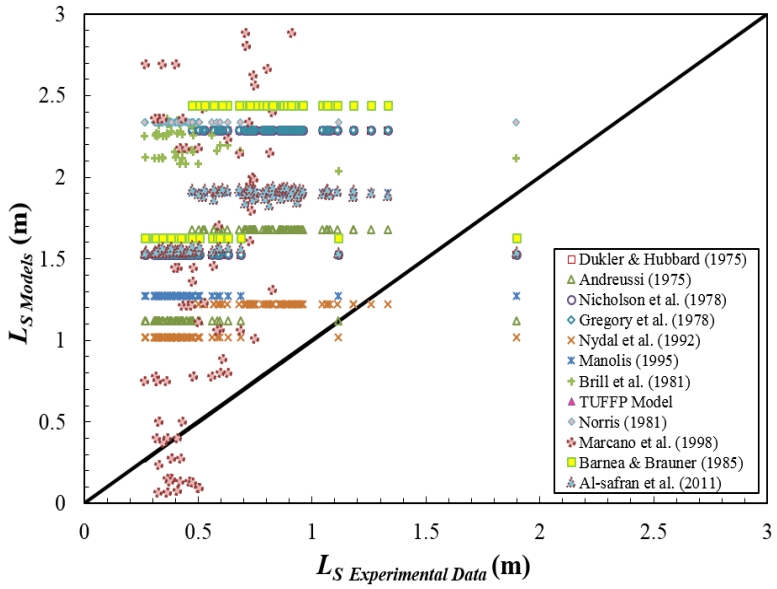

Figure 5.100 Comparison of model predictions against the measured slug length for μ_{Oil} = 155 cP acquired from both 2- and 3-in. ID pipes.

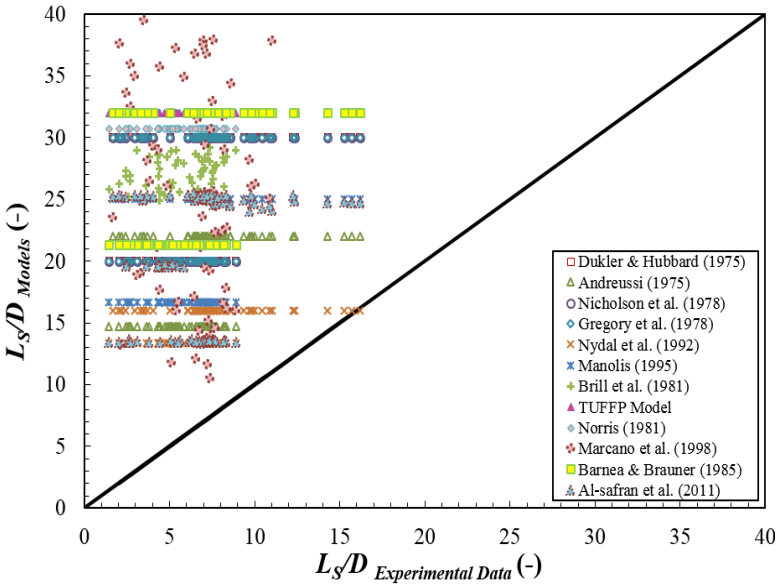

Figure 5.101 Comparison of model predictions against the measured dimensionless slug length for μ_{Oil} = 155 cP acquired from both 2- and 3-in. ID pipes.

5.4.5 Slug frequency

Comparison between model and experimental data for slug frequency is presented below.

5.4.5.1 3-in. ID pipes

The slug frequency data has been compared with Taitel & Dukler (1977), Gregory & Scott (1969), Greskovich & Shrier (1972), Heywood & Richardson (1979), Hill & Wood I (1990), Hill & Wood II (1990), Stapelberg & Mews (1994), TUFFP Unified, Zabaras (1999), Schulkes (2011), Gokcal (2008), and Tronconi (1990) models.

Gregory & Scott (1969) and Greskovich & Shrier (1972) models use the same correlation to predict the slug frequency. For 'all' of oil viscosities, these models under-predict the slug frequency with the average relative and absolute average relative errors of $\varepsilon_{1\ (3\text{-}in.)}$ = -28% and $\varepsilon_{2\ (3\text{-}in.)}$ = 50%. TUFFP Unified model also produces a negative value of $\varepsilon_{1\ (3\text{-}in.)}$ = -19%, indicating under-estimation of the slug frequency. In contrast, Heywood & Richardson (1979) model slightly over-estimates the slug frequency with an average relative error of $\varepsilon_{1\ (3\text{-}in.)}$ = 5.5%. This model gives the lowest absolute average relative error, $\varepsilon_{2\ (3\text{-}in.)}$, value of 49%. For these four models, there is no significant change of the average relative errors with an increase of the oil viscosity. Figure 5.110 shows the comparison of the best five models against the measured slug frequency for 'all' oil viscosities.

Taitel & Dukler (1997) and Hill & Wood II (1990) models present

higher average relative error, $\varepsilon_{1\ (3\text{-in.})}$, with values of 836% and 520%, respectively, indicating severe over-prediction of the slug frequency.

The model evaluation results for the slug frequency are presented in Figure 5.102. Figures 5.103 through 5.109 show the measured versus the predicted slug frequency for different oil viscosities. The details of the error analysis are tabled in Appendix F.

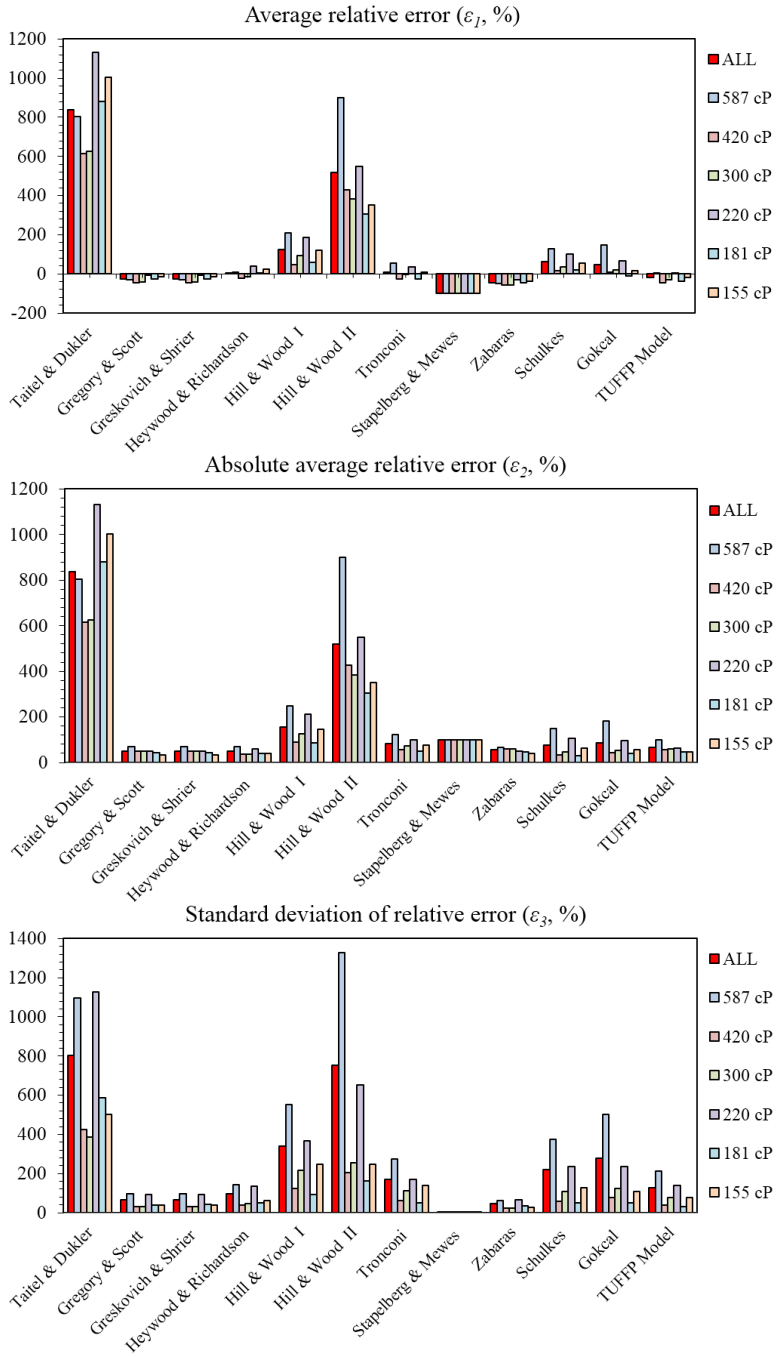

Figure 5.102 Model evaluation using the slug frequency experimental data acquired from 3-in. ID pipes.

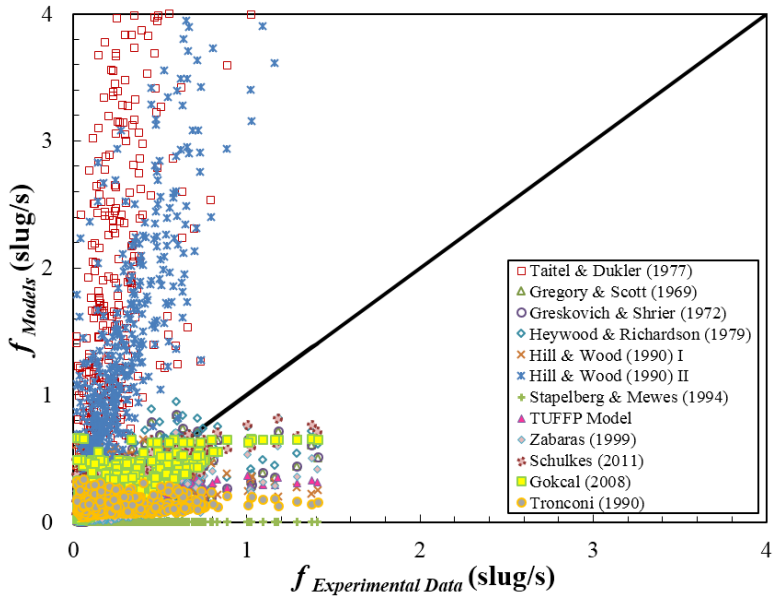

Figure 5.103 Comparison of model predictions against the measured slug frequency for 'all' oil viscosities when the pipe diameters is 3-in.

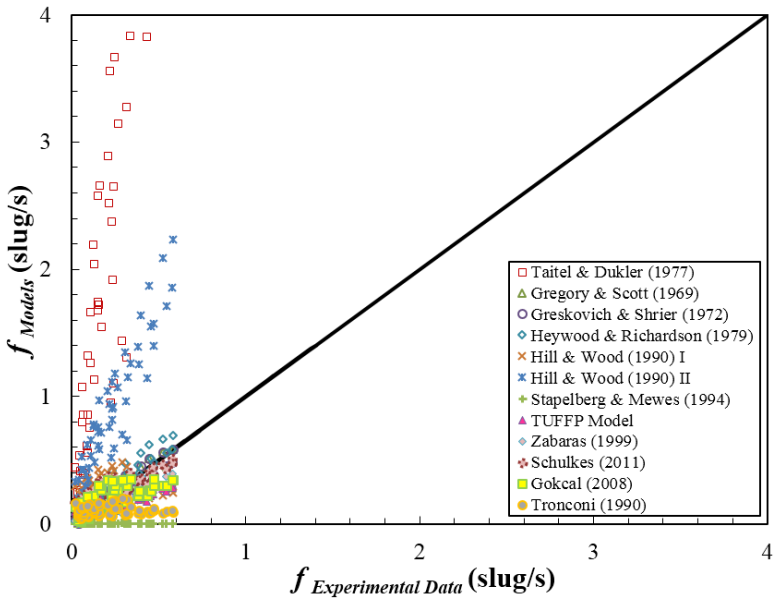

Figure 5.104 Comparison of model predictions against the measured slug frequency for μ_{Oil} = 155 cP when the pipe diameters is 3-in.

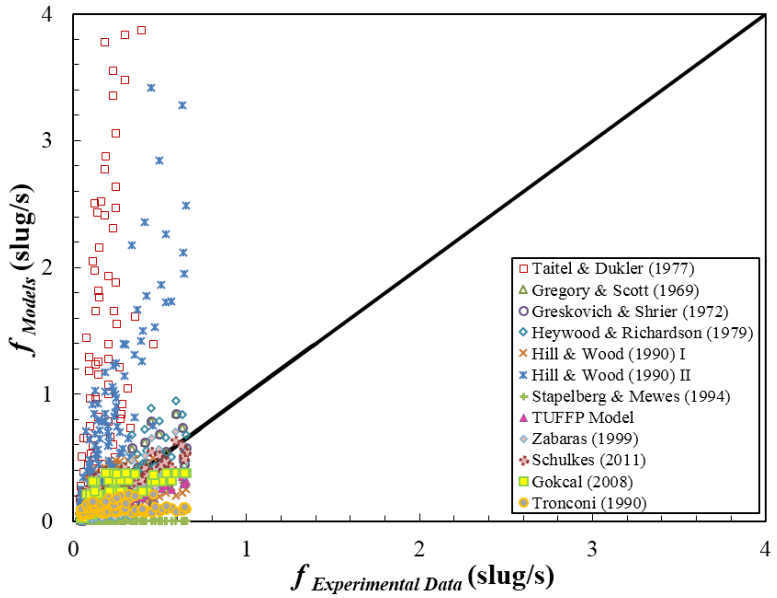

Figure 5.105 Comparison of model predictions against the measured slug frequency for μ_{Oil} = 181 cP when the pipe diameters is 3-in.

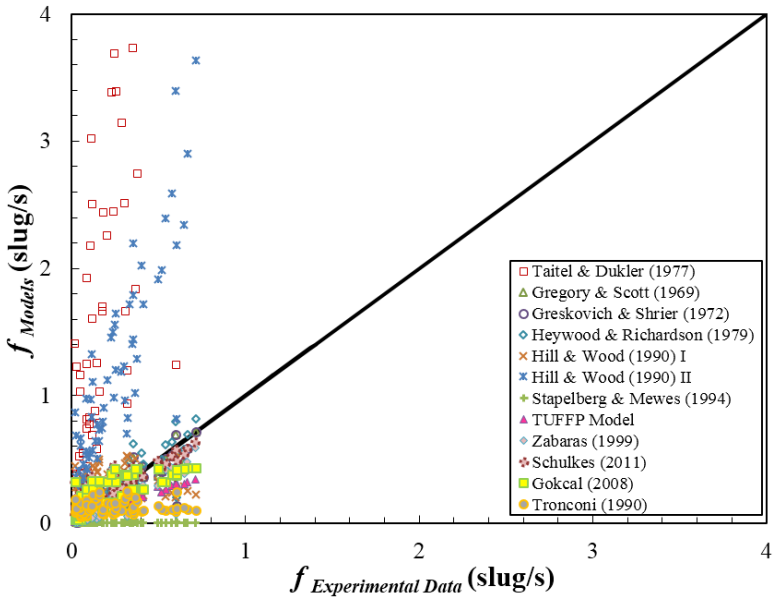

Figure 5.106 Comparison of model predictions against the measured slug frequency for μ_{Oil} = 220 cP when the pipe diameters is 3-in.

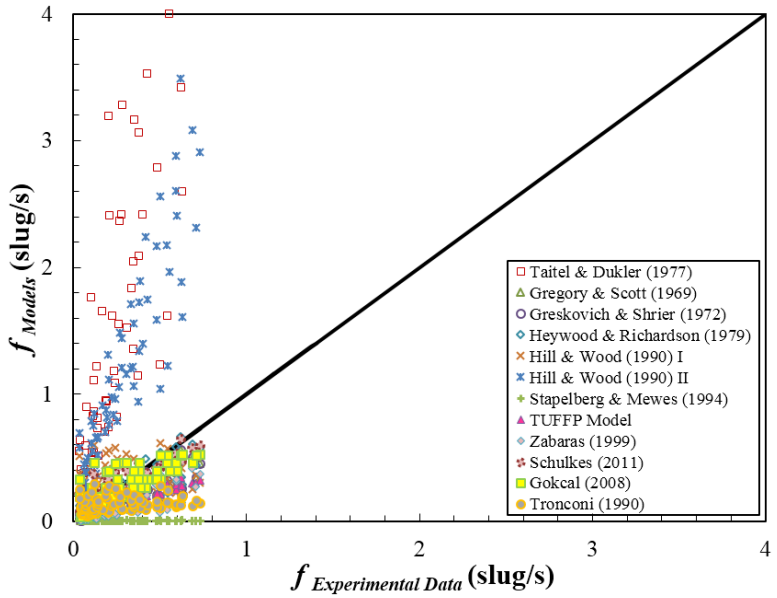

Figure 5.107 Comparison of model predictions against the measured slug frequency for μ_{Oil} = 300 cP when the pipe diameters is 3-in.

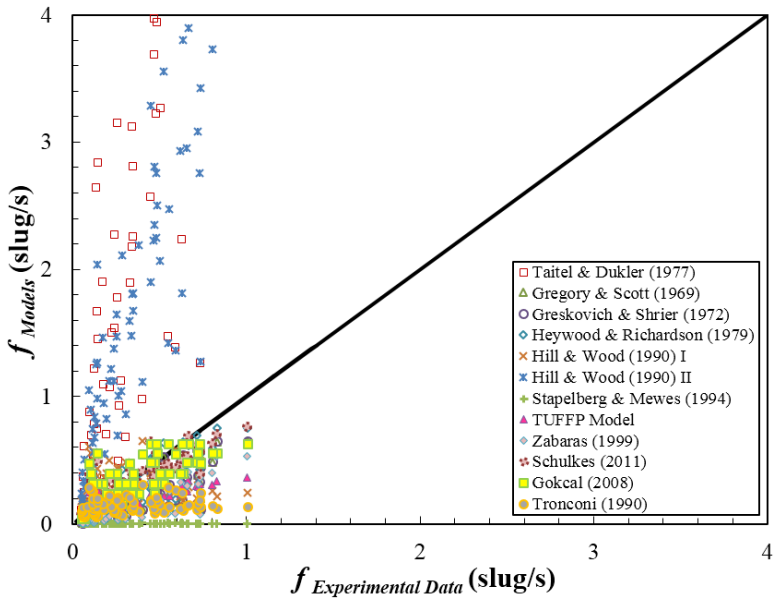

Figure 5.108 Comparison of model predictions against the measured slug frequency for μ_{Oil} = 420 cP when the pipe diameters is 3-in.

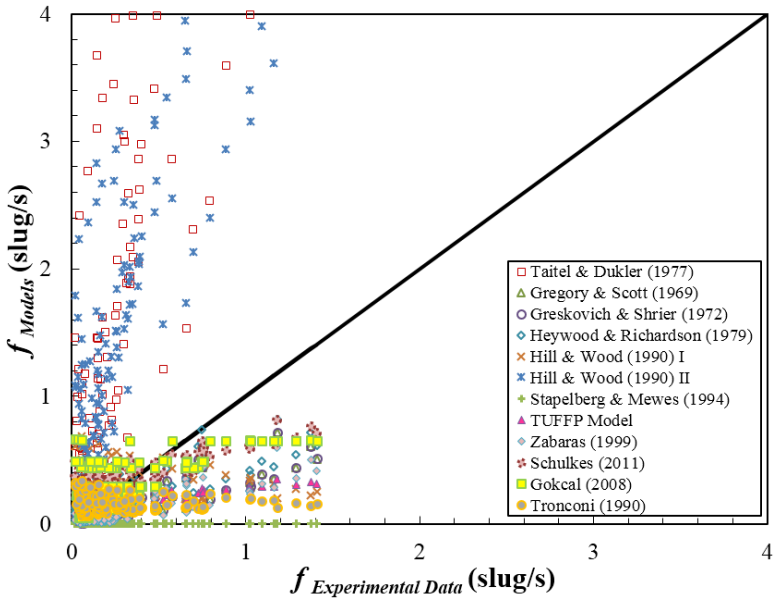

Figure 5.109 Comparison of model predictions against the measured slug frequency for μ_{Oil} = 587 cP when the pipe diameters is 3-in.

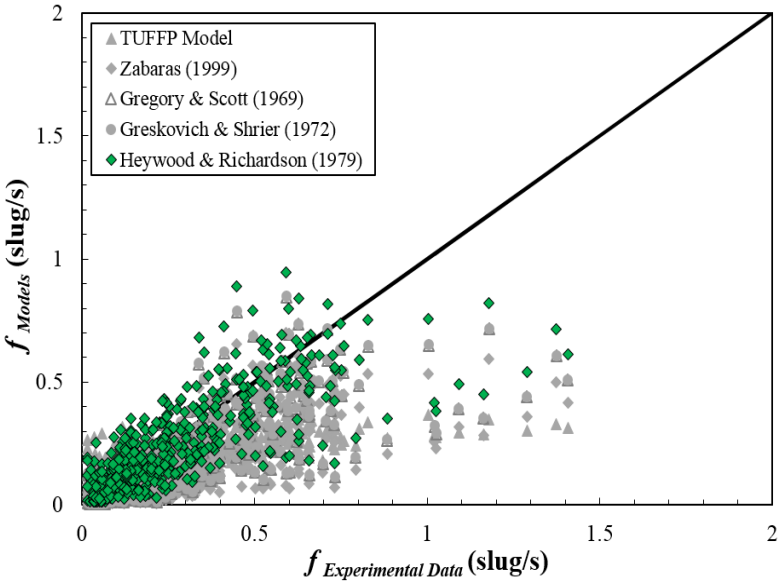

Figure 5.110 Comparison of the best five model predictions against the measured slug frequency for 'all' oil viscosities when the pipe diameters is 3-in.

5.4.5.2 2-in. ID pipes

The model evaluation results for the slug frequency are shown in Figure 5.111 when the pipe diameter is 2-in. Same as 3-in. ID pipes case, the considered models are the Taitel & Dukler (1977), Gregory & Scott (1969), Greskovich & Shrier (1972), Heywood & Richardson (1979), Hill & Wood I (1990), Hill & Wood II (1990), Stapelberg & Mews (1994), TUFFP Unified, Zabaras (1999), Schulkes (2011), Gokcal (2008), and Tronconi (1990) models.

For the 2-in. ID pipes case, Gokcal (2008) and Schulkes (2011) models present lower average relative and absolute average relative errors. The average relative, $\varepsilon_{1\ (2\text{-in.})}$, and the absolute average relative, $\varepsilon_{2\ (2\text{-in.})}$, errors calculated by Gokcal (2008) model are the values of 18% and 29%, respectively. Comparatively, Shulkes (2011) model presents a better agreement with a less over-estimation of the slug frequency with the average relative error of 4.6%. The details of the error analysis are tabled in Appendix F.

Figure 5.112 presents the comparison of the existing slug frequency prediction models against the measured slug frequency for μ_{Oil}=155 cP, and D=2-in. A graphical presentation using the selected models which give the suitable predictions is shown in Figure 5.113.

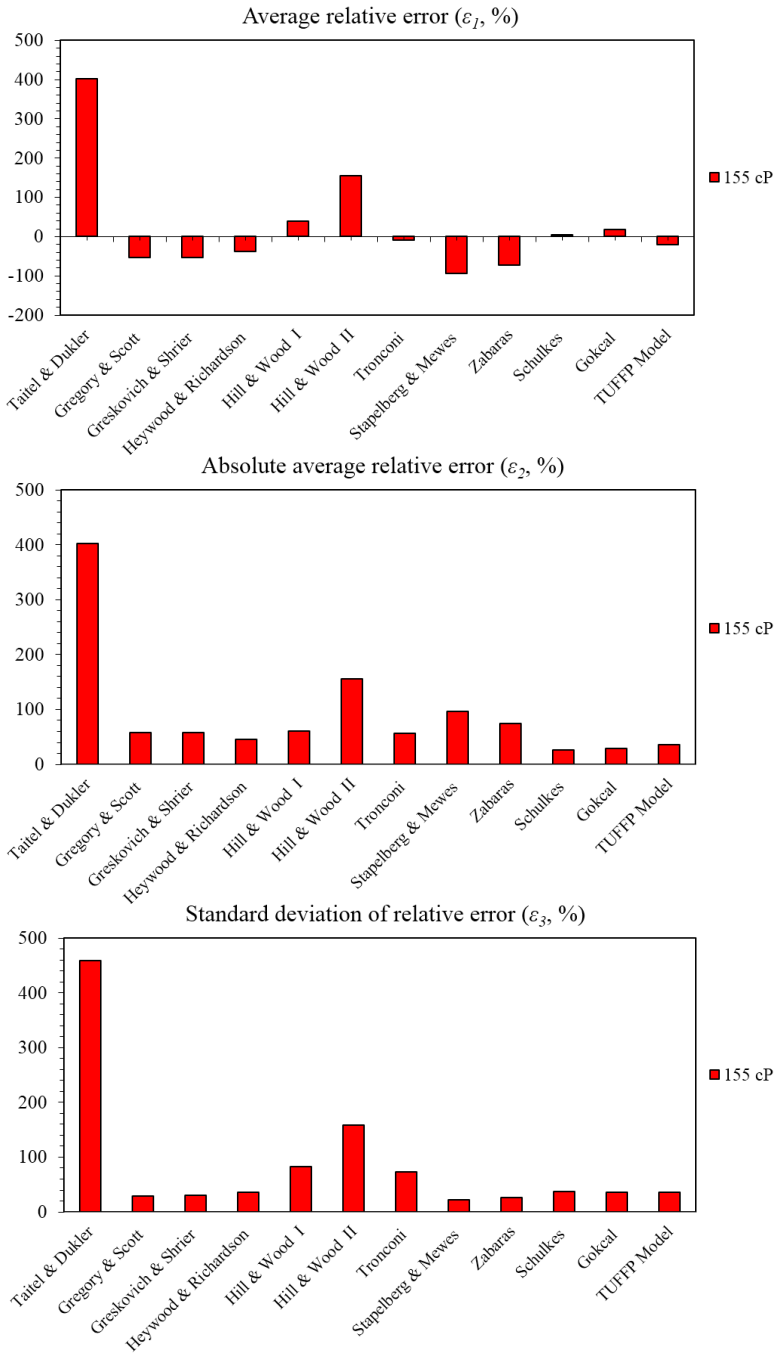

Figure 5.111 Model evaluation using the slug frequency experimental data reported by Brito (2012) from 2-in. ID pipes.

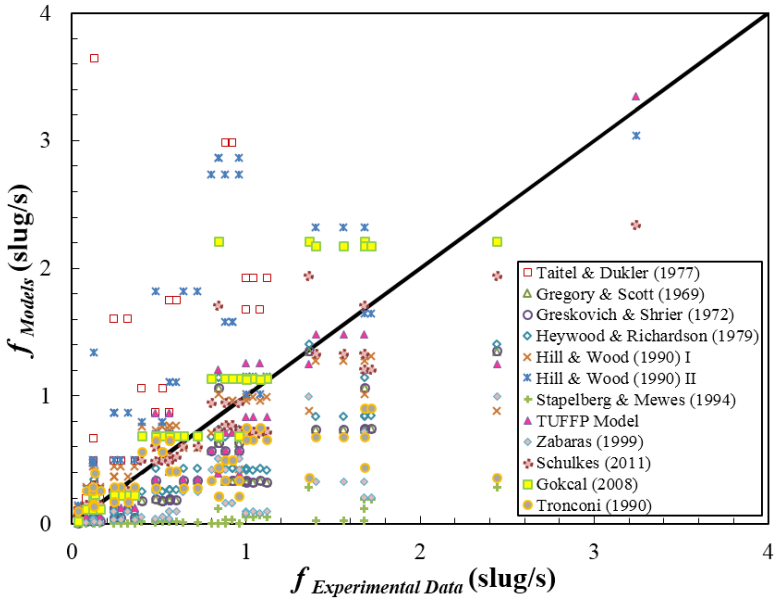

Figure 5.112 Comparison of model predictions against the Brito's (2012) measured slug frequency for μ_{Oil} = 155 cP when the pipe diameters is 2-in.

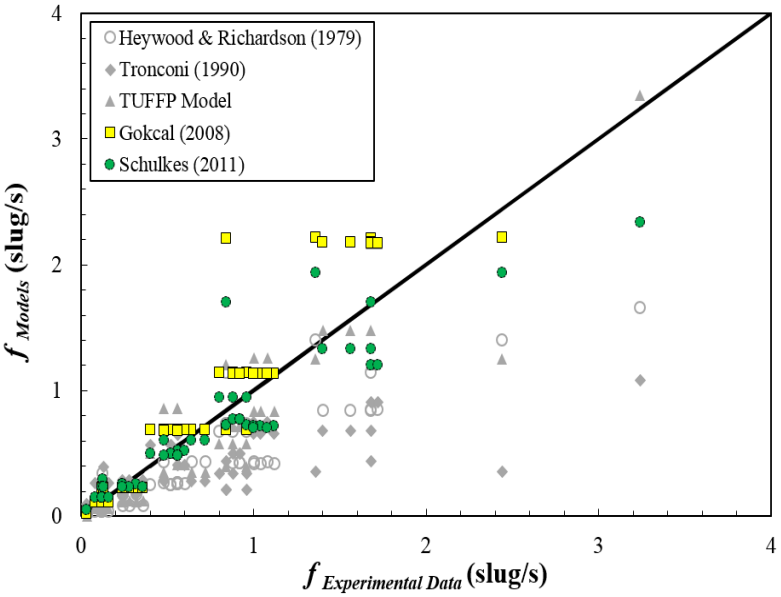

Figure 5.113 Comparison of the best five model predictions against the Brito's (2012) measured slug frequency for μ_{Oil} = 155 cP when the pipe diameters is 2-in.

5.4.5.3 Combined data of 2- and 3-in. ID pipes

When the data of 2- and 3-in. are combined, the models which can give the proper slug frequency predictions for both 2- and 3-in. ID pipes cases can be narrowed by TUFFP Unified, Gregory & Scott (1969), Greskovich & Shier (1972), Zabaras (1999), and Heywood & Richardson (1979). Among them, the model with lower average relative error ($\varepsilon_{1\ (2\text{-in.}+3\text{-in.})}$ = -5.8%) and absolute average relative error ($\varepsilon_{2\ (2\text{-in.}+3\text{-in.})}$ = 42.7%) correspond to the Heywood & Richardson (1979) model. The model evaluation results for the slug frequency are shown in Figures 5.114 and 5.115. Figures 5.116 and 5.117 present the comparison of the slug frequency experimental data acquired from both 2- and 3-in. ID pipes against the existing models.

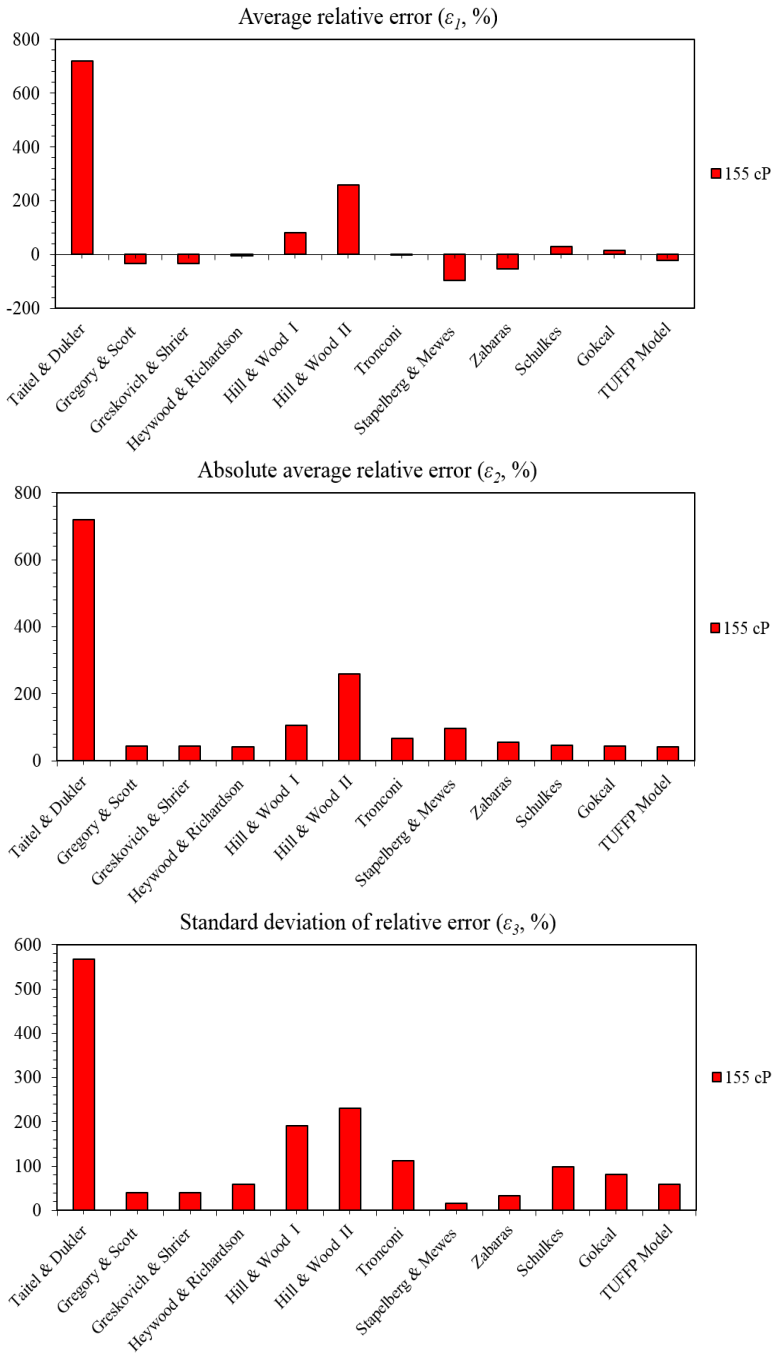

Figure 5.114 Model evaluation using the slug frequency experimental data acquired from both 2- and 3-in. ID pipes.

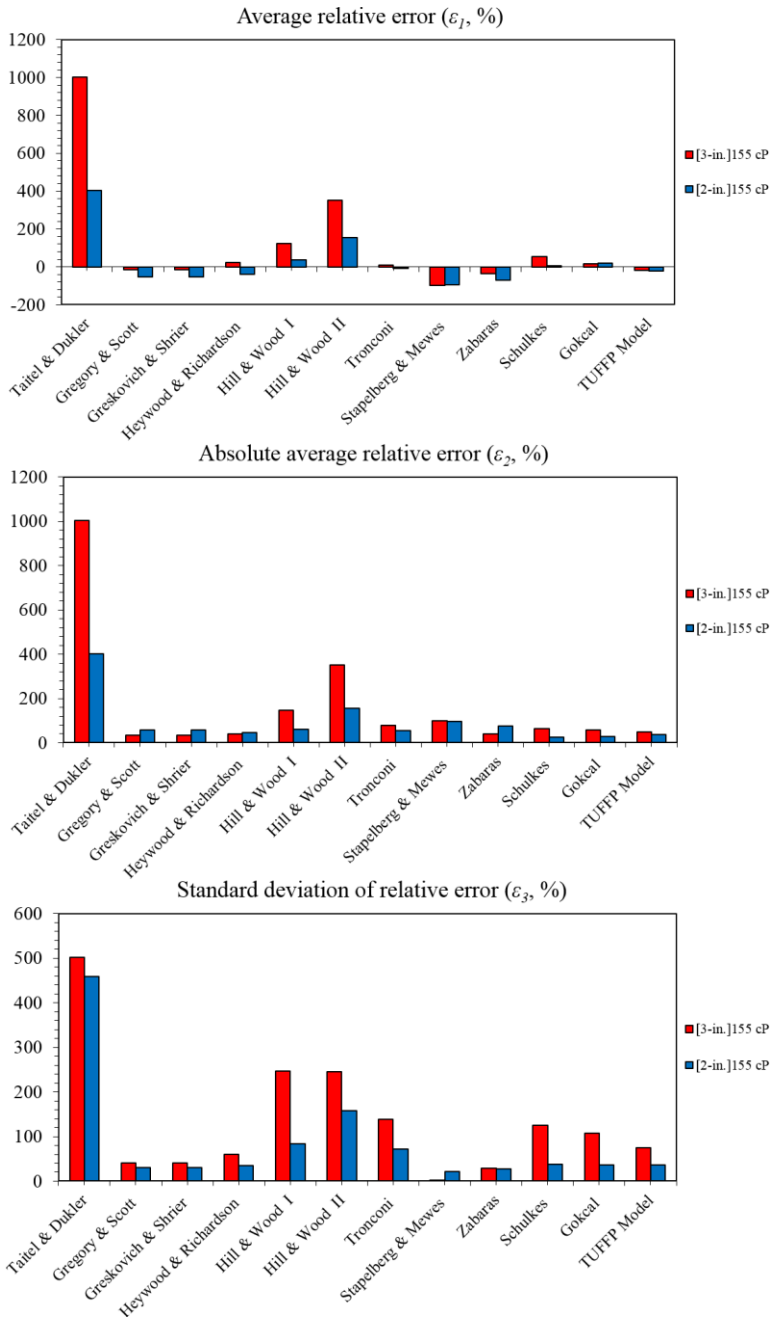

Figure 5.115 Model evaluation using the slug frequency experimental data acquired from 2- and 3-in. ID pipes, respectively.

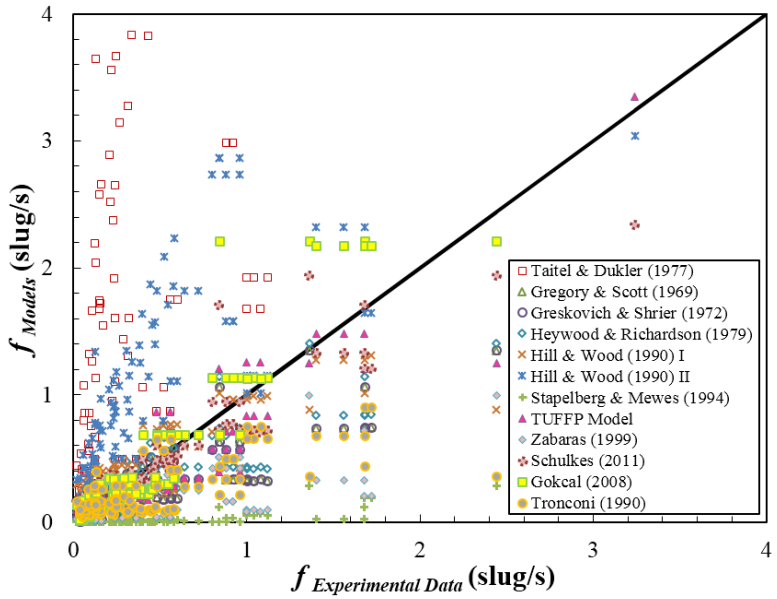

Figure 5.116 Comparison of model predictions against the measured slug frequency for μ_{Oil} = 155 cP acquired from both 2- and 3-in. ID pipes.

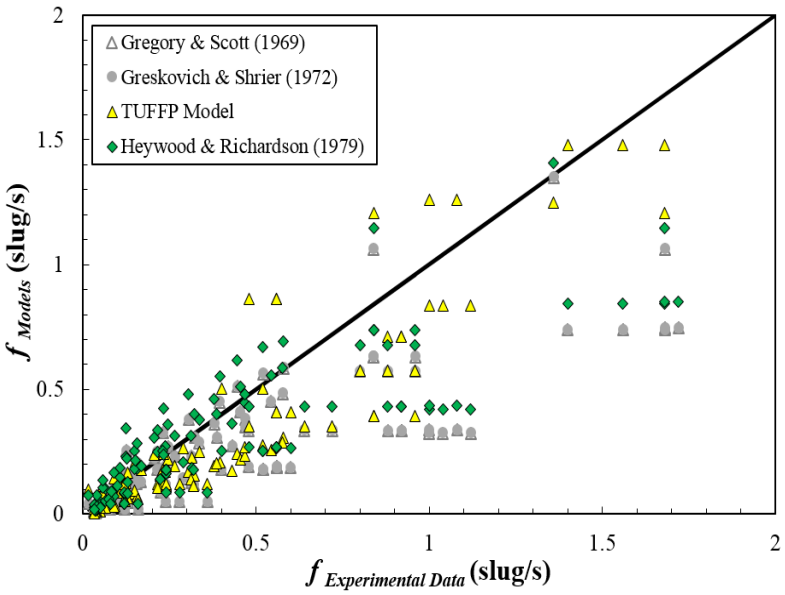

Figure 5.117 Comparison of the best four model predictions against the measured slug frequency for μ_{Oil} = 155 cP acquired from both 2- and 3-in. ID pipes.

5.4.6 Summary

This section presents the summarized table which shows the best models for each variables. These variables are pressure gradient, average liquid holdup, and slug characteristics such as slug and film liquid holdup, translational velocity, slug length, and slug frequency. The criteria to evaluate is based on the results of statistical analysis for 'all' oil viscosities and for each oil viscosity. Appendix F shows the more details of the statistical parameters.

Table 5.1 Best prediction models for variables.

					Statistical Parameter					
D_{pipe}	Variables	Model	No. of Data	Oil Viscosity (cP)	ε_1 (%)	ε_2 (%)	ε_3 (%)	ε_4	ε_5	ε_6
3-in.	Pressure Gradient dP/dL (Pa/m)	**TUFFP Model**	489	ALL	-22	26	16	-139	139	127
		TUFFP Model	119	587 cP	-28	28	8	-233	233	161
		TUFFP Model	72	420 cP	-24	25	10	-177	178	131
		TUFFP Model	71	300 cP	-19	24	19	-129	130	104
		TUFFP Model	70	220 cP	-21	22	12	-96	97	71
		TUFFP Model	96	181 cP	-19	23	16	-75	75	61
		TUFFP Model	61	155 cP	-16	26	26	-69	71	57
2-in.		**TUFFP Model**	82	ALL	-7	7	5	-80	87	87
		TUFFP Model	38	587 cP	-4	5	4	-79	93	101
		TUFFP Model	44	181 cP	-10	10	4	-81	81	74
2- and 3-in.		**TUFFP Model**	297	ALL	-19	21	13	-140	142	139
		TUFFP Model	157	587 cP	-22	22	12	-196	199	162
		TUFFP Model	140	181 cP	-16	19	14	-77	77	65
3-in.	Average Liquid Holdup $H_{LAverage}$ (-)	**TUFFP Model**	489	ALL	0.7	7.5	10.1	0.004	0.047	0.062
		TUFFP Model	119	587 cP	0.6	5.2	6.7	0.003	0.033	0.042
		TUFFP Model	72	420 cP	1.4	5.6	7.8	0.010	0.034	0.046
		TUFFP Model	71	300 cP	-13.5	14.2	9.3	-0.091	0.096	0.057
		TUFFP Model	70	220 cP	3.6	7.0	7.8	0.025	0.042	0.045
		TUFFP Model	96	181 cP	5.5	7.1	7.8	0.035	0.043	0.046
		TUFFP Model	61	155 cP	6.2	7.9	9.8	0.035	0.044	0.049
2-in.		**Xiao *et al* . (1990)**	82	ALL	5.5	9.7	11.5	0.033	0.063	0.077
		Xiao *et al* . (1990)	38	587 cP	4.8	11.7	13.8	0.026	0.077	0.094
		Xiao *et al* . (1990)	44	181 cP	6.1	7.9	9.2	0.039	0.051	0.058
2- and 3-in.		**TUFFP Model**	297	ALL	4.0	6.9	8.6	0.025	0.043	0.053
		TUFFP Model	157	587 cP	2.6	6.3	8.4	0.015	0.040	0.052
		TUFFP Model	140	181 cP	5.7	7.6	8.5	0.036	0.047	0.052
		Xiao *et al* . (1990)	297	ALL	4.0	6.8	8.5	0.023	0.043	0.055
		Xiao *et al* . (1990)	157	587 cP	1.7	6.3	8.8	0.007	0.042	0.059
		Xiao *et al* . (1990)	140	181 cP	6.6	7.3	7.3	0.040	0.045	0.045
3-in.	Slug Liquid Holdup H_{LLS} (-)	**Gregory (1978)**	489	ALL	-1.0	2.9	4.2	-0.010	0.027	0.037
		Gregory (1978)	119	587 cP	-1.4	4.1	5.8	-0.014	0.038	0.053
		Gregory (1978)	72	420 cP	-0.8	2.9	4.0	-0.008	0.026	0.035
		Gregory (1978)	71	300 cP	-2.8	3.1	3.0	-0.026	0.028	0.026
		Gregory (1978)	70	220 cP	-1.0	2.2	3.0	-0.009	0.020	0.027
		Gregory (1978)	96	181 cP	-0.5	1.7	2.0	-0.004	0.015	0.019
		Gregory (1978)	61	155 cP	0.6	3.2	4.4	0.004	0.029	0.038
2-in.		**Kora (2010)**	72	ALL	-0.6	0.8	0.9	-0.006	0.008	0.008
		Kora (2010)	36	587 cP	-0.9	1.0	0.8	-0.008	0.009	0.008
		Kora (2010)	36	181 cP	-0.3	0.7	0.9	-0.003	0.006	0.008
2- and 3-in.		**Gregory (1978)**	287	ALL	-1.7	3.2	4.5	-0.016	0.029	0.040
		Gregory (1978)	155	587 cP	-1.8	3.9	5.4	-0.017	0.035	0.048
		Gregory (1978)	132	181 cP	-1.5	2.4	3.1	-0.014	0.021	0.027
		Kora (2010)	287	ALL	1.6	2.8	3.7	0.015	0.025	0.032
		Kora (2010)	155	587 cP	0.9	2.8	4.1	0.008	0.025	0.037
		Kora (2010)	132	181 cP	2.5	2.7	2.8	0.022	0.025	0.024

3-in.	Film Liquid Holdup $H_{LAverage}$ (-)	**TUFFP Model**	489	ALL	3.0	10.4	13.0	0.016	0.058	0.072
		TUFFP Model	119	587 cP	0.4	9.8	12.0	0.000	0.057	0.070
		TUFFP Model	72	420 cP	2.5	11.6	14.4	0.013	0.066	0.081
		TUFFP Model	71	300 cP	1.1	11.2	14.2	0.006	0.061	0.077
		TUFFP Model	70	220 cP	2.8	9.8	11.9	0.017	0.054	0.066
		TUFFP Model	96	181 cP	6.1	9.9	12.2	0.035	0.055	0.066
		TUFFP Model	61	155 cP	6.1	11.0	12.9	0.032	0.058	0.067
2-in.		**TUFFP Model**	71	ALL	-15.8	18.3	14.1	-0.097	0.113	0.084
		TUFFP Model	35	587 cP	-12.8	15.5	13.2	-0.074	0.090	0.076
		TUFFP Model	36	181 cP	-18.8	21.1	14.5	-0.119	0.134	0.087
2- and 3-in.		**TUFFP Model**	286	ALL	-1.7	11.9	15.2	-0.012	0.070	0.089
		TUFFP Model	154	587 cP	-2.6	11.1	13.5	-0.017	0.065	0.078
		TUFFP Model	132	181 cP	-0.7	12.9	17.0	-0.007	0.077	0.100
3-in.	Translational Velocity v_T (m/s)	**Choi *et al* . (2012)**	465	ALL	-6.4	9.6	9.2	-0.096	0.222	0.280
		Choi *et al* . (2012)	112	587 cP	-3.7	8.7	9.6	-0.004	0.212	0.330
		Choi *et al* . (2012)	72	420 cP	-4.1	9.2	11.0	-0.015	0.226	0.348
		Choi *et al* . (2012)	65	300 cP	-6.3	9.6	8.6	-0.084	0.220	0.242
		Choi *et al* . (2012)	63	220 cP	-8.3	10.1	8.0	-0.160	0.222	0.204
		Choi *et al* . (2012)	92	181 cP	-8.0	9.9	8.3	-0.156	0.217	0.209
		Choi *et al* . (2012)	61	155 cP	-9.8	10.7	7.1	-0.215	0.244	0.201
2-in.		**Choi *et al* . (2012)**	82	ALL	-0.1	10.1	13.6	-0.032	0.173	0.231
		Choi *et al* . (2012)	38	587 cP	-6.8	10.2	10.3	-0.089	0.197	0.251
		Choi *et al* . (2012)	44	181 cP	5.6	9.9	13.5	0.016	0.152	0.202
2- and 3-in.		**Choi *et al* . (2012)**	286	ALL	-4.1	9.5	10.9	-0.061	0.202	0.275
		Choi *et al* . (2012)	150	587 cP	-4.5	9.1	9.9	-0.026	0.208	0.313
		Choi *et al* . (2012)	136	181 cP	-3.6	9.9	12.0	-0.100	0.196	0.221
3-in.	Slug Length L_S (m)	**None of the models show a satisfactory result**								
2-in.		**None of the models show a satisfactory result**								
2- and 3-in.		**None of the models show a satisfactory result**								
3-in.	Slug Frequency f_S (slug/s)	**Heywood & Richardson (1979)**	489	ALL	5.5	49.0	97.3	-0.034	0.095	0.143
		Heywood & Richardson (1979)	119	587 cP	7.8	71.2	144.0	-0.102	0.141	0.195
		Heywood & Richardson (1979)	72	420 cP	-23.5	36.9	37.4	-0.083	0.108	0.125
		Heywood & Richardson (1979)	71	300 cP	-15.2	35.3	46.0	-0.060	0.081	0.096
		Heywood & Richardson (1979)	70	220 cP	39.6	58.4	136.2	0.027	0.068	0.097
		Heywood & Richardson (1979)	96	181 cP	3.7	39.5	48.9	0.017	0.084	0.118
		Heywood & Richardson (1979)	61	155 cP	23.4	39.9	60.6	0.036	0.056	0.066
2-in.		**Schulkes (2011)**	55	155 cP	4.6	26.1	37.7	-0.091	0.186	0.301
2- and 3-in.		**Heywood & Richardson (1979)**	116	155 cP	-5.8	42.7	58.8	-0.143	0.202	0.357

Chapter 6 Simplified Lockhart and Martinelli's Separated Pressure Gradient Prediction Model

As can be seen in section 5.2, available pressure gradient prediction models and correlations do not perform well for 3-in. ID pipes. Most of the existing models calculate the pressure gradient by using a force balance over a slug unit. However, the used variables for this term such as slug and film length are calculated by being based on the experimenter's subjectivity, showing some degree of discrepancy with larger pipe diameter. This may occurs enormous errors to predict pressure gradient. Reinvestigation for more accurate prediction of the pressure gradient is needed in this study.

In the original Lockhart and Martinelli's (1949) separated model, there are some values showing extreme gap between the present data and original separated model due to the over-prediction or minus values (see Figures 6.2(b) and 6.3). This is mainly caused by the misapplication of Reynolds numbers that should be separately calculated by being based on the fluid phase. This model was modified and simplified to predict pressure gradient changing the Chisholm's (1967) coefficients. Figure 6.1 summarizes the solution procedure and Table 6.1 shows coefficient values of C.

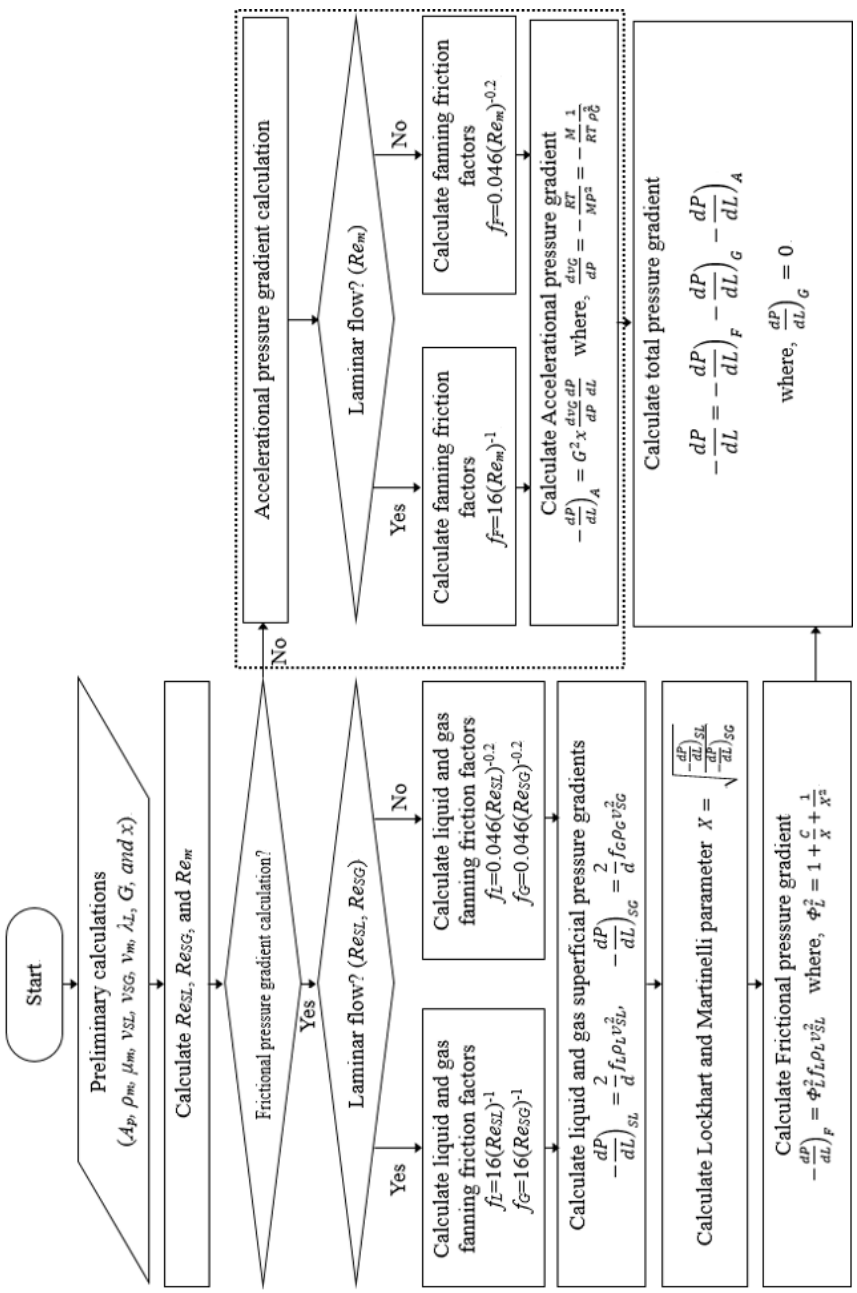

Figure 6.1 The solution procedure of the original Lockhart and Martinelli's (1949) separated model. In the procedure, correlation coefficient C was changed by the input variables such as v_{SL}, μ_{Oil}, and d, fundamentally based on the Chisholm's (1967) classification.

Table 6.1 Chisholm's (1967) correlation coefficients.

Liquid-Phase	Gas-Phase	C
Turbulent	Turbulent	20
Laminar	Turbulent	12
Turbulent	Laminar	10
Laminar	Laminar	5

The Lockhart and Martinelli's (1949) separated model is limited to the calculation of the frictional pressure losses in horizontal pipes, so the accelerational pressure gradient is calculated by homogeneous no-slip model. The Reynolds numbers in the Lockhart and Martinelli's model to calculate the frictional pressure gradient are separated to Re_{SL} and Re_{SG}. Because of high viscous oil in this study, Re_{SL} always shows laminar flow and Re_{SG} shows turbulent flow, indicating other ways to calculate the Fanning friction factors. On the other hands, the Reynolds number used in the homogeneous no-slip model is mixture Reynolds number, assuming no slippage occurs between the phases. Moreover, the steady-state flow was able to be assumed in relatively shorter time because of high viscous oil property in this experiment, so the accelerational pressure gradient term can be subtracted from the original separated model. It also has little effect on the total pressure gradient ($\leq$ 10%) in high viscous oil flow.

As can be seen in Figures 6.2 and 6.3, there are some values showing extreme gap between the present data and original separated model due to the over-prediction or minus values occurred by using the accelerational pressure gradient. The prediction from simplified Lockhart and Martinelli's separated model are relatively stable and presents lower absolute average relative error, subtracting the accelerational pressure gradient term.

Chisholm's (1967) correlation coefficients were also reconsidered to predict pressure gradient more properly. Previous coefficient was calculated by Eqs (111) and (112) to use it in Eq. (113), assuming annular flow and zero slip conditions. The coefficients for other flow patterns were empirically predicted and recommended to be modified by further study in Chisholm (1967).

$$Z = \left(\frac{\rho_L}{\rho_G} \right)^{0.5} \tag{111}$$

$$C = Z + \frac{1}{Z} \tag{112}$$

$$\varphi^2{}_L = 1 + \frac{C}{X} + \frac{1}{X^2} \tag{113}$$

where X is the square root of the ratio of the liquid superficial pressure gradient to the gas superficial pressure gradient.

However, the square roots of liquid-gas density ratio are higher than 20 in this study, so the sensitivity analysis was performed to investigate suitable value. As can be seen in Eq. (114), putting weight to the coefficients depending on the input variables such as superficial liquid velocity and oil viscosity shows better performance for predicting pressure gradient in both pipe diameters and viscosities. The absolute average relative errors are much lower than the existing models and original separated model (see Tables 6.2).

$$\begin{aligned} v_{SL} * \mu_{Oil} &< 30, \qquad C = 12 \\ v_{SL} * \mu_{Oil} &> 30, \qquad C = 20 \end{aligned} \tag{114}$$

where v_{SL} is superficial liquid velocity in m/s and μ_{Oil} is oil viscosity in cP.

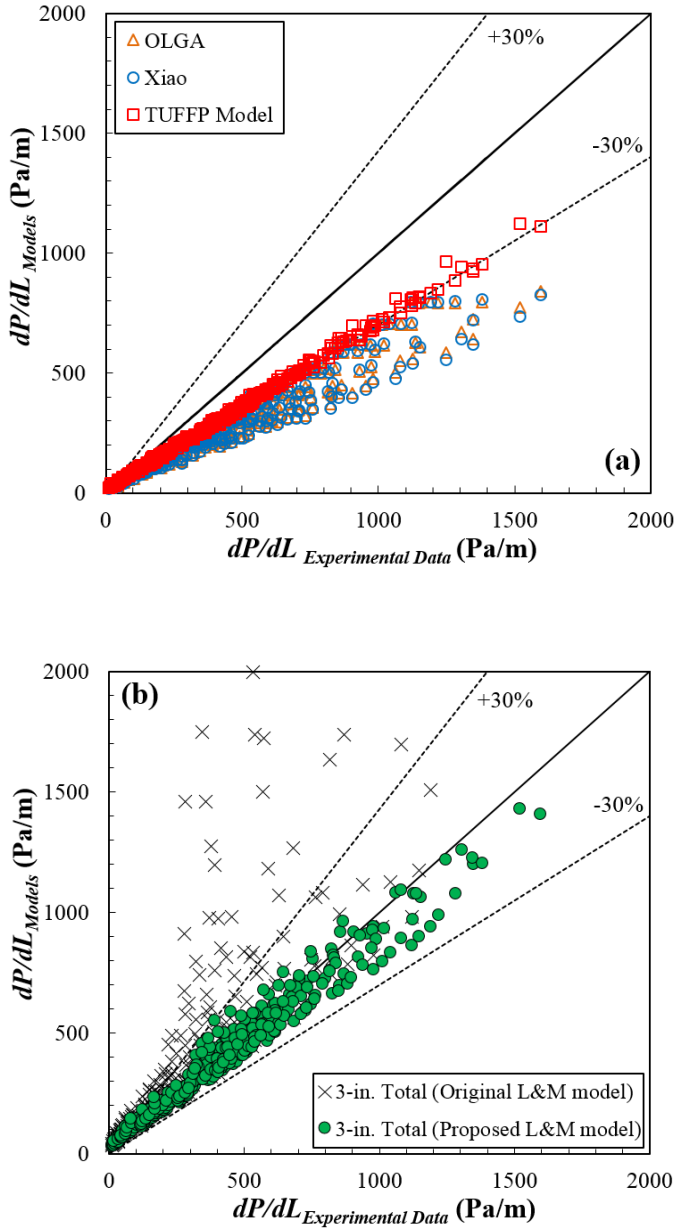

Figure 6.2 (a) Comparison between TUFFP, OLGA, and Xiao *et al*. (1990) model prediction and measured pressure gradients for 'all' oil viscosities when *d*=3-in. (b) Comparison between original and simplified Lockhart and Martinelli's (1949) separated model prediction with measured pressure gradients for *d*=3-in.

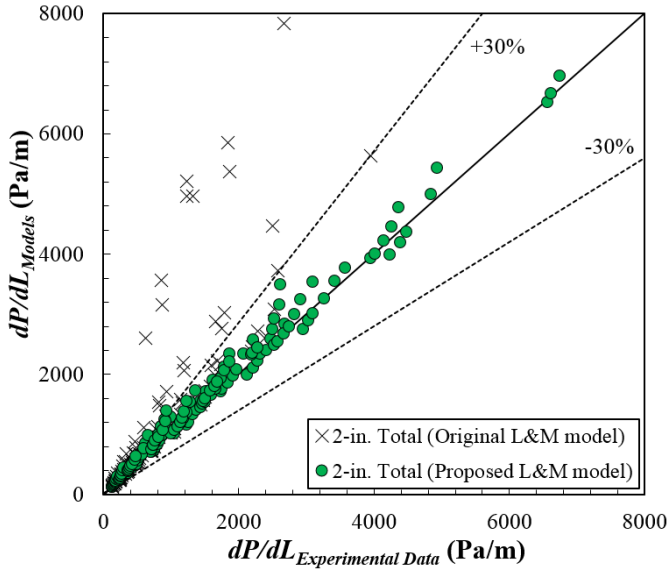

Figure 6.3 Comparison between original and simplified Lockhart and Martinelli's (1949) separated model prediction with the Gokcal's (2008) measured pressure gradients for *d*=2-in.

Table 6.2 Model evaluation using the measured pressure gradient of 3-in. ID pipes.

Model	No. of Data	Oil Viscosity (cP)	Statistical Parameter					
			ε_1 (%)	ε_2 (%)	ε_3 (%)	ε_4 (Pa/m)	ε_5 (Pa/m)	ε_6 (Pa/m)
TUFFP Model	489	ALL	-22	26	16	-139	139	127
OLGA	489	ALL	-31	33	17	-185	186	173
Xiao	489	ALL	-32	34	17	-186	187	175
Original Lockhart&Marintelli's Separated Model ALL	489	ALL	-388	1115	6619	-631	1751	8719
Proposed Model ALL	**489**	**ALL**	**6**	**19**	**32**	**-32**	**64**	**91**
TUFFP Model	119	587 cP	-28	28	8	-233	233	161
OLGA	119	587 cP	-34	34	10	-286	286	209
Xiao	119	587 cP	-34	34	10	-287	288	211
Original Lockhart&Martinelli's Separated Model 587cP	119	587 cP	-43	119	466	-512	1236	4419
Proposed Model 587cP	**119**	**587 cP**	**-4**	**15**	**17**	**-80**	**118**	**138**
TUFFP Model	72	420 cP	-24	25	10	-177	178	131
OLGA	72	420 cP	-31	32	12	-229	229	187
Xiao	72	420 cP	-32	32	12	-231	231	190
Original Lockhart&Martinelli's Separated Model 420cP	72	420 cP	-221	294	1815	-2418	2874	18484
Proposed Model 420cP	**72**	**420 cP**	**1**	**17**	**23**	**-54**	**88**	**100**
TUFFP Model	71	300 cP	-19	24	19	-129	130	104
OLGA	71	300 cP	-30	33	22	-189	190	173
Xiao	71	300 cP	-30	34	21	-190	191	176
Original Lockhart&Martinelli's Separated Model 300cP	71	300 cP	-28	147	337	-500	982	2706
Proposed Model 300cP	**71**	**300 cP**	**10**	**20**	**34**	**-15**	**52**	**65**
TUFFP Model	70	220 cP	-21	22	12	-96	97	71
OLGA	70	220 cP	-32	33	15	-144	145	126
Xiao	70	220 cP	-33	33	15	-145	145	128
Original Lockhart&Martinelli's Separated Model 220cP	70	220 cP	-224	340	1667	-1226	1636	8131
Proposed Model 220cP	**70**	**220 cP**	**10**	**19**	**29**	**-5**	**38**	**48**
TUFFP Model	96	181 cP	-19	23	16	-75	75	61
OLGA	96	181 cP	-31	33	18	-109	109	99
Xiao	96	181 cP	-31	34	18	-109	110	99
Original Lockhart&Martinelli's Separated Model 181cP	96	181 cP	149	222	794	497	890	3406
Proposed Model 181cP	**96**	**181 cP**	**11**	**20**	**33**	**-5**	**29**	**36**
TUFFP Model	61	155 cP	-16	26	26	-69	71	57
OLGA	61	155 cP	-28	35	25	-100	102	89
Xiao	61	155 cP	-29	35	24	-101	102	88
Original Lockhart&Martinelli's Separated Model 155cP	61	155 cP	108	518	2276	2	1846	8419
Proposed Model 155cP	**61**	**155 cP**	**18**	**29**	**53**	**-8**	**27**	**31**

Figure 6.4 presents the comparison of the proposed model against the Brito's (2012) measured pressure gradient data for low and medium viscous oils (39, 60, and 108 cP) using 2-in. ID pipes. Figure 6.4(a) shows a great agreement between the proposed model and experimental data, including the similar range of superficial liquid and gas velocities with this 3-in. study. However, as oil viscosity decreases, the effect of accelerational pressure gradient on the total pressure gradient becomes increasing (≥ 30%) especially for higher superficial liquid and gas velocities, showing the gap between the measured and predicted values (see Figure 6.4(b)). Further studies are needed to reflect the effect of accelerational term when the oil viscosity is relatively low and superficial liquid and gas velocities are high.

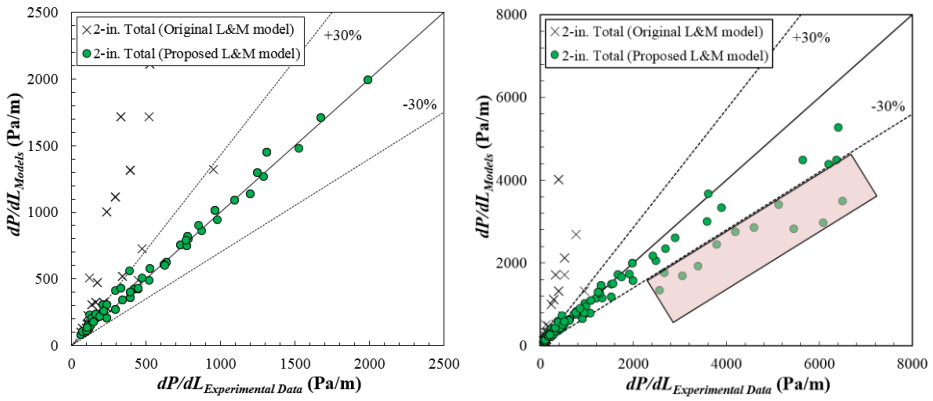

Figure 6.4 Comparison between original and simplified Lockhart and Martinelli's (1949) separated model prediction with the Brito's (2012) measured pressure gradients for d=2-in, (a) using the similar range of v_{SL} and v_{SG} with this study and (b) using the entire range of v_{SL} and v_{SG} of Brito's (2012) study.

Chapter 7 Conclusions and Recommendations

This experimental study presents the pipe diameter effect on oil and gas two-phase slug flow characteristics in horizontal pipes. The performed experiments include two different pipe diameters (2- and 3-in. ID) with three different oil viscosities (155, 181, and 587 cP). Based on pipe diameters, the changing aspect of slug flow characteristics were qualitatively analyzed and the existing closure relationships were quantitatively tested to evaluate their performance. The suitable correlations were presented by this study for matching specific cases. Moreover, simplified Lockhart and Martinelli's (1949) separated pressure gradient prediction model was suggested comparing with present data. The following conclusions summarize the experimental results and model evaluations in this study.

7.1 Conclusions

7.1.1 3-in. ID pipes results

7.1.1.1 Flow pattern map

1. Three types of the existing flow patterns: Elongated Bubble, Slug, and Annular flow were observed for the studied flow conditions.
2. Transition boundaries between Elongated Bubble to Slug, Slug to Annular, and Slug to Dispersed Bubble flow were monitored

corresponding to the studied flow conditions.

3. Most of the experimental points observed in this study are located on intermittent flow regime. Among them, the main flow regime is slug flow.
4. Classification between elongated bubble and slug flow was based on slippage and eddy structure at the slug front.
5. The range of the elongated bubble flow regime is slightly narrowed when oil viscosity increases.
6. The range of the slug flow regime slightly expands when oil viscosity increases, because slug front eddy formation is delayed as the oil viscosity decreases.
7. As oil viscosity increases, annular flow occurs at relatively high superficial gas velocity.
8. The observed flow pattern data are compared with Taitel & Dukler (1976), Barnea (1985), and TUFFP unified (2003) models, indicating that all of the models present some discrepancies to predict transition boundaries.

7.1.1.2 Pressure gradient

1. For a given superficial liquid velocity and oil viscosity, pressure gradient increases with increasing superficial gas velocity.
2. For a given superficial gas velocity and oil viscosity, pressure gradient increases with superficial liquid velocity increase.
3. For a given superficial liquid and gas velocity, pressure gradient

increases for higher oil viscosities.

4. The measured pressure gradient is compared with TUFFP Unified, OLGA, and Xiao *et al*. (1990) models. Statistical parameters present that the three models give relatively large absolute average relative errors of 26%, 33%, and 34%, respectively, under-estimating in all of the cases.
5. Simplified Lockhart and Martinelli's (1949) separated model was suggested subtracting the accelerational pressure gradient term from the original equation. This model presents much better performance than other relationships but also requiring further theoretical studies.

7.1.1.3 Average liquid holdup

1. The results of static calibration show linear trend of capacitance sensor voltage and liquid level. The minimum voltage values were able to be estimated with static calibration.
2. For a constant oil viscosity and superficial gas velocity, average liquid holdup increases as superficial liquid velocity increases.
3. At a given superficial liquid and gas velocity, average liquid holdup slightly increases with oil viscosity increase.
4. Experimental results for the average liquid holdup are compared with predictions by TUFFP Unified, OLGA, and Xiao *et al*. (1990) models. The absolute average relative errors of all models slightly increase as oil viscosity decreases. TUFFP Unified model presents the lowest absolute average relative errors, $\varepsilon_{2\,(3\text{-in.})}$, for all viscosities.

7.1.1.4 Slug liquid holdup

1. Slug liquid holdup slightly increases with an increase of superficial liquid velocity.
2. As superficial gas velocity increases, slug liquid holdup decreases for all oil viscosities.
3. When superficial liquid velocities are lower than 0.1 m/s, the highest slug liquid holdups are acquired for the lowest oil viscosity.
4. Slug liquid holdups are almost same for different oil viscosities with relatively higher superficial liquid velocities (v_{SL}>1.0 m/s).
5. For the relatively higher oil viscosities and superficial liquid velocities (v_{SL}>1.0 m/s), the effect of the bubble amount decreases and liquid rate influence becomes dominant factor.
6. Different existing models and correlations are used to evaluate the performance. Barnea & Brauner (1985) model gives the lowest average relative error value of 0.3% with the slightly higher absolute average relative error of 5.8%.

7.1.1.5 Film liquid holdup

1. For a given superficial liquid velocity and oil viscosity, film liquid holdup decreases as superficial gas velocity increases.
2. With increase of superficial liquid velocity, film liquid holdup increases owing to the increase in the interfacial shear stress.
3. Slight increase of the film liquid holdup is observed with increasing

oil viscosity when superficial liquid velocities are higher than 1 m/s and superficial gas velocities are less than 1 m/s.

4. It can be concluded that the impact of superficial liquid velocity on the film liquid holdup is greater than does to oil viscosity.
5. TUFFP Unified model is compared with the experimental results for the average film liquid holdup, showing absolute average relative and average relative errors of 10.43% and 3% for 'all' oil viscosities, respectively. The degree of scattering increases with the superficial liquid velocity increase.

7.1.1.6 Translational velocity

1. For a constant mixture velocity, translational velocity increases with the increase of oil viscosity.
2. Above some points of mixture velocities, the degree of scattering is high due to increase amount of gas passing through the top of the slug region.
3. With Nicklin *et al*. (1962) equation, initially, calculated drift velocities and C_0 coefficients were decided for different oil viscosities. After considering other components such as void fraction and mixture Reynolds number, C_0 coefficients were re-calculated by Choi *et al.* (2012) correlation showing about 2.0 at highest oil viscosity.
4. Different models are compared against experimental data for translational velocity. Choi *et al.* (2012) model presents the lowest absolute average relative error for 'all' oil viscosities, but errors

increase as the oil viscosity decreases. This makes this model less suitable for low viscous oils.

7.1.1.7 Slug length

1. For a given superficial liquid velocity and oil viscosity, slug length decreases with superficial gas velocity increase, indicating that there might be additional variables affecting the slug length.
2. For a given superficial liquid and gas velocity, slug length decreases as oil viscosity increases.
3. The approximate minimum slug length of 4*D* are observed for all of the superficial liquid velocities.
4. Most of the slug length distribution shape present a gamma (or gamma 3p) or log-normal (or log-normal 3p) distribution.
5. All of the considered models present the high positive values of absolute average relative and average relative errors. It can be concluded that none of the existing models are completely suitable to predict the slug length, indicating that all possible variables are not considered in these models.

7.1.1.8 Slug frequency

1. For a constant superficial gas velocity and oil viscosity, slug frequency increases as superficial liquid velocity increases.
2. For a given superficial liquid velocity and oil viscosity, slug frequency

slightly increases until v_{SG}=0.4 m/s. However, in general, slug frequency decreases with increasing superficial gas velocity above v_{SG}=0.4 m/s.

3. Slug frequency and slug length show an inversely proportional relationship like the correlations proposed by Al-safran *et al*. (2011).
4. Different models are compared against the experimental data for slug frequency showing that Gregory & Scott (1969), Greskovich & Shrier (1972), TUFFP Unified, and Heywood & Richardson (1979) give better predictions of slug frequency.

7.1.2 Comparison between 2- and 3-in. ID pipes results

7.1.2.1 Flow pattern map

1. Slug flow region expands and elongated bubble flow region shrinks with the increase of oil viscosity in both cases.
2. Taitel and Dukler (1976) model satisfactorily predicts intermittent flow region and transition boundary between slug and dispersed bubble flow in 3-in. case while this model is inappropriate for 2-in. case.
3. Barnea (1985) model shows a large discrepancy in predicting the transition boundary between slug flow and annular flow in both cases. However this model gives a proper prediction for the transition boundary from elongated bubble flow to slug flow in 2-in. case.
4. TUFFP Unified model is appropriate to predict intermittent flow regime and transition boundary between slug and annular flow for both cases. On the other hand, as oil viscosity increases, a wide gap is

observed to predict transition boundary from slug to annular flow in both cases.

7.1.2.2 Pressure gradient

1. For a constant superficial liquid and gas velocity, and oil viscosity, pressure gradient decreases for larger pipe diameters.
2. It can be concluded that, as pipe diameter increases, frictional component reduces and total pressure gradient decreases.
3. TUFFP Unified mechanistic model produces the best pressure gradient prediction for the both pipe diameter, but also showing relatively higher absolute average relative errors.

7.1.2.3 Average liquid holdup

1. Average liquid holdup of 3-in. are little higher than 2-in. case.
2. Film liquid holdup and ratio of slug length to slug unit length can be effective on the average liquid holdup. In this study, although film liquid holdup between 2- and 3-in. cases are almost same, the average liquid holdup can be increased with the increasing proportion of slug length for larger pipe diameter.
3. At a higher oil viscosity (587 cP), the difference of average liquid holdup between 2- and 3-in. ID pipes increases in less-slip condition. This is because, for high no-slip liquid holdup, the gas phase tends to be dragged more easily by the liquid phase especially at lower oil viscosity case.

4. TUFFP Unified and Xiao *et al*. (1990) models present lower absolute average relative errors in both cases, indicating that these models give a proper prediction for the average liquid holdup.

7.1.2.4 Slug liquid holdup

1. When the oil viscosity is 181 cP, the slug liquid holdups of 2- and 3-in. ID pipes are almost same. However, as oil viscosity increases, the results of 3-in. are slightly higher than 2-in. case.
2. The different effect of gas amount which pass through the top of the slug region, and gas bubble amount which was entrained in the slug region has to be considered. However, because the quantification of these components was challenge in this study, future research is needed to investigate the effect of these components.
3. Gregory *et al*. (1978), Kora (2010), and TUFFP Unified models give a proper prediction for the slug liquid holdup in 3-in. case while Andreussi & Bendiksen (1989), Kora (2010), and TUFFP Unified models are suitable for prediction this parameter in 2-in. case.

7.1.2.5 Film liquid holdup

1. For the similar flow and relatively low oil viscosity (181 cP), the film liquid holdup of 2-in. are higher than that of 3-in. However, as oil viscosity increases, the difference of film liquid holdup decreases.
2. When v_{SL}/v_m is higher than 0.3, the film liquid holdup of 3-in. are slightly higher than that of 2-in.
3. Similar with the average liquid holdup and the slug liquid holdup, this

discrepancy can occur due to the different effect of drag force.

4. The results of film liquid holdup show analogous trend with Ben-Mansour *et al*. (2010).

7.1.2.6 Translational velocity

1. At low mixture velocities, v_m < 2.0 m/s, the results of 3-in. are little higher than those of 2-in. ID pipes due to the small difference of drift velocity. As previously stated in Ben-Mansour *et al*. (2010), the drift increases with larger pipe diameter.
2. For v_m > 2.0 m/s, translational velocity slightly decreases as pipe diameter increases due to the effect of different bubble size on the top of the slug region.
3. In both pipe diameter cases, C_0 coefficient shows the value of 2.0 indicating that the experiments were in the laminar flow.
4. Choi *et al*. (2012) model gives the best agreement to predict the translational velocity, presenting the lowest absolute average relative error in both cases.

7.1.2.7 Slug length

1. For a constant mixture velocity and oil viscosity, L_s/D values of 3-in. are slightly higher than 2-in. case.
2. Same as 3-in. case, there is no model gives a satisfactory result to predict the slug length in 2-in. case.

7.1.2.8 Slug frequency

1. For the same superficial liquid and gas velocities with the same oil viscosity, slug frequency of 2-in. is higher than that of 3-in. Due to the inversely proportional trend between slug length and frequency, the comparison of slug frequency between 2- and 3-in. cases shows an opposite trend of slug length discrepancy.
2. Gokcal (2008) and Schulkes (2011) models present lower absolute average relative errors for 2-in. while Heywood & Richardson (1979) model gives the lowest absolute average relative error for 3-in. case to predict the slug frequency.

7.2 Recommendations

(1) A greater variety of experiments need to be conducted for larger pipe diameter conditions; the pipe diameters are above 6-in, which are frequently used in field-scale production system.

(2) The experimental matrices of both pipe diameters are recommended to be exactly same to quantitatively analyze the gap between the results. For safety reasons related with pressure problem, the experiments of 3-in. ID pipes were performed by being based on the superficial liquid and gas velocities of 2-in. ID pipes.

(3) More optional dimensionless coefficients and variables such as Froud and Lockhar-Martinelli numbers that can offset the effect of pipe diameter, need to be used to elaborately check the reasonability of

scale-up study.

(4) More theoretical studies are needed to be researched to modify the simplified Lockhart and Martinelli's separated model and to give better pressure gradient prediction in relatively higher values.

(5) The used VBA Excel Macro program are better to be changed using other software to reduce the processing speed of the obtained data sets.

References

Abdul-Majeed, G. H. (2000). Liquid slug holdup in horizontal and slightly inclined two-phase slug flow. *Journal of Petroleum Science and Engineering* 27: 27-32.

Al-Safran, E., Gokcal, B., and Sarica, C. (2011). Analysis and prediction of heavy oil two-phase slug length in horizontal pipelines. Paper No. SPE 150572. *SPE Heavy Oil Conference and Exhibition*, Kuwait City, Kuwait, December 12-14.

Al-Safran, E., Kora, C., and Sarica, C. (2013). Prediction of liquid volume fraction in slugs in two-phase horizontal pipe flow with high viscosity liquid. *BHR Group 16th International Conference on Multiphase Production Technology*, Cannes, France, June 12-14.

Andreussi, P. and Bendiksen, K. (1989). An investigation of void fraction in liquid slugs for horizontal and inclined gas-liquid pipe flow. *International Journal of Multiphase Flow* 15: 937-946.

Andreussi, P., Bendiksen, K., and Nydal, O. J. (1993). Void distribution in slug flow. *International Journal of Multiphase Flow* 19: 817-823.

Barnea, D. (1987). A unified model for predicting flow-pattern transitions for the whole range of pipe inclinations. *International Journal of Multiphase Flow* 13: 1-12.

Barnea, D., Shoham, O., and., and Taitel, Y. (1980). Flow pattern transition for gas-liquid flow in horizontal and inclined pipes. *International Journal of Multiphase Flow* 6: 217-225.

Barnea, D. and Brauner, N. (1985). Holdup of the liquid slug in two phase intermittent flow. *International Journal of Multiphase Flow* 11: 43-49.

Beattie, D. R. H. and Sugawara, S. (1986). Steam-water void fraction for vertical upflow in a 73.9 mm pipe. *International Journal of Multiphase Flow* 12: 641-653.

Bendiksen, K. H. (1984). An experimental investigation of the motion of long bubbles in inclined tubes. *International Journal of Multiphase Flow* 10: 467-483.

Ben-Mansour, R., Sharma, A. K., Jeyachandra, B. C., Gokcal, B., Al-Sarkhi, A., and Sarica, C. (2010). Effect of pipe diameter and high oil viscosity on drift velocity for horizontal pipes. *BHR Group 7th North American Conference on Multiphase Technology,* Banff, Canada, June 2-4.

Bhagwat, S. M. and Ghajar, A. J. (2014). A flow pattern independent drift flux model based void fraction correlation for a wide range of gas-liquid two phase flow. *International Journal of Multiphase Flow* 59: 186-205.

Bonnecaze, R. H., Erskine, and Greskovich, E. J. (1971). Holdup and pressure drop for two phase slug flow in inclined pipelines. *American Institute of Chemical Engineers Journal* 17: 1109-1113.

Brill, J. P., Schmidt, Z., Coberly, W. A., Herring, J. D., and Moore, D. W. (1981). Analysis of two-phase tests in large-diameter flow lines in Prudhoe Bay field. *SPE Journal*: 363-378.

Brito, R. (2012). *Effect of Medium Oil Viscosity on Two-phase Oil-gas Flow Behavior in Horizontal Pipes*. Master of Science Thesis, University of Tulsa, Tulsa, OK, USA.

Brito, R., Pereyra, E., Sarica, C., and Torres, C. (2013). A simplified slug flow model for highly viscous oil-gas flow in horizontal pipes. Paper No. SPE 166454. *SPE Annual Technical Conference and Exhibition*, New Orleans, Louisiana, USA, September 30-October 2.

Chisholm, D. (1967). A theoretical basis for the Lockhart-Martinelli correlation for two-phase flow. *International Journal of Heat and Mass Transfer* 10: 1767-1778.

Choi, J., Pereyra, E., Sarica, C., Park, C., and Kang, J.M. (2012). An efficient drift flux closure relationship to estimate liquid holdups of gas-liquid two phase flow in pipes. *Energies* 5: 5294-5306.

Clark, N. N. and Flemmer, R. L. (1985). Predicting the holdup in two phase bubble upflow and downflow using the Zuber and Findlay drift flux model. *American Institute of Chemical Engineers Journal* 31: 500-503.

Colmenares, J., Ortega, P., Padrino, J., and Trallero, J. L. (2001). Slug flow model for the prediction of pressure drop for high viscosity oils in a horizontal pipeline. Paper No. SPE 71111. *SPE International Thermal Operations and Heavy Oil Symposium*, Porlamar, Margarita Island, Venezuela, March 12-14.

Dieck, R. H. (2006). *Measurement Uncertainty: Methods and Application*, ISA Books.

Dukler, A. E. and Hubbard, M. G. (1975). A model for gas-liquid slug flow in horizontal and near horizontal tubes. *Industrial & Engineering Chemistry Fundamentals* 14(4): 337-347.

Fabre, J. (1994). Advancements in two-phase slug flow modeling. Paper No. SPE 27961. *University of Tulsa Centennial Petroleum Engineering Symposium*, Tulsa, Oklahoma, USA, August 29-31.

Felizola, H. (1992). *Slug Flow in Extended Reach Directional Wells*. Master of Science Thesis, University of Tulsa, Tulsa, Oklahoma, USA.

Gokcal, B. (2005). *Effects of High Oil Viscosity on Two-Phase Oil-Gas Flow Behavior in Horizontal Pipes*. Master of Science Thesis, University of Tulsa, Tulsa, Oklahoma, USA.

Gokcal, B. (2008). *An Experimental and Theoretical Investigation of Slug Flow for High Oil Viscosity in Horizontal Pipes*. Ph.D. Dissertation, University of Tulsa, Tulsa, Oklahoma, USA.

Gokcal, B., Al-Sarkhi, A. S., Sarica, C., and Al-Safran, E. M. (2009). Prediction of slug frequency for high-viscosity oils in horizontal pipes. Paper No.

SPE 124057. *SPE European Formation Damage Conference*, New Orleans, Louisiana, USA, October 4-7.

Gokcal, B., Wang, Q., Zhang, H., and Sarica, C. (2006). Effects of high oil viscosity on oil/gas flow behavior in horizontal pipes. Paper No. SPE 102727. *SPE Annual Technical Conference and Exhibition*, San Antonio, Texas, USA, September 24-27.

Gomez, L. E., Shoham, O., Schmidt, Z., Chokshi, R. N., Brown, A., and Northug, T. (1999). A unified mechanistic model for steady-state two-phase flow in wellbores and pipelines. Paper No. SPE 56520. *SPE Annual Technical Conference and Exhibition*, Houston, Texas, USA, October 3-6.

Gomez, L. E., Shoham, O., Schmidt, Z., Chokshi, R. N., and Northug, T. (2000). Unified mechanistic model for steady-state two-phase flow: horizontal to vertical upward flow. *SPE Journal* 5(3): 339-350.

Gregory, G. A. and Scott, D. S. (1969). Correlation of liquid slug velocity and frequency in horizontal, concurrent gas liquid flow. *American Institute of Chemical Engineers Journal* 15: 933-935.

Gregory, G. A., Nicholson, M. K., and Aziz, K. (1978). Correlation of the liquid volume fraction in the slug for horizontal gas-liquid slug flow. *International Journal of Multiphase Flow* 4: 33-39.

Greskovich, E. J. and Cooper, W. T. (1975). Correlation and prediction of gas-liquid holdups in inclined upflows. *American Institute of Chemical Engineers Journal* 21: 1189-1192.

Greskovich, E. J. and Shrier, A. L. (1972). Slug frequency in horizontal gas-liquid slug flow. *Industrial & Engineering Chemistry Process Design and Development* 11(2): 317-318.

Heywood, N. I. and Richardson, J. F. (1979). Slug flow of air-water mixtures in a horizontal pipe: determination of liquid holdup by γ-ray absorption. *Chemical Engineering Science* 34: 17-30.

Hibiki, T. and Ishii, M. (2003). One-dimensional drift-flux model for two-phase flow in a large diameter pipe. *International Journal of Heat and Mass Transfer* 46: 1773-1790.

Hill, T. J. and Wood, D. G. (1990). A new approach to the prediction of slug frequency. Paper No. SPE 20629. *SPE Annual Technical Conference and Exhibition*, New Orleans, Louisiana, USA, September 23-26.

Jeyachandra, B. C. (2011). *Effect of Pipe Inclination on Flow Characteristics of High Viscosity Oil-Gas Two-Phase Flow*. Master of Science Thesis, University of Tulsa, Tulsa, Oklahoma, USA.

Jeyachandra, B. C., Gokcal, B., Al-Sarkhi, A., Sarica, C., and Sharma, A. K. (2010). Drift-velocity closure relationships for slug two-phase high-viscosity oil flow in pipes. Paper No. SPE 151616. *SPE Annual Technical Conference and Exhibition*, Tuscany, Italy, September 20-22.

Jeyachandra, B. C., Sarica, C., Zhang, H., and Pereyra, E. (2012). Inclination effects on flow characteristics of high viscosity oil/gas two-phase flow. Paper No. SPE 159217. *SPE Annual Technical Conference and Exhibition*, San Antonio, Texas, USA, October 8-10.

Kataoka, I. and Ishii, M. (1987). Drift flux model for large diameter pipe and new correlation for pool void fraction. *International Journal of Heat and Mass Transfer* 30(9): 1927-1939.

Kokal, S. L. (1987). *An Experimental Study of Two Phase Flow in Inclined Pipes*. Ph.D. Dissertation, University of Calgary, Calgary, Alberta, Canada.

Kora, C. (2010). *Effects of High Oil Viscosity on Slug Liquid Holdup in Horizontal Pipes*. Master of Science Thesis, University of Tulsa, Tulsa, Oklahoma, USA.

Kouba, G. E. (1986). *Horizontal Slug Flow Modeling and Metering*. Ph.D. Dissertation, University of Tulsa, Tulsa, Oklahoma, USA.

Lockhart, R. W. and Martinelli, R. C. (1949). Proposed correlation of data for isothermal two-phase component flow in pipes. *Chemical Engineering Progress* 45(1): 39-48.

Londono, F. E., Archer, R. A., and Blasingame, T. A. (2002). Simplified correlations for hydrocarbon gas viscosity and gas density validation and correlation of behavior using a large-scale database. Paper No. SPE 75721. *SPE Gas Technology Symposium*, Calgary, Alberta, Canada, April 30-May 2.

Maley, L. C. and Jepson, W. P. (1998). Liquid holdup in large-diameter horizontal multiphase pipelines. *ASME Journal of Energy Resources Technology* 120: 185-192.

Manolis, I. G. (1995). *High Pressure Gas-Liquid Slug Flow*. Ph.D. Dissertation, Department of Chemical Engineering and Chemical Technology, Imperial College of Science, Technology & Medicine, UK.

Marcano, R., Chen, X. T., Sarica, C., and Brill, J. P. (1998). A study of slug characteristics for two-phase horizontal flow. Paper No. SPE 39856. *International Petroleum Conference and Exhibition*, Villahermosa, Mexico, March 3-5.

Marquez, J., Manzanilla, C., and Trujillo, J. (2009). Slug catcher conceptual design as separator for heavy oil. Paper No. SPE 122829. *SPE Latin American and Caribbean Petroleum Engineering Conference*, Cartagena, Colombia, May 31-June 3.

Mazza, R. A., Rosa, E. S., and Yoshizawa, C. J. (2010). Analyses of liquid film models applied to horizontal and near horizontal gas-liquid slug flows. *Chemical Engineering Science* 65: 3876-3892.

Mishima, K. and Hibiki, T. (1996). Some characteristics of air-water two-phase flow in small diameter vertical tubes. *International Journal of Multiphase Flow* 22(4): 703-712.

Moreiras, J. (2012). *Experimental Determination of Drift Velocity in Medium Oil Viscosities for Horizontal and Upward Inclined Pipes*. Undergraduate Research Project, University of Tulsa, Tulsa, Oklahoma, USA.

Nädler, M. and Mewes, D. (1995). Effects of the liquid viscosity on the phase distributions in horizontal gas-liquid slug flow. *International Journal of Multiphase Flow* 21(2): 253-266.

Nicholson, M. K., Aziz, K., and Gregory, G. A. (1978). Intermittent two phase flow in horizontal pipes: predictive models. *The Canadian Journal of Chemical Engineering* 56: 653-663.

Nicklin, D. J. and Davidson, J. F. (1962). Two-phase flow in vertical tubes. *Transactions of the Institution of Chemical Engineers* 40.

Norris, L. (1981). Correlation of Prudhoe Bay liquid slug lengths and holdups including 1981 large diameter flow line tests. *Internal Report, Exxon Production Research Co*, Houston, Texas, USA.

Nuland, S. (1990). Bubble fraction in slugs in two-phase flow with high viscosity liquid. *International Symposium on Two Phase Flow Modeling and Experimentation*, Pisa, Italy.

Nossen, J. and Lawrence, C. J. (2012). Pressure drop in laminar slug flow with heavy oil. *BHR Group 8th North American Conference on Multiphase Technology*, Banff, Alberta, Canada, June 20-22.

Nydal, O. J., Pintus, S., and Andreussi, P. (1992). Statistical characterization of slug flow in horizontal pipes. *International Journal of Multiphase Flow* 18(3): 439-453.

Petalas, N. and Aziz, K. (1998). A mechanistic model for multiphase flow in pipes. *The 49th Annual Technical Meeting of the Petroleum Society*, Calgary, Alberta, Canada, June 8-10.

Petalas, N. and Aziz, K. (2000). A mechanistic model for multiphase flow in pipes. *Journal of Canadian Petroleum Technology* 39(6): 43-55.

Rosa, E. S. and Netto, J. R. F. (2004). Viscosity effect and flow development in horizontal slug flows. *The 5th International Conference on Multiphase Flow*, Yokohama, Japan, May 20-Jun 4.

Rouhani, S. Z. and Axelsson, E. (1970). Calculation of void volume fraction in the subcooled and quality boiling regions. *International Journal of Heat and Mass Transfer* 13: 383-393.

Schulkes, R. (2011). Slug frequencies revisited. *BHR Group 15th International Conference on Multiphase Production Technology*, Cannes, France, June 15-17.

Scott, S. L., Shoham, O., and Brill, J. P. (1986). Prediction of slug length in horizontal large diameter pipes. Paper No. SPE 15103. *SPE 56th Annual California Regional Meeting*, Oakland, California, USA, April 2-4.

Scott, S. L. and Kouba, G. E. (1990). Advances in slug flow characterization for horizontal and slightly inclined pipelines. Paper No. SPE 20628. *SPE Annual Technical Conference and Exhibition*, New Orleans, Louisiana, USA, September 23-26.

Shipley, D. G. (1982). Two phase flow in large diameter pipes. *Chemical Engineering Science* 39: 163-165.

Shoham, O. (1982). *Flow-Pattern Transition and Characterization in Gas-Liquid Two-Phase Flow in Inclined Pipes*. Ph.D. Dissertation, Tel Aviv University, Tel Aviv, Israel.

Shoham, O. (2005). *Mechanistic Modeling of Gas-Liquid Two-Phase Flow in Pipes*. SPE Books.

Stapelberg, H. and Mewes, D. (1994). The pressure loss and slug frequency of liquid-liquid-gas slug flow in horizontal pipes. *International Journal of Multiphase Flow* 20(2): 285-303.

Taitel, Y. and Barnea, D. (1990). Two-phase slug flow. *Advances in Heat Transfer* 20: 83-132.

Taitel, Y. and Dukler, A. E. (1976). A model for predicting flow regime transition in horizontal and near horizontal gas-liquid flow. *American Institute of Chemical Engineers Journal* 22(1): 47-55.

Taitel, Y. and Dukler, A. E. (1977). A model for slug frequency during gas-liquid flow in horizontal and near horizontal pipes. *International Journal of Multiphase Flow* 3: 585-596.

Tronconi, E. (1990). Prediction of slug frequency in horizontal two-phase slug flow. *American Institute of Chemical Engineers Journal* 36(5): 701-709.

Vázquez E. G. and Fairuzov, Y. V. (2007). A study of normal slug flow in an offshore production facility with a large-diameter flowline. Paper No. SPE 108752. *The 2007 International Oil Conference and Exhibition*, Veracruz, Mexico, June 27-30.

Wang, S., Zhang, H., Sarica, C., and Pereyra, E. (2013). A Mechanistic slug liquid holdup model for wide ranges of liquid viscosity and pipe inclination angle. Paper No. OTC 24046. *The Offshore Technology Conference*, Houston, Texas, USA, May 6-9.

Xiao, J. J., Shoham, O., and Brill, J. P. (1990). A comprehensive mechanistic model for two-phase flow in pipelines. Paper No. SPE 20631. *SPE Annual Technical Conference and Exhibition*, New Orleans, Louisiana, USA, September 23-26.

Zabaras, G. J. (2000). Prediction of slug frequency for gas/liquid flows. *SPE Journal* 5(3): 252-258.

Zhang, H., Wang, Q., Sarica, C., and Brill, J. P. (2003). Unified model for gas-liquid pipe flow via slug dynamics – part 1: model development. *ASME Journal of Energy Resources Technology* 125: 266-273.

Zhang, H., Wang, Q., Sarica, C., and Brill, J. P. (2003). Unified model for gas-liquid pipe flow via slug dynamics – part 2: model validation. *ASME Journal of Energy Resources Technology* 125: 274-283.

Nomenclature

Symbol	Description	Unit
A	Cross-sectional area of the pipe	m^2
α	Void fraction	dimensionless
B_O	Bond number	dimensionless
B_R	Combined uncertainty	dimensionless
C	Chisholm's coefficient	dimensionless
C_0	Flow coefficient, Distribution parameter	dimensionless
CP	Capacitance sensor	abbreviation
D	Pipe diameter	mm
D_p	Pipe diameter	literature unit
dP/dL	Pressure gradient	Pa/m
$(dP/dL)_A$	Accelerational pressure gradient	Pa/m
$(dP/dL)_F$	Frictional pressure gradient	Pa/m
$(dP/dL)_G$	Gravitational pressure gradient	Pa/m
$(dP/dL)_T$	Total Pressure gradient	Pa/m
e_i	Actual error	dimensionless
e_j	Relative error	dimensionless

$\varepsilon_1 \sim \varepsilon_6$	Statistical parameters	dimensionless
F_E	Entrainment fraction of liquid in gas core	dimensionless
f_F	Fanning friction factor	dimensionless
f_M	Moody friction factor	dimensionless
f_s	Friction factor for the slug	dimensionless
f_f	Friction factor for the film	dimensionless
f_S	Slug frequency	dimensionless
G	Total (Mixture) mass flux	kg/m^{2}s
g	Gravity acceleration	m/s^2
γ	Specific gravity	dimensionless
H_L	Liquid holdup	dimensionless
$H_{LAverage}$	Average liquid holdup	dimensionless
H_{LF}	Liquid Film holdup	dimensionless
H_{LFe}	Liquid Film holdup just before pickup	dimensionless
H_{LLS}	Liquid holdup in slug body	dimensionless
ID	Inner diameter	abbreviation
L_F	Film length	m
L_S	Slug length	m
L_S / D	Dimensionless slug length	dimensionless

L_U	Slug unit length	m
λ_L	No-slip liquid holdup	dimensionless
μ_{air}	Air viscosity	Pa·s
μ_{Oil}	Oil viscosity	Pa·s
μ_G	Gas phase viscosity	Pa·s
μ_L	Liquid phase viscosity	Pa·s
N	Number of data points	dimensionless
N_{Fr}	Froude number	dimensionless
N_{μ}	Viscosity number	dimensionless
Re	Reynolds number	dimensionless
$\mathrm{Re}_{\mathrm{SL}}$	Liquid Reynolds number	dimensionless
$\mathrm{Re}_{\mathrm{SG}}$	Gas Reynolds number	dimensionless
Re_{m}	Mixture Reynolds number	dimensionless
ρ_G	Gas phase density	kg/m^3
ρ_L	Liquid phase density	kg/m^3
ρ_S	Mixture density in the slug body	kg/m^3
S_X	Standard deviation of a population	dimensionless
$S_{\overline{X}}$	Standard deviation of a population average	dimensionless
σ	Surface tension	N/m

T	Temperature	°F
t_{95}	Student's t	dimensionless
θ	Inclination angle from horizontal	dimensionless
U_{95}	Combined uncertainty with 95% confidence	dimensionless
V	Voltage	Volt
V'	Dimensionless voltage	dimensionless
v_C	Gas core velocity	m/s
v_D	Drift velocity	m/s
v_F	Average velocity of fluid in the film	m/s
v_m	Mixture velocity	m/s
v_{SG}	Superficial gas velocity	m/s
v_{SL}	Superficial liquid velocity	m/s
v_S	Average velocity of fluid in the slug	m/s
v_T	Translational velocity	m/s
W_G	Gas mass flow rate	kg/s
W_L	Liquid mass flow rate	kg/s
X_i	i^{th} element in the population	dimensionless
$\overline{X}$	Population average	dimensionless
x	Flow quality	dimensionless

Appendix A

Experimental Results

Table A.1 Flow Pattern, fluid properties average and uncertainty for the all oil viscosities of both gas and liquid phases.

	File name	FP	TT (°F)	U_{TT} (°F)	ρ_L (kg/m^3)	$U\rho_L$ (kg/m^3)	ρ_G (kg/m^3)	$U\rho_G$ (kg/m^3)	μ_L (cP)	$U\mu_L$ (cP)	μ_G (cP)	$U\mu_G$ (cP)
1	Vsl_0.022_Vsg_0.333	SL	62	1.4	883.6	0.642	1.2	1.46E-01	578.7	48.6	9.28E-03	1.95E-05
2	Vsl_0.022_Vsg_0.385	SL	61	1.4	883.6	0.642	1.2	1.27E-01	582.7	49.8	9.27E-03	1.95E-05
3	Vsl_0.022_Vsg_0.431	SL	61	1.4	883.6	0.642	1.2	1.19E-01	582.8	49.9	9.27E-03	1.95E-05
4	Vsl_0.022_Vsg_0.496	SL	61	1.4	883.6	0.643	1.2	2.67E-01	581.2	49.4	9.27E-03	1.96E-05
5	Vsl_0.022_Vsg_0.656	SL	61	1.4	883.7	0.642	1.2	3.11E-01	586.3	51.1	9.27E-03	1.97E-05
6	Vsl_0.022_Vsg_0.755	SL	61	1.4	883.7	0.642	1.2	3.22E-01	587.3	51.4	9.27E-03	1.97E-05
7	Vsl_0.022_Vsg_0.946	SL	61	1.4	883.7	0.642	1.2	3.37E-01	588.0	51.7	9.27E-03	1.97E-05
8	Vsl_0.022_Vsg_1.213	SL	60	1.4	883.9	0.652	1.2	2.71E-01	608.9	62.8	9.25E-03	1.96E-05
9	Vsl_0.022_Vsg_1.496	SL	60	1.4	884.0	0.643	1.2	1.09E-01	611.7	63.6	9.25E-03	1.95E-05
10	Vsl_0.022_Vsg_1.754	SL	60	1.4	884.0	0.643	1.2	8.29E-02	615.5	66.1	9.25E-03	1.95E-05
11	Vsl_0.022_Vsg_1.965	SL	60	1.4	884.0	0.643	1.2	9.03E-02	619.3	68.7	9.25E-03	1.95E-05
12	Vsl_0.050_Vsg_0.331	SL	61	1.4	883.6	0.642	1.2	6.22E-02	582.0	49.6	9.27E-03	1.94E-05
13	Vsl_0.050_Vsg_0.367	SL	61	1.4	883.6	0.642	1.2	6.21E-02	581.3	49.3	9.27E-03	1.94E-05
14	Vsl_0.050_Vsg_0.418	SL	61	1.4	883.6	0.642	1.2	1.66E-01	581.1	49.3	9.27E-03	1.95E-05
15	Vsl_0.050_Vsg_0.464	SL	61	1.4	883.6	0.642	1.2	1.61E-01	581.1	49.3	9.27E-03	1.95E-05
16	Vsl_0.050_Vsg_0.530	SL	61	1.4	883.6	0.642	1.2	1.90E-01	581.2	49.3	9.27E-03	1.95E-05
17	Vsl_0.050_Vsg_0.670	SL	61	1.4	883.6	0.642	1.2	2.50E-01	581.0	49.2	9.27E-03	1.96E-05
18	Vsl_0.050_Vsg_0.764	SL	61	1.4	883.6	0.642	1.2	3.39E-01	580.6	49.1	9.27E-03	1.98E-05
19	Vsl_0.050_Vsg_1.017	SL	61	1.4	883.6	0.644	1.2	3.19E-01	582.3	49.8	9.27E-03	1.98E-05
20	Vsl_0.050_Vsg_1.306	SL	61	1.5	883.9	0.662	1.2	3.00E-01	605.9	62.1	9.26E-03	1.99E-05
21	Vsl_0.050_Vsg_1.557	SL	61	1.4	883.8	0.642	1.2	2.10E-01	596.8	55.5	9.26E-03	1.96E-05
22	Vsl_0.050_Vsg_1.797	SL	61	1.4	883.8	0.642	1.2	2.15E-01	596.0	55.0	9.26E-03	1.96E-05
23	Vsl_0.050_Vsg_2.007	SL	61	1.4	883.9	0.642	1.2	1.80E-01	600.3	57.1	9.26E-03	1.95E-05
24	Vsl_0.050_Vsg_2.370	SL	61	1.4	883.8	0.642	1.2	1.23E-01	598.2	56.1	9.26E-03	1.94E-05
25	Vsl_0.089_Vsg_0.282	SL	62	1.4	883.6	0.642	1.2	1.21E-01	575.9	47.7	9.28E-03	1.94E-05
26	Vsl_0.089_Vsg_0.330	SL	61	1.4	883.7	0.644	1.2	1.21E-01	585.8	51.1	9.27E-03	1.95E-05
27	Vsl_0.089_Vsg_0.397	SL	61	1.4	883.7	0.642	1.2	1.64E-01	583.2	50.0	9.27E-03	1.95E-05
28	Vsl_0.089_Vsg_0.448	SL	61	1.4	883.6	0.642	1.2	1.83E-01	582.2	49.7	9.27E-03	1.95E-05
29	Vsl_0.089_Vsg_0.505	SL	61	1.4	883.6	0.642	1.2	2.13E-01	581.4	49.4	9.27E-03	1.96E-05
30	Vsl_0.089_Vsg_0.573	SL	61	1.4	883.6	0.642	1.2	1.98E-01	580.9	49.2	9.27E-03	1.95E-05
31	Vsl_0.089_Vsg_0.721	SL	61	1.4	883.6	0.642	1.2	2.66E-01	580.8	49.2	9.27E-03	1.97E-05
32	Vsl_0.089_Vsg_0.844	SL	61	1.4	883.6	0.642	1.2	2.74E-01	581.0	49.3	9.27E-03	1.97E-05
33	Vsl_0.089_Vsg_1.128	SL	61	1.4	883.6	0.642	1.2	2.61E-01	582.8	49.9	9.27E-03	1.97E-05
34	Vsl_0.089_Vsg_1.400	SL	61	1.4	883.7	0.650	1.2	3.08E-01	586.5	51.8	9.27E-03	1.99E-05
35	Vsl_0.089_Vsg_1.765	SL	61	1.4	883.7	0.642	1.2	3.04E-01	583.8	50.2	9.27E-03	1.98E-05
36	Vsl_0.089_Vsg_2.028	SL	61	1.4	883.7	0.642	1.3	3.07E-01	583.7	50.1	9.27E-03	1.98E-05
37	Vsl_0.089_Vsg_2.281	SL	61	1.4	883.7	0.642	1.3	2.91E-01	590.0	52.5	9.27E-03	1.97E-05
38	Vsl_0.089_Vsg_2.577	SL	61	1.4	883.7	0.642	1.3	2.21E-01	591.2	53.0	9.27E-03	1.96E-05
39	Vsl_0.089_Vsg_2.908	SL	61	1.4	883.8	0.649	1.3	2.31E-01	593.5	54.6	9.26E-03	1.96E-05
40	Vsl_0.100_Vsg_0.229	SL	61	1.4	883.6	0.642	1.2	1.33E-01	581.7	49.5	9.27E-03	1.94E-05
41	Vsl_0.100_Vsg_0.283	SL	61	1.4	883.6	0.642	1.2	1.20E-01	581.8	49.5	9.27E-03	1.94E-05
42	Vsl_0.100_Vsg_0.334	SL	61	1.4	883.7	0.643	1.2	1.56E-01	587.0	51.4	9.27E-03	1.95E-05
43	Vsl_0.100_Vsg_0.404	SL	61	1.4	883.7	0.642	1.2	1.53E-01	584.6	50.5	9.27E-03	1.94E-05
44	Vsl_0.100_Vsg_0.464	SL	61	1.4	883.7	0.642	1.2	1.59E-01	583.7	50.1	9.27E-03	1.94E-05
45	Vsl_0.100_Vsg_0.515	SL	61	1.4	883.7	0.642	1.2	1.78E-01	583.2	50.0	9.27E-03	1.95E-05
46	Vsl_0.100_Vsg_0.593	SL	61	1.4	883.6	0.642	1.2	1.95E-01	582.7	49.8	9.27E-03	1.95E-05
47	Vsl_0.100_Vsg_0.738	SL	61	1.4	883.6	0.642	1.2	2.42E-01	582.1	49.6	9.27E-03	1.96E-05
48	Vsl_0.100_Vsg_0.863	SL	61	1.4	883.6	0.642	1.3	2.91E-01	582.0	49.6	9.27E-03	1.97E-05
49	Vsl_0.100_Vsg_1.153	SL	61	1.4	883.7	0.642	1.3	2.87E-01	583.3	50.0	9.27E-03	1.97E-05
50	Vsl_0.100_Vsg_1.448	SL	61	1.4	883.7	0.642	1.3	3.10E-01	586.3	51.1	9.27E-03	1.98E-05
51	Vsl_0.100_Vsg_1.803	SL	61	1.4	883.7	0.642	1.3	3.42E-01	586.3	51.1	9.27E-03	1.99E-05
52	Vsl_0.100_Vsg_2.032	SL	61	1.4	883.7	0.642	1.3	3.30E-01	587.2	51.4	9.27E-03	1.99E-05
53	Vsl_0.100_Vsg_2.488	SL	61	1.4	883.7	0.643	1.3	3.25E-01	588.9	52.1	9.27E-03	1.99E-05
54	Vsl_0.100_Vsg_2.653	SL	61	1.4	883.7	0.642	1.3	2.82E-01	590.5	52.7	9.27E-03	1.97E-05
55	Vsl_0.100_Vsg_3.013	SL	61	1.4	883.8	0.643	1.3	2.16E-01	591.9	53.3	9.27E-03	1.96E-05
56	Vsl_0.133_Vsg_0.230	SL	61	1.4	883.7	0.642	1.3	1.14E-01	587.2	51.4	9.27E-03	1.94E-05
57	Vsl_0.133_Vsg_0.305	SL	61	1.4	883.7	0.643	1.3	1.19E-01	588.7	52.0	9.27E-03	1.94E-05
58	Vsl_0.133_Vsg_0.365	SL	61	1.4	883.7	0.642	1.3	1.38E-01	585.6	50.8	9.27E-03	1.94E-05
59	Vsl_0.133_Vsg_0.426	SL	61	1.4	883.7	0.642	1.3	1.31E-01	584.8	50.6	9.27E-03	1.94E-05
60	Vsl_0.133_Vsg_0.489	SL	61	1.4	883.7	0.642	1.3	1.54E-01	584.4	50.4	9.27E-03	1.94E-05

61	Vsl_0.133_Vsg_0.547	SL	61	1.4	883.7	0.642	1.3	1.70E-01	584.0	50.3	9.27E-03	1.94E-05
62	Vsl_0.133_Vsg_0.624	SL	61	1.4	883.7	0.642	1.3	1.82E-01	583.8	50.2	9.27E-03	1.95E-05
63	Vsl_0.133_Vsg_0.796	SL	61	1.4	883.7	0.642	1.3	2.37E-01	583.9	50.2	9.27E-03	1.96E-05
64	Vsl_0.133_Vsg_0.911	SL	61	1.4	883.8	0.649	1.3	2.82E-01	594.2	54.9	9.26E-03	1.98E-05
65	Vsl_0.133_Vsg_1.211	SL	61	1.4	883.8	0.642	1.3	2.75E-01	593.4	53.9	9.26E-03	1.97E-05
66	Vsl_0.133_Vsg_1.530	SL	61	1.4	883.8	0.646	1.3	3.10E-01	593.1	54.1	9.26E-03	1.99E-05
67	Vsl_0.133_Vsg_1.821	SL	61	1.4	883.7	0.642	1.3	3.09E-01	588.6	51.9	9.27E-03	1.98E-05
68	Vsl_0.133_Vsg_2.226	SL	61	1.4	883.7	0.642	1.3	3.08E-01	589.7	52.3	9.27E-03	1.98E-05
69	Vsl_0.133_Vsg_2.521	SL	61	1.4	883.7	0.642	1.3	3.22E-01	591.0	52.9	9.27E-03	1.99E-05
70	Vsl_0.133_Vsg_2.891	SL	61	1.4	883.7	0.642	1.3	3.28E-01	590.9	52.9	9.27E-03	1.99E-05
71	Vsl_0.133_Vsg_3.145	SL	61	1.4	883.8	0.642	1.3	2.84E-01	592.6	53.5	9.26E-03	1.97E-05
72	Vsl_0.200_Vsg_0.201	SL	61	1.4	883.7	0.642	1.3	1.26E-01	586.9	51.3	9.27E-03	1.93E-05
73	Vsl_0.200_Vsg_0.263	SL	61	1.4	883.7	0.642	1.3	1.38E-01	586.0	51.0	9.27E-03	1.93E-05
74	Vsl_0.200_Vsg_0.333	SL	61	1.4	883.7	0.642	1.3	1.38E-01	585.2	50.7	9.27E-03	1.93E-05
75	Vsl_0.200_Vsg_0.401	SL	61	1.4	883.7	0.644	1.3	1.51E-01	586.1	51.2	9.27E-03	1.94E-05
76	Vsl_0.200_Vsg_0.462	SL	61	1.4	883.6	0.642	1.3	1.51E-01	583.0	49.9	9.27E-03	1.93E-05
77	Vsl_0.200_Vsg_0.544	SL	61	1.4	883.6	0.642	1.3	1.67E-01	580.8	49.2	9.27E-03	1.94E-05
78	Vsl_0.200_Vsg_0.613	SL	61	1.4	883.6	0.642	1.3	1.82E-01	580.1	49.0	9.27E-03	1.94E-05
79	Vsl_0.200_Vsg_0.696	SL	61	1.4	883.6	0.642	1.3	2.06E-01	580.8	49.2	9.27E-03	1.95E-05
80	Vsl_0.200_Vsg_0.842	SL	62	1.4	883.6	0.642	1.3	2.37E-01	579.5	48.8	9.28E-03	1.96E-05
81	Vsl_0.200_Vsg_1.007	SL	61	1.4	883.6	0.642	1.3	2.64E-01	579.9	48.9	9.27E-03	1.97E-05
82	Vsl_0.200_Vsg_1.339	SL	61	1.4	883.6	0.642	1.3	2.83E-01	580.9	49.2	9.27E-03	1.97E-05
83	Vsl_0.200_Vsg_1.709	SL	61	1.4	883.7	0.645	1.3	2.99E-01	588.1	52.0	9.27E-03	1.98E-05
84	Vsl_0.200_Vsg_2.093	SL	61	1.4	883.7	0.642	1.3	3.25E-01	586.0	51.0	9.27E-03	1.99E-05
85	Vsl_0.200_Vsg_2.468	SL	61	1.4	883.7	0.642	1.3	3.70E-01	586.1	51.0	9.27E-03	2.01E-05
86	Vsl_0.200_Vsg_2.957	SL	61	1.4	883.7	0.642	1.3	3.83E-01	587.7	51.6	9.27E-03	2.02E-05
87	Vsl_0.200_Vsg_3.167	SL	61	1.4	883.7	0.642	1.3	3.58E-01	588.8	52.0	9.27E-03	2.01E-05
88	Vsl_0.222_Vsg_0.146	SL	62	1.4	883.6	0.642	1.3	1.30E-01	579.0	48.6	9.28E-03	1.93E-05
89	Vsl_0.222_Vsg_0.198	SL	62	1.4	883.6	0.642	1.3	1.36E-01	578.3	48.4	9.28E-03	1.93E-05
90	Vsl_0.222_Vsg_0.275	SL	62	1.4	883.6	0.642	1.3	1.41E-01	577.5	48.2	9.28E-03	1.93E-05
91	Vsl_0.222_Vsg_0.340	SL	61	1.4	883.6	0.644	1.3	1.48E-01	581.1	49.4	9.27E-03	1.94E-05
92	Vsl_0.222_Vsg_0.412	SL	62	1.4	883.6	0.643	1.3	1.59E-01	577.6	48.3	9.28E-03	1.93E-05
93	Vsl_0.222_Vsg_0.478	SL	62	1.4	883.6	0.642	1.3	1.65E-01	575.9	47.7	9.28E-03	1.93E-05
94	Vsl_0.222_Vsg_0.562	SL	62	1.4	883.5	0.642	1.3	1.76E-01	574.6	47.3	9.28E-03	1.94E-05
95	Vsl_0.222_Vsg_0.627	SL	62	1.4	883.5	0.642	1.3	1.82E-01	573.8	47.1	9.28E-03	1.94E-05
96	Vsl_0.222_Vsg_0.695	SL	62	1.4	883.5	0.642	1.3	2.01E-01	573.3	47.0	9.28E-03	1.94E-05
97	Vsl_0.222_Vsg_0.891	SL	62	1.4	883.6	0.644	1.3	2.23E-01	578.1	48.5	9.28E-03	1.95E-05
98	Vsl_0.222_Vsg_1.055	SL	62	1.4	883.6	0.642	1.3	2.49E-01	575.7	47.7	9.28E-03	1.96E-05
99	Vsl_0.222_Vsg_1.418	SL	62	1.4	883.5	0.642	1.3	2.84E-01	574.8	47.4	9.28E-03	1.97E-05
100	Vsl_0.222_Vsg_1.781	SL	61	1.4	883.7	0.646	1.3	3.05E-01	590.8	53.1	9.27E-03	1.99E-05
101	Vsl_0.222_Vsg_2.204	SL	61	1.4	883.7	0.642	1.3	3.46E-01	586.6	51.2	9.27E-03	2.00E-05
102	Vsl_0.222_Vsg_2.577	SL	61	1.4	883.7	0.642	1.3	3.48E-01	587.9	51.7	9.27E-03	2.00E-05
103	Vsl_0.222_Vsg_3.021	SL	61	1.4	883.7	0.642	1.3	3.74E-01	589.1	52.1	9.27E-03	2.02E-05
104	Vsl_0.222_Vsg_3.472	SL	61	1.4	883.7	0.642	1.3	3.72E-01	589.7	52.4	9.27E-03	2.02E-05
105	Vsl_0.300_Vsg_0.150	SL	62	1.4	883.5	0.642	1.3	1.69E-01	570.2	46.2	9.28E-03	1.93E-05
106	Vsl_0.300_Vsg_0.218	SL	62	1.4	883.5	0.644	1.3	1.77E-01	573.5	47.2	9.28E-03	1.94E-05
107	Vsl_0.300_Vsg_0.304	SL	62	1.4	883.5	0.643	1.3	1.80E-01	569.8	46.2	9.28E-03	1.93E-05
108	Vsl_0.300_Vsg_0.385	SL	62	1.4	883.5	0.642	1.3	1.83E-01	567.9	45.6	9.28E-03	1.93E-05
109	Vsl_0.300_Vsg_0.459	SL	62	1.4	883.4	0.642	1.3	1.88E-01	566.9	45.4	9.29E-03	1.93E-05
110	Vsl_0.300_Vsg_0.530	SL	62	1.4	883.4	0.642	1.3	1.90E-01	566.4	45.3	9.29E-03	1.93E-05
111	Vsl_0.300_Vsg_0.604	SL	62	1.4	883.5	0.646	1.3	2.00E-01	571.6	46.8	9.28E-03	1.94E-05
112	Vsl_0.300_Vsg_0.690	SL	62	1.4	883.4	0.642	1.3	2.11E-01	567.6	45.6	9.29E-03	1.94E-05
113	Vsl_0.300_Vsg_0.781	SL	62	1.4	883.4	0.642	1.3	2.14E-01	565.8	45.2	9.29E-03	1.94E-05
114	Vsl_0.300_Vsg_1.012	SL	62	1.4	883.4	0.642	1.3	2.47E-01	564.4	44.9	9.29E-03	1.95E-05
115	Vsl_0.300_Vsg_1.155	SL	62	1.4	883.5	0.645	1.3	2.59E-01	569.9	46.4	9.28E-03	1.96E-05
116	Vsl_0.300_Vsg_1.578	SL	62	1.4	883.4	0.642	1.3	2.97E-01	566.9	45.4	9.29E-03	1.97E-05
117	Vsl_0.300_Vsg_2.036	SL	61	1.4	883.7	0.648	1.3	3.50E-01	584.9	51.1	9.27E-03	2.02E-05
118	Vsl_0.300_Vsg_2.457	SL	61	1.4	883.6	0.642	1.3	3.56E-01	581.4	49.4	9.27E-03	2.01E-05
119	Vsl_0.300_Vsg_2.921	SL	62	1.4	883.5	0.642	1.3	3.96E-01	572.6	46.8	9.28E-03	2.04E-05
120	Vsl_0.022_Vsg_0.324	SL	69	1.4	881.2	0.642	1.2	3.78E-01	429.0	30.2	9.43E-03	1.97E-05
121	Vsl_0.022_Vsg_0.504	SL	69	1.4	881.1	0.642	1.2	3.09E-01	428.2	30.1	9.43E-03	1.96E-05
122	Vsl_0.022_Vsg_0.719	SL	69	1.4	881.1	0.642	1.2	2.96E-01	427.6	30.1	9.43E-03	1.96E-05
123	Vsl_0.022_Vsg_0.969	SL	69	1.4	881.2	0.642	1.2	3.05E-01	428.6	30.1	9.43E-03	1.96E-05
124	Vsl_0.022_Vsg_1.418	SL	69	1.4	881.1	0.642	1.2	1.48E-01	427.9	30.1	9.43E-03	1.95E-05
125	Vsl_0.022_Vsg_1.900	SL	70	1.4	881.1	0.642	1.2	8.27E-02	426.7	30.0	9.43E-03	1.94E-05
126	Vsl_0.022_Vsg_2.403	SL	70	1.4	881.1	0.642	1.2	5.01E-02	427.2	30.0	9.43E-03	1.94E-05
127	Vsl_0.044_Vsg_0.160	SL	70	1.4	881.1	0.642	1.2	8.63E-02	423.9	29.7	9.43E-03	1.94E-05
128	Vsl_0.044_Vsg_0.255	SL	70	1.4	881.0	0.642	1.2	2.02E-01	423.2	29.7	9.44E-03	1.95E-05
129	Vsl_0.044_Vsg_0.345	SL	70	1.4	881.0	0.642	1.2	3.43E-01	422.8	29.6	9.44E-03	1.97E-05
130	Vsl_0.044_Vsg_0.517	SL	70	1.4	881.0	0.642	1.2	1.70E-01	422.6	29.6	9.44E-03	1.95E-05
131	Vsl_0.044_Vsg_0.738	SL	70	1.4	881.0	0.642	1.2	3.05E-01	422.9	29.7	9.44E-03	1.96E-05
132	Vsl_0.044_Vsg_1.015	SL	70	1.4	881.0	0.642	1.2	2.92E-01	423.1	29.7	9.44E-03	1.96E-05
133	Vsl_0.044_Vsg_1.499	SL	70	1.4	881.0	0.643	1.2	2.69E-01	419.0	29.4	9.44E-03	1.96E-05
134	Vsl_0.044_Vsg_1.994	SL	70	1.4	881.0	0.642	1.2	1.60E-01	418.8	29.3	9.44E-03	1.95E-05
135	Vsl_0.044_Vsg_2.485	SL	70	1.4	880.9	0.642	1.2	1.05E-01	418.0	29.2	9.44E-03	1.94E-05
136	Vsl_0.089_Vsg_0.164	SL	70	1.4	880.9	0.642	1.2	5.05E-02	415.4	29.0	9.45E-03	1.94E-05
137	Vsl_0.089_Vsg_0.267	SL	70	1.4	880.9	0.642	1.2	5.57E-02	416.4	29.1	9.44E-03	1.94E-05
138	Vsl_0.089_Vsg_0.379	SL	70	1.4	880.9	0.642	1.2	1.62E-01	416.7	29.1	9.44E-03	1.94E-05
139	Vsl_0.089_Vsg_0.558	SL	70	1.4	880.9	0.642	1.2	2.38E-01	416.7	29.1	9.44E-03	1.95E-05

140	Vsl_0.089_Vsg_0.772	SL	70	1.4	880.9	0.642	1.2	2.57E-01	417.1	29.1	9.44E-03	1.96E-05
141	Vsl_0.089_Vsg_1.094	SL	70	1.4	880.9	0.642	1.2	2.64E-01	417.4	29.2	9.44E-03	1.96E-05
142	Vsl_0.089_Vsg_1.617	SL	70	1.4	880.9	0.642	1.2	3.11E-01	417.8	29.2	9.44E-03	1.97E-05
143	Vsl_0.089_Vsg_2.147	SL	70	1.4	880.9	0.642	1.2	3.82E-01	417.6	29.2	9.44E-03	1.99E-05
144	Vsl_0.089_Vsg_2.758	SL	70	1.4	881.0	0.644	1.2	2.76E-01	419.5	29.4	9.44E-03	1.97E-05
145	Vsl_0.133_Vsg_0.172	SL	70	1.4	880.9	0.642	1.2	7.06E-02	414.7	28.9	9.45E-03	1.93E-05
146	Vsl_0.133_Vsg_0.279	SL	70	1.4	880.9	0.642	1.2	1.02E-01	414.3	28.9	9.45E-03	1.93E-05
147	Vsl_0.133_Vsg_0.404	SL	70	1.4	880.8	0.642	1.2	1.25E-01	414.0	28.9	9.45E-03	1.94E-05
148	Vsl_0.133_Vsg_0.592	SL	70	1.4	880.8	0.642	1.2	1.79E-01	413.8	28.9	9.45E-03	1.94E-05
149	Vsl_0.133_Vsg_0.858	SL	70	1.4	880.9	0.644	1.2	1.94E-01	415.0	29.1	9.45E-03	1.95E-05
150	Vsl_0.133_Vsg_1.134	SL	70	1.4	880.9	0.642	1.2	2.31E-01	414.1	28.9	9.45E-03	1.95E-05
151	Vsl_0.133_Vsg_1.749	SL	70	1.4	880.8	0.642	1.2	3.34E-01	413.2	28.8	9.45E-03	1.98E-05
152	Vsl_0.133_Vsg_2.429	SL	70	1.4	880.8	0.642	1.2	3.40E-01	413.3	28.8	9.45E-03	1.98E-05
153	Vsl_0.178_Vsg_0.165	SL	71	1.4	880.8	0.642	1.2	8.41E-02	411.5	28.7	9.45E-03	1.93E-05
154	Vsl_0.178_Vsg_0.272	SL	71	1.4	880.8	0.642	1.2	9.24E-02	411.2	28.6	9.45E-03	1.93E-05
155	Vsl_0.178_Vsg_0.410	SL	71	1.4	880.8	0.642	1.2	1.27E-01	410.9	28.6	9.45E-03	1.93E-05
156	Vsl_0.178_Vsg_0.608	SL	71	1.4	880.8	0.642	1.2	1.94E-01	410.8	28.6	9.45E-03	1.94E-05
157	Vsl_0.178_Vsg_0.913	SL	71	1.4	880.8	0.642	1.2	1.97E-01	410.6	28.6	9.45E-03	1.95E-05
158	Vsl_0.178_Vsg_1.191	SL	71	1.4	880.8	0.642	1.2	2.15E-01	410.2	28.6	9.45E-03	1.95E-05
159	Vsl_0.178_Vsg_1.833	SL	71	1.4	880.8	0.642	1.2	3.06E-01	409.5	28.5	9.45E-03	1.97E-05
160	Vsl_0.178_Vsg_2.444	SL	71	1.4	880.8	0.642	1.2	3.66E-01	409.4	28.5	9.45E-03	2.00E-05
161	Vsl_0.178_Vsg_3.205	SL	71	1.4	880.8	0.642	1.2	4.27E-01	410.2	28.6	9.45E-03	2.03E-05
162	Vsl_0.222_Vsg_0.198	SL	71	1.4	880.7	0.642	1.2	9.83E-02	407.2	28.3	9.46E-03	1.93E-05
163	Vsl_0.222_Vsg_0.329	SL	71	1.4	880.7	0.642	1.2	1.11E-01	406.9	28.3	9.46E-03	1.93E-05
164	Vsl_0.222_Vsg_0.456	SL	71	1.4	880.7	0.642	1.2	1.39E-01	406.6	28.3	9.46E-03	1.93E-05
165	Vsl_0.222_Vsg_0.643	SL	71	1.4	880.7	0.642	1.2	1.65E-01	405.7	28.2	9.46E-03	1.94E-05
166	Vsl_0.222_Vsg_0.957	SL	71	1.4	880.7	0.642	1.2	1.96E-01	405.3	28.1	9.46E-03	1.94E-05
167	Vsl_0.222_Vsg_1.224	SL	71	1.4	880.7	0.642	1.2	2.15E-01	405.0	28.1	9.46E-03	1.95E-05
168	Vsl_0.222_Vsg_2.006	SL	71	1.4	880.7	0.642	1.3	3.22E-01	405.7	28.2	9.46E-03	1.98E-05
169	Vsl_0.222_Vsg_3.046	SL	71	1.4	880.7	0.642	1.3	4.94E-01	405.2	28.1	9.46E-03	2.07E-05
170	Vsl_0.267_Vsg_0.204	SL	70	1.4	880.9	0.642	1.2	1.15E-01	418.7	29.3	9.44E-03	1.93E-05
171	Vsl_0.267_Vsg_0.333	SL	70	1.4	881.0	0.642	1.3	1.24E-01	418.9	29.3	9.44E-03	1.93E-05
172	Vsl_0.267_Vsg_0.442	SL	70	1.4	880.9	0.642	1.3	1.35E-01	417.4	29.2	9.44E-03	1.93E-05
173	Vsl_0.267_Vsg_0.674	SL	70	1.4	880.9	0.642	1.3	1.83E-01	416.7	29.1	9.44E-03	1.94E-05
174	Vsl_0.267_Vsg_1.008	SL	70	1.4	880.9	0.642	1.3	2.17E-01	415.0	29.0	9.45E-03	1.95E-05
175	Vsl_0.267_Vsg_1.388	SL	70	1.4	880.9	0.642	1.3	2.34E-01	414.4	28.9	9.45E-03	1.95E-05
176	Vsl_0.267_Vsg_2.082	SL	70	1.4	880.8	0.642	1.3	3.03E-01	413.3	28.8	9.45E-03	1.98E-05
177	Vsl_0.267_Vsg_2.988	SL	71	1.4	880.8	0.643	1.3	3.65E-01	412.3	28.8	9.45E-03	2.01E-05
178	Vsl_0.311_Vsg_0.199	SL	71	1.4	880.8	0.643	1.3	1.26E-01	410.0	28.6	9.45E-03	1.93E-05
179	Vsl_0.311_Vsg_0.339	SL	71	1.4	880.7	0.642	1.3	1.35E-01	408.5	28.4	9.46E-03	1.93E-05
180	Vsl_0.311_Vsg_0.490	SL	71	1.4	880.7	0.642	1.3	1.45E-01	407.8	28.4	9.46E-03	1.93E-05
181	Vsl_0.311_Vsg_0.727	SL	71	1.4	880.7	0.642	1.3	1.75E-01	407.3	28.3	9.46E-03	1.93E-05
182	Vsl_0.311_Vsg_1.059	SL	71	1.4	880.7	0.644	1.3	2.09E-01	406.6	28.3	9.46E-03	1.94E-05
183	Vsl_0.311_Vsg_2.223	SL	71	1.4	880.6	0.642	1.3	3.23E-01	403.9	28.0	9.46E-03	1.98E-05
184	Vsl_0.311_Vsg_3.174	SL	71	1.4	880.6	0.642	1.3	4.12E-01	403.4	28.0	9.46E-03	2.03E-05
185	Vsl_0.356_Vsg_0.227	SL	71	1.4	880.6	0.642	1.3	1.41E-01	403.1	28.0	9.46E-03	1.92E-05
186	Vsl_0.356_Vsg_0.369	SL	71	1.4	880.6	0.642	1.3	1.48E-01	402.1	27.9	9.46E-03	1.93E-05
187	Vsl_0.356_Vsg_0.515	SL	71	1.4	880.6	0.644	1.3	1.62E-01	402.6	28.0	9.46E-03	1.93E-05
188	Vsl_0.356_Vsg_0.716	SL	71	1.4	880.6	0.642	1.3	1.77E-01	400.9	27.8	9.47E-03	1.93E-05
189	Vsl_0.356_Vsg_1.053	SL	71	1.4	880.6	0.644	1.3	2.06E-01	401.3	27.9	9.47E-03	1.94E-05
190	Vsl_0.356_Vsg_1.571	SL	71	1.4	880.6	0.644	1.3	2.64E-01	401.4	27.9	9.47E-03	1.96E-05
191	Vsl_0.356_Vsg_2.426	SL	71	1.4	880.6	0.645	1.3	3.07E-01	401.8	28.0	9.46E-03	1.98E-05
192	Vsl_0.022_Vsg_0.228	SL	80	1.4	878.0	0.642	1.2	1.36E-02	301.9	19.9	9.63E-03	1.94E-05
193	Vsl_0.022_Vsg_0.331	SL	80	1.4	878.0	0.642	1.2	1.37E-02	301.8	19.9	9.63E-03	1.94E-05
194	Vsl_0.022_Vsg_0.461	SL	80	1.4	878.0	0.642	1.2	1.42E-02	301.8	19.9	9.63E-03	1.94E-05
195	Vsl_0.022_Vsg_0.698	SL	80	1.4	878.0	0.642	1.2	2.31E-01	302.1	19.9	9.63E-03	1.94E-05
196	Vsl_0.022_Vsg_0.944	SL	80	1.4	878.0	0.642	1.2	2.41E-01	302.4	19.9	9.63E-03	1.95E-05
197	Vsl_0.022_Vsg_1.416	SL	80	1.4	878.0	0.642	1.2	2.36E-01	303.6	20.0	9.63E-03	1.95E-05
198	Vsl_0.022_Vsg_1.871	SL	80	1.4	878.0	0.642	1.2	4.79E-02	303.6	20.0	9.63E-03	1.94E-05
199	Vsl_0.022_Vsg_2.392	SL	80	1.4	878.0	0.642	1.2	5.44E-02	303.0	20.0	9.63E-03	1.94E-05
200	Vsl_0.044_Vsg_0.241	SL	80	1.4	877.9	0.642	1.2	9.90E-02	301.3	19.8	9.63E-03	1.94E-05
201	Vsl_0.044_Vsg_0.345	SL	80	1.4	877.9	0.642	1.2	7.69E-02	301.3	19.8	9.63E-03	1.94E-05
202	Vsl_0.044_Vsg_0.493	SL	80	1.4	877.9	0.642	1.2	2.32E-01	301.6	19.9	9.63E-03	1.95E-05
203	Vsl_0.044_Vsg_0.730	SL	80	1.4	877.9	0.642	1.2	2.76E-01	301.7	19.9	9.63E-03	1.95E-05
204	Vsl_0.044_Vsg_0.976	SL	80	1.4	877.9	0.642	1.2	2.91E-01	301.7	19.9	9.63E-03	1.95E-05
205	Vsl_0.044_Vsg_1.491	SL	80	1.4	878.0	0.642	1.2	3.40E-01	302.3	19.9	9.63E-03	1.96E-05
206	Vsl_0.044_Vsg_1.948	SL	80	1.4	878.0	0.642	1.2	2.34E-01	302.1	19.9	9.63E-03	1.95E-05
207	Vsl_0.044_Vsg_2.427	SL	80	1.4	878.0	0.642	1.2	1.64E-01	302.5	19.9	9.63E-03	1.94E-05
208	Vsl_0.089_Vsg_0.263	SL	80	1.4	877.9	0.642	1.2	1.38E-01	300.5	19.8	9.63E-03	1.94E-05
209	Vsl_0.089_Vsg_0.356	SL	80	1.4	877.9	0.642	1.2	9.22E-02	300.4	19.8	9.63E-03	1.93E-05
210	Vsl_0.089_Vsg_0.520	SL	80	1.4	877.9	0.642	1.2	1.56E-01	300.2	19.7	9.63E-03	1.94E-05
211	Vsl_0.089_Vsg_0.760	SL	80	1.4	877.9	0.642	1.2	2.11E-01	300.3	19.8	9.63E-03	1.94E-05
212	Vsl_0.089_Vsg_1.019	SL	80	1.4	878.0	0.642	1.2	2.63E-01	302.7	19.9	9.63E-03	1.95E-05
213	Vsl_0.089_Vsg_1.536	SL	80	1.4	878.0	0.642	1.2	3.26E-01	302.3	19.9	9.63E-03	1.97E-05
214	Vsl_0.089_Vsg_2.041	SL	80	1.4	878.0	0.642	1.2	4.13E-01	302.1	19.9	9.63E-03	1.99E-05
215	Vsl_0.089_Vsg_2.819	SL	80	1.4	878.0	0.642	1.2	4.43E-01	302.1	19.9	9.63E-03	2.00E-05
216	Vsl_0.133_Vsg_0.278	SL	80	1.4	877.7	0.644	1.2	7.91E-02	295.3	19.4	9.64E-03	1.94E-05
217	Vsl_0.133_Vsg_0.382	SL	81	1.4	877.7	0.642	1.2	1.03E-01	294.1	19.3	9.64E-03	1.93E-05
218	Vsl_0.133_Vsg_0.531	SL	81	1.4	877.6	0.642	1.2	1.49E-01	291.7	19.1	9.65E-03	1.94E-05

219	Vsl_0.133_Vsg_0.796	SL	81	1.4	877.7	0.642	1.2	1.79E-01	293.3	19.2	9.65E-03	1.94E-05
220	Vsl_0.133_Vsg_1.081	SL	81	1.4	877.7	0.642	1.2	2.01E-01	293.9	19.3	9.64E-03	1.94E-05
221	Vsl_0.133_Vsg_1.681	SL	80	1.4	877.7	0.642	1.2	3.05E-01	295.0	19.4	9.64E-03	1.96E-05
222	Vsl_0.133_Vsg_2.189	SL	80	1.4	877.8	0.642	1.2	3.71E-01	296.0	19.4	9.64E-03	1.98E-05
223	Vsl_0.133_Vsg_2.909	SL	80	1.4	877.8	0.642	1.2	4.67E-01	296.8	19.5	9.64E-03	2.02E-05
224	Vsl_0.178_Vsg_0.264	SL	80	1.4	878.0	0.642	1.2	9.09E-02	303.4	20.0	9.63E-03	1.93E-05
225	Vsl_0.178_Vsg_0.366	SL	80	1.4	878.0	0.642	1.2	1.13E-01	303.2	20.0	9.63E-03	1.93E-05
226	Vsl_0.178_Vsg_0.533	SL	80	1.4	878.0	0.642	1.2	1.50E-01	303.1	20.0	9.63E-03	1.94E-05
227	Vsl_0.178_Vsg_0.848	SL	80	1.4	878.0	0.642	1.2	1.62E-01	303.0	20.0	9.63E-03	1.94E-05
228	Vsl_0.178_Vsg_1.117	SL	80	1.4	878.0	0.642	1.2	1.88E-01	303.0	19.9	9.63E-03	1.94E-05
229	Vsl_0.178_Vsg_1.806	SL	80	1.4	878.0	0.642	1.2	2.91E-01	303.0	20.0	9.63E-03	1.96E-05
230	Vsl_0.178_Vsg_2.385	SL	80	1.4	878.0	0.642	1.2	3.64E-01	302.1	19.9	9.63E-03	1.99E-05
231	Vsl_0.178_Vsg_3.061	SL	80	1.4	878.0	0.642	1.2	4.26E-01	302.0	19.9	9.63E-03	2.01E-05
232	Vsl_0.222_Vsg_0.282	SL	80	1.4	877.9	0.642	1.2	8.39E-02	301.0	19.8	9.63E-03	1.93E-05
233	Vsl_0.222_Vsg_0.389	SL	80	1.4	877.9	0.642	1.2	1.01E-01	300.7	19.8	9.63E-03	1.93E-05
234	Vsl_0.222_Vsg_0.589	SL	80	1.4	877.9	0.642	1.2	1.47E-01	300.6	19.8	9.63E-03	1.93E-05
235	Vsl_0.222_Vsg_0.892	SL	80	1.4	877.9	0.642	1.2	1.82E-01	300.5	19.8	9.63E-03	1.94E-05
236	Vsl_0.222_Vsg_1.183	SL	80	1.4	877.9	0.642	1.2	2.13E-01	300.4	19.8	9.63E-03	1.94E-05
237	Vsl_0.222_Vsg_1.885	SL	80	1.4	877.9	0.642	1.2	2.74E-01	300.4	19.8	9.63E-03	1.96E-05
238	Vsl_0.222_Vsg_2.594	SL	80	1.4	877.9	0.642	1.2	3.60E-01	300.7	19.8	9.63E-03	1.99E-05
239	Vsl_0.222_Vsg_3.322	SL	80	1.4	877.9	0.642	1.2	4.69E-01	301.0	19.8	9.63E-03	2.04E-05
240	Vsl_0.267_Vsg_0.293	SL	80	1.4	877.9	0.642	1.2	9.74E-02	300.1	19.7	9.63E-03	1.93E-05
241	Vsl_0.267_Vsg_0.416	SL	80	1.4	877.9	0.642	1.2	1.10E-01	300.3	19.7	9.63E-03	1.93E-05
242	Vsl_0.267_Vsg_0.612	SL	80	1.4	877.9	0.642	1.2	1.35E-01	299.9	19.7	9.63E-03	1.93E-05
243	Vsl_0.267_Vsg_0.923	SL	80	1.4	877.9	0.642	1.2	1.92E-01	299.9	19.7	9.63E-03	1.94E-05
244	Vsl_0.267_Vsg_1.253	SL	80	1.4	877.9	0.642	1.2	2.19E-01	300.0	19.7	9.63E-03	1.94E-05
245	Vsl_0.267_Vsg_1.935	SL	80	1.4	877.9	0.642	1.2	2.64E-01	300.1	19.7	9.63E-03	1.96E-05
246	Vsl_0.267_Vsg_2.747	SL	80	1.4	877.8	0.644	1.2	3.43E-01	296.9	19.6	9.64E-03	1.99E-05
247	Vsl_0.267_Vsg_3.546	SL	80	1.4	877.9	0.644	1.2	4.79E-01	299.0	19.7	9.63E-03	2.06E-05
248	Vsl_0.311_Vsg_0.322	SL	80	1.4	877.9	0.642	1.2	1.03E-01	300.6	19.8	9.63E-03	1.92E-05
249	Vsl_0.311_Vsg_0.447	SL	80	1.4	877.9	0.642	1.2	1.16E-01	300.5	19.8	9.63E-03	1.93E-05
250	Vsl_0.311_Vsg_0.628	SL	80	1.4	877.9	0.642	1.2	1.49E-01	299.9	19.7	9.63E-03	1.93E-05
251	Vsl_0.311_Vsg_0.972	SL	80	1.4	877.9	0.642	1.2	2.01E-01	299.6	19.7	9.63E-03	1.94E-05
252	Vsl_0.311_Vsg_1.285	SL	80	1.4	877.9	0.642	1.2	2.24E-01	299.2	19.7	9.63E-03	1.94E-05
253	Vsl_0.311_Vsg_2.028	SL	80	1.4	877.8	0.642	1.2	2.65E-01	298.5	19.6	9.64E-03	1.96E-05
254	Vsl_0.311_Vsg_2.849	SL	80	1.4	877.8	0.642	1.2	3.39E-01	298.2	19.6	9.64E-03	1.99E-05
255	Vsl_0.311_Vsg_3.615	SL	80	1.4	877.9	0.642	1.2	4.27E-01	298.9	19.7	9.63E-03	2.03E-05
256	Vsl_0.356_Vsg_0.305	SL	80	1.4	877.8	0.642	1.2	1.07E-01	297.3	19.5	9.64E-03	1.92E-05
257	Vsl_0.356_Vsg_0.437	SL	80	1.4	877.8	0.645	1.2	1.19E-01	298.4	19.7	9.64E-03	1.93E-05
258	Vsl_0.356_Vsg_0.674	SL	80	1.4	877.8	0.642	1.2	1.49E-01	297.1	19.5	9.64E-03	1.93E-05
259	Vsl_0.356_Vsg_0.986	SL	80	1.4	877.8	0.642	1.2	1.87E-01	297.3	19.5	9.64E-03	1.93E-05
260	Vsl_0.356_Vsg_1.337	SL	80	1.4	877.8	0.642	1.2	2.07E-01	297.8	19.6	9.64E-03	1.94E-05
261	Vsl_0.356_Vsg_2.202	SL	80	1.4	877.8	0.642	1.2	3.25E-01	296.8	19.5	9.64E-03	1.98E-05
262	Vsl_0.356_Vsg_2.902	SL	80	1.4	877.8	0.642	1.3	3.48E-01	296.9	19.5	9.64E-03	1.99E-05
263	Vsl_0.022_Vsg_0.486	SL	90	1.4	874.8	0.644	1.1	1.34E-02	217.5	13.9	9.83E-03	1.93E-05
264	Vsl_0.022_Vsg_0.710	SL	90	1.4	874.9	0.648	1.1	1.38E-02	219.1	14.1	9.82E-03	1.93E-05
265	Vsl_0.022_Vsg_0.941	SL	89	1.4	875.1	0.646	1.1	2.04E-01	225.1	14.5	9.80E-03	1.95E-05
266	Vsl_0.022_Vsg_1.397	SL	89	1.4	875.2	0.643	1.1	2.56E-01	226.5	14.5	9.80E-03	1.94E-05
267	Vsl_0.022_Vsg_1.908	SL	90	1.4	874.7	0.649	1.1	2.79E-02	215.9	13.9	9.83E-03	1.94E-05
268	Vsl_0.022_Vsg_2.374	SL	89	1.4	875.1	0.642	1.1	3.24E-02	225.0	14.4	9.80E-03	1.93E-05
269	Vsl_0.044_Vsg_0.336	SL	89	1.4	875.1	0.644	1.1	3.21E-01	223.0	14.3	9.81E-03	1.95E-05
270	Vsl_0.044_Vsg_0.499	SL	89	1.4	875.0	0.646	1.1	2.16E-01	222.5	14.3	9.81E-03	1.95E-05
271	Vsl_0.044_Vsg_0.715	SL	90	1.4	874.9	0.644	1.1	2.33E-01	219.9	14.1	9.82E-03	1.95E-05
272	Vsl_0.044_Vsg_0.954	SL	90	1.4	874.9	0.642	1.1	2.72E-01	219.2	14.0	9.82E-03	1.94E-05
273	Vsl_0.044_Vsg_1.438	SL	89	1.4	875.0	0.648	1.2	3.31E-01	221.5	14.3	9.81E-03	1.97E-05
274	Vsl_0.044_Vsg_1.906	SL	90	1.4	874.9	0.643	1.2	3.81E-01	219.6	14.0	9.82E-03	1.96E-05
275	Vsl_0.044_Vsg_2.394	SL	90	1.4	874.9	0.642	1.2	2.10E-01	219.8	14.0	9.82E-03	1.94E-05
276	Vsl_0.089_Vsg_0.352	SL	89	1.4	875.0	0.642	1.2	1.60E-01	222.4	14.2	9.81E-03	1.94E-05
277	Vsl_0.089_Vsg_0.508	SL	89	1.4	875.0	0.643	1.2	1.58E-01	222.0	14.2	9.81E-03	1.94E-05
278	Vsl_0.089_Vsg_0.731	SL	90	1.4	874.9	0.654	1.2	2.10E-01	218.8	14.2	9.82E-03	1.96E-05
279	Vsl_0.089_Vsg_1.000	SL	90	1.4	874.9	0.642	1.2	2.45E-01	218.7	14.0	9.82E-03	1.95E-05
280	Vsl_0.089_Vsg_1.525	SL	90	1.4	874.9	0.642	1.2	3.07E-01	220.0	14.0	9.82E-03	1.96E-05
281	Vsl_0.089_Vsg_2.007	SL	89	1.4	875.0	0.642	1.2	4.02E-01	220.7	14.1	9.82E-03	1.97E-05
282	Vsl_0.089_Vsg_2.638	SL	89	1.4	875.0	0.642	1.2	4.65E-01	221.5	14.1	9.81E-03	1.99E-05
283	Vsl_0.133_Vsg_0.240	SL	89	1.4	875.0	0.642	1.2	9.22E-02	221.8	14.2	9.81E-03	1.93E-05
284	Vsl_0.133_Vsg_0.368	SL	89	1.4	875.0	0.642	1.2	1.21E-01	221.7	14.1	9.81E-03	1.93E-05
285	Vsl_0.133_Vsg_0.525	SL	90	1.4	874.9	0.645	1.2	1.55E-01	218.9	14.0	9.82E-03	1.94E-05
286	Vsl_0.133_Vsg_0.777	SL	90	1.4	874.8	0.643	1.2	1.76E-01	217.3	13.9	9.83E-03	1.94E-05
287	Vsl_0.133_Vsg_1.042	SL	90	1.4	874.8	0.643	1.2	2.10E-01	216.7	13.8	9.83E-03	1.94E-05
288	Vsl_0.133_Vsg_1.602	SL	90	1.4	874.8	0.642	1.2	2.97E-01	216.6	13.8	9.83E-03	1.95E-05
289	Vsl_0.133_Vsg_2.207	SL	90	1.4	874.9	0.642	1.2	3.53E-01	219.1	14.0	9.82E-03	1.97E-05
290	Vsl_0.133_Vsg_2.684	SL	90	1.4	874.9	0.642	1.2	4.59E-01	219.5	14.0	9.82E-03	2.00E-05
291	Vsl_0.178_Vsg_0.171	SL	90	1.4	874.7	0.650	1.2	5.30E-02	215.7	13.9	9.83E-03	1.95E-05
292	Vsl_0.178_Vsg_0.271	SL	91	1.4	874.6	0.645	1.2	7.45E-02	212.7	13.6	9.84E-03	1.94E-05
293	Vsl_0.178_Vsg_0.373	SL	91	1.4	874.5	0.644	1.2	1.10E-01	211.1	13.5	9.84E-03	1.94E-05
294	Vsl_0.178_Vsg_0.537	SL	91	1.4	874.5	0.642	1.2	1.37E-01	210.2	13.4	9.85E-03	1.93E-05
295	Vsl_0.178_Vsg_0.795	SL	91	1.4	874.5	0.642	1.2	1.46E-01	210.1	13.4	9.85E-03	1.93E-05
296	Vsl_0.178_Vsg_1.081	SL	90	1.4	874.7	0.648	1.2	2.03E-01	214.5	13.8	9.83E-03	1.95E-05
297	Vsl_0.178_Vsg_1.657	SL	90	1.4	874.7	0.642	1.2	2.79E-01	214.7	13.7	9.83E-03	1.95E-05

298	Vsl_0.178_Vsg_2.275	SL	90	1.4	874.7	0.642	1.2	3.47E-01	215.2	13.7	9.83E-03	1.97E-05
299	Vsl_0.178_Vsg_2.847	SL	90	1.4	874.8	0.643	1.2	4.06E-01	216.8	13.8	9.83E-03	1.99E-05
300	Vsl_0.222_Vsg_0.274	SL	91	1.4	874.6	0.642	1.2	8.16E-02	212.0	13.5	9.84E-03	1.93E-05
301	Vsl_0.222_Vsg_0.370	SL	91	1.4	874.6	0.642	1.2	9.48E-02	212.3	13.5	9.84E-03	1.93E-05
302	Vsl_0.222_Vsg_0.552	SL	91	1.4	874.6	0.642	1.2	1.21E-01	212.5	13.5	9.84E-03	1.93E-05
303	Vsl_0.222_Vsg_0.860	SL	91	1.4	874.6	0.642	1.2	1.62E-01	212.8	13.6	9.84E-03	1.93E-05
304	Vsl_0.222_Vsg_1.128	SL	90	1.4	874.8	0.645	1.2	1.92E-01	216.3	13.9	9.83E-03	1.95E-05
305	Vsl_0.222_Vsg_1.726	SL	90	1.4	874.7	0.644	1.2	2.54E-01	214.8	13.7	9.83E-03	1.95E-05
306	Vsl_0.222_Vsg_2.438	SL	90	1.4	874.8	0.643	1.2	3.12E-01	216.4	13.8	9.83E-03	1.97E-05
307	Vsl_0.222_Vsg_3.084	SL	90	1.4	874.8	0.643	1.2	3.66E-01	217.2	13.9	9.83E-03	1.98E-05
308	Vsl_0.267_Vsg_0.270	SL	90	1.4	874.9	0.642	1.2	7.73E-02	218.5	13.9	9.82E-03	1.93E-05
309	Vsl_0.267_Vsg_0.390	SL	90	1.4	874.9	0.642	1.2	9.07E-02	218.8	14.0	9.82E-03	1.93E-05
310	Vsl_0.267_Vsg_0.562	SL	90	1.4	874.9	0.642	1.2	1.19E-01	219.4	14.0	9.82E-03	1.93E-05
311	Vsl_0.267_Vsg_0.846	SL	89	1.4	875.0	0.644	1.2	1.56E-01	221.0	14.2	9.82E-03	1.94E-05
312	Vsl_0.267_Vsg_1.156	SL	90	1.4	874.9	0.644	1.2	1.96E-01	219.9	14.1	9.82E-03	1.94E-05
313	Vsl_0.267_Vsg_1.865	SL	90	1.4	874.9	0.642	1.2	2.77E-01	218.8	14.0	9.82E-03	1.95E-05
314	Vsl_0.267_Vsg_2.541	SL	90	1.4	874.9	0.642	1.2	3.28E-01	218.7	14.0	9.82E-03	1.97E-05
315	Vsl_0.267_Vsg_3.346	SL	89	1.4	875.0	0.644	1.2	3.76E-01	222.7	14.3	9.81E-03	2.00E-05
316	Vsl_0.311_Vsg_0.169	SL	90	1.4	874.8	0.643	1.2	6.55E-02	217.3	13.9	9.83E-03	1.93E-05
317	Vsl_0.311_Vsg_0.290	SL	90	1.4	874.8	0.643	1.2	8.04E-02	218.2	13.9	9.82E-03	1.93E-05
318	Vsl_0.311_Vsg_0.403	SL	90	1.4	874.8	0.643	1.2	9.22E-02	218.2	13.9	9.82E-03	1.92E-05
319	Vsl_0.311_Vsg_0.589	SL	90	1.4	874.8	0.642	1.2	1.15E-01	217.9	13.9	9.82E-03	1.93E-05
320	Vsl_0.311_Vsg_0.870	SL	90	1.4	874.8	0.642	1.2	1.41E-01	217.9	13.9	9.82E-03	1.93E-05
321	Vsl_0.311_Vsg_1.207	SL	90	1.4	874.8	0.642	1.2	1.80E-01	218.4	13.9	9.82E-03	1.93E-05
322	Vsl_0.311_Vsg_1.851	SL	90	1.4	874.7	0.642	1.2	2.49E-01	214.3	13.7	9.83E-03	1.95E-05
323	Vsl_0.311_Vsg_2.588	SL	89	1.4	875.0	0.655	1.2	2.99E-01	222.0	14.5	9.81E-03	2.00E-05
324	Vsl_0.311_Vsg_3.323	SL	90	1.4	874.7	0.643	1.2	3.42E-01	215.4	13.8	9.83E-03	1.98E-05
325	Vsl_0.356_Vsg_0.182	SL	90	1.4	874.8	0.644	1.2	7.48E-02	217.5	13.9	9.83E-03	1.93E-05
326	Vsl_0.356_Vsg_0.283	SL	90	1.4	874.8	0.642	1.2	8.26E-02	216.6	13.8	9.83E-03	1.92E-05
327	Vsl_0.356_Vsg_0.413	SL	91	1.4	874.6	0.647	1.2	9.21E-02	212.2	13.6	9.84E-03	1.93E-05
328	Vsl_0.356_Vsg_0.610	SL	91	1.4	874.6	0.642	1.2	1.14E-01	212.5	13.5	9.84E-03	1.93E-05
329	Vsl_0.356_Vsg_0.902	SL	90	1.4	874.6	0.646	1.2	1.58E-01	213.8	13.7	9.84E-03	1.94E-05
330	Vsl_0.356_Vsg_1.263	SL	91	1.4	874.5	0.652	1.2	1.89E-01	210.6	13.6	9.84E-03	1.96E-05
331	Vsl_0.356_Vsg_1.932	SL	91	1.4	874.4	0.643	1.2	2.41E-01	208.6	13.3	9.85E-03	1.95E-05
332	Vsl_0.356_Vsg_2.887	SL	92	1.4	874.3	0.648	1.2	3.10E-01	206.5	13.3	9.86E-03	1.98E-05
333	Vsl_0.022_Vsg_0.382	SL	96	1.4	873.1	0.642	1.1	1.31E-02	181.6	11.5	9.93E-03	1.93E-05
334	Vsl_0.022_Vsg_0.490	SL	95	1.4	873.1	0.643	1.1	1.32E-02	182.2	11.6	9.93E-03	1.93E-05
335	Vsl_0.022_Vsg_0.739	SL	95	1.4	873.1	0.644	1.1	1.34E-02	183.4	11.7	9.93E-03	1.94E-05
336	Vsl_0.022_Vsg_0.980	SL	95	1.5	873.4	0.665	1.1	9.70E-02	187.7	12.4	9.91E-03	1.97E-05
337	Vsl_0.022_Vsg_1.206	SL	94	1.4	873.5	0.648	1.1	1.56E-01	190.0	12.2	9.91E-03	1.94E-05
338	Vsl_0.022_Vsg_1.491	SL	94	1.4	873.5	0.645	1.1	2.25E-01	190.0	12.1	9.91E-03	1.95E-05
339	Vsl_0.022_Vsg_1.680	SL	94	1.4	873.5	0.645	1.1	1.68E-01	189.9	12.1	9.91E-03	1.95E-05
340	Vsl_0.022_Vsg_1.914	SL	94	1.4	873.5	0.643	1.1	2.81E-02	190.3	12.1	9.91E-03	1.93E-05
341	Vsl_0.022_Vsg_2.124	SL	94	1.4	873.6	0.643	1.1	3.03E-02	191.6	12.2	9.90E-03	1.93E-05
342	Vsl_0.050_Vsg_0.370	SL	95	1.4	873.1	0.645	1.1	2.13E-01	182.8	11.7	9.93E-03	1.95E-05
343	Vsl_0.050_Vsg_0.485	SL	95	1.4	873.1	0.643	1.1	1.84E-01	182.5	11.6	9.93E-03	1.94E-05
344	Vsl_0.050_Vsg_0.695	SL	95	1.4	873.1	0.643	1.1	2.13E-01	183.4	11.7	9.93E-03	1.94E-05
345	Vsl_0.050_Vsg_0.976	SL	95	1.4	873.2	0.642	1.1	2.46E-01	184.1	11.7	9.93E-03	1.94E-05
346	Vsl_0.050_Vsg_1.203	SL	95	1.4	873.2	0.642	1.1	3.03E-01	184.3	11.7	9.93E-03	1.95E-05
347	Vsl_0.050_Vsg_1.493	SL	95	1.4	873.2	0.643	1.1	3.36E-01	184.7	11.8	9.92E-03	1.95E-05
348	Vsl_0.050_Vsg_1.710	SL	95	1.4	873.2	0.643	1.1	3.90E-01	184.9	11.8	9.92E-03	1.96E-05
349	Vsl_0.050_Vsg_1.958	SL	95	1.4	873.3	0.648	1.1	4.12E-01	186.3	12.0	9.92E-03	1.98E-05
350	Vsl_0.089_Vsg_0.340	SL	96	1.4	872.9	0.642	1.1	1.65E-01	178.5	11.3	9.95E-03	1.93E-05
351	Vsl_0.089_Vsg_0.399	SL	96	1.4	872.9	0.642	1.1	1.73E-01	178.6	11.4	9.94E-03	1.93E-05
352	Vsl_0.089_Vsg_0.489	SL	96	1.4	873.0	0.646	1.1	1.84E-01	181.5	11.6	9.93E-03	1.95E-05
353	Vsl_0.089_Vsg_0.733	SL	96	1.4	873.0	0.642	1.1	2.17E-01	181.1	11.5	9.94E-03	1.94E-05
354	Vsl_0.089_Vsg_1.006	SL	96	1.4	873.0	0.642	1.1	2.72E-01	181.4	11.5	9.94E-03	1.94E-05
355	Vsl_0.089_Vsg_1.243	SL	96	1.4	872.9	0.652	1.1	3.09E-01	179.6	11.6	9.94E-03	1.97E-05
356	Vsl_0.089_Vsg_1.495	SL	96	1.4	872.9	0.643	1.1	3.29E-01	178.6	11.4	9.94E-03	1.96E-05
357	Vsl_0.089_Vsg_1.740	SL	96	1.4	872.9	0.642	1.1	3.82E-01	178.1	11.3	9.95E-03	1.96E-05
358	Vsl_0.089_Vsg_1.903	SL	96	1.4	872.8	0.642	1.1	4.07E-01	177.8	11.3	9.95E-03	1.97E-05
359	Vsl_0.100_Vsg_0.244	SL	96	1.4	872.9	0.642	1.1	9.41E-02	179.1	11.4	9.94E-03	1.93E-05
360	Vsl_0.100_Vsg_0.345	SL	96	1.4	872.9	0.642	1.1	1.37E-01	179.0	11.4	9.94E-03	1.93E-05
361	Vsl_0.100_Vsg_0.400	SL	96	1.4	872.9	0.642	1.1	1.55E-01	179.2	11.4	9.94E-03	1.93E-05
362	Vsl_0.100_Vsg_0.503	SL	96	1.4	872.9	0.642	1.1	1.81E-01	179.6	11.4	9.94E-03	1.93E-05
363	Vsl_0.100_Vsg_0.763	SL	96	1.4	873.0	0.642	1.1	2.23E-01	180.3	11.5	9.94E-03	1.94E-05
364	Vsl_0.100_Vsg_0.987	SL	96	1.4	873.0	0.652	1.1	2.35E-01	180.9	11.7	9.94E-03	1.96E-05
365	Vsl_0.100_Vsg_1.235	SL	96	1.4	873.0	0.643	1.1	2.56E-01	179.9	11.5	9.94E-03	1.95E-05
366	Vsl_0.100_Vsg_1.523	SL	96	1.4	872.9	0.642	1.1	2.85E-01	179.5	11.4	9.94E-03	1.95E-05
367	Vsl_0.100_Vsg_1.760	SL	96	1.4	872.9	0.642	1.1	3.19E-01	179.4	11.4	9.94E-03	1.95E-05
368	Vsl_0.100_Vsg_2.126	SL	96	1.4	872.9	0.642	1.1	3.80E-01	179.6	11.4	9.94E-03	1.97E-05
369	Vsl_0.133_Vsg_0.254	SL	96	1.4	872.9	0.642	1.1	1.15E-01	179.1	11.4	9.94E-03	1.93E-05
370	Vsl_0.133_Vsg_0.350	SL	96	1.4	872.9	0.642	1.1	1.39E-01	178.8	11.4	9.94E-03	1.93E-05
371	Vsl_0.133_Vsg_0.414	SL	96	1.4	872.9	0.642	1.1	1.41E-01	178.7	11.4	9.94E-03	1.93E-05
372	Vsl_0.133_Vsg_0.521	SL	96	1.4	872.9	0.642	1.1	1.56E-01	178.2	11.3	9.95E-03	1.93E-05
373	Vsl_0.133_Vsg_0.782	SL	96	1.4	872.9	0.642	1.1	1.78E-01	178.0	11.3	9.95E-03	1.93E-05
374	Vsl_0.133_Vsg_1.038	SL	96	1.4	872.8	0.642	1.1	2.09E-01	177.7	11.3	9.95E-03	1.94E-05
375	Vsl_0.133_Vsg_1.293	SL	96	1.4	872.8	0.642	1.1	2.64E-01	177.8	11.3	9.95E-03	1.94E-05
376	Vsl_0.133_Vsg_1.582	SL	96	1.4	872.9	0.642	1.1	2.75E-01	178.1	11.3	9.95E-03	1.95E-05

377	Vsl_0.133_Vsg_1.859	SL	95	1.4	873.1	0.650	1.1	3.33E-01	182.7	11.8	9.93E-03	1.97E-05
378	Vsl_0.133_Vsg_2.037	SL	96	1.4	873.0	0.644	1.1	3.47E-01	181.2	11.6	9.94E-03	1.97E-05
379	Vsl_0.133_Vsg_2.408	SL	96	1.4	873.0	0.644	1.1	3.76E-01	180.3	11.5	9.94E-03	1.98E-05
380	Vsl_0.200_Vsg_0.159	SL	96	1.5	872.9	0.662	1.1	5.05E-02	179.7	11.8	9.94E-03	1.95E-05
381	Vsl_0.200_Vsg_0.264	SL	96	1.4	872.8	0.647	1.1	6.66E-02	177.1	11.4	9.95E-03	1.94E-05
382	Vsl_0.200_Vsg_0.366	SL	97	1.4	872.8	0.642	1.1	8.53E-02	176.2	11.2	9.95E-03	1.93E-05
383	Vsl_0.200_Vsg_0.412	SL	97	1.4	872.7	0.642	1.1	1.06E-01	175.7	11.2	9.95E-03	1.93E-05
384	Vsl_0.200_Vsg_0.538	SL	97	1.4	872.7	0.643	1.1	1.21E-01	175.5	11.2	9.96E-03	1.93E-05
385	Vsl_0.200_Vsg_0.798	SL	97	1.4	872.7	0.642	1.1	1.53E-01	175.1	11.1	9.96E-03	1.93E-05
386	Vsl_0.200_Vsg_1.075	SL	97	1.4	872.7	0.645	1.1	2.07E-01	175.9	11.2	9.95E-03	1.95E-05
387	Vsl_0.200_Vsg_1.349	SL	96	1.4	872.8	0.642	1.1	2.41E-01	177.3	11.3	9.95E-03	1.94E-05
388	Vsl_0.200_Vsg_1.639	SL	96	1.4	872.9	0.643	1.2	2.55E-01	178.0	11.3	9.95E-03	1.95E-05
389	Vsl_0.200_Vsg_1.915	SL	96	1.4	872.9	0.642	1.2	2.83E-01	178.7	11.4	9.94E-03	1.95E-05
390	Vsl_0.200_Vsg_2.262	SL	96	1.4	872.9	0.642	1.2	3.47E-01	179.1	11.4	9.94E-03	1.97E-05
391	Vsl_0.200_Vsg_2.594	SL	96	1.4	872.9	0.642	1.2	3.54E-01	179.0	11.4	9.94E-03	1.97E-05
392	Vsl_0.222_Vsg_0.153	SL	97	1.4	872.6	0.642	1.1	5.12E-02	174.2	11.1	9.96E-03	1.93E-05
393	Vsl_0.222_Vsg_0.269	SL	97	1.4	872.7	0.644	1.1	7.05E-02	174.8	11.2	9.96E-03	1.93E-05
394	Vsl_0.222_Vsg_0.375	SL	97	1.4	872.7	0.645	1.1	7.97E-02	176.0	11.2	9.95E-03	1.93E-05
395	Vsl_0.222_Vsg_0.418	SL	96	1.4	872.8	0.643	1.1	1.14E-01	177.0	11.3	9.95E-03	1.93E-05
396	Vsl_0.222_Vsg_0.529	SL	96	1.4	872.8	0.642	1.1	1.30E-01	177.6	11.3	9.95E-03	1.93E-05
397	Vsl_0.222_Vsg_0.816	SL	96	1.4	872.8	0.646	1.1	1.59E-01	177.2	11.3	9.95E-03	1.94E-05
398	Vsl_0.222_Vsg_1.100	SL	97	1.4	872.7	0.644	1.2	1.97E-01	175.8	11.2	9.95E-03	1.94E-05
399	Vsl_0.222_Vsg_1.396	SL	97	1.4	872.7	0.643	1.2	2.29E-01	174.8	11.1	9.96E-03	1.94E-05
400	Vsl_0.222_Vsg_1.698	SL	97	1.4	872.7	0.642	1.2	2.51E-01	174.5	11.1	9.96E-03	1.94E-05
401	Vsl_0.222_Vsg_2.003	SL	97	1.4	872.8	0.642	1.2	3.01E-01	176.1	11.2	9.95E-03	1.96E-05
402	Vsl_0.222_Vsg_2.322	SL	96	1.4	872.8	0.643	1.2	3.12E-01	176.9	11.3	9.95E-03	1.96E-05
403	Vsl_0.222_Vsg_2.649	SL	96	1.4	872.8	0.642	1.2	3.17E-01	177.5	11.3	9.95E-03	1.96E-05
404	Vsl_0.300_Vsg_0.116	SL	97	1.4	872.6	0.642	1.2	5.05E-02	173.7	11.1	9.96E-03	1.92E-05
405	Vsl_0.300_Vsg_0.167	SL	97	1.4	872.6	0.642	1.2	5.41E-02	173.9	11.1	9.96E-03	1.92E-05
406	Vsl_0.300_Vsg_0.264	SL	97	1.4	872.7	0.644	1.2	6.15E-02	175.5	11.2	9.96E-03	1.92E-05
407	Vsl_0.300_Vsg_0.385	SL	97	1.4	872.7	0.642	1.2	8.60E-02	175.3	11.2	9.96E-03	1.92E-05
408	Vsl_0.300_Vsg_0.441	SL	97	1.4	872.7	0.642	1.2	8.52E-02	175.6	11.2	9.95E-03	1.92E-05
409	Vsl_0.300_Vsg_0.559	SL	97	1.4	872.7	0.653	1.2	1.21E-01	175.0	11.3	9.96E-03	1.95E-05
410	Vsl_0.300_Vsg_0.845	SL	97	1.4	872.6	0.643	1.2	1.49E-01	173.9	11.1	9.96E-03	1.93E-05
411	Vsl_0.300_Vsg_1.166	SL	97	1.4	872.6	0.642	1.2	1.91E-01	173.6	11.0	9.96E-03	1.93E-05
412	Vsl_0.300_Vsg_1.445	SL	97	1.4	872.6	0.643	1.2	2.25E-01	174.0	11.1	9.96E-03	1.94E-05
413	Vsl_0.300_Vsg_1.794	SL	97	1.4	872.7	0.643	1.2	2.42E-01	174.6	11.1	9.96E-03	1.94E-05
414	Vsl_0.300_Vsg_2.129	SL	97	1.4	872.8	0.643	1.2	3.06E-01	176.5	11.2	9.95E-03	1.96E-05
415	Vsl_0.300_Vsg_2.447	SL	96	1.4	872.8	0.642	1.2	3.28E-01	176.6	11.2	9.95E-03	1.97E-05
416	Vsl_0.300_Vsg_2.848	SL	96	1.4	872.8	0.642	1.2	3.48E-01	177.1	11.3	9.95E-03	1.97E-05
417	Vsl_0.356_Vsg_0.108	SL	96	1.4	872.8	0.644	1.2	5.91E-02	177.3	11.3	9.95E-03	1.93E-05
418	Vsl_0.356_Vsg_0.168	SL	96	1.4	872.9	0.643	1.2	6.13E-02	178.1	11.3	9.95E-03	1.92E-05
419	Vsl_0.356_Vsg_0.291	SL	96	1.4	872.9	0.644	1.2	7.08E-02	178.9	11.4	9.94E-03	1.93E-05
420	Vsl_0.356_Vsg_0.389	SL	96	1.4	872.8	0.654	1.2	8.09E-02	176.6	11.5	9.95E-03	1.95E-05
421	Vsl_0.356_Vsg_0.453	SL	97	1.4	872.7	0.642	1.2	8.53E-02	175.4	11.2	9.96E-03	1.92E-05
422	Vsl_0.356_Vsg_0.572	SL	97	1.4	872.7	0.642	1.2	1.08E-01	175.5	11.2	9.96E-03	1.92E-05
423	Vsl_0.356_Vsg_0.861	SL	97	1.4	872.8	0.642	1.2	1.41E-01	176.1	11.2	9.95E-03	1.93E-05
424	Vsl_0.356_Vsg_1.198	SL	96	1.4	872.8	0.643	1.2	1.77E-01	176.6	11.2	9.95E-03	1.93E-05
425	Vsl_0.356_Vsg_1.517	SL	97	1.5	872.8	0.660	1.2	2.31E-01	176.2	11.6	9.95E-03	1.99E-05
426	Vsl_0.356_Vsg_1.886	SL	97	1.5	872.6	0.665	1.2	2.73E-01	172.7	11.4	9.97E-03	2.02E-05
427	Vsl_0.356_Vsg_2.204	SL	98	1.4	872.4	0.649	1.2	2.53E-01	169.2	10.9	9.98E-03	1.96E-05
428	Vsl_0.356_Vsg_2.558	SL	98	1.4	872.3	0.642	1.2	3.03E-01	167.8	10.7	9.98E-03	1.96E-05
429	Vsl_0.022_Vsg_0.458	SL	99	1.4	871.9	0.645	1.1	1.30E-02	161.3	10.3	1.00E-02	1.93E-05
430	Vsl_0.022_Vsg_0.686	SL	99	1.4	872.0	0.646	1.1	1.32E-02	163.1	10.5	1.00E-02	1.94E-05
431	Vsl_0.022_Vsg_0.935	SL	98	1.4	872.2	0.655	1.1	1.44E-02	166.0	10.8	9.99E-03	1.97E-05
432	Vsl_0.022_Vsg_1.395	SL	97	1.5	872.5	0.662	1.1	1.63E-01	172.2	11.3	9.97E-03	1.96E-05
433	Vsl_0.022_Vsg_1.917	SL	97	1.4	872.7	0.645	1.1	2.62E-02	175.1	11.2	9.96E-03	1.94E-05
434	Vsl_0.022_Vsg_2.399	SL	96	1.5	872.9	0.666	1.1	3.03E-02	178.5	11.8	9.95E-03	1.99E-05
435	Vsl_0.044_Vsg_0.476	SL	100	1.5	871.8	0.667	1.1	2.17E-01	159.7	10.6	1.00E-02	2.06E-05
436	Vsl_0.044_Vsg_0.701	SL	99	1.4	872.0	0.654	1.1	2.33E-01	162.5	10.6	1.00E-02	1.97E-05
437	Vsl_0.044_Vsg_0.950	SL	99	1.4	872.0	0.644	1.1	2.75E-01	162.2	10.4	1.00E-02	1.94E-05
438	Vsl_0.044_Vsg_1.435	SL	99	1.4	872.0	0.643	1.1	3.35E-01	162.7	10.4	1.00E-02	1.95E-05
439	Vsl_0.044_Vsg_1.925	SL	99	1.4	872.0	0.647	1.1	3.75E-01	163.3	10.5	1.00E-02	1.97E-05
440	Vsl_0.044_Vsg_2.236	SL	99	1.4	872.1	0.643	1.1	1.57E-01	164.5	10.5	9.99E-03	1.94E-05
441	Vsl_0.089_Vsg_0.332	SL	100	1.4	871.6	0.644	1.1	1.31E-01	156.9	10.0	1.00E-02	1.93E-05
442	Vsl_0.089_Vsg_0.501	SL	100	1.4	871.7	0.642	1.1	2.01E-01	158.3	10.1	1.00E-02	1.93E-05
443	Vsl_0.089_Vsg_0.750	SL	99	1.5	872.1	0.666	1.1	2.39E-01	164.3	10.9	1.00E-02	2.01E-05
444	Vsl_0.089_Vsg_0.973	SL	98	1.4	872.2	0.643	1.1	2.66E-01	166.1	10.6	9.99E-03	1.94E-05
445	Vsl_0.089_Vsg_1.490	SL	98	1.4	872.2	0.642	1.1	3.07E-01	166.7	10.6	9.99E-03	1.95E-05
446	Vsl_0.089_Vsg_2.004	SL	98	1.4	872.2	0.642	1.1	4.06E-01	167.1	10.7	9.98E-03	1.97E-05
447	Vsl_0.133_Vsg_0.249	SL	101	1.4	871.4	0.644	1.1	8.83E-02	152.6	9.8	1.00E-02	1.93E-05
448	Vsl_0.133_Vsg_0.348	SL	101	1.4	871.3	0.643	1.1	1.28E-01	151.7	9.7	1.00E-02	1.93E-05
449	Vsl_0.133_Vsg_0.510	SL	101	1.4	871.3	0.644	1.1	1.55E-01	151.1	9.7	1.00E-02	1.94E-05
450	Vsl_0.133_Vsg_0.770	SL	101	1.4	871.2	0.644	1.1	1.87E-01	150.5	9.7	1.00E-02	1.93E-05
451	Vsl_0.133_Vsg_1.014	SL	101	1.4	871.2	0.643	1.1	2.33E-01	150.5	9.7	1.00E-02	1.94E-05
452	Vsl_0.133_Vsg_1.557	SL	101	1.4	871.3	0.645	1.1	2.91E-01	151.9	9.8	1.00E-02	1.96E-05
453	Vsl_0.133_Vsg_1.997	SL	101	1.4	871.4	0.644	1.1	3.42E-01	153.7	9.9	1.00E-02	1.96E-05
454	Vsl_0.133_Vsg_2.707	SL	100	1.4	871.7	0.642	1.1	4.41E-01	157.5	10.1	1.00E-02	1.98E-05
455	Vsl_0.178_Vsg_0.274	SL	101	1.4	871.4	0.645	1.1	8.19E-02	153.8	9.9	1.00E-02	1.94E-05

456	Vsl_0.178_Vsg_0.365	SL	101	1.4	871.4	0.649	1.1	1.02E-01	152.7	9.9	1.00E-02	1.94E-05
457	Vsl_0.178_Vsg_0.513	SL	101	1.4	871.3	0.643	1.1	1.36E-01	151.6	9.7	1.00E-02	1.93E-05
458	Vsl_0.178_Vsg_0.789	SL	101	1.4	871.3	0.644	1.1	1.84E-01	151.3	9.7	1.00E-02	1.94E-05
459	Vsl_0.178_Vsg_1.043	SL	101	1.4	871.3	0.642	1.1	2.21E-01	150.9	9.7	1.00E-02	1.94E-05
460	Vsl_0.178_Vsg_1.597	SL	101	1.4	871.2	0.642	1.1	2.96E-01	150.8	9.7	1.00E-02	1.95E-05
461	Vsl_0.178_Vsg_2.218	SL	101	1.4	871.2	0.643	1.1	3.29E-01	150.8	9.7	1.00E-02	1.96E-05
462	Vsl_0.222_Vsg_0.269	SL	100	1.4	871.7	0.642	1.1	7.06E-02	158.2	10.1	1.00E-02	1.92E-05
463	Vsl_0.222_Vsg_0.370	SL	100	1.4	871.7	0.642	1.1	8.94E-02	158.0	10.1	1.00E-02	1.92E-05
464	Vsl_0.222_Vsg_0.535	SL	100	1.4	871.7	0.643	1.1	1.28E-01	157.9	10.1	1.00E-02	1.93E-05
465	Vsl_0.222_Vsg_0.808	SL	100	1.4	871.6	0.648	1.1	1.94E-01	156.8	10.1	1.00E-02	1.95E-05
466	Vsl_0.222_Vsg_1.062	SL	101	1.4	871.5	0.651	1.1	1.97E-01	154.1	10.0	1.00E-02	1.96E-05
467	Vsl_0.222_Vsg_1.637	SL	101	1.4	871.3	0.649	1.1	2.65E-01	152.3	9.9	1.00E-02	1.96E-05
468	Vsl_0.222_Vsg_2.254	SL	101	1.4	871.3	0.642	1.1	3.05E-01	151.4	9.7	1.00E-02	1.95E-05
469	Vsl_0.267_Vsg_0.264	SL	101	1.4	871.4	0.644	1.1	6.50E-02	152.8	9.8	1.00E-02	1.93E-05
470	Vsl_0.267_Vsg_0.376	SL	101	1.4	871.3	0.642	1.1	8.25E-02	152.2	9.8	1.00E-02	1.92E-05
471	Vsl_0.267_Vsg_0.564	SL	101	1.4	871.3	0.642	1.1	1.09E-01	152.2	9.7	1.00E-02	1.92E-05
472	Vsl_0.267_Vsg_0.809	SL	100	1.4	871.7	0.644	1.1	1.59E-01	157.5	10.1	1.00E-02	1.93E-05
473	Vsl_0.267_Vsg_1.096	SL	100	1.4	871.6	0.642	1.1	1.61E-01	157.1	10.0	1.00E-02	1.93E-05
474	Vsl_0.267_Vsg_1.702	SL	100	1.4	871.7	0.642	1.1	2.49E-01	157.3	10.0	1.00E-02	1.94E-05
475	Vsl_0.267_Vsg_2.384	SL	100	1.4	871.6	0.647	1.2	3.07E-01	156.4	10.1	1.00E-02	1.97E-05
476	Vsl_0.311_Vsg_0.263	SL	101	1.5	871.3	0.665	1.1	6.39E-02	151.5	10.1	1.00E-02	1.96E-05
477	Vsl_0.311_Vsg_0.384	SL	102	1.4	871.2	0.643	1.1	7.80E-02	149.5	9.6	1.01E-02	1.92E-05
478	Vsl_0.311_Vsg_0.559	SL	102	1.4	871.1	0.642	1.1	1.05E-01	149.2	9.6	1.01E-02	1.92E-05
479	Vsl_0.311_Vsg_0.791	SL	101	1.4	871.2	0.654	1.1	1.46E-01	150.8	9.9	1.00E-02	1.95E-05
480	Vsl_0.311_Vsg_1.137	SL	102	1.4	871.2	0.642	1.1	2.07E-01	149.9	9.6	1.01E-02	1.93E-05
481	Vsl_0.311_Vsg_1.768	SL	102	1.4	871.2	0.645	1.1	2.50E-01	150.4	9.7	1.00E-02	1.95E-05
482	Vsl_0.311_Vsg_2.372	SL	101	1.4	871.3	0.644	1.2	3.05E-01	151.6	9.7	1.00E-02	1.96E-05
483	Vsl_0.356_Vsg_0.281	SL	102	1.4	871.2	0.652	1.1	6.74E-02	150.2	9.8	1.00E-02	1.95E-05
484	Vsl_0.356_Vsg_0.399	SL	102	1.4	871.1	0.644	1.1	7.29E-02	148.6	9.6	1.01E-02	1.92E-05
485	Vsl_0.356_Vsg_0.575	SL	101	1.4	871.5	0.647	1.1	1.03E-01	154.6	10.0	1.00E-02	1.94E-05
486	Vsl_0.356_Vsg_0.862	SL	101	1.4	871.4	0.655	1.1	1.36E-01	152.8	10.0	1.00E-02	1.96E-05
487	Vsl_0.356_Vsg_1.192	SL	102	1.5	871.2	0.665	1.1	2.06E-01	150.1	10.0	1.00E-02	2.01E-05
488	Vsl_0.356_Vsg_1.845	SL	102	1.5	871.0	0.667	1.2	3.08E-01	146.9	9.8	1.01E-02	2.03E-05
489	Vsl_0.356_Vsg_2.489	SL	102	1.4	871.2	0.656	1.2	3.33E-01	150.1	9.9	1.00E-02	1.98E-05

Table A.2 Average and uncertainty for flow conditions, mixture Reynolds number, pressure gradient, and average liquid holdup for all oil viscosities.

1	0.022	7.98E-04	0.333	0.04	0.355	1.00E-03	42	3	79	1.70E-01	0.588
2	0.022	5.85E-04	0.385	0.04	0.407	9.95E-04	47	4	71	1.18E-01	0.577
3	0.022	6.61E-04	0.431	0.05	0.453	1.06E-03	53	5	66	1.02E-01	0.570
4	0.022	1.50E-03	0.496	0.11	0.518	2.60E-03	60	5	78	1.40E-01	0.572
5	0.022	2.25E-03	0.656	0.17	0.678	4.07E-03	78	7	85	1.44E-01	0.570
6	0.022	2.17E-03	0.755	0.20	0.777	4.82E-03	90	8	92	1.60E-01	0.563
7	0.022	2.38E-03	0.946	0.27	0.968	6.55E-03	112	10	102	1.70E-01	0.545
8	0.022	2.17E-03	1.213	0.27	1.235	6.66E-03	137	14	104	2.00E-01	0.520
9	0.022	1.96E-03	1.496	0.14	1.518	4.24E-03	168	17	121	2.24E-01	0.529
10	0.022	1.96E-03	1.754	0.12	1.776	4.44E-03	195	21	118	2.22E-01	0.504
11	0.022	2.13E-03	1.965	0.15	1.987	5.35E-03	217	24	127	2.48E-01	0.506
12	0.050	5.83E-04	0.331	0.02	0.381	1.13E-03	44	4	179	8.06E-02	0.621
13	0.050	5.40E-04	0.367	0.02	0.417	1.20E-03	48	4	184	4.90E-02	0.619
14	0.050	7.01E-04	0.418	0.06	0.468	2.89E-03	54	5	195	1.02E-01	0.609
15	0.050	6.95E-04	0.464	0.06	0.514	3.10E-03	60	5	199	8.40E-02	0.598
16	0.050	9.09E-04	0.530	0.08	0.580	4.12E-03	67	6	205	1.35E-01	0.601
17	0.050	1.09E-03	0.670	0.14	0.720	6.75E-03	84	7	210	1.04E-01	0.583
18	0.050	1.62E-03	0.764	0.21	0.814	1.04E-02	95	8	210	1.45E-01	0.581
19	0.050	1.70E-03	1.017	0.27	1.067	1.30E-02	124	11	239	1.81E-01	0.570
20	0.050	2.62E-03	1.306	0.32	1.356	1.59E-02	151	16	267	2.00E-01	0.548
21	0.050	2.00E-03	1.557	0.27	1.607	1.33E-02	182	17	275	2.13E-01	0.534
22	0.050	1.85E-03	1.797	0.32	1.847	1.57E-02	210	19	262	2.46E-01	0.516
23	0.050	1.81E-03	2.007	0.30	2.057	1.49E-02	232	22	269	2.59E-01	0.489
24	0.050	1.44E-03	2.370	0.24	2.420	1.21E-02	274	26	258	2.22E-01	0.459
25	0.089	7.16E-04	0.282	0.03	0.371	2.81E-03	44	4	358	6.71E-02	0.704
26	0.089	6.42E-04	0.330	0.04	0.419	3.18E-03	48	4	379	7.11E-02	0.681
27	0.089	6.94E-04	0.397	0.05	0.486	4.90E-03	56	5	390	7.05E-02	0.669
28	0.089	7.05E-04	0.448	0.07	0.537	6.10E-03	62	5	397	6.70E-02	0.657
29	0.089	7.66E-04	0.505	0.09	0.594	7.94E-03	69	6	406	1.00E-01	0.654
30	0.089	7.48E-04	0.573	0.09	0.662	8.34E-03	77	7	413	1.05E-01	0.646
31	0.089	8.55E-04	0.721	0.16	0.810	1.40E-02	94	8	432	9.93E-02	0.616
32	0.089	9.30E-04	0.844	0.19	0.933	1.68E-02	109	9	437	1.49E-01	0.609
33	0.089	9.67E-04	1.128	0.24	1.217	2.13E-02	141	12	470	1.66E-01	0.583
34	0.089	1.51E-03	1.400	0.35	1.489	3.11E-02	172	16	491	1.91E-01	0.577
35	0.089	1.71E-03	1.765	0.43	1.854	3.87E-02	215	19	506	2.11E-01	0.535
36	0.089	1.50E-03	2.028	0.50	2.117	4.48E-02	245	22	521	2.01E-01	0.502
37	0.089	1.47E-03	2.281	0.53	2.370	4.79E-02	272	25	511	2.07E-01	0.497
38	0.089	1.26E-03	2.577	0.46	2.666	4.11E-02	305	28	516	1.97E-01	0.466
39	0.089	1.04E-03	2.908	0.54	2.997	4.84E-02	341	32	512	2.07E-01	0.449
40	0.100	7.33E-04	0.229	0.03	0.329	2.97E-03	39	3	426	4.64E-02	0.751
41	0.100	7.25E-04	0.283	0.03	0.383	3.22E-03	45	4	437	4.99E-02	0.718
42	0.100	6.79E-04	0.334	0.04	0.434	4.65E-03	51	4	456	5.90E-02	0.701
43	0.100	7.11E-04	0.404	0.05	0.504	5.42E-03	59	5	466	5.88E-02	0.684
44	0.100	7.28E-04	0.464	0.06	0.564	6.40E-03	66	6	479	6.97E-02	0.674
45	0.100	7.29E-04	0.515	0.08	0.615	7.88E-03	72	6	482	8.15E-02	0.667
46	0.100	7.37E-04	0.593	0.09	0.693	9.87E-03	81	7	500	9.03E-02	0.659
47	0.100	7.80E-04	0.738	0.14	0.838	1.51E-02	98	9	512	1.03E-01	0.630
48	0.100	8.26E-04	0.863	0.20	0.963	2.11E-02	112	10	533	1.23E-01	0.611
49	0.100	9.11E-04	1.153	0.27	1.253	2.78E-02	146	13	549	1.71E-01	0.601
50	0.100	1.13E-03	1.448	0.36	1.548	3.76E-02	179	16	588	1.94E-01	0.575
51	0.100	1.22E-03	1.803	0.49	1.903	5.14E-02	220	20	593	1.80E-01	0.542
52	0.100	1.45E-03	2.032	0.54	2.132	5.60E-02	246	22	602	2.18E-01	0.522
53	0.100	1.24E-03	2.488	0.65	2.588	6.72E-02	297	27	611	2.16E-01	0.488
54	0.100	1.18E-03	2.653	0.60	2.753	6.22E-02	316	29	611	2.21E-01	0.469
55	0.100	9.87E-04	3.013	0.52	3.113	5.42E-02	356	33	610	1.94E-01	0.453
56	0.133	7.33E-04	0.230	0.03	0.363	3.40E-03	42	4	578	4.74E-02	0.770
57	0.133	7.34E-04	0.305	0.03	0.438	4.35E-03	50	4	603	5.28E-02	0.734
58	0.133	7.24E-04	0.365	0.04	0.498	5.72E-03	58	5	618	5.34E-02	0.717
59	0.133	7.35E-04	0.426	0.05	0.559	6.30E-03	65	6	628	5.77E-02	0.700
60	0.133	7.37E-04	0.489	0.06	0.622	8.31E-03	72	6	640	5.76E-02	0.690

61	0.133	7.48E-04	0.547	0.08	0.680	1.02E-02	79	7	647	6.20E-02	0.674
62	0.133	7.52E-04	0.624	0.09	0.757	1.23E-02	88	8	657	7.11E-02	0.668
63	0.133	7.71E-04	0.796	0.15	0.929	2.03E-02	108	10	682	9.74E-02	0.636
64	0.133	8.08E-04	0.911	0.20	1.044	2.74E-02	119	11	700	1.19E-01	0.624
65	0.133	7.68E-04	1.211	0.27	1.344	3.57E-02	154	15	743	1.71E-01	0.598
66	0.133	8.39E-04	1.530	0.38	1.663	5.03E-02	189	18	777	1.81E-01	0.570
67	0.133	8.89E-04	1.821	0.44	1.954	5.94E-02	224	21	788	1.81E-01	0.545
68	0.133	9.45E-04	2.226	0.54	2.359	7.25E-02	270	25	802	1.86E-01	0.499
69	0.133	9.46E-04	2.521	0.64	2.654	8.56E-02	303	29	810	1.82E-01	0.486
70	0.133	9.00E-04	2.891	0.75	3.024	9.98E-02	346	33	811	2.02E-01	0.463
71	0.133	9.02E-04	3.145	0.71	3.278	9.40E-02	374	35	802	1.98E-01	0.456
72	0.200	5.90E-04	0.201	0.02	0.401	4.81E-03	46	4	885	3.00E-02	0.861
73	0.200	5.60E-04	0.263	0.03	0.463	6.33E-03	53	5	912	3.55E-02	0.828
74	0.200	5.18E-04	0.333	0.04	0.533	7.73E-03	61	5	934	4.36E-02	0.798
75	0.200	6.13E-04	0.401	0.05	0.601	9.91E-03	69	6	965	4.38E-02	0.778
76	0.200	5.87E-04	0.462	0.06	0.662	1.13E-02	77	7	972	4.42E-02	0.761
77	0.200	5.51E-04	0.544	0.07	0.744	1.45E-02	86	8	978	5.70E-02	0.736
78	0.200	5.85E-04	0.613	0.09	0.813	1.77E-02	95	8	990	5.96E-02	0.721
79	0.200	6.51E-04	0.696	0.11	0.896	2.28E-02	104	9	1010	6.53E-02	0.698
80	0.200	5.70E-04	0.842	0.16	1.042	3.14E-02	121	11	1027	8.36E-02	0.668
81	0.200	5.57E-04	1.007	0.21	1.207	4.16E-02	140	13	1058	1.31E-01	0.641
82	0.200	5.95E-04	1.339	0.30	1.539	5.91E-02	179	17	1101	1.51E-01	0.617
83	0.200	6.95E-04	1.709	0.40	1.909	7.90E-02	219	21	1166	1.66E-01	0.572
84	0.200	6.79E-04	2.093	0.53	2.293	1.05E-01	264	26	1203	1.53E-01	0.531
85	0.200	7.59E-04	2.468	0.71	2.668	1.40E-01	307	31	1229	1.63E-01	0.495
86	0.200	7.39E-04	2.957	0.87	3.157	1.73E-01	362	37	1278	1.94E-01	0.476
87	0.200	7.43E-04	3.167	0.88	3.367	1.74E-01	385	39	1293	2.09E-01	0.470
88	0.222	6.11E-04	0.146	0.02	0.368	4.49E-03	43	4	967	3.27E-02	0.914
89	0.222	5.29E-04	0.198	0.03	0.420	5.60E-03	49	4	983	3.54E-02	0.888
90	0.222	6.17E-04	0.275	0.03	0.497	7.42E-03	58	5	1011	3.86E-02	0.844
91	0.222	5.92E-04	0.340	0.04	0.562	9.25E-03	65	6	1053	4.68E-02	0.808
92	0.222	6.10E-04	0.412	0.05	0.634	1.18E-02	74	6	1061	4.56E-02	0.785
93	0.222	6.16E-04	0.478	0.06	0.700	1.40E-02	82	7	1071	4.69E-02	0.766
94	0.222	6.21E-04	0.562	0.08	0.784	1.74E-02	92	8	1084	6.46E-02	0.745
95	0.222	5.78E-04	0.627	0.09	0.849	2.00E-02	100	9	1095	5.77E-02	0.726
96	0.222	5.66E-04	0.695	0.11	0.917	2.43E-02	108	9	1109	7.53E-02	0.708
97	0.222	6.52E-04	0.891	0.15	1.113	3.44E-02	130	12	1167	9.40E-02	0.663
98	0.222	6.39E-04	1.055	0.20	1.277	4.53E-02	150	13	1180	1.07E-01	0.647
99	0.222	6.08E-04	1.418	0.31	1.640	6.92E-02	192	18	1228	1.48E-01	0.604
100	0.222	7.00E-04	1.781	0.42	2.003	9.23E-02	228	23	1312	1.57E-01	0.571
101	0.222	7.08E-04	2.204	0.59	2.426	1.29E-01	279	28	1349	1.59E-01	0.529
102	0.222	7.52E-04	2.577	0.69	2.799	1.51E-01	321	33	1417	1.75E-01	0.493
103	0.222	7.69E-04	3.021	0.87	3.243	1.90E-01	371	39	1444	2.04E-01	0.475
104	0.222	7.68E-04	3.472	0.99	3.694	2.17E-01	422	45	1500	1.95E-01	0.461
105	0.300	6.96E-04	0.150	0.02	0.450	7.15E-03	53	4	1338	3.64E-02	0.980
106	0.300	7.64E-04	0.218	0.03	0.518	9.82E-03	61	5	1392	3.94E-02	0.923
107	0.300	7.31E-04	0.304	0.04	0.604	1.33E-02	72	6	1413	4.38E-02	0.880
108	0.300	7.16E-04	0.385	0.06	0.685	1.68E-02	82	7	1430	4.19E-02	0.843
109	0.300	7.53E-04	0.459	0.07	0.759	2.04E-02	91	8	1439	4.98E-02	0.820
110	0.300	6.89E-04	0.530	0.08	0.830	2.36E-02	99	8	1451	5.00E-02	0.796
111	0.300	7.10E-04	0.604	0.09	0.904	2.82E-02	107	9	1502	5.84E-02	0.764
112	0.300	7.14E-04	0.690	0.11	0.990	3.38E-02	118	10	1510	7.15E-02	0.740
113	0.300	7.29E-04	0.781	0.13	1.081	3.88E-02	129	11	1526	6.21E-02	0.726
114	0.300	7.33E-04	1.012	0.19	1.312	5.75E-02	157	14	1560	1.03E-01	0.680
115	0.300	7.77E-04	1.155	0.23	1.455	6.84E-02	172	16	1615	1.22E-01	0.661
116	0.300	7.40E-04	1.578	0.35	1.878	1.07E-01	223	22	1674	1.27E-01	0.611
117	0.300	7.91E-04	2.036	0.53	2.336	1.62E-01	269	30	1843	1.49E-01	0.570
118	0.300	7.90E-04	2.457	0.65	2.757	1.98E-01	319	36	1912	1.70E-01	0.520
119	0.300	8.11E-04	2.921	0.86	3.221	2.59E-01	379	43	1954	1.73E-01	0.486
120	0.022	3.06E-03	0.324	0.10	0.346	2.58E-03	55	4	48	1.05E-01	0.559
121	0.022	3.13E-03	0.504	0.13	0.526	3.43E-03	83	6	44	1.41E-01	0.545
122	0.022	3.63E-03	0.719	0.18	0.741	4.89E-03	117	8	59	1.66E-01	0.552
123	0.022	4.08E-03	0.969	0.25	0.991	6.94E-03	156	11	63	1.63E-01	0.542
124	0.022	2.50E-03	1.418	0.18	1.440	5.42E-03	228	16	68	1.87E-01	0.544
125	0.022	2.95E-03	1.900	0.14	1.922	6.45E-03	305	21	83	2.08E-01	0.507
126	0.022	2.60E-03	2.403	0.11	2.425	6.79E-03	384	27	82	1.98E-01	0.479
127	0.044	6.57E-04	0.160	0.02	0.204	8.78E-04	33	2	119	3.49E-02	0.705
128	0.044	1.18E-03	0.255	0.05	0.299	2.12E-03	48	3	116	5.95E-02	0.635
129	0.044	1.06E-03	0.345	0.10	0.389	4.59E-03	62	4	121	1.02E-01	0.595
130	0.044	1.54E-03	0.517	0.08	0.561	3.52E-03	90	6	123	1.37E-01	0.585
131	0.044	2.63E-03	0.738	0.19	0.782	8.82E-03	125	9	136	1.74E-01	0.578
132	0.044	2.94E-03	1.015	0.25	1.059	1.17E-02	169	12	151	1.70E-01	0.574
133	0.044	3.46E-03	1.499	0.34	1.543	1.62E-02	249	18	168	2.09E-01	0.562
134	0.044	3.02E-03	1.994	0.27	2.038	1.37E-02	329	23	169	2.30E-01	0.512
135	0.044	2.54E-03	2.485	0.22	2.529	1.19E-02	409	29	165	2.17E-01	0.480
136	0.089	4.98E-04	0.164	0.02	0.253	1.51E-03	41	3	256	2.49E-02	0.757
137	0.089	5.23E-04	0.267	0.02	0.356	1.80E-03	58	4	254	4.44E-02	0.685
138	0.089	7.69E-04	0.379	0.05	0.468	4.86E-03	76	5	263	7.35E-02	0.648
139	0.089	1.10E-03	0.558	0.11	0.647	1.01E-02	105	8	281	9.02E-02	0.627

140	0.089	1.38E-03	0.772	0.17	0.861	1.51E-02	140	10	294	1.43E-01	0.611
141	0.089	1.69E-03	1.094	0.24	1.183	2.19E-02	192	14	318	1.69E-01	0.609
142	0.089	2.68E-03	1.617	0.42	1.706	3.80E-02	276	20	345	1.72E-01	0.564
143	0.089	3.23E-03	2.147	0.68	2.236	6.17E-02	362	27	366	2.02E-01	0.509
144	0.089	2.97E-03	2.758	0.63	2.847	5.75E-02	458	33	390	2.42E-01	0.465
145	0.133	5.90E-04	0.172	0.02	0.305	2.44E-03	50	4	405	2.69E-02	0.787
146	0.133	6.34E-04	0.279	0.03	0.412	3.78E-03	67	5	408	4.08E-02	0.723
147	0.133	7.09E-04	0.404	0.04	0.537	6.01E-03	88	6	423	5.53E-02	0.683
148	0.133	8.63E-04	0.592	0.09	0.725	1.21E-02	119	9	447	7.34E-02	0.657
149	0.133	1.10E-03	0.858	0.14	0.991	1.87E-02	162	12	476	1.33E-01	0.636
150	0.133	1.13E-03	1.134	0.22	1.267	2.92E-02	207	15	494	1.42E-01	0.612
151	0.133	1.79E-03	1.749	0.48	1.882	6.49E-02	308	24	534	1.73E-01	0.569
152	0.133	1.92E-03	2.429	0.68	2.562	9.13E-02	419	33	573	1.98E-01	0.488
153	0.178	6.60E-04	0.165	0.02	0.343	3.45E-03	56	4	528	3.10E-02	0.819
154	0.178	6.85E-04	0.272	0.03	0.450	4.50E-03	74	5	540	4.07E-02	0.751
155	0.178	6.90E-04	0.410	0.05	0.588	8.02E-03	96	7	563	4.82E-02	0.705
156	0.178	7.67E-04	0.608	0.10	0.786	1.72E-02	129	9	593	8.51E-02	0.678
157	0.178	8.26E-04	0.913	0.15	1.091	2.61E-02	179	13	618	1.17E-01	0.652
158	0.178	9.79E-04	1.191	0.21	1.369	3.70E-02	225	17	645	1.57E-01	0.624
159	0.178	1.16E-03	1.833	0.46	2.011	8.02E-02	331	27	706	1.68E-01	0.561
160	0.178	1.44E-03	2.444	0.73	2.622	1.27E-01	431	37	747	1.72E-01	0.507
161	0.178	2.09E-03	3.205	1.10	3.383	1.93E-01	555	50	865	2.54E-01	0.453
162	0.222	6.17E-04	0.198	0.02	0.420	4.87E-03	70	5	684	2.65E-02	0.831
163	0.222	6.48E-04	0.329	0.03	0.551	7.43E-03	92	6	711	4.69E-02	0.765
164	0.222	6.63E-04	0.456	0.05	0.678	1.20E-02	113	8	732	4.63E-02	0.731
165	0.222	6.82E-04	0.643	0.09	0.865	1.96E-02	144	11	761	8.16E-02	0.701
166	0.222	7.24E-04	0.957	0.15	1.179	3.42E-02	196	15	790	9.32E-02	0.663
167	0.222	7.33E-04	1.224	0.22	1.446	4.83E-02	241	19	818	1.20E-01	0.638
168	0.222	1.09E-03	2.006	0.52	2.228	1.16E-01	370	32	930	1.61E-01	0.547
169	0.222	1.24E-03	3.046	1.38	3.268	3.07E-01	543	63	1081	1.96E-01	0.479
170	0.267	6.92E-04	0.204	0.02	0.471	6.34E-03	76	5	851	3.31E-02	0.847
171	0.267	6.97E-04	0.333	0.04	0.600	9.63E-03	96	7	882	3.08E-02	0.780
172	0.267	6.78E-04	0.442	0.05	0.709	1.33E-02	114	8	896	4.41E-02	0.760
173	0.267	6.79E-04	0.674	0.10	0.941	2.66E-02	152	11	938	7.65E-02	0.709
174	0.267	7.37E-04	1.008	0.18	1.275	4.66E-02	207	16	971	1.17E-01	0.665
175	0.267	7.49E-04	1.388	0.26	1.655	6.89E-02	269	22	1019	1.17E-01	0.630
176	0.267	9.37E-04	2.082	0.50	2.349	1.33E-01	382	34	1137	1.54E-01	0.548
177	0.267	1.18E-03	2.988	0.86	3.255	2.26E-01	531	52	1305	2.08E-01	0.474
178	0.311	7.98E-04	0.199	0.02	0.510	7.65E-03	83	6	980	2.95E-02	0.875
179	0.311	7.73E-04	0.339	0.04	0.650	1.22E-02	107	8	1012	3.66E-02	0.802
180	0.311	7.50E-04	0.490	0.06	0.801	1.81E-02	132	10	1040	4.29E-02	0.763
181	0.311	7.61E-04	0.727	0.10	1.038	3.16E-02	171	13	1081	8.88E-02	0.714
182	0.311	8.27E-04	1.059	0.18	1.370	5.46E-02	226	18	1124	1.07E-01	0.664
183	0.311	8.51E-04	2.223	0.56	2.534	1.74E-01	422	41	1346	1.44E-01	0.537
184	0.311	9.87E-04	3.174	1.02	3.485	3.13E-01	580	66	1520	2.13E-01	0.468
185	0.356	8.51E-04	0.227	0.03	0.583	1.04E-02	97	7	1119	3.05E-02	0.862
186	0.356	8.13E-04	0.369	0.05	0.725	1.62E-02	121	9	1148	3.87E-02	0.808
187	0.356	8.78E-04	0.515	0.07	0.871	2.40E-02	145	11	1191	4.65E-02	0.763
188	0.356	8.12E-04	0.716	0.10	1.072	3.58E-02	179	14	1219	6.39E-02	0.721
189	0.356	8.90E-04	1.053	0.17	1.409	6.13E-02	236	19	1282	8.71E-02	0.668
190	0.356	9.25E-04	1.571	0.33	1.927	1.16E-01	323	30	1380	1.03E-01	0.609
191	0.356	1.00E-03	2.426	0.58	2.782	2.05E-01	465	47	1596	1.38E-01	0.514
192	0.022	1.42E-03	0.228	0.02	0.250	4.93E-04	56	4	33	5.67E-02	0.638
193	0.022	1.63E-03	0.331	0.02	0.353	6.81E-04	79	5	34	8.25E-02	0.579
194	0.022	2.00E-03	0.461	0.02	0.483	1.01E-03	108	7	18	1.08E-01	0.550
195	0.022	4.33E-03	0.698	0.14	0.720	4.41E-03	161	11	34	1.26E-01	0.565
196	0.022	5.02E-03	0.944	0.20	0.966	6.56E-03	216	14	43	1.30E-01	0.566
197	0.022	4.49E-03	1.416	0.29	1.438	9.20E-03	320	21	47	1.59E-01	0.554
198	0.022	4.28E-03	1.871	0.08	1.893	8.30E-03	421	28	50	1.81E-01	0.542
199	0.022	5.02E-03	2.392	0.15	2.414	1.26E-02	538	36	61	2.03E-01	0.492
200	0.044	1.41E-03	0.241	0.03	0.285	1.25E-03	64	4	77	6.24E-02	0.639
201	0.044	1.11E-03	0.345	0.03	0.389	1.34E-03	87	6	80	5.82E-02	0.593
202	0.044	2.66E-03	0.493	0.10	0.537	4.75E-03	121	8	86	1.19E-01	0.576
203	0.044	3.71E-03	0.730	0.17	0.774	8.40E-03	174	12	93	1.24E-01	0.582
204	0.044	5.32E-03	0.976	0.24	1.020	1.23E-02	229	15	103	1.71E-01	0.582
205	0.044	6.40E-03	1.491	0.44	1.535	2.21E-02	343	23	119	1.74E-01	0.557
206	0.044	6.86E-03	1.948	0.39	1.992	2.24E-02	445	30	133	2.35E-01	0.531
207	0.044	5.45E-03	2.427	0.40	2.471	2.26E-02	552	37	125	2.49E-01	0.495
208	0.089	1.14E-03	0.263	0.03	0.352	3.07E-03	79	5	169	6.03E-02	0.656
209	0.089	1.01E-03	0.356	0.03	0.445	2.86E-03	99	7	172	7.04E-02	0.618
210	0.089	2.05E-03	0.520	0.07	0.609	6.33E-03	136	9	185	9.67E-02	0.601
211	0.089	2.42E-03	0.760	0.14	0.849	1.22E-02	190	13	198	1.07E-01	0.591
212	0.089	3.73E-03	1.019	0.24	1.108	2.12E-02	247	17	211	1.47E-01	0.591
213	0.089	4.42E-03	1.536	0.43	1.625	3.79E-02	362	25	232	1.84E-01	0.560
214	0.089	7.30E-03	2.041	0.72	2.130	6.43E-02	475	34	250	2.12E-01	0.504
215	0.089	8.12E-03	2.819	1.09	2.908	9.79E-02	649	48	295	2.79E-01	0.448
216	0.133	6.81E-04	0.278	0.02	0.411	3.31E-03	95	6	290	3.65E-02	0.684
217	0.133	1.00E-03	0.382	0.04	0.515	5.05E-03	119	8	293	6.49E-02	0.644
218	0.133	1.40E-03	0.531	0.07	0.664	9.57E-03	154	10	301	8.55E-02	0.625

219	0.133	1.99E-03	0.796	0.12	0.929	1.63E-02	214	14	311	9.69E-02	0.621
220	0.133	2.42E-03	1.081	0.19	1.214	2.52E-02	278	19	325	1.33E-01	0.594
221	0.133	3.36E-03	1.681	0.44	1.814	5.81E-02	414	30	373	1.54E-01	0.533
222	0.133	5.20E-03	2.189	0.69	2.322	9.16E-02	529	40	403	1.89E-01	0.487
223	0.133	6.92E-03	2.909	1.19	3.042	1.58E-01	691	58	451	2.46E-01	0.421
224	0.178	6.45E-04	0.264	0.03	0.442	4.55E-03	98	7	394	3.17E-02	0.751
225	0.178	8.23E-04	0.366	0.04	0.544	6.81E-03	121	8	402	4.90E-02	0.707
226	0.178	1.11E-03	0.533	0.07	0.711	1.27E-02	162	11	424	6.63E-02	0.683
227	0.178	1.37E-03	0.848	0.12	1.026	2.10E-02	228	16	440	8.12E-02	0.659
228	0.178	1.82E-03	1.117	0.18	1.295	3.22E-02	288	20	467	1.11E-01	0.636
229	0.178	2.53E-03	1.806	0.44	1.984	7.79E-02	441	34	540	1.74E-01	0.558
230	0.178	3.28E-03	2.385	0.73	2.563	1.29E-01	571	47	593	1.74E-01	0.491
231	0.178	4.05E-03	3.061	1.09	3.239	1.92E-01	722	64	644	2.10E-01	0.450
232	0.222	6.83E-04	0.282	0.03	0.504	5.63E-03	113	8	504	3.60E-02	0.770
233	0.222	7.32E-04	0.389	0.04	0.611	8.51E-03	137	9	516	3.58E-02	0.737
234	0.222	9.53E-04	0.589	0.08	0.811	1.68E-02	182	13	540	7.65E-02	0.709
235	0.222	1.15E-03	0.892	0.14	1.114	3.04E-02	249	18	564	8.01E-02	0.674
236	0.222	1.41E-03	1.183	0.21	1.405	4.71E-02	315	23	588	1.36E-01	0.638
237	0.222	1.87E-03	1.885	0.43	2.107	9.53E-02	472	38	672	1.32E-01	0.552
238	0.222	2.75E-03	2.594	0.77	2.816	1.71E-01	630	56	753	1.94E-01	0.492
239	0.222	2.99E-03	3.322	1.29	3.544	2.84E-01	792	82	856	2.15E-01	0.442
240	0.267	7.34E-04	0.293	0.03	0.560	7.59E-03	125	8	612	2.95E-02	0.786
241	0.267	7.78E-04	0.416	0.04	0.683	1.11E-02	153	10	634	4.17E-02	0.756
242	0.267	8.82E-04	0.612	0.08	0.879	2.03E-02	197	14	649	6.39E-02	0.718
243	0.267	9.96E-04	0.923	0.15	1.190	4.01E-02	267	20	680	8.54E-02	0.673
244	0.267	1.23E-03	1.253	0.23	1.520	6.19E-02	342	26	733	1.02E-01	0.628
245	0.267	1.64E-03	1.935	0.42	2.202	1.14E-01	494	41	832	1.51E-01	0.550
246	0.267	1.93E-03	2.747	0.79	3.014	2.14E-01	683	66	979	2.31E-01	0.466
247	0.267	2.51E-03	3.546	1.39	3.813	3.75E-01	858	101	1062	2.26E-01	0.425
248	0.311	8.04E-04	0.322	0.03	0.633	9.92E-03	142	10	727	3.32E-02	0.793
249	0.311	8.13E-04	0.447	0.05	0.758	1.43E-02	170	12	747	4.52E-02	0.762
250	0.311	9.17E-04	0.628	0.08	0.939	2.46E-02	211	15	765	5.65E-02	0.730
251	0.311	9.59E-04	0.972	0.16	1.283	5.05E-02	288	22	799	8.03E-02	0.682
252	0.311	1.12E-03	1.285	0.24	1.596	7.43E-02	359	29	841	1.09E-01	0.650
253	0.311	1.25E-03	2.028	0.44	2.339	1.37E-01	527	46	974	1.36E-01	0.557
254	0.311	3.52E-03	2.849	0.79	3.160	2.44E-01	712	72	1126	1.89E-01	0.491
255	0.311	2.05E-03	3.615	1.25	3.926	3.86E-01	882	104	1247	2.40E-01	0.452
256	0.356	8.22E-04	0.305	0.03	0.661	1.11E-02	149	10	826	2.96E-02	0.806
257	0.356	9.06E-04	0.437	0.05	0.793	1.63E-02	178	12	853	4.25E-02	0.771
258	0.356	8.91E-04	0.674	0.08	1.030	3.00E-02	233	17	870	6.41E-02	0.730
259	0.356	9.47E-04	0.986	0.15	1.342	5.49E-02	304	23	923	8.40E-02	0.684
260	0.356	9.94E-04	1.337	0.23	1.693	8.16E-02	383	31	988	8.83E-02	0.638
261	0.356	1.13E-03	2.202	0.59	2.558	2.12E-01	580	61	1154	1.47E-01	0.548
262	0.356	1.31E-03	2.902	0.84	3.258	3.00E-01	758	84	1349	1.88E-01	0.484
263	0.022	2.59E-03	0.486	0.02	0.508	1.34E-03	158	10	21	1.11E-01	0.577
264	0.022	3.21E-03	0.710	0.02	0.732	2.36E-03	226	15	28	1.26E-01	0.571
265	0.022	4.94E-03	0.941	0.17	0.963	6.07E-03	289	19	29	1.32E-01	0.572
266	0.022	6.43E-03	1.397	0.32	1.419	1.16E-02	423	27	40	1.61E-01	0.567
267	0.022	4.03E-03	1.908	0.05	1.930	7.89E-03	604	39	40	1.76E-01	0.519
268	0.022	5.28E-03	2.374	0.07	2.396	1.28E-02	719	46	46	1.87E-01	0.514
269	0.044	3.58E-03	0.336	0.10	0.380	4.62E-03	116	8	53	9.07E-02	0.569
270	0.044	3.78E-03	0.499	0.10	0.543	4.83E-03	165	11	62	1.31E-01	0.569
271	0.044	4.93E-03	0.715	0.15	0.759	7.72E-03	233	15	64	1.18E-01	0.569
272	0.044	6.03E-03	0.954	0.23	0.998	1.21E-02	308	20	71	1.48E-01	0.564
273	0.044	8.44E-03	1.438	0.42	1.482	2.28E-02	452	30	81	1.72E-01	0.534
274	0.044	9.70E-03	1.906	0.64	1.950	3.48E-02	600	40	89	1.82E-01	0.494
275	0.044	6.58E-03	2.394	0.44	2.438	2.60E-02	749	48	104	2.21E-01	0.488
276	0.089	1.63E-03	0.352	0.05	0.441	4.65E-03	133	9	121	4.39E-02	0.644
277	0.089	2.35E-03	0.508	0.07	0.597	6.49E-03	181	12	129	1.08E-01	0.635
278	0.089	3.17E-03	0.731	0.14	0.820	1.22E-02	252	17	141	1.06E-01	0.549
279	0.089	4.22E-03	1.000	0.22	1.089	1.94E-02	335	22	152	1.42E-01	0.536
280	0.089	5.58E-03	1.525	0.41	1.614	3.70E-02	494	33	180	1.60E-01	0.496
281	0.089	6.90E-03	2.007	0.71	2.096	6.34E-02	640	45	193	1.81E-01	0.457
282	0.089	1.02E-02	2.638	1.07	2.727	9.72E-02	830	61	220	2.24E-01	0.391
283	0.133	9.75E-04	0.240	0.02	0.373	3.33E-03	113	7	203	3.88E-02	0.742
284	0.133	1.31E-03	0.368	0.04	0.501	5.68E-03	152	10	210	6.69E-02	0.688
285	0.133	1.59E-03	0.525	0.07	0.658	9.78E-03	202	13	218	7.38E-02	0.666
286	0.133	2.03E-03	0.777	0.12	0.910	1.62E-02	282	19	230	1.02E-01	0.649
287	0.133	2.64E-03	1.042	0.19	1.175	2.58E-02	365	25	242	1.23E-01	0.630
288	0.133	3.83E-03	1.602	0.42	1.735	5.56E-02	540	38	283	1.55E-01	0.571
289	0.133	5.76E-03	2.207	0.68	2.340	9.07E-02	719	54	322	2.05E-01	0.514
290	0.133	6.46E-03	2.684	1.07	2.817	1.42E-01	864	70	344	2.16E-01	0.479
291	0.178	6.30E-04	0.171	0.02	0.349	3.21E-03	109	7	269	2.60E-02	0.815
292	0.178	6.87E-04	0.271	0.02	0.449	4.29E-03	142	9	275	3.63E-02	0.743
293	0.178	8.60E-04	0.373	0.04	0.551	7.08E-03	176	11	278	4.85E-02	0.702
294	0.178	1.06E-03	0.537	0.07	0.715	1.19E-02	229	15	287	6.88E-02	0.688
295	0.178	1.63E-03	0.795	0.10	0.973	1.84E-02	312	21	303	7.02E-02	0.659
296	0.178	2.45E-03	1.081	0.19	1.259	3.44E-02	395	28	331	1.10E-01	0.626
297	0.178	3.10E-03	1.657	0.40	1.835	7.18E-02	576	43	372	1.76E-01	0.575

298	0.178	3.58E-03	2.275	0.68	2.453	1.22E-01	768	62	426	1.90E-01	0.518
299	0.178	3.94E-03	2.847	0.99	3.025	1.77E-01	939	81	490	1.84E-01	0.475
300	0.222	7.34E-04	0.274	0.03	0.496	5.58E-03	157	10	349	3.00E-02	0.722
301	0.222	8.13E-04	0.370	0.03	0.592	7.64E-03	187	12	357	4.62E-02	0.695
302	0.222	9.77E-04	0.552	0.06	0.774	1.36E-02	245	16	378	6.57E-02	0.672
303	0.222	1.38E-03	0.860	0.12	1.082	2.74E-02	343	23	400	7.95E-02	0.635
304	0.222	1.61E-03	1.128	0.19	1.350	4.20E-02	420	30	432	9.93E-02	0.611
305	0.222	2.30E-03	1.726	0.38	1.948	8.47E-02	611	47	490	1.51E-01	0.548
306	0.222	2.83E-03	2.438	0.65	2.660	1.46E-01	828	69	564	1.76E-01	0.500
307	0.222	3.06E-03	3.084	0.97	3.306	2.15E-01	1025	93	629	1.99E-01	0.453
308	0.267	7.68E-04	0.270	0.02	0.537	6.61E-03	167	11	447	2.75E-02	0.751
309	0.267	8.02E-04	0.390	0.03	0.657	9.30E-03	202	13	452	3.12E-02	0.712
310	0.267	1.15E-02	0.562	0.06	0.829	1.73E-02	254	17	464	5.90E-02	0.686
311	0.267	1.06E-03	0.846	0.11	1.113	3.09E-02	339	24	499	6.70E-02	0.646
312	0.267	1.31E-03	1.156	0.19	1.423	5.23E-02	436	32	534	9.05E-02	0.606
313	0.267	1.84E-03	1.865	0.44	2.132	1.18E-01	656	55	615	1.60E-01	0.528
314	0.267	2.08E-03	2.541	0.72	2.808	1.91E-01	864	80	704	1.64E-01	0.466
315	0.267	2.34E-03	3.346	1.06	3.613	2.82E-01	1091	110	824	2.29E-01	0.415
316	0.311	7.92E-04	0.169	0.02	0.480	5.69E-03	148	10	498	2.05E-02	0.838
317	0.311	8.30E-04	0.290	0.03	0.601	7.94E-03	184	12	514	2.78E-02	0.768
318	0.311	8.57E-04	0.403	0.04	0.714	1.11E-02	219	14	536	3.76E-02	0.733
319	0.311	8.94E-04	0.589	0.06	0.900	1.88E-02	277	19	546	5.10E-02	0.698
320	0.311	9.87E-04	0.870	0.11	1.181	3.30E-02	364	25	570	9.15E-02	0.657
321	0.311	1.08E-03	1.207	0.19	1.518	5.76E-02	467	35	614	9.95E-02	0.610
322	0.311	1.51E-03	1.851	0.39	2.162	1.20E-01	676	57	696	1.37E-01	0.532
323	0.311	1.63E-03	2.588	0.65	2.899	2.03E-01	878	84	829	1.84E-01	0.465
324	0.311	1.67E-03	3.323	0.96	3.634	3.01E-01	1135	118	906	1.87E-01	0.424
325	0.356	8.78E-04	0.182	0.02	0.538	7.03E-03	167	11	586	2.19E-02	0.775
326	0.356	8.84E-04	0.283	0.03	0.639	9.19E-03	199	13	596	2.55E-02	0.729
327	0.356	9.17E-04	0.413	0.04	0.769	1.32E-02	245	16	614	3.36E-02	0.703
328	0.356	9.46E-04	0.610	0.06	0.966	2.24E-02	307	21	628	6.24E-02	0.669
329	0.356	1.00E-03	0.902	0.12	1.258	4.45E-02	397	29	666	6.28E-02	0.615
330	0.356	1.08E-03	1.263	0.20	1.619	7.42E-02	518	41	712	9.32E-02	0.574
331	0.356	1.29E-03	1.932	0.40	2.288	1.43E-01	739	66	816	1.34E-01	0.500
332	0.356	1.53E-03	2.887	0.76	3.243	2.74E-01	1056	111	955	1.73E-01	0.426
333	0.022	2.42E-03	0.382	0.02	0.404	1.04E-03	150	10	14	8.55E-02	0.518
334	0.022	2.95E-03	0.490	0.02	0.512	1.56E-03	190	12	17	8.66E-02	0.515
335	0.022	3.00E-03	0.739	0.02	0.762	2.32E-03	280	18	23	1.03E-01	0.535
336	0.022	4.90E-03	0.980	0.09	1.002	5.27E-03	360	24	30	1.24E-01	0.530
337	0.022	5.85E-03	1.206	0.17	1.229	8.10E-03	437	28	33	1.38E-01	0.519
338	0.022	6.88E-03	1.491	0.30	1.513	1.24E-02	538	35	35	1.41E-01	0.503
339	0.022	4.53E-03	1.680	0.25	1.702	9.57E-03	605	39	30	1.47E-01	0.493
340	0.022	4.75E-03	1.914	0.05	1.936	9.30E-03	687	44	45	1.85E-01	0.502
341	0.022	4.82E-03	2.124	0.07	2.146	1.05E-02	756	48	42	1.62E-01	0.480
342	0.050	2.49E-03	0.370	0.07	0.420	3.76E-03	155	10	47	7.93E-02	0.585
343	0.050	3.39E-03	0.485	0.08	0.535	4.45E-03	198	13	47	9.24E-02	0.566
344	0.050	4.26E-03	0.695	0.13	0.745	7.36E-03	274	18	56	1.06E-01	0.571
345	0.050	5.07E-03	0.976	0.22	1.026	1.18E-02	376	24	65	1.15E-01	0.562
346	0.050	7.89E-03	1.203	0.33	1.253	1.88E-02	459	30	67	1.33E-01	0.527
347	0.050	8.87E-03	1.493	0.45	1.543	2.61E-02	564	37	71	1.71E-01	0.514
348	0.050	1.00E-02	1.710	0.60	1.760	3.43E-02	642	43	77	1.86E-01	0.499
349	0.050	1.15E-02	1.958	0.72	2.008	4.24E-02	727	49	85	1.80E-01	0.476
350	0.089	1.85E-03	0.340	0.05	0.429	4.71E-03	161	10	97	5.20E-02	0.631
351	0.089	2.07E-03	0.399	0.06	0.488	5.70E-03	184	12	97	6.94E-02	0.622
352	0.089	2.53E-03	0.489	0.08	0.578	7.38E-03	214	14	103	9.38E-02	0.620
353	0.089	3.54E-03	0.733	0.14	0.822	1.29E-02	306	20	111	9.81E-02	0.600
354	0.089	4.51E-03	1.006	0.24	1.095	2.19E-02	406	27	125	1.27E-01	0.580
355	0.089	6.38E-03	1.243	0.34	1.331	3.11E-02	499	34	133	1.66E-01	0.562
356	0.089	6.15E-03	1.495	0.44	1.584	3.96E-02	598	41	144	1.55E-01	0.525
357	0.089	7.07E-03	1.740	0.59	1.829	5.34E-02	692	48	149	1.77E-01	0.509
358	0.089	9.12E-03	1.903	0.69	1.992	6.29E-02	755	53	150	1.75E-01	0.498
359	0.100	1.20E-03	0.244	0.03	0.344	2.77E-03	130	8	115	4.01E-02	0.693
360	0.100	1.75E-03	0.345	0.05	0.445	4.78E-03	169	11	119	4.85E-02	0.644
361	0.100	1.89E-03	0.400	0.06	0.500	6.04E-03	189	12	124	6.57E-02	0.628
362	0.100	2.10E-03	0.503	0.08	0.603	8.68E-03	227	15	130	7.30E-02	0.623
363	0.100	3.09E-03	0.763	0.15	0.863	1.60E-02	324	21	137	1.08E-01	0.611
364	0.100	3.99E-03	0.987	0.21	1.087	2.18E-02	406	27	159	1.14E-01	0.585
365	0.100	4.95E-03	1.235	0.28	1.335	2.97E-02	501	34	167	1.42E-01	0.554
366	0.100	5.65E-03	1.523	0.39	1.623	4.07E-02	610	42	180	1.75E-01	0.530
367	0.100	6.10E-03	1.760	0.50	1.860	5.23E-02	700	49	188	1.76E-01	0.518
368	0.100	7.06E-03	2.126	0.72	2.226	7.51E-02	836	60	204	1.73E-01	0.478
369	0.133	1.19E-03	0.254	0.03	0.387	4.19E-03	145	9	163	3.40E-02	0.696
370	0.133	1.34E-03	0.350	0.05	0.484	6.29E-03	182	12	170	3.95E-02	0.654
371	0.133	1.51E-03	0.414	0.05	0.547	7.36E-03	206	13	172	5.22E-02	0.635
372	0.133	2.05E-03	0.521	0.07	0.654	1.01E-02	247	16	179	5.41E-02	0.624
373	0.133	2.71E-03	0.782	0.13	0.915	1.69E-02	346	23	190	9.19E-02	0.605
374	0.133	3.45E-03	1.038	0.19	1.171	2.61E-02	444	30	200	1.29E-01	0.594
375	0.133	4.33E-03	1.293	0.30	1.427	4.08E-02	541	38	218	1.28E-01	0.540
376	0.133	4.43E-03	1.582	0.39	1.716	5.17E-02	649	46	234	1.52E-01	0.530

377	0.133	5.30E-03	1.859	0.55	1.992	7.34E-02	734	54	264	1.80E-01	0.506
378	0.133	5.44E-03	2.037	0.63	2.171	8.36E-02	807	60	281	2.04E-01	0.494
379	0.133	5.97E-03	2.408	0.80	2.541	1.07E-01	950	72	279	1.82E-01	0.468
380	0.200	6.79E-04	0.159	0.02	0.359	3.77E-03	135	9	262	2.18E-02	0.759
381	0.200	7.55E-04	0.264	0.02	0.464	4.89E-03	176	11	266	3.08E-02	0.685
382	0.200	9.84E-04	0.366	0.03	0.566	6.61E-03	216	14	267	3.80E-02	0.658
383	0.200	1.06E-03	0.412	0.05	0.612	9.16E-03	235	15	272	4.90E-02	0.644
384	0.200	1.04E-03	0.538	0.06	0.738	1.22E-02	283	19	283	5.74E-02	0.628
385	0.200	1.60E-03	0.798	0.11	0.998	2.21E-02	384	26	286	1.03E-01	0.606
386	0.200	2.40E-03	1.075	0.20	1.275	4.00E-02	488	35	317	1.15E-01	0.566
387	0.200	2.56E-03	1.349	0.29	1.549	5.81E-02	589	43	335	1.39E-01	0.536
388	0.200	3.27E-03	1.639	0.37	1.839	7.43E-02	696	52	359	1.53E-01	0.517
389	0.200	3.06E-03	1.918	0.48	2.118	9.62E-02	798	62	393	1.59E-01	0.485
390	0.200	3.85E-03	2.262	0.69	2.462	1.38E-01	926	78	433	1.89E-01	0.458
391	0.200	4.08E-03	2.594	0.81	2.794	1.61E-01	1051	90	461	1.71E-01	0.423
392	0.222	7.01E-04	0.153	0.02	0.375	5.37E-03	145	9	284	2.20E-02	0.862
393	0.222	7.87E-04	0.269	0.02	0.491	5.37E-03	189	12	291	2.61E-02	0.764
394	0.222	8.84E-04	0.375	0.03	0.597	7.16E-03	228	15	301	3.86E-02	0.730
395	0.222	9.21E-04	0.418	0.05	0.640	1.02E-02	243	16	307	4.01E-02	0.720
396	0.222	9.84E-04	0.529	0.07	0.751	1.54E-02	285	19	313	6.26E-02	0.705
397	0.222	1.48E-03	0.816	0.12	1.038	2.61E-02	395	27	337	8.30E-02	0.657
398	0.222	2.19E-03	1.100	0.19	1.322	4.31E-02	506	36	361	1.06E-01	0.618
399	0.222	2.50E-03	1.396	0.28	1.619	6.35E-02	623	46	378	1.38E-01	0.591
400	0.222	2.99E-03	1.698	0.38	1.920	8.39E-02	741	57	417	1.37E-01	0.554
401	0.222	3.06E-03	2.003	0.53	2.225	1.18E-01	850	70	437	1.47E-01	0.530
402	0.222	3.23E-03	2.322	0.64	2.544	1.41E-01	968	81	463	1.83E-01	0.503
403	0.222	3.68E-03	2.649	0.73	2.871	1.63E-01	1089	92	503	2.12E-01	0.482
404	0.300	7.77E-04	0.116	0.02	0.416	5.23E-03	161	10	377	1.89E-02	0.899
405	0.300	7.95E-04	0.167	0.02	0.467	5.74E-03	181	12	387	2.05E-02	0.852
406	0.300	8.16E-04	0.264	0.02	0.564	6.99E-03	216	14	405	2.31E-02	0.786
407	0.300	8.55E-04	0.385	0.03	0.685	1.06E-02	263	17	416	3.48E-02	0.753
408	0.300	8.64E-04	0.441	0.04	0.741	1.15E-02	284	19	423	4.50E-02	0.740
409	0.300	9.96E-04	0.559	0.06	0.859	1.89E-02	330	23	434	5.89E-02	0.715
410	0.300	1.15E-03	0.845	0.11	1.145	3.42E-02	444	31	455	8.95E-02	0.675
411	0.300	1.29E-03	1.166	0.20	1.466	5.96E-02	568	43	490	9.36E-02	0.631
412	0.300	1.57E-03	1.445	0.29	1.745	8.63E-02	675	54	524	1.14E-01	0.599
413	0.300	1.67E-03	1.794	0.38	2.094	1.14E-01	807	67	568	1.34E-01	0.558
414	0.300	2.17E-03	2.129	0.57	2.429	1.73E-01	927	88	610	1.74E-01	0.533
415	0.300	2.10E-03	2.447	0.69	2.747	2.11E-01	1048	104	668	1.73E-01	0.502
416	0.300	2.14E-03	2.848	0.86	3.148	2.60E-01	1197	124	733	1.92E-01	0.478
417	0.356	8.76E-04	0.108	0.02	0.464	6.14E-03	175	11	461	1.71E-02	0.852
418	0.356	8.87E-04	0.168	0.02	0.523	6.76E-03	197	13	472	1.98E-02	0.803
419	0.356	8.97E-04	0.291	0.02	0.646	8.82E-03	242	16	491	2.25E-02	0.741
420	0.356	9.19E-04	0.389	0.03	0.744	1.21E-02	283	19	510	3.01E-02	0.725
421	0.356	9.21E-04	0.453	0.04	0.808	1.39E-02	309	20	510	3.78E-02	0.711
422	0.356	9.51E-04	0.572	0.06	0.927	2.08E-02	355	24	522	5.27E-02	0.689
423	0.356	1.00E-03	0.861	0.11	1.216	3.85E-02	464	33	546	7.32E-02	0.645
424	0.356	1.06E-03	1.198	0.19	1.554	6.68E-02	591	45	592	8.80E-02	0.606
425	0.356	1.35E-03	1.517	0.30	1.872	1.08E-01	713	62	636	1.10E-01	0.570
426	0.356	1.43E-03	1.886	0.45	2.241	1.58E-01	872	84	678	1.52E-01	0.536
427	0.356	1.40E-03	2.204	0.49	2.559	1.72E-01	1016	94	708	1.56E-01	0.501
428	0.356	1.61E-03	2.558	0.67	2.913	2.37E-01	1166	120	758	2.06E-01	0.479
429	0.022	2.79E-03	0.458	0.02	0.480	1.36E-03	201	13	12	8.55E-02	0.520
430	0.022	3.17E-03	0.686	0.02	0.708	2.26E-03	293	19	12	8.76E-02	0.515
431	0.022	3.47E-03	0.935	0.03	0.957	3.35E-03	389	25	15	1.08E-01	0.516
432	0.022	4.86E-03	1.395	0.21	1.417	8.25E-03	556	37	24	1.34E-01	0.507
433	0.022	3.62E-03	1.917	0.06	1.939	7.17E-03	747	48	29	1.49E-01	0.477
434	0.022	4.48E-03	2.399	0.09	2.421	1.11E-02	916	61	44	1.86E-01	0.461
435	0.044	3.25E-03	0.476	0.10	0.520	4.67E-03	221	15	31	9.41E-02	0.525
436	0.044	4.29E-03	0.701	0.15	0.745	7.53E-03	310	20	46	1.02E-01	0.518
437	0.044	5.53E-03	0.950	0.24	0.994	1.22E-02	415	27	51	1.24E-01	0.521
438	0.044	7.45E-03	1.435	0.44	1.479	2.28E-02	615	40	56	1.59E-01	0.479
439	0.044	8.14E-03	1.925	0.65	1.969	3.18E-02	813	54	69	1.78E-01	0.453
440	0.044	4.18E-03	2.236	0.32	2.280	1.66E-02	935	60	62	1.87E-01	0.454
441	0.089	1.82E-03	0.332	0.04	0.421	3.85E-03	180	12	84	6.77E-02	0.644
442	0.089	2.22E-03	0.501	0.09	0.590	8.25E-03	251	16	90	9.34E-02	0.618
443	0.089	3.38E-03	0.750	0.16	0.839	1.45E-02	344	24	106	1.08E-01	0.480
444	0.089	4.16E-03	0.973	0.23	1.062	2.10E-02	431	29	111	1.28E-01	0.486
445	0.089	5.22E-03	1.490	0.41	1.579	3.69E-02	639	43	133	1.49E-01	0.421
446	0.089	6.63E-03	2.004	0.73	2.093	6.52E-02	844	60	150	1.93E-01	0.382
447	0.133	1.13E-03	0.249	0.03	0.382	3.54E-03	169	11	140	3.98E-02	0.721
448	0.133	1.33E-03	0.348	0.04	0.481	5.91E-03	214	14	144	4.97E-02	0.671
449	0.133	1.72E-03	0.510	0.07	0.643	9.88E-03	286	19	151	6.36E-02	0.646
450	0.133	2.68E-03	0.770	0.13	0.903	1.77E-02	404	27	162	9.83E-02	0.618
451	0.133	3.40E-03	1.014	0.21	1.147	2.88E-02	513	35	175	1.25E-01	0.597
452	0.133	4.39E-03	1.557	0.41	1.690	5.48E-02	750	54	209	1.41E-01	0.541
453	0.133	4.80E-03	1.997	0.61	2.130	8.20E-02	934	70	232	1.68E-01	0.495
454	0.133	5.72E-03	2.707	1.07	2.840	1.42E-01	1215	98	281	2.12E-01	0.439
455	0.178	8.39E-04	0.274	0.03	0.452	4.81E-03	198	13	197	4.14E-02	0.744

456	0.178	1.11E-03	0.365	0.04	0.543	6.79E-03	239	16	208	3.01E-02	0.693
457	0.178	1.24E-03	0.513	0.07	0.691	1.18E-02	307	20	215	6.75E-02	0.669
458	0.178	2.13E-03	0.789	0.13	0.967	2.37E-02	430	30	225	9.49E-02	0.649
459	0.178	2.48E-03	1.043	0.21	1.221	3.73E-02	545	39	241	1.04E-01	0.613
460	0.178	3.39E-03	1.597	0.42	1.775	7.58E-02	793	61	278	1.38E-01	0.552
461	0.178	4.12E-03	2.218	0.65	2.396	1.16E-01	1071	86	318	1.91E-01	0.501
462	0.222	7.85E-04	0.269	0.02	0.491	5.32E-03	208	13	261	3.46E-02	0.760
463	0.222	8.50E-04	0.370	0.03	0.592	7.60E-03	251	16	268	3.48E-02	0.723
464	0.222	1.00E-03	0.535	0.06	0.757	1.41E-02	322	21	282	6.12E-02	0.695
465	0.222	1.42E-03	0.808	0.14	1.030	3.13E-02	441	31	297	7.79E-02	0.663
466	0.222	1.67E-03	1.062	0.19	1.284	4.22E-02	562	41	321	1.08E-01	0.620
467	0.222	2.44E-03	1.637	0.39	1.859	8.69E-02	823	65	364	1.59E-01	0.560
468	0.222	2.72E-03	2.254	0.61	2.476	1.37E-01	1102	93	417	1.88E-01	0.500
469	0.267	7.96E-04	0.264	0.02	0.531	6.17E-03	232	15	311	2.79E-02	0.787
470	0.267	8.49E-04	0.376	0.03	0.643	8.74E-03	283	19	319	4.18E-02	0.751
471	0.267	9.43E-04	0.564	0.06	0.831	1.55E-02	366	24	334	6.87E-02	0.715
472	0.267	1.12E-03	0.809	0.12	1.076	3.08E-02	458	32	363	1.00E-01	0.671
473	0.267	1.26E-03	1.096	0.16	1.363	4.28E-02	584	41	391	9.73E-02	0.637
474	0.267	1.81E-03	1.702	0.38	1.969	1.01E-01	843	69	453	1.61E-01	0.561
475	0.267	2.05E-03	2.384	0.65	2.651	1.73E-01	1141	104	525	1.87E-01	0.495
476	0.311	8.42E-04	0.263	0.02	0.574	7.04E-03	254	17	369	2.15E-02	0.793
477	0.311	8.69E-04	0.384	0.03	0.695	9.97E-03	311	20	375	3.57E-02	0.758
478	0.311	9.31E-04	0.559	0.06	0.870	1.72E-02	391	26	388	6.10E-02	0.722
479	0.311	1.09E-03	0.791	0.10	1.102	3.24E-02	490	35	413	6.17E-02	0.670
480	0.311	1.14E-03	1.137	0.21	1.448	6.52E-02	649	51	440	9.96E-02	0.640
481	0.311	1.50E-03	1.768	0.39	2.079	1.22E-01	929	80	523	1.38E-01	0.550
482	0.311	1.57E-03	2.372	0.64	2.683	1.97E-01	1189	115	586	1.80E-01	0.497
483	0.356	9.10E-04	0.281	0.02	0.637	8.45E-03	284	19	421	2.37E-02	0.759
484	0.356	9.33E-04	0.399	0.03	0.755	1.12E-02	340	22	430	3.34E-02	0.724
485	0.356	9.59E-04	0.575	0.06	0.931	1.99E-02	404	27	462	4.69E-02	0.694
486	0.356	1.01E-03	0.862	0.11	1.218	3.76E-02	535	39	484	8.94E-02	0.649
487	0.356	1.05E-03	1.192	0.22	1.548	7.77E-02	693	58	517	9.77E-02	0.601
488	0.356	1.30E-03	1.845	0.50	2.201	1.78E-01	1007	105	589	1.59E-01	0.531
489	0.356	1.73E-03	2.489	0.73	2.845	2.57E-01	1273	141	700	1.73E-01	0.464

Table A.3 Slug flow characterizations for all oil viscosities.

1	4.71E-04	0.538	1.32E-04	7.20E-03	0.998	3.85E-04	0.000	0.058	0.000	0.889	0.07	15.27	0.36
2	6.79E-04	0.534	5.23E-04	1.51E-02	0.998	1.18E-03	0.000	0.083	0.000	0.956	0.16	9.84	0.54
3	9.37E-04	0.536	6.37E-04	2.42E-02	0.975	1.26E-02	0.000	0.091	0.000	0.951	0.37	7.58	0.75
4	1.15E-03	0.537	1.36E-03	3.32E-02	0.951	3.89E-02	0.000	0.089	0.000	1.140	1.43	10.38	1.35
5	1.16E-03	0.550	1.29E-03	3.35E-02	0.948	3.68E-02	0.000	0.067	0.008	1.520	1.78	11.02	1.77
6	2.09E-03	0.544	1.03E-03	6.47E-02	0.951	3.55E-02	0.067	0.100	0.000	1.726	1.45	9.62	3.29
7	4.68E-04	0.535	9.26E-04	2.14E-02	0.865	4.89E-02	0.000	0.075	0.008	1.933	3.04	12.36	1.58
8	1.81E-03	0.512	3.60E-03	3.25E-02	0.823	7.13E-02	0.000	0.092	0.000	2.540	5.07	13.95	2.68
9	1.81E-03	0.523	1.88E-03	6.26E-02	0.803	9.45E-02	0.000	0.067	0.000	3.066	8.12	16.15	7.14
10	1.80E-03	0.498	1.55E-03	5.43E-02	0.779	4.61E-02	0.033	0.125	0.008	3.704	3.88	15.01	9.65
11	9.56E-04	0.503	4.43E-04	8.89E-02	0.863	6.57E-02	0.025	0.050	0.000	3.486	2.07	8.04	3.05
12	1.17E-03	0.541	6.37E-04	1.05E-02	0.996	2.52E-03	0.000	0.138	0.000	0.903	0.14	9.98	0.43
13	1.96E-03	0.545	2.54E-03	2.04E-02	0.987	9.89E-03	0.000	0.192	0.000	0.972	0.17	7.58	0.60
14	1.20E-03	0.548	8.75E-04	1.63E-02	0.989	8.59E-03	0.000	0.158	0.000	1.091	0.23	9.23	0.56
15	2.98E-03	0.545	1.06E-03	4.13E-02	0.988	1.01E-02	0.000	0.183	0.000	1.185	0.25	7.61	1.37
16	1.85E-03	0.558	1.14E-03	3.01E-02	0.978	1.54E-02	0.000	0.167	0.000	1.357	0.46	8.42	1.18
17	3.49E-03	0.554	3.59E-03	5.99E-02	0.936	5.48E-02	0.008	0.158	0.017	1.677	1.68	8.34	3.40
18	2.59E-03	0.550	4.45E-03	3.66E-02	0.909	8.74E-02	0.025	0.201	0.000	1.833	2.94	10.15	3.04
19	3.88E-03	0.548	2.08E-03	6.59E-02	0.929	4.67E-02	0.000	0.177	0.000	-	1.49	7.89	3.63
20	3.54E-03	0.531	2.64E-03	7.54E-02	0.938	5.05E-02	0.000	0.201	0.000	2.778	1.27	6.54	3.30
21	2.27E-03	0.524	1.56E-03	8.80E-02	0.943	4.35E-02	0.017	0.167	0.008	3.233	0.86	6.10	2.54
22	2.49E-03	0.506	1.68E-03	7.27E-02	0.881	5.97E-02	0.042	0.192	0.017	3.355	1.56	6.06	2.57
23	1.48E-03	0.480	9.50E-04	5.14E-02	0.927	3.29E-02	0.000	0.151	0.034	3.556	0.59	4.91	0.68
24	2.99E-03	0.452	2.51E-03	5.74E-02	0.848	5.30E-02	0.042	0.192	0.079	3.783	0.47	3.89	0.82
25	4.80E-03	0.564	7.08E-03	1.90E-02	0.990	7.26E-03	0.000	0.292	0.000	0.847	0.20	8.13	0.56
26	4.60E-03	0.560	3.10E-03	3.02E-02	0.984	9.83E-03	0.008	0.325	0.000	0.961	0.35	7.60	0.95
27	7.81E-03	0.577	3.98E-02	2.76E-02	0.992	6.22E-03	0.234	0.293	0.033	1.118	1.48	6.51	0.87
28	7.21E-03	0.574	4.25E-02	3.22E-02	0.985	1.41E-02	0.037	0.332	0.000	1.218	1.10	6.88	1.05
29	9.46E-03	0.595	4.00E-02	2.82E-02	0.967	2.72E-02	0.062	0.308	0.008	1.337	2.17	7.44	0.72
30	2.59E-02	0.610	2.71E-02	5.42E-02	0.969	2.89E-02	0.121	0.310	0.008	1.457	1.20	7.10	2.05
31	2.61E-02	0.606	1.05E-02	9.56E-01	0.956	4.22E-02	0.174	0.249	0.008	1.852	1.23	6.47	3.57
32	2.16E-02	0.603	5.17E-03	9.41E-01	0.941	5.88E-02	0.129	0.209	0.025	2.092	3.48	9.77	1.22
33	6.00E-03	0.570	1.15E-02	9.24E-02	0.945	4.98E-02	0.100	0.100	0.158	2.577	0.96	9.24	4.08
34	1.05E-02	0.573	4.25E-03	8.83E-01	0.883	9.88E-02	0.059	0.059	0.117	3.066	1.51	6.53	3.15
35	4.27E-03	0.526	4.22E-03	7.91E-02	0.900	7.87E-02	0.058	0.084	0.125	3.556	2.15	6.40	2.94
36	2.71E-03	0.494	3.19E-03	4.27E-02	0.950	1.60E-02	0.108	0.188	0.063	4.135	0.27	3.50	0.85
37	9.91E-04	0.493	2.44E-03	1.46E-02	0.948	1.12E-02	0.062	0.083	0.050	4.041	0.13	3.53	0.21
38	9.49E-04	0.464	9.06E-04	2.88E-02	0.950	7.06E-03	0.063	0.100	0.071	4.041	0.49	2.39	0.13
39	4.79E-04	0.448	6.72E-04	2.40E-02	0.937	1.82E-02	0.054	0.075	0.042	-	0.09	1.68	0.11
40	5.70E-03	0.574	5.62E-03	1.29E-02	0.989	7.84E-03	0.000	0.351	0.000	0.776	0.35	8.25	0.55
41	4.78E-03	0.565	4.33E-03	1.72E-02	0.990	7.62E-03	0.000	0.357	0.000	0.872	0.37	7.80	0.56
42	3.91E-03	0.576	1.52E-02	1.38E-02	0.995	3.27E-03	0.008	0.359	0.000	1.005	0.46	6.64	0.59
43	6.11E-03	0.585	1.81E-02	2.94E-02	0.992	6.44E-03	0.033	0.388	0.000	1.155	0.44	6.62	0.96
44	8.32E-03	0.592	4.31E-02	2.96E-02	0.979	1.98E-02	0.108	0.358	0.017	1.288	1.13	7.17	1.04
45	9.99E-03	0.600	4.18E-02	4.94E-02	0.976	1.90E-02	0.169	0.330	0.025	1.411	1.23	7.42	1.79
46	1.61E-02	0.615	3.15E-02	6.73E-02	0.975	2.44E-02	0.187	0.316	0.033	1.560	2.64	6.67	2.39
47	1.85E-02	0.608	2.02E-02	5.68E-02	0.963	3.61E-02	0.250	0.300	0.033	1.852	1.82	6.90	1.35
48	1.77E-02	0.604	7.20E-03	9.83E-01	0.983	1.53E-02	0.170	0.217	0.113	2.067	0.70	6.56	1.66
49	1.13E-02	0.597	3.86E-03	9.33E-01	0.933	4.54E-02	0.083	0.083	0.179	2.654	4.71	9.46	1.24
50	6.95E-03	0.564	1.08E-02	9.46E-01	0.946	3.74E-02	0.000	0.032	0.103	3.066	1.59	6.41	2.09
51	3.51E-03	0.538	3.57E-03	3.07E-02	0.958	2.93E-02	0.008	0.058	0.079	3.704	1.98	2.62	0.92
52	1.33E-03	0.513	2.58E-03	1.48E-02	0.945	1.76E-02	0.062	0.062	0.078	3.865	0.20	3.55	0.34
53	7.85E-04	0.483	1.44E-03	2.38E-02	0.943	1.35E-02	0.075	0.134	0.059	4.559	0.52	3.29	0.56
54	1.10E-03	0.466	1.03E-03	2.50E-02	0.950	1.46E-02	0.050	0.100	0.075	4.041	0.27	2.13	0.27
55	2.12E-04	0.453	8.31E-04	9.12E-01	0.912	4.01E-02	0.000	0.017	0.033	-	0.60	1.73	0.31
56	6.85E-03	0.568	6.82E-03	1.76E-02	0.993	5.34E-03	0.000	0.451	0.000	0.827	0.21	7.43	0.32
57	5.25E-03	0.572	3.09E-02	1.19E-02	0.993	5.09E-03	0.008	0.486	0.008	0.977	0.58	6.96	0.40
58	6.27E-03	0.587	2.31E-02	1.78E-02	0.995	3.60E-03	0.008	0.483	0.025	1.104	0.31	6.58	0.59
59	1.37E-02	0.605	4.90E-02	2.76E-02	0.991	9.10E-03	0.004	0.467	0.000	1.261	0.40	6.90	0.80
60	2.19E-02	0.618	4.30E-02	4.26E-02	0.982	1.45E-02	0.000	0.498	0.000	1.389	0.54	6.46	0.96

61	2.21E-02	0.624	3.53E-02	4.14E-02	0.969	3.02E-02	0.000	0.442	0.000	1.560	1.10	7.09	1.24
62	1.56E-02	0.626	2.53E-02	4.17E-02	0.969	2.57E-02	0.058	0.426	0.008	1.646	0.73	7.04	1.20
63	1.55E-02	0.617	1.70E-02	4.18E-02	0.981	1.65E-02	0.088	0.425	0.017	1.998	0.62	6.03	4.95
64	1.31E-02	0.587	2.13E-02	8.26E-02	0.928	4.13E-02	0.141	0.408	0.025	2.223	0.85	7.92	4.41
65	0.00E+00	0.578	0.00E+00	0.00E+00	0.952	0.00E+00	0.000	0.350	0.000	2.822	0.00	6.17	0.00
66	6.92E-03	0.555	7.94E-03	7.66E-02	0.939	3.03E-02	0.152	0.280	0.074	3.556	0.73	6.88	2.23
67	4.89E-03	0.530	5.16E-03	1.18E-01	0.922	4.25E-02	0.185	0.261	0.076	3.783	0.63	5.04	2.75
68	1.54E-03	0.498	1.50E-03	9.53E-01	0.953	4.26E-03	0.017	0.033	0.059	4.041	0.19	3.85	1.98
69	1.01E-03	0.481	1.40E-03	2.58E-02	0.939	1.92E-02	0.072	0.093	0.072	4.233	0.15	3.08	0.15
70	1.45E-03	0.462	6.91E-04	1.13E-02	0.873	5.99E-02	0.033	0.042	0.033	-	0.49	2.90	0.37
71	9.20E-04	0.455	7.23E-04	7.11E-02	0.934	1.40E-02	0.026	0.026	0.051	-	0.26	1.63	0.17
72	3.55E-02	0.644	1.13E-01	2.63E-02	0.981	9.25E-03	0.234	0.509	0.063	0.867	0.64	6.25	1.38
73	3.94E-02	0.652	8.59E-02	3.53E-02	0.974	2.01E-02	0.284	0.535	0.050	0.982	0.68	6.61	1.38
74	3.18E-02	0.658	8.98E-02	3.29E-02	0.953	3.45E-02	0.399	0.557	0.116	1.155	0.82	6.89	1.25
75	5.73E-02	0.700	6.75E-02	4.27E-02	0.920	4.15E-02	0.310	0.410	0.163	1.337	2.27	8.13	2.30
76	4.37E-02	0.725	3.01E-02	4.92E-02	0.924	7.51E-02	0.196	0.250	0.275	1.482	2.48	8.29	1.76
77	5.53E-02	0.705	2.95E-02	5.86E-02	0.910	7.01E-02	0.366	0.424	0.245	1.646	1.86	9.23	2.80
78	4.02E-02	0.708	1.12E-02	7.05E-02	0.903	9.70E-02	0.225	0.317	0.292	1.778	4.19	6.40	4.80
79	5.22E-02	0.689	8.57E-03	8.95E-01	0.895	6.67E-02	0.196	0.217	0.355	2.020	1.94	6.54	4.46
80	2.47E-02	0.597	4.10E-02	8.51E-02	0.913	6.21E-02	0.407	0.473	0.237	2.279	1.45	7.23	4.93
81	3.28E-02	0.612	2.50E-02	9.26E-02	0.932	5.60E-02	0.198	0.244	0.345	2.694	3.10	7.29	3.94
82	1.65E-02	0.608	8.00E-03	4.91E-01	0.930	2.27E-02	0.050	0.050	0.213	3.355	0.69	7.37	1.18
83	1.29E-02	0.564	6.33E-03	9.20E-02	0.912	3.31E-02	0.213	0.230	0.254	4.041	0.81	7.17	2.09
84	6.44E-03	0.523	4.60E-03	1.41E-02	0.926	1.89E-03	0.128	0.190	0.186	4.559	0.14	4.58	0.31
85	2.53E-03	0.491	1.71E-03	3.08E-02	0.932	2.98E-02	0.057	0.097	0.218	4.559	0.17	2.04	0.43
86	1.94E-03	0.475	5.44E-04	2.68E-02	0.918	5.04E-02	0.058	0.058	0.112	4.939	0.34	2.50	0.49
87	2.01E-04	0.469	6.95E-04	1.95E-02	0.916	4.37E-02	0.020	0.030	0.056	-	0.06	2.68	1.14
88	2.94E-02	0.614	3.59E-02	2.95E-02	0.980	1.49E-02	0.116	0.740	0.017	0.801	0.76	7.64	1.56
89	2.00E-02	0.637	5.66E-02	2.04E-02	0.988	7.82E-03	0.067	0.701	0.033	0.903	0.65	6.99	0.95
90	3.21E-02	0.652	9.32E-02	3.33E-02	0.965	2.76E-02	0.614	0.660	0.134	1.058	1.32	7.18	1.30
91	5.03E-02	0.684	9.85E-02	4.29E-02	0.946	4.38E-02	0.276	0.769	0.042	1.235	1.34	7.29	1.80
92	6.84E-02	0.705	7.16E-02	5.26E-02	0.928	5.97E-02	0.477	0.861	0.033	1.389	1.83	7.56	2.81
93	6.92E-02	0.733	2.90E-02	5.76E-02	0.925	4.66E-02	0.524	0.665	0.158	1.560	2.64	7.65	2.89
94	4.74E-02	0.731	1.14E-02	4.95E-02	0.909	7.58E-02	0.325	0.417	0.313	1.743	5.14	7.60	3.98
95	4.78E-02	0.707	1.64E-02	5.89E-02	0.924	7.58E-02	0.433	0.492	0.238	1.872	2.90	7.91	2.67
96	5.16E-02	0.684	2.32E-02	7.50E-02	0.975	2.24E-02	0.555	0.786	0.141	1.998	1.99	4.91	2.31
97	2.46E-02	0.660	2.67E-03	3.76E-02	0.958	2.91E-02	0.383	0.466	0.325	2.469	1.55	5.51	1.11
98	2.56E-02	0.618	2.68E-02	7.97E-02	0.940	5.53E-02	0.341	0.441	0.212	2.778	2.62	6.72	2.70
99	1.26E-02	0.566	1.59E-02	1.43E-01	0.925	3.02E-02	0.239	0.535	0.156	3.556	1.37	6.38	5.93
100	5.05E-03	0.551	1.01E-02	1.80E-02	0.939	1.79E-02	0.337	0.591	0.119	3.865	0.69	4.41	0.56
101	4.13E-03	0.521	5.10E-03	8.91E-03	0.926	2.79E-02	0.157	0.182	0.195	4.939	0.55	4.22	0.21
102	3.60E-03	0.491	1.38E-03	8.42E-02	0.920	3.16E-02	0.034	0.034	0.118	5.388	0.49	3.47	1.88
103	1.71E-03	0.472	1.41E-03	2.83E-02	0.904	2.71E-02	0.051	0.051	0.111	4.939	0.22	2.34	0.45
104	5.06E-04	0.461	1.24E-04	4.90E-01	0.958	4.43E-03	0.000	0.040	0.071	-	0.36	2.45	0.41
105	3.59E-02	0.736	4.27E-02	1.66E-02	0.980	6.81E-03	0.008	1.187	0.017	0.941	0.67	5.79	0.89
106	3.14E-02	0.731	4.13E-02	2.18E-02	0.968	1.41E-02	0.008	1.417	0.000	1.104	0.69	4.81	0.86
107	2.93E-02	0.729	4.13E-02	2.92E-02	0.962	1.27E-02	0.000	1.446	0.000	1.307	0.59	4.64	1.43
108	3.88E-02	0.750	4.99E-02	3.19E-02	0.943	1.70E-02	0.008	1.514	0.000	1.482	0.80	4.29	1.42
109	3.54E-02	0.739	3.41E-02	3.46E-02	0.940	2.75E-02	0.017	1.333	0.008	1.646	0.65	4.86	1.70
110	3.17E-02	0.717	3.53E-02	3.32E-02	0.963	1.55E-02	0.013	1.386	0.009	1.833	0.29	4.38	0.96
111	2.90E-02	0.701	3.87E-02	2.42E-02	0.962	1.70E-02	0.004	1.339	0.000	2.044	0.33	4.30	0.94
112	2.02E-02	0.676	2.76E-02	1.66E-02	0.974	6.10E-03	0.004	1.268	0.000	2.195	0.20	4.32	0.55
113	1.98E-02	0.677	2.83E-02	1.73E-02	0.967	4.09E-03	0.000	1.227	0.008	2.371	0.53	4.29	0.42
114	1.85E-02	0.646	2.35E-02	1.46E-02	0.965	6.70E-03	0.125	1.010	0.013	2.915	0.28	5.36	0.47
115	9.16E-03	0.622	1.76E-02	1.35E-02	0.950	6.81E-03	0.392	0.977	0.042	3.233	0.63	5.11	0.36
116	1.16E-02	0.599	8.17E-03	5.75E-03	0.927	1.89E-02	0.321	0.883	0.058	4.041	0.39	4.97	0.25
117	4.79E-03	0.569	3.10E-04	8.45E-01	0.845	4.72E-02	0.008	0.008	0.188	4.559	0.12	3.59	0.98
118	9.66E-04	0.519	6.87E-04	8.93E-01	0.893	5.77E-02	0.063	0.063	0.310	5.388	1.30	3.84	0.90
119	5.11E-04	0.485	7.65E-04	2.37E-02	0.874	5.99E-02	0.008	0.008	0.037	5.388	0.51	3.28	0.30
120	6.13E-04	0.513	4.26E-04	2.12E-02	0.989	5.68E-03	0.000	0.066	0.000	0.831	0.29	13.46	0.65
121	1.20E-03	0.519	7.66E-04	4.91E-02	0.959	2.29E-02	0.000	0.065	0.000	1.307	1.25	14.51	2.52
122	1.62E-03	0.535	2.25E-03	6.29E-02	0.877	5.40E-02	0.000	0.062	0.000	1.646	2.57	15.67	4.68
123	3.37E-03	0.531	1.99E-03	6.61E-02	0.838	9.91E-02	0.000	0.075	0.000	2.067	4.47	12.97	6.46
124	2.53E-03	0.540	1.60E-03	1.58E-01	0.907	6.60E-02	0.000	0.056	0.004	3.066	1.30	8.45	13.18
125	1.43E-03	0.503	9.43E-04	1.04E-01	0.835	7.27E-02	0.021	0.057	0.008	3.783	2.35	9.77	7.12
126	1.27E-03	0.476	1.43E-03	5.89E-02	0.780	1.23E-01	0.000	0.025	0.041	3.355	2.81	6.50	3.58
127	1.89E-03	0.595	2.02E-03	1.14E-02	0.983	6.16E-03	0.000	0.125	0.000	0.577	0.41	12.71	0.58
128	1.27E-03	0.546	1.09E-03	2.04E-02	0.977	1.30E-02	0.000	0.139	0.000	0.711	0.45	11.03	0.74
129	1.43E-03	0.527	1.20E-03	2.72E-02	0.968	1.60E-02	0.000	0.124	0.000	0.956	0.69	12.81	1.08
130	1.76E-03	0.546	2.11E-03	3.45E-02	0.945	3.48E-02	0.000	0.123	0.008	1.368	1.53	12.16	1.67
131	2.45E-03	0.554	4.08E-03	4.57E-02	0.948	4.38E-02	0.000	0.127	0.000	1.833	1.83	10.27	2.71
132	2.68E-03	0.561	7.83E-04	7.74E-02	0.965	2.58E-02	0.000	0.124	0.000	2.279	0.88	7.63	3.54
133	3.46E-03	0.553	7.18E-04	1.26E-01	0.935	2.68E-02	0.024	0.114	0.008	2.915	0.98	6.99	4.83
134	1.54E-03	0.508	7.19E-04	3.66E-02	0.884	3.67E-02	0.017	0.058	0.025	3.556	0.91	6.10	1.25
135	1.61E-03	0.475	2.03E-03	5.21E-02	0.860	9.12E-02	0.010	0.081	0.030	3.556	0.30	3.60	1.51
136	6.41E-03	0.587	5.57E-03	1.30E-02	0.990	4.41E-03	0.000	0.285	0.000	0.640	0.39	9.56	0.60
137	2.01E-03	0.556	1.18E-03	1.19E-02	0.993	3.00E-03	0.000	0.253	0.000	0.812	0.15	9.87	0.39
138	3.29E-03	0.554	2.21E-03	2.77E-02	0.982	1.14E-02	0.000	0.237	0.000	1.091	0.46	10.75	1.10
139	4.45E-03	0.577	2.07E-03	4.47E-02	0.988	5.84E-03	0.008	0.263	0.000	1.533	0.22	8.85	1.68

140	4.51E-03	0.575	4.79E-03	5.82E-02	0.941	4.63E-02	0.008	0.193	0.008	1.998	2.01	12.53	3.44
141	1.30E-03	0.595	1.76E-03	2.63E-02	0.964	2.45E-02	0.016	0.179	0.000	2.577	0.79	8.19	0.94
142	3.70E-03	0.558	1.41E-03	9.39E-02	0.943	3.33E-02	0.025	0.180	0.008	3.355	0.78	6.17	3.17
143	1.83E-03	0.501	1.82E-03	5.52E-02	0.891	4.76E-02	0.058	0.140	0.025	4.041	0.54	5.34	0.89
144	1.38E-03	0.462	1.15E-03	4.68E-02	0.890	2.78E-02	0.049	0.106	0.094	4.041	0.61	3.63	0.30
145	5.82E-03	0.570	1.15E-02	1.48E-02	0.986	6.80E-03	0.000	0.468	0.000	0.703	0.44	8.12	0.45
146	6.61E-03	0.564	3.78E-03	2.60E-02	0.984	9.08E-03	0.000	0.382	0.000	0.903	0.36	9.20	0.78
147	6.21E-03	0.569	5.82E-03	3.69E-02	0.968	2.13E-02	0.000	0.341	0.000	1.210	0.93	10.90	1.67
148	2.97E-03	0.600	4.71E-03	2.91E-02	0.983	1.38E-02	0.008	0.362	0.008	1.616	0.27	8.00	0.88
149	6.13E-03	0.611	5.86E-03	5.35E-02	0.957	3.34E-02	0.033	0.286	0.016	2.223	0.85	8.69	2.19
150	1.24E-02	0.592	4.64E-03	1.34E-01	0.949	3.14E-02	0.050	0.377	0.013	2.778	0.49	6.89	5.78
151	2.05E-03	0.560	3.16E-03	3.77E-02	0.940	2.22E-02	0.042	0.234	0.050	3.629	0.50	5.43	1.11
152	2.54E-03	0.480	1.70E-03	3.52E-02	0.882	3.20E-02	0.034	0.271	0.068	4.679	0.86	4.71	0.51
153	1.39E-02	0.567	1.56E-02	2.63E-02	0.972	1.56E-02	0.000	0.517	0.000	0.744	0.69	9.15	1.04
154	1.02E-02	0.575	1.45E-02	2.39E-02	0.978	1.54E-02	0.000	0.489	0.000	0.956	0.49	9.04	0.74
155	1.06E-02	0.584	1.07E-02	5.66E-02	0.973	1.55E-02	0.000	0.467	0.000	1.279	0.75	9.31	2.22
156	1.23E-02	0.624	2.23E-02	7.66E-02	0.921	5.96E-02	0.000	0.414	0.000	1.726	2.19	10.34	4.67
157	9.76E-03	0.634	7.23E-03	9.47E-02	0.940	3.61E-02	0.029	0.329	0.025	2.403	2.01	9.57	4.53
158	4.25E-03	0.614	6.45E-03	5.27E-02	0.899	8.10E-02	0.080	0.302	0.053	2.915	3.02	7.78	2.59
159	3.27E-03	0.550	2.56E-03	5.58E-02	0.909	8.84E-03	0.060	0.342	0.043	4.041	0.67	6.25	1.20
160	1.75E-03	0.500	2.39E-03	3.64E-02	0.900	2.31E-02	0.128	0.420	0.086	4.559	0.50	3.40	0.40
161	1.64E-03	0.451	1.02E-03	1.70E-02	0.894	2.26E-02	0.058	0.127	0.046	5.388	0.27	2.96	0.20
162	1.05E-02	0.592	1.06E-02	8.52E-03	0.992	5.08E-03	0.000	0.633	0.000	0.867	0.35	8.34	0.41
163	8.55E-03	0.601	5.12E-03	2.41E-02	0.988	7.67E-03	0.000	0.620	0.000	1.185	0.36	8.55	0.86
164	7.36E-03	0.618	3.65E-03	3.77E-02	0.986	7.77E-03	0.000	0.572	0.000	1.494	0.30	9.25	1.25
165	8.92E-03	0.644	6.22E-03	7.88E-02	0.981	9.88E-03	0.016	0.569	0.016	1.891	0.25	7.37	2.86
166	1.07E-02	0.636	6.65E-03	6.25E-02	0.970	1.16E-02	0.091	0.453	0.062	2.577	0.27	7.07	1.60
167	6.05E-03	0.622	6.86E-03	3.18E-02	0.947	2.01E-02	0.147	0.425	0.061	3.066	0.38	6.96	0.84
168	2.29E-03	0.539	3.71E-03	9.02E-02	0.896	3.73E-02	0.049	0.155	0.065	4.233	0.61	5.93	2.61
169	3.34E-03	0.476	1.88E-03	7.71E-02	0.871	3.75E-02	0.026	0.044	0.035	5.388	0.68	5.30	1.50
170	1.29E-02	0.608	9.07E-03	8.93E-03	0.992	4.91E-03	0.008	0.728	0.000	0.972	0.31	8.75	0.31
171	7.25E-03	0.628	5.83E-03	2.27E-02	0.991	5.61E-03	0.000	0.742	0.000	1.279	0.16	7.86	0.68
172	5.96E-03	0.650	1.83E-03	2.76E-02	0.993	3.34E-03	0.000	0.674	0.004	1.560	0.20	8.44	0.92
173	1.00E-02	0.656	5.02E-03	4.60E-02	0.981	5.47E-03	0.016	0.599	0.016	2.067	0.16	8.44	1.58
174	6.42E-03	0.634	7.69E-03	7.30E-02	0.955	1.29E-02	0.120	0.513	0.066	2.778	0.15	7.48	2.33
175	3.73E-03	0.612	4.87E-03	5.78E-02	0.955	1.39E-02	0.143	0.360	0.078	3.556	0.40	6.99	1.49
176	2.23E-03	0.528	1.92E-03	2.78E-02	0.903	1.73E-02	0.017	0.777	0.031	4.559	0.46	4.13	0.54
177	2.39E-03	0.472	1.21E-03	1.54E-02	0.870	4.46E-02	0.111	0.213	0.075	5.735	0.79	4.56	0.27
178	1.98E-02	0.643	1.86E-02	3.52E-02	0.980	1.45E-02	0.000	0.862	0.008	1.052	1.03	8.93	1.85
179	1.64E-02	0.656	2.34E-02	6.78E-02	0.955	3.38E-02	0.000	0.827	0.008	1.389	0.94	9.06	4.25
180	2.54E-02	0.665	2.33E-02	1.02E-01	0.961	2.59E-02	0.000	0.810	0.008	1.778	0.96	9.01	5.92
181	9.90E-03	0.669	2.15E-02	6.78E-02	0.951	3.24E-02	0.037	0.716	0.049	2.279	0.74	8.72	2.78
182	5.61E-03	0.655	7.43E-03	4.43E-02	0.937	5.08E-02	0.129	0.431	0.094	3.066	1.77	7.83	1.45
183	3.90E-03	0.521	3.96E-03	4.49E-02	0.885	2.20E-02	0.049	0.715	0.094	4.939	0.42	4.80	0.78
184	2.83E-03	0.461	2.45E-03	2.92E-02	0.849	2.11E-02	0.213	0.594	0.098	5.388	0.26	3.54	0.18
185	1.50E-02	0.663	1.75E-02	3.48E-02	0.977	1.33E-02	0.032	1.053	0.000	1.210	0.78	8.33	1.93
186	3.52E-02	0.720	6.72E-02	2.31E-02	0.990	3.04E-03	0.262	0.916	0.008	1.573	0.23	8.33	0.64
187	3.88E-02	0.723	3.54E-02	3.77E-02	0.986	6.63E-03	0.695	0.919	0.041	1.933	0.43	7.61	1.18
188	1.62E-02	0.662	3.03E-02	6.27E-02	0.959	1.83E-02	0.125	0.917	0.019	2.371	0.48	7.47	2.53
189	1.43E-02	0.640	1.74E-02	3.41E-02	0.930	2.37E-02	0.306	0.687	0.074	3.014	0.81	7.38	1.36
190	6.10E-03	0.584	8.65E-03	3.49E-02	0.908	2.04E-02	0.141	0.736	0.116	4.041	0.54	6.22	1.04
191	3.10E-03	0.499	5.63E-03	2.46E-02	0.860	2.84E-02	0.159	0.668	0.115	5.388	0.71	5.21	0.49
192	3.64E-04	0.578	7.82E-04	6.45E-03	0.988	3.12E-03	0.000	0.075	0.000	0.673	0.37	14.55	0.30
193	5.37E-04	0.532	4.71E-04	1.56E-02	0.981	9.52E-03	0.000	0.068	0.000	0.889	0.48	15.10	0.65
194	8.82E-04	0.529	9.18E-04	4.93E-02	0.946	3.42E-02	0.000	0.043	0.000	1.162	1.49	15.59	3.10
195	3.24E-03	0.552	2.85E-04	9.44E-02	0.965	7.36E-03	0.000	0.062	0.000	1.646	0.38	10.34	6.02
196	5.34E-04	0.560	1.30E-03	9.02E-03	0.961	1.67E-02	0.000	0.059	0.000	2.223	0.84	7.49	1.08
197	1.37E-03	0.550	1.89E-03	6.86E-02	0.901	6.69E-02	0.000	0.044	0.000	3.066	1.20	9.51	4.56
198	4.78E-04	0.539	1.94E-04	5.50E-02	0.891	2.57E-02	0.000	0.038	0.000	3.233	0.95	6.84	3.17
199	1.39E-04	0.490	6.36E-04	2.67E-02	0.905	1.07E-02	0.009	0.017	0.009	-	0.56	6.61	0.48
200	6.12E-04	0.553	6.04E-04	4.90E-03	0.991	2.18E-03	0.000	0.112	0.000	0.747	0.22	14.66	0.25
201	1.43E-03	0.530	7.87E-04	1.58E-02	0.988	4.46E-03	0.000	0.132	0.000	0.941	0.24	10.87	0.59
202	1.58E-03	0.531	6.39E-04	2.83E-02	0.986	5.84E-03	0.000	0.103	0.000	1.261	0.36	12.95	1.24
203	6.31E-04	0.562	1.84E-03	7.44E-03	0.979	7.12E-03	0.009	0.120	0.009	1.833	1.14	9.09	0.43
204	1.61E-03	0.574	1.49E-03	2.05E-02	0.974	9.17E-03	0.026	0.097	0.007	2.371	0.87	8.18	0.92
205	7.01E-04	0.553	1.69E-03	1.89E-02	0.965	2.01E-02	0.024	0.056	0.032	2.915	0.25	5.94	0.39
206	2.43E-03	0.526	4.38E-04	5.85E-02	0.871	4.09E-02	0.027	0.062	0.013	3.556	1.86	9.84	1.60
207	1.20E-03	0.491	3.74E-04	2.25E-02	0.882	1.55E-02	0.035	0.078	0.013	-	0.48	5.58	0.63
208	2.79E-03	0.529	2.25E-03	1.23E-02	0.989	3.76E-03	0.000	0.200	0.000	0.790	0.30	12.58	0.54
209	2.67E-03	0.529	2.72E-03	8.68E-03	0.992	3.55E-03	0.000	0.205	0.000	1.016	0.28	11.39	0.37
210	9.43E-04	0.549	7.22E-04	3.24E-03	0.990	1.61E-03	0.004	0.199	0.000	1.422	0.22	12.49	0.30
211	3.03E-03	0.570	1.53E-03	8.27E-03	0.974	2.08E-03	0.021	0.158	0.000	1.933	0.64	10.48	0.31
212	1.12E-03	0.579	6.17E-03	1.15E-02	0.978	2.14E-03	0.044	0.148	0.030	2.469	0.18	7.24	0.55
213	3.24E-03	0.551	9.53E-04	5.74E-02	0.930	2.19E-02	0.018	0.115	0.044	3.355	0.65	7.37	1.58
214	2.94E-03	0.500	2.04E-03	4.71E-02	0.902	4.32E-02	0.043	0.052	0.017	3.556	0.80	6.79	1.54
215	8.52E-04	0.443	9.78E-04	6.10E-02	0.851	2.21E-02	0.031	0.079	0.026	-	0.63	5.99	1.26
216	3.95E-03	0.537	3.39E-03	7.91E-03	0.992	3.37E-03	0.000	0.332	0.000	0.903	0.26	9.99	0.38
217	3.95E-03	0.539	9.32E-03	4.84E-03	0.994	2.18E-03	0.000	0.281	0.000	1.170	0.44	11.61	0.34
218	1.53E-03	0.554	2.01E-02	5.74E-03	0.989	4.20E-03	0.000	0.288	0.000	1.533	1.05	10.54	0.38

219	3.34E-03	0.595	2.94E-03	1.56E-02	0.980	1.77E-03	0.080	0.275	0.009	2.142	0.16	7.92	0.59
220	2.70E-03	0.576	7.66E-03	1.19E-02	0.971	4.15E-03	0.100	0.244	0.022	2.577	0.38	6.73	0.83
221	1.79E-03	0.525	2.39E-03	1.87E-02	0.929	2.46E-02	0.015	0.077	0.050	3.233	0.65	6.41	0.21
222	1.60E-03	0.486	1.28E-03	2.28E-02	0.928	3.91E-02	0.009	0.009	0.034	3.783	0.50	5.54	0.92
223	1.20E-03	0.418	1.54E-03	3.21E-02	0.873	3.71E-02	0.034	0.084	0.017	4.939	0.46	4.34	0.60
224	7.18E-03	0.582	5.59E-03	7.63E-03	0.995	2.64E-03	0.000	0.416	0.000	0.931	0.37	9.77	0.54
225	7.50E-03	0.583	4.65E-03	1.63E-02	0.994	2.60E-03	0.000	0.412	0.000	1.193	0.37	10.53	0.36
226	5.65E-03	0.614	1.01E-02	2.56E-02	0.982	1.28E-02	0.018	0.385	0.000	1.693	0.54	10.43	0.92
227	3.99E-03	0.629	6.98E-03	3.77E-02	0.961	1.36E-02	0.066	0.396	0.009	2.371	0.58	7.32	1.33
228	5.46E-03	0.619	3.29E-03	4.95E-02	0.963	9.03E-03	0.102	0.351	0.023	2.694	0.51	6.28	1.03
229	5.23E-03	0.549	2.78E-03	2.63E-02	0.938	2.73E-02	0.087	0.227	0.061	3.783	0.53	5.75	0.88
230	2.80E-03	0.484	1.43E-03	4.75E-02	0.910	1.95E-02	0.009	0.217	0.041	4.041	0.27	4.58	0.75
231	1.74E-03	0.447	9.14E-04	2.44E-02	0.899	1.07E-02	0.083	0.123	0.018	4.939	0.36	4.33	0.23
232	6.90E-03	0.602	5.50E-03	6.21E-03	0.995	2.90E-03	0.000	0.513	0.000	1.071	0.28	9.86	0.31
233	4.13E-03	0.616	1.30E-02	2.75E-03	0.998	1.05E-03	0.011	0.492	0.000	1.337	0.34	9.91	0.12
234	7.86E-03	0.648	7.53E-03	1.07E-02	0.987	3.41E-03	0.009	0.475	0.014	1.833	0.20	8.86	0.40
235	7.69E-03	0.646	4.90E-03	2.21E-02	0.966	9.29E-03	0.059	0.484	0.025	2.469	0.46	6.57	0.54
236	5.94E-03	0.619	7.96E-03	1.42E-02	0.960	9.07E-03	0.069	0.397	0.028	2.915	0.51	6.12	0.46
237	3.78E-03	0.536	3.28E-03	4.10E-02	0.914	2.89E-02	0.124	0.363	0.040	4.041	0.63	5.87	1.09
238	2.74E-03	0.482	3.52E-03	3.19E-02	0.855	2.93E-02	0.081	0.170	0.116	4.559	0.72	5.85	0.55
239	5.34E-05	0.441	6.03E-04	9.17E-03	0.882	5.84E-02	0.000	0.009	0.014	-	1.03	4.76	0.27
240	6.14E-03	0.611	8.14E-03	1.45E-02	0.989	6.45E-03	0.000	0.599	0.000	1.185	0.34	10.51	0.50
241	3.80E-03	0.651	3.15E-02	3.08E-03	0.997	1.12E-03	0.084	0.647	0.000	1.520	0.21	8.73	0.21
242	8.35E-03	0.654	6.40E-03	1.27E-02	0.982	4.78E-03	0.024	0.608	0.016	1.954	0.38	8.19	0.43
243	2.15E-03	0.635	3.79E-03	1.93E-02	0.951	6.16E-03	0.100	0.549	0.008	2.577	0.29	7.90	0.78
244	6.07E-03	0.606	5.69E-03	2.57E-02	0.948	1.35E-02	0.071	0.471	0.059	3.233	0.33	6.99	0.71
245	2.24E-03	0.535	3.45E-03	2.14E-02	0.908	1.43E-02	0.067	0.446	0.045	4.041	0.65	6.10	0.36
246	3.67E-03	0.458	1.89E-03	5.96E-02	0.872	1.20E-02	0.050	0.075	0.038	4.939	0.29	6.07	0.53
247	1.91E-03	0.419	2.76E-03	2.78E-02	0.827	4.29E-02	0.041	0.057	0.110	-	0.58	4.50	0.46
248	6.25E-03	0.648	1.11E-02	8.33E-03	0.992	3.15E-03	0.004	0.695	0.000	1.368	0.51	9.85	0.37
249	6.73E-03	0.668	1.75E-02	8.20E-03	0.985	7.97E-03	0.013	0.672	0.009	1.693	0.61	10.04	0.21
250	1.03E-02	0.679	1.71E-02	2.32E-02	0.974	4.91E-03	0.159	0.644	0.052	2.067	0.20	8.09	0.91
251	9.81E-03	0.660	1.20E-02	1.92E-02	0.953	3.40E-03	0.222	0.521	0.065	2.778	0.20	7.08	0.53
252	7.00E-03	0.637	9.55E-03	8.73E-03	0.936	1.68E-02	0.194	0.406	0.099	3.355	1.22	6.92	0.30
253	5.21E-03	0.546	5.27E-03	1.82E-02	0.923	1.95E-02	0.178	0.381	0.087	4.559	0.70	5.74	0.32
254	3.21E-03	0.485	4.66E-03	2.19E-02	0.893	2.44E-02	0.140	0.240	0.140	5.388	0.59	4.64	0.44
255	1.83E-03	0.449	2.02E-03	1.95E-02	0.815	8.71E-02	0.067	0.168	0.084	-	1.55	5.54	0.39
256	4.34E-02	0.708	9.32E-02	3.83E-03	0.994	2.93E-03	0.596	0.817	0.009	1.422	2.38	9.26	0.30
257	8.73E-03	0.672	3.82E-02	9.43E-03	0.982	6.18E-03	0.021	0.781	0.008	1.778	0.37	9.34	0.42
258	9.01E-03	0.673	1.97E-02	1.45E-02	0.967	4.29E-03	0.139	0.774	0.025	2.371	0.24	8.03	0.57
259	6.56E-03	0.651	1.56E-02	1.45E-02	0.944	9.74E-03	0.199	0.722	0.058	2.915	0.40	6.65	0.47
260	4.35E-03	0.609	4.02E-03	2.18E-02	0.925	8.07E-03	0.182	0.677	0.083	3.556	0.54	6.52	0.73
261	4.01E-03	0.530	4.44E-03	2.11E-02	0.882	2.33E-02	0.222	0.527	0.084	4.939	0.78	5.87	0.99
262	3.84E-03	0.473	3.49E-03	2.61E-02	0.866	2.15E-02	0.136	0.527	0.123	5.388	0.38	3.93	0.55
263	4.45E-03	0.552	2.48E-03	5.73E-02	0.964	2.68E-02	0.000	0.042	0.017	1.162	0.73	17.65	2.18
264	3.80E-04	0.559	1.95E-03	1.21E-02	0.962	2.75E-02	0.025	0.058	0.000	1.693	2.78	12.98	0.76
265	1.10E-03	0.563	1.59E-03	5.16E-02	0.927	3.15E-02	0.000	0.034	0.008	2.223	1.38	13.60	3.88
266	9.44E-04	0.566	9.90E-04	7.35E-02	0.943	3.19E-02	0.013	0.034	0.000	2.778	2.33	9.35	2.65
267	2.17E-03	0.518	9.53E-05	7.52E-02	0.889	2.69E-02	0.033	0.033	0.000	3.783	1.09	7.70	4.83
268	1.92E-04	0.512	5.12E-04	2.06E-02	0.870	5.53E-02	0.025	0.034	0.000	3.556	0.64	6.44	1.82
269	4.53E-04	0.498	4.84E-04	4.41E-03	0.992	2.39E-03	0.000	0.084	0.000	0.956	0.25	19.90	0.22
270	1.46E-03	0.530	4.17E-04	6.95E-03	0.982	2.63E-03	0.000	0.092	0.000	1.337	0.72	17.42	0.39
271	2.59E-03	0.558	2.44E-03	3.14E-02	0.972	1.46E-02	0.000	0.083	0.000	2.067	0.44	11.28	1.31
272	8.95E-04	0.554	4.89E-04	1.54E-02	0.939	2.08E-03	0.008	0.080	0.000	2.279	0.57	11.03	0.45
273	1.29E-03	0.529	1.90E-03	3.34E-02	0.947	9.21E-03	0.021	0.051	0.017	3.066	0.58	7.86	1.42
274	4.43E-04	0.491	1.19E-04	5.50E-02	0.892	1.03E-02	0.020	0.060	0.013	3.355	0.42	7.03	2.23
275	1.00E-03	0.484	2.20E-04	3.91E-02	0.864	1.57E-02	0.012	0.060	0.036	4.041	0.84	8.30	1.19
276	3.24E-03	0.555	1.60E-03	2.37E-02	0.989	5.10E-03	0.000	0.182	0.000	1.016	0.37	12.98	1.13
277	2.33E-03	0.584	1.70E-03	1.84E-02	0.987	5.60E-03	0.008	0.183	0.000	1.494	0.50	12.71	1.06
278	6.63E-03	0.541	7.94E-03	1.70E-02	0.962	2.98E-02	0.008	0.166	0.000	1.998	0.94	9.52	5.41
279	2.24E-03	0.524	4.24E-03	5.93E-03	0.935	2.41E-03	0.029	0.134	0.000	2.469	0.20	9.54	0.14
280	2.26E-03	0.493	2.38E-03	4.62E-01	0.914	4.01E-02	0.029	0.084	0.017	2.822	2.24	7.09	0.43
281	2.65E-03	0.455	1.31E-03	8.96E-01	0.896	1.58E-02	0.050	0.067	0.025	-	0.32	4.91	0.97
282	1.80E-03	0.389	8.36E-04	2.10E-02	0.895	2.46E-02	0.014	0.072	0.018	4.337	0.73	3.97	0.52
283	4.04E-03	0.581	3.27E-03	7.89E-03	0.996	2.34E-03	0.000	0.237	0.008	0.851	0.31	14.46	0.59
284	3.07E-03	0.596	7.35E-03	5.34E-03	0.996	1.70E-03	0.000	0.255	0.000	1.132	0.63	11.30	0.54
285	4.14E-03	0.607	1.92E-02	1.41E-02	0.987	2.83E-03	0.000	0.250	0.000	1.573	1.39	11.70	0.79
286	4.20E-03	0.628	1.46E-02	1.93E-02	0.981	5.63E-03	0.084	0.227	0.008	2.117	0.20	8.82	0.77
287	4.51E-03	0.628	2.51E-03	9.51E-01	0.951	5.89E-03	0.055	0.076	0.059	2.469	1.18	9.33	2.08
288	2.85E-03	0.564	4.61E-03	5.38E-02	0.910	4.29E-02	0.038	0.094	0.009	3.233	1.63	8.18	3.24
289	2.36E-03	0.511	1.68E-03	1.55E-02	0.894	3.55E-02	0.008	0.016	0.070	3.783	0.54	5.59	0.66
290	2.20E-03	0.475	1.25E-03	4.75E-02	0.856	2.42E-02	0.000	0.020	0.030	-	0.19	5.87	0.65
291	1.24E-02	0.598	1.37E-02	1.96E-02	0.985	9.07E-03	0.000	0.353	0.000	0.763	0.75	13.15	1.24
292	5.98E-03	0.595	1.67E-02	3.29E-03	0.996	1.80E-03	0.000	0.332	0.000	0.972	0.73	12.19	0.23
293	4.77E-03	0.595	4.06E-02	4.98E-03	0.993	1.59E-03	0.000	0.345	0.000	1.210	0.47	10.99	0.57
294	8.28E-03	0.638	3.05E-02	1.75E-02	0.977	8.18E-03	0.059	0.351	0.017	1.646	0.36	9.84	0.97
295	8.10E-03	0.647	7.65E-03	1.65E-02	0.981	2.70E-03	0.138	0.201	0.025	2.223	0.40	9.02	1.93
296	6.92E-03	0.615	7.41E-03	4.98E-02	0.953	2.75E-02	0.071	0.108	0.075	2.654	1.41	8.72	1.78
297	2.15E-03	0.571	3.32E-03	2.67E-02	0.949	2.11E-02	0.050	0.059	0.059	3.233	1.21	8.72	0.48

298	7.98E-04	0.514	1.79E-03	4.65E-02	0.918	8.13E-03	0.034	0.042	0.046	4.041	0.17	6.31	1.26
299	1.44E-03	0.470	1.83E-03	4.09E-02	0.880	2.52E-02	0.072	0.136	0.047	-	0.61	5.00	0.70
300	6.53E-03	0.573	7.44E-03	5.17E-03	0.986	3.10E-03	0.017	0.408	0.008	1.052	0.31	11.70	0.29
301	4.81E-03	0.584	8.49E-03	6.46E-03	0.979	3.45E-03	0.008	0.393	0.013	1.307	0.23	11.30	0.54
302	8.30E-03	0.620	1.18E-02	1.36E-02	0.963	8.59E-03	0.200	0.391	0.017	1.778	0.26	9.71	0.66
303	3.90E-03	0.622	4.70E-03	1.60E-02	0.957	3.70E-03	0.075	0.218	0.034	2.469	0.21	10.86	0.78
304	5.10E-03	0.605	5.49E-03	2.31E-02	0.938	4.57E-02	0.105	0.193	0.050	2.694	0.95	7.62	0.57
305	2.86E-03	0.540	5.31E-03	2.71E-02	0.902	1.66E-02	0.064	0.080	0.048	3.556	0.37	7.47	0.95
306	2.68E-03	0.494	2.54E-03	4.26E-02	0.877	1.80E-02	0.067	0.117	0.075	4.559	0.58	7.33	1.49
307	1.15E-03	0.449	2.23E-03	1.11E-02	0.874	2.35E-02	0.086	0.163	0.050	-	0.40	4.41	0.44
308	6.63E-03	0.609	6.76E-03	5.65E-03	0.982	3.19E-03	0.017	0.549	0.000	1.162	0.40	10.39	0.41
309	4.12E-03	0.604	9.13E-03	6.24E-03	0.973	2.78E-03	0.234	0.510	0.007	1.494	0.17	10.84	0.33
310	1.58E-02	0.649	3.43E-02	3.77E-03	0.962	1.29E-02	0.303	0.383	0.066	1.872	1.84	10.73	0.57
311	6.64E-03	0.638	8.59E-03	9.49E-01	0.949	1.57E-02	0.158	0.275	0.102	2.577	1.40	8.33	0.53
312	4.24E-03	0.594	6.48E-03	5.35E-03	0.932	9.10E-03	0.205	0.286	0.090	3.066	0.55	6.91	0.49
313	3.85E-03	0.527	8.03E-04	8.87E-01	0.887	1.69E-02	0.089	0.127	0.076	4.041	1.07	6.95	3.28
314	2.73E-03	0.461	3.66E-03	1.76E-02	0.878	2.79E-02	0.091	0.299	0.087	4.559	0.24	4.79	0.38
315	1.95E-03	0.412	2.55E-03	9.94E-03	0.847	3.59E-02	0.135	0.317	0.059	-	0.54	3.70	0.19
316	1.61E-02	0.643	1.68E-02	8.16E-03	0.989	4.59E-03	0.000	0.599	0.008	0.972	0.61	11.03	0.50
317	5.79E-03	0.628	1.20E-02	5.93E-03	0.982	3.61E-03	0.100	0.583	0.000	1.288	0.43	10.91	0.37
318	1.08E-02	0.635	2.86E-02	1.17E-02	0.974	4.66E-03	0.264	0.621	0.017	1.602	0.24	9.68	0.56
319	1.30E-02	0.658	2.11E-02	1.35E-02	0.955	8.78E-03	0.059	0.485	0.046	2.142	0.80	10.28	0.46
320	7.81E-03	0.638	1.08E-02	8.48E-03	0.936	2.07E-02	0.134	0.336	0.042	2.654	0.55	9.14	0.26
321	9.58E-03	0.590	6.56E-03	3.38E-02	0.899	2.18E-02	0.159	0.293	0.092	3.066	0.72	8.39	1.50
322	3.21E-03	0.517	6.48E-03	2.26E-02	0.860	2.16E-02	0.132	0.271	0.051	4.041	0.40	7.30	0.85
323	4.01E-03	0.452	3.11E-03	3.26E-02	0.832	1.03E-02	0.146	0.320	0.094	4.939	0.72	7.04	0.79
324	3.66E-03	0.415	2.27E-03	3.45E-02	0.814	2.34E-02	0.063	0.292	0.127	-	0.86	5.25	0.43
325	1.54E-02	0.603	5.95E-02	9.75E-03	0.939	5.74E-03	0.218	0.729	0.000	1.125	1.44	10.50	0.70
326	7.05E-03	0.593	4.50E-02	7.57E-03	0.932	4.20E-03	0.545	0.672	0.008	1.422	0.94	11.07	0.39
327	1.16E-02	0.612	2.83E-02	1.64E-02	0.931	7.04E-03	0.392	0.680	0.033	1.778	0.45	10.21	0.77
328	1.53E-02	0.620	2.07E-02	2.53E-02	0.905	1.20E-02	0.373	0.495	0.093	2.309	0.38	10.58	1.21
329	1.30E-02	0.598	1.01E-02	2.20E-02	0.894	2.19E-02	0.232	0.423	0.089	2.778	1.26	8.29	0.48
330	5.83E-03	0.551	8.53E-03	3.08E-02	0.866	2.47E-02	0.154	0.362	0.106	3.355	0.92	8.34	0.91
331	4.70E-03	0.484	4.44E-03	2.55E-02	0.853	1.49E-02	0.173	0.497	0.020	4.337	0.30	7.27	0.76
332	2.41E-03	0.410	2.87E-03	2.10E-02	0.809	2.14E-02	0.123	0.550	0.047	-	0.43	4.15	0.95
333	7.01E-04	0.492	4.07E-04	4.49E-03	0.991	2.03E-03	0.000	0.048	0.000	1.046	0.28	15.00	0.52
334	1.83E-03	0.494	9.38E-04	5.62E-03	0.978	4.90E-03	0.000	0.057	0.000	1.185	0.57	12.04	1.21
335	1.40E-03	0.528	1.08E-03	6.08E-03	0.919	1.52E-02	0.000	0.036	0.009	1.693	0.50	9.20	1.37
336	1.10E-03	0.526	3.32E-03	2.00E-02	0.929	3.23E-02	0.019	0.038	0.019	2.223	0.69	9.55	2.15
337	7.45E-04	0.514	1.17E-03	3.54E-03	0.914	4.28E-03	0.016	0.043	0.011	2.577	0.71	9.34	0.08
338	2.92E-04	0.499	6.92E-04	1.38E-02	0.892	2.75E-02	0.013	0.039	0.000	2.577	1.59	6.44	0.63
339	2.77E-04	0.490	5.66E-04	2.65E-02	0.875	2.95E-02	0.009	0.035	0.000	3.066	2.14	7.76	1.21
340	4.01E-04	0.498	4.28E-04	2.46E-02	0.878	1.56E-03	0.000	0.042	0.007	3.355	1.19	9.50	0.53
341	1.01E-04	0.477	9.45E-05	1.90E-02	0.852	9.58E-03	0.000	0.064	0.000	2.915	0.37	5.13	0.43
342	9.69E-04	0.519	2.09E-03	2.86E-03	0.994	2.73E-03	0.000	0.093	0.000	1.028	0.56	17.75	0.46
343	1.38E-03	0.528	8.73E-04	7.12E-03	0.984	3.44E-03	0.000	0.095	0.000	1.185	0.41	13.31	0.65
344	6.47E-03	0.558	8.27E-04	2.59E-02	0.943	1.21E-02	0.024	0.096	0.019	1.833	1.13	13.35	0.82
345	1.03E-03	0.553	4.77E-03	2.49E-02	0.946	2.37E-02	0.011	0.076	0.022	2.309	1.32	7.98	1.34
346	6.85E-04	0.518	9.75E-04	2.59E-02	0.936	9.05E-03	0.010	0.089	0.010	2.371	0.25	6.06	0.57
347	2.27E-03	0.510	1.03E-03	1.07E-02	0.919	8.07E-03	0.044	0.088	0.000	2.778	0.61	7.04	0.54
348	6.88E-04	0.493	5.24E-04	1.55E-02	0.897	1.65E-02	0.000	0.082	0.000	3.233	0.95	7.78	1.21
349	4.84E-04	0.470	8.29E-04	1.72E-02	0.879	1.87E-02	0.015	0.121	0.008	3.783	0.38	7.05	0.67
350	1.24E-03	0.535	1.66E-03	5.13E-03	0.992	3.70E-03	0.000	0.152	0.000	0.982	0.33	15.12	0.35
351	2.13E-03	0.547	1.03E-03	3.39E-03	0.992	1.93E-03	0.000	0.151	0.000	1.140	0.40	15.30	0.52
352	1.03E-03	0.561	1.09E-03	3.49E-03	0.990	1.71E-03	0.000	0.158	0.000	1.368	0.42	15.66	0.37
353	4.05E-03	0.578	1.80E-03	2.78E-02	0.980	4.68E-03	0.008	0.142	0.008	1.891	0.34	9.19	1.65
354	2.38E-03	0.562	1.90E-03	1.60E-02	0.952	8.55E-03	0.034	0.146	0.000	2.309	0.39	9.35	0.76
355	5.26E-03	0.553	2.07E-03	1.61E-02	0.911	8.49E-03	0.026	0.123	0.018	2.778	0.64	10.75	0.37
356	1.86E-03	0.517	1.02E-03	2.34E-02	0.917	8.89E-03	0.037	0.110	0.028	2.915	0.27	7.43	0.59
357	1.53E-03	0.500	1.12E-03	2.62E-02	0.903	1.52E-02	0.024	0.164	0.010	3.066	0.69	5.20	1.17
358	4.94E-04	0.491	1.33E-03	1.37E-02	0.908	9.00E-03	0.011	0.187	0.000	3.556	0.14	4.88	0.34
359	6.23E-03	0.563	6.54E-03	7.62E-03	0.992	5.94E-03	0.000	0.174	0.009	0.790	0.33	14.95	0.79
360	1.41E-03	0.552	2.33E-03	3.92E-03	0.994	2.96E-03	0.000	0.183	0.000	1.052	0.39	14.18	0.32
361	1.05E-03	0.551	2.69E-03	3.46E-03	0.994	3.02E-03	0.000	0.182	0.000	1.279	0.57	14.51	0.29
362	1.33E-03	0.573	9.02E-04	8.03E-03	0.989	2.95E-03	0.000	0.201	0.008	1.494	0.25	11.27	0.45
363	4.18E-03	0.589	8.04E-03	1.58E-02	0.964	8.91E-03	0.025	0.159	0.017	1.998	0.63	10.55	0.46
364	3.10E-03	0.571	2.56E-03	1.40E-02	0.954	1.26E-02	0.026	0.154	0.026	2.469	0.77	9.24	0.91
365	4.65E-03	0.546	3.10E-03	2.26E-02	0.953	9.75E-03	0.044	0.131	0.017	2.694	0.14	7.67	0.26
366	2.16E-03	0.522	3.68E-03	1.78E-02	0.935	2.70E-02	0.091	0.155	0.000	-	1.08	7.70	0.55
367	2.38E-03	0.512	2.19E-03	1.65E-02	0.932	8.21E-03	0.069	0.130	0.043	2.915	0.51	4.78	1.20
368	1.52E-03	0.473	2.07E-03	1.26E-02	0.892	1.70E-02	0.075	0.170	0.020	3.556	0.19	4.68	0.14
369	4.34E-03	0.548	5.74E-03	7.26E-03	0.987	6.31E-03	0.000	0.246	0.000	0.843	0.62	13.64	0.54
370	1.97E-03	0.552	2.22E-03	3.71E-03	0.993	2.47E-03	0.000	0.227	0.000	1.104	0.33	14.05	0.33
371	1.41E-03	0.550	6.08E-03	3.60E-03	0.988	3.08E-03	0.009	0.246	0.000	1.307	0.17	13.23	0.14
372	5.73E-03	0.575	1.25E-02	5.49E-03	0.983	7.52E-03	0.072	0.252	0.018	1.560	0.45	9.76	0.17
373	4.62E-03	0.592	1.05E-02	1.49E-02	0.982	8.55E-03	0.088	0.117	0.058	2.142	0.44	7.92	0.45
374	3.30E-03	0.580	4.58E-03	1.33E-02	0.949	8.08E-03	0.036	0.144	0.009	2.469	0.37	10.17	0.94
375	1.06E-03	0.530	5.77E-03	4.25E-03	0.915	3.08E-02	0.097	0.140	0.011	2.915	0.88	8.01	0.20
376	1.59E-03	0.517	3.09E-03	1.11E-02	0.902	1.39E-02	0.032	0.203	0.028	3.066	0.48	6.92	0.66

377	1.78E-03	0.495	1.10E-03	1.51E-02	0.893	1.03E-02	0.067	0.221	0.029	3.233	0.88	5.55	0.49
378	1.60E-03	0.485	1.70E-03	2.34E-02	0.908	2.01E-02	0.010	0.280	0.015	4.041	0.67	4.56	0.48
379	1.38E-03	0.461	1.38E-03	2.58E-02	0.863	2.58E-02	0.045	0.231	0.030	4.041	0.16	3.92	0.57
380	1.06E-02	0.576	1.85E-02	4.53E-03	0.989	3.37E-03	0.000	0.338	0.000	0.773	0.88	12.59	0.55
381	5.67E-03	0.545	2.45E-02	4.47E-03	0.972	3.48E-03	0.000	0.367	0.000	0.982	0.75	11.32	0.44
382	5.75E-03	0.564	5.07E-02	4.38E-03	0.960	6.90E-03	0.010	0.307	0.019	1.279	0.50	13.59	0.28
383	1.05E-02	0.570	5.22E-02	9.07E-03	0.957	9.82E-03	0.024	0.355	0.024	1.422	1.57	10.08	1.07
384	1.11E-02	0.580	2.83E-02	1.58E-02	0.951	3.83E-03	0.126	0.342	0.023	1.726	1.47	9.60	0.69
385	4.10E-03	0.588	9.79E-03	1.82E-02	0.921	4.14E-03	0.108	0.152	0.051	2.279	0.30	11.29	1.12
386	4.33E-03	0.552	7.03E-03	1.30E-02	0.916	1.11E-02	0.060	0.186	0.066	2.778	1.59	10.10	0.75
387	5.85E-03	0.530	2.76E-03	2.48E-02	0.906	1.09E-02	0.064	0.148	0.042	3.066	0.63	8.26	0.77
388	5.86E-03	0.511	4.36E-03	1.55E-02	0.875	1.28E-02	0.081	0.139	0.046	3.355	1.19	7.92	0.44
389	2.40E-03	0.475	3.69E-03	2.62E-02	0.880	2.03E-02	0.040	0.173	0.080	3.783	0.39	6.16	0.48
390	2.82E-03	0.447	2.15E-03	2.55E-02	0.867	1.70E-02	0.056	0.356	0.017	3.556	0.66	4.42	0.60
391	1.43E-03	0.413	1.50E-03	2.50E-02	0.826	1.92E-02	0.020	0.338	0.051	4.337	0.51	4.37	0.54
392	2.03E-02	0.632	2.36E-02	7.85E-03	0.988	7.32E-03	0.000	0.412	0.000	0.783	1.04	13.16	0.95
393	6.20E-03	0.614	6.74E-03	7.30E-03	0.991	4.90E-03	0.000	0.422	0.000	1.052	0.53	11.36	0.55
394	4.48E-03	0.621	8.13E-03	3.33E-03	0.996	2.07E-03	0.009	0.403	0.000	1.307	0.14	11.50	0.43
395	3.62E-03	0.624	3.25E-03	6.52E-03	0.989	3.26E-03	0.020	0.400	0.000	1.457	0.20	12.08	0.19
396	6.52E-03	0.637	3.32E-03	1.64E-02	0.979	5.74E-03	0.103	0.383	0.029	1.778	0.41	10.97	0.57
397	7.48E-03	0.633	5.40E-03	2.47E-02	0.964	8.97E-03	0.145	0.159	0.056	2.371	0.46	9.15	1.03
398	7.63E-03	0.608	2.83E-03	1.98E-02	0.949	1.85E-03	0.134	0.161	0.054	2.694	0.36	9.08	0.44
399	4.58E-03	0.570	8.62E-03	2.68E-02	0.925	1.60E-02	0.079	0.112	0.074	3.066	0.83	9.24	1.56
400	4.00E-03	0.542	5.15E-03	3.21E-02	0.917	2.18E-02	0.087	0.126	0.102	3.556	0.50	7.30	1.09
401	2.48E-03	0.519	5.30E-03	2.33E-02	0.895	2.01E-02	0.071	0.091	0.076	3.556	0.58	6.82	0.86
402	2.34E-03	0.490	3.05E-03	2.48E-02	0.869	2.36E-02	0.068	0.291	0.018	4.041	1.06	6.60	0.50
403	2.22E-03	0.471	2.27E-03	2.04E-02	0.856	1.90E-02	0.072	0.251	0.036	4.559	1.16	6.27	0.58
404	2.85E-02	0.675	2.02E-02	1.17E-02	0.991	5.49E-03	0.010	0.459	0.000	0.863	0.85	14.87	1.02
405	1.64E-02	0.659	1.36E-02	1.01E-02	0.990	5.34E-03	0.000	0.496	0.000	0.956	0.72	12.79	0.89
406	7.94E-03	0.634	7.78E-03	9.13E-03	0.990	4.60E-03	0.000	0.536	0.019	1.210	0.57	11.95	0.37
407	6.88E-03	0.647	4.93E-03	8.17E-03	0.986	3.52E-03	0.153	0.540	0.000	1.560	0.23	11.47	0.60
408	5.53E-03	0.649	8.43E-03	9.42E-03	0.981	3.89E-03	0.245	0.555	0.026	1.693	0.24	10.25	0.53
409	4.78E-03	0.651	8.32E-03	1.04E-02	0.962	3.84E-03	0.333	0.444	0.039	1.998	0.18	11.15	0.39
410	6.42E-03	0.654	6.31E-03	1.35E-02	0.957	5.22E-03	0.156	0.193	0.083	2.577	0.38	9.51	1.00
411	3.69E-03	0.621	3.31E-03	5.43E-03	0.947	1.31E-02	0.095	0.161	0.057	3.066	0.30	9.33	0.38
412	4.33E-03	0.591	3.76E-03	1.38E-02	0.928	1.90E-02	0.110	0.156	0.064	3.355	1.04	8.54	0.38
413	4.39E-03	0.546	5.35E-03	3.17E-02	0.913	5.94E-03	0.049	0.235	0.099	3.783	0.61	7.00	1.23
414	4.89E-03	0.524	5.23E-03	1.66E-02	0.884	2.52E-02	0.131	0.252	0.055	-	0.65	7.34	0.99
415	3.45E-03	0.489	1.73E-03	3.12E-02	0.884	9.40E-03	0.118	0.237	0.069	-	0.76	7.65	0.86
416	1.74E-03	0.466	3.77E-03	1.26E-02	0.856	1.79E-02	0.096	0.354	0.048	5.388	0.32	6.85	0.25
417	2.11E-02	0.670	2.91E-02	7.80E-03	0.980	6.59E-03	0.017	0.601	0.000	0.931	1.13	11.62	0.69
418	1.33E-02	0.638	3.54E-02	5.71E-03	0.963	4.41E-03	0.008	0.627	0.000	1.084	1.10	11.44	0.63
419	7.96E-03	0.611	7.46E-02	4.52E-03	0.950	5.24E-03	0.113	0.660	0.017	1.389	0.65	10.72	0.37
420	5.78E-03	0.620	2.17E-02	4.59E-03	0.958	4.56E-03	0.219	0.652	0.000	1.693	0.31	10.86	0.20
421	6.04E-03	0.623	9.01E-03	1.38E-02	0.948	7.15E-03	0.266	0.630	0.000	1.891	0.58	10.23	0.77
422	7.76E-03	0.626	1.52E-02	1.26E-02	0.935	1.02E-02	0.295	0.477	0.085	2.142	0.78	10.54	0.65
423	6.65E-03	0.618	1.08E-02	1.38E-02	0.919	1.05E-02	0.158	0.202	0.123	2.778	0.76	10.70	0.25
424	8.87E-03	0.592	4.63E-03	1.78E-02	0.916	1.01E-02	0.083	0.092	0.108	3.233	0.68	9.74	0.62
425	1.01E-02	0.557	2.85E-03	4.54E-02	0.899	1.70E-02	0.134	0.219	0.080	3.556	0.45	8.12	2.29
426	5.92E-03	0.520	4.58E-03	3.51E-02	0.869	1.05E-02	0.144	0.226	0.077	4.041	1.41	9.20	1.16
427	3.20E-03	0.486	4.09E-03	2.16E-02	0.866	1.52E-02	0.139	0.410	0.067	4.559	0.67	6.85	0.20
428	3.77E-03	0.461	3.63E-03	3.68E-02	0.835	2.38E-02	0.092	0.481	0.037	-	0.58	7.31	1.14
429	1.75E-04	0.494	2.40E-04	2.05E-03	0.962	1.84E-03	0.000	0.049	0.000	1.185	0.39	17.49	0.19
430	1.01E-03	0.499	9.77E-04	2.07E-02	0.913	1.83E-02	0.000	0.050	0.000	1.602	1.57	15.36	1.61
431	8.08E-04	0.511	7.94E-04	4.04E-02	0.916	7.64E-03	0.000	0.024	0.008	2.223	0.73	11.82	1.15
432	5.35E-04	0.502	9.96E-04	3.73E-02	0.818	4.16E-02	0.016	0.032	0.000	2.577	0.97	11.54	3.73
433	2.97E-04	0.474	6.82E-04	5.92E-02	0.839	1.57E-02	0.015	0.030	0.008	3.066	0.88	9.52	2.50
434	5.48E-04	0.459	4.53E-04	4.74E-02	0.821	2.39E-02	0.025	0.036	0.000	4.233	0.62	10.61	1.56
435	2.22E-03	0.489	1.16E-03	2.74E-02	0.946	1.02E-02	0.000	0.092	0.000	1.279	0.72	14.15	1.64
436	1.66E-03	0.498	3.86E-04	1.65E-02	0.935	6.94E-03	0.033	0.098	0.000	1.778	0.40	11.75	0.45
437	2.09E-03	0.511	1.01E-04	2.33E-02	0.906	2.15E-03	0.024	0.056	0.016	2.067	0.17	10.83	0.72
438	6.98E-04	0.476	7.85E-04	3.07E-02	0.836	5.81E-03	0.000	0.040	0.009	3.233	1.49	12.71	3.22
439	8.27E-04	0.450	1.14E-03	2.86E-02	0.867	2.26E-02	0.008	0.024	0.032	3.066	0.49	6.91	0.90
440	1.04E-03	0.450	1.35E-03	6.10E-02	0.815	3.08E-02	0.008	0.025	0.008	3.556	1.10	9.69	1.47
441	1.92E-03	0.550	1.19E-03	1.03E-02	0.993	3.25E-03	0.000	0.150	0.000	0.993	0.29	16.48	0.72
442	9.18E-04	0.565	1.42E-03	5.06E-03	0.988	3.22E-03	0.000	0.156	0.000	1.422	0.46	13.73	0.33
443	3.78E-03	0.460	9.85E-03	2.47E-02	0.874	8.43E-03	0.057	0.154	0.016	1.933	1.17	9.86	0.91
444	3.60E-03	0.477	6.91E-03	2.68E-02	0.863	2.02E-02	0.062	0.115	0.016	2.279	2.67	10.50	0.65
445	3.91E-03	0.417	2.69E-03	4.76E-02	0.832	2.10E-02	0.033	0.041	0.033	3.066	0.81	10.41	1.16
446	5.09E-04	0.378	1.24E-03	2.14E-02	0.785	1.64E-02	0.029	0.050	0.067	3.556	0.48	7.36	0.40
447	4.84E-03	0.565	5.25E-03	9.05E-03	0.988	5.37E-03	0.008	0.240	0.000	0.855	0.57	15.43	0.22
448	3.46E-03	0.573	3.34E-03	8.03E-03	0.994	2.94E-03	0.000	0.215	0.000	1.084	0.38	13.98	0.20
449	2.85E-03	0.585	1.84E-03	8.54E-03	0.984	6.34E-03	0.017	0.224	0.000	1.602	0.61	13.98	0.40
450	4.14E-03	0.595	4.78E-03	1.70E-02	0.971	6.59E-03	0.058	0.149	0.021	1.998	0.25	10.74	0.18
451	2.97E-03	0.582	3.48E-03	1.91E-02	0.961	9.22E-03	0.083	0.107	0.041	2.469	0.32	11.01	0.52
452	3.69E-03	0.536	2.08E-03	3.82E-02	0.950	1.64E-02	0.025	0.083	0.042	3.066	0.23	8.24	1.72
453	1.65E-03	0.489	3.11E-03	8.84E-03	0.910	6.93E-03	0.075	0.108	0.046	3.556	0.33	7.75	1.21
454	4.53E-04	0.438	8.74E-04	8.77E-01	0.877	1.00E-02	0.025	0.025	0.025	4.233	1.31	6.19	0.63
455	5.36E-03	0.584	7.40E-03	1.17E-02	0.984	7.81E-03	0.000	0.297	0.008	0.956	0.39	14.54	0.75

456	2.30E-03	0.588	2.45E-03	5.09E-03	0.993	3.12E-03	0.000	0.322	0.000	1.235	0.33	12.14	0.33
457	4.05E-03	0.601	4.45E-03	1.01E-02	0.980	5.09E-03	0.012	0.313	0.008	1.602	0.26	11.24	0.59
458	5.08E-03	0.632	5.67E-03	9.89E-03	0.969	1.21E-02	0.083	0.141	0.033	2.371	1.52	12.41	0.46
459	7.27E-03	0.601	3.52E-03	2.32E-02	0.959	1.41E-02	0.041	0.140	0.058	2.371	0.24	9.35	0.26
460	4.63E-03	0.547	3.10E-03	2.07E-02	0.944	2.89E-03	0.057	0.139	0.008	3.066	0.59	10.00	2.30
461	2.62E-03	0.495	3.10E-03	3.61E-02	0.910	2.54E-02	0.074	0.131	0.049	3.783	0.51	6.64	0.84
462	5.70E-03	0.606	7.17E-03	6.00E-03	0.992	4.54E-03	0.000	0.396	0.000	1.034	0.35	12.44	0.54
463	4.78E-03	0.617	3.86E-03	7.34E-03	0.990	3.34E-03	0.012	0.396	0.008	1.337	0.50	12.29	0.38
464	3.87E-03	0.631	6.59E-03	1.22E-02	0.978	6.21E-03	0.083	0.406	0.017	1.726	0.41	9.18	1.00
465	3.60E-03	0.634	7.29E-03	1.37E-02	0.967	1.01E-02	0.095	0.198	0.049	2.223	0.39	10.15	0.46
466	7.70E-03	0.608	4.92E-03	1.91E-02	0.953	1.96E-02	0.120	0.223	0.040	2.694	0.79	9.79	0.69
467	7.23E-03	0.553	3.23E-03	2.14E-02	0.906	1.17E-02	0.070	0.082	0.033	3.233	0.24	9.52	0.96
468	3.32E-03	0.489	2.68E-03	3.31E-02	0.883	1.91E-02	0.066	0.191	0.058	4.337	0.79	7.03	0.74
469	7.08E-03	0.631	6.88E-03	7.13E-03	0.992	4.27E-03	0.008	0.437	0.000	1.104	0.29	12.55	0.64
470	4.87E-03	0.644	3.11E-03	7.97E-03	0.989	3.66E-03	0.008	0.462	0.000	1.422	0.36	11.84	0.48
471	9.34E-03	0.657	8.96E-03	1.63E-02	0.969	7.72E-03	0.144	0.403	0.016	1.891	0.73	11.18	0.47
472	8.13E-03	0.646	7.43E-03	1.68E-02	0.955	6.74E-03	0.141	0.166	0.124	2.371	0.41	9.73	0.99
473	3.38E-03	0.616	7.33E-03	1.47E-02	0.954	6.14E-03	0.107	0.115	0.128	2.778	0.95	9.42	0.70
474	1.96E-03	0.547	1.57E-03	1.53E-02	0.926	6.50E-03	0.098	0.112	0.084	3.355	0.23	9.32	0.25
475	4.27E-03	0.482	6.18E-03	2.10E-02	0.861	1.18E-02	0.091	0.141	0.083	4.041	0.57	7.89	0.57
476	6.64E-03	0.658	1.42E-02	3.89E-03	0.994	2.37E-03	0.066	0.529	0.008	1.210	0.33	11.60	0.30
477	3.34E-03	0.651	1.96E-02	3.13E-03	0.989	2.44E-03	0.146	0.543	0.016	1.560	0.43	11.33	0.41
478	7.77E-03	0.655	1.20E-02	1.05E-02	0.970	6.48E-03	0.300	0.403	0.086	1.998	0.26	11.44	0.93
479	1.22E-02	0.645	8.70E-03	1.50E-02	0.954	1.15E-02	0.114	0.133	0.152	2.469	0.66	10.48	0.49
480	1.15E-02	0.627	3.70E-03	2.51E-02	0.957	6.95E-03	0.079	0.091	0.141	2.915	0.58	8.98	0.40
481	6.55E-03	0.541	2.30E-03	1.84E-02	0.915	2.62E-03	0.059	0.092	0.105	3.783	1.07	7.40	0.59
482	4.48E-03	0.480	4.42E-03	3.70E-02	0.839	3.06E-02	0.095	0.215	0.095	4.939	1.08	9.67	2.18
483	5.57E-03	0.628	1.24E-02	4.40E-03	0.963	2.86E-03	0.517	0.579	0.033	1.389	0.34	12.02	0.23
484	8.82E-03	0.623	1.92E-02	4.60E-03	0.956	4.45E-03	0.045	0.594	0.008	1.693	0.52	11.56	0.41
485	1.39E-02	0.631	1.02E-02	2.40E-02	0.936	7.13E-03	0.226	0.238	0.214	2.067	0.60	11.90	0.91
486	1.48E-02	0.617	1.04E-02	2.67E-02	0.918	7.55E-03	0.176	0.287	0.098	2.654	0.26	11.04	1.48
487	1.02E-02	0.585	4.70E-03	1.99E-02	0.905	5.58E-03	0.148	0.181	0.132	3.066	0.33	9.57	0.95
488	6.65E-03	0.514	5.66E-03	1.81E-02	0.869	1.23E-02	0.075	0.224	0.066	4.041	0.51	10.66	0.23
489	3.33E-03	0.451	3.30E-03	3.42E-02	0.831	2.73E-02	0.091	0.265	0.091	4.939	0.78	7.85	0.98

Appendix B

Effect of High Viscous Oil on Two-Phase Oil-Gas Flow Behavior in Horizontal Pipes

Experiments were conducted using 3-in. ID horizontal to investigate the effect of high oil viscosity on two-phase oil-gas flow behavior. 628 data sets were acquired for 587 cP, 420 cP, 300 cP, 220 cP, 181 cP, and 155 cP oil viscosities. Superficial oil and gas velocities had ranges of 0.02 m/s to 0.35 m/s, and 0.1 m/s to 3.6 m/s, respectively. The following subsections explain the experimental matrix, single-phase, and two-phase flow tests. Flow pattern, pressure gradient, average liquid holdup, and slug characterization are presented for two-phase flow tests. The slug flow characteristics are subdivided into slug liquid holdup, film liquid holdup, translational velocity, slug length, slug length distribution, and slug frequency.

B.1 Experimental matrix

In this study, most experiments were simultaneously performed in both 2- and 3-in. ID pipes. The experimental matrix was set for 2-in. ID pipes at first. Based on the 2-in. ID test matrix, the matrix for 3-in. ID pipe was calculated using the experimental parameters such as gas mass flow rate and pressure. The superficial gas velocity of 3-in. ID pipes was calculated using Eq. (115) derived from gas law equation. The superficial liquid velocity was computed by

considering the pipe diameter as Eq. (116).

$$v_{SG\,(3-in.\ Test\,section\,)} = \frac{W_{G\,(3-in.\ Test\,section\,)}(286.99T + 131920.7)}{1886.42\ P_{(3-in.\ Test\,section\,)}} \tag{115}$$

$$v_{SL(3-in.\ Test\,section\,)} = \frac{4}{9} v_{SL(2-in.\ Test\,section)} \tag{116}$$

where W_G is gas mass flow rate in kg/s, T is temperature in ℉, P is pressure in psi, v_{SG} is superficial gas velocity in m/s, and v_{SL} is superficial liquid velocity in m/s.

Because of the maximum allowable pressure in 2-in. ID pipe section, the superficial liquid and gas velocities of 3-in. ID pipe section were not able to be increased larger than 0.4 m/s and 4 m/s, respectively. The sample of test matrix is given in Table B.1.

Figures B.1 to B.3 present the ranges of experimental matrix on the flow pattern maps by Taitel & Dukler, Barnea, and TUFFP Unified models when the oil viscosities are 181 cP and 587 cP.

Table B.1 Experimental matrix when oil viscosity is 70 ℉

	v_{SL} (m/s)	v_{SG} (m/s)		v_{SL} (m/s)	v_{SG} (m/s)
1	0.022	0.324	37	0.178	0.608
2	0.022	0.504	38	0.178	0.913
3	0.022	0.719	39	0.178	1.191
4	0.022	0.969	40	0.178	1.833
5	0.022	1.418	41	0.178	2.444
6	0.022	1.900	42	0.178	3.205
7	0.022	2.403	43	0.222	0.198
8	0.044	0.160	44	0.222	0.329
9	0.044	0.255	45	0.222	0.456
10	0.044	0.345	46	0.222	0.643
11	0.044	0.517	47	0.222	0.957
12	0.044	0.738	48	0.222	1.224
13	0.044	1.015	49	0.222	2.006
14	0.044	1.499	50	0.222	3.046
15	0.044	1.994	51	0.267	0.204
16	0.044	2.485	52	0.267	0.333
17	0.089	0.164	53	0.267	0.442
18	0.089	0.267	54	0.267	0.674
19	0.089	0.379	55	0.267	1.008
20	0.089	0.558	56	0.267	1.388
21	0.089	0.772	57	0.267	2.082
22	0.089	1.094	58	0.267	2.988
23	0.089	1.617	59	0.311	0.199
24	0.089	2.147	60	0.311	0.339
25	0.089	2.758	61	0.311	0.490
26	0.133	0.172	62	0.311	0.727
27	0.133	0.279	63	0.311	1.059
28	0.133	0.404	64	0.311	2.223
29	0.133	0.592	65	0.311	3.174
30	0.133	0.858	66	0.356	0.227
31	0.133	1.134	67	0.356	0.369
32	0.133	1.749	68	0.356	0.515
33	0.133	2.429	69	0.356	0.716
34	0.178	0.165	70	0.356	1.053
35	0.178	0.272	71	0.356	1.571
36	0.178	0.410	72	0.356	2.426

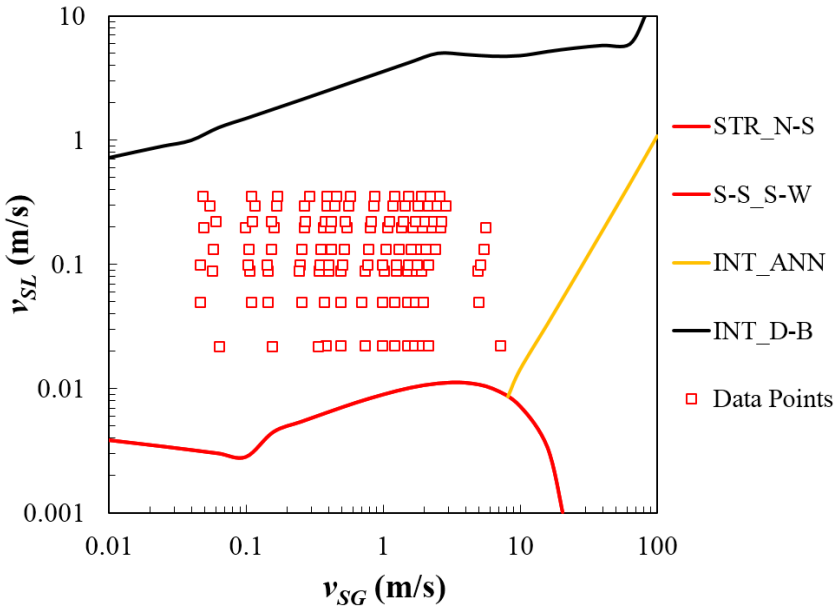

(a) μ_{Oil} = 181 cP

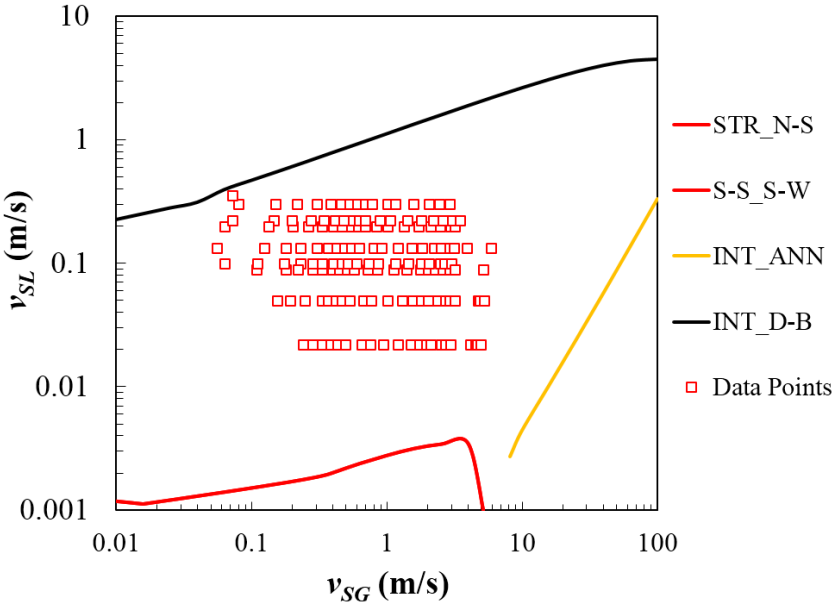

(b) μ_{Oil} = 587 cP

Figure B.1 Experimental matrix and Taitel & Dukler flow pattern map for (a) oil viscosity of 181 cP and (b) oil viscosity of 587 cP.

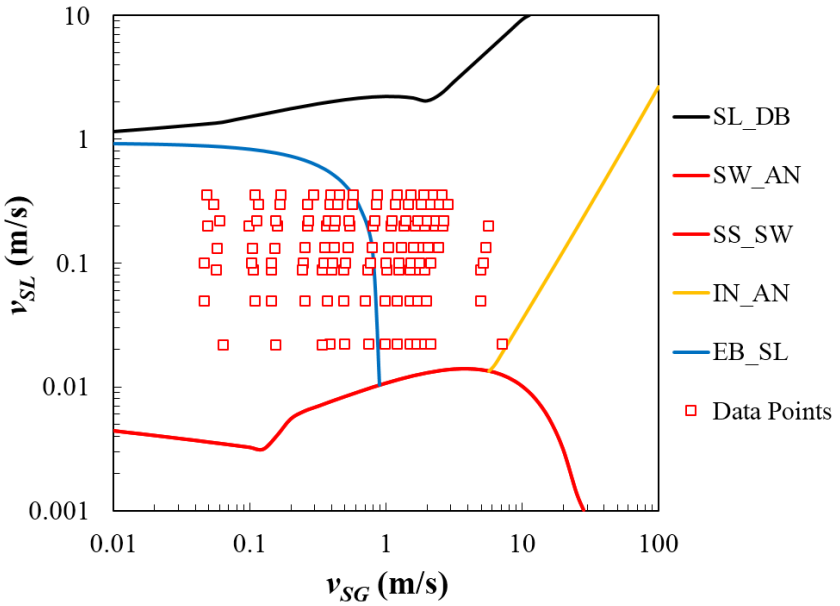

(a) μ_{Oil} = 181 cP

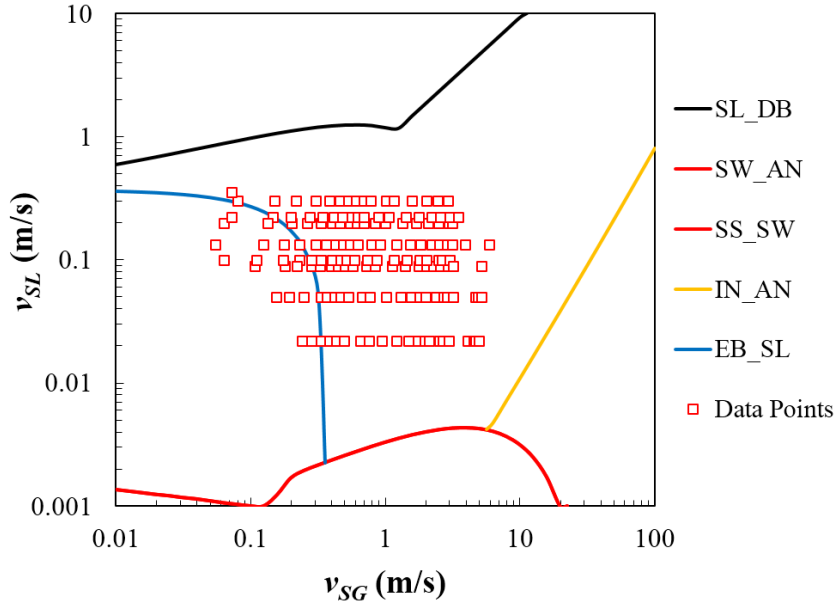

(b) μ_{Oil} = 587 cP

Figure B.2 Experimental matrix and Barnea flow pattern map for (a) oil viscosity of 181 cP and (b) oil viscosity of 587 cP.

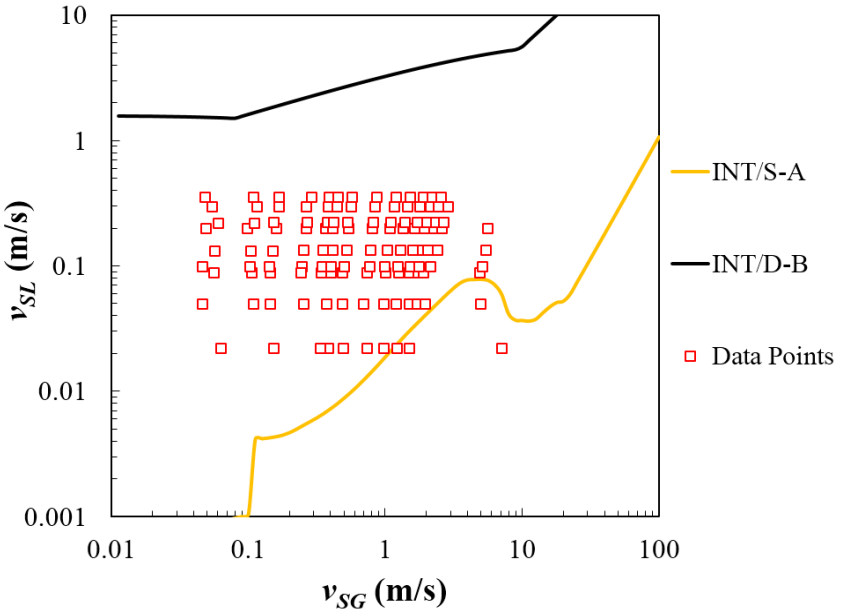

(a) μ_{Oil} = 181 cP

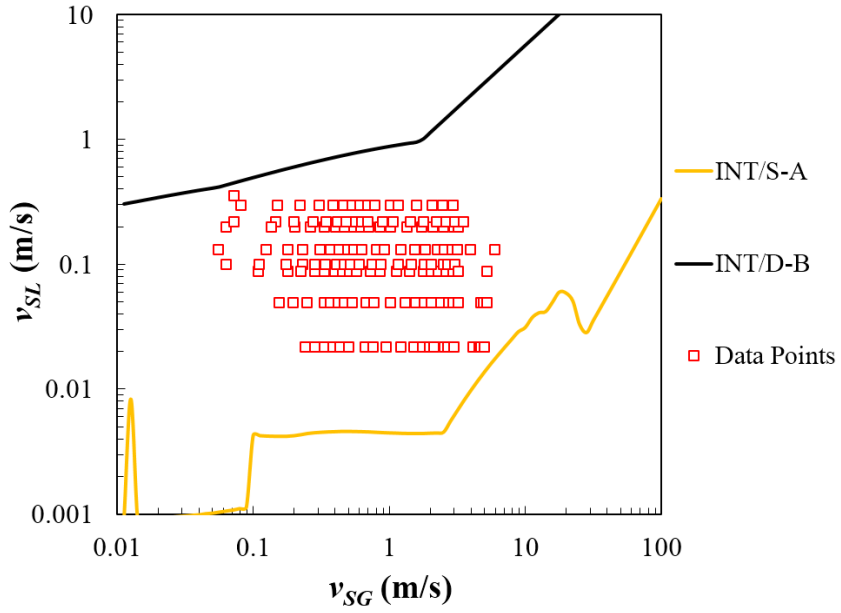

(b) μ_{Oil} = 587 cP

Figure B.3 Experimental matrix and TUFFP Unified flow pattern map for (a) oil viscosity of 181 cP and (b) oil viscosity of 587 cP.

B.2 Single-phase flow test

A set of single-phase flow experiments was executed for the facility commissioning. The purpose of these tests was to ensure the valid calibration of all instrumentation installed on 3-in ID pipeline. For these single-phase flow tests, the superficial liquid velocity ranged from 0.1 m/s to 0.5 m/s and temperature was varied from 70 °F to 110 °F. The oil viscosities were changed from 587 cP to 125 cP corresponding to the designated temperatures. Total 59 tests were carried out. Figure B.4 shows the measured pressure gradients against the calculated pressure gradients using viscosity which was obtained by rheometer. The data points are within ±10% error. It is concluded that the experimental facility and data acquisition system reasonably work and the acquired data is credible. Appendix B presents the equations for the used single-phase tests analysis.

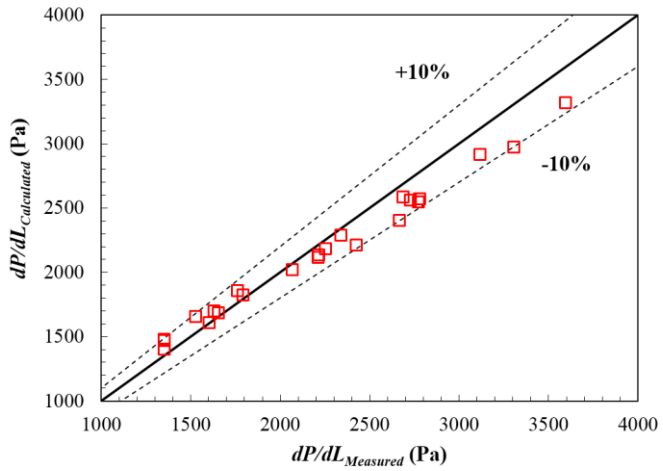

Figure B.4 Measured pressure gradients vs. calculated pressure gradients for oil temperatures of 70 °F, 75 °F, 80 °F, 85 °F, 90 °F, 95 °F, 100 °F, and 110 °F.

B.3 Two-phase flow tests

This section has the following subcategories: flow pattern map, pressure gradient, average liquid holdup, and slug flow characterizations such as slug and film liquid holdup, translational velocity, slug length, and slug frequency.

B.3.1 Flow pattern map

A high speed video camera, FASTCAM SA4 was used to take snapshots for the flow pattern investigation. Three types of the existing flow patterns: elongated bubble, slug, and annular flow, were observed. Transition boundaries between elongated bubble to slug flow, slug to annular flow, and slug to dispersed bubble flow were monitored corresponding to the above flow patterns.

In this study, classification between elongated bubble and slug flow is significant to discriminate the range of experimental matrix supposed to be in the slug flow region. Elongated bubble and slug flow have the same flow mechanism. The elongated bubble flow is considered as the limiting case of slug flow, when the liquid slug is free of entrained bubbles (Shoham, 2006). This occurs at relatively lower gas rates ($v_{SG} < 0.5$ m/s) when the flow is calmer. Figure B.5 shows the front and the end of slug in elongated bubble flow. As can be seen, there is no slippage and eddy current in this flow pattern. The interface between two phases is very smooth, without any perturbation. The number of data points located in the elongated bubble region slightly decreases when oil viscosity increases from 155 cP to 587 cP.

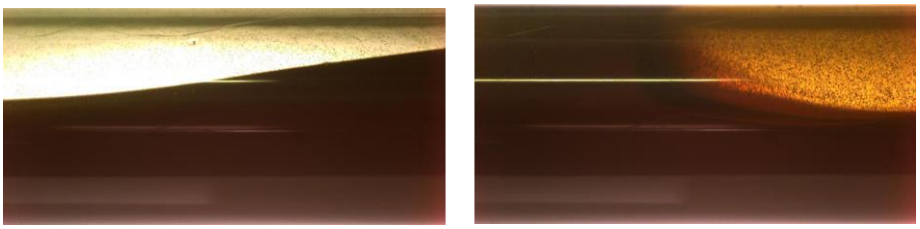

(a) Slug front and tail for v_{SL} = 0.044 m/s, v_{SG} = 0.150 m/s and μ_{Oil} = 220 cP.

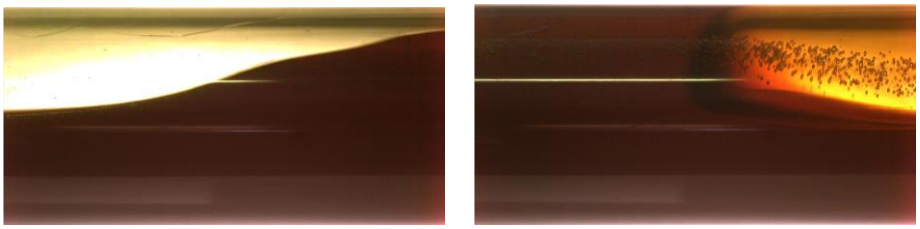

(b) Slug front and tail for v_{SL} = 0.089 m/s, v_{SG} = 0.159 m/s and μ_{Oil} = 220 cP.

Figure B.5 Elongated bubble flow for different superficial liquid and gas velocities.

Transition from elongated bubble to slug flow occurs at relatively low superficial gas velocity with increase of superficial liquid velocity. At this boundary, the behavior change in slug front is observed (see Figure B.6). The inclination angle of the slug front increases comparing to elongated bubble flow. Additionally, a little slippage is observed and this means that the velocity difference between the liquid film and the gas phase increases.

On the other hand, from Figure B.7, it is obviously observed that there are eddy and recirculation current from the liquid film to the slug body. For this flow regime, the amount of gas entrained in both the film and slug region increases comparing to the elongated bubble flow. The perturbation in the interface region increases as the superficial gas and liquid velocities increase. Because slug front eddy formation is delayed as the oil viscosity decreases, the number of data points having slug flow regime slightly expands when oil

viscosity increases. This trend was also reported by Colmenares *et al*. (2001). This phenomenon is observed because, the liquid level for stratified flow increases as viscosity increases facilitating that any perturbation block the top of the pipe promoting slug flow.

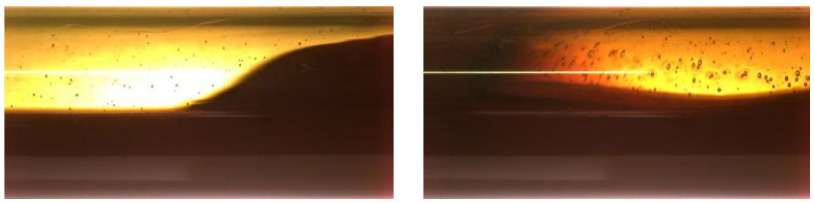

Figure B.6 Slug front and tail of transition boundary between elongated bubble to slug flow when v_{SL} = 0.311 m/s, v_{SG} = 0.062 m/s and μ_{Oil} = 220 cP.

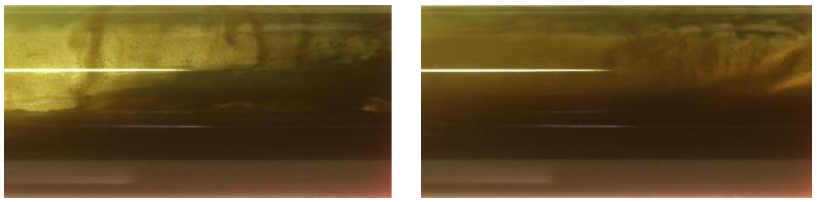

(a) Slug front and tail for v_{SL} = 0.133 m/s, v_{SG} = 3.0 m/s and μ_{Oil} = 420 cP.

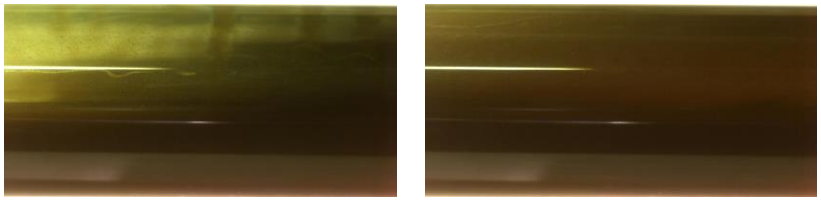

(b) Slug front and tail for v_{SL} = 0.133 m/s, v_{SG} = 3.0 m/s and μ_{Oil} = 300 cP.

Figure B.7 Slug flow behavior for different oil viscosities.

Annular flow occurs for high superficial gas velocity (v_{SG} > 4.5 m/s) in this study. Because the transition boundary between slug and annular flow occurs at relatively high superficial gas velocity as oil viscosity increases, this flow regime was hard to be observed. In general, the gas phase which contain

entrained liquid droplets flows in a core at high velocity. The liquid flows as a thin film around the pipe wall. Sufficient turbulent kinetic energy is offered to segregate the mass of liquid into small droplets, which can be delivered to the top of the pipe making a liquid film around the pipe. Thus, the feature of this flow is a fast-moving gas core with entrained liquid droplets and a slow-moving liquid film flowing around the pipe wall. The annular flow observation during this experimental study was a challenge due to the limitation of the air compressor pressure.

Slug to dispersed bubble transition occurs at very high liquid-flow rates and, the liquid-phase is the continuous-phase, in which the gas-phase is dispersed as discrete bubbles (Shoham, 2006). Due to the limitations of the oil pump capacity and maximum allowable pipe pressure, it was not possible to observe dispersed bubble flow regime in this study.

Figures B.8 through B.16 show the comparison between the acquired flow pattern data for different oil viscosities (181 cP, 300 cP, and 587 cP) and the existing flow pattern prediction models such as Taitel and Dukler (1976), Barnea (1987) and TUFFP Unified model. For all oil viscosities, Barnea model shows a large discrepancy in predicting the transition boundary between slug and annular flow. As liquid viscosity decreases, small differences are observed for the transition boundary from elongated bubble flow to slug flow in this model. TUFFP unified model gives satisfactory results to predict slug-annular flow transition except when oil viscosity is 587 cP, however it is not properly predicted for the transition boundary between slug and dispersed bubble flow. Although Taitel & Dukler model is good at predicting the slug-dispersed bubble transition, this model poorly predicts the slug-annular transition boundary.

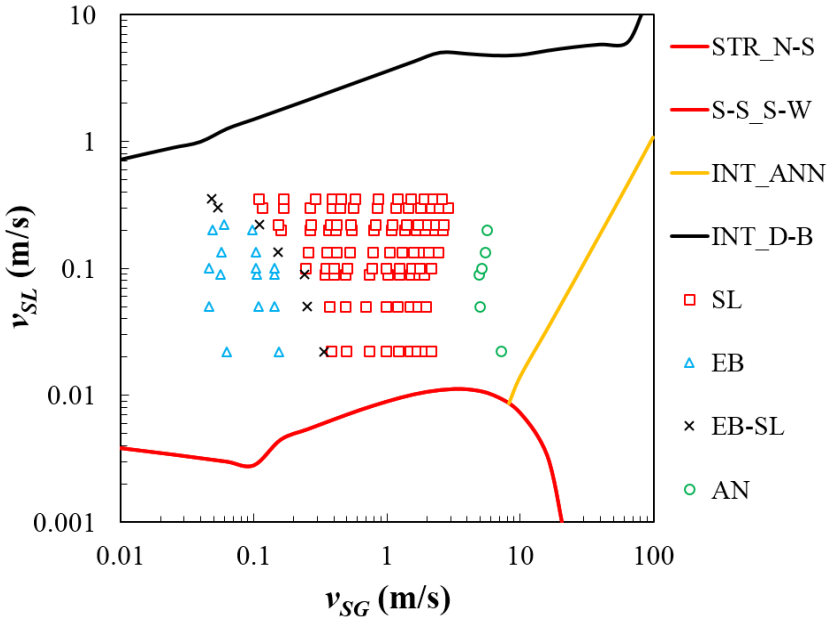

Figure B.8 Observed flow patterns for μ_{Oil}=181 cP vs. Taitel & Dukler (1976) flow pattern prediction model.

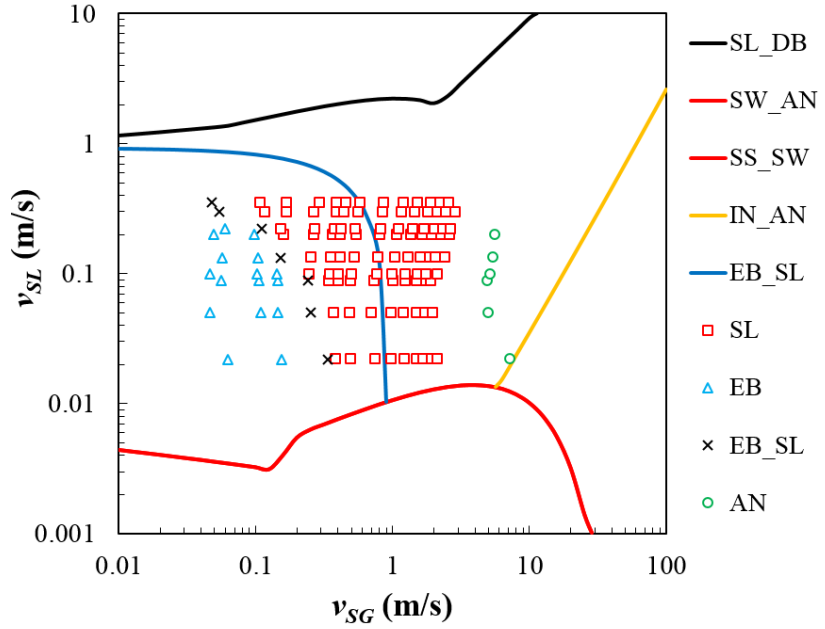

Figure B.9 Observed flow patterns for μ_{Oil}=181 cP vs. Barnea (1987) flow pattern prediction model.

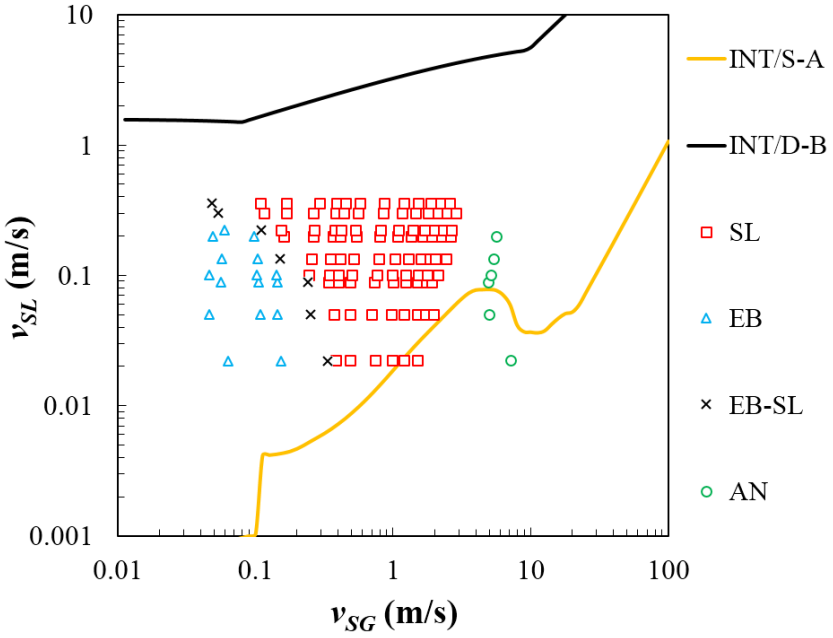

Figure B.10 Observed flow patterns for μ_{Oil}=181 cP vs. TUFFP Unified flow pattern prediction model.

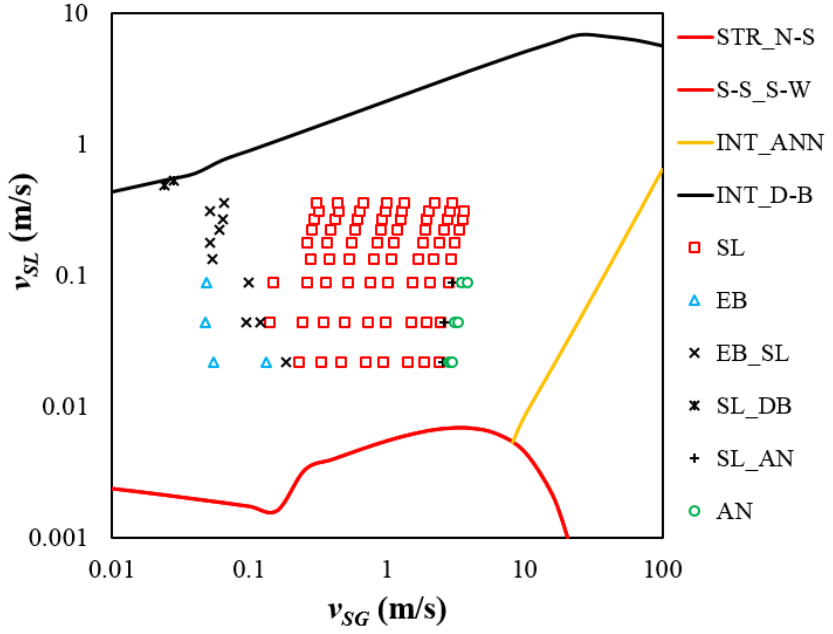

Figure B.11 Observed flow patterns for μ_{Oil}=300 cP vs. Taitel & Dukler (1976) flow pattern prediction model.

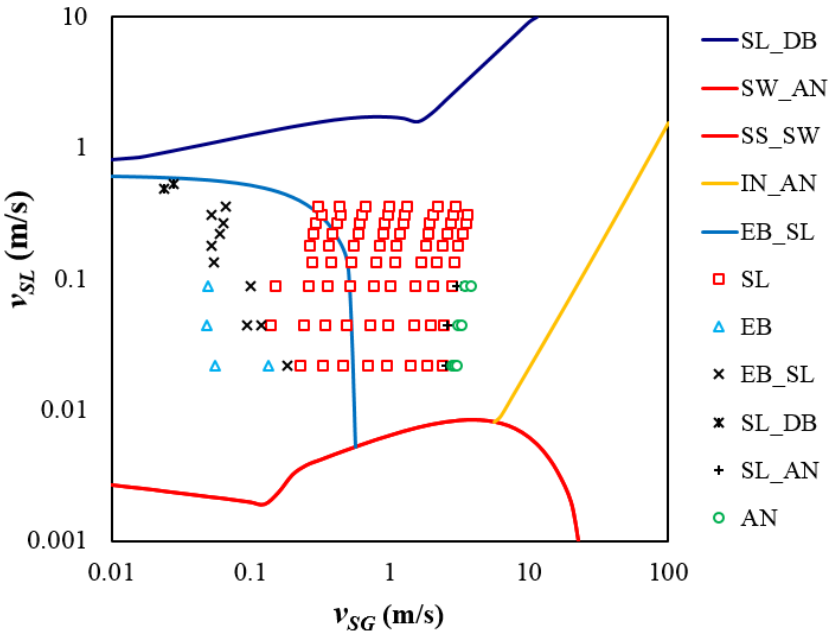

Figure B.12 Observed flow patterns for μ_{Oil}=300 cP vs. Barnea (1987) flow pattern prediction model.

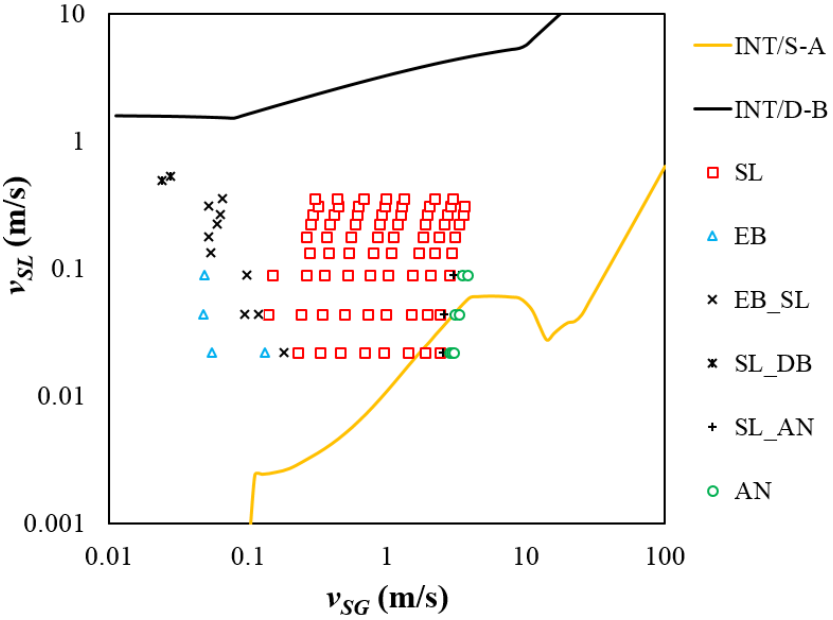

Figure B.13 Observed flow patterns for μ_{Oil}=300 cP vs. TUFFP Unified flow pattern prediction model.

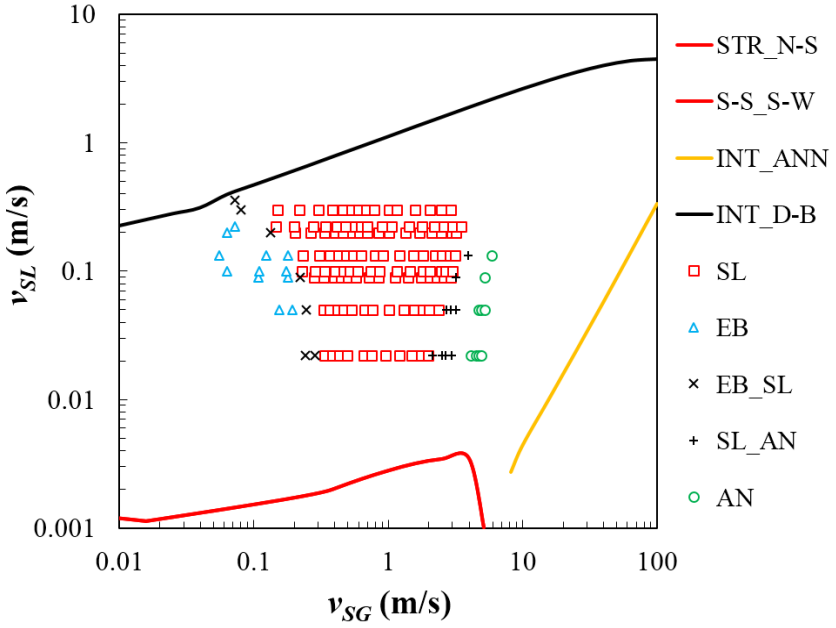

Figure B.14 Observed flow patterns for μ_{Oil}=587 cP vs. Taitel & Dukler (1976) flow pattern prediction model.

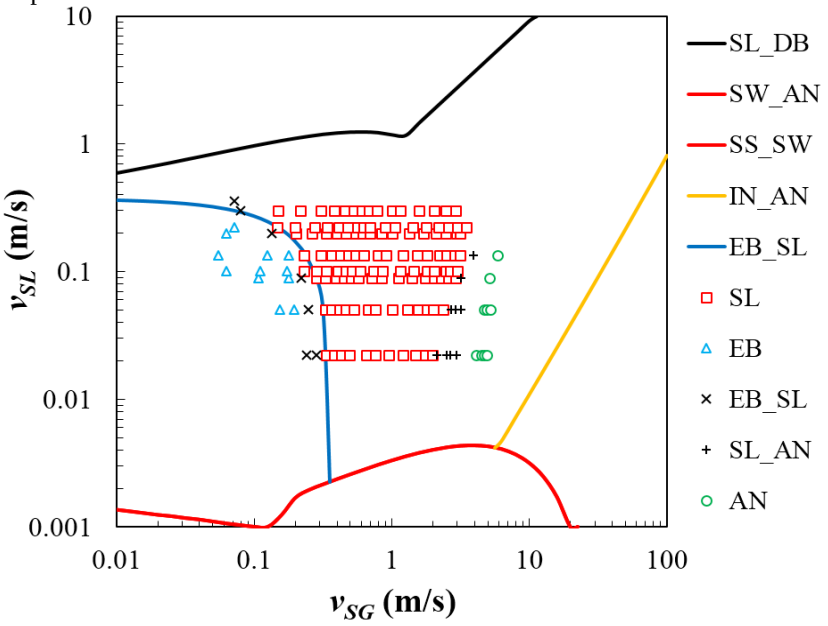

Figure B.15 Observed flow patterns for μ_{Oil}=587 cP vs. Barnea (1987) flow pattern prediction model.

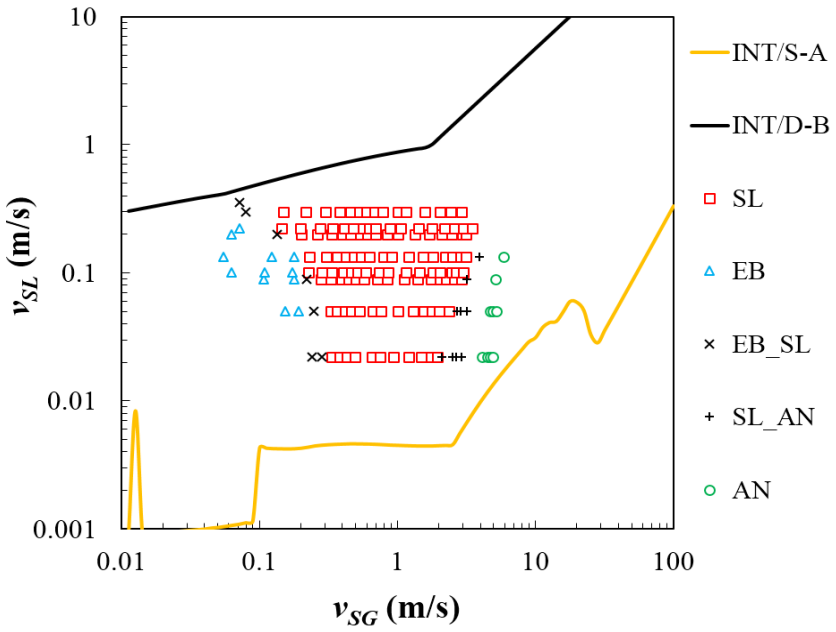

Figure B.16 Observed flow patterns for μ_{Oil}=587 cP vs. TUFFP Unified flow pattern prediction model.

B.3.2 Pressure gradient

Figures B.17 to B.22 present the measured pressure gradient vs. superficial gas velocity for all oil viscosities (155 cP, 181 cP, 220 cP, 300 cP, 420 cP, and 587 cP). Same as Gokcal (2008), Jeyachandra (2011) and Brito (2012), pressure gradient increases as superficial gas velocity increases. Similarly, at given superficial liquid and gas velocities, pressure gradient increases as oil viscosity increases. As can be seen, oil viscosity plays a leading role on the pressure gradient. Finally, for a given superficial gas velocity and oil viscosity, pressure gradient increases as superficial liquid velocity increases.

Figures B.23 to B.27 show the measured pressure gradients against superficial gas velocities for specific superficial liquid velocities (0.022 m/s, 0.089 m/s, 0.133 m/s, 0.222 m/s, and 0.356 m/s).

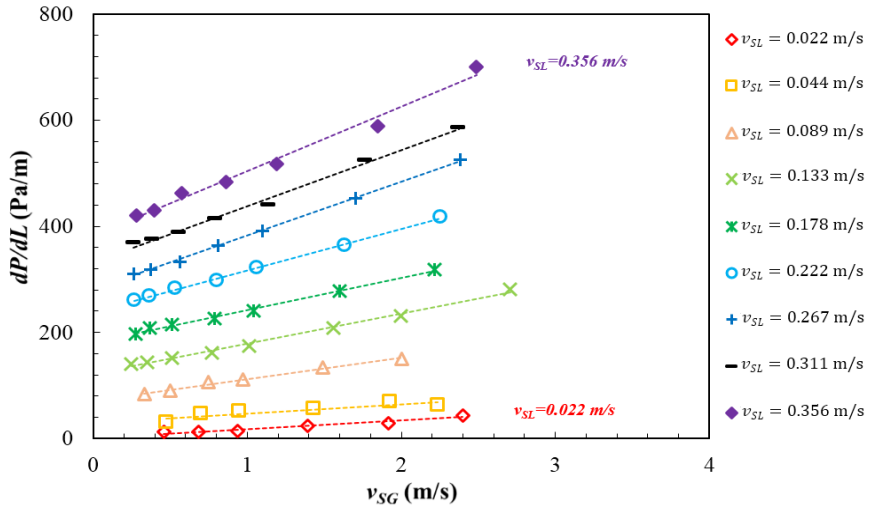

Figure B.17 Pressure gradient vs. superficial gas velocity for μ_{Oil} = 155 cP.

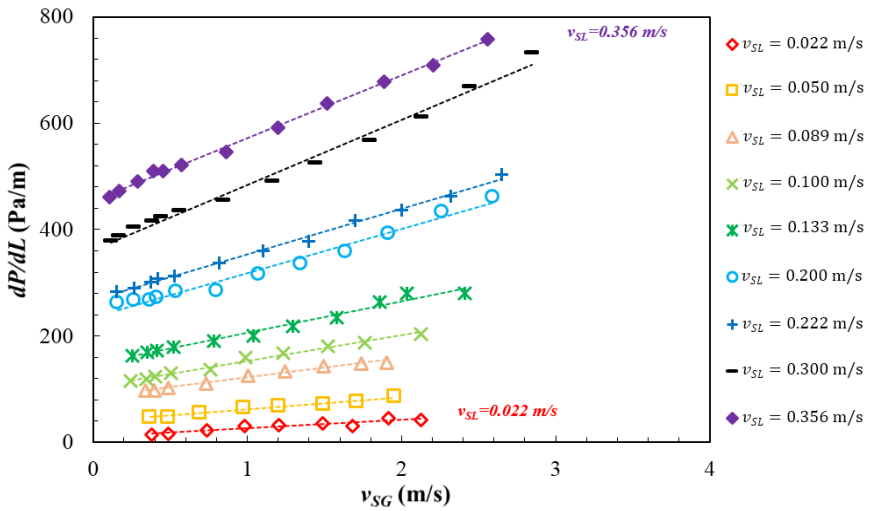

Figure B.18 Pressure gradient vs. superficial gas velocity for μ_{Oil} = 181 cP.

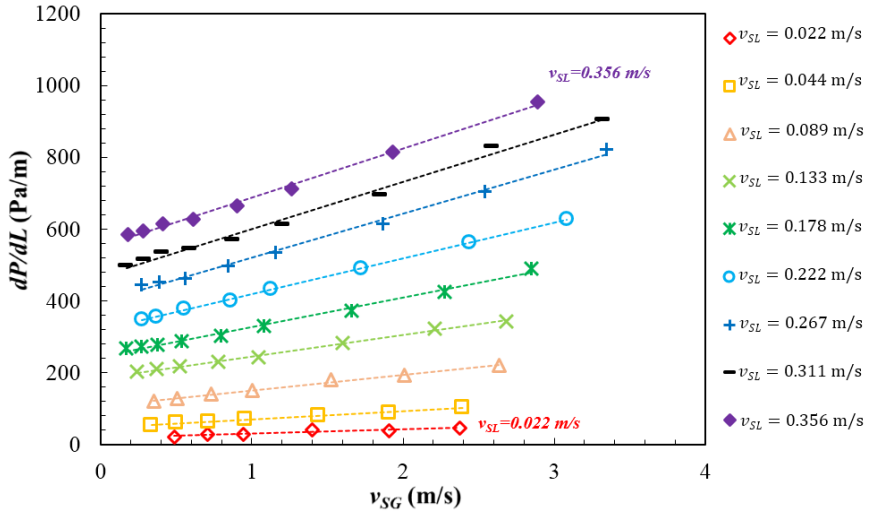

Figure B.19 Pressure gradient vs. superficial gas velocity for μ_{Oil} = 220 cP.

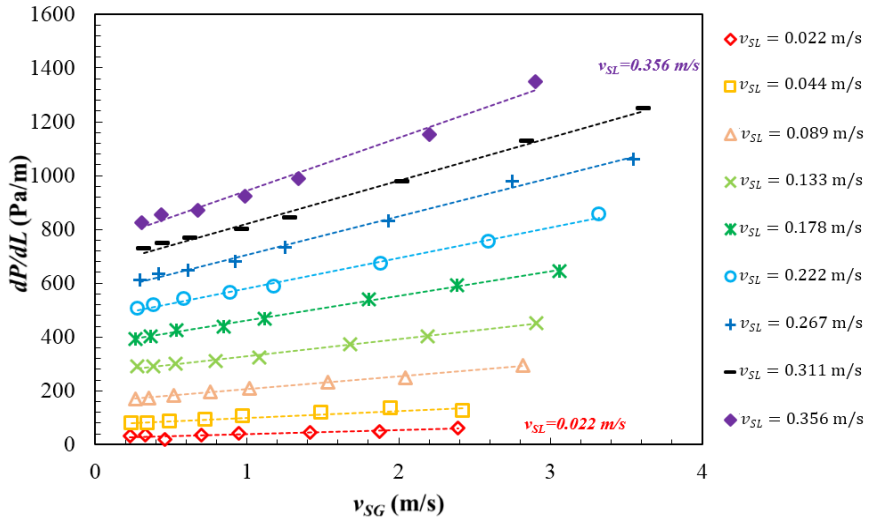

Figure B.20 Pressure gradient vs. superficial gas velocity for μ_{Oil} = 300 cP.

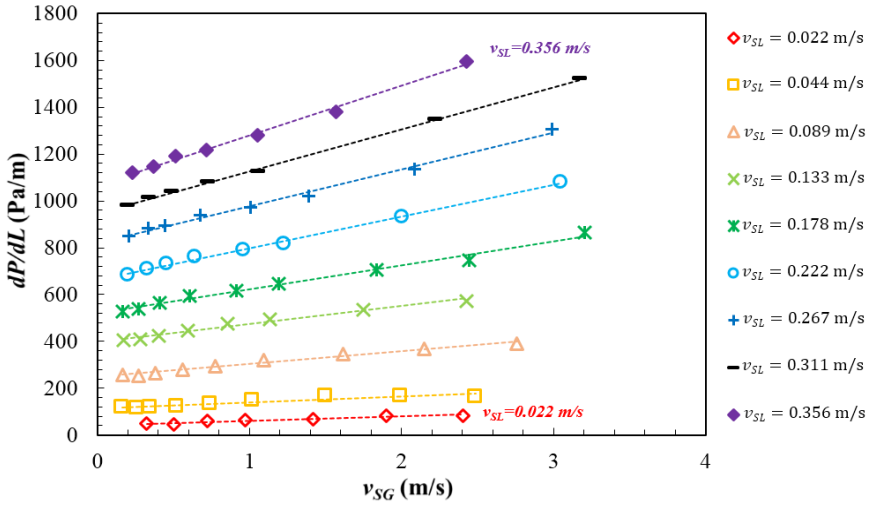

Figure B.21 Pressure gradient vs. superficial gas velocity for μ_{Oil} = 420 cP.

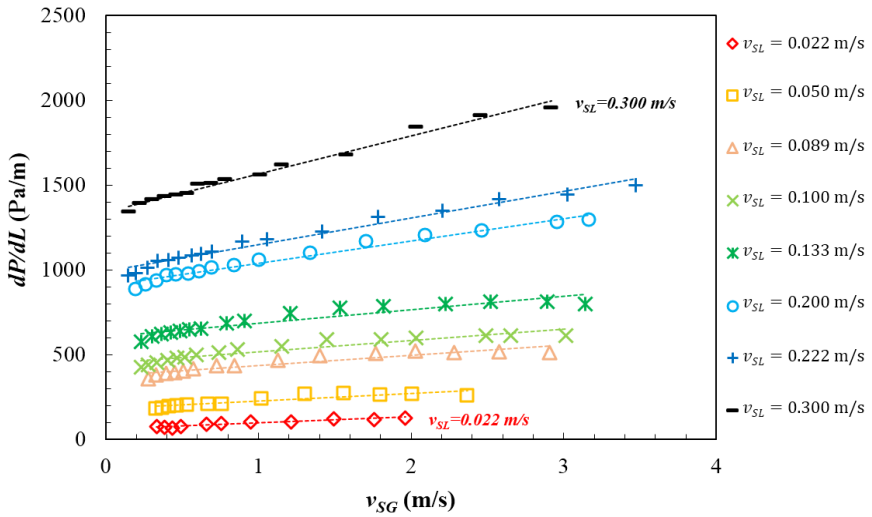

Figure B.22 Pressure gradient vs. superficial gas velocity for μ_{Oil} = 587 cP.

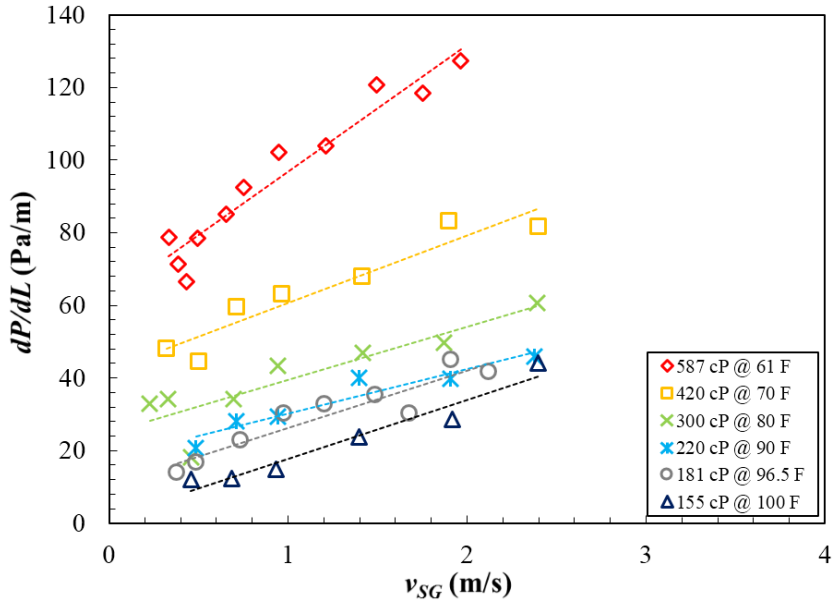

Figure B.23 Pressure gradient comparison for v_{SL}=0.022 m/s.

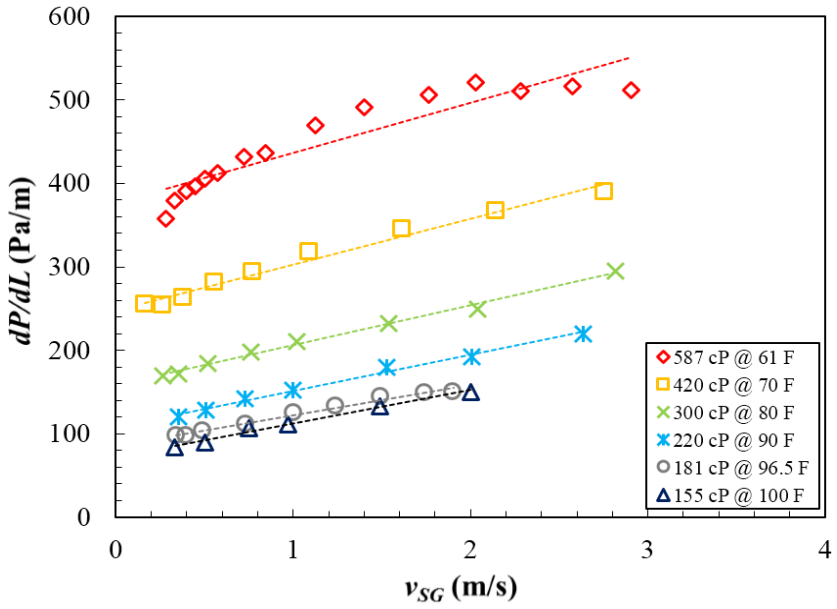

Figure B.24 Pressure gradient comparison for v_{SL}=0.089 m/s.

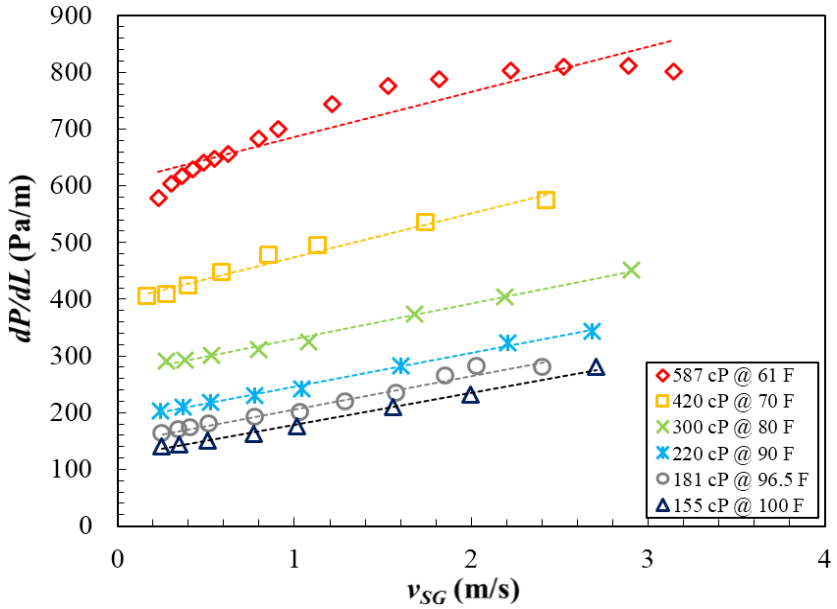

Figure B.25 Pressure gradient comparison for v_{SL}=0.133 m/s.

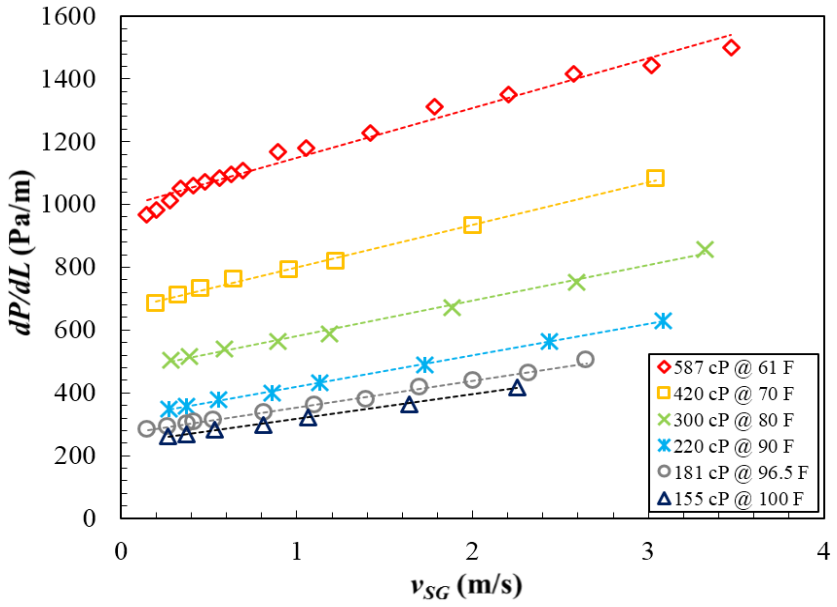

Figure B.26 Pressure gradient comparison for v_{SL}=0.222 m/s.

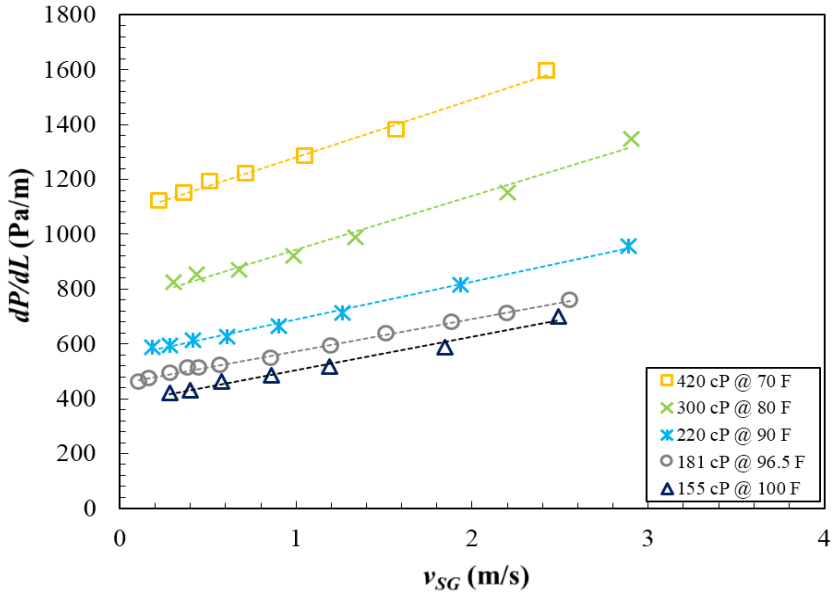

Figure B.27 Pressure gradient comparison for v_{SL}=0.356 m/s.

B.3.3 Average liquid holdup

Two capacitance sensors were used to measure the dimensionless voltage values. A Static calibration was conducted for each oil viscosity conditions because of the residual oil in the pipe. The minimum voltage values can be estimated through static calibration. During the static calibration, drainage of the trapped volume was not acceptable because of the viscous nature of the oil. Accordingly, a graduated tape mounted on the outside wall of the pipe was used to measure the trapped volume of oil. Figure B.28 presents the results of the static calibration for all oil viscosities. As can be seen, there is a linear trend between the dimensionless voltage (from the sensor) and the liquid level. It is also observed that maximum voltage values increases constantly as oil temperature increases (see Figure B.29).

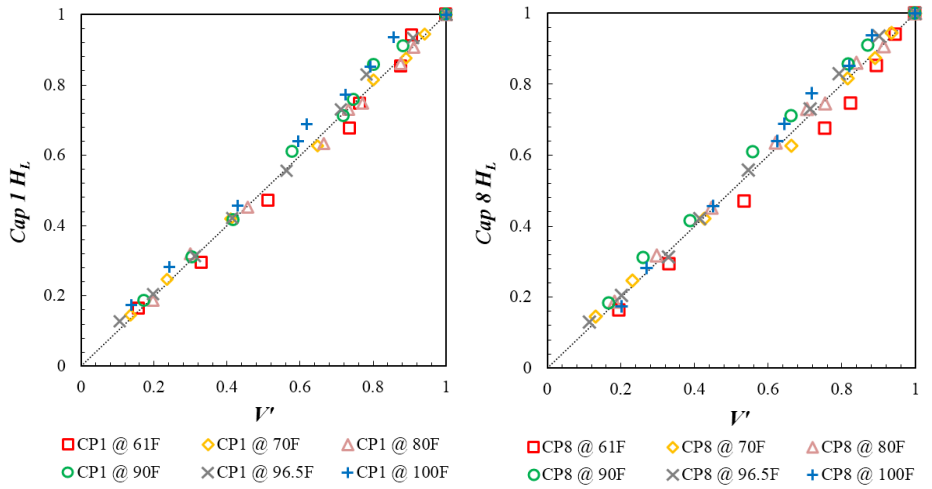

(a) Static calibration results of CP1 (b) Static Calibration results of CP 8

Figure B.28 Static calibration results of (a) Capacitance sensor 1 and (b) Capacitance sensor 8. Trend lines are almost linear according to capacitance sensor property.

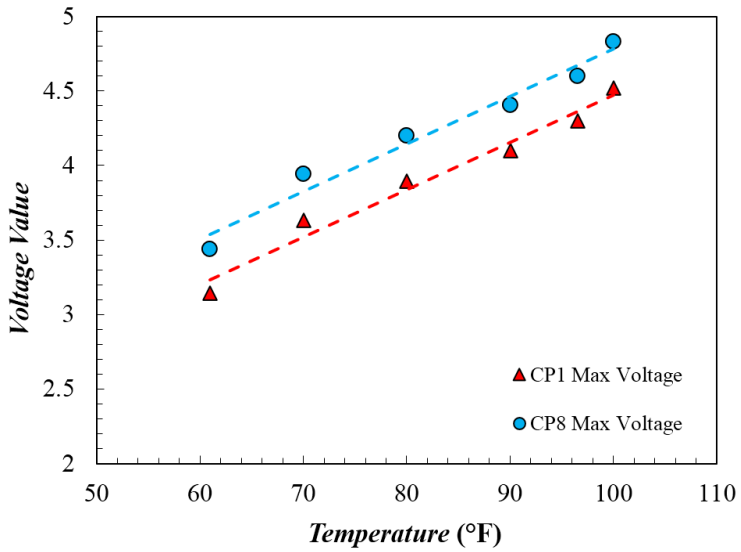

Figure B.29 The maximum voltage value at different temperature for two capacitance sensors. The amount of increase in voltage values are almost constant with respect to every temperature-step.

Figures B.30 to B.39 present the average liquid holdup against superficial gas velocity for all oil viscosities (155 cP, 181 cP, 220 cP, 300 cP, 420 cP, and 587 cP) and different superficial liquid velocities. For a constant oil viscosity and superficial gas velocity, average liquid holdup increases as superficial liquid velocity increases. In Brito (2012), average liquid holdup did not change much when oil viscosity increases (39 – 166 cP), however, average liquid holdup slightly increases with oil viscosity increase at given superficial liquid and gas velocities in this study.

The best fit corresponds to a power curve through a regression analysis showing the average R^2 value as 0.92. Uncertainty was calculated using uncertainty values of slug and film liquid holdup, therefore, uncertainty values of average liquid holdup are relatively high (± 17%) due to the wave propagation of slug flow regime. These average liquid holdups are related with film liquid holdup. The film liquid holdup increases when liquid flow rate increases yielding in a larger average liquid holdup. Section B.3.4.2 presents more details about the film liquid holdup.

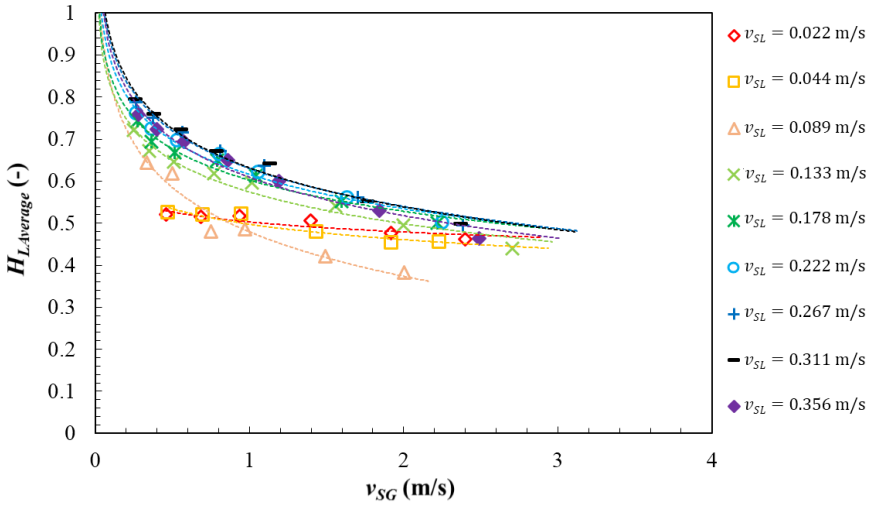

Figure B.30 Average liquid holdup vs. superficial gas velocity μ_{Oil} = 155 cP.

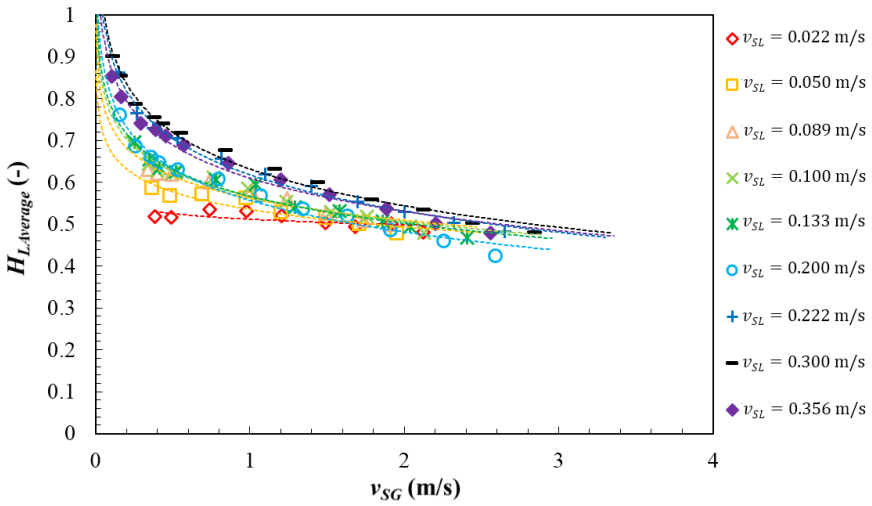

Figure B.31 Average liquid holdup vs. superficial gas velocity μ_{Oil} = 181 cP.

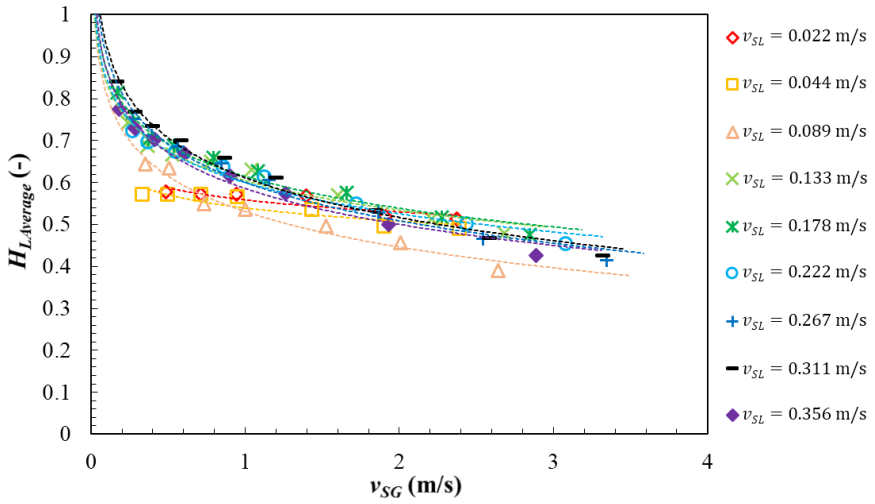

Figure B.32 Average liquid holdup vs. superficial gas velocity μ_{Oil} = 220 cP.

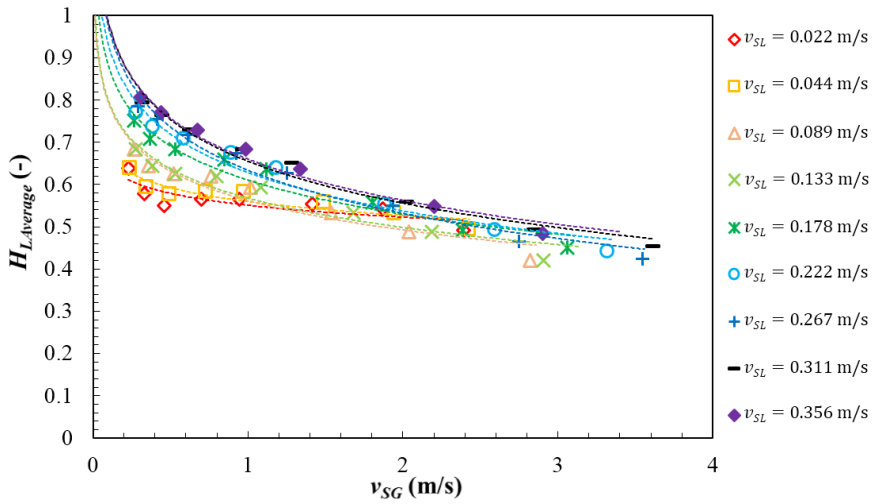

Figure B.33 Average liquid holdup vs. superficial gas velocity μ_{Oil} = 300 cP.

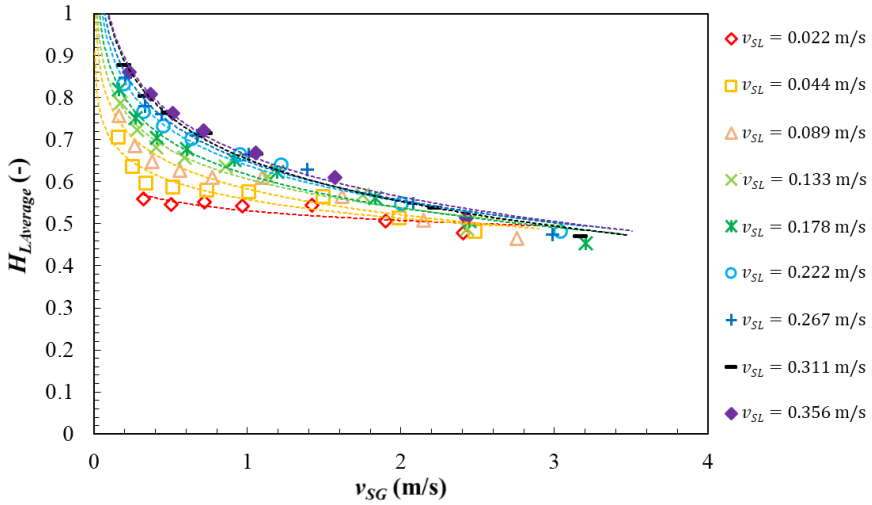

Figure B.34 Average liquid holdup vs. superficial gas velocity μ_{Oil} = 420 cP.

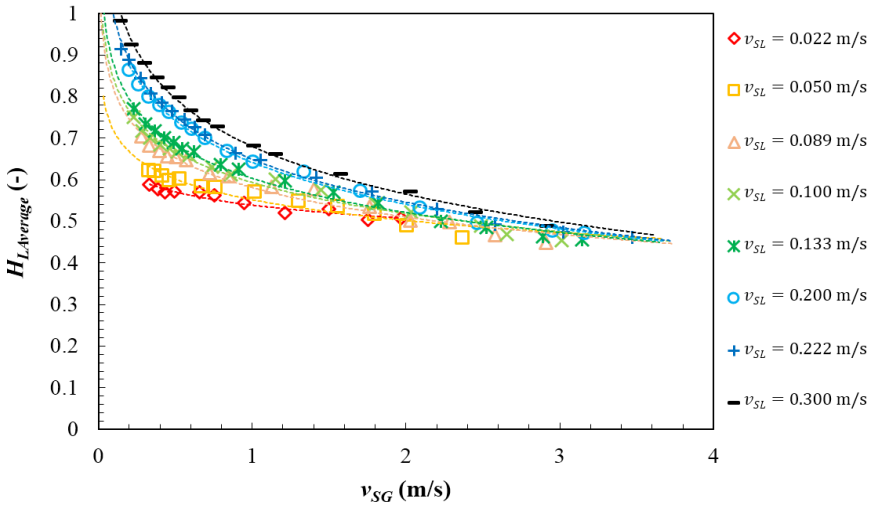

Figure B.35 Average liquid holdup vs. superficial gas velocity μ_{Oil} = 587 cP.

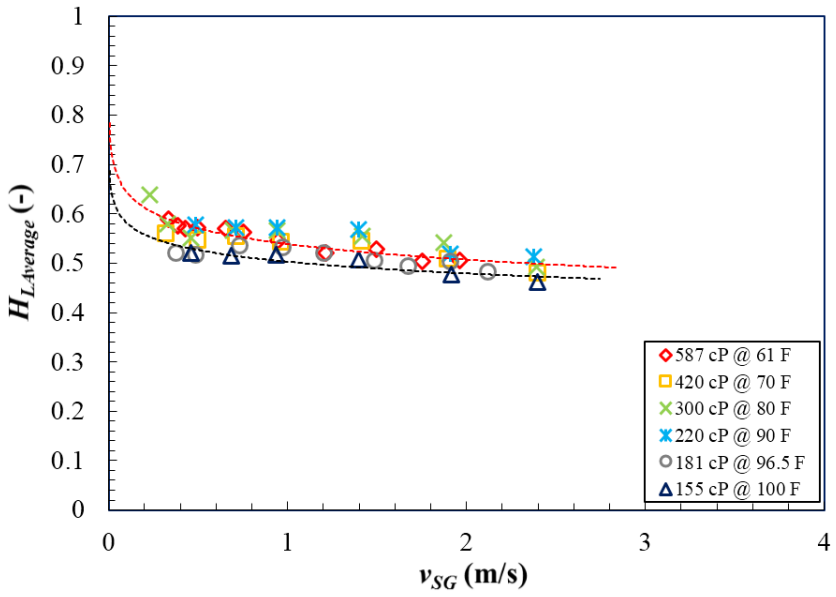

Figure B.36 Average liquid holdup comparison for v_{SL}=0.022 m/s.

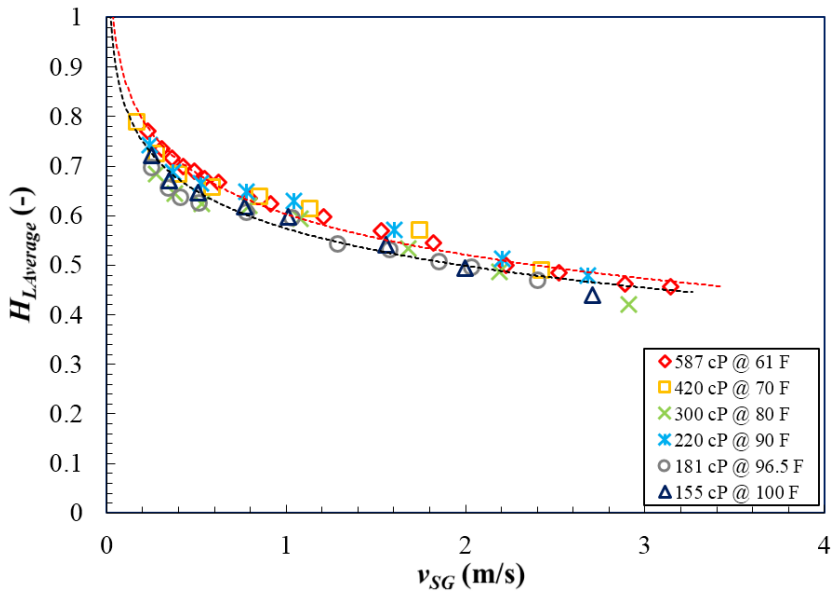

Figure B.37 Average liquid holdup comparison for v_{SL}=0.133 m/s.

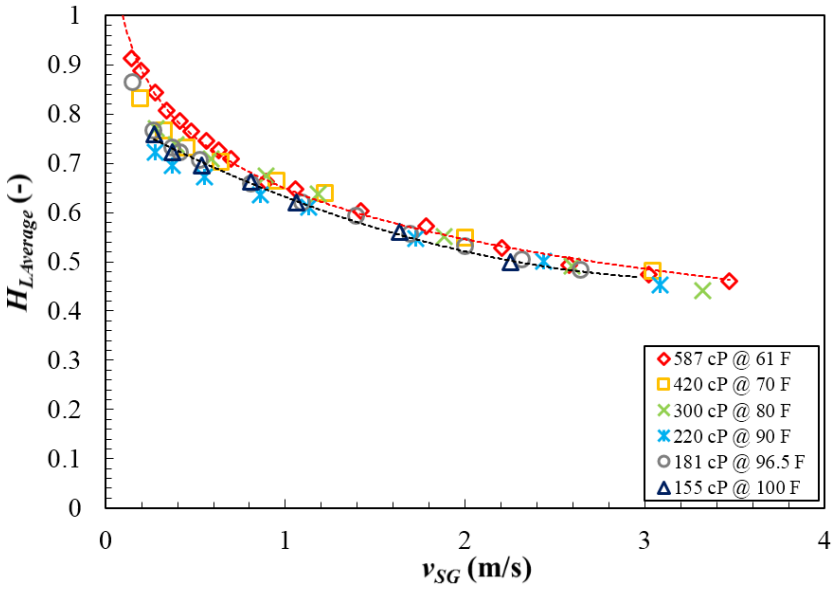

Figure B.38 Average liquid holdup comparison for v_{SL}=0.222 m/s.

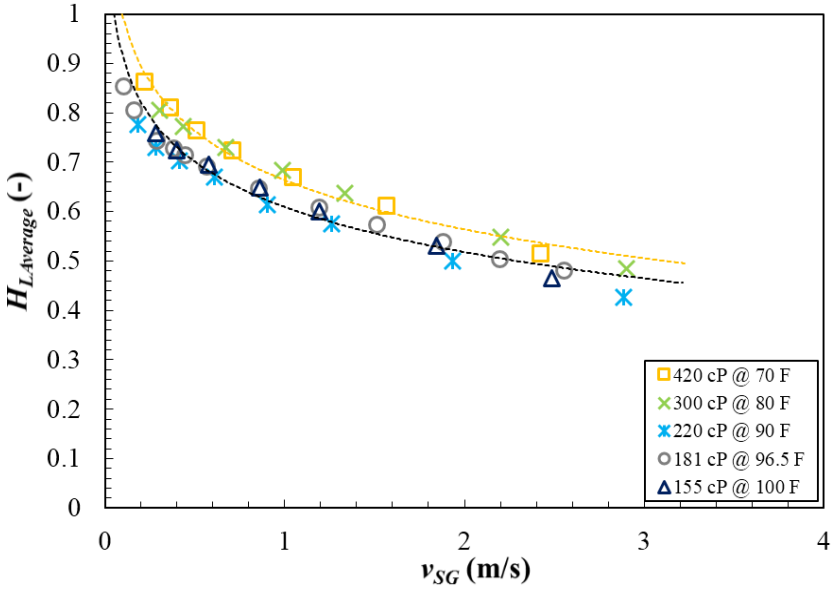

Figure B.39 Average liquid holdup comparison for v_{SL}=0.356 m/s.

Figure B.40 presents a comparison of the average liquid holdup vs. superficial gas velocity. Figure B.41 illustrates a comparison of the average liquid holdup against v_{SG}/v_m. Using v_{SG}/v_m instead of v_m is more efficient to emphasize superficial gas velocity influence because superficial gas velocity values are much higher than superficial liquid velocities in most cases. As can be seen, the average liquid holdup increases when oil viscosity increases. These trends are the same as Nädler & Mewes (1995) and Gokcal's (2005 and 2008) experimental results. Furthermore, in Brito (2012), when oil viscosities are varied from 1 cP to 587 cP, the trend is similar to this experimental study.

Figure B.42 shows a comparison of the average liquid holdup against v_{SL}/v_m, namely, no-slip liquid holdup. As no-slip liquid holdup increases, the average liquid holdups become closer to the inlet liquid fraction, indicating that the slippages between the phases decreases. This means that, for high no-slip liquid holdup, namely in less-slip conditions, the gas phase tends to be dragged more easily by the liquid phase especially for lower oil viscosity case. Consequently, the average liquid holdup becomes closer to the no-slip liquid holdup as oil viscosity decreases and the average liquid holdup difference between each oil viscosity increases as no-slip liquid holdup increases.

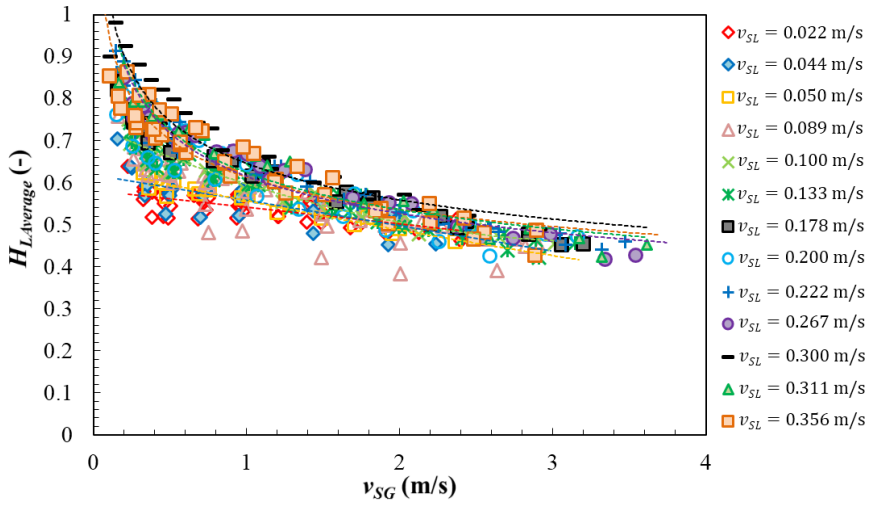

Figure B.40 Average liquid holdup vs. superficial gas velocity for all oil viscosities.

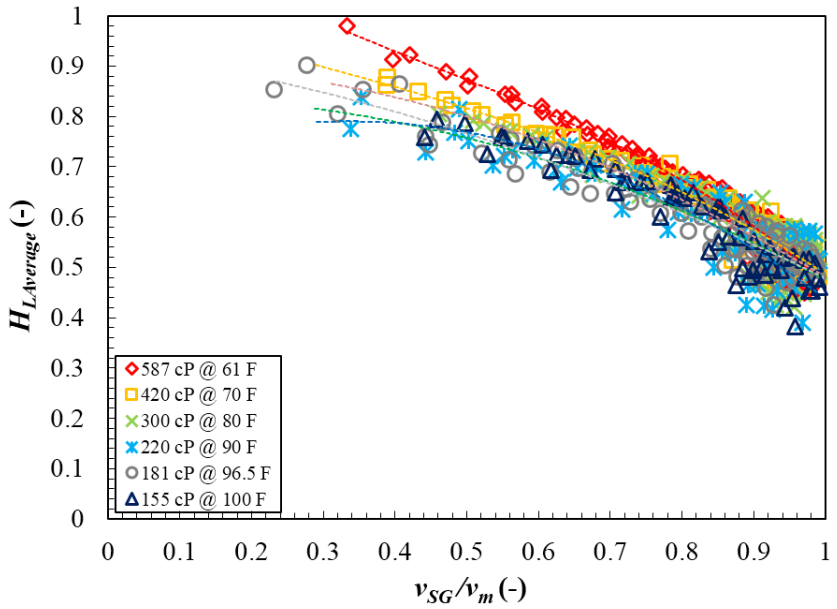

Figure B.41 Average liquid holdup vs. v_{SG}/v_m for all average liquid holdup data.

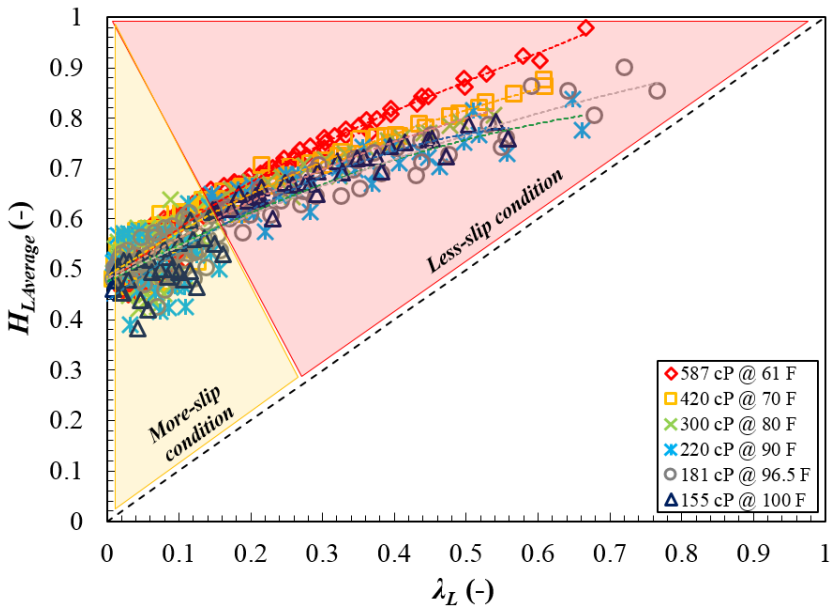

Figure B.42 Average liquid holdup vs. no-slip liquid holdup($\lambda_L=v_{SL}/v_m$) for all average liquid holdup data.

B.3.4 Slug flow characterizations

This section presents the slug characteristics. Following subsections are slug and film liquid holdup, translational velocity, slug length, slug length distribution, and slug frequency. From 628 entire experimental data acquired in this study, 489 data points located in slug flow regime are used to investigate slug characteristics.

B.3.4.1 Slug liquid holdup

From the capacitance sensor measurements, slug and film region were

distinguished using a modified VBA Excel Macro program which was initially made by Brito (2012). This program distinguishes slug and film region with good accuracy, but it is not easy to average dimensionless voltage values due to the severe fluctuation in relatively high oil viscosity tests.

Figure B.43 shows a comparison of the capacitance sensor's voltage value vs. time for superficial liquid velocity of 0.089 m/s and superficial gas velocity of 0.3 m/s when oil viscosities are 181 cP, 220 cP, 420 cP, and 587 cP. As can be seen, the degree of fluctuation increases when oil viscosity increases. Therefore, the uncertainty values of slug characteristics in higher oil viscosity tests are larger than lower oil viscosity tests. Appendix A gives more details of the uncertainty values for slug liquid holdups.

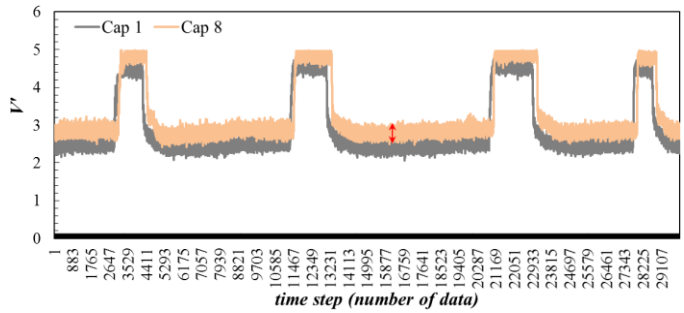

(a) Oil viscosity is 181 cP

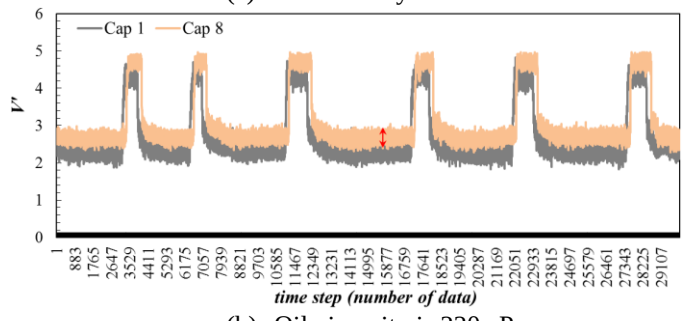

(b) Oil viscosity is 220 cP

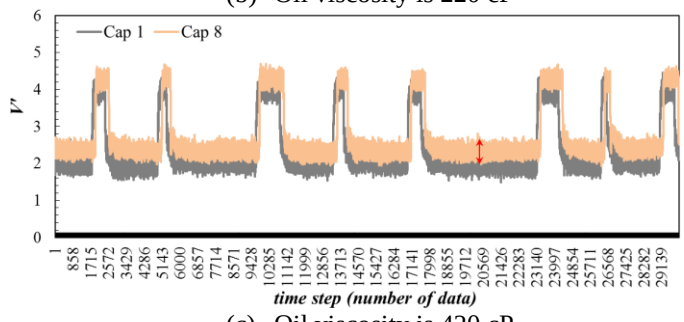

(c) Oil viscosity is 420 cP

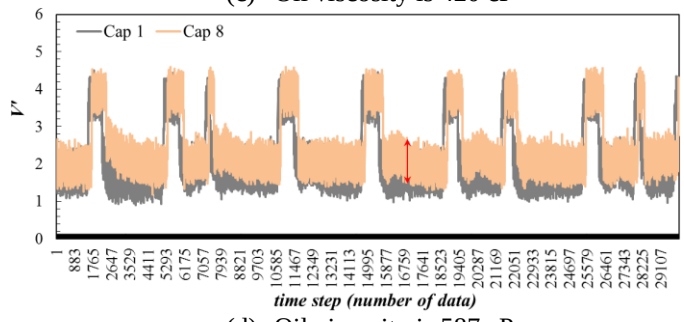

(d) Oil viscosity is 587 cP

Figure B.43 Capacitance sensor's voltage vs. time when v_{SL}=0.089 m/s and v_{SG}=0.3 m/s for μ_{Oil}=(a) 181 cP, (b) 220 cP, (c) 420 cP and (d) 587 cP.

Figures B.44 to B.48 present measured slug liquid holdup vs. superficial gas velocity for different oil viscosities (155 cP, 181 cP, 300 cP, 420 cP and 587 cP). Slug liquid holdup slightly increases with an increase of superficial liquid velocity similar with average and film liquid holdup results. This the opposite result of Kora's (2010) study, which reported that a slight decrease in slug liquid holdup was observed with superficial liquid velocity increase because of the high gas bubble entrainment rate at slug front for higher superficial liquid velocities. On the other hand, the observation of this study is in agreement with Brito (2012), who studied viscosities from 39 cP to 166 cP, and Nuland (1999), who used viscosities from 50 cP to 400 cP. As superficial gas velocity increases, slug liquid holdup decreases for every oil viscosity cases. Although Kouba (1986), Nuland (1999) and Brito (2012) reported that significant data scattering occurred at higher mixture velocities (v_m > 4 m/s), no severe scattering was observed in this study due to the limitation of superficial gas velocity allowance.

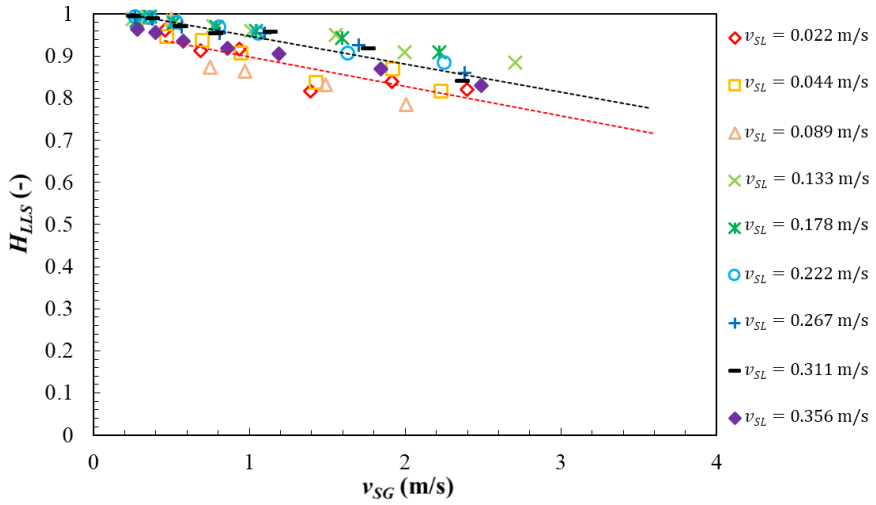

Figure B.44 Slug liquid holdup vs. superficial gas velocity for μ_{Oil}=155 cP.

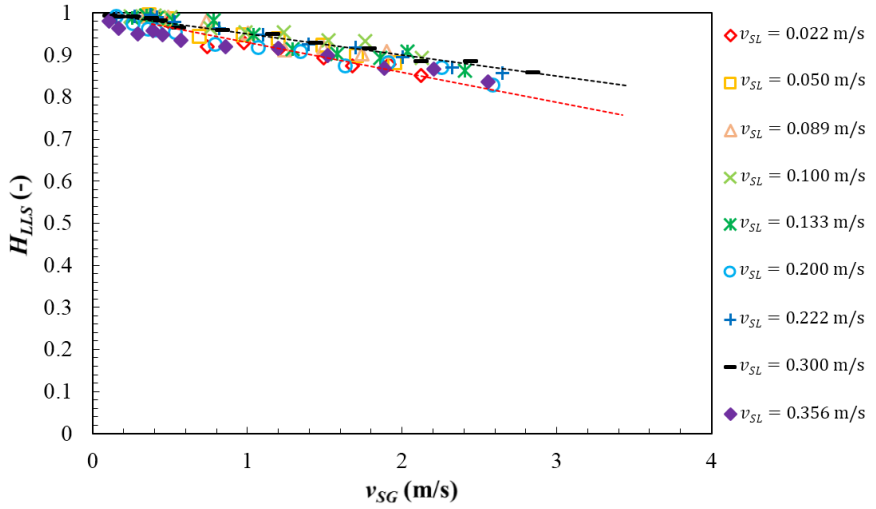

Figure B.45 Slug liquid holdup vs. superficial gas velocity for μ_{Oil}=181 cP.

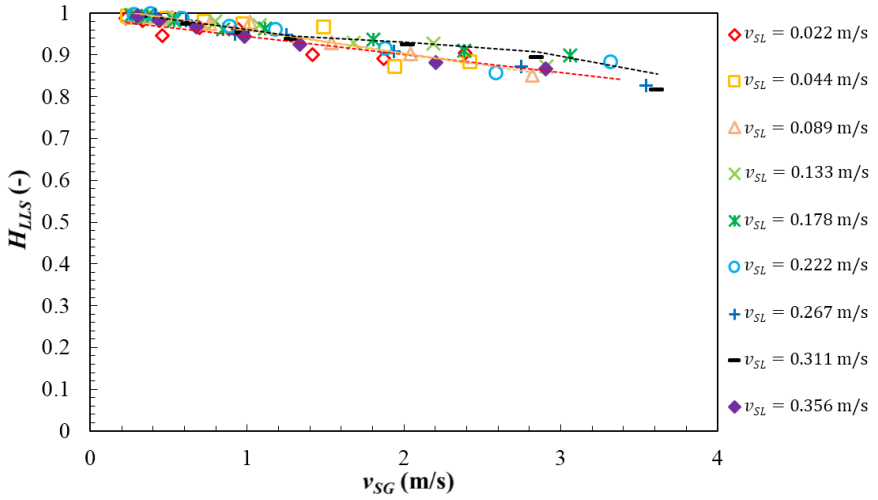

Figure B.46 Slug liquid holdup vs. superficial gas velocity for μ_{Oil}=300 cP.

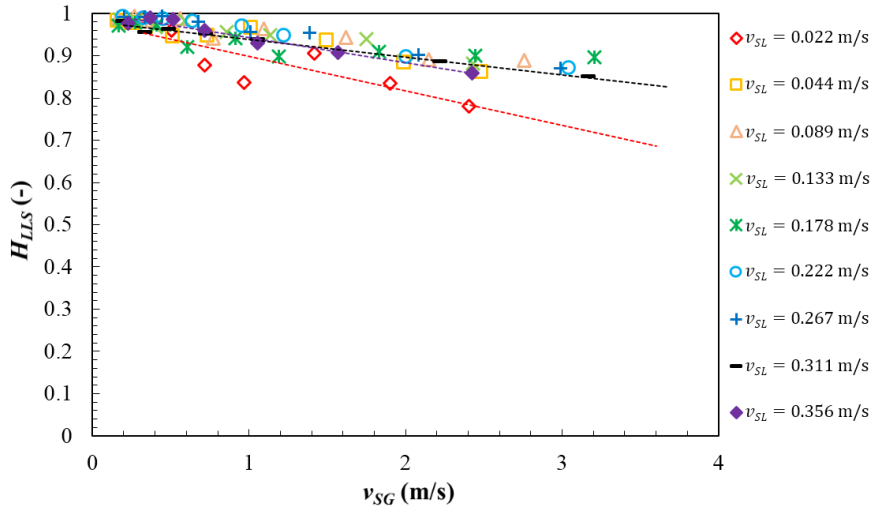

Figure B.47 Slug liquid holdup vs. superficial gas velocity for μ_{Oil}=420 cP.

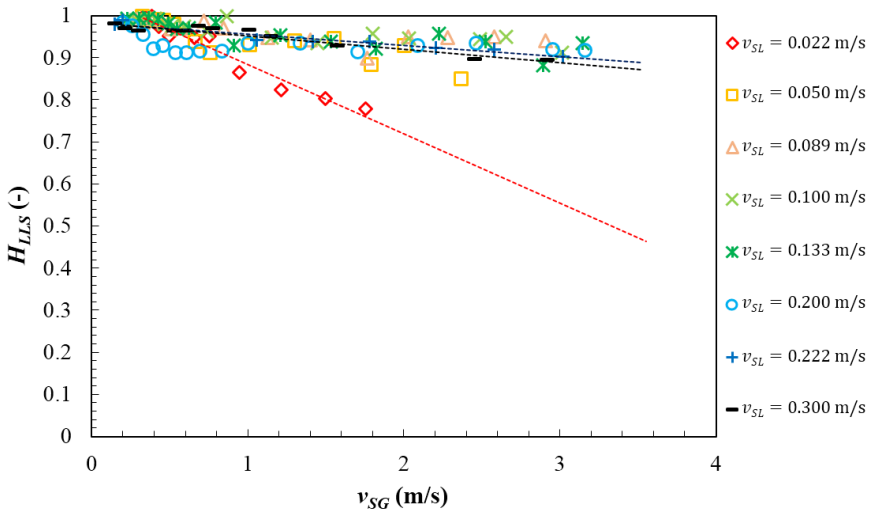

Figure B.48 Slug liquid holdup vs. superficial gas velocity for μ_{Oil}=587 cP.

Additionally, Figures B.49 to B.52 show measured slug liquid holdup against superficial gas velocity for constant superficial liquid velocities of 0.022 m/s, 0.133 m/s, 0.222 m/s and 0.356 m/s. Slug liquid holdup has no significant change with oil viscosity increase when superficial liquid velocity is higher than 1.0 m/s. This result agrees with Kora's (2010) experimental data, which showed that viscosity change did not affect much on slug liquid holdup within the oil viscosity range of 587 cP to 181 cP. However, Kora (2010) reported that slightly high slug liquid holdups appeared at high mixture velocities for the lowest oil viscosity, 181 cP, and it was caused by small bubble entrainment decrease as oil viscosity decreases. Slug liquid holdups obtained by Brito (2012) had a similar trend as Kora's (2010) for lower oil viscosities (39 – 166 cP). Brito (2012) reported that the slug liquid holdup reduction owing to liquid viscosity increase can be explained with following reasons.

1. When oil viscosity increased from 39 cP to 166 cP, the number of bubbles in the slug front increased. The higher viscosity is, the more gas was entrained in the slug front.
2. When the oil viscosity increased from 39 cP to 166 cP, the number of bubbles in the film region increased due to difficulty of gas separation.
3. Less gas was introduced back to the gas pocket downstream of the slug body. Perhaps, the drag of the liquid over the gas phase increased as oil viscosity increased. Thus, it was expected that the amount of gas head back reduced when oil viscosity increased.

Additionally, Brito (2012) explained that the reason of this phenomenon was different size and number of eddies in slug front, dividing the range of superficial liquid and gas velocity.

In this study, both Kora's (2010) and Brito's (2012) experimental opinions are able to be applied to explain grounds of the results.

1. At a relatively low superficial liquid velocity (v_{SL} < 0.1 m/s), the size of bubbles in the slug front can have an effect on slug liquid holdup when oil viscosities are regarded as medium viscosities (39 - 181 cP). As a result, slug liquid holdup decreases with oil viscosity increase.
2. On the other hand, for higher oil viscosities, the effect of the bubble amount decreases and liquid rate influence becomes more dominant.
3. When superficial gas velocities are lower than 0.5 m/s, there is no variation of slug liquid holdups for all cases.

As a result, the highest slug liquid holdups are acquired at the lowest oil viscosity, 181 cP, when superficial liquid velocities are lower than 0.1 m/s. In contrast, the slug liquid holdups are almost same for different oil viscosities with higher superficial liquid velocities. With increase of superficial liquid velocities, the slug liquid holdup increases slightly.

In previous study, Nädler & Mewes (1995) indicated that liquid holdup in the slug region increased when the surface tension increased. To prove this investigation, more studies are required with various oils which have higher or lower surface tension.

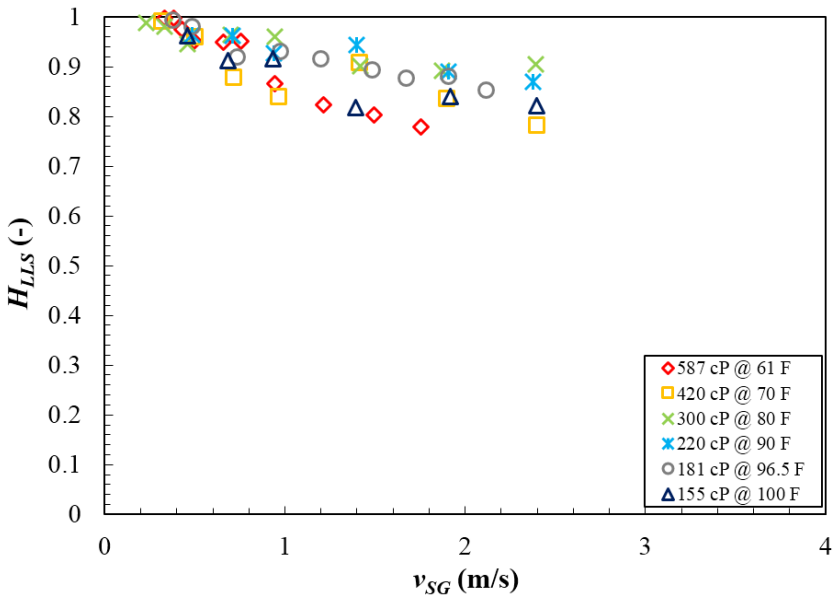

Figure B.49 Slug liquid holdup vs. superficial gas velocity for v_{SL}=0.022 m/s.

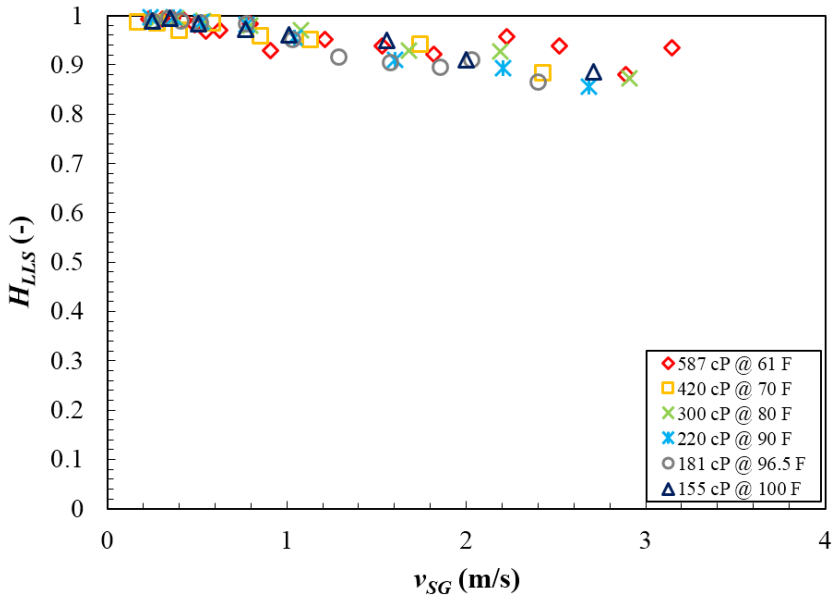

Figure B.50 Slug liquid holdup vs. superficial gas velocity for v_{SL}=0.133 m/s.

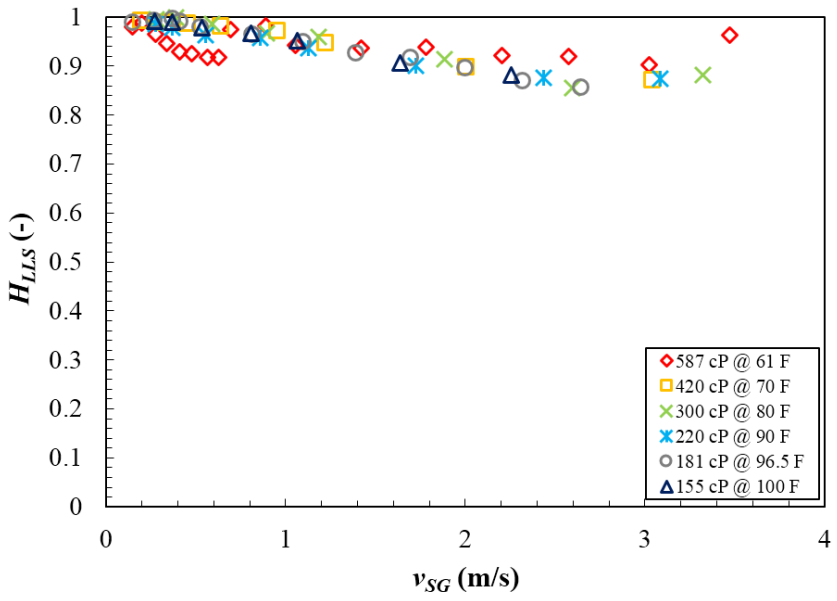

Figure B.51 Slug liquid holdup vs. superficial gas velocity for v_{SL}=0.222 m/s.

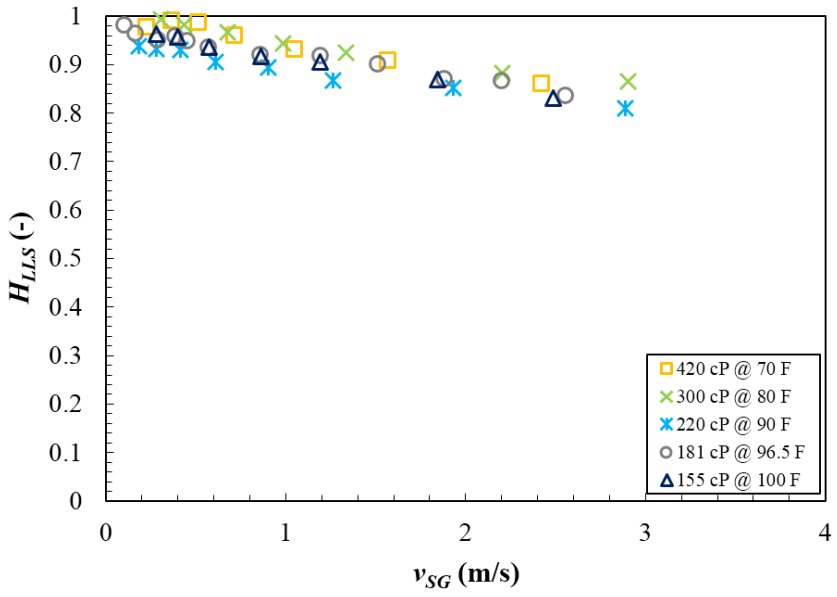

Figure B.52 Slug liquid holdup vs. superficial gas velocity for v_{SL}=0.356 m/s.

Figure B.53 shows a comparison of slug liquid holdup against mixture velocity for all oil viscosities. Figure B.54 presents slug liquid holdup vs. v_{SG}/v_m using all of the data, which is better to show the entire trend. As can be seen, there is no extreme variation of slug liquid holdups for different oil viscosities. The slug liquid holdup decreases as superficial gas velocity increases.

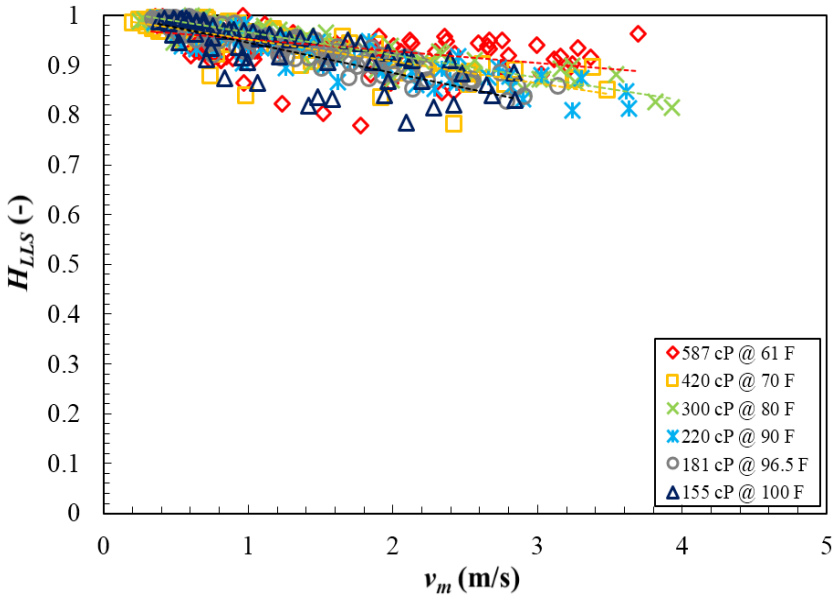

Figure B.53 Slug liquid holdup vs. mixture velocity for all oil viscosities.

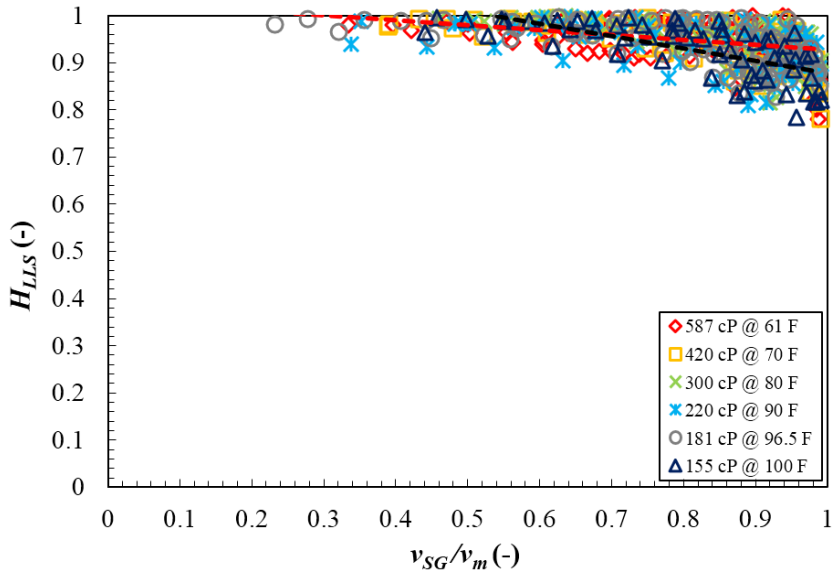

Figure B.54 Slug liquid holdup vs. v_{SG}/v_m for all oil viscosities.

B.3.4.2 Film liquid holdup

The results of the measured film liquid holdup are presented in Figures B.55 to B.60 at 155 cP, 181 cP, 220 cP, 300 cP, 420 cP and 587 cP oil viscosities, respectively. Superficial liquid and gas velocities were varied from 0.022 to 0.356 m/s and 0.1 to 3.6 m/s, respectively. As can be seen, the film liquid holdup decreases as superficial gas velocity increases. With increase of superficial gas velocity, the film liquid holdup decreases owing to the increase in the interfacial shear stress. This trend is same as the experimental data reported by Brito (2012) who stated that liquid film velocity increases as interfacial shear stress increases, requiring less area of the pipe to transport the same amount of liquid.

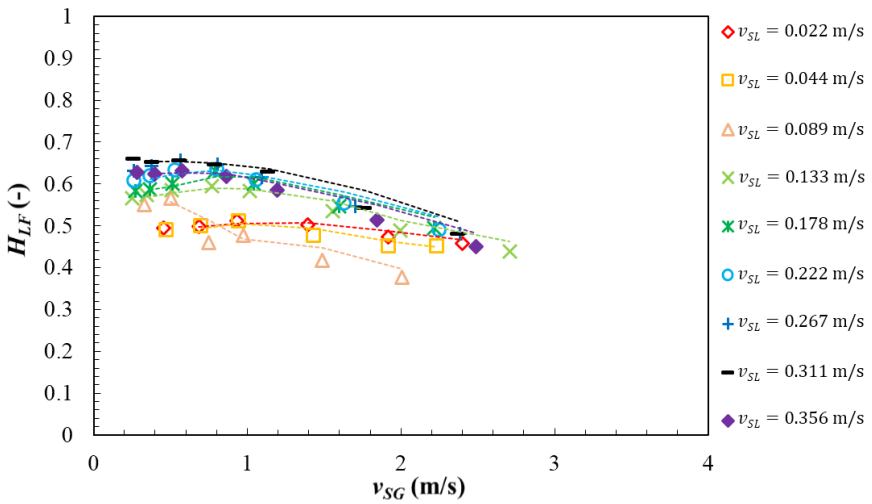

Figure B.55 Film liquid holdup vs. superficial gas velocity for μ_{Oil}=155 cP.

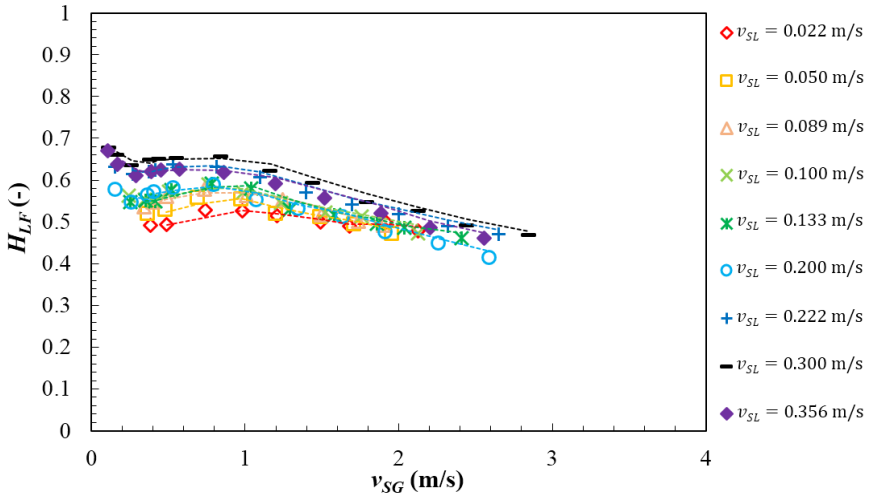

Figure B.56 Film liquid holdup vs. superficial gas velocity for μ_{Oil}=181 cP.

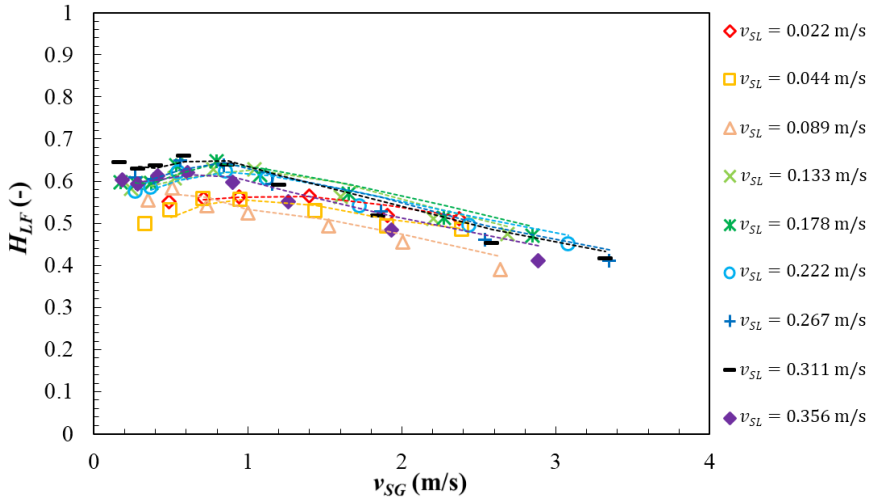

Figure B.57 Film liquid holdup vs. superficial gas velocity for μ_{Oil}=220 cP.

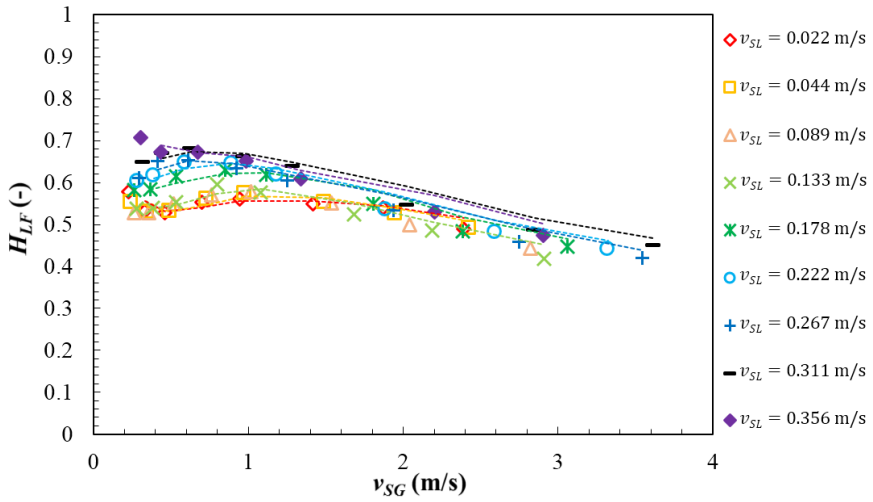

Figure B.58 Film liquid holdup vs. superficial gas velocity for μ_{Oil}=300 cP.

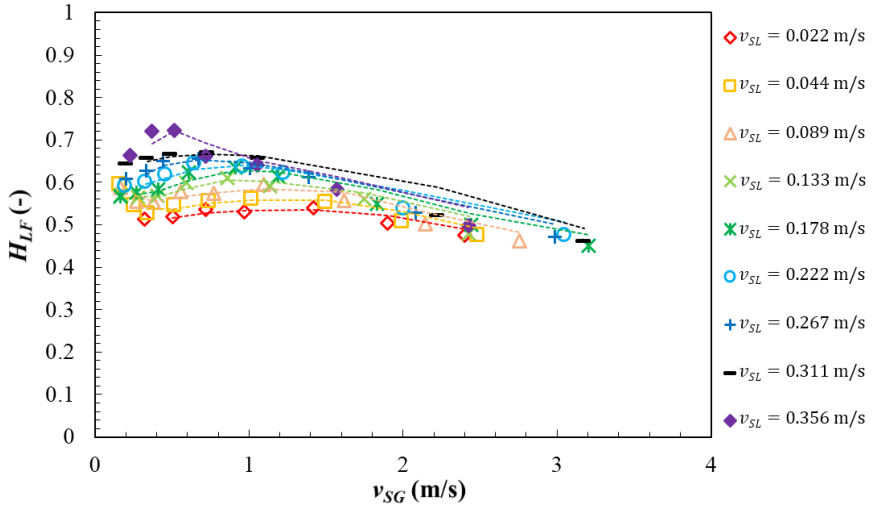

Figure B.59 Film liquid holdup vs. superficial gas velocity for μ_{Oil}=420 cP.

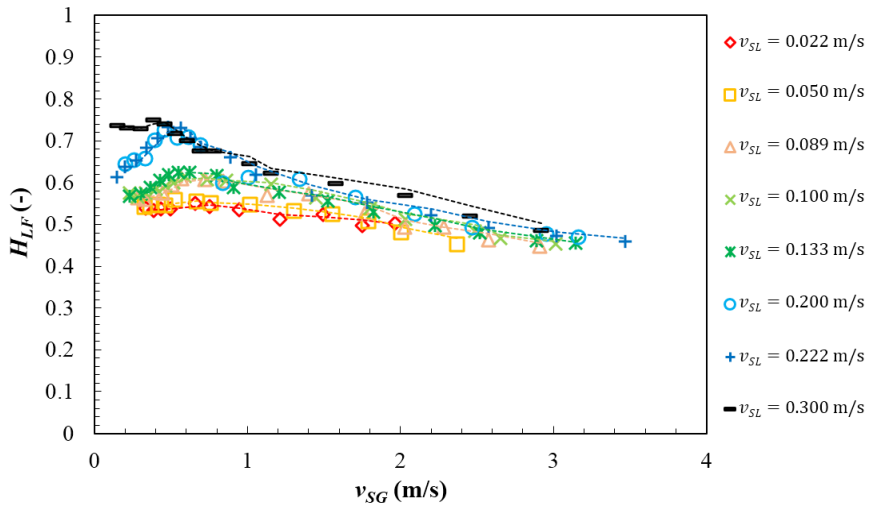

Figure B.60 Film liquid holdup vs. superficial gas velocity for μ_{Oil}=587 cP.

Figures B.61 to B.64 show the film liquid holdup against superficial gas velocity for various superficial liquid velocities and all oil viscosities. As can be seen, there is no significant increase of the film liquid holdup with oil viscosity increase. Nevertheless, a slight increase of the film liquid holdup is observed with increasing oil viscosity when superficial liquid velocities are higher than 1 m/s and superficial gas velocities are less than 1 m/s. Otherwise, Kora (2010) observed that, as liquid viscosity decreased, liquid film height slightly increased due to higher drainage rate of top oil film. In contrast with Kora's (2010) experimental results, Brito (2012) investigated that film liquid holdups for medium viscous oil were always higher than film liquid holdups for water-air flow, however, the film liquid holdups for liquid viscosities from 7 cP to 166 cP had no significant changes. Thus, it can be concluded that the impact of superficial liquid velocity on the film liquid holdup is greater than oil viscosity.

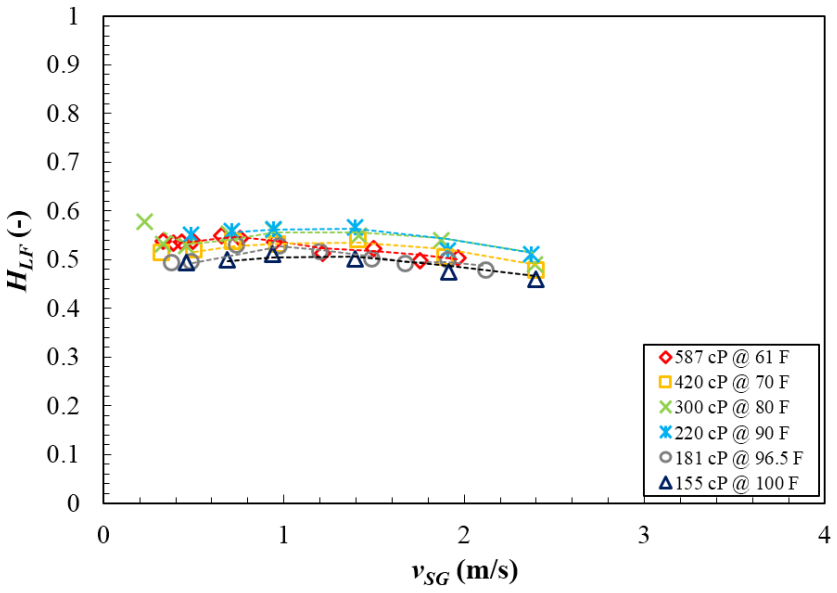

Figure B.61 Film liquid holdup vs. superficial gas velocity for v_{SL}=0.022 m/s.

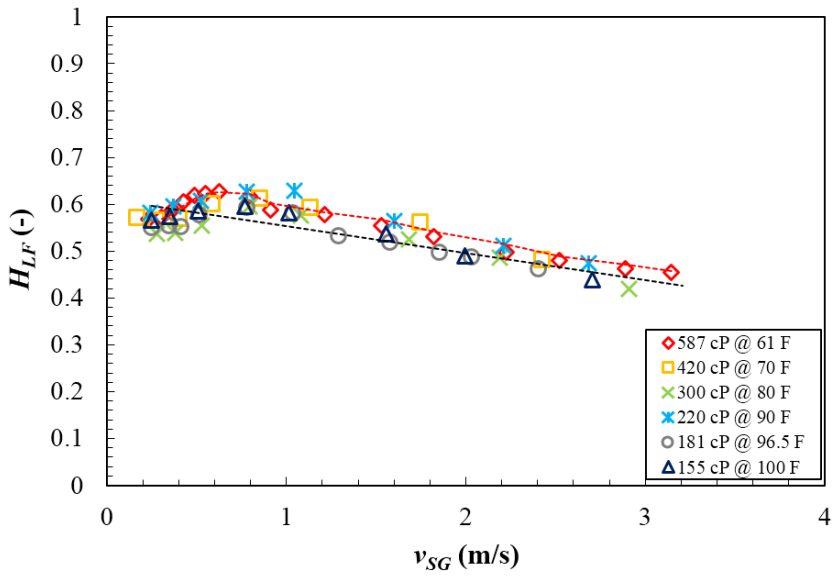

Figure B.62 Film liquid holdup vs. superficial gas velocity for v_{SL}=0.133 m/s.

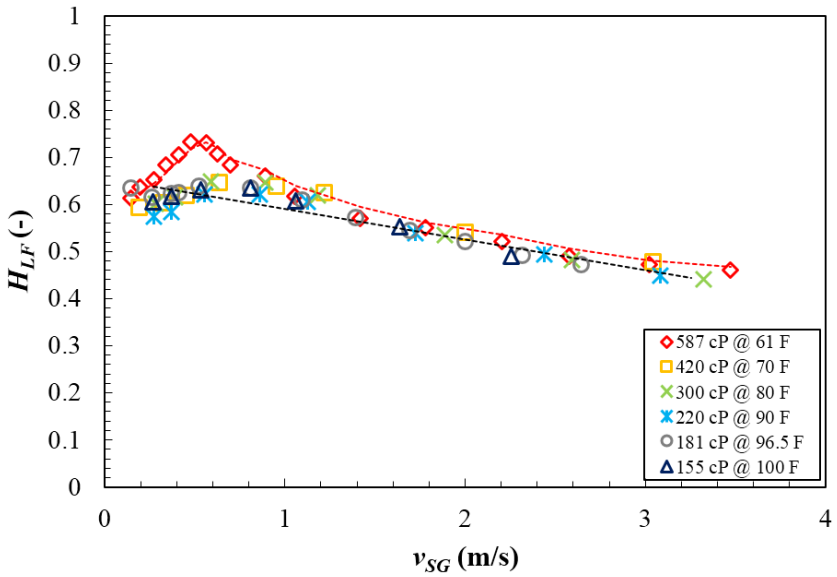

Figure B.63 Film liquid holdup vs. superficial gas velocity for v_{SL}=0.222 m/s.

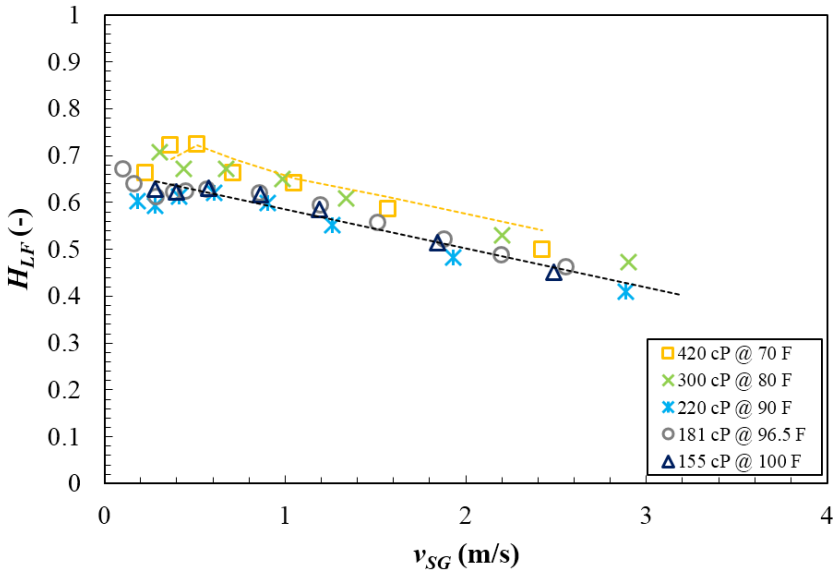

Figure B.64 Film liquid holdup vs. superficial gas velocity for v_{SL}=0.356 m/s.

Figure B.65 illustrates a comparison of film liquid holdup to mixture velocity for all obtained data. When mixture velocities are less than 1 m/s, the film liquid holdup increases as oil viscosity increases. Above the 1.5 m/s of mixture velocity, the film liquid holdups of all oil viscosities are almost same.

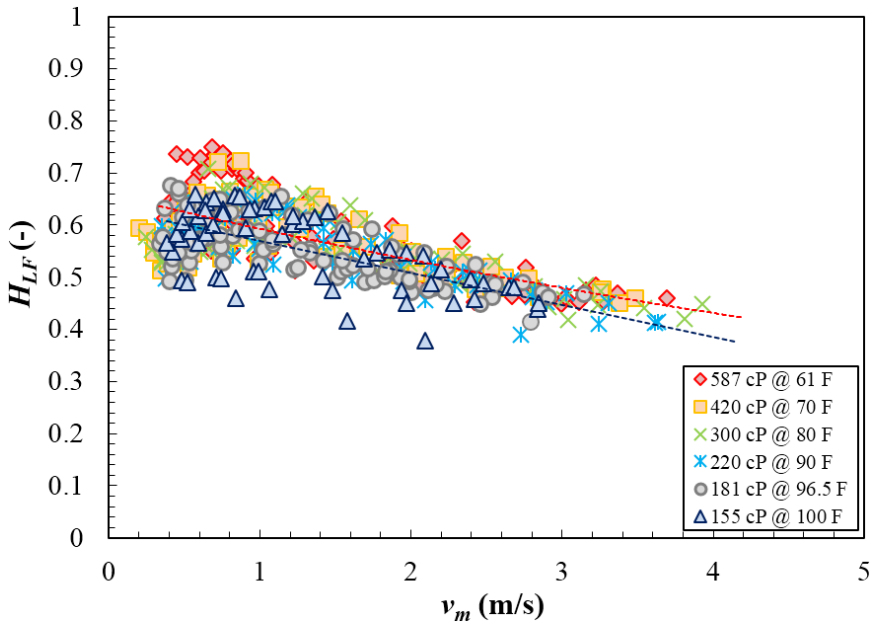

Figure B.65 Film liquid holdup vs. mixture velocity for all oil viscosities.

B.3.4.3 Translational velocity

Cross correlation of time traces from the two capacitance sensors was used to determine the slug translational velocity. Time delay between consecutive slug front (Δt_{cr}) and the distance between two different capacitance sensors were used to calculate translational velocity.

Figure B.66 shows translational velocity vs. mixture velocity for all oil viscosities of 155 cP, 181 cP, 220 cP, 300 cP, 420 cP, and 587 cP. Additionally, Figure B.67 presents translational velocity against mixture velocity including Brito's (2012) medium oil viscosity experimental data. As expected, translational velocity increases with mixture velocity increase and similar trend was reported by Gokcal (2008) and Brito (2012).

Figure B.68 illustrates translational velocity against mixture Reynolds number for all different oil viscosities. As can be seen in Eq. (117), since the only different term in this formulation is oil viscosity at given superficial gas and liquid velocities, the effect of the oil viscosity can be visualized. Figure B.69 presents similar plot as Figure B.68 including Brito's (2012) medium oil viscosity experimental data. This study covered a smaller range of Re_{Mix} than Brito's (2012) due to high oil viscosity.

$$\mathrm{Re}_{Mix} = \frac{\rho_{Oil} v_m D}{\mu_{Oil}} \tag{117}$$

Above some points of mixture velocities, the degree of scattering is high due to increase amount of gas passing through the top of the slug region. In this sections, top portion of the slug region is hard to reach the top of pipe.

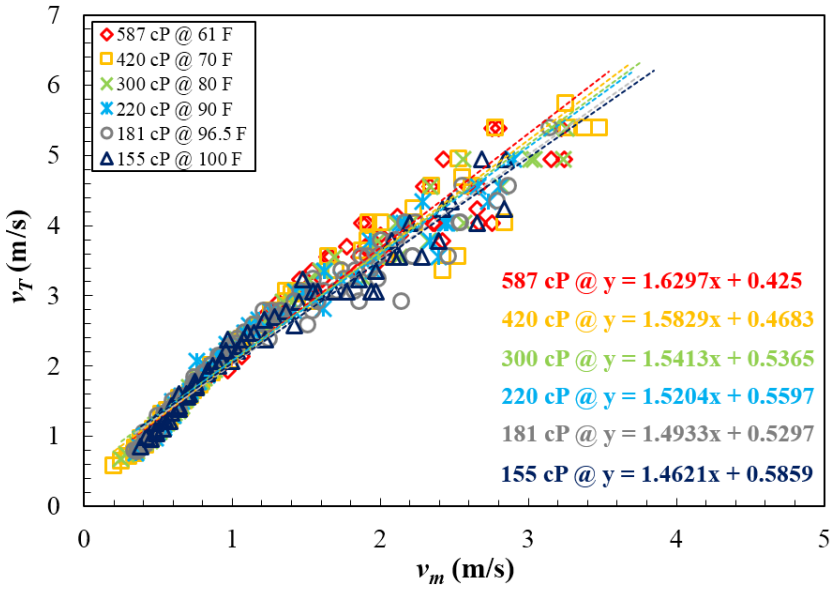

Figure B.66 Translational velocity vs. mixture velocity for all oil viscosities.

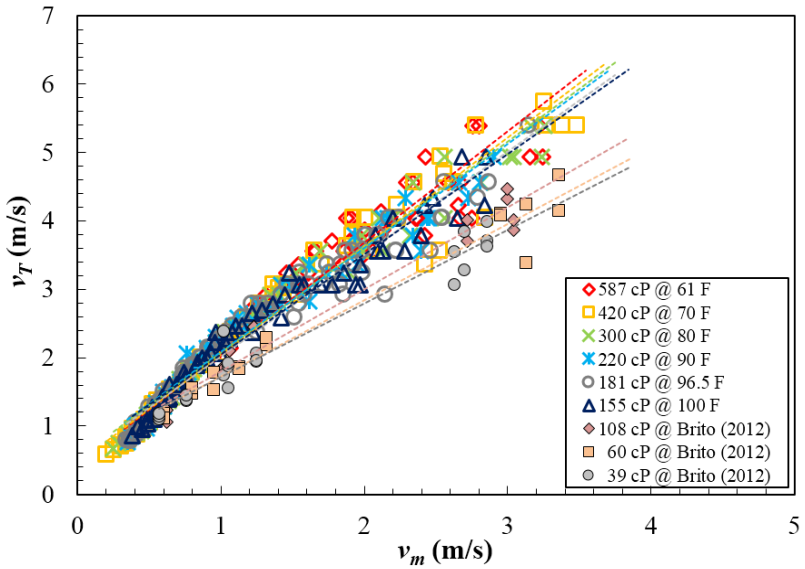

Figure B.67 Translational velocity vs. mixture velocity including Brito's (2012) experimental data.

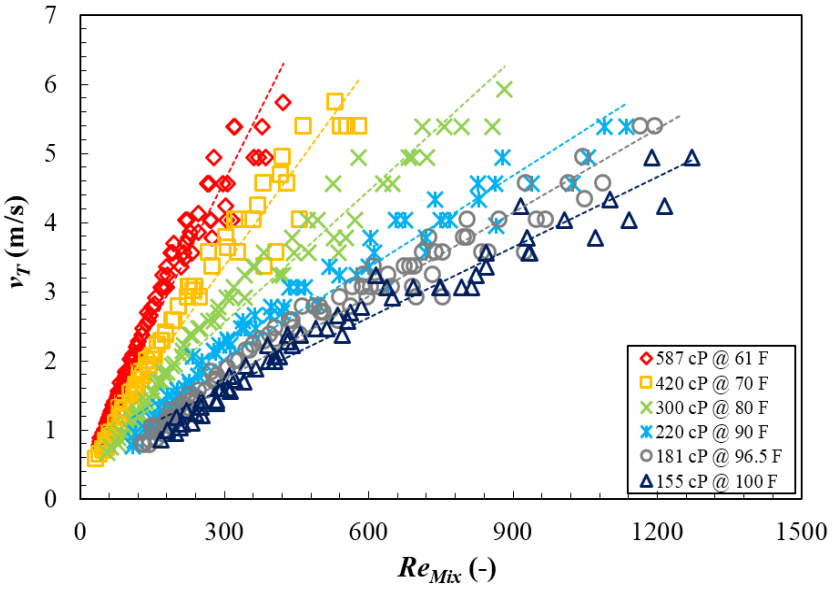

Figure B.68 Translational velocity vs. mixture Reynolds number for all oil viscosities.

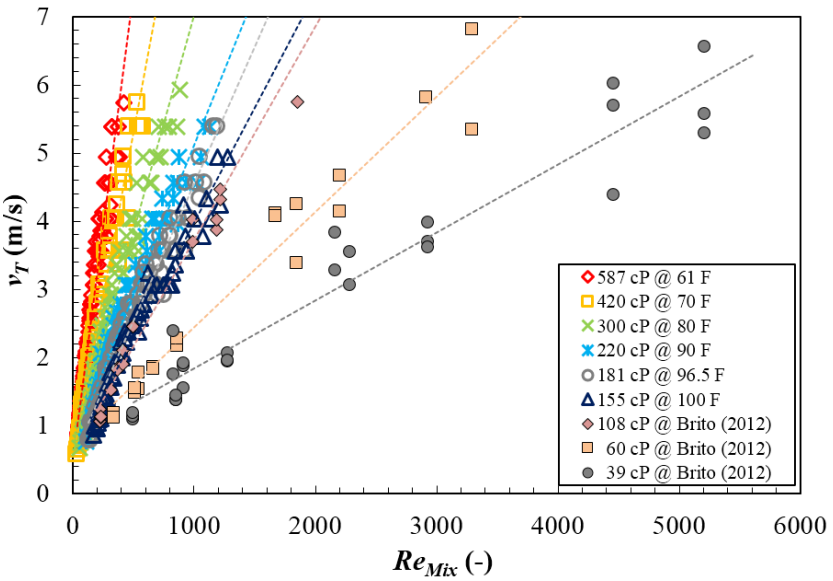

Figure B.69 Translational velocity vs. mixture Reynolds number including Brito's (2012) experimental data.

Figure B.66 illustrates the linear correlation between the mixture velocity and the measured drift velocity at different oil viscosities. By using the Eq. (118) proposed by Nicklin *et al.* (1962), initially, calculated drift velocities and C_0 coefficients were decided for different oil viscosities. From trend line in Figure B.66, it was decided that the slope of the graph (m) gave C_0 coefficients and the y intercept represented drift velocities at different oil viscosities. Figure B.70 shows obtained drift velocity values for different oil viscosities. Figures B.71 and B.72 are comparison of the C_0 coefficients against mixture Reynolds number and oil viscosity, respectively, based on linearly plotted trend line.

$$v_T = C_0 v_m + v_D \tag{118}$$

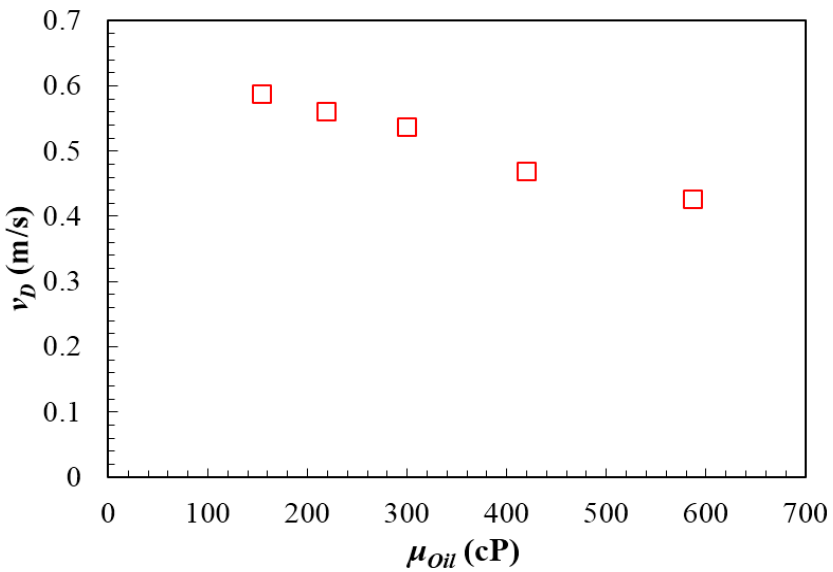

Figure B.70 Obtained drift velocity vs. oil viscosity. In this plot, drift velocities were calculated by using $v_T = C_0 v_m + v_D$ propsed by Nicklin *et al.* (1962).

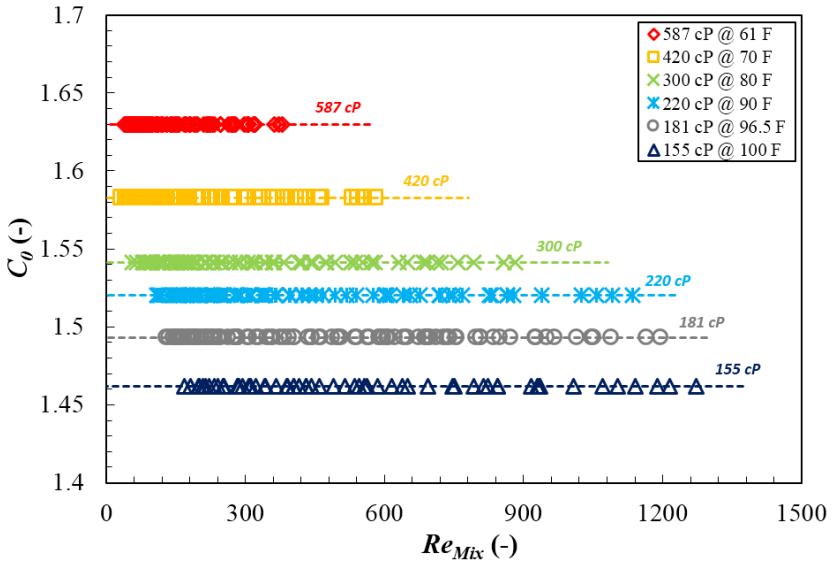

Figure B.71 Obtained C_0 coefficient vs. mixture Reynolds number. In this plot, C_0 were calculated by using $v_T = C_0 v_m + v_D$ proposed by Nicklin *et al*. (1962).

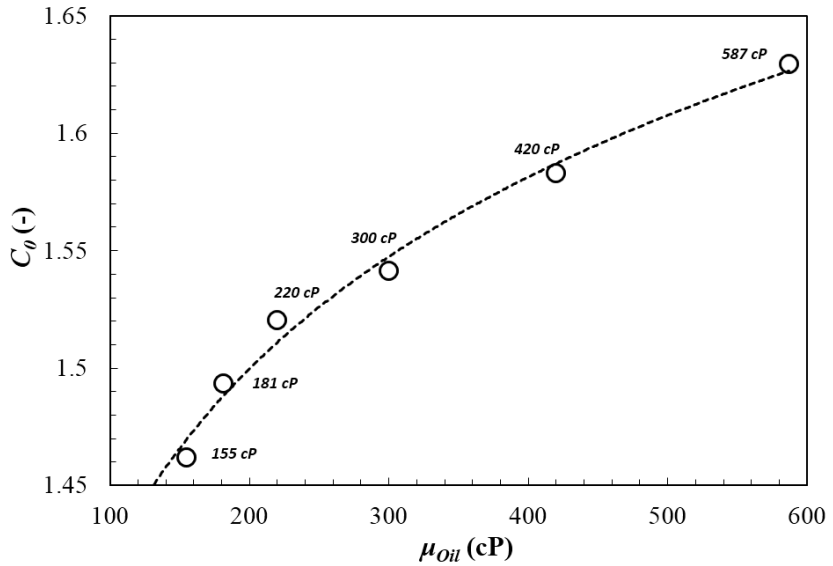

Figure B.72 Obtained C_0 coefficient vs. oil viscosity. In this plot, C_0 coefficients were calculated by using $v_T = C_0 v_m + v_D$ propsed by Nicklin *et al*. (1962).

In this study, distribution parameter, C_0, was initially not a fixed value. It varied from 1.5 to 1.65 when the oil viscosities were increased from 181 to 587 cP. Gokcal (2008) showed that the liquid viscosity increase led to an increase in drift velocity but did not have a significant effect on the flow coefficient C_0. In Gokcal's (2008) experimental study, the C_0 value was fixed as 2.0 confirming that the experiments were in the laminar flow regime, which was higher than the results of this study.

Similarly, Brito (2012) discussed that although, for the lowest viscosity (39 cP), C_0 value is near 1.2 at high mixture Reynolds number indicating that the flow regime tend to be turbulent flow, when oil viscosity increases, C_0 was near 2.0, indicating that the flow regime tended to be laminar flow for high viscosities.

Therefore, it was necessary to be investigated for other elements which can have an effect on C_0 coefficient or drift velocity. One of the recent studies, Bhagwat and Ghajar (2014) showed that new equations for distribution parameter (C_0) and drift velocity were essentially needed to be developed using the void fraction correlation. They discussed that the distribution parameter (C_0) and the drift velocity were expressed as the average of the product of void fraction.

Similarly, some of the existing drift flux model are based on specific correlations using some variables such as void fraction, flow quality (x), pipe diameter, liquid density, mixture mass flux, and mixture Reynolds number. Some recommended correlations are summarized in Table B.2. It is concluded that, for different pipe diameter, more constituents have to be considered. Among the existing models, Choi *et al*. (2012) model gives the lowest absolute

average relative error. Thus, C_0 coefficient values need to be recalculated by using Eqs (119) and (120) proposed by Choi *et al*. (2012).

$$C_0 = \frac{2}{1+(\mathrm{Re}_{tp}/1000)^2} + \frac{1.2 - 0.2\sqrt{\frac{\rho_G}{\rho_L}}(1-e^{(-18\alpha)})}{1+(1000/\mathrm{Re}_{tp})^2} \tag{119}$$

$$v_D = 0.0246\cos\theta + 1.606(g\sigma\Delta\rho/\rho_L{}^2)^{0.25}\sin\theta \tag{120}$$

where Re_{tp} is two-phase mixture Reynolds number, ρ_g is gas density in kg/m^3, ρ_L is liquid density in kg/m^3, g is gravity acceleration in m/s^2, v_D is drift velocity in m/s and σ is surface tension in N/m.

Figures B.73 and B.74 show re-calculated C_0 coefficient vs. oil viscosity and mixture Reynolds number, respectively. As can be seen, C_0 coefficient increases from 1.8 to 2.0 with oil viscosity increase and reaches 2.0 at highest oil viscosity (587 cP). Additionally, there is no change of C_0 coefficient between different oil viscosities with variation of mixture Reynolds number. Translational velocity model comparison including other existing models are treated in the section 5.4.3.

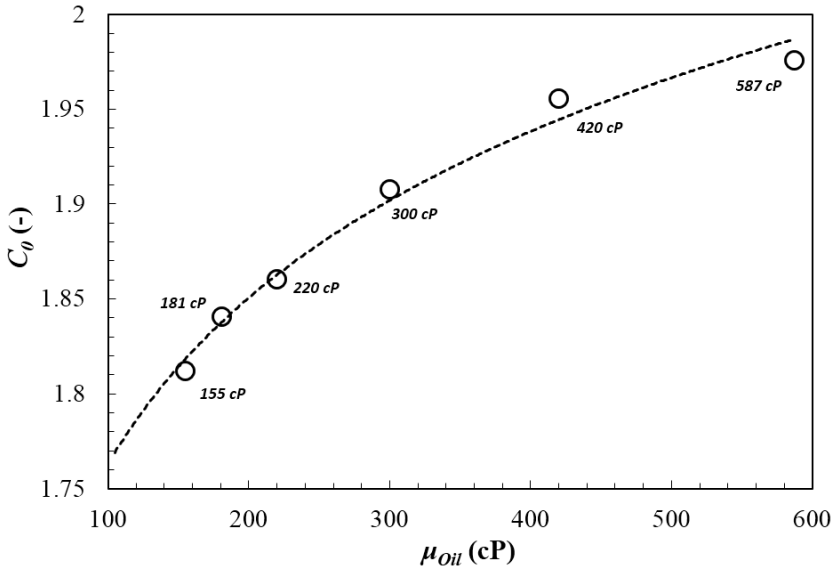

Figure B.73 Recalculated C_0 coefficient vs. oil viscosity. In this plot, C_0 coefficients were calculated by using Eq. (119) proposed by Choi *et al*. (2012).

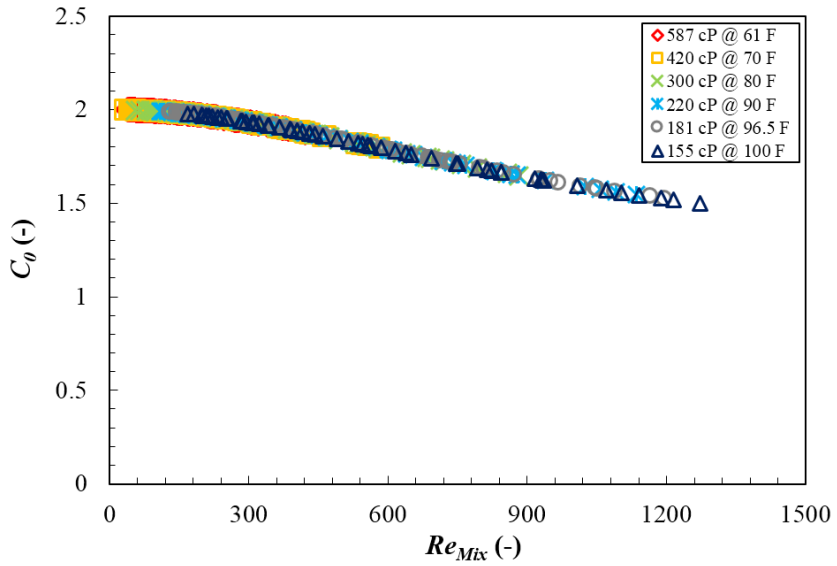

Figure B.74 Recalculated C_0 coefficient vs. mixture Reynolds number. In this plot, C_0 coefficients were calculated by using Eq. (119) proposed by Choi *et al*. (2012).

Table B.2 The existing drift flux models considering void fraction correlations (Bhagwat & Ghajar, 2014).

Correlation	Distribution parameter	Drift velocity (m/s)
Rouhanni and Axelsson (1970)	$C_0 = 1+0.2(1-x)(gD\rho_G{}^2/G^2)^{0.25}$ (*for* $\alpha \le 0.1$) $C_0 = 1+0.2(1-x)$ (*for* $\alpha > 0.1$) $C_0 = 1+0.12(1-x)$ (*for* $\theta = 0$)	$v_D = 1.18(g\sigma\Delta\rho/\rho_L{}^2)^{0.25}$
Bonnecaze et al. (1971)	$C_0 = 1.2$	$v_D = 0.35\sqrt{gD\Delta\rho/\rho_L}$ *where* $\Delta\rho = (\rho_L - \rho_G)$
Greskovich and Cooper (1975)	$C_0 = 1.0$	$v_D = 0.671\sqrt{gD}(\sin\theta)^{0.263}$
Sun et al. (1981)	$C_0 = (0.82+0.18(P_{sys}/P_{crit}))^{-1}$	$v_D = 1.41(g\sigma\Delta\rho/\rho_L{}^2)^{0.25}$
Shipley (1982)	$C_0 = 1.2$	$v_D = 0.24+0.35(v_{SG}/v_m)^2\sqrt{gD\alpha}$
Clark and Flemmer (1985)	$C_0 = 0.934(1+1.42\alpha)$	$v_D = 1.53(g\sigma\Delta\rho/\rho_L{}^2)^{0.25}$
Beattie and Sugawara (1985)	$C_0 = 1+2.6\sqrt{f_{tp}}$ *where* $f_{tp} = 0.0716\mathrm{Re}_{tp}{}^{-0.237}+0.008$	$v_D = 0.35\sqrt{gD\Delta\rho/\rho_L}$ *where* $\Delta\rho = (\rho_L - \rho_G)$
Kataoka and Ishii (1987)	$C_0 = 1.2-0.2\sqrt{\rho_G/\rho_L}$	$v_D = 0.03(\rho_G/\rho_L)^{-0.157}(g\sigma\Delta\rho/\rho_L{}^2)^{0.25}N_{\mu_L}{}^{-0.562}$ *for* $D_h{}^* \le 40$ $v_D = 0.92(\rho_G/\rho_L)^{-0.157}(g\sigma\Delta\rho/\rho_L{}^2)^{0.25}N_{\mu_L}{}^{-0.562}$ *for* $D_h{}^* > 40$
Mishima and Hibiki (1996)	$C_0 = 1.2+0.51\exp(-0.691(D/1000))$	$v_D = 0$
Gomez et al. (2000)	$C_0 = 1.15$	$v_D = 1.53(g\sigma\Delta\rho/\rho_L{}^2)^{0.25}\sqrt{1-\alpha}\sin\theta$
Hibiki and Ishii (2003)	$C_0 = 1.2-0.2\sqrt{\rho_G/\rho_L}(1-\exp(-18\alpha))$ (*B*) $C_0 = 1.2-0.2\sqrt{\rho_G/\rho_L}$ (*S*) $C_0 = 1+(1-\alpha)/(\alpha+4\sqrt{\rho_G/\rho_L})$ (*A*)	$v_D = 1.41(g\sigma\Delta\rho/\rho_L{}^2)^{0.25}(1-\alpha)^{1.75}$ (*B*) $v_D = 0.35\sqrt{gD\Delta\rho/\rho_L}$ (*S*) $v_D = (1-\alpha)/(\alpha+4\sqrt{\rho_G/\rho_L}(\sqrt{gD\Delta\rho}(1-\alpha))/0.015\rho_G)$ (*A*)
Woldesemayat and Ghajar (2007)	$C_0 = (v_{SG}/v_m)[1+((v_{SL}/v_{SG})^{(\rho_G/\rho_L)^{0.1}})]$	$v_D = 2.9(\frac{gD\sigma(1+\cos\theta)\Delta\rho}{\rho_G{}^2})^{0.25}(1.22+1.22\sin\theta)^{\frac{P_{atm}}{P_{sys}}}$
Choi et al. (2012)	$C_0 = \frac{2}{1+(\mathrm{Re}_{tp}/1000)^2}+\frac{1.2-0.2\sqrt{\rho_G/\rho_L}(1-e^{(-18\alpha)})}{1+(1000/\mathrm{Re}_{tp})^2}$	$v_D = 0.0246\cos\theta+1.606(g\sigma\Delta\rho/\rho_G{}^2)^{0.25}\sin\theta$

B.3.4.4 Slug length

Figures B.75 to B.79 present the average dimensionless slug length against the superficial gas velocity for constant superficial liquid velocities. The existing slug length prediction models show that the slug length is independent of superficial gas and liquid velocity. Nevertheless, as can be seen, slug length decreases with superficial gas velocity increase indicating that there might be additional variables affecting the slug length. Until v_{SG} < 0.7 m/s, slug length decreases more rapidly comparing to higher superficial gas velocity areas. This trend is similar with Brito's (2012) experimental results showing that slug length remained approximately constant for high superficial gas velocities. Jeyachandra (2011) addressed the effect of pipe inclination on flow characteristics of gas and high viscous oil two-phase flow and also investigated that the slug length decreased with increasing mixture velocity. It was observed that slug length decreased as oil viscosity increased.

The best fit corresponds to a power curve following a regression analysis and the correlation coefficient, R^2, varied from 0.7 to 0.9. The approximate minimum slug length of 4*D* are observed for all of the superficial liquid velocity (0.022 m/s, 0.089 m/s, 0.133 m/s, 0.222 m/s and 0.356 m/s). Figure B.80 shows a comparison of the average dimensionless slug length vs. superficial gas velocity using all the experimental data. Effect of oil viscosity can be visualized more clearly in this plot.

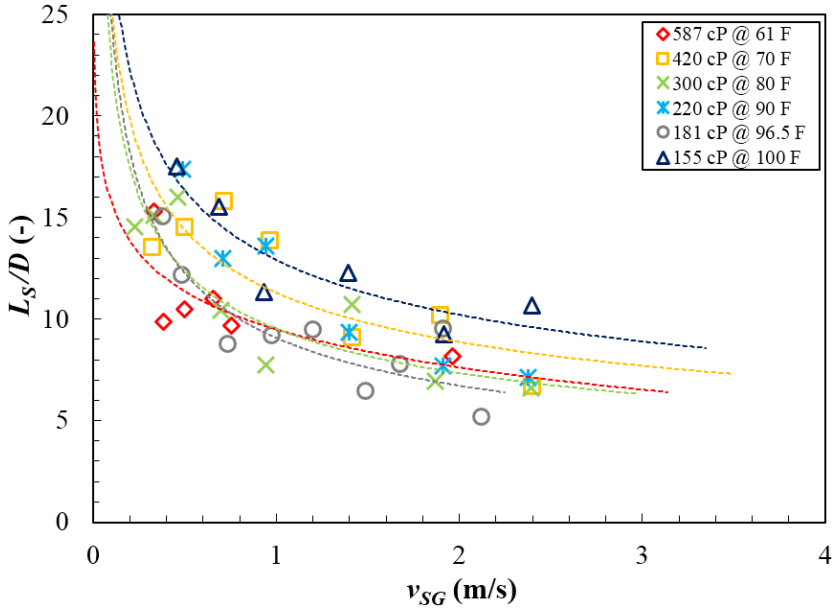

Figure B.75 Average dimensionless slug length vs. superficial gas velocity for v_{SL}=0.022 m/s.

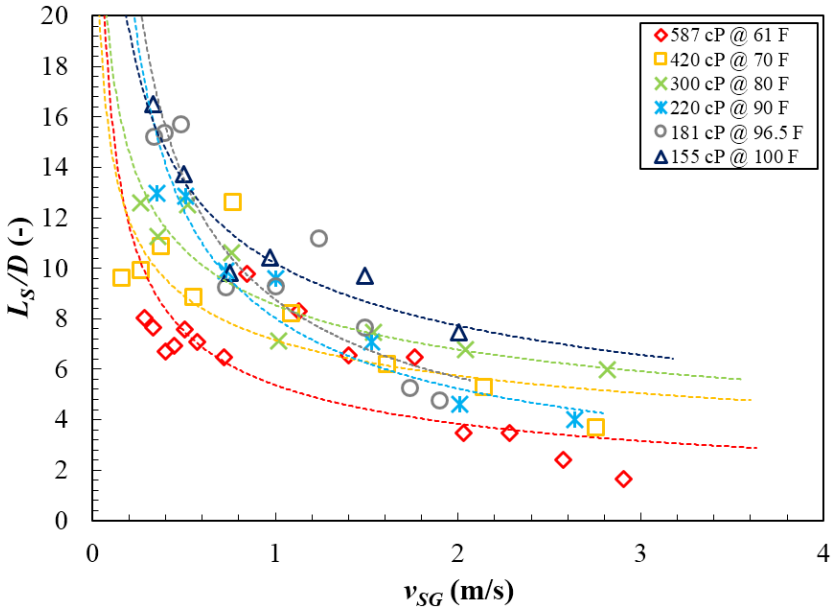

Figure B.76 Average dimensionless slug length vs. superficial gas velocity for v_{SL}=0.089 m/s.

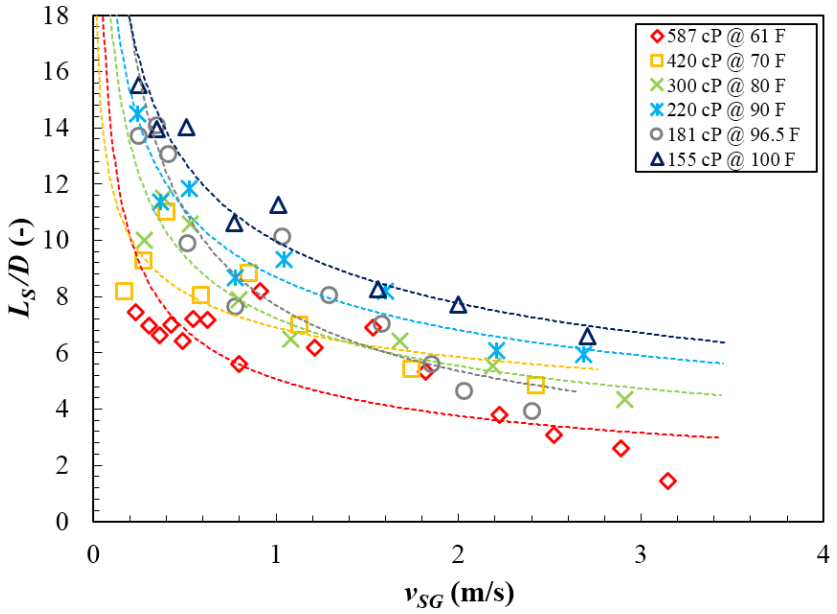

Figure B.77 Average dimensionless slug length vs. superficial gas velocity for v_{SL}=0.133 m/s.

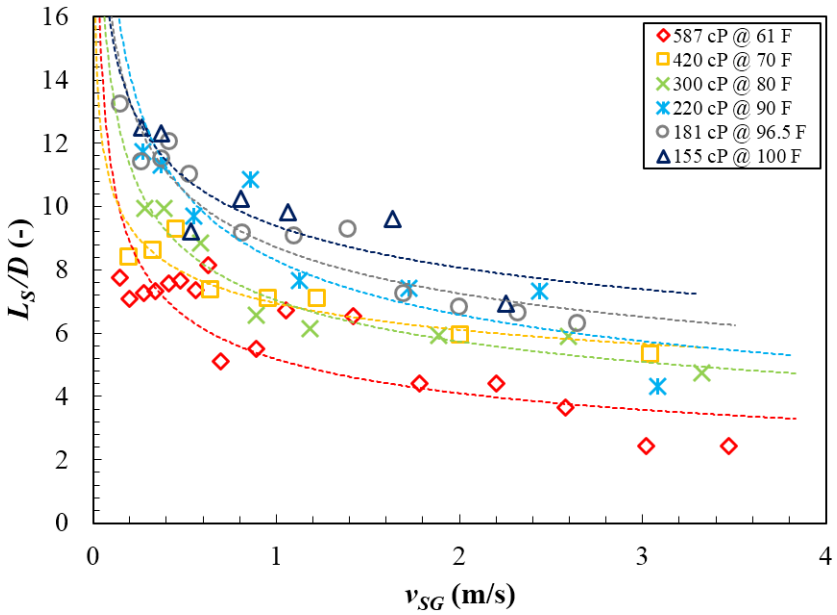

Figure B.78 Average dimensionless slug length vs. superficial gas velocity for v_{SL}=0.222 m/s.

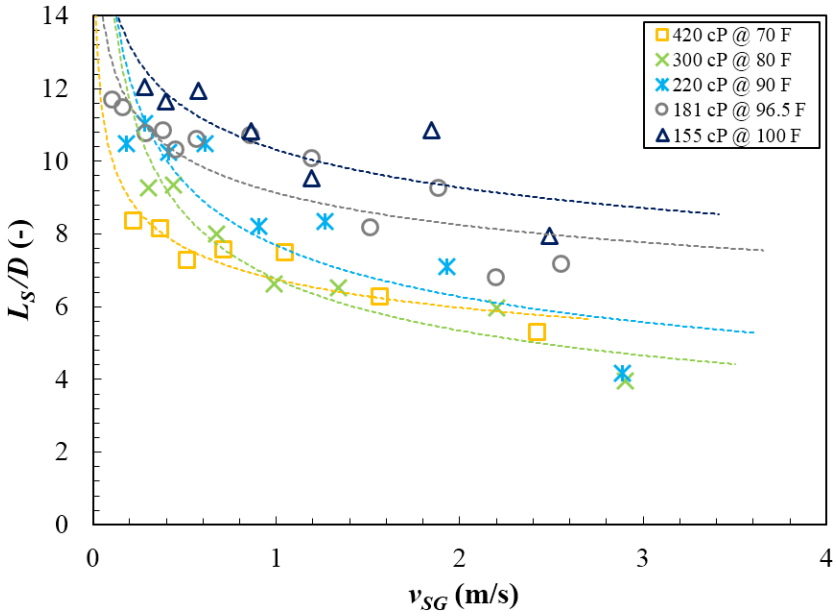

Figure B.79 Average dimensionless slug length vs. superficial gas velocity for v_{SL}=0.356 m/s.

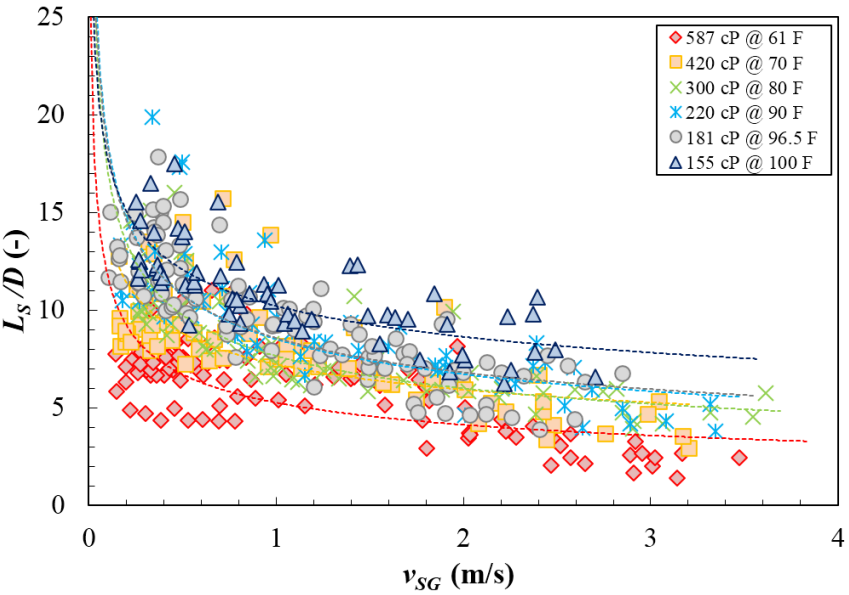

Figure B.80 Average dimensionless slug length vs. superficial gas velocity including all experimental data.

B.3.4.5 Slug length distribution

Brill *et al*. (1981) presented that the nature of the statistical distribution of liquid-slug lengths is the right-skewed log-normal shape. Analysis of the Marcano *et al*. (1998), Gokcal (2008), and Brito's (2012) experimental results showed that the shape of slug length distribution follows a log-normal pattern. This characteristic is also verified in this study, and Appendix D shows the histogram of probability density for dimensionless slug length.

Among the functions included in the EasyFit 5.5 software, the proper high ranked three functions are plotted on the probability density histogram. As can be seen in Appendix C, most of the distribution shape present a gamma (or gamma 3p) or log-normal (or log-normal 3p) distribution.

Figure B.81 shows dimensionless slug length distributions for v_{SL}=0.2 m/s, v_{SG}=1.0 m/s, and oil viscosities from 155 cP to 587 cP. As oil viscosity increases, the degree of right-skewed in log-normal shape also increases. This is in agreement with Brito (2012) who observed similar trend with using medium oil viscosities (39 cP to 166 cP).

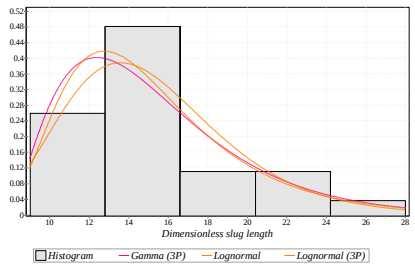

(a)μ_{Oil}=155cP, v_{SL}=0.2m/s, v_{SG}=1.0m/s

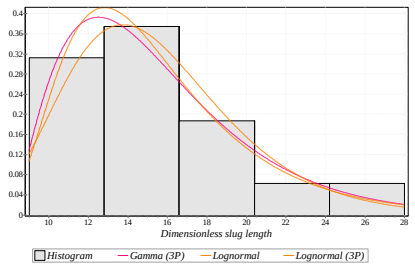

(b)μ_{Oil}=181cP, v_{SL}=0.2m/s, v_{SG}=1.0m/s

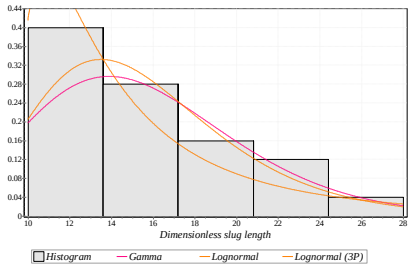

(c)μ_{Oil}=220cP, v_{SL}=0.2m/s, v_{SG}=1.0m/s

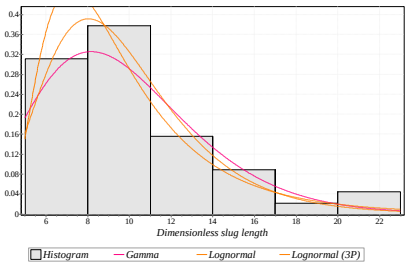

(d)μ_{Oil}=300cP, v_{SL}=0.2m/s, v_{SG}=1.0m/s

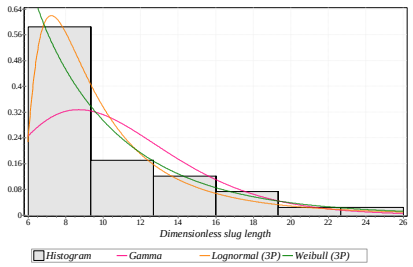

(e)μ_{Oil}=420cP, v_{SL}=0.2m/s, v_{SG}=1.0m/s

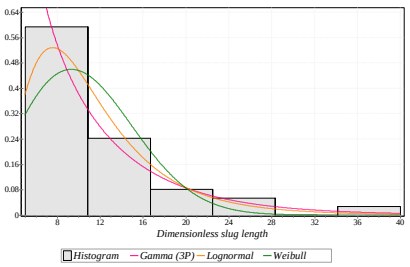

(f)μ_{Oil}=587cP, v_{SL}=0.2m/s, v_{SG}=1.0m/s

Figure B.81 Dimensionless slug length distribution for v_{SL}=0.2 m/s, v_{SG}=1.0 m/s at different oil viscosities (155 cP, 181 cP, 220 cP, 300 cP, 420 cP, and 587 cP).

B.3.4.6 Slug frequency

A modified VBA Excel macro was used to calculate the slug frequency automatically. Slug frequency was obtained by dividing the total number of slugs by the total recorded time. Figures B.82 to B.86 show that the slug frequency increases as superficial liquid velocity increases. A similar trend was observed in Jeyachandra (2011) indicating that this is attributed to the increased chances to create more interfacial waves that can bridge the pipe cross section. As superficial gas velocity increases, slug frequency slightly increases up to

v_{SG}=0.4 m/s. However, in general, slug frequency decreases with increasing superficial gas velocity due to increase in interfacial shear stress reducing the change of waves bridging the top of the pipe. As superficial liquid velocity increases, the slug length decreases, while slug frequency increases indicating that slug length and frequency have inversely proportional relationship. It has been also reported (Scott, 1986) that the slug frequency decreases and the mean slug length increases in long pipelines. Most existing models could capture this relationship. Eqs (121) to (123) are correlations for slug frequency and dimensionless slug length proposed by Al-safran *et al*. (2011).

$$N_f = \frac{N_{Fr}}{N_\mu} = \frac{D^{3/2}\sqrt{\rho_L(\rho_L - \rho_g)g}}{\mu_L} \tag{121}$$

$$f_s = 2.623\left(\frac{N_f{}^{-0.612} v_{SL}}{D}\right) \tag{122}$$

$$\frac{L_s}{D} = 2.63\left(\frac{D^{3/2}\sqrt{\rho_L(\rho_L - \rho_g)g}}{\mu_L}\right)^{0.321} \tag{123}$$

where f_s is slug frequency in 1/s, D is pipe diameter in m, g is gravity acceleration in m/s^2, ρ_g is gas density in kg/m^3, ρ_L is liquid density in kg/m^3, and μ_L is liquid viscosity in Pa·s.

Sections 4.4.4 and 4.4.6 present more detailed relationship between the slug length and the slug frequency obtained from different pipe diameters. The entire result of slug frequency is summarized in Figure B.87.

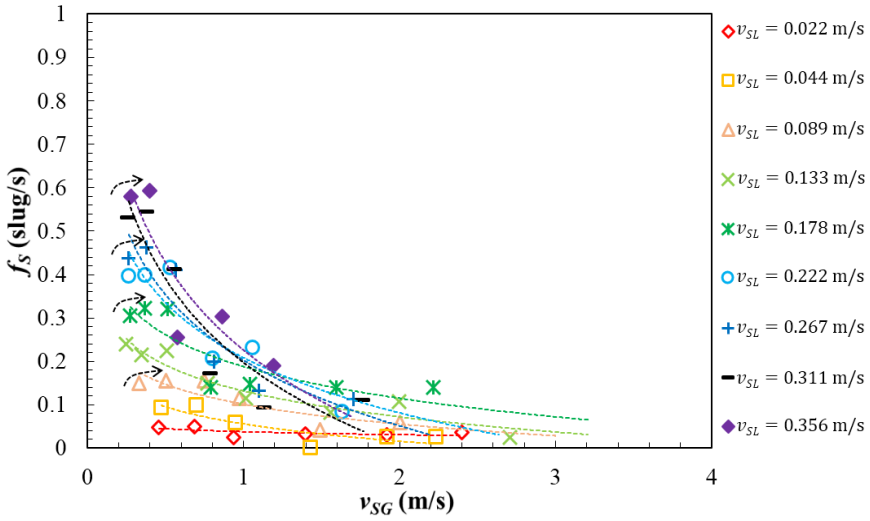

Figure B.82 Slug frequency vs. superficial gas velocity for μ_{Oil} = 155 cP.

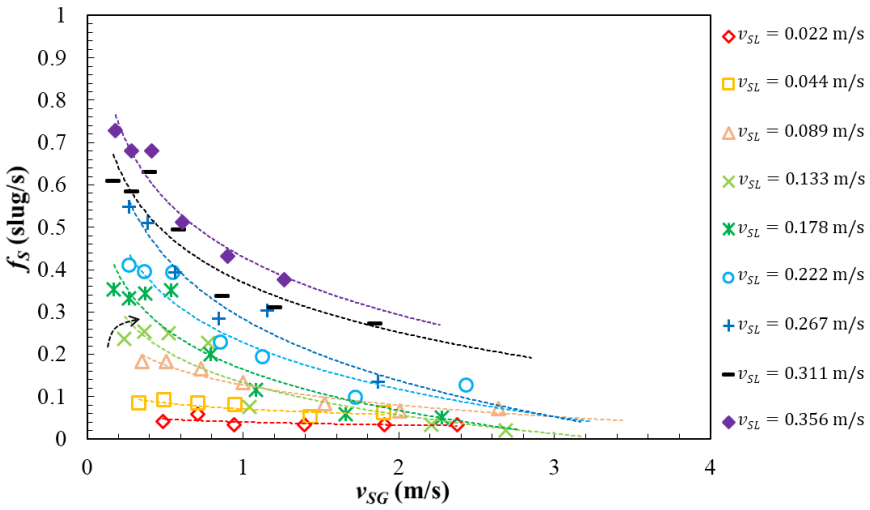

Figure B.83 Slug frequency vs. superficial gas velocity for μ_{Oil} = 220 cP.

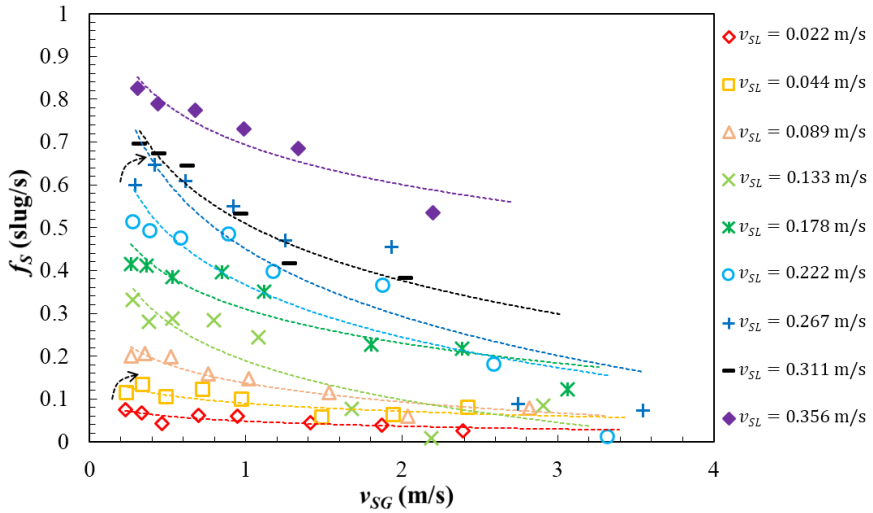

Figure B.84 Slug frequency vs. superficial gas velocity for μ_{Oil} = 300 cP.

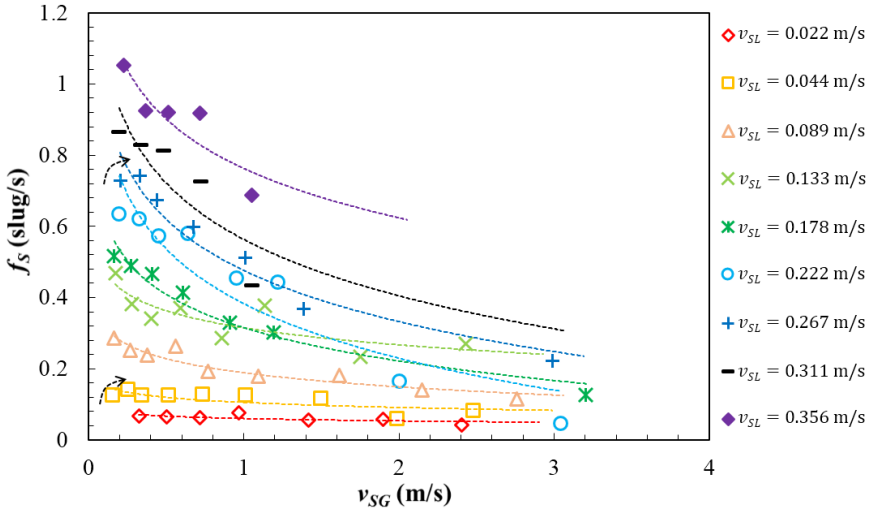

Figure B.85 Slug frequency vs. superficial gas velocity for μ_{Oil} = 420 cP.

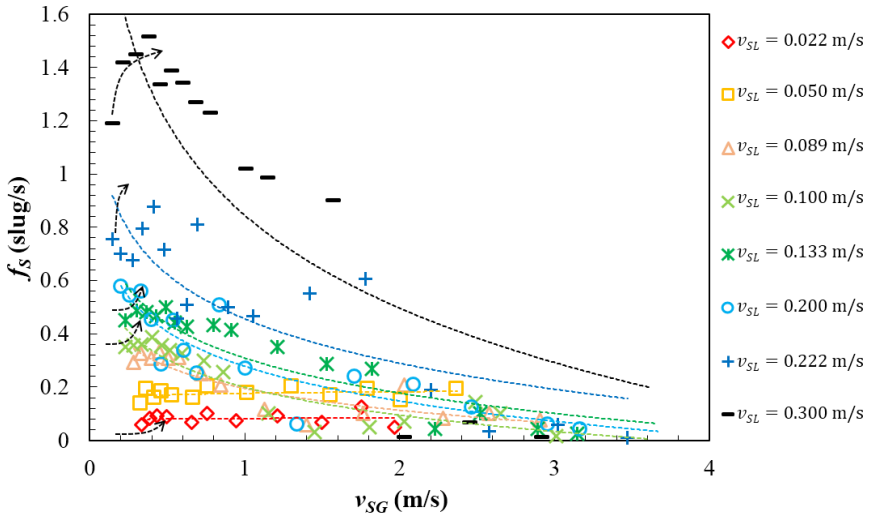

Figure B.86 Slug frequency vs. superficial gas velocity for μ_{Oil} = 587 cP.

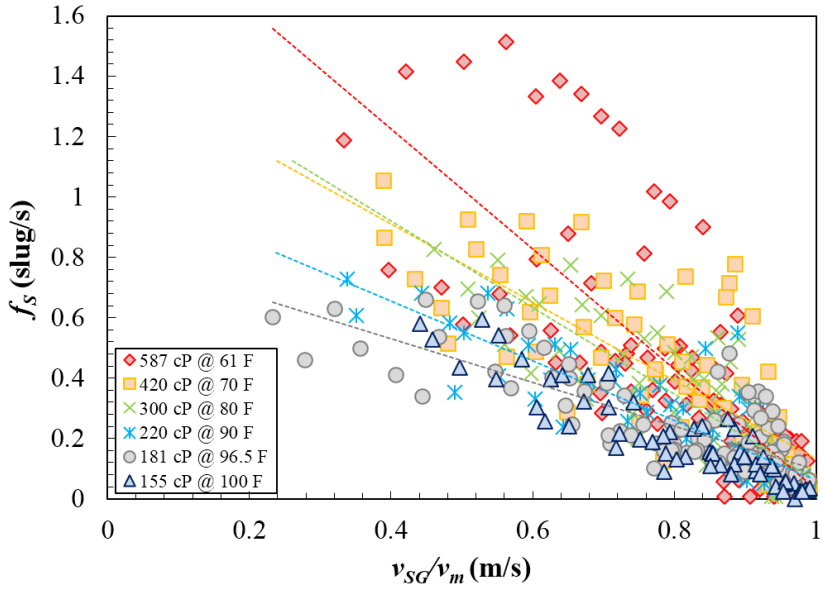

Figure B.87 Slug Frequency vs. v_{SG}/v_m using all of slug frequency data.

Appendix C

Single Phase Flow Test (Brito, 2012)

C.1 Pressure gradient calculation

For single-phase flow, the steady state pressure gradient equation is expressed with the following equation.

$$\frac{dP}{dL} = -\frac{2}{D} f_F \rho v^2 + \rho g \sin\theta + \rho v \frac{dv}{dL} \tag{124}$$

For horizontal flow ignoring acceleration, Eq. (124) can be written as:

$$\frac{dP}{dL} = -\frac{2}{D} f_F \rho v^2 \tag{125}$$

where f_F is the fanning friction factor. The friction factor can be calculated with Eq. (126) for a smooth pipe.

$$f_F = C_F * \mathrm{Re}^{-n} \tag{126}$$

For laminar flow, C_F=16 and n=1, and C_F=0.046 and n=0.2, values can be used for laminar and turbulent flows, respectively. Reynolds number is defined as:

$$\mathrm{Re} = \frac{\rho v D}{\mu} \tag{127}$$

where ρ is the liquid density calculated with Eq. (81), v is the liquid velocity, D

is the pipe diameter, and μ is the liquid viscosity calculated with Eq. (80).

After calculating friction factor, Eq. (125) is used to calculate the pressure gradient.

C.2 Viscosity calculation

Oil viscosity is calculated for different oil temperature to verify the measurements obtained from the laboratory measurements. For this, Eq. (125) is first used to determine the friction factor, where dP/dL is the pressure gradient obtained from the experiments. Then, Eq. (126) is used to calculate Reynolds number and Eq. (127) is solved for the oil viscosity.

Appendix D

Slug Length Distribution

The slug length distribution acquired for different oil viscosities (155 cP, 181 cP, 220 cP, 300 cP, 420 cP, and 587 cP), superficial liquid and gas velocities are presented in the following section, respectively. The investigated distribution functions were calculated using the EasyFit 5.5 software and the proper high rank three models are plotted on the slug length distribution histograms. As can be seen, most of the experimental points present a gamma or log-normal distribution. The probability density functions of gamma and log-normal distribution are shown in Eqs (128) and (129), respectively.

$$f(x;k,\theta)=\frac{x^{k-1}e^{-\frac{x}{\theta}}}{\theta^{k}\Gamma(k)} \qquad for\ \ x>0\ and\ k,\theta>0 \tag{128}$$

$$f(x;\mu,\sigma)=\frac{1}{x\sigma\sqrt{2\pi}}e^{-\frac{(\ln x-\mu)^2}{2\sigma^2}} \qquad for\ \ x>0 \tag{129}$$

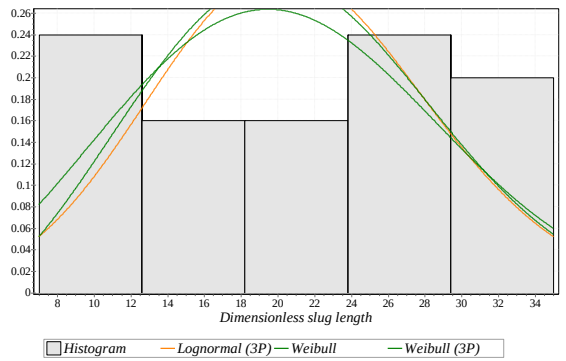

(a) v_{SL}= 0.133 *m/s* and v_{SG}= 0.348 *m/s*.

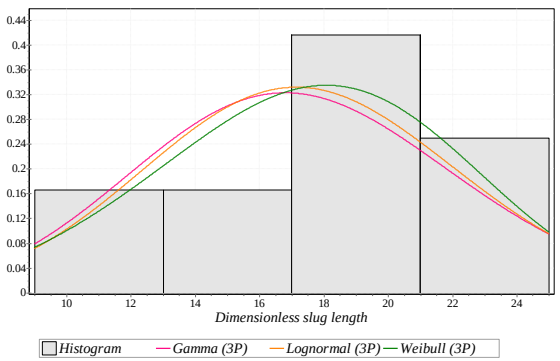

(b) v_{SL}= 0.133 *m/s* and v_{SG}= 1.014 *m/s*.

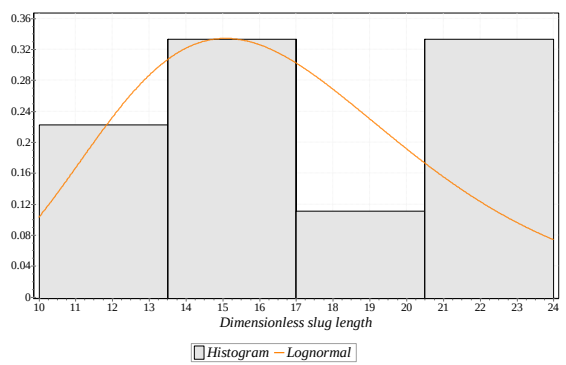

(c) v_{SL}= 0.133 *m/s* and v_{SG}= 1.557 *m/s*.

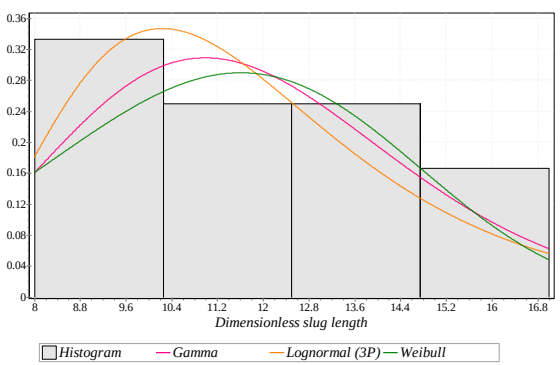

(d) v_{SL}= 0.133 *m/s* and v_{SG}= 1.997 *m/s*.

Figure D.1 Slug length distribution for v_{SL}=0.133 m/s and different v_{SG} values when μ_{Oil}=155 cP.

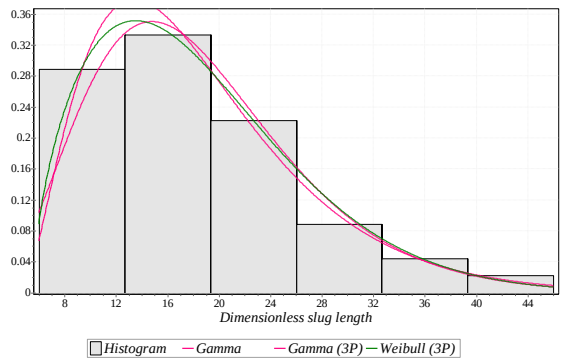

(a) v_{SL}= 0.222 *m/s* and v_{SG}= 0.370 *m/s*.

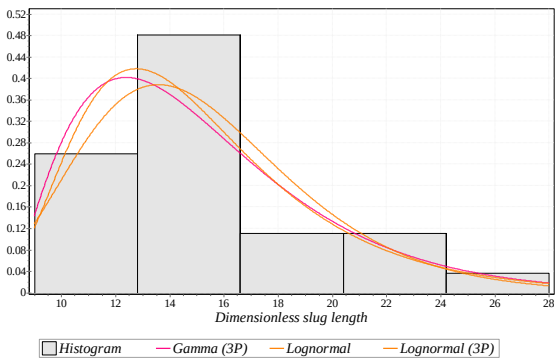

(b) v_{SL}= 0.222 *m/s* and v_{SG}= 0.808 *m/s*.

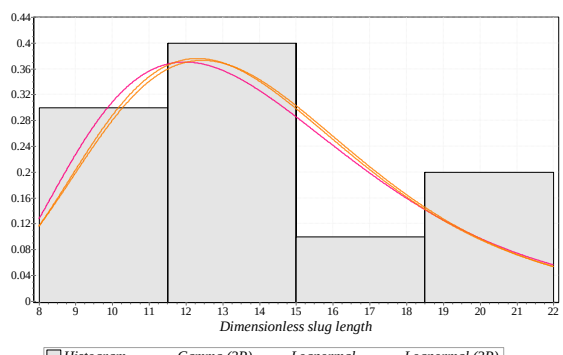

(c) v_{SL}= 0.222 *m/s* and v_{SG}= 1.637 *m/s*.

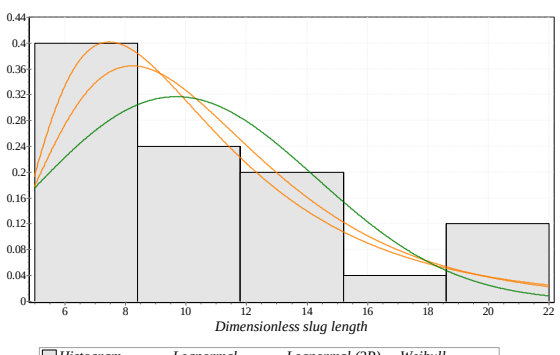

(d) v_{SL}= 0.222 *m/s* and v_{SG}= 2.254 *m/s*.

Figure D.2 Slug length distribution for v_{SL}=0.222 m/s and different v_{SG} values when μ_{Oil}=155 cP.

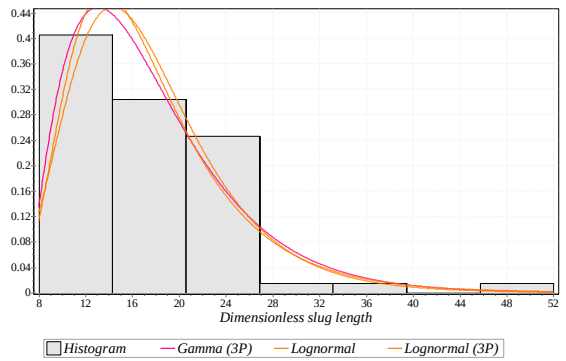

(a) v_{SL}= 0.356 *m/s* and v_{SG}= 0.399 *m/s*.

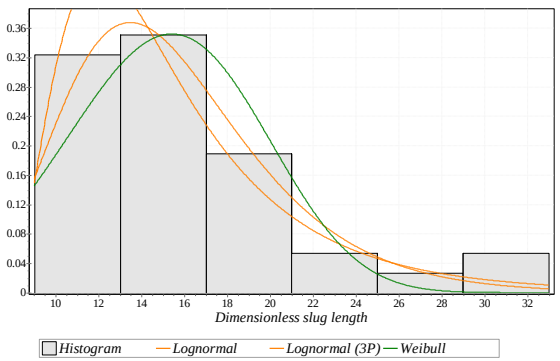

(b) v_{SL}= 0.356 *m/s* and v_{SG}= 0.862 *m/s*.

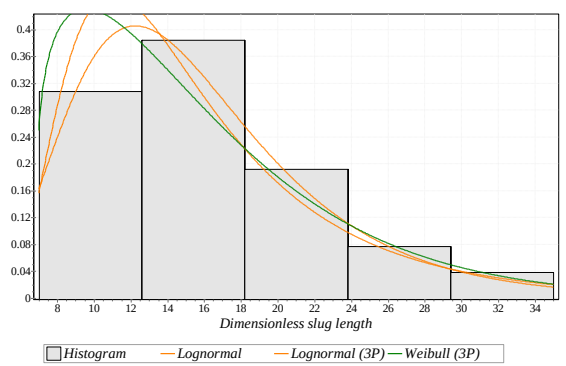

(c) v_{SL}= 0.356 *m/s* and v_{SG}= 1.845 *m/s*.

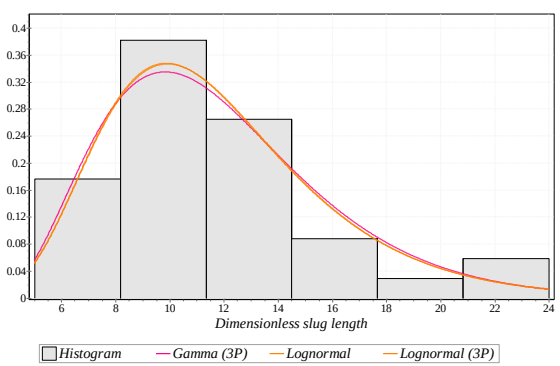

(d) v_{SL}= 0.356 *m/s* and v_{SG}= 2.849 *m/s*.

Figure D.3 Slug length distribution for v_{SL}=0.356 m/s and different v_{SG} values when μ_{Oil}=155 cP.

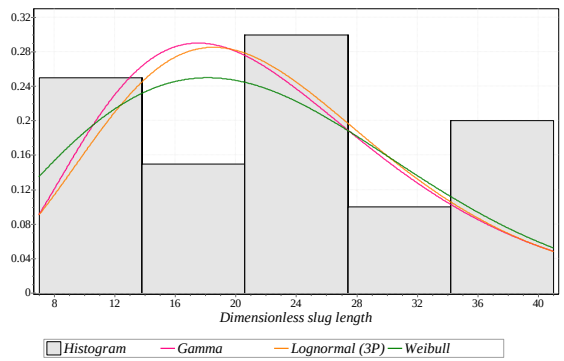

(a) v_{SL}= 0.100 *m/s* and v_{SG}= 0.400 *m/s*.

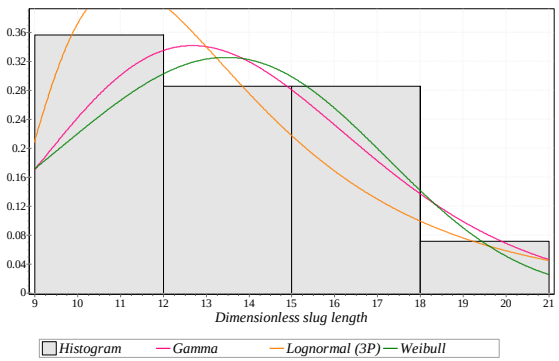

(b) v_{SL}= 0.100 *m/s* and v_{SG}= 0.987 *m/s*.

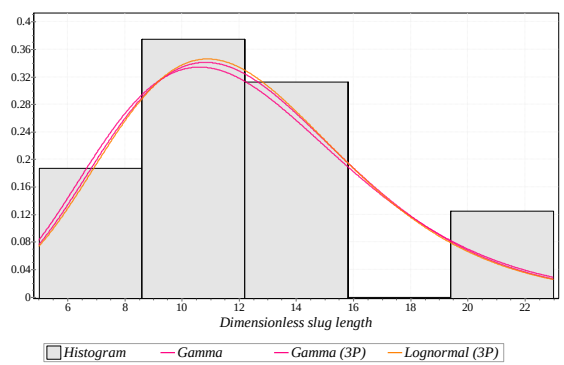

(c) v_{SL}= 0.100 *m/s* and v_{SG}= 1.523 *m/s*.

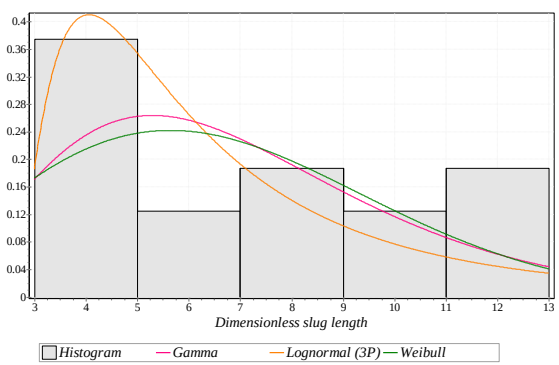

(d) v_{SL}= 0.100 *m/s* and v_{SG}= 2.126 *m/s*.

Figure D.4 Slug length distribution for v_{SL}=0.1 m/s and different v_{SG} values when μ_{Oil}=181 cP.

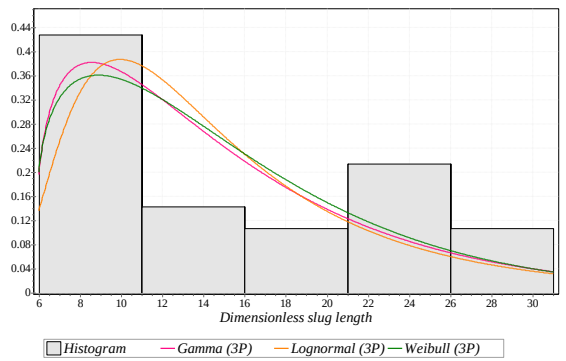

(a) v_{SL}= 0.200 *m/s* and v_{SG}= 0.412 *m/s*.

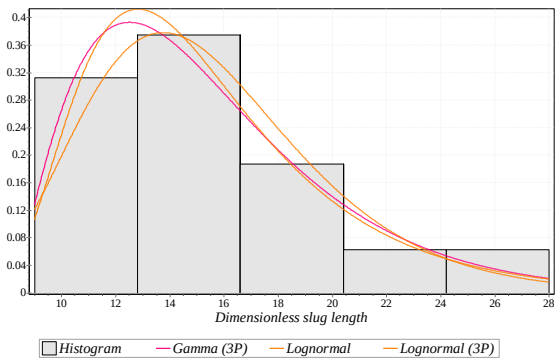

(b) v_{SL}= 0.200 *m/s* and v_{SG}= 1.075 *m/s*.

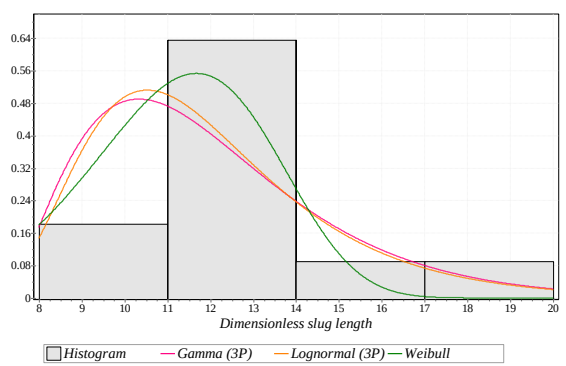

(c) v_{SL}= 0.200 *m/s* and v_{SG}= 1.639 *m/s*.

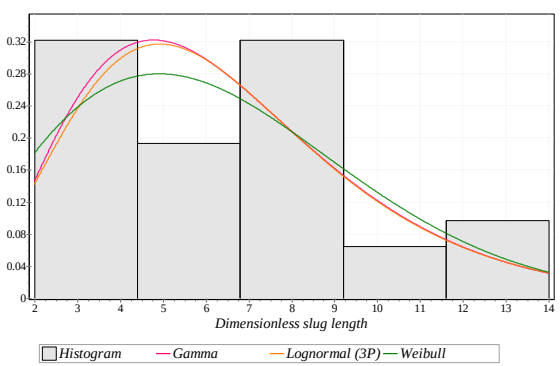

(d) v_{SL}= 0.200 *m/s* and v_{SG}= 2.594 *m/s*.

Figure D.5 Slug length distribution for v_{SL}=0.2 m/s and different v_{SG} values when μ_{Oil}=181 cP.

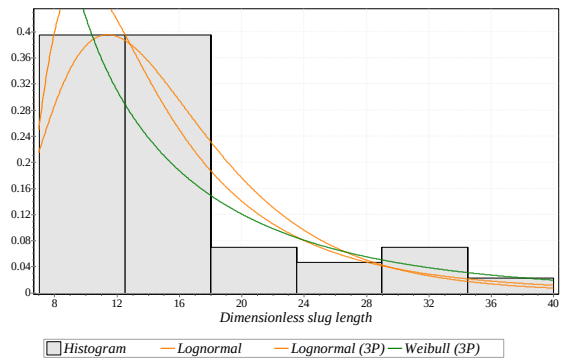

(a) v_{SL}= 0.300 *m/s* and v_{SG}= 0.441 *m/s*.

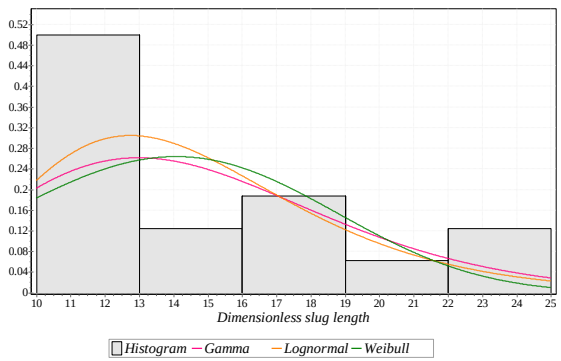

(b) v_{SL}= 0.300 *m/s* and v_{SG}= 1.166 *m/s*.

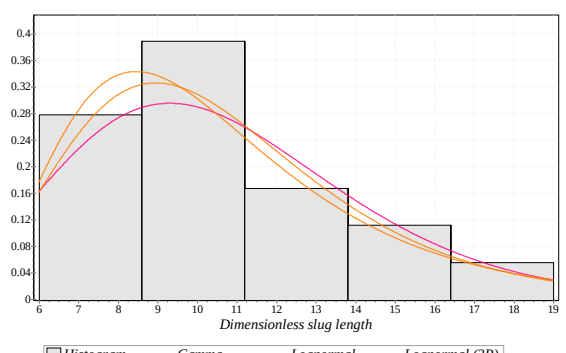

(c) v_{SL}= 0.300 *m/s* and v_{SG}= 1.794 *m/s*.

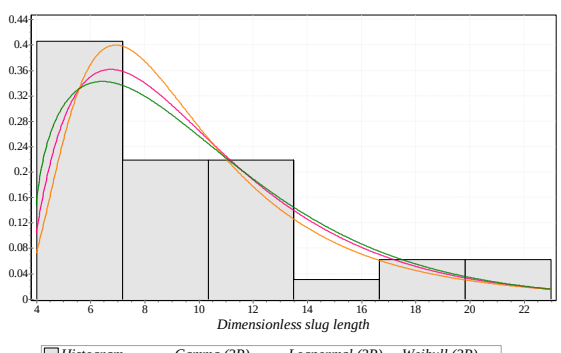

(d) v_{SL}= 0.300 *m/s* and v_{SG}= 2.848 *m/s*.

Figure D.6 Slug length distribution for v_{SL}=0.3 m/s and different v_{SG} values when μ_{Oil}=181 cP.

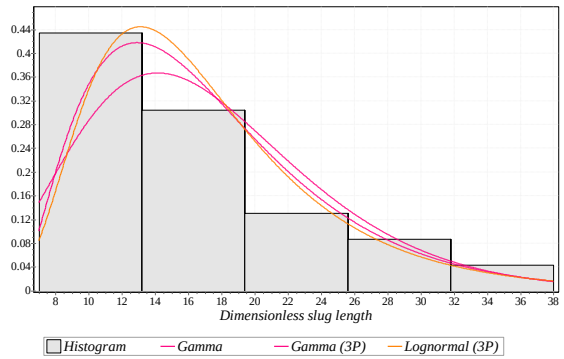

(a) v_{SL}= 0.133 *m/s* and v_{SG}= 0.368 *m/s*.

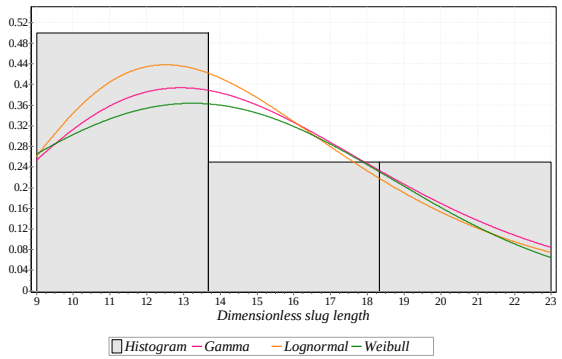

(b) v_{SL}= 0.133 *m/s* and v_{SG}= 1.042 *m/s*.

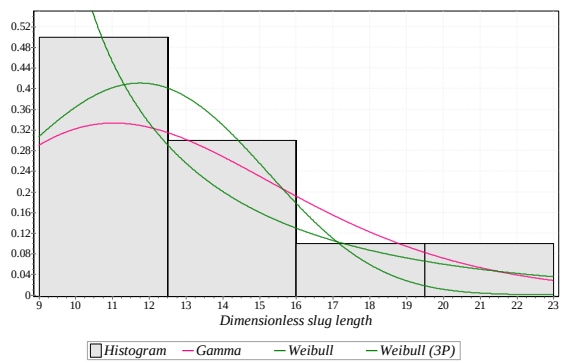

(c) v_{SL}= 0.133 *m/s* and v_{SG}= 1.602 *m/s*.

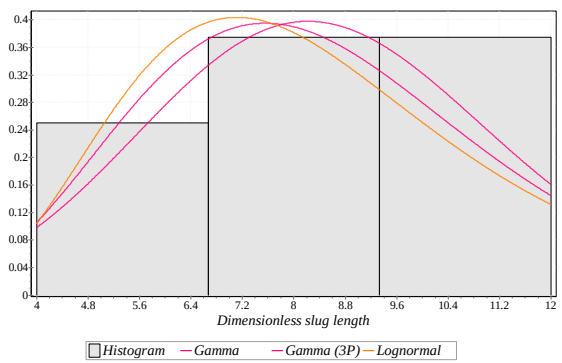

(d) v_{SL}= 0.133 *m/s* and v_{SG}= 2.684 *m/s*.

Figure D.7 Slug length distribution for v_{SL}=0.133 m/s and different v_{SG} values when μ_{Oil}=220 cP.

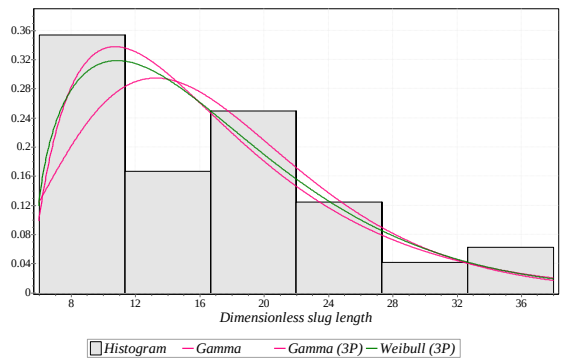

(a) v_{SL}= 0.222 *m/s* and v_{SG}= 0.370 *m/s*.

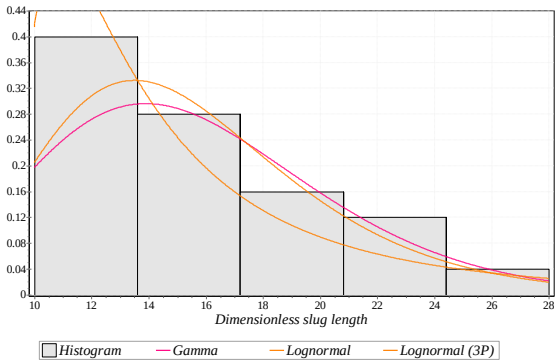

(b) v_{SL}= 0.222 *m/s* and v_{SG}= 0.860 *m/s*.

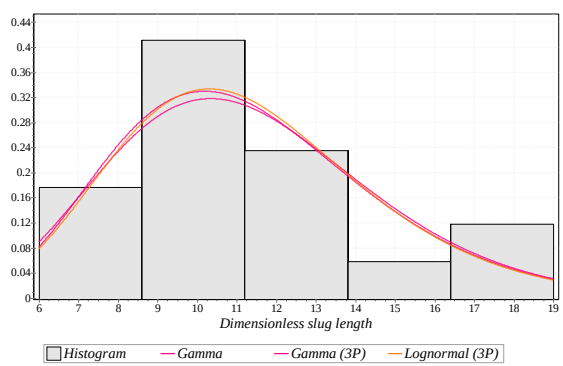

(c) v_{SL}= 0.222 *m/s* and v_{SG}= 1.726 *m/s*.

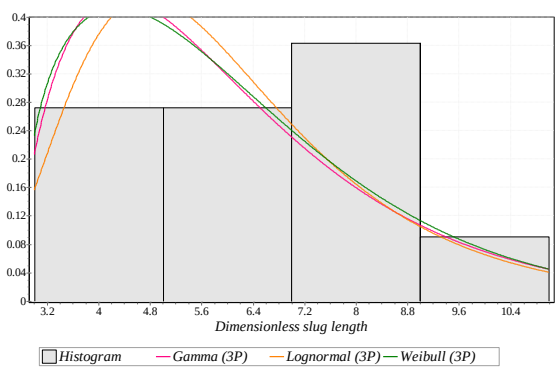

(d) v_{SL}= 0.222 *m/s* and v_{SG}= 3.084 *m/s*.

Figure D.8 Slug length distribution for v_{SL}=0.222 m/s and different v_{SG} values when μ_{Oil}=220 cP.

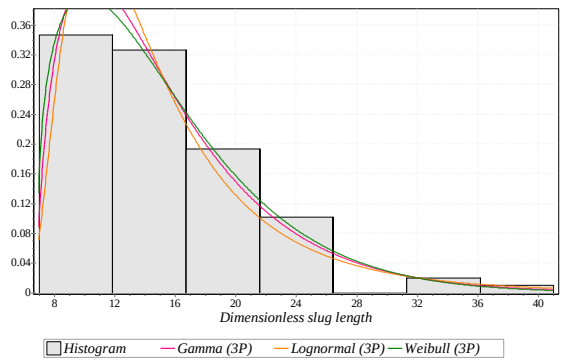

(a) v_{SL}= 0.356 *m/s* and v_{SG}= 0.413 *m/s*.

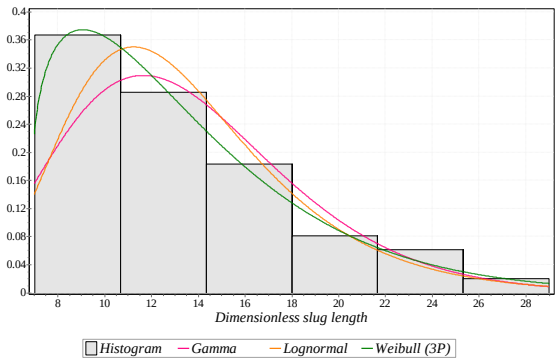

(b) v_{SL}= 0.356 *m/s* and v_{SG}= 0.902 *m/s*.

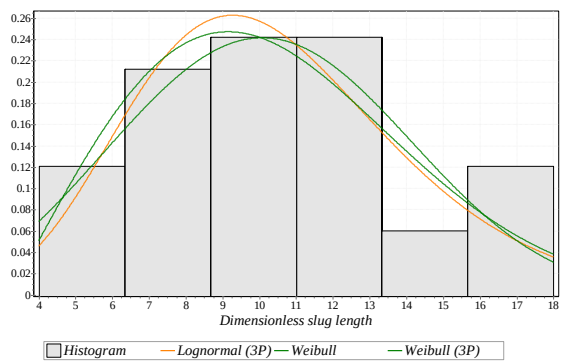

(c) v_{SL}= 0.356 *m/s* and v_{SG}= 1.932 *m/s*.

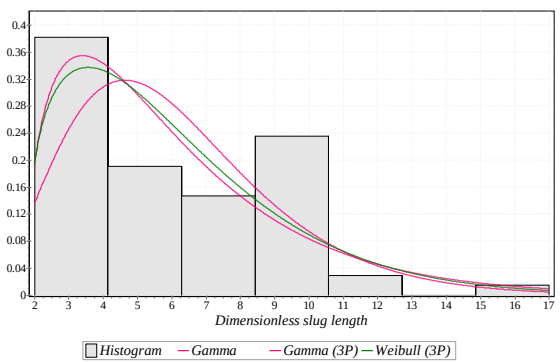

(d) v_{SL}= 0.356 *m/s* and v_{SG}= 2.887 *m/s*.

Figure D.9 Slug length distribution for v_{SL}=0.356 m/s and different v_{SG} values when μ_{Oil}=220 cP.

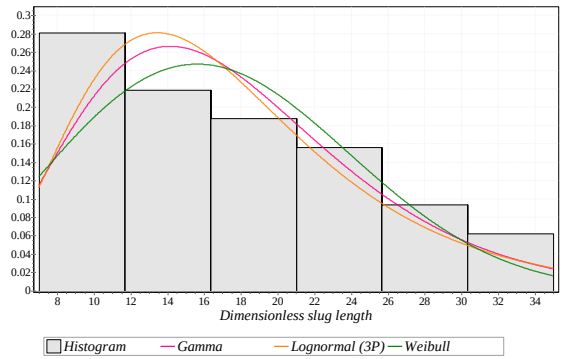

(a) v_{SL}= 0.133 *m/s* and v_{SG}= 0.382 *m/s*.

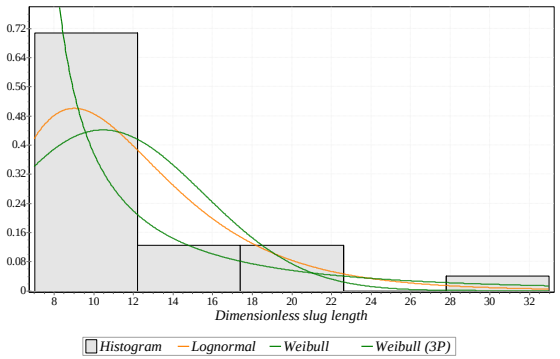

(b) v_{SL}= 0.133 *m/s* and v_{SG}= 0.796 *m/s*.

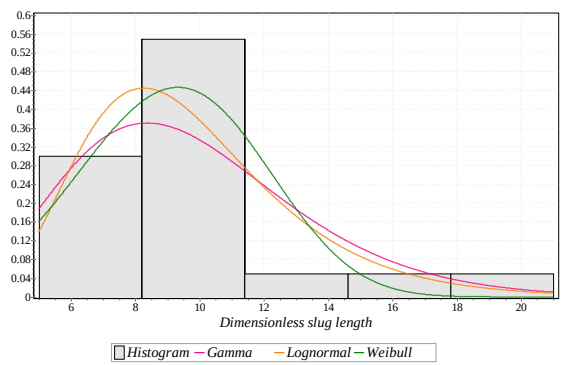

(c) v_{SL}= 0.133 *m/s* and v_{SG}= 1.081 *m/s*.

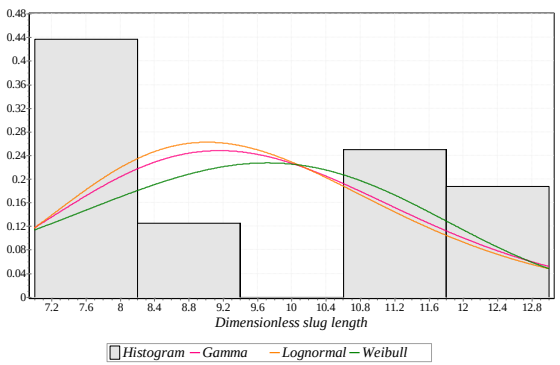

(d) v_{SL}= 0.133 *m/s* and v_{SG}= 1.681 *m/s*.

Figure D.10 Slug length distribution for v_{SL}=0.133 m/s and different v_{SG} values when μ_{Oil}=300 cP.

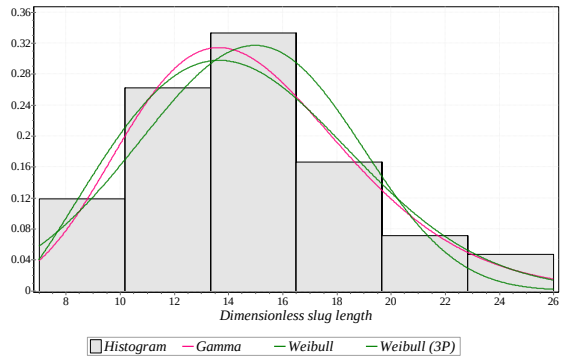

(a) v_{SL}= 0.222 *m/s* and v_{SG}= 0.389 *m/s*.

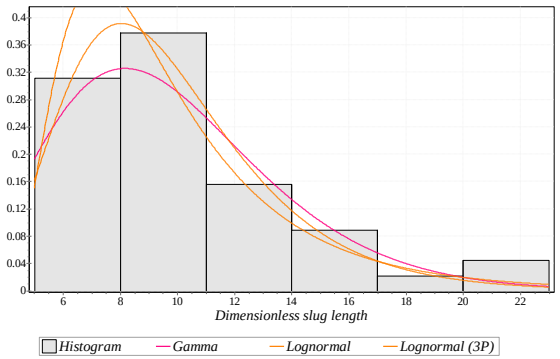

(b) v_{SL}= 0.222 *m/s* and v_{SG}= 0.892 *m/s*.

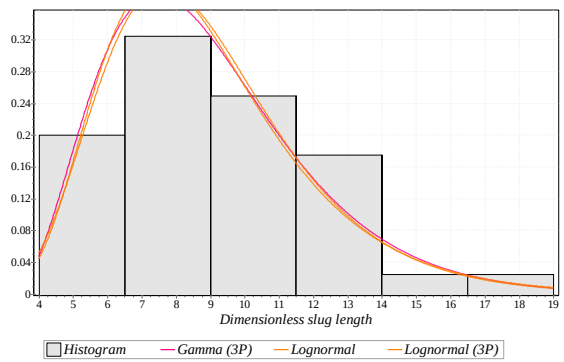

(c) v_{SL}= 0.222 *m/s* and v_{SG}= 1.885 *m/s*.

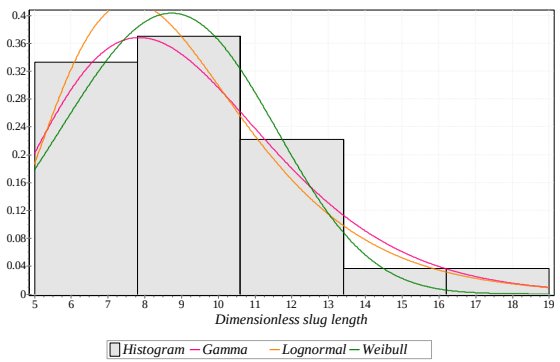

(d) v_{SL}= 0.222 *m/s* and v_{SG}= 2.594 *m/s*.

Figure D.11 Slug length distribution for v_{SL}=0.222 m/s and different v_{SG} values when μ_{Oil}=300 cP.

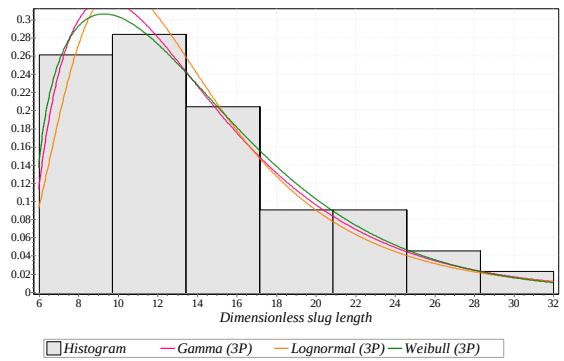

(a) v_{SL}= 0.356 *m/s* and v_{SG}= 0.437 *m/s*.

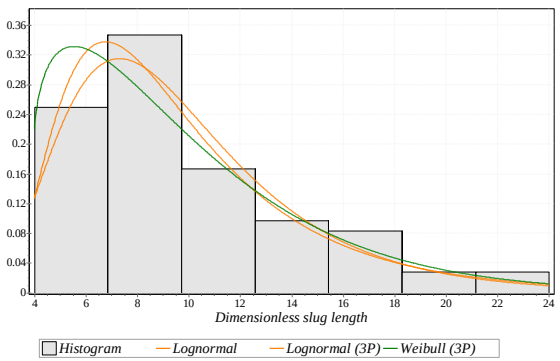

(b) v_{SL}= 0.356 *m/s* and v_{SG}= 0.986 *m/s*.

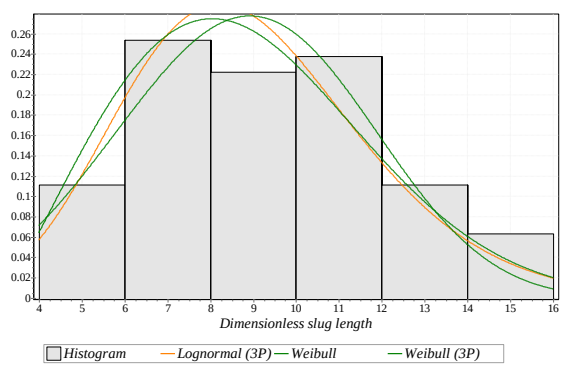

(c) v_{SL}= 0.356 *m/s* and v_{SG}= 2.202 *m/s*.

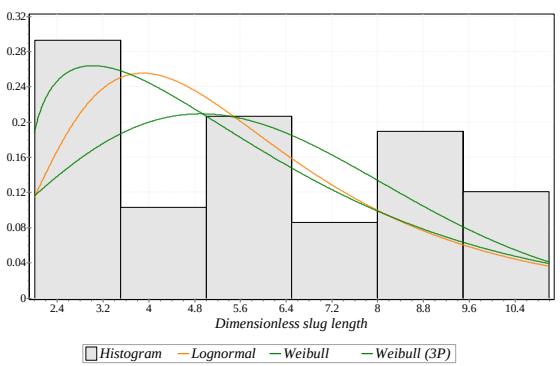

(d) v_{SL}= 0.356 *m/s* and v_{SG}= 2.902 *m/s*.

Figure D.12 Slug length distribution for v_{SL}=0.356 m/s and different v_{SG} values when μ_{Oil}=300 cP.

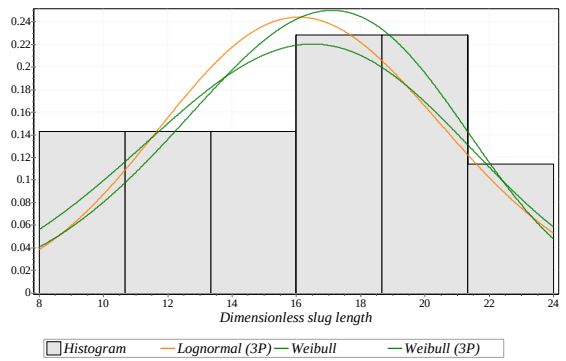

(a) v_{SL}= 0.133 *m/s* and v_{SG}= 0.404 *m/s*.

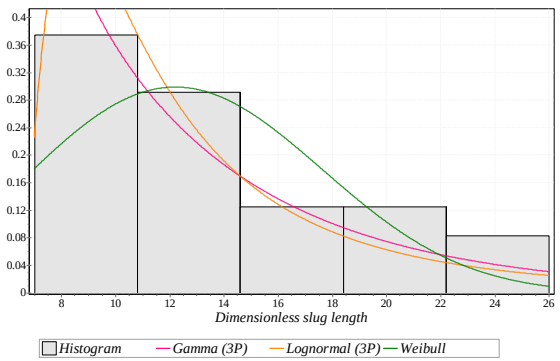

(b) v_{SL}= 0.133 *m/s* and v_{SG}= 0.858 *m/s*.

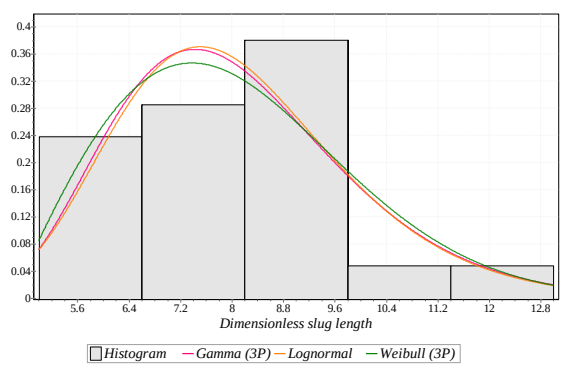

(c) v_{SL}= 0.133 *m/s* and v_{SG}= 1.749 *m/s*.

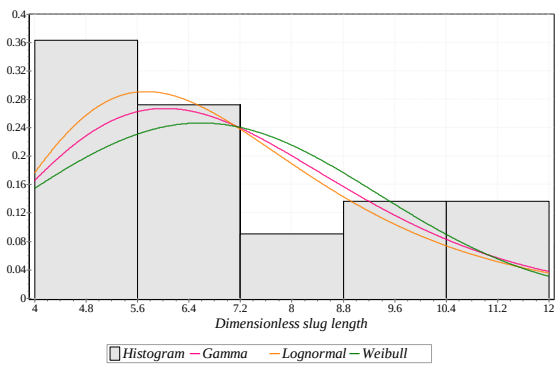

(d) v_{SL}= 0.133 *m/s* and v_{SG}= 2.429 *m/s*.

Figure D.13 Slug length distribution for v_{SL}=0.133 m/s and different v_{SG} values when μ_{Oil}=420 cP.

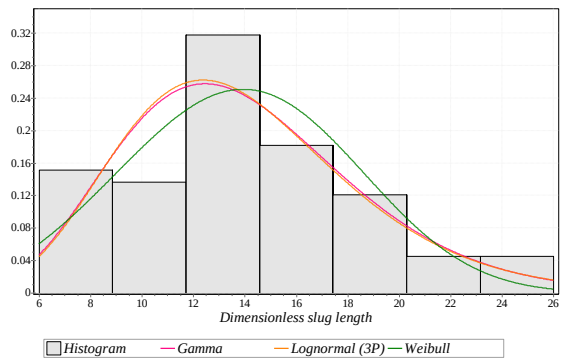

(a) v_{SL}= 0.222 *m/s* and v_{SG}= 0.456 *m/s*.

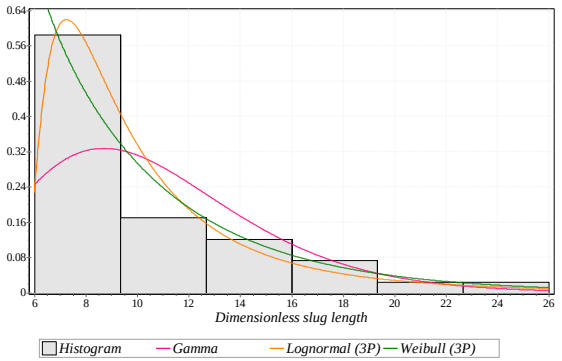

(b) v_{SL}= 0.222 *m/s* and v_{SG}= 0.957 *m/s*.

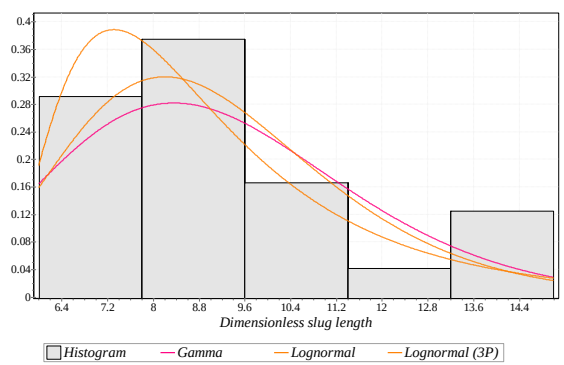

(c) v_{SL}= 0.222 *m/s* and v_{SG}= 2.006 *m/s*.

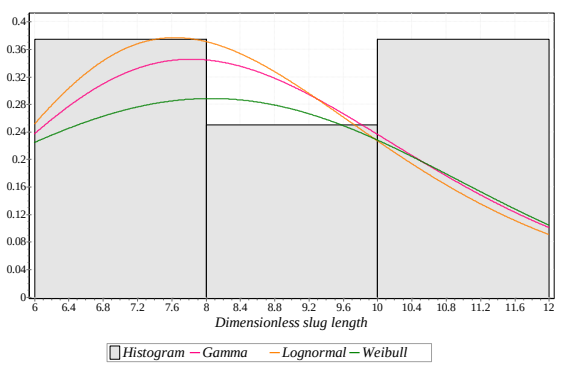

(d) v_{SL}= 0.222 *m/s* and v_{SG}= 3.046 *m/s*.

Figure D.14 Slug length distribution for v_{SL}=0.222 m/s and different v_{SG} values when μ_{Oil}=420 cP.

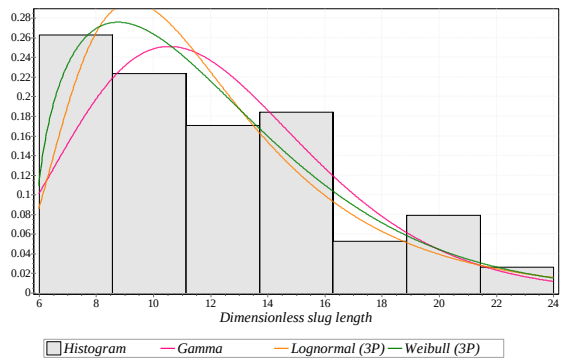

(a) v_{SL}= 0.356 *m/s* and v_{SG}= 0.369 *m/s*.

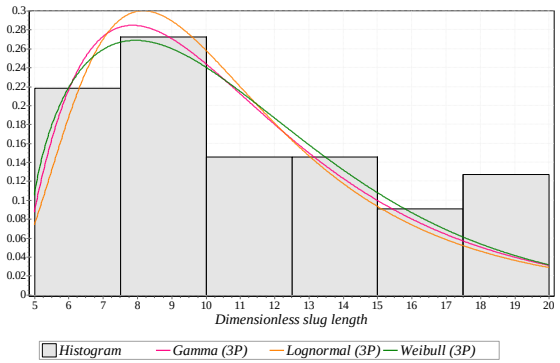

(b) v_{SL}= 0.356 *m/s* and v_{SG}= 1.053 *m/s*.

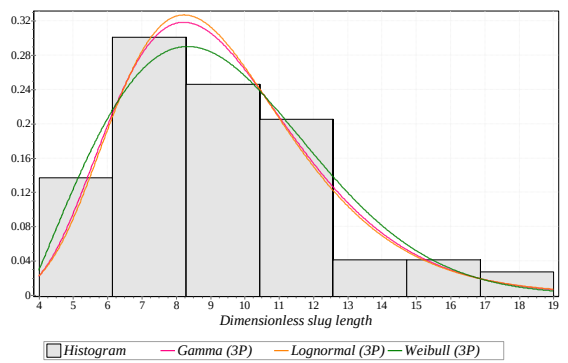

(c) v_{SL}= 0.356 *m/s* and v_{SG}= 1.571 *m/s*.

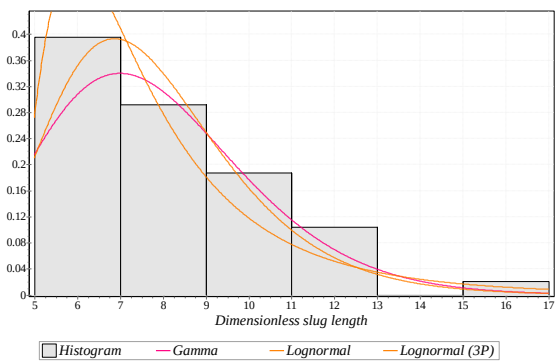

(d) v_{SL}= 0.356 *m/s* and v_{SG}= 2.426 *m/s*.

Figure D.15 Slug length distribution for v_{SL}=0.356 m/s and different v_{SG} values when μ_{Oil}=420 cP.

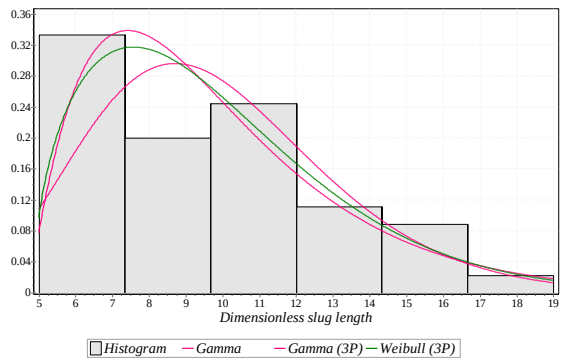

(a) v_{SL}= 0.100 *m/s* and v_{SG}= 0.404 *m/s*.

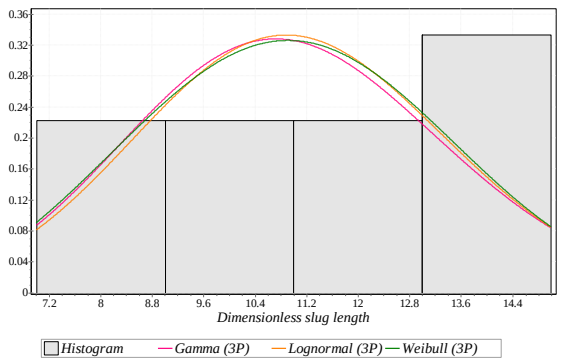

(b) v_{SL}= 0.100 *m/s* and v_{SG}= 1.153 *m/s*.

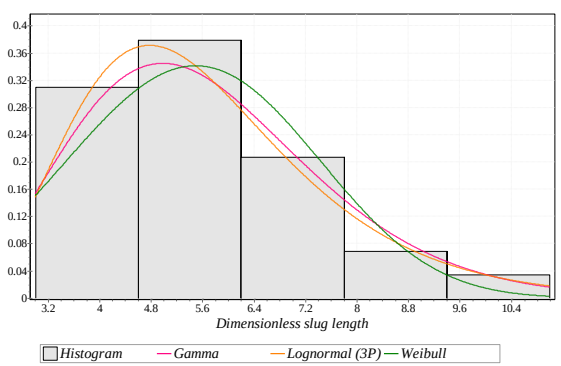

(c) v_{SL}= 0.100 *m/s* and v_{SG}= 2.032 *m/s*.

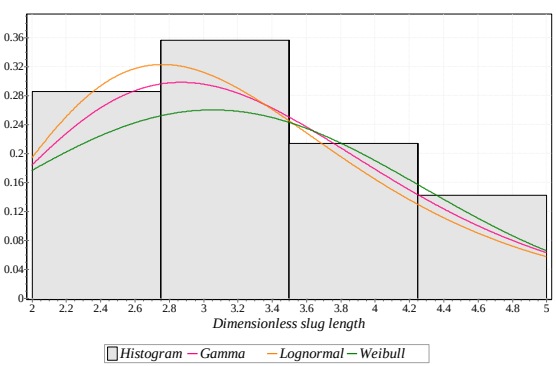

(d) v_{SL}= 0.100 *m/s* and v_{SG}= 2.653 *m/s*.

Figure D.16 Slug length distribution for v_{SL}=0.1 m/s and different v_{SG} values when μ_{Oil}=587 cP.

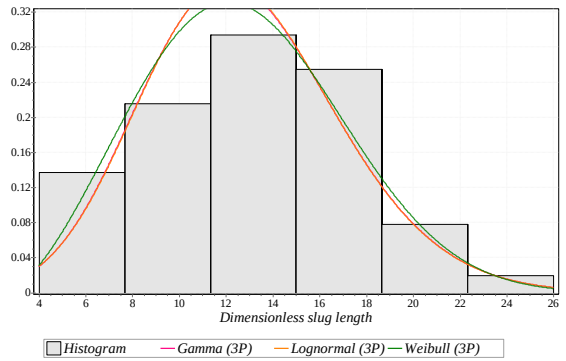

(a) v_{SL}= 0.200 *m/s* and v_{SG}= 0.401 *m/s*.

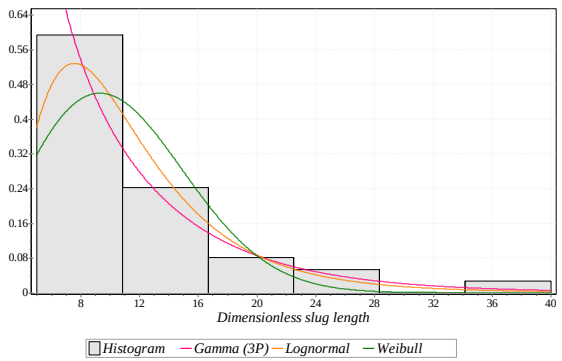

(b) v_{SL}= 0.200 *m/s* and v_{SG}= 1.007 *m/s*.

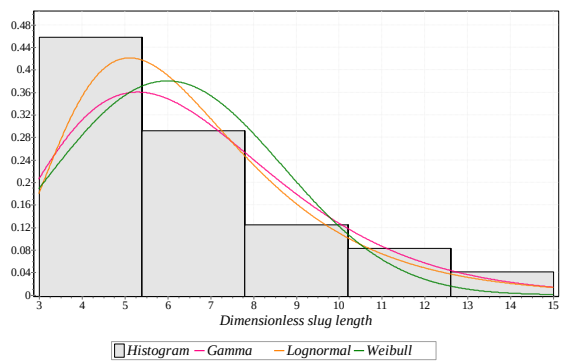

(c) v_{SL}= 0.200 *m/s* and v_{SG}= 2.093 *m/s*.

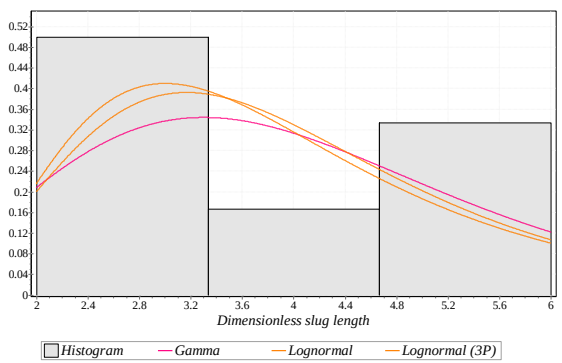

(d) v_{SL}= 0.200 *m/s* and v_{SG}= 2.957 *m/s*.

Figure D.17 Slug length distribution for v_{SL}=0.2 m/s and different v_{SG} values when μ_{Oil}=587 cP.

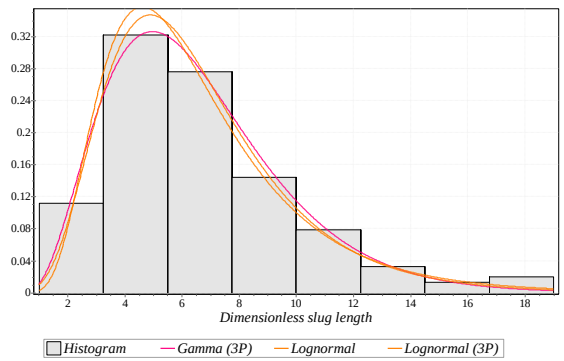

(a) v_{SL}= 0.300 *m/s* and v_{SG}= 0.385 *m/s*.

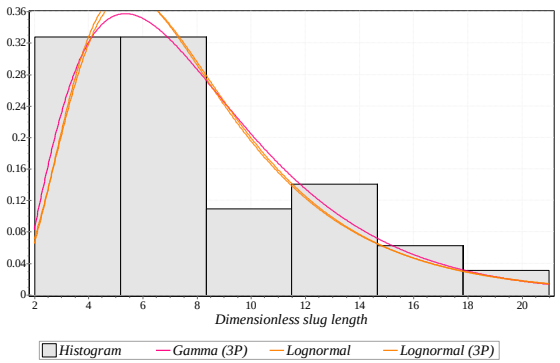

(b) v_{SL}= 0.300 *m/s* and v_{SG}= 1.012 *m/s*.

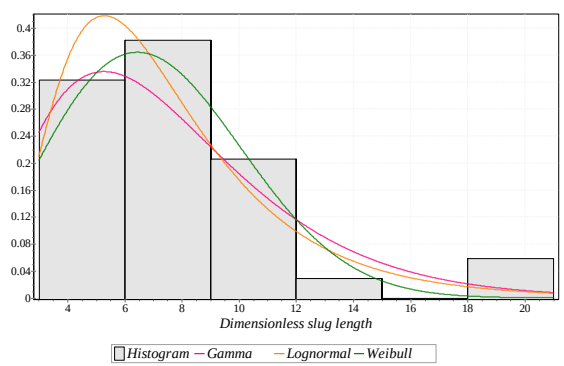

(c) v_{SL}= 0.300 *m/s* and v_{SG}= 1.578 *m/s*.

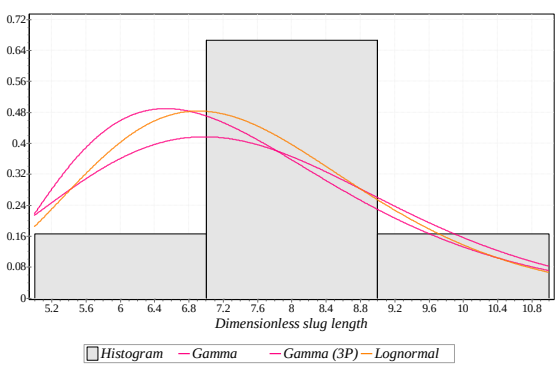

(d) v_{SL}= 0.300 *m/s* and v_{SG}= 2.457 *m/s*.

Figure D.18 Slug length distribution for v_{SL}=0.3 m/s and different v_{SG} values when μ_{Oil}=587 cP.

Appendix E

Slug Frequency Comparison with the Gokcal's (2008)

In previous study, Gokcal (2008) used different equipment, lase sensors, to conduct experimental study for the slug frequency. Although the different methodology was used to measure this parameter, the acquired data showed a great accuracy. Thus, in this section, the comparison between 3-in. ID pipes results and Gokcal's (2008) 2-in. ID pipes results are presented for the slug frequency.

Figures E.1 to E.3 show that the slug frequency of 2-in. is always higher than 3-in. ID pipes and this trend is similar with the one of section 4.4.5.

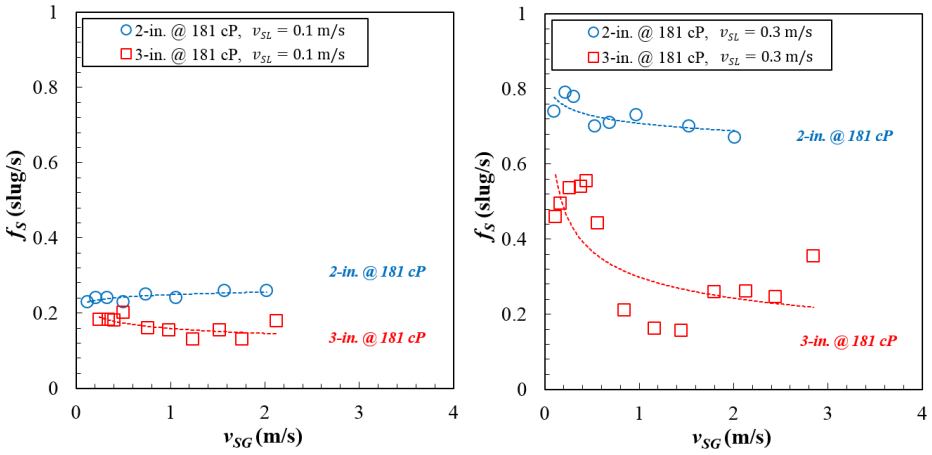

(a) v_{SL} = 0.1 m/s (b) v_{SL} = 0.3 m/s

Figure E.1 Slug frequency obtained from different pipe diameters vs. superficial gas velocity for μ_{Oil} = 181 cP, (a) v_{SL}=0.1 m/s and (b) v_{SL}=0.3 m/s.

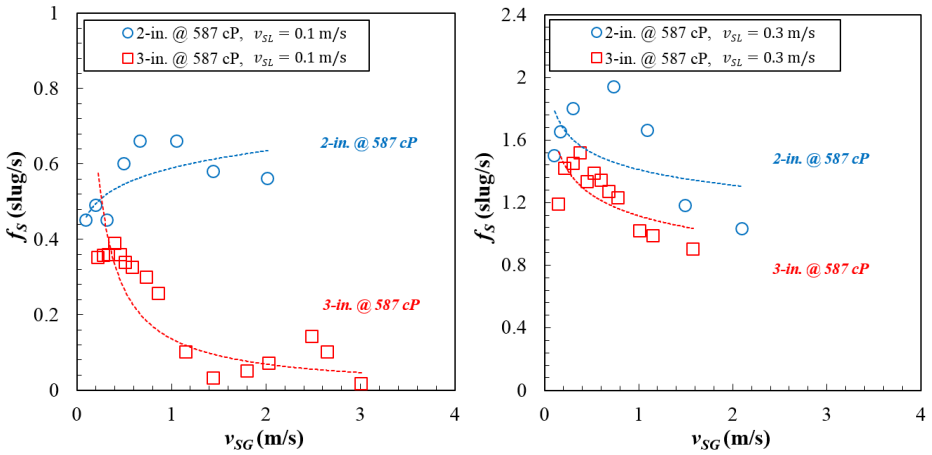

(a) v_{SL} = 0.1 m/s (b) v_{SL} = 0.3 m/s

Figure E.2 Slug frequency obtained from different pipe diameters vs. superficial gas velocity for μ_{Oil} = 587 cP, (a) v_{SL}=0.1 m/s and (b) v_{SL}=0.3 m/s.

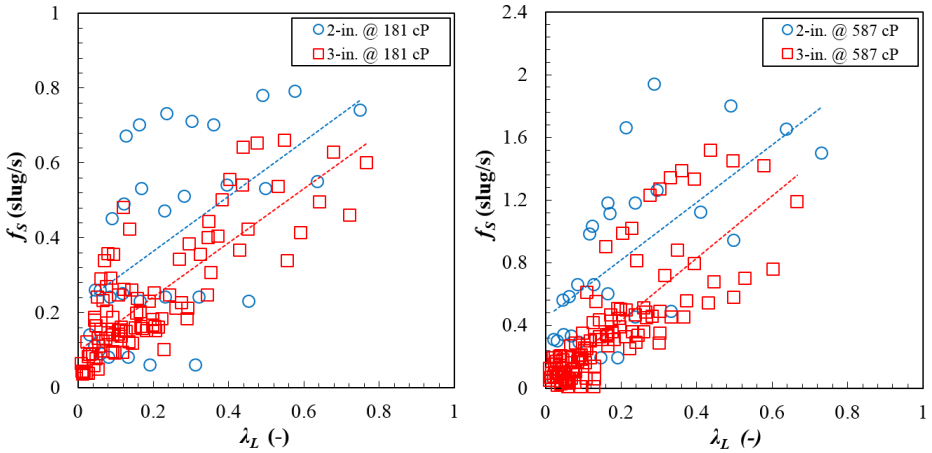

(a) μ_{Oil} = 181 cP (b) μ_{Oil} = 587 cP

Figure E.3 Slug frequency obtained from different pipe diameters vs. superficial gas velocity for (a) μ_{Oil} = 181 cP, and (b) μ_{Oil} = 587 cP.

Appendix F

Model Evaluation Statistical Parameters

The following tables summarize the statistical parameter values, obtained for the different existing correlations and models to predict pressure gradient, average liquid holdup, slug and film liquid holdup, translational velocity, slug length, and slug frequency under different viscosity conditions.

Table F.1 Model evaluation using the measured pressure gradient of 3-in. ID pipes.

			Statistical Parameter					
Model	No. of Data	Oil Viscosity (cP)	ε_1 (%)	ε_2 (%)	ε_3 (%)	ε_4 (Pa/m)	ε_5 (Pa/m)	ε_6 (Pa/m)
TUFFP Model	489	ALL	-22	26	16	-139	139	127
OLGA	489	ALL	-31	33	17	-185	186	173
Xiao *et al* . (1990)	489	ALL	-32	34	17	-186	187	175
TUFFP Model	119	587 cP	-28	28	8	-233	233	161
OLGA	119	587 cP	-34	34	10	-286	286	209
Xiao *et al* . (1990)	119	587 cP	-34	34	10	-287	288	211
TUFFP Model	72	420 cP	-24	25	10	-177	178	131
OLGA	72	420 cP	-31	32	12	-229	229	187
Xiao *et al* . (1990)	72	420 cP	-32	32	12	-231	231	190
TUFFP Model	71	300 cP	-19	24	19	-129	130	104
OLGA	71	300 cP	-30	33	22	-189	190	173
Xiao *et al* . (1990)	71	300 cP	-30	34	21	-190	191	176
TUFFP Model	70	220 cP	-21	22	12	-96	97	71
OLGA	70	220 cP	-32	33	15	-144	145	126
Xiao *et al* . (1990)	70	220 cP	-33	33	15	-145	145	128
TUFFP Model	96	181 cP	-19	23	16	-75	75	61
OLGA	96	181 cP	-31	33	18	-109	109	99
Xiao *et al* . (1990)	96	181 cP	-31	34	18	-109	110	99
TUFFP Model	61	155 cP	-16	26	26	-69	71	57
OLGA	61	155 cP	-28	35	25	-100	102	89
Xiao *et al* . (1990)	61	155 cP	-29	35	24	-101	102	88

Table F.2 Model evaluation using the measured pressure gradient of 2-in. ID pipes.

Model	No. of Data	Oil Viscosity (cP)	Statistical Parameter					
			ε_1 (%)	ε_2 (%)	ε_3 (%)	ε_4 (Pa/m)	ε_5 (Pa/m)	ε_6 (Pa/m)
TUFFP Model	82	ALL	-7	7	5	-80	87	87
OLGA	82	ALL	-14	14	8	-191	193	215
Xiao *et al* . (1990)	82	ALL	-13	14	10	-142	161	188
TUFFP Model	38	587 cP	-4	5	4	-79	93	101
OLGA	38	587 cP	-9	9	7	-215	220	256
Xiao *et al* . (1990)	38	587 cP	-7	8	8	-109	151	196
TUFFP Model	44	181 cP	-10	10	4	-81	81	74
OLGA	44	181 cP	-18	18	7	-170	170	172
Xiao *et al* . (1990)	44	181 cP	-18	18	7	-171	171	178

Table F.3 Model evaluation using the measured pressure gradient of 2- and 3-in. ID pipes.

Model	No. of Data	Oil Viscosity (cP)	Statistical Parameter					
			ε_1 (%)	ε_2 (%)	ε_3 (%)	ε_4 (Pa/m)	ε_5 (Pa/m)	ε_6 (Pa/m)
TUFFP Model	297	All	-19	21	13	-140	142	139
OLGA	297	All	-27	28	15	-202	203	197
Xiao *et al* . (1990)	297	All	-27	28	16	-190	195	193
TUFFP Model	157	587 cP	-22	22	12	-196	199	162
OLGA	157	587 cP	-28	28	14	-268	270	222
Xiao *et al* . (1990)	157	587 cP	-28	28	15	-244	254	220
TUFFP Model	140	181 cP	-16	19	14	-77	77	65
OLGA	140	181 cP	-27	28	16	-128	129	129
Xiao *et al* . (1990)	140	181 cP	-27	29	16	-128	129	132

Table F.4 Model evaluation using the measured average liquid holdup of 3-in. ID pipes.

Model	No. of Data	Oil Viscosity (cP)	Statistical Parameter					
			ε_1 (%)	ε_2 (%)	ε_3 (%)	ε_4 (-)	ε_5 (-)	ε_6 (-)
TUFFP Model	489	ALL	0.7	7.5	10.1	0.004	0.05	0.06
OLGA	489	ALL	6.9	9.7	9.5	0.04	0.06	0.06
Xiao *et al* . (1990)	489	ALL	1.8	7.0	9.3	0.01	0.04	0.06
TUFFP Model	119	587 cP	0.6	5.2	6.7	0.003	0.03	0.04
OLGA	119	587 cP	5.5	7.2	6.6	0.03	0.04	0.04
Xiao *et al* . (1990)	119	587 cP	0.7	4.6	6.2	0.001	0.03	0.04
TUFFP Model	72	420 cP	1.4	5.6	7.8	0.01	0.03	0.05
OLGA	72	420 cP	6.5	6.6	6.2	0.04	0.04	0.04
Xiao *et al* . (1990)	72	420 cP	1.8	4.8	6.9	0.01	0.03	0.04
TUFFP Model	71	300 cP	-13.5	14.2	9.3	-0.09	0.10	0.06
OLGA	71	300 cP	-7.8	8.6	5.4	-0.05	0.06	0.04
Xiao *et al* . (1990)	71	300 cP	-12.2	12.8	7.2	-0.08	0.09	0.05
TUFFP Model	70	220 cP	3.6	7.0	7.8	0.02	0.04	0.05
OLGA	70	220 cP	11.1	11.1	6.6	0.06	0.06	0.03
Xiao *et al* . (1990)	70	220 cP	5.6	6.6	6.4	0.03	0.04	0.04
TUFFP Model	96	181 cP	5.5	7.1	7.8	0.03	0.04	0.05
OLGA	96	181 cP	12.4	12.4	6.0	0.07	0.07	0.03
Xiao *et al* . (1990)	96	181 cP	6.9	7.0	6.3	0.04	0.04	0.04
TUFFP Model	61	155 cP	6.2	7.9	9.8	0.03	0.04	0.05
OLGA	61	155 cP	13.4	13.4	9.7	0.07	0.07	0.04
Xiao *et al* . (1990)	61	155 cP	7.8	8.0	8.8	0.04	0.04	0.04

Table F.5 Model evaluation using the measured average liquid holdup of 2-in. ID pipes.

Model	No. of Data	Oil Viscosity (cP)	Statistical Parameter					
			ε_1 (%)	ε_2 (%)	ε_3 (%)	ε_4 (-)	ε_5 (-)	ε_6 (-)
TUFFP Model	82	ALL	7.4	9.3	10.0	0.05	0.06	0.06
OLGA	82	ALL	10.6	10.8	8.2	0.07	0.07	0.05
Xiao *et al* . (1990)	82	ALL	5.5	9.7	11.5	0.03	0.06	0.08
TUFFP Model	38	587 cP	8.7	9.9	10.0	0.06	0.06	0.06
OLGA	38	587 cP	11.5	11.6	8.6	0.07	0.07	0.05
Xiao *et al* . (1990)	38	587 cP	4.8	11.7	13.8	0.03	0.08	0.09
TUFFP Model	44	181 cP	6.2	8.8	10.0	0.04	0.06	0.06
OLGA	44	181 cP	9.9	10.1	8.0	0.06	0.06	0.05
Xiao *et al* . (1990)	44	181 cP	6.1	7.9	9.2	0.04	0.05	0.06

Table F.6 Model evaluation using the measured average liquid holdup of 2- and 3-in. ID pipes.

Model	No. of Data	Oil Viscosity (cP)	Statistical Parameter					
			ε_1 (%)	ε_2 (%)	ε_3 (%)	ε_4 (-)	ε_5 (-)	ε_6 (-)
TUFFP Model	297	All	4.0	6.9	8.6	0.03	0.04	0.05
OLGA	297	All	9.2	9.9	7.5	0.05	0.06	0.05
Xiao *et al* . (1990)	297	All	4.0	6.8	8.5	0.02	0.04	0.05
TUFFP Model	157	587 cP	2.6	6.3	8.4	0.02	0.04	0.05
OLGA	157	587 cP	7.0	8.2	7.6	0.04	0.05	0.05
Xiao *et al* . (1990)	157	587 cP	1.7	6.3	8.8	0.01	0.04	0.06
TUFFP Model	140	181 cP	5.7	7.6	8.5	0.04	0.05	0.05
OLGA	140	181 cP	11.6	11.7	6.7	0.07	0.07	0.04
Xiao *et al* . (1990)	140	181 cP	6.6	7.3	7.3	0.04	0.04	0.04

Table F.7 Model evaluation using the measured slug liquid holdup of 3-in. ID pipes.

Model	No. of Data	Oil Viscosity (cP)	Statistical Parameter					
			ε_1 (%)	ε_2 (%)	ε_3 (%)	ε_4 (-)	ε_5 (-)	ε_6 (-)
Gregory *et al* . (1978)	489	ALL	-1.0	2.9	4.2	-0.01	0.03	0.04
Gomez *et al* . (2000)	489	ALL	5.7	5.8	5.6	0.05	0.05	0.05
Barnea & Brauner (1985)	489	ALL	0.3	5.8	9.8	0.004	0.05	0.09
Andreussi & Bendiksen (1989)	489	ALL	4.7	5.0	4.6	0.04	0.05	0.04
Abdul-Majeed (2000)	489	ALL	6.6	6.6	5.5	0.06	0.06	0.05
Kora (2010)	489	ALL	2.6	3.2	3.7	0.02	0.03	0.03
Felizola (1992)	489	ALL	-16.7	16.7	3.8	-0.16	0.16	0.04
TUFFP Model	489	ALL	-0.8	3.8	6.0	-0.01	0.03	0.05
Gregory *et al* . (1978)	119	587 cP	-1.4	4.1	5.8	-0.01	0.04	0.05
Gomez *et al* . (2000)	119	587 cP	4.9	5.0	4.8	0.04	0.05	0.04
Barnea & Brauner (1985)	119	587 cP	-1.5	7.6	12.7	-0.01	0.07	0.12
Andreussi & Bendiksen (1989)	119	587 cP	3.9	5.0	5.6	0.04	0.05	0.05
Abdul-Majeed (2000)	119	587 cP	5.8	5.8	4.8	0.05	0.05	0.04
Kora (2010)	119	587 cP	1.5	3.3	4.6	0.01	0.03	0.04
Felizola (1992)	119	587 cP	-17.3	17.3	4.2	-0.16	0.16	0.04
TUFFP Model	119	587 cP	-0.2	4.7	7.1	-0.003	0.04	0.06
Gregory *et al* . (1978)	72	420 cP	-0.8	2.9	4.0	-0.01	0.03	0.04
Gomez *et al* . (2000)	72	420 cP	5.6	5.6	5.7	0.05	0.05	0.05
Barnea & Brauner (1985)	72	420 cP	-0.2	5.6	9.7	-0.001	0.05	0.09
Andreussi & Bendiksen (1989)	72	420 cP	4.5	4.7	4.3	0.04	0.04	0.04
Abdul-Majeed (2000)	72	420 cP	6.5	6.5	5.6	0.06	0.06	0.05
Kora (2010)	72	420 cP	2.4	2.6	3.4	0.02	0.02	0.03
Felizola (1992)	72	420 cP	-16.8	16.8	3.7	-0.16	0.16	0.04
TUFFP Model	72	420 cP	0.0	3.5	5.5	0.0002	0.03	0.05
Gregory *et al* . (1978)	71	300 cP	-2.8	3.1	3.0	-0.03	0.03	0.03
Gomez *et al* . (2000)	71	300 cP	4.9	5.0	5.5	0.04	0.04	0.05
Barnea & Brauner (1985)	71	300 cP	-3.0	6.0	11.6	-0.02	0.05	0.10
Andreussi & Bendiksen (1989)	71	300 cP	3.0	3.2	3.0	0.03	0.03	0.03
Abdul-Majeed (2000)	71	300 cP	5.8	5.8	5.2	0.05	0.05	0.04
Kora (2010)	71	300 cP	1.2	1.5	1.9	0.01	0.01	0.02
Felizola (1992)	71	300 cP	-18.0	18.0	2.5	-0.17	0.17	0.03
TUFFP Model	71	300 cP	-3.0	3.7	6.0	-0.03	0.03	0.05
Gregory *et al* . (1978)	70	220 cP	-1.0	2.2	3.0	-0.01	0.02	0.03
Gomez *et al* . (2000)	70	220 cP	6.5	6.5	5.8	0.06	0.06	0.05
Barnea & Brauner (1985)	70	220 cP	0.5	5.6	8.6	0.01	0.05	0.07
Andreussi & Bendiksen (1989)	70	220 cP	4.9	5.0	3.6	0.04	0.05	0.03
Abdul-Majeed (2000)	70	220 cP	7.4	7.4	5.6	0.07	0.07	0.05
Kora (2010)	70	220 cP	3.3	3.3	2.7	0.03	0.03	0.02
Felizola (1992)	70	220 cP	-16.3	16.3	3.1	-0.15	0.15	0.03
TUFFP Model	70	220 cP	-1.6	4.0	6.2	-0.01	0.04	0.05
Gregory *et al* . (1978)	96	181 cP	-0.5	1.7	2.0	-0.004	0.02	0.02
Gomez *et al* . (2000)	96	181 cP	5.9	5.9	5.2	0.05	0.05	0.04
Barnea & Brauner (1985)	96	181 cP	2.8	3.9	4.2	0.03	0.04	0.04
Andreussi & Bendiksen (1989)	96	181 cP	5.5	5.5	3.7	0.05	0.05	0.03
Abdul-Majeed (2000)	96	181 cP	6.9	6.9	5.1	0.06	0.06	0.04
Kora (2010)	96	181 cP	3.5	3.5	2.5	0.03	0.03	0.02
Felizola (1992)	96	181 cP	-16.1	16.1	3.2	-0.15	0.15	0.04
TUFFP Model	96	181 cP	-0.7	2.8	4.2	-0.01	0.03	0.04
Gregory *et al* . (1978)	61	155 cP	0.6	3.2	4.4	0.004	0.03	0.04
Gomez *et al* . (2000)	61	155 cP	7.0	7.0	6.9	0.06	0.06	0.06
Barnea & Brauner (1985)	61	155 cP	4.3	5.1	5.7	0.04	0.04	0.05
Andreussi & Bendiksen (1989)	61	155 cP	6.6	6.6	5.8	0.06	0.06	0.05
Abdul-Majeed (2000)	61	155 cP	8.0	8.0	6.9	0.07	0.07	0.06
Kora (2010)	61	155 cP	4.8	4.8	5.0	0.04	0.04	0.04
Felizola (1992)	61	155 cP	-15.1	15.1	4.8	-0.14	0.14	0.05
TUFFP Model	61	155 cP	0.2	4.0	5.8	0.001	0.04	0.05

Table F.8 Model evaluation using the measured slug liquid holdup of 2-in. ID pipes.

Model	No. of Data	Oil Viscosity (cP)	Statistical Parameter					
			ε_1 (%)	ε_2 (%)	ε_3 (%)	ε_4 (-)	ε_5 (-)	ε_6 (-)
Gregory *et al* . (1978)	72	All	-3.7	3.7	3.5	-0.03	0.03	0.03
Gomez *et al* . (2000)	72	All	7.8	8.0	6.4	0.07	0.07	0.05
Barnea & Brauner (1985)	72	All	-17.9	19.4	26.9	-0.15	0.17	0.23
Andreussi & Bendiksen (1989)	72	All	0.8	2.0	2.3	0.01	0.02	0.02
Abdul-Majeed (2000)	72	All	8.5	8.5	6.0	0.08	0.08	0.05
Kora (2010)	72	All	-0.6	0.8	0.9	-0.01	0.01	0.01
Felizola (1992)	72	All	-17.8	17.8	3.5	-0.16	0.16	0.03
TUFFP Model	72	All	-4.3	5.1	7.6	-0.04	0.04	0.06
Gregory *et al* . (1978)	36	587 cP	-3.1	3.1	3.1	-0.03	0.03	0.03
Gomez *et al* . (2000)	36	587 cP	8.6	8.6	6.9	0.07	0.08	0.06
Barnea & Brauner (1985)	36	587 cP	-19.9	21.3	28.4	-0.17	0.18	0.24
Andreussi & Bendiksen (1989)	36	587 cP	1.4	2.0	1.8	0.01	0.02	0.02
Abdul-Majeed (2000)	36	587 cP	9.2	9.2	6.4	0.08	0.08	0.05
Kora (2010)	36	587 cP	-0.9	1.0	0.8	-0.01	0.01	0.01
Felizola (1992)	36	587 cP	-17.3	17.3	3.4	-0.16	0.16	0.03
TUFFP Model	36	587 cP	-2.5	3.7	5.8	-0.02	0.03	0.05
Gregory *et al* . (1978)	36	181 cP	-4.3	4.3	3.8	-0.04	0.04	0.03
Gomez *et al* . (2000)	36	181 cP	7.1	7.3	5.9	0.06	0.06	0.05
Barnea & Brauner (1985)	36	181 cP	-15.8	17.5	25.5	-0.14	0.15	0.22
Andreussi & Bendiksen (1989)	36	181 cP	0.2	2.1	2.6	0.003	0.02	0.02
Abdul-Majeed (2000)	36	181 cP	7.8	7.8	5.4	0.07	0.07	0.05
Kora (2010)	36	181 cP	-0.3	0.7	0.9	-0.003	0.01	0.01
Felizola (1992)	36	181 cP	-18.4	18.4	3.5	-0.17	0.17	0.03
TUFFP Model	36	181 cP	-6.1	6.5	8.8	-0.05	0.06	0.07

Table F.9 Model evaluation using the measured slug liquid holdup of 2- and 3-in. ID pipes.

Model	No. of Data	Oil Viscosity (cP)	Statistical Parameter					
			ε_1 (%)	ε_2 (%)	ε_3 (%)	ε_4 (-)	ε_5 (-)	ε_6 (-)
Gregory *et al* . (1978)	287	All	-1.7	3.2	4.5	-0.02	0.03	0.04
Gomez *et al* . (2000)	287	All	6.0	6.1	5.5	0.05	0.05	0.05
Barnea & Brauner (1985)	287	All	-4.2	9.3	17.8	-0.035	0.08	0.15
Andreussi & Bendiksen (1989)	287	All	3.7	4.4	4.7	0.03	0.04	0.04
Abdul-Majeed (2000)	287	All	6.9	6.9	5.3	0.06	0.06	0.04
Kora (2010)	287	All	1.6	2.8	3.7	0.01	0.03	0.03
Felizola (1992)	287	All	-17.0	17.0	3.8	-0.16	0.16	0.04
TUFFP Model	287	All	-1.4	4.2	6.6	-0.01	0.04	0.06
Gregory *et al* . (1978)	155	587 cP	-1.8	3.9	5.4	-0.02	0.04	0.05
Gomez *et al* . (2000)	155	587 cP	5.8	5.9	5.6	0.05	0.05	0.05
Barnea & Brauner (1985)	155	587 cP	-5.8	10.8	19.2	-0.05	0.10	0.17
Andreussi & Bendiksen (1989)	155	587 cP	3.3	4.3	5.1	0.03	0.04	0.04
Abdul-Majeed (2000)	155	587 cP	6.6	6.6	5.4	0.06	0.06	0.04
Kora (2010)	155	587 cP	0.9	2.8	4.1	0.01	0.03	0.04
Felizola (1992)	155	587 cP	-17.3	17.3	4.0	-0.16	0.16	0.04
TUFFP Model	155	587 cP	-0.8	4.5	6.8	-0.01	0.04	0.06
Gregory *et al* . (1978)	132	181 cP	-1.5	2.4	3.1	-0.01	0.02	0.03
Gomez *et al* . (2000)	132	181 cP	6.2	6.3	5.4	0.06	0.06	0.05
Barnea & Brauner (1985)	132	181 cP	-2.2	7.6	16.0	-0.02	0.07	0.14
Andreussi & Bendiksen (1989)	132	181 cP	4.1	4.6	4.1	0.04	0.04	0.04
Abdul-Majeed (2000)	132	181 cP	7.1	7.1	5.2	0.06	0.06	0.04
Kora (2010)	132	181 cP	2.5	2.7	2.8	0.02	0.02	0.02
Felizola (1992)	132	181 cP	-16.7	16.7	3.4	-0.16	0.16	0.04
TUFFP Model	132	181 cP	-2.2	3.8	6.3	-0.02	0.03	0.05

Table F.10 Model evaluation using the measured film liquid holdup of 3-in. ID pipes.

Model	No. of Data	Oil Viscosity (cP)	Statistical Parameter					
			ε_1 (%)	ε_2 (%)	ε_3 (%)	ε_4 (-)	ε_5 (-)	ε_6 (-)
TUFFP Model	489	All	3.0	10	13	0.02	0.06	0.07
TUFFP Model	119	587 cP	0.4	10	12	0.0003	0.06	0.07
TUFFP Model	72	420 cP	2.5	12	14	0.01	0.07	0.08
TUFFP Model	71	300 cP	1.1	11	14	0.01	0.06	0.08
TUFFP Model	70	220 cP	2.8	10	12	0.02	0.05	0.07
TUFFP Model	96	181 cP	6.1	10	12	0.03	0.06	0.07
TUFFP Model	61	155 cP	6.1	11	13	0.03	0.06	0.07

Table F.11 Model evaluation using the measured film liquid holdup of 2-in. ID pipes.

Model	No. of Data	Oil Viscosity (cP)	Statistical Parameter					
			ε_1 (%)	ε_2 (%)	ε_3 (%)	ε_4 (-)	ε_5 (-)	ε_6 (-)
TUFFP Model	71	All	-16	18	14	-0.10	0.11	0.08
TUFFP Model	35	587 cP	-13	15	13	-0.07	0.09	0.08
TUFFP Model	36	181 cP	-19	21	15	-0.12	0.13	0.09

Table F.12 Model evaluation using the measured film liquid holdup of 2- and 3-in. ID pipes.

Model	No. of Data	Oil Viscosity (cP)	Statistical Parameter					
			ε_1 (%)	ε_2 (%)	ε_3 (%)	ε_4 (-)	ε_5 (-)	ε_6 (-)
TUFFP Model	286	All	-1.7	12	15	-0.012	0.07	0.09
TUFFP Model	154	587 cP	-2.6	11	13	-0.02	0.06	0.08
TUFFP Model	132	181 cP	-0.7	13	17	-0.01	0.08	0.10

Table F.13 Model evaluation using the translational velocity of 3-in. ID pipes.

Model	No. of Data	Oil Viscosity (cP)	Statistical Parameter					
			ε_1 (%)	ε_2 (%)	ε_3 (%)	ε_4 (m/s)	ε_5 (m/s)	ε_6 (m/s)
Gokcal (2008)	465	All	19	19	13	0.40	0.40	0.36
Bendiksen (1984)	465	All	23	23	13	0.52	0.52	0.43
Beattie & Sugawara (1986)	465	All	-17	17	9	-0.45	0.45	0.31
Bonnecaze *et al* . (1971)	465	All	-25	25	8	-0.63	0.63	0.37
Choi *et al* . (2012)	465	All	-6	10	9	-0.10	0.22	0.28
Clark & Flemmer (1985)	465	All	-18	20	12	-0.35	0.43	0.33
Fabre (1994)	465	All	29	29	14	0.63	0.63	0.38
Gomez *et al* . (2000)	465	All	-33	33	7	-0.79	0.79	0.40
Greskovich & Cooper (1975)	465	All	-51	51	7	-1.18	1.18	0.50
Hibiki & Ishii (2003)	465	All	-25	25	8	-0.64	0.64	0.38
Kataoka & Ishii (1987)	465	All	-41	41	8	-0.93	0.93	0.38
Mishima & Hibiki (2003)	465	All	-17	19	12	-0.30	0.38	0.28
Petalas & Aziz (2000)	465	All	-9	13	12	-0.28	0.33	0.30
Rouhani & Axelsson (1970)	465	All	-37	37	6	-0.88	0.88	0.42
Shipley (1982)	465	All	-22	22	8	-0.56	0.57	0.35
Shoham (1982)	465	All	-12	16	13	-0.40	0.43	0.37
Gokcal (2008)	112	587 cP	14	14	11	0.28	0.29	0.32
Bendiksen (1984)	112	587 cP	23	23	12	0.48	0.48	0.39
Beattie & Sugawara (1986)	112	587 cP	-16	16	8	-0.42	0.42	0.34
Bonnecaze *et al* . (1971)	112	587 cP	-25	25	7	-0.63	0.63	0.42
Choi *et al* . (2012)	112	587 cP	-4	9	10	0.00	0.21	0.33
Clark & Flemmer (1985)	112	587 cP	-20	21	11	-0.39	0.44	0.32
Fabre (1994)	112	587 cP	34	34	12	0.74	0.74	0.48
Gomez *et al* . (2000)	112	587 cP	-33	33	6	-0.79	0.79	0.46
Greskovich & Cooper (1975)	112	587 cP	-52	52	6	-1.17	1.17	0.56
Hibiki & Ishii (2003)	112	587 cP	-25	25	7	-0.64	0.64	0.43
Kataoka & Ishii (1987)	112	587 cP	-42	42	7	-0.93	0.93	0.43
Mishima & Hibiki (2003)	112	587 cP	-18	19	10	-0.33	0.38	0.27
Petalas & Aziz (2000)	112	587 cP	-7	12	12	-0.25	0.30	0.33
Rouhani & Axelsson (1970)	112	587 cP	-37	37	5	-0.87	0.87	0.48
Shipley (1982)	112	587 cP	-22	22	8	-0.56	0.56	0.40
Shoham (1982)	112	587 cP	-11	16	14	-0.39	0.43	0.42
Gokcal (2008)	72	420 cP	18	18	15	0.36	0.36	0.40
Bendiksen (1984)	72	420 cP	24	24	15	0.53	0.53	0.48
Beattie & Sugawara (1986)	72	420 cP	-16	17	10	-0.45	0.46	0.38
Bonnecaze *et al* . (1971)	72	420 cP	-24	24	10	-0.65	0.65	0.45
Choi *et al* . (2012)	72	420 cP	-4	9	11	-0.02	0.23	0.35
Clark & Flemmer (1985)	72	420 cP	-19	21	13	-0.38	0.47	0.39
Fabre (1994)	72	420 cP	34	34	15	0.74	0.74	0.48
Gomez *et al* . (2000)	72	420 cP	-32	32	7	-0.81	0.81	0.49
Greskovich & Cooper (1975)	72	420 cP	-52	52	7	-1.21	1.21	0.60
Hibiki & Ishii (2003)	72	420 cP	-25	25	10	-0.66	0.66	0.46
Kataoka & Ishii (1987)	72	420 cP	-42	42	8	-0.95	0.95	0.46
Mishima & Hibiki (2003)	72	420 cP	-17	20	12	-0.31	0.41	0.33
Petalas & Aziz (2000)	72	420 cP	-6	14	15	-0.28	0.37	0.37
Rouhani & Axelsson (1970)	72	420 cP	-36	36	7	-0.90	0.90	0.51
Shipley (1982)	72	420 cP	-22	22	10	-0.59	0.59	0.43
Shoham (1982)	72	420 cP	-10	18	17	-0.41	0.47	0.45
Gokcal (2008)	65	300 cP	19	19	13	0.42	0.42	0.36
Bendiksen (1984)	65	300 cP	22	22	12	0.52	0.52	0.45
Beattie & Sugawara (1986)	65	300 cP	-18	18	8	-0.48	0.48	0.30
Bonnecaze *et al* . (1971)	65	300 cP	-26	26	7	-0.67	0.67	0.37
Choi *et al* . (2012)	65	300 cP	-6	10	9	-0.08	0.22	0.24
Clark & Flemmer (1985)	65	300 cP	-19	20	12	-0.39	0.45	0.34
Fabre (1994)	65	300 cP	29	29	12	0.66	0.66	0.35
Gomez *et al* . (2000)	65	300 cP	-33	33	6	-0.83	0.83	0.40
Greskovich & Cooper (1975)	65	300 cP	-52	52	7	-1.24	1.24	0.51
Hibiki & Ishii (2003)	65	300 cP	-26	26	7	-0.68	0.68	0.38
Kataoka & Ishii (1987)	65	300 cP	-42	42	8	-0.97	0.97	0.38
Mishima & Hibiki (2003)	65	300 cP	-17	19	11	-0.32	0.38	0.28
Petalas & Aziz (2000)	65	300 cP	-10	13	11	-0.32	0.35	0.29
Rouhani & Axelsson (1970)	65	300 cP	-37	37	6	-0.92	0.92	0.43
Shipley (1982)	65	300 cP	-23	23	9	-0.60	0.61	0.35
Shoham (1982)	65	300 cP	-13	17	13	-0.44	0.47	0.37

Gokcal (2008)	63	220 cP	20	20	14	0.43	0.43	0.34
Bendiksen (1984)	63	220 cP	21	21	13	0.49	0.50	0.42
Beattie & Sugawara (1986)	63	220 cP	-19	19	8	-0.48	0.48	0.28
Bonnecaze *et al* . (1971)	63	220 cP	-26	26	8	-0.65	0.65	0.33
Choi *et al* . (2012)	63	220 cP	-8	10	8	-0.16	0.22	0.20
Clark & Flemmer (1985)	63	220 cP	-19	20	12	-0.37	0.42	0.30
Fabre (1994)	63	220 cP	26	26	13	0.55	0.55	0.26
Gomez *et al* . (2000)	63	220 cP	-34	34	7	-0.81	0.81	0.35
Greskovich & Cooper (1975)	63	220 cP	-52	52	7	-1.20	1.20	0.44
Hibiki & Ishii (2003)	63	220 cP	-27	27	8	-0.66	0.66	0.33
Kataoka & Ishii (1987)	63	220 cP	-42	42	8	-0.94	0.94	0.33
Mishima & Hibiki (2003)	63	220 cP	-18	19	12	-0.33	0.38	0.27
Petalas & Aziz (2000)	63	220 cP	-11	14	11	-0.32	0.34	0.27
Rouhani & Axelsson (1970)	63	220 cP	-38	38	6	-0.89	0.89	0.37
Shipley (1982)	63	220 cP	-24	24	7	-0.58	0.58	0.30
Shoham (1982)	63	220 cP	-14	17	12	-0.41	0.44	0.33
Gokcal (2008)	92	181 cP	21	21	14	0.46	0.46	0.36
Bendiksen (1984)	92	181 cP	24	24	13	0.56	0.56	0.43
Beattie & Sugawara (1986)	92	181 cP	-17	18	9	-0.43	0.43	0.27
Bonnecaze *et al* . (1971)	92	181 cP	-24	24	8	-0.59	0.59	0.31
Choi *et al* . (2012)	92	181 cP	-8	10	8	-0.16	0.22	0.21
Clark & Flemmer (1985)	92	181 cP	-16	18	13	-0.29	0.37	0.31
Fabre (1994)	92	181 cP	27	27	15	0.53	0.53	0.24
Gomez *et al* . (2000)	92	181 cP	-32	32	7	-0.74	0.74	0.34
Greskovich & Cooper (1975)	92	181 cP	-51	51	7	-1.14	1.14	0.42
Hibiki & Ishii (2003)	92	181 cP	-25	25	8	-0.60	0.60	0.32
Kataoka & Ishii (1987)	92	181 cP	-40	40	9	-0.88	0.88	0.32
Mishima & Hibiki (2003)	92	181 cP	-15	18	13	-0.26	0.35	0.28
Petalas & Aziz (2000)	92	181 cP	-9	13	11	-0.26	0.31	0.26
Rouhani & Axelsson (1970)	92	181 cP	-36	36	7	-0.83	0.83	0.35
Shipley (1982)	92	181 cP	-22	22	8	-0.52	0.52	0.29
Shoham (1982)	92	181 cP	-11	15	13	-0.35	0.39	0.31
Gokcal (2008)	61	155 cP	22	22	12	0.52	0.52	0.36
Bendiksen (1984)	61	155 cP	23	23	11	0.57	0.57	0.44
Beattie & Sugawara (1986)	61	155 cP	-19	19	7	-0.46	0.46	0.25
Bonnecaze *et al* . (1971)	61	155 cP	-25	25	7	-0.62	0.62	0.29
Choi *et al* . (2012)	61	155 cP	-10	11	7	-0.21	0.24	0.20
Clark & Flemmer (1985)	61	155 cP	-16	19	13	-0.30	0.39	0.32
Fabre (1994)	61	155 cP	23	23	12	0.47	0.47	0.22
Gomez *et al* . (2000)	61	155 cP	-33	33	6	-0.78	0.78	0.31
Greskovich & Cooper (1975)	61	155 cP	-50	50	7	-1.18	1.18	0.40
Hibiki & Ishii (2003)	61	155 cP	-26	26	7	-0.63	0.63	0.29
Kataoka & Ishii (1987)	61	155 cP	-40	40	8	-0.91	0.91	0.29
Mishima & Hibiki (2003)	61	155 cP	-15	17	13	-0.27	0.35	0.28
Petalas & Aziz (2000)	61	155 cP	-11	12	9	-0.30	0.31	0.24
Rouhani & Axelsson (1970)	61	155 cP	-36	36	6	-0.86	0.86	0.33
Shipley (1982)	61	155 cP	-23	23	7	-0.55	0.55	0.27
Shoham (1982)	61	155 cP	-13	15	10	-0.38	0.40	0.29

Table F.14 Model evaluation using the translational velocity of 2-in. ID pipes.

Model	No. of Data	Oil Viscosity (cP)	Statistical Parameter					
			ε_1 (%)	ε_2 (%)	ε_3 (%)	ε_4 (m/s)	ε_5 (m/s)	ε_6 (m/s)
Gokcal (2008)	82	All	7	14	18	0.05	0.20	0.25
Bendiksen (1984)	82	All	28	28	24	0.40	0.40	0.24
Beattie & Sugawara (1986)	82	All	-12	19	17	-0.41	0.46	0.42
Bonnecaze *et al* . (1971)	82	All	-22	24	15	-0.60	0.62	0.50
Choi *et al* . (2012)	82	All	-0.1	10	14	-0.03	0.17	0.23
Clark & Flemmer (1985)	82	All	-15	18	15	-0.39	0.42	0.38
Fabre (1994)	82	All	39	39	26	0.59	0.59	0.27
Gomez *et al* . (2000)	82	All	-27	28	13	-0.69	0.70	0.53
Greskovich & Cooper (1975)	82	All	-50	50	7	-1.06	1.06	0.62
Hibiki & Ishii (2003)	82	All	-22	24	15	-0.61	0.62	0.50
Kataoka & Ishii (1987)	82	All	-39	39	9	-0.84	0.84	0.50
Mishima & Hibiki (2003)	82	All	-14	16	12	-0.30	0.32	0.25
Petalas & Aziz (2000)	82	All	-4	19	22	-0.29	0.39	0.41
Rouhani & Axelsson (1970)	82	All	-32	32	11	-0.77	0.77	0.55
Shipley (1982)	82	All	-17	22	18	-0.53	0.56	0.49
Shoham (1982)	82	All	-0.2	25	30	-0.31	0.48	0.50
Gokcal (2008)	38	587 cP	-5	9	9	-0.11	0.19	0.23
Bendiksen (1984)	38	587 cP	18	19	17	0.28	0.29	0.26
Beattie & Sugawara (1986)	38	587 cP	-17	19	12	-0.46	0.47	0.35
Bonnecaze *et al* . (1971)	38	587 cP	-28	28	11	-0.67	0.67	0.44
Choi *et al* . (2012)	38	587 cP	-7	10	10	-0.09	0.20	0.25
Clark & Flemmer (1985)	38	587 cP	-21	21	10	-0.47	0.47	0.34
Fabre (1994)	38	587 cP	30	30	17	0.54	0.54	0.35
Gomez *et al* . (2000)	38	587 cP	-33	33	9	-0.76	0.76	0.47
Greskovich & Cooper (1975)	38	587 cP	-54	54	6	-1.12	1.12	0.55
Hibiki & Ishii (2003)	38	587 cP	-28	28	11	-0.68	0.68	0.45
Kataoka & Ishii (1987)	38	587 cP	-45	45	6	-0.92	0.92	0.45
Mishima & Hibiki (2003)	38	587 cP	-21	22	10	-0.40	0.41	0.24
Petalas & Aziz (2000)	38	587 cP	-9	17	17	-0.34	0.39	0.34
Rouhani & Axelsson (1970)	38	587 cP	-38	38	7	-0.84	0.84	0.49
Shipley (1982)	38	587 cP	-23	24	13	-0.60	0.60	0.43
Shoham (1982)	38	587 cP	-7	23	25	-0.38	0.48	0.44
Gokcal (2008)	44	181 cP	17	18	18	0.19	0.21	0.17
Bendiksen (1984)	44	181 cP	37	37	26	0.50	0.50	0.17
Beattie & Sugawara (1986)	44	181 cP	-8	19	19	-0.37	0.45	0.46
Bonnecaze *et al* . (1971)	44	181 cP	-17	21	17	-0.54	0.57	0.54
Choi *et al* . (2012)	44	181 cP	6	10	13	0.02	0.15	0.20
Clark & Flemmer (1985)	44	181 cP	-9	16	16	-0.32	0.37	0.40
Fabre (1994)	44	181 cP	46	46	30	0.64	0.64	0.17
Gomez *et al* . (2000)	44	181 cP	-22	23	14	-0.63	0.64	0.57
Greskovich & Cooper (1975)	44	181 cP	-46	46	6	-1.01	1.01	0.67
Hibiki & Ishii (2003)	44	181 cP	-17	21	17	-0.55	0.57	0.54
Kataoka & Ishii (1987)	44	181 cP	-34	34	7	-0.77	0.77	0.54
Mishima & Hibiki (2003)	44	181 cP	-8	12	10	-0.21	0.24	0.23
Petalas & Aziz (2000)	44	181 cP	1.5	21	24	-0.24	0.40	0.45
Rouhani & Axelsson (1970)	44	181 cP	-28	28	12	-0.71	0.71	0.59
Shipley (1982)	44	181 cP	-12	21	20	-0.46	0.53	0.53
Shoham (1982)	44	181 cP	6	27	33	-0.24	0.47	0.54

Table F.15 Model evaluation using the translational velocity of 2- and 3-in. ID pipes.

Model	No. of Data	Oil Viscosity (cP)	Statistical Parameter					
			ε_1 (%)	ε_2 (%)	ε_3 (%)	ε_4 (m/s)	ε_5 (m/s)	ε_6 (m/s)
Gokcal (2008)	286	All	14	16	15	0.27	0.32	0.35
Bendiksen (1984)	286	All	25	25	17	0.48	0.48	0.37
Beattie & Sugawara (1986)	286	All	-15	17	12	-0.42	0.44	0.34
Bonnecaze *et al* . (1971)	286	All	-24	24	11	-0.61	0.61	0.42
Choi *et al* . (2012)	286	All	-4	9	11	-0.06	0.20	0.28
Clark & Flemmer (1985)	286	All	-17	19	13	-0.36	0.41	0.34
Fabre (1994)	286	All	33	33	19	0.63	0.63	0.37
Gomez *et al* . (2000)	286	All	-31	31	9	-0.75	0.75	0.45
Greskovich & Cooper (1975)	286	All	-51	51	7	-1.13	1.13	0.54
Hibiki & Ishii (2003)	286	All	-24	25	11	-0.62	0.62	0.42
Kataoka & Ishii (1987)	286	All	-41	41	8	-0.89	0.89	0.42
Mishima & Hibiki (2003)	286	All	-16	18	11	-0.30	0.35	0.27
Petalas & Aziz (2000)	286	All	-6	14	15	-0.27	0.33	0.33
Rouhani & Axelsson (1970)	286	All	-35	35	8	-0.83	0.83	0.46
Shipley (1982)	286	All	-21	22	12	-0.54	0.55	0.39
Shoham (1982)	286	All	-8	18	20	-0.35	0.43	0.42
Gokcal (2008)	150	587 cP	9	13	13	0.18	0.27	0.35
Bendiksen (1984)	150	587 cP	22	22	13	0.43	0.43	0.37
Beattie & Sugawara (1986)	150	587 cP	-16	17	9	-0.43	0.43	0.34
Bonnecaze *et al* . (1971)	150	587 cP	-26	26	9	-0.64	0.64	0.43
Choi *et al* . (2012)	150	587 cP	-5	9	10	-0.03	0.21	0.31
Clark & Flemmer (1985)	150	587 cP	-20	21	11	-0.41	0.45	0.33
Fabre (1994)	150	587 cP	33	33	14	0.69	0.69	0.46
Gomez *et al* . (2000)	150	587 cP	-33	33	7	-0.78	0.78	0.46
Greskovich & Cooper (1975)	150	587 cP	-53	53	6	-1.16	1.16	0.55
Hibiki & Ishii (2003)	150	587 cP	-26	26	9	-0.65	0.65	0.43
Kataoka & Ishii (1987)	150	587 cP	-43	43	7	-0.93	0.93	0.43
Mishima & Hibiki (2003)	150	587 cP	-19	20	10	-0.35	0.39	0.26
Petalas & Aziz (2000)	150	587 cP	-7	13	13	-0.28	0.33	0.33
Rouhani & Axelsson (1970)	150	587 cP	-37	37	6	-0.86	0.86	0.48
Shipley (1982)	150	587 cP	-22	23	9	-0.57	0.57	0.40
Shoham (1982)	150	587 cP	-10	17	17	-0.39	0.45	0.43
Gokcal (2008)	136	181 cP	20	20	15	0.37	0.38	0.33
Bendiksen (1984)	136	181 cP	28	28	19	0.54	0.54	0.37
Beattie & Sugawara (1986)	136	181 cP	-14	18	14	-0.41	0.44	0.34
Bonnecaze *et al* . (1971)	136	181 cP	-22	23	12	-0.57	0.58	0.40
Choi *et al* . (2012)	136	181 cP	-4	10	12	-0.10	0.20	0.22
Clark & Flemmer (1985)	136	181 cP	-14	17	14	-0.30	0.37	0.34
Fabre (1994)	136	181 cP	33	33	23	0.57	0.57	0.23
Gomez *et al* . (2000)	136	181 cP	-29	29	11	-0.71	0.71	0.43
Greskovich & Cooper (1975)	136	181 cP	-49	49	7	-1.09	1.09	0.52
Hibiki & Ishii (2003)	136	181 cP	-22	23	12	-0.58	0.59	0.40
Kataoka & Ishii (1987)	136	181 cP	-38	38	9	-0.84	0.84	0.41
Mishima & Hibiki (2003)	136	181 cP	-13	16	12	-0.25	0.31	0.26
Petalas & Aziz (2000)	136	181 cP	-5	15	17	-0.26	0.34	0.33
Rouhani & Axelsson (1970)	136	181 cP	-33	33	10	-0.79	0.79	0.45
Shipley (1982)	136	181 cP	-18	21	14	-0.50	0.52	0.38
Shoham (1982)	136	181 cP	-6	19	23	-0.32	0.42	0.40

Table F.16 Model evaluation using the measured slug length of 3-in. ID pipes.

Model	No. of Data	Oil Viscosity (cP)	Statistical Parameter					
			ε_1 (%)	ε_2 (%)	ε_3 (%)	ε_4 (m)	ε_5 (m)	ε_6 (m)
Dukler & Hubbard (1975)	489	All	314	314	218	1.63	1.63	0.24
Andreussi (1975)	489	All	204	204	160	1.02	1.02	0.24
Nicholson *et al* . (1978)	489	All	314	314	218	1.63	1.63	0.24
Gregory *et al* . (1978)	489	All	314	314	218	1.63	1.63	0.24
Nydal *et al* . (1992)	489	All	121	121	117	0.56	0.57	0.24
Manolis (1995)	489	All	245	245	182	1.25	1.25	0.24
Scott *et al* . (1986)	489	All	1504	1504	846	8.20	8.20	0.24
Brill *et al* . (1981)	489	All	1156	1156	710	6.20	6.20	0.47
Norris (1981)	489	All	1107	1107	637	6.01	6.01	0.24
Marcano *et al* . (1998)	489	All	411	411	203	2.68	2.68	1.53
Barnea & Brauner (1985)	489	All	341	341	233	1.78	1.78	0.24
Al-safran *et al* . (2011)	489	All	177	177	122	0.92	0.92	0.26
TUFFP Model	489	All	341	341	233	1.78	1.78	0.24
Dukler & Hubbard (1975)	119	587 cP	468	468	327	1.79	1.79	0.21
Andreussi (1975)	119	587 cP	316	316	240	1.18	1.18	0.21
Nicholson *et al* . (1978)	119	587 cP	468	468	327	1.79	1.79	0.21
Gregory *et al* . (1978)	119	587 cP	468	468	327	1.79	1.79	0.21
Nydal *et al* . (1992)	119	587 cP	203	203	174	0.72	0.72	0.21
Manolis (1995)	119	587 cP	373	373	273	1.40	1.40	0.21
Scott *et al* . (1986)	119	587 cP	2100	2100	1267	8.36	8.36	0.21
Brill *et al* . (1981)	119	587 cP	1625	1625	1070	6.34	6.34	0.43
Norris (1981)	119	587 cP	1556	1556	954	6.16	6.16	0.21
Marcano *et al* . (1998)	119	587 cP	601	601	224	3.01	3.01	1.61
Barnea & Brauner (1985)	119	587 cP	506	506	349	1.94	1.94	0.21
Al-safran *et al* . (2011)	119	587 cP	211	211	179	0.75	0.75	0.21
TUFFP Model	119	587 cP	506	506	349	1.94	1.94	0.21
Dukler & Hubbard (1975)	72	420 cP	312	312	166	1.66	1.66	0.21
Andreussi (1975)	72	420 cP	202	202	122	1.05	1.05	0.21
Nicholson *et al* . (1978)	72	420 cP	312	312	166	1.66	1.66	0.21
Gregory *et al* . (1978)	72	420 cP	312	312	166	1.66	1.66	0.21
Nydal *et al* . (1992)	72	420 cP	120	120	89	0.59	0.59	0.21
Manolis (1995)	72	420 cP	243	243	138	1.28	1.28	0.21
Scott *et al* . (1986)	72	420 cP	1497	1497	643	8.23	8.23	0.21
Brill *et al* . (1981)	72	420 cP	1146	1146	555	6.20	6.20	0.46
Norris (1981)	72	420 cP	1101	1101	484	6.04	6.04	0.21
Marcano *et al* . (1998)	72	420 cP	428	428	162	2.86	2.86	1.66
Barnea & Brauner (1985)	72	420 cP	340	340	177	1.81	1.81	0.21
Al-safran *et al* . (2011)	72	420 cP	153	153	102	0.77	0.77	0.21
TUFFP Model	72	420 cP	340	340	177	1.81	1.81	0.21
Dukler & Hubbard (1975)	71	300 cP	304	304	132	1.66	1.66	0.21
Andreussi (1975)	71	300 cP	196	196	97	1.05	1.05	0.21
Nicholson *et al* . (1978)	71	300 cP	304	304	132	1.66	1.66	0.21
Gregory *et al* . (1978)	71	300 cP	304	304	132	1.66	1.66	0.21
Nydal *et al* . (1992)	71	300 cP	116	116	71	0.59	0.59	0.21
Manolis (1995)	71	300 cP	237	237	110	1.28	1.28	0.21
Scott *et al* . (1986)	71	300 cP	1466	1466	512	8.23	8.23	0.21
Brill *et al* . (1981)	71	300 cP	1132	1132	449	6.25	6.25	0.49
Norris (1981)	71	300 cP	1078	1078	386	6.04	6.04	0.21
Marcano *et al* . (1998)	71	300 cP	379	379	172	2.62	2.62	1.75
Barnea & Brauner (1985)	71	300 cP	331	331	141	1.81	1.81	0.21
Al-safran *et al* . (2011)	71	300 cP	174	174	90	0.92	0.92	0.21
TUFFP Model	71	300 cP	331	331	141	1.81	1.81	0.21
Dukler & Hubbard (1975)	70	220 cP	261	261	138	1.57	1.57	0.24
Andreussi (1975)	70	220 cP	165	165	101	0.96	0.96	0.24
Nicholson *et al* . (1978)	70	220 cP	261	261	138	1.57	1.57	0.24
Gregory *et al* . (1978)	70	220 cP	261	261	138	1.57	1.57	0.24
Nydal *et al* . (1992)	70	220 cP	93	94	74	0.51	0.52	0.24
Manolis (1995)	70	220 cP	201	201	115	1.19	1.19	0.24
Scott *et al* . (1986)	70	220 cP	1301	1301	534	8.14	8.14	0.24
Brill *et al* . (1981)	70	220 cP	1002	1002	462	6.17	6.17	0.49
Norris (1981)	70	220 cP	954	954	402	5.95	5.95	0.24
Marcano *et al* . (1998)	70	220 cP	313	313	118	2.39	2.39	1.37
Barnea & Brauner (1985)	70	220 cP	286	286	147	1.73	1.73	0.24
Al-safran *et al* . (2011)	70	220 cP	172	172	104	1.00	1.00	0.24
TUFFP Model	70	220 cP	286	286	147	1.73	1.73	0.24

Dukler & Hubbard (1975)	96	181 cP	248	248	127	1.55	1.55	0.23
Andreussi (1975)	96	181 cP	155	155	93	0.94	0.94	0.23
Nicholson *et al* . (1978)	96	181 cP	248	248	127	1.55	1.55	0.23
Gregory *et al* . (1978)	96	181 cP	248	248	127	1.55	1.55	0.23
Nydal *et al* . (1992)	96	181 cP	86	86	68	0.48	0.49	0.23
Manolis (1995)	96	181 cP	190	190	106	1.17	1.17	0.23
Scott *et al* . (1986)	96	181 cP	1249	1249	494	8.12	8.12	0.23
Brill *et al* . (1981)	96	181 cP	955	955	419	6.12	6.12	0.47
Norris (1981)	96	181 cP	915	915	371	5.93	5.93	0.23
Marcano *et al* . (1998)	96	181 cP	343	343	145	2.55	2.55	1.35
Barnea & Brauner (1985)	96	181 cP	271	271	136	1.70	1.70	0.23
Al-safran *et al* . (2011)	96	181 cP	178	178	101	1.09	1.09	0.23
TUFFP Model	96	181 cP	271	271	136	1.70	1.70	0.23
Dukler & Hubbard (1975)	61	155 cP	191	191	68	1.46	1.46	0.18
Andreussi (1975)	61	155 cP	113	113	50	0.85	0.85	0.18
Nicholson *et al* . (1978)	61	155 cP	191	191	68	1.46	1.46	0.18
Gregory *et al* . (1978)	61	155 cP	191	191	68	1.46	1.46	0.18
Nydal *et al* . (1992)	61	155 cP	55	55	36	0.39	0.40	0.18
Manolis (1995)	61	155 cP	142	142	57	1.08	1.08	0.18
Scott *et al* . (1986)	61	155 cP	1026	1026	263	8.03	8.03	0.18
Brill *et al* . (1981)	61	155 cP	778	778	231	6.03	6.03	0.40
Norris (1981)	61	155 cP	748	748	198	5.84	5.84	0.18
Marcano *et al* . (1998)	61	155 cP	277	277	112	2.40	2.40	1.30
Barnea & Brauner (1985)	61	155 cP	210	210	72	1.61	1.61	0.18
Al-safran *et al* . (2011)	61	155 cP	143	143	57	1.08	1.08	0.19
TUFFP Model	61	155 cP	210	210	72	1.61	1.61	0.18

Table F.17 Model evaluation using the measured slug length of 2-in. ID pipes.

			Statistical Parameter					
Model	No. of Data	Oil Viscosity (cP)	ε_1 (%)	ε_2 (%)	ε_3 (%)	ε_4 (m)	ε_5 (m)	ε_6 (m)
Dukler & Hubbard (1975)	55	155 cP	277	278	93	1.07	1.09	0.24
Andreussi (1975)	55	155 cP	177	178	68	0.67	0.70	0.24
Nicholson *et al* . (1978)	55	155 cP	277	278	93	1.07	1.09	0.24
Gregory *et al* . (1978)	55	155 cP	277	278	93	1.07	1.09	0.24
Nydal *et al* . (1992)	55	155 cP	151	153	62	0.57	0.60	0.24
Manolis (1995)	55	155 cP	214.3	216	78	0.82	0.84	0.24
Scott *et al* . (1986)	55	155 cP	500	500	148	1.98	1.98	0.24
Brill *et al* . (1981)	55	155 cP	453	453	140	1.78	1.78	0.28
Norris (1981)	55	155 cP	479	479	143	1.89	1.89	0.24
Marcano *et al* . (1998)	55	155 cP	132	174	236	0.55	0.72	0.89
Barnea & Brauner (1985)	55	155 cP	302	303	99	1.18	1.19	0.24
Al-safran *et al* . (2011)	55	155 cP	284	285	94	1.10	1.11	0.24
TUFFP Model	55	155 cP	302	303	99	1.18	1.19	0.24

Table F.18 Model evaluation using the measured slug length of 2- and 3-in. ID pipes.

			Statistical Parameter					
Model	No. of Data	Oil Viscosity (cP)	ε_1 (%)	ε_2 (%)	ε_3 (%)	ε_4 (m)	ε_5 (m)	ε_6 (m)
Dukler & Hubbard (1975)	116	155 cP	232	232	91	1.28	1.28	0.29
Andreussi (1975)	116	155 cP	143	144	67	0.76	0.78	0.23
Nicholson *et al* . (1978)	116	155 cP	232	232	91	1.28	1.28	0.29
Gregory *et al* . (1978)	116	155 cP	232	232	91	1.28	1.28	0.29
Nydal *et al* . (1992)	116	155 cP	101	102	70	0.47	0.49	0.23
Manolis (1995)	116	155 cP	176	177	76	0.96	0.97	0.25
Scott *et al* . (1986)	116	155 cP	777	777	341	5.16	5.16	3.04
Brill *et al* . (1981)	116	155 cP	624	624	252	4.02	4.02	2.16
Norris (1981)	116	155 cP	620	620	220	3.96	3.96	1.99
Marcano *et al* . (1998)	116	155 cP	208	228	195	1.52	1.60	1.45
Barnea & Brauner (1985)	116	155 cP	254	254	98	1.40	1.41	0.30
Al-safran *et al* . (2011)	116	155 cP	210	210	104	1.09	1.10	0.21
TUFFP Model	116	155 cP	254	254	98	1.40	1.41	0.30

Table F.19 Model evaluation using the measured slug frequency of 3-in. ID pipes.

Model	No. of Data	Oil Viscosity (cP)	Statistical Parameter					
			ε_1 (%)	ε_2 (%)	ε_3 (%)	ε_4 (slug/s)	ε_5 (slug/s)	ε_6 (slug/s)
Taitel & Dukler (1977)	489	ALL	836	837	804	2.13	2.13	2.20
Gregory & Scott (1969)	489	ALL	-28	50	66	-0.09	0.12	0.15
Greskovich & Shrier (1972)	489	ALL	-28	50	66	-0.09	0.12	0.15
Heywood & Richardson (1979)	489	ALL	6	49	97	-0.03	0.10	0.14
Hill & Wood I (1990)	489	ALL	124	157	340	0.02	0.20	0.26
Hill & Wood II (1990)	489	ALL	520	520	753	1.02	1.02	0.86
Tronconi (1990)	489	ALL	10	82	168	-0.13	0.18	0.23
Stapelberg & Mewes (1994)	489	ALL	-99	99	2	-0.27	0.27	0.23
Zabaras (1999)	489	ALL	-46	55	46	-0.13	0.14	0.15
Schulkes (2011)	489	ALL	64	77	221	0.02	0.09	0.13
Gokcal (2008)	489	ALL	49	87	278	-0.02	0.11	0.16
TUFFP Model	489	ALL	-19	65	126	-0.12	0.14	0.17
Taitel & Dukler (1977)	119	587 cP	803	803	1098	1.81	1.81	1.89
Gregory & Scott (1969)	119	587 cP	-28	68	96	-0.16	0.18	0.21
Greskovich & Shrier (1972)	119	587 cP	-28	68	97	-0.16	0.18	0.21
Heywood & Richardson (1979)	119	587 cP	8	71	144	-0.10	0.14	0.20
Hill & Wood I (1990)	119	587 cP	208	247	554	-0.001	0.27	0.37
Hill & Wood II (1990)	119	587 cP	899	899	1328	1.49	1.49	1.05
Tronconi (1990)	119	587 cP	55	123	273	-0.15	0.23	0.32
Stapelberg & Mewes (1994)	119	587 cP	-99	99	4	-0.31	0.31	0.31
Zabaras (1999)	119	587 cP	-48	68	62	-0.19	0.20	0.22
Schulkes (2011)	119	587 cP	127	147	376	0.01	0.15	0.21
Gokcal (2008)	119	587 cP	147	180	501	0.01	0.18	0.24
TUFFP Model	119	587 cP	4	98	211	-0.17	0.21	0.26
Taitel & Dukler (1977)	72	420 cP	615	615	424	2.30	2.30	2.28
Gregory & Scott (1969)	72	420 cP	-47	50	29	-0.15	0.15	0.13
Greskovich & Shrier (1972)	72	420 cP	-46	49	30	-0.15	0.15	0.13
Heywood & Richardson (1979)	72	420 cP	-24	37	37	-0.08	0.11	0.12
Hill & Wood I (1990)	72	420 cP	46	90	124	-0.04	0.21	0.26
Hill & Wood II (1990)	72	420 cP	428	428	206	1.33	1.33	0.98
Tronconi (1990)	72	420 cP	-26	58	63	-0.19	0.22	0.23
Stapelberg & Mewes (1994)	72	420 cP	-99	99	1	-0.34	0.34	0.24
Zabaras (1999)	72	420 cP	-59	60	25	-0.19	0.19	0.14
Schulkes (2011)	72	420 cP	17	32	60	-0.01	0.08	0.11
Gokcal (2008)	72	420 cP	7	45	79	-0.03	0.11	0.15
TUFFP Model	72	420 cP	-45	56	40	-0.17	0.19	0.16
Taitel & Dukler (1977)	71	300 cP	625	625	388	1.85	1.85	1.83
Gregory & Scott (1969)	71	300 cP	-43	48	31	-0.12	0.12	0.11
Greskovich & Shrier (1972)	71	300 cP	-43	48	31	-0.12	0.12	0.11
Heywood & Richardson (1979)	71	300 cP	-15	35	46	-0.06	0.08	0.10
Hill & Wood I (1990)	71	300 cP	95	125	218	0.02	0.18	0.22
Hill & Wood II (1990)	71	300 cP	383	383	255	0.89	0.89	0.62
Tronconi (1990)	71	300 cP	-3	72	110	-0.14	0.18	0.20
Stapelberg & Mewes (1994)	71	300 cP	-99	99	2	-0.28	0.28	0.20
Zabaras (1999)	71	300 cP	-58	58	22	-0.16	0.16	0.12
Schulkes (2011)	71	300 cP	34	46	108	0.01	0.06	0.09
Gokcal (2008)	71	300 cP	19	54	122	-0.02	0.09	0.12
TUFFP Model	71	300 cP	-31	59	76	-0.12	0.14	0.13
Taitel & Dukler (1977)	70	220 cP	1131	1131	1126	2.34	2.34	2.37
Gregory & Scott (1969)	70	220 cP	-5	48	92	-0.04	0.07	0.09
Greskovich & Shrier (1972)	70	220 cP	-5	48	92	-0.04	0.07	0.09
Heywood & Richardson (1979)	70	220 cP	40	58	136	0.03	0.07	0.10
Hill & Wood I (1990)	70	220 cP	185	211	367	0.06	0.19	0.21
Hill & Wood II (1990)	70	220 cP	551	551	652	0.84	0.84	0.63
Tronconi (1990)	70	220 cP	36	98	169	-0.10	0.15	0.19
Stapelberg & Mewes (1994)	70	220 cP	-98	98	3	-0.22	0.22	0.19
Zabaras (1999)	70	220 cP	-29	51	64	-0.08	0.09	0.10
Schulkes (2011)	70	220 cP	101	107	236	0.05	0.08	0.09
Gokcal (2008)	70	220 cP	66	97	237	0.005	0.10	0.13
TUFFP Model	70	220 cP	5	64	141	-0.07	0.10	0.12

Taitel & Dukler (1977)	96	181 cP	879	879	588	2.36	2.36	2.62
Gregory & Scott (1969)	96	181 cP	-27	42	41	-0.04	0.09	0.10
Greskovich & Shrier (1972)	96	181 cP	-27	42	41	-0.04	0.09	0.10
Heywood & Richardson (1979)	96	181 cP	4	40	49	0.02	0.08	0.12
Hill & Wood I (1990)	96	181 cP	57	84	94	0.02	0.14	0.17
Hill & Wood II (1990)	96	181 cP	304	304	162	0.69	0.69	0.64
Tronconi (1990)	96	181 cP	-28	48	49	-0.12	0.14	0.16
Stapelberg & Mewes (1994)	96	181 cP	-99	99	1	-0.23	0.23	0.16
Zabaras (1999)	96	181 cP	-44	48	34	-0.08	0.10	0.10
Schulkes (2011)	96	181 cP	20	31	49	0.01	0.05	0.07
Gokcal (2008)	96	181 cP	-10	40	50	-0.04	0.09	0.10
TUFFP Model	96	181 cP	-38	46	32	-0.09	0.10	0.09
Taitel & Dukler (1977)	61	155 cP	1003	1003	503	2.28	2.28	2.07
Gregory & Scott (1969)	61	155 cP	-16	33	40	-0.03	0.05	0.06
Greskovich & Shrier (1972)	61	155 cP	-16	33	40	-0.03	0.05	0.06
Heywood & Richardson (1979)	61	155 cP	23	40	61	0.04	0.06	0.07
Hill & Wood I (1990)	61	155 cP	122	147	247	0.04	0.15	0.17
Hill & Wood II (1990)	61	155 cP	351	351	246	0.60	0.60	0.39
Tronconi (1990)	61	155 cP	8	77	138	-0.10	0.13	0.16
Stapelberg & Mewes (1994)	61	155 cP	-99	99	1	-0.21	0.21	0.16
Zabaras (1999)	61	155 cP	-37	39	29	-0.07	0.07	0.06
Schulkes (2011)	61	155 cP	55	63	126	0.03	0.06	0.07
Gokcal (2008)	61	155 cP	15	56	107	-0.03	0.08	0.11
TUFFP Model	61	155 cP	-19	48	75	-0.07	0.09	0.10

Table F.20 Model evaluation using the measured slug frequency of 2-in. ID pipes.

			Statistical Parameter					
Model	No. of Data	Oil Viscosity (cP)	ε_1 (%)	ε_2 (%)	ε_3 (%)	ε_4 (slug/s)	ε_5 (slug/s)	ε_6 (slug/s)
Taitel & Dukler (1977)	55	155 cP	402	402	459	3.21	3.21	4.06
Gregory & Scott (1969)	55	155 cP	-53	58	30	-0.41	0.43	0.44
Greskovich & Shrier (1972)	55	155 cP	-53	58	30	-0.41	0.42	0.43
Heywood & Richardson (1979)	55	155 cP	-38	46	35	-0.34	0.36	0.44
Hill & Wood I (1990)	55	155 cP	38	61	83	-0.10	0.29	0.51
Hill & Wood II (1990)	55	155 cP	155	156	159	0.85	0.87	1.08
Tronconi (1990)	55	155 cP	-9	56	72	-0.39	0.45	0.66
Stapelberg & Mewes (1994)	55	155 cP	-94	96	22	-0.65	0.74	0.71
Zabaras (1999)	55	155 cP	-72	74	27	-0.59	0.60	0.62
Schulkes (2011)	55	155 cP	5	26	38	-0.09	0.19	0.30
Gokcal (2008)	55	155 cP	18	29	36	0.17	0.22	0.30
TUFFP Model	55	155 cP	-21	36	36	-0.13	0.24	0.34

Table F.21 Model evaluation using the measured slug frequency of 2- and 3-in. ID pipes.

			Statistical Parameter					
Model	No. of Data	Oil Viscosity (cP)	ε_1 (%)	ε_2 (%)	ε_3 (%)	ε_4 (slug/s)	ε_5 (slug/s)	ε_6 (slug/s)
Taitel & Dukler (1977)	116	155 cP	718	718	567	2.72	2.72	3.19
Gregory & Scott (1969)	116	155 cP	-34	45	40	-0.21	0.23	0.36
Greskovich & Shrier (1972)	116	155 cP	-33	45	40	-0.21	0.23	0.36
Heywood & Richardson (1979)	116	155 cP	-6	43	59	-0.14	0.20	0.36
Hill & Wood I (1990)	116	155 cP	82	106	192	-0.02	0.22	0.38
Hill & Wood II (1990)	116	155 cP	258	258	230	0.72	0.73	0.81
Tronconi (1990)	116	155 cP	0	67	112	-0.24	0.29	0.49
Stapelberg & Mewes (1994)	116	155 cP	-96	97	15	-0.42	0.46	0.55
Zabaras (1999)	116	155 cP	-53	56	33	-0.32	0.32	0.50
Schulkes (2011)	116	155 cP	31	46	98	-0.03	0.12	0.22
Gokcal (2008)	116	155 cP	16	43	81	0.07	0.15	0.24
TUFFP Model	116	155 cP	-20	42	60	-0.10	0.16	0.24

요약(국문초록)

본 연구에서는 관 직경에 따른 고점성도 수평 슬러그 유동 특성을 실험적으로 분석한다. 슬러그 유동은 수평관 내 오일-가스 2상 유동에서 가장 일반적인 유동 패턴이다. 각각의 슬러그 인자들은 생산 시스템 설계에 필수적인 압력 구배, 평균 액체 점유율을 예측하는데 매우 중요한 역할을 한다.

이전의 실험들은 대부분 저, 중점성도 오일에 대한 평가이므로 고점성도 오일의 경우 유동인자 예측의 정확도에 대한 검증이 필요하다. 몇몇 기존 가스와 고점성도 오일 2상 유동 실험은 모두 직경 2인치에 한정적이므로 관직경이 변화될 경우 예측과정에서 어떤 영향이 있는지 분석하는 것 또한 필요하다.

따라서 본 연구에서는 수평 3인치 관과 고점성도 오일을 이용하여 압력 구배, 평균 액체 점유율, 슬러그 액체 점유율, 필름 액체 점유율, 슬러그 속도, 슬러그 길이, 그리고 슬러그 빈도가 관 직경에 따라 어떻게 변화하는지 보여준다.

실험에서는 서로 다른 6가지 오일 점성도와 지정된 범위 내의 공탑 액체 속도(0.02 m/s ~ 0.35 m/s), 공탑 기체 속도(0.1 m/s ~ 3.6 m/s)를 사용하였다. 이 중 587cP, 181cP, 155cP 오일을 사용하여 얻어진 데이터와 기존의 2인치 데이터를 정성적으로 비교하였다. 정적교정이 완료된 커패시턴스 센서를 통해 액체 점유율을 측정하였고 압력 구배, 온도, 압력 변환기를 이용하여 추가적인 유동 특성들을 측정하였다.

결과적으로 관 직경이 증가함에 따라 압력 구배는 감소하였고 평균 액체 점유율은 증가하였다. 또한 필름 액체 점유율과 슬러그 길이는 감소하였고 슬러그 액체 점유율과 슬러그 빈도는 증가하였다.

나아가 본 연구에서는 측정된 결과와 기존의 2상 유동 예측 모델들을 통해 예측한 결과를 정량적으로 비교하였다. 대부분의 경우 편차를 보였으며 이를 통해 기존의 모델들이 고점성도 오일과 관 직경에 따른 결합적 영향을 잘 반영하지 못하고 있다는 것이 나타났다. 각각의 유동 인자에 대해 가장 오차가 적은 기존 모델들을 최적 모델로 제시하였다.

직경 3인치의 경우, 기존의 압력 구배 예측 모델들을 통해 계산된 결과는 획일화된 과소예측의 문제점을 보이며 측정된 결과와 큰 오차를 나타내므로 적합한 최적 모델 선정을 제한하였다. 이를 위해 본 연구에서는 유체의 상에 따라 레이놀즈 수 계산을 달리하는 간소화된 Lockhart and Martinelli 부분 압력 구배 예측 모델을 제안하였다. 제안한 모델은 실험 자료 예측 시험 결과 OLGA, Xiao *et al.* (1990) 모델에 비해 15%p, TUFFP 모델에 비해 7%p 낮은 오차를 나타내었고 획일화된 과소예측의 문제를 해결하였다.

주요어: 2상 유동, 관 직경, 고점성도, 수평 유동, 관 유동, 슬러그 유동, 압력 구배, 평균 액체 점유율, 슬러그 인자, 슬러그 액체 점유율, 필름 액체 점유율, 슬러그 속도, 슬러그 길이, 슬러그 빈도, 압력 구배 예측 모델

학 번: 2012-23280